Report LR-761

A method for the determination of the effect of propeller slipstream on static longitudinal stability and control of multi-engined aircraft

December 1994

E. Obert

TU Delft
Delft University of Technology

Faculty of Aerospace Engineering

A method for the determination of the effect of propeller slipstream on static longitudinal stability and control of multi-engined aircraft

E. Obert

Publisher: Delft University of Technology
Faculty of Aerospace Engineering
P.O. Box 5058
2600 GB Delft
The Netherlands.
tel: (015)782058
fax: (015)781822

Date December 1994

Report LR- 761

ISBN: 90-5623-009-3

Title	:	A method for the determination of the effect of propeller slipstream on static longitudinal stability and control of multi-engined aricraft.
Author(s)	:	E. Obert
Abstract	:	The method makes possible the determination of slipstream effects on wing lift, tail-off pitching moment and flow conditions at the horizontal tail.
Keyword(s)	:	Longitudinal stability. Longitudinal control. Propeller slipstream.

Date	December 1994
Prepared	E. Obert
Verified	
Approved	Th. van Holten
Authorized EB	P.G. Bakker

Summary

A method is presented for the determination of slipstream effects on static longitudinal stability and control of multi-engined propeller aircraft.
The method is partly based on elementary momentum considerations partly on a correlation of windtunnel data.
The method allows the determination of:

- The increase in lift due to propeller slipstream,
- The change in tail-off pitching moment, both with flaps retracted and deflected.
- The location of the propeller slipstream relative to the horizontal tailplane and the associated effect on average dynamic pressure at the tailplane.
- The change in average downwash angle due to slipstream at the tailplane.

For a number of aircraft configurations a comparison is shown between calculated results and windtunnel data.

Preface

This report consists basically of two parts.
The first part, the main body and Appendix I to V were originally published as paper 7.3.4 in the Proceedings of the 19th Congress of the International Council of the Aeronautical Sciences, ICAS held in Anaheim, Cal. USA on 18-23 September, 1994.

The second and the largest part of this report consists of Appendix VI to XVIII. In these appendices the various subjects mentioned in the original publication are covered in much greater depth. Many more aircraft configurations are analysed by means of computations compared with test data and all calculation procedures are explained via step-by-step calculations for specific examples.

Contents

THE EFFECT OF PROPELLER SLIPSTREAM ON THE STATIC LONGITUDINAL STABILITY AND CONTROL OF MULTI- ENGINED PROPELLER AIRCRAFT

1. Abstract

A method is presented for the determination of slipstream effects on static longitudinal stability and control of multi-engined propeller aircraft.
The method is partly based on elementary momentum considerations partly on a correlation of windtunnel data.
The method allows the determination of:

- o The increase in lift due to propeller slipstream,
- o The change in tail-off pitching moment, both with flaps retracted and deflected.
- o The location of the propeller slipstream relative to the horizontal tailplane and the associated effect on average dynamic pressure at the tailplane.
- o The change in average downwash angle due to slipstream at the tailplane.

For a number of aircraft configurations a comparison is shown between calculated results and windtunnel data.

2. Notation

Symbol	Description	Unit
A_s	Aspect ratio of wing part immersed in the slipstream of a single propeller.	(-)
$A_{s,eff}$	Effective aspect ratio of wing part immersed in the slipstream of a single propeller at low thrust coefficients.	(-)
A_s'	Total cross-sectional area of the combined fully contracted slipstream tubes: $\left(A_S' = n_e \frac{\pi}{4} D^{*2}\right)$	(m^2)
A_W	Wing aspect ratio ($A_W = b^2/S_W$)	(-)
A^*	Cross-sectional area of the part of the outer flow stream tube affected by the slipstream (see Appendix IV).	(m^2)
1+b	Square-root of the average dynamic pressure ratio at the horizontal tailplane $\left[b=\sqrt{q_h/q-1}\right]$	(-)
b_s	Width of the tailplane part covered by the slipstream of a single propeller in idealized flow.	(m)
b_w	Wing span.	(m)
c	Wing section chord.	(m)
c'	Extended wing chord (chord extension due to flap deflection).	(m)
$\bar{c}$	Mean aerodynamic chord.	(m)
c_f	Flap chord.	(m)
C_L	Lift coefficient $\left[C_L=\frac{lift}{\frac{1}{2}\rho V_o^2 S_W}\right]$	
c_l	Two-dimensional lift curve referred to the extended section chord c'.	(-)
C_{Lp}	Total normal-force coefficient of the combined propellers $\left[C_{L_p}=\frac{n_e N_p}{\frac{1}{2}\rho V_o^2 S_W}\right]$	(-)
$(C_L)_{p-o}$	Power-off lift coefficient.	(-)
ΔC_{L_s}	Lift coefficient due to slipstream deflection by the wing.	(-)
$\Delta C_{L_{s,o}}$	Lift coefficient due to slipstream deflection by the wing at the zero-lift angle for the wing with flaps retracted. (See fig. 20).	(-)
$\Delta C_{L_{s,\alpha}}$	Lift coefficient due to slipstream deflection at a given angle-of-attack.	(-)
$c_{l_{s,o}}$	Local lift coefficient at the propeller axis location in the absence of slipstream.	(-)
C_{LT}	Vertical component of total thrust coefficient. $\left[C_T=\frac{T_{tot}\times\sin\alpha_R}{\frac{1}{2}\rho V_o^2 S_W}\right]$	

C_{Lw+s} Total wing lift coefficient in the presence of slipstream.

$C_{L\alpha}$ Wing lift curve slope. (1/deg)

$C_{L\alpha h}$ Horizontal tailplane lift curve slope (1/deg)

$C_{L\alpha s}$ Lift curve slope of a wing in free air with aspect ratio A_S (1/deg)

$C_{L\alpha s,eff}$ Lift curve slope of a wing in free air with aspect ratio $A_{s,eff}$ (1/deg)

$c_{l\alpha}$ Airfoil section lift curve slope. - Lift coefficient-versus-angle of attack. (1/deg)

$c_{l\alpha s}$ Airfoil section lift curve slope at the propeller axis location. (1/deg)

$c_{l\delta}$ Airfoil section lift curve slope. -Lift coefficient-versus-flap angle (1/deg)

C_M Pitching moment coefficient (-)

$$\left[C_M = \frac{M}{\frac{1}{2}\rho V_o^2 S_w \bar{c}}\right]$$

ΔC_{MFS} Additional pitching moment contribution to the calculated pitching moment due to slipstream C_{Ms} to improve comparison with test data. (-)

$c_{mo,s}$ Zero-lift pitching moment coefficient of the wing section at the propeller axis location. (-)

$c'_{m0.25c'}$ Airfoil pitching moment coefficient about the quarter-chord point referred to the extended section chord c'. (-)

ΔC_{Mp} Pitching moment coefficient due to total propeller normal force. (-)

ΔC_{Ms} (= C_{Ms}) Total pitching moment coefficient due to propeller forces and slipstream. (-)

c_s Wing section chord at propeller location. (m)

ΔC_{MT} Pitching moment coefficient due to total propeller thrust. (-)

C_T Thrust coefficient

$$\left[C_T = \frac{T_{tot}}{\frac{1}{2}\rho V_o^2 S_w}\right]$$

D Propeller diameter (m)

D^* Diameter of fully contracted slipstream. (m)

Δh^* The (assumed) vertical displacement of the slipstream centre line due to the propeller axis at the propeller plane not coinciding with the stream-line leading to the forward stagnation point. (m)

h_{tot} Total distance in the Z-direction between slipstream centreline and horizontal tailplane. (m)

Δh_i Vertical displacement due to angle-of-attack of the quarterchord point of the tailplane section at the propeller location. (m)

h_t Vertical distance between the tailplane section at the propeller location and the propeller axis. (m)

$(\Delta_{hl})_{upw}$ Vertical displacement of slipstream centre line due to upwash in front of the wing due to flap deflection (m)

$(\Delta h_l)_\alpha$ Vertical displacement of slipstream centre line due to angle-of-attack. (m)

$(\Delta h_l)_{\delta f}$ Vertical displacement of slip-stream centre line due to flap deflection. (m)

i_{cs} Incidence of wing section chord at the propeller location (deg

L_W Wing lift not affected by slipstream. (N)

L_S Wing lift due to slipstream. (N)

l_h Tail arm. (Measured between wing and tailplane quarter-mean-aerodynamic chord points). (m)

l^*_h Distance between wing trailing-edge and tailplane quarter-chord points at the propeller axis location. (m)

K_e Downwash factor. ($K_e = Z_w/Z_e$) (-)

n_e Number of propellers. (-)

N_p Normal force of a single propeller (N)

P Coefficient in downwash formula (-)

q (= q_o) Dynamic pressure of the undisturbed flow (N/m^2)

q_h Average dynamic pressure at the horizontal tailplane. (N/m^2)

q_s (= q_j) Average dynamic pressure in the fully contracted slipstream. (N/m^2)

S_h Horizontal tail area. (m^2)

S_s (= $S_{h,s}$). Area of horizontal tail surface immersed in the idealized slipstream.

S_w Wing reference area (m^2)

T_{tot} (=T) Total propeller thrust (N)

ΔV Increase in velocity in the fully contracted slipstream (m/s)

V_O Velocity of undisturbed airflow. (m/s)

X Coordinate parallel to the fuselage reference line. (m)

X_{CG} Centre-of-gravity position along the X-axes. (m)

$X_{FS}/\bar{c}$ Dimensionless distance over which the lift due to slipstream is assumed to be displaced to obtain calculated pitching moment data due to

	slipstream with flaps deflected which match with test data.	(-)
X_{prop}	Propeller plane coordinate along the X-axis.	(m)
$X_{0.25cs}$	Quarter-chord coordinate along the X-axis of the wing section at the propeller location.	(m)
Y	Lateral coordinate.	(m)
$Y_{s,o}$	Distance between propeller axis and fuselage centre line.	(m)
Z	Coordinate in the plane of symmetry prependicular tot he fuselage reference line. Positive upward.	(m)
Z_{CG}	Centre-of-gravity position along the Z-axis.	(m)
Z_h	Distance along the Z-axis between the wing trailing-edge and the horizontal tailplane at the propeller axis location.	(m)
Z_t	Distance along the Z-axis between the propeller axis and the wing trailing edge.	(m)
Z_w	Actual vertical displacement of the wing wake relative to the wing trailing edge at the horizontal tailplane position.	(m)
Z_ε	Wing wake displacement calculated with the lifting line theory	(m)
α	Angle-of-attack.	(deg)
α^*	Change in flow direction immediately behind the propeller relative to the direction of the undisturbed flow	(deg)
α_o	Airfoil section zero-lift angle-of-attack.	(deg)
$\Delta\alpha_{o,f}$	Change in airfoil section zero-lift angle-of-attack due to flap deflection.	(deg)
α_R	Angle-of-attack related to the fuselage reference line.	(deg)
α_S	Angle-of-attack of the wing part immersed in the propeller slipstream.	(deg)
$\alpha_{S,eff}$	Effective angle-of-attack of the wing part immersed in the slip stream at low thrust coefficients.	(deg)
δ	(Plain) flap defection angle	(deg)
δ_f	Flap setting.	(deg)
ε	Downwash angle.	(deg)
ε'	Estimated average downwash angle of the flow affected by slipstream.	(deg)
$(\varepsilon_o)_{p-o}$	The average downwash angle at the horizontal tailplane at zero lift in the power-off condition.	(deg)
	The slope of the downwash-angle versus-lift curve at the power-off condition.	(deg)
ε_S	Calculated downwash angle in the slipstream.	(deg)
$\varepsilon_{\alpha=o}$	Downwash angle at α_R = O at the power-off condition.	(deg)
	The increase in average downwash angle at the tail due to inflow into the slipstream when the slipstream velocity is twice the velocity of the undisturbed flow.	(deg)
ϕ	Angle defined in Appendix IV.	(-)
λ	1: Wing taper ratio 2: Parameter used in ref. 6	(-)
ϱ	Air density.	(kg/m^3)
σ	Parameter defined in Appendix II	(-)
Θ	Slipstream turning angle.	(deg)

3. Introduction

The effect of propeller slipstream on the longitudinal characteristics of an aircraft has caught the attention of aircraft designers since the early days of aviation. In particular on multi-engined aircraft propeller slipstream often leads to a decrease in longitudinal stability and non-linear control characteristics when speed or power setting is varied.
This may severely limit the allowable centre-of-gravity range in particular on high-performance aircraft.
But most of all the unpredictability of slipstream effects is a matter of concern, in particular when no windtunnel data with powered propellers are available for the configuration under consideration.
For preliminary design purposes open literature provides guidelines for the estimation of the effect of propeller slipstream on lift and drag. Tail-off pitching moments, in particular with flaps deflected, downwash at the tail and the location of the slipstream relative to the tail and consequently the average dynamic pressure at the tail with slipstream present are to the author's knowledge not covered in open literature. In the present paper a semi-empirical method is presented which allows the estimation of these parameters. With these data available a first-order estimate of the effect of propeller slipstream on longitudinal stability and control should be possible.

4. Historical Overview

In the '20's and '30's the analysis of propeller slipstream effects was mainly limited to gathering data collections from which some general trends were derived (refs. 1-3). Some relevant work was also performed on the analysis of the characteristics of a two-dimensional model wing placed in an open windtunnel test section. This resembled a wing partly immersed in a slipstream at very low flight speeds (refs. 4, 5).

The first systematic investigation concerning the increase in lift on a multi-engined aircraft due to propeller slipstream was performed by Smelt and Davies in 1936. This resulted in the classic semi-empirical method reported in ref. 6. No configurations with high-lift devices were considered. The method was primarily aimed at conditions with low thrust coefficients. The increase in lift due to slipstream was thought to be primarily caused by an increase in dynamic pressure of the flow about the part of the wing immersed in the slipstream. The downwash was not considered explicitly.

In the late 1930's and early 1940's efforts were made to describe slipstream effects with theoretical models. Numerical values for the required coefficients of proportionality could not be determined however (ref. 7-12). Also more testdata were published (refs. 13, 14).

With the increase in engine power in the 1940's the need for better insight in slipstream effects on aircraft characteristics lead to several systematic windtunnel investigations such as presented in refs. 15-17.

With the advent of the turbojet engine the interest in conventional propeller aircraft disappeared in the 1950's in particular from the research programme's of the large research institutes.

However, in the late 1950's and throughout the 1960's extensive research into the feasibility of V/STOL-aircraft lead to a renewed interest in propellers (refs. 18-32). Because of the emphasis on V/STOL-characteristics most of the research was performed at very low speed (and thus very high thrust coefficients). Also, most configurations investigated (except those of refs. 33-37) had the greater part of the wing immersed in the propeller slipstream. Based on these latter investigations Kuhn (ref. 38,1959) developed a semi-empirical method which allows the estimation of the increase in lift due to propeller slipstream with flaps deflected and at very low flight speeds up to V = 0 .

In ref. 39 some results are presented of the application of the method by Kuhn.
In refs. 40 and 41 more recent analyses are presented of the effect of slipstream on longitudinal characteristics.

Although two oil crises and the deregulation in the US and subsequent developments in airline operation renewed the interest in conventional propeller aircraft no method has been published since then which allows the analysis of the combined slipstream effects on longitudinal aircraft characteristics.

Numerous investigations were performed and reported on propellers and propeller-airframe interaction. These were however mainly aimed at obtaining better insight in details of the flow and at the development of computer codes based on full-potential, Euler or Navier-Stokes flow equations. None of these studies produced results up to now which could be used to determine overall aircraft characteristics.

5. Some remarks on the methods by Smelt and Davies and Kuhn

As mentioned before the method by Smelt and Davies (ref. 6) has the following characteristics:

a. Only clean wings are considered.

b. Only low thrust coefficients are considered

c. The increase in lift due to slipstream can be written as (in the present report's notation):

$$\Delta C_{L_s} = \frac{D^* C_S}{S_W} \Delta V \left[\lambda C_{l_{s,o}} - 0.6 C_{l_{\alpha_s}} (\alpha_R - \alpha^*)\right]$$

In the first term between brackets λ is estimated for two extreme cases:

$\lambda = 2$ when the ratio between slipstream diameter and average chord of the part of the wing immersed in the slipstream is large. This leads effectively to the assumption that the spanwise lift distribution over this part of the wing can be treated as a two-dimensional flow problem.

$\lambda = 1$ when the ratio between slipstream diameter and average chord of the part of the wing in the slipstream is very small. The reasoning behind the latter is rather qualitative.

Comparison with windtunnel data lead to a correlation curve where λ varied between 1 and 1.8 as a function of the aspect ratio of the total part of the wing immersed in the combined slipstreams.

The second term between brackets takes into account the change in local angle-of-attack due to downwash behind the propeller(s). The factor 0.6 is an empirical constant.

Although for very low thrust coefficients the method by Smelt and Davies may in certain cases give reliable results many cases have been reported where the comparison between theory and testdata was unsatisfactory.

The method by Kuhn (ref. 38) approaches the problem from the other side. The starting point is the static condition ($V_0 = 0$) where the lift is entirely determined

by the propeller slipstream. Windtunnel test data show that the slipstream momentum is effectively rotated over an angle Θ by flap deflection. Although Kuhn suggests that the degree of rotation is a function of the ratio of flap chord and propeller diameter C_f/D the shape of the resultant empirical curve is identical to the curve that gives the ratio of lift curve slopes due do flap deflection and change in angle of attack (see fig. 8). Furthermore a thrust-recovery factor F/T is introduced to incorporate viscous effects. (See fig. Ic, Appendix I).

Having established empirical relations between propeller thrust and the total force on the wing-propeller(s) combination as a function of angle-of-attack and flap deflection for different flap types at static conditions (V_0=0) Kuhn then proceeds in formulating a model for the total lift on wing-propeller(s) combinations at low flying speeds.

Basically it is assumed that the total lift on the wing is determined by the vertical component of the outgoing momentum of the stream tubes determined by the propeller diameters and the wing span. The downwash angle of the propeller slipstream behind the wing is assumed to remain equal to the value found for static conditions. Thus no effect of forward speed or thrust coefficient is considered. The downwash angle of the remaining stream tube determined by the wing span is taken according to lifting line theory for the condition with power off:

$$\varepsilon = 57.3 \frac{2C_{L_{p=0}}}{\pi A_W} \qquad \text{(deg)}$$

As the slipstream turning angle Θ is kept constant a correction factor is added to obtain the correct power-off lift when the thrust coefficient approaches $C_T = 0$ and consequently the turning angle Θ approaches the power-off downwash angle ε.

Also, a comparison with test data required the addition of a multiplication factor K = 1.6 to the calculated extra lift due to slipstream.

Thus, although the method by Kuhn allows the estimation of lift due to propeller slipstream with flaps deflected it shows much room for improvement in particular at lower thrust coefficients.

6. Determination of the effect of propeller slipstream on static longitudinal stability

When at constant speed propeller thrust is increased the total flow condition about an aircraft changes.

Four elements can be distinguished.

1. The wing lift increases.
2. The tail-off pitching moment increases in a negative sense, in particular with flaps deflected.
3. The average downwash angle at the horizontal tail changes.
4. The average dynamic pressure at the horizontal tail changes if the tail is partly immersed in the slipstream.

6.1 The increase in wing lift due to propeller slipstream

Two established methods have been mentioned for the estimation of the increase in wing lift due to propeller slipstream, the methods by Smelt and Davies (ref. 6) and Kuhn. (ref. 38).

In the following a method is presented which offers certain improvements over the methods previously described.

The basic concept is identical to that of the method of ref. 38
The total lift is assumed to be the sum of the vertical components of the outgoing momentum of the stream tubes determined by the fully contracted propeller slipstream and the stream tube determined by the wing span. The cross-sectional area of this latter stream tube is a circle determined by the wing span minus the total cross-sectional area of the fully contracted propeller slipstream. (Fig. 1).

According to lifting line theory (valid for high-aspect-ratio wings) the turning angle of the stream tube determined by the wing span is equal to the downwash angle:

$$\varepsilon = 57.3 \frac{2C_L}{\pi A_W} \qquad \text{(deg.)}$$

For very high lift this leads, when the same stream tube analogy is used, to:

$$\sin \varepsilon = \frac{2C_L}{\pi A_W}$$

The lifting theory developed by R.T. Jones (ref. 42) states that for very low aspect ratios ($A \leq 1$) the same expression is valid. However, in this case the lift-curve slope, when the wing aspect ratio approaches zero, can be written as:

$$C_{L_\alpha} = \frac{1}{57,3} \times \frac{\pi}{2} A_W \qquad \text{(per deg.)}$$

and

$$C_L = C_{L_\alpha} \times \alpha = \frac{1}{57.3} \times \frac{\pi}{2} A_W \times \alpha \quad \text{(per deg.)}$$

or, for very high angles-of-attack:

$$C_L = \frac{\pi}{2} A_W \sin \alpha$$

Thus: $\sin \varepsilon = \sin \alpha$
and $\varepsilon = \alpha$

Stepniewsky (ref. 44 page 13) suggested that at least for clean wings for higher thrust coefficients the increase in lift due to slipstream could be estimated by considering the flow of the slipstream over the wing to be equivalent to the flow about a wing in a free stream of which the span was equal to the diameter of the fully contracted slipstream and the chord equal to the actual wing's chord at the propeller axis.

The dynamic pressure to be considered is equal to the dynamic pressure in the slipstream and the angle of attack α_s should be measured between the airfoil section's zero-lift angle-of-attack and the centre-line of the propeller slipstream. On a propeller at a given angle-of-attack the latter means that with increasing thrust coefficient the slipstream is deflected more downward and the angle-of-attack α_s of the equivalent wing decreases.

The validity of this concept was first checked on the test data from ref. 28.
In front of a wing, spanning the windtunnel test section a propeller was fitted driven by an electric motor. The propeller and electric motor were mounted separately and were physically detached from the 2-d wing model. The model was constructed such that spanwise lift distribution coul be measured directly. With the propeller in a fixed position the angle of attack of the model could be varied.

Because the model extended from wall to wall in the test section the "free-air" lift could not be determined on the basis of a stream tube being deflected over an angle ε. The downwash angle was taken as zero. Then the lift due to slipstream was taken as:

$$L_s = \rho \, (V_o + \Delta V)^2 \, \frac{\pi}{4} D^{*2} \sin \varepsilon_s$$

or

$$L_s = \rho \, (V_o + \Delta V)^2 \, \frac{\pi}{4} D^{*2} \sin \alpha_s$$

as the propeller was fixed to the tunnel, $\alpha_s = \alpha$
The test data of ref. 28 and the calculated data obtained according to the procedure outlined above are presented Appendix II and in fig. 11.

This comparison shows that the principle is proved although the effect of varying angle-of-attack is not incorporated in the calculation method. It is unclear if this is a viscous effect or if it is more fundamental.

The increase in lift due to slipstream was then calculated according to the method described for a number of aircraft configurations for which data were available.
Figs. 2-6 show measured and calculated lift curves at various thrust coefficients for some of the clean wing configurations analysed. Ref. 49 presents a more extensive overvieuw.
Fig. 7 shows that in general a comparison between test data and calculated data for the increase in lift due to slipstream on wings without flaps shows satisfactory results and that no correction factors need be applied.

As mentioned before, in ref. 38 a relation is suggested for wings with flaps deflected between the slipstream turning angle Θ per degree of flap deflection at zero flight speed (Θ/δ) and the ratio between flap chord and propeller diameter (c_f/D). This relation is, however, identical to the relation between the ratio of the slope of the lift curves due to flap deflection and due to change in angle-of-attack ($C_{l\delta}/C_{l\alpha}$) as a function of flap-chord-to-section chord ratio (fig. 8). (In the test data considered the propeller diameter was roughly equal to the wing chord).

In the present analysis the latter relation is taken as more relevant. This allows the model previously described for plain wings to be extended to wings with flaps.
This is not strictly in line with a later extension of Jones's theory for small-aspect-ratio wings (ref. 42) which states that when the aspect ratio approaches zero the lift on a flapped wing is determined only by the inclination of the trailing edge of the camber line i.e. the sum of angle-of-attack and flap angle. The theory of ref. 43 was developed for small angles only however. Also the approach as described above produces data far more in line with experimental results.

Again it is assumed that the lift due to slipstream is equal to the lift on a wing in free flow with a span equal to the diameter of the fully contracted slipstream and an airfoil section equal to the wing section at the propeller axes with flaps deflected. The angle of attack α_s is measured between the zero-lift angle-of-attack with flaps deflected and the effective propeller slipstream centre line.

In figs. 12-16 examples are presented of the lift curves for several aircraft configurations with flaps deflected and varying thrust coefficient.

In fig. 17 the measured and calculated increase in lift due to slipstream is compared for a number of aircraft configurations. Note that no correction factor is required in the calculation procedure.

More examples are presented in Appendix XI.

Up to now fairly high thrust coefficients have been considered. It will be clear that when the thrust coefficient approaches zero the assumption

$$\sin \varepsilon_s = \sin \alpha_s$$

can no longer be maintained.
Following the suggestion from ref. 44 to assume an arbitrary fairing function for the downwash angle ε_s the (slightly modified) function from ref. 44 was adopted. Here the gradual change from $\varepsilon_s = \alpha_s$ to ε was accomplished by considering an imaginary aspect ratio:

$$A_{s_{eff}} = A_s + (A_w - A_s)\left[\frac{V_o}{V_o+\Delta V}\right]^{(A_w-A_s)}$$

such that

$$\sin \varepsilon_s = \frac{2C_{L_{\alpha_s}} \times \sin \alpha_s}{\pi A_{s_{eff}}}$$

where $C_{L_{\alpha_s}}$ is related to $A_{s_{eff}}$.

A derivation of the formulae used in the calculations is presented in Appendix I.

In the method just described the lift due to slipstream has been compared to the lift of a wing with small aspect ratio.
In refs. 5, 28, 31 the lift due to slipstream at zero flight speed has been analysed both theoretically and experimentally. The results obtained in these investigations indicate that when zero flight speed is approached this assumption seems no longer to hold (figs. 9, 10). This is also suggested by the data of fig. 11 when σ approaches 1 and thus q_s/q_o approaches infinity. For practical values of the thrust coefficient the approach followed produces satisfactory results however.

In the foregoing it has been assumed that the vertical position of the propeller axis does not affect the lift due to slipstream. This assumption is valid when the propeller axis is not more than 0.5 propeller diameter above or below the wing chord (fig. 18). However, recent wind tunnel tests performed at the Delft University of Technology suggest that at more extreme positions large variations in lift can occur. This will be reported on in the near future. Some tesst data obtained in this investigation is presented in Appendix **XVII**.

6.2 Change in tail-off pitching moment due to propeller slipstream

For clean wings the effect of slipstream on the tail-off pitching moment of an aircraft is limited to a term:

$$C_{M_{s,o}} = n_e \frac{D^* c_s}{S_w} C_{m_{o,s}} \left[\frac{V_o + \Delta V}{V_o}\right]^2$$

Windtunnel tests show that on clean wings the additional lift due to slipstream applies at the quarter-chord point of the wing section at the propeller axis.

With flaps deflected the situation is different. Glauert has shown in ref. 45 (see also ref. 46, p. 215) a relation between the increase in lift due to flap deflection and the change in pitching moment at constant angle-of-attack (see fig. 19a). This relation derived for potential flow is valid for small flap angles only and can be approximated by the formula:

$$\left[\frac{dc'_{m_{0.25c'}}}{dc'_1}\right]_{\alpha=const.} = -0.25+0.32\frac{c_f}{c'}$$

where c'_m, c'_1 and c' refer to the extended chord when flap deflection also leads to chord extension.

Numerous windtunnel tests have shown that in viscous flow the pitching moment is more negative.
Good correlation with test data is obtained by the following modified formula (see fig. 19b):

$$\left[\frac{dc'_{m_{0.25c'}}}{dc'_1}\right]_{\alpha=const.} = \left(-0.25+0.32\frac{c_f}{c'}\right)$$

$$\times \left(1 + 0.2\left(1 - \sqrt{2}\sin\delta_f\right)\right)$$

In this formula the reference length c' is the extended chord and the moment reference point is also referred to this extended chord. If the reference length is the chord of the airfoil section with flap retracted c and the pitching moment is taken about the 0.25c-point this formula should be written as:

$$\left[\frac{dc_{m_{0.25c}}}{dc_1}\right]_{\alpha=const.} = \frac{c'}{c}\left[-0.25+0.32\frac{c_f}{c'}\right]$$

$$\times \left[1+0.2\left(1-\sqrt{2}\sin\delta_f\right)\right] - 0.25\left[\frac{c'}{c}-1\right]$$

For a cambered airfoil this increase in pitching moment due to flap deflection and extension should be considered at the zero-lift angle-of-attack for the clean

airfoil in order to distinguish between flap effects and angle-off-attack effects.
In the present calculation procedure (fig. 20) for a tail-off aircraft configuration the zero-lift angle for this configuration is taken.
At other angles-of-attack an extra change in pitching moment occurs due to a change in lift. This extra lift is assumed to apply at 25 percent of the extended chord c'.
Thus:

$$\left[\frac{dc_{m_{0.25c}}}{dc_l}\right]_{\delta_f=const.} = -\Delta c_l \times 0.25\left(\frac{c'}{c}-1\right)$$

It is now assumed that the lift due to slipstream produces a change in pitching moment according to the same relations as apply to free stream conditions
This idea was first suggested in ref. 49.
Thus:

$$[\Delta C_{M_s}]_{\delta_f=const.} = \frac{c'}{c}\left[-0.25 + 0.32\ \frac{c_f}{c'}\right]$$

$$\times\left[1\times 0.2\,(1-\sqrt{2}\sin\delta_f)\right]\Delta C_{L_{s,o}} -$$

$$-0.25\left[\frac{c'}{c}-1\right]\Delta C_{L_{s,\alpha}}$$

If the moment reference centre differs from the quarter-chord point an extra change in pitching moment should be added:

$$\Delta C_{M_s} = \frac{X_{CG} - X_{0.25c_s}}{\bar{c}} \times \Delta C_{L_{s,\alpha}}$$

Furthermore, both the direct thrust force and the propeller normal force produce pitching moment contributions:

$$\Delta C_{M_T} = -\frac{Z_T - Z_{CG}}{\bar{c}} \times C_{T_{eff}}$$

$$\Delta C_{M_p} = \frac{X_{CG} - X_{prop}}{\bar{c}} \times C_{L_p}$$

The determination of C_{Lp} is covered in ref. 24 (see also Appendix I).
Finally, a comparison was made between the sum of the pitching moment contributions described above and test data. The difference was assumed to be caused by a shift in the point op application of the wing lift due to slipstream.

$$\Delta C_{M_{FS}} = \left[C_{M_{S,test}} - C_{M_{S,calc}}\right] = -\frac{\Delta X_{FS}}{\bar{c}}\Delta C_{L_{s,\alpha}}$$

$\Delta X_{FS}/\bar{c}$ has been determined for a large number of configurations and test conditions. Fig. 21 shows representative examples and the curve faired through the data points. The curve adopted is:

$$\frac{\Delta X_{FS}}{\bar{c}} = 0.05 + 0.5\left[\frac{c'}{c}-1\right]$$

The total change in pitching moment coefficient due to operating propellers on a tail-off aircraft configuration can then be described as:

$$[C_{M_s}]_{\alpha=const.} = \frac{c'}{c}\left[-0.25+0.32\,\frac{c_f}{c}\right]$$

$$\times\left[1+0.2\,(1-\sqrt{2}\,\sin\delta_f)\right]\Delta C_{L_{s,o}}$$

$$+\left[-0.25\,(\frac{c'}{c}-1) + \frac{X_{CG}-X_{0.25c_s}}{\bar{c}}\right]\Delta C_{L_{s,\alpha}}$$

$$+\ \frac{X_{CG}-X_{prop}}{\bar{c}}\ C_{L_p} - \frac{Z_T-Z_{CG}}{\bar{c}}\ C_T$$

$$-\left[0.05 + 0.5\ (\frac{c'}{c}-1)\right]\Delta C_{L_{s,\alpha}}$$

Examples of tail-off pitching moment curves for configurations with running propellers at different thrust coefficients, both as calculated and as obtained from windtunnel tests are presented in figs. 22-26. More examples are presented in Appendix XIV.

6.3 The vertical position of the slipstream centre lines

When lift due to slipstream was discussed in chapter 6.1 the average downwash angle for slipstream and the outer flow were assumed to have different values ε_s and ε with no interaction between the two flows.

Measured average downwash angles at tailplane locations sufficiently far above the propeller slipstream show however (to a first order) a unique linear relationship between average downwash angle and total lift coefficient.
Whether high lift is generated by a high angle-of-attack, a very efficient flap system or by propeller slipstream, rougly the same C_L -versus - ε curve is found (see figs. 27, 28).

Apparently, the interaction between slipstream and outer flow is such that, at least in the region of convential horizontal tail surfaces slipstream and outer flow can be considered as if they produce the same average downwash angle in the part of the outer flow stream tube between the outboard edges of the propeller slipstream tubes.

As a check the following analysis was performed:

In fig. 29 a cross section of the idealised flow behind a wing with two propellers is shown. The flow is assumed to consist of two stream tubes defined by the fully contracted propeller slipstream and the outer flow stream tube. In Appendix IV the formulae used in the analysis have been derived.

It is now assumed that the vertical components of the outgoing momentum of the flow through area A* (with downwash angle ε) and of the slipstream with total area $A'_S = 2 \times \pi/4\ D^{*2}$ and downwash angle ε_S can be combined into the vertical component of a total momentum with different velocities but a single downwash angle ε'.
with

$$\sin\varepsilon = \frac{\rho V_O^2 A^* \sin\varepsilon + \rho (V_O+\Delta V)^2 A'_S \sin\varepsilon_S}{\rho V_O^2 A^* + \rho (V_O+\Delta V)^2 A'_S}$$

With the above equation and some of the formulae from Appendix I the downwash angle ε' has been calculated for a number of aircraft configurations. As an example ε' versus C_L for the configuration of ref. 36 with the flaps deflected to 60 deg and the ailerons to 30 deg for thrust coefficients $C_T = 0$ and $C_T = 2.15$ is presented in fig. 30.

Thus, the assumption that the average downwash far behind the wing is only dependent on the total lift coefficient, irrespective of the way this lift coefficient is achieved seems to hold.

In real flow the downwash angle, averaged over the tailplane's span is dependent on the height above the wing wake.
Fig. 31 shows that:

$$\varepsilon = 57.3\ \frac{P\ C_L}{\pi\ A_W}$$

where P varies on average between 1.5 and 2.5. When it is assumed that this relation also applies with propeller slipstream present it follows that with engines mounted on the wing the centre line of the slipstream should show a downwash angle corresponding tot a value for P close to 2.5. Varying P between 2.5 and 2.0 showed best correspondence with test values for P = 2.2.

So, far behind the wing the inclination of the slipstream centre line is:

$$\varepsilon_{s,cl} = 57.3 \times \frac{2.2\ C_L}{\pi\ A_W}$$

In particular at high lift coefficients the wing wake is not flat but curved with a higher downwash angle near the wing trailing edge.

For a straight wing with $A_W = 8$ and taper ratio λ = 0.3 the flow field has been calculated for C_L = 1, 2 and 3.
Fig. 32a shows the flow field for $C_L = 2$. The vertical displacement of the wake relative to the wing trailing edge Z_W is clearly larger than $Z_\varepsilon = l_h \sin\varepsilon$. The ratio $K_\varepsilon = Z_W/Z_\varepsilon$ as a function of l_h/c_s, as derived from the analysis mentioned above is presented in fig. 32b. It is assumed to be valid for wing aspect ratio's $5 < A_W < 14$. Fig. 35 shows that $K_\varepsilon \approx 1.5$ when l_h/c_s = 3.0 to 4.0 .

With the data from fig. 32b the slipstream centre line can be determined for clean wings when the propeller axis lies on or close to the streamline that leads to the forward stagnation point on the airfoil. The slipstream centre line coincides, in the present model, with the wing wake.

The vertical distance between the horizontal tail surface and the slipstream centre line is than the sum of the geometrical distance between the tail surface and the propeller axis (h_t) at zero angle-of-attack, the vertical displacement of the slipstream centre line (or wing wake) passing through (or assuming its origin at) the clean wing's trailing edge (Δh_ε) and the vertical displacement of the horizontal tail due to angle of attack (Δh_l):

$$h_t = Z_h - Z_T$$

$$\Delta h_\varepsilon = l_h^* \times tg \left[K_\varepsilon \frac{d\varepsilon}{dC_L} \frac{dC_L}{d\alpha} \alpha_R + K_\varepsilon \frac{d\varepsilon}{dC_L} \Delta C_{L_s} + K_\varepsilon \varepsilon_{\alpha=0} \right]$$

$$\Delta h_l = -l_h\ tg\ \alpha_R$$

where l_h = distance from wing quarter-chord point to tailplane quarter-chord point.
l_h^* = distance from wing trailing edge to tailplane quarter chord point.

On most aircraft configurations the propeller axis is situated above or below the wing chord plane at a distance Z_T and is located 0.50 c_s to 1.00 c_s in front of the wing. Also when the angle-of-attack increases the propeller centre line moves up. When flaps are deflected the streamline leading to the forward stagnation point moves down with respect to the propeller axis.

In all these cases the slipstream centre line will not coincide with the wing wake.

In the present analysis it is assumed that the slipstream centre line is off-set from the wing wake for a clean wing at the same C_L over a constant distance Δh^* . This distance is the sum of (see fig. 33):

1. $(\Delta h_t)_\alpha$: The (upward) vertical displacement of the propeller disc centre due to angle-of-attack.

$$(\Delta h_t)_\alpha = -(X_{0.25c_s} - X_{prop}) \sin \alpha_R$$

2. $(\Delta h_t)_{\delta f}$: The (downward) vertical displacement of the wing trailing-edge when the flaps are deflected.

$$(\Delta h_t)_{\delta_f} = c_f \times \sin \delta_f$$

3. $(\Delta h_t)_{upw}$: The (upward) vertical displacement due to flap deflection of the streamline running through the propeller disc centre between the propeller and the quarterchord point on the airfoil.

$$(\Delta h_t)_{upw} = +0.25\left[X_{0.25c_s} - X_{prop}\right] \sin \Delta\alpha_{0,f}$$

The coefficient 0.25 was chosen somewhat arbitrarily after regarding the streamline pattern about a number of airfoil configurations such as presented in fig. 33.

The vertical displacement of the wing trailing edge relative to the propeller due to angle-of-attack is assumed to be compensated by an increased upwash of the slipstream between the propeller and the airfoil quarter-chord point.

The total vertical displacement of the slipstream can be written as:

$$\Delta h^* = (\Delta h_t)_\alpha + (\Delta h_t)_{\delta_f} + (\Delta h_t)_{upw}$$

The total height of the horizontal tail surface above the slipstream centre line can then be written as:

$$h_{tot} = h_t + \Delta h_s + \Delta h_l + \Delta h^*$$

or:

$$h_{tot} = h_t$$

$$+ l_h^* t_g \left[k_\varepsilon \frac{d\varepsilon}{dc_L} \frac{dc_L}{d\alpha} \alpha_R + K_\varepsilon \frac{d\varepsilon}{dc_L} \Delta C_{L_s} + K_\varepsilon \varepsilon_\alpha = 0 \right]$$

$$- l_h tg\alpha_R - \left[X_{0.25c_s} - X_{prop}\right] \sin \alpha_R$$

$$+ c_f \sin \delta_f + 0.25 \left(X_{0.25c_s} - X_{prop}\right) \sin \Delta\alpha_{o,f}$$

6.4 The average dynamic pressure at the horizontal tailplane

A model has now been established for the propeller slipstream centre line shape and location. If it is assumed that the slipstream cross section remains circular with diameter D^* and that no mixing with the outer flow or deformation occurs the position of the propeller slipstream relative to the horizontal tail surface can then be determined.

It is further assumed that:

a. Slipstream rotation and resultant lateral translation of the slipstream can be neglected. Handed propellers are not considered.

b. On configurations with more than two engines (four or six) only the two inboard engines affect the flow over the tail.

The average dynamic pressure at the tail can now be determined as a function of the vertical distance between the tail surface and the slipstream centre line and of the ratio between slipstream diameter and tailspan.

As shown in Appendix III the average dynamic pressure can then be written as:

$$\frac{q_h}{q} = \left[1 + \left(\frac{\Delta V}{V_o}\right)_{AV}\right]^2 = (1+b)^2$$

$$= \left[1 + \frac{\Delta V}{V_o}\right]^2 \frac{S_{h,s}}{S_h} + \frac{S_h - S_{h,s}}{S_h}$$

where:

$$\frac{S_{h,s}}{S_h} = \frac{2 \times c_s}{S_h} \times D^* \sqrt{1 - \left[\frac{h_{tot}}{D^*/2}\right]^2}$$

In ref. 16 a detailed windtunnel test programme is reported where on a four-engined aircraft model downwash and average dynamic pressure at the tail were investigated for a large number of tailplane positions relative to the wing both with single- and counter-rotating propellers and both with split flaps retracted and deflected 60 degrees.
For this configuration the slipstream location for the inboard engines and the average dynamic pressure at the tail has been determined according to the procedure indicated above for a thrust coefficient
$T_C = 0.40$.
$\Delta V/V_o$ (= b) as a function of $h_{tot}/D^*/2$ as calculated is shown as a dotted line in fig. 34.

Figure 34 also shows test data on $\Delta V/V_o$ as derived from ref. 16 again plotted versus the calculated relative slipstream centre line position. The test data substantiate the assumptions concerning the relative position of the slipstream centre line.

However the average dynamic pressure starts to increase at larger distances between tailplane and slipstream centre line than indicated by the dotted line. This indicates that the assumption that no mixing between slipstream and outer flow or that no deformation occurs does not hold.
Mixing and possibly also deformation apparently does occur with consequently a widening of the slipstream.

As no other detailed analysis data is available the continuous curve as drawn in fig. 34 is assumed to apply for all conventional aircraft configurations. The curve is redrawn in fig. 35 in a generalised form.

As a further check on the validity of the procedure given above for the determination of the average dynamic pressure at the tail two further examples are presented.

In fig. 36 $\sqrt{q_h/q_o}$ as calculated and measured is presented for the DHC-5 Caribon in the clean configuration. The testdata were teken from ref. 47.

In fig.37 $\sqrt{q_h/q_o}$ is presented for the Fokker 50 for three flap settings. The testdata were taken from unpublished windtunnel test data. Note how flap deflection lowers the position of the slipstream relative to the horizontail tailplane.

6.5 The average downwash angle at the horizontal tailplane

In chapter 6.3 (and figs. 27, 28) it was shown that, when the horizontal tailplane lies sufficiently far above the propeller slipstream for practical purposes a single linear relationship can be assumed between the average downwash angle ε of the horizontal tailplane and the lift-coefficient for the aircraft-less-tail. Whether a given high lift coefficient is generated through a high angle-of-attack without slipstream or at a lower angle-of-attack combined with propeller slipstream, the same average downwash angle ε occurs.

When the distance between slipstream centre line and tailplane becomes less than one nominal slipstream diameter D^* this is no longer true however. In the mixing region on the boundary between slipstream and outer flow an inflow into the slipstream occurs which causes the average downwash to increase when the tailplane is located in that area. This is illustrated in fig. 38a to g. This inflow angle increases with increasing thrust coefficent. For the present analysis it has been assumed that $\Delta\varepsilon$ is proportional to $\Delta V/V_o$.

A large amount of available test data has been analysed on this extra downwash angle $\Delta\varepsilon$ above the increase in downwash directly related to the increase in wing lift due to slipstream.
When the testdata are normalised to a slipstream strength $\Delta V/V0=1$ the data points are shown to lie in a fairly narrow band as is illustrated in fig. 39.
Note that the datapoints are not only taken from ref. 16 but also from refs. 7,21,36 and other sources.
The drawn line in fig. 39 repeated in fig. 40 is the curve adopted for use in the present method for the determination of the downwash at the tailplane in the presence of propeller slipstream.

The average downwash angle can then be written as:

$$\varepsilon = (\varepsilon_o)_{P-O} + \left[\frac{d\varepsilon}{dC_L}\right]_{P-O} \times C_{L_{w+s}} + \\ + (\Delta\varepsilon)_{\Delta V/V_o=1} \times \frac{\Delta V}{V_O}$$

The distance between slipstream centre line and tailplane, required to determine $(\Delta\varepsilon)_{\Delta V/V_o=1}$ is determined according to the procedure outlined in chapter 6.3.

Tail-on and tail-off windtunnel test data on the C-160 Transall with and without running propellers were analysed to compare downwash data as calculated according to the equation given above and as derived from the test data. The average dynamic pressure at the tail was calculated according to chapter 6.4.
The comparison is presented in fig. 41. The effect of the vertical displacement of the slipstream due to flap deflection and the associated effect on the average downwash at the tail is clearly reproduced in the calculation.
More testdata on downwash characteristics are presented in Appendix XVII and Appendix XVIII.

7. Two examples of the decrease in longitudinal stability due to slipstream

Finally, the method to determine the effect of propeller slipstream on static longitudinal stability as described in the present report has been applied to the aircraft configuration from refs. 36,37 with both flaps retracted and with flaps deflected 60 deg. and ailerons deflected 30 deg.
C_M-versus-C_L curves for the tail-off and tail-on configurations are presented in figs. 42, 43.
The tail-on curves were calculated according to the following equations valid for a given angle-of-attack,

α_R and thrust coefficient C_T with horizontal tail setting i_h = 4.3 deg. and elevator in neutral position:

$$C_L = C_{L_{T-O}} + C_{L_{\alpha_h}}\left[\alpha_R\left(1 - \frac{d_\epsilon}{dC_L}\left(\frac{dc_L}{d\alpha}\right)_{T-O}\right) - \epsilon_{\alpha=0}\ \epsilon_O + i_h\right] \times \frac{q_h}{q}\ \frac{S}{S}$$

$$C_{M_{CG}} = C_{M_{T-O}}$$

$$- C_{L_{\alpha_h}}\left[\alpha_R\left[1 - \frac{d\epsilon}{dC_L}\left(\frac{dC_L}{d\alpha}\right)_{T-O}\right] - \epsilon_{\alpha=0} + i_h\right]\frac{q_h}{q}\ \frac{S_h}{S_w}\ \frac{l_h}{\bar{c}}$$

2. When figures 42 and 43 were prepared it was noticed that better agreement between calculated and test data was obtained when the pitching moment contribution from the fuselage due to the upwash in front of the wing was extended to the increase in lift due to slipstream. Then, at a given angle-of-attack the following pitching moment contribution has to be added to the pitching moment calculated with the formulae given in the main part of this paper:

$$\Delta C_M = \Delta C_{L_a} \times \Delta \frac{X_{ac.fus}}{\bar{c}}$$

where $\Delta \frac{X_{ac.fus}}{\bar{c}}$ is the forward shift in aerodynamic centre due to the presence of the fuselage.
This subject is analysed in more detail in Appendix XV.

8. Conclusions

A method has been presented for the analysis of the effect of propeller slipstream on the static longitudinal stability and control of multi-engined aircraft. The method allows the determination of the increase in lift and the change in tail-off pitching moment due to slipstream, the location of the slipstream relative to the horizontal tailplane and the average downwash angle and dynamic pressure at the tailplane. A comparison of calculated and windtunnel test data showed the method to be suitable for preliminary design purposes.

9. Acknowledgement

The author gratefully acknowledges the assistance of Ms. Yvonne Spronk in the preparation of this paper.

References

1. Simmons, L.F.G. and Ower, E.:
An investigation of downwash in the slipstream, ARC R&M
No. 882, 1923

2. Bradfield, F.B. et al.:
Windtunnel data on the effect of slipstream on the downwash and velocity at the tailplane, ARC R&M No. 1488, 1932.

3. Stüper, J.:
Einfluss des Schraubenstrahls auf Flügel und Leitwerk, Luftfahrtforschung 1938, p. 181.

4. Glauert, H.:
The lift and drag of a wing spanning a free jet, ARC R&M No. 1603, 1934.

5. Stüper, J.:
Beitrag zum Problem des durch einen Freistrahl hindurch gesteckten Tragflugels, Luftfahrt forschung 1935, P. 267.

6. Smelt, R. and Davies, H.:
Estimation of increase in lift due to slipstream, ARC R&M No. 1788, 1937

7. Bryant, L.W. and McMillan, G.A.:
The longitudinal stability of a twin-engined monoplane with airscrews running, ARC R&M No. 2310, 1938.

8. Millikan C.B.:
The influence of running propellers on airplane characteristics, Journal of the Aeronautical Sciences, Jan. 1940, p. 85

9. Falkner, V.M.; Nixon, H.L. and Sweeting, N.E.:
An experimental investigation of the effect of airscrews on the longitudinal stability of a twin-engined monoplane,
ARC R&M No. 2070, 1941

10. Schubert, R.:
Zur Berechnung der statischen Längsstabilität im Motorflug,
Luftfahrtforschung 1942,
p. 271

11. Baranoff, von, A.;
Beitrag zur Frage der Beeinflüssung des Abwindes durch den Schraubenstrahl, Luftfahrt forschung 1942, p 1.

12. Priestley, E.:
A general treatment of static longitudinal stability with propellers, with application to single-engined aircraft, ARC R&M No. 2732, 1944

13. Stiess, Von, W.:
Uber den Einfluss des Luftschraubendrehsinnes auf die Längsstabilität von zweimotorigen Flugzeugen, Jahrbuch 1938 der deutschen Luftfahrtforschung, p.206.

14. Katzoff, S.:
Longitudinal stability and control with special reference to slipstream effects,
NACA report No 690, 1940.

15. Spence, A.:
The effect of propeller thrust on downwash and velocity at tailplane. - A collection of data from low speed windtunnel tests, ARC Current Paper No 21, 1947.

16. Hartley, D.E.; Spence, A and Kirby, D.A.:
Model tests on the effect of slipstream on the flow at various tailplane positions on a four-engined aircraft, ARC R&M No. 2747, 1951.

17. Morris, D.E. and Morall, J.C.:
The effect of slipstream on the longitudinal stability of multi-engined aircraft,
ARC R&M 2701, 1948.

18. Draper, J.W. and Kuhn, R.E.:
Investigation of the aerodynamic characteristics of a model wing-propeller combination and of the wing and propeller separately at angles-of-attack up to 90°, NACA TN 3304, 1956 (Also NACA Report 1263).

19. Kuhn, R.E. and Grunwald, K.J.:
Longitudinal aerodynamic characteristics of a four-propeller deflected slipstream VTOL model including the effects of ground proximity.
NASA TN D-248, 1960.

20. Weiberg, J.A. and
Holzhauser C.A.:
Large-scale windtunnel tests of an airplane model with an unswept, tilt wing of aspect ratio 5.5 and with four propellers and blowing flaps.
NASA TN D-1034, 1961.

21. Margason, R.J.; Hammond, A.D. and Gentry, G.L.:
Longitudinal stability and control characteristics of a powered model of a twin-propeller deflected-slipstream STOL aircraft configuration.
NASA TN D-3438, 1966.

22. Page, V.R.; Dickinson, S.O. and Deckert, W.H.:
Large-scale windtunnel tests of a deflected slipstream STOL model with wings of various aspect ratio's.
NASA TN D-4448, 1968.

23. Page, V.R. and Aiken, T.N.:
Stability and control characteristics of a large-scale deflected slipstream STOL model with a wing of 5.7-aspect ratio. NASA TN D-6393, 1971.

24. De Young, J.:
Propeller at high incidence, Journal of Aircraft, May-June 1965, p. 241.

25. Strand, T.; Levinsky, E.S. and Wei, H.Y.:
Unified performance theory for V/STOL aircraft in equilibrium flight, Journal of Aircraft, 1967.

Part I : March-April 1967, p. 105
Part II: May-June 1967, p. 193

26. Levinsky, F.S.; Thommen, H.U.; Yager, P.M. and Holland, C.H.: Lifting surface theory for V/STOL aircraft in transition and cruise.
Journal of Aircraft,
1969-1970.
Part I , Nov.-Dec. 1969, p. 488
Part II , Jan.-Febr. 1970, p. 58

27. Fowler, H.D.:
Determination of the influence of propeller thrust on C_L and C_D of an airplane using a triple-slotted flap at various deflections.
SAE Paper No 690724, 1969.

28. Brenckmann, M.:
Experimental investigation of the aerodynamics of a wing in a slipstream,
University of Toronto, UTIA Technical Note No. 11, 1957
Also in: Journal of the Aeronautical Sciences, May 1958.

29. Ribner, H.S.:
Theory of wings in slipstreams, University of Toronto, UTIA Technical Note No. 60, 1959.

30. Ellis, N.D.:
A computer study of a wing in a slipstream, University of Toronto, UTIA Technical Note No. 101, 1967.

31. Jameson, A.:
Analysis of wing slipstream flow interaction.
NASA CR-1632, 1970.

32. Rethorst, S.:
Aerodynamics of Non-uniform flows as related to an airfoil extending through a circular jet, Journal of the Aeronautical Sciences, 1958.

33. Fink, M.P.; Cocke, B.W. and Lipson, S.:
A wind-tunnel investigation of a 0.4-scale model of an assault-transport airplane with boundary-layer control applied,
NACA RM L55G26a, 1955.

34. Weiberg, J.A.; Griffin, R.N. and Florman, G.L.:
Large-scale wind-tunnel tests of an airplane model with an unswept, aspect-ratio-10 wing, two propellers, and area-suction flaps,
NACA TN 4365, 1958.

35. Griffin, R.N.; Holzhauser, C.A. and Weiberg, J.A.:
Large-scale windtunnel tests of an airplane model with an unswept, aspect-ratio-10 wing, two propellers, and blowing flaps.
NASA Memo 12-3-58A, 1958.

36. Weiberg, J.A. and Page, V.R.:
Large-scale windtunnel tests of an airplane model with an unswept, aspect-ratio-10 wing, four propellers, and blowing flaps.
NASA TN D-25, 1959.

37. Weiberg, J.A. and Holzhauser, C.A.:
STOL characteristics of a propeller-driven, aspect-ratio-10, straight-wing airplane with boundary-layer control flaps, as estimated from large-scale windtunnel tests.
NASA TN D-1032, 1961

38. Kuhn, R.E.:
Semi-empirical procedure for estimating lift and drag characteristics of propeller-wing-flaps configurations for vertical- and short-take-off-and-landing airplanes.
NASA Memo 1-16-59A, 1958.

39. Eliraz, Y.:
Aircraft power-on polars corrected for propeller slipstream deflection, Israel Journal of Technology, Vol. 9 Nos 1-2, 1971, p. 195.

40. Marr, R.L.:
A method for analyzing Power-on static longitudinal stability, SAE Paper
No 700238, 1970.

41. Segall, R.N. and Gajdjis, S.:
An enhanced method for reducing power-on lift coefficent data to power-off lift coefficient data for multi-engined propeller aircraft.
AIAA Paper No. 91-0683, 1991.

42. Jones, R.T.:
Properties of low-aspect-ratio pointed wings at speeds below and above the speed of sound,
NACA report 835, 1946.

43. De Young, J.:
Spanwise loading for wings and control surfaces of low aspect ratio, NACA TN 2011, 1949.

44. Stepniewski, W.Z.:
Expérience tirée des essais en vol d'un appareil VTOL à aile basculante. Technique et Science Aeronautiques, 1960, No. 1, p. 1.

45. Glauert, H.:
Theoretical relationships for an airfoil with hinged flap, ARC R&M No. 1095, 1927.

46. Abbott, I.H. and Doenhoff, von, A.E.: Theory of wing section, Dover Publications, Inc, New York, 1958, p. 215.

47. Nettleton, T.R.:
Handling qualities research in the development of a STOL utility transport aircraft, Canadian Aeronautical and Space Journal, March 1966, p. 93.

48. Borne, van den, P.C.M. and Hengst, van, J.:
Investigation of propeller slipstream effects on the Fokker 50 through in-flight pressure measurements,
AIAA Paper No. 90-3084, 1990.

49. Verweij, A.:
A preliminary design study of an aircraft equipped with two high-power, wing mounted tractor propeller engines with special emphasis on longitudinal and lateral stability and control.
Thesis, Delft University of Technology, June 1992.

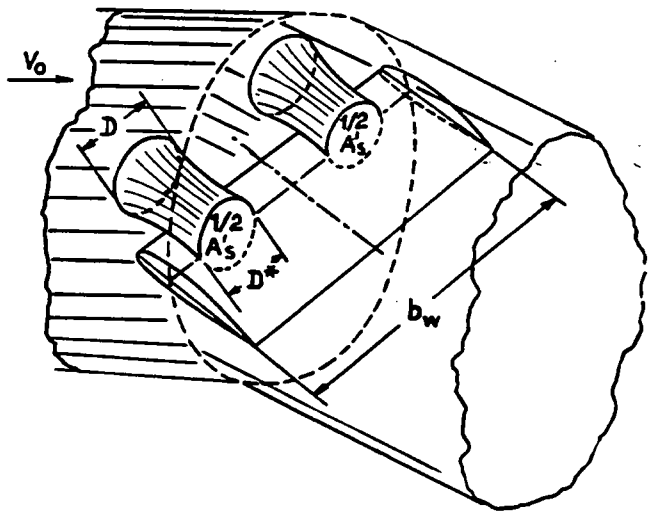

Figure 1 - Lift generation concept.

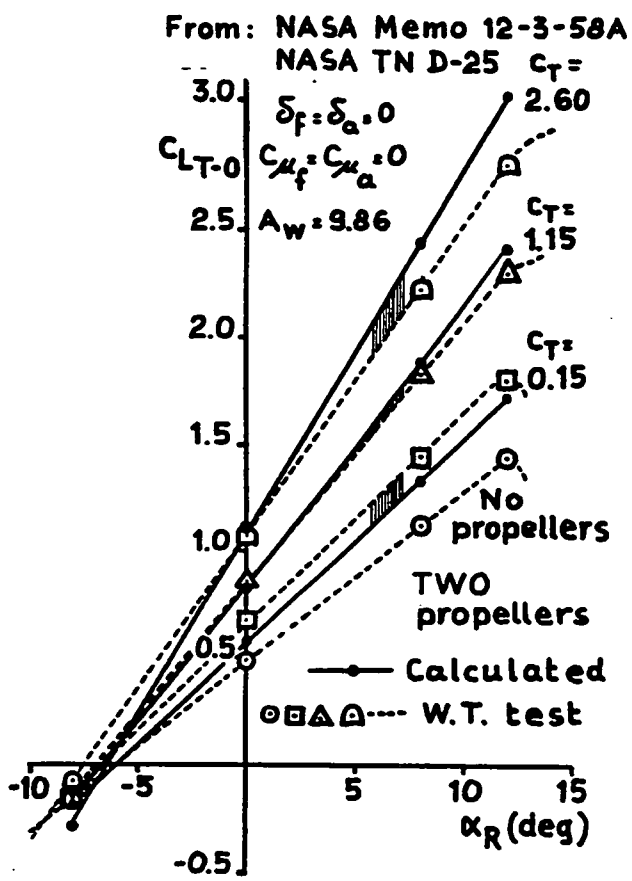

Figure 2 - Lift curves. Configuration ref. 35 with clean wing.

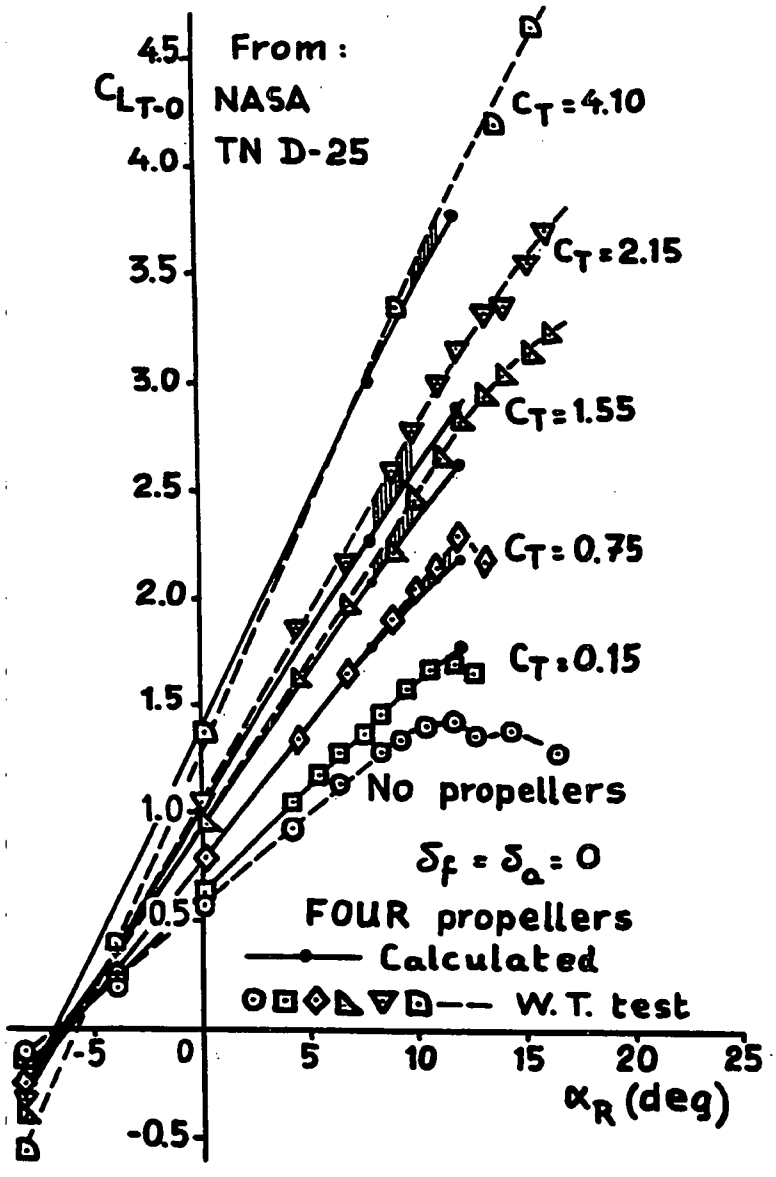

Figure 3 - Lift curves. Configuration of ref. 36 with clean wing.

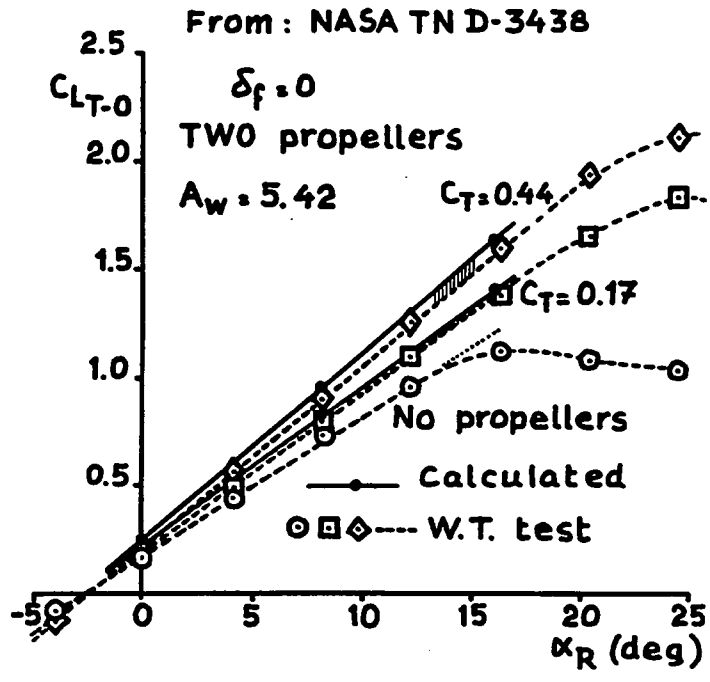

Figure 4 - Lift curves. Configuration of ref. 21 with clean wing.

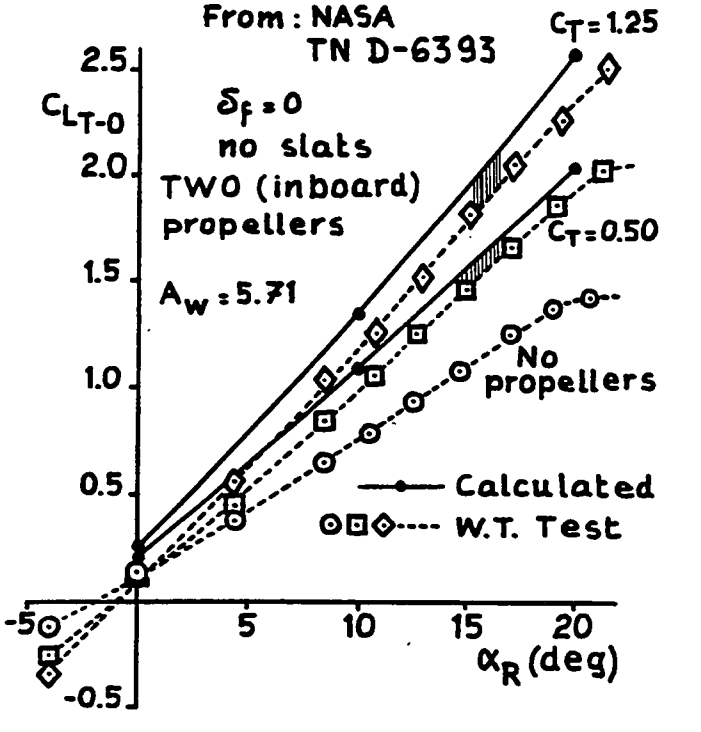

Figure 5 - Lift curves. Configuration of ref. 23 with clean wing.

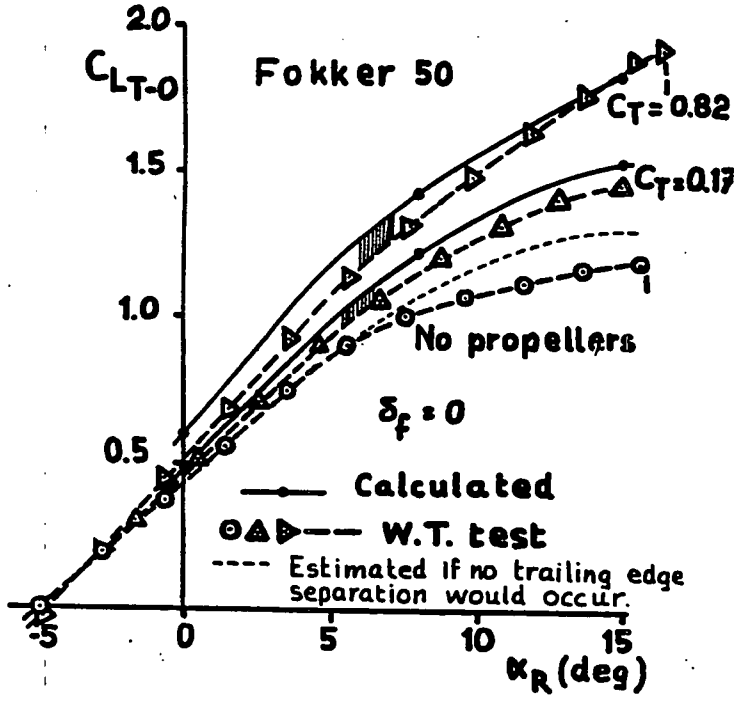

Figure 6 - Lift curves. Fokker 50 with clean wing.

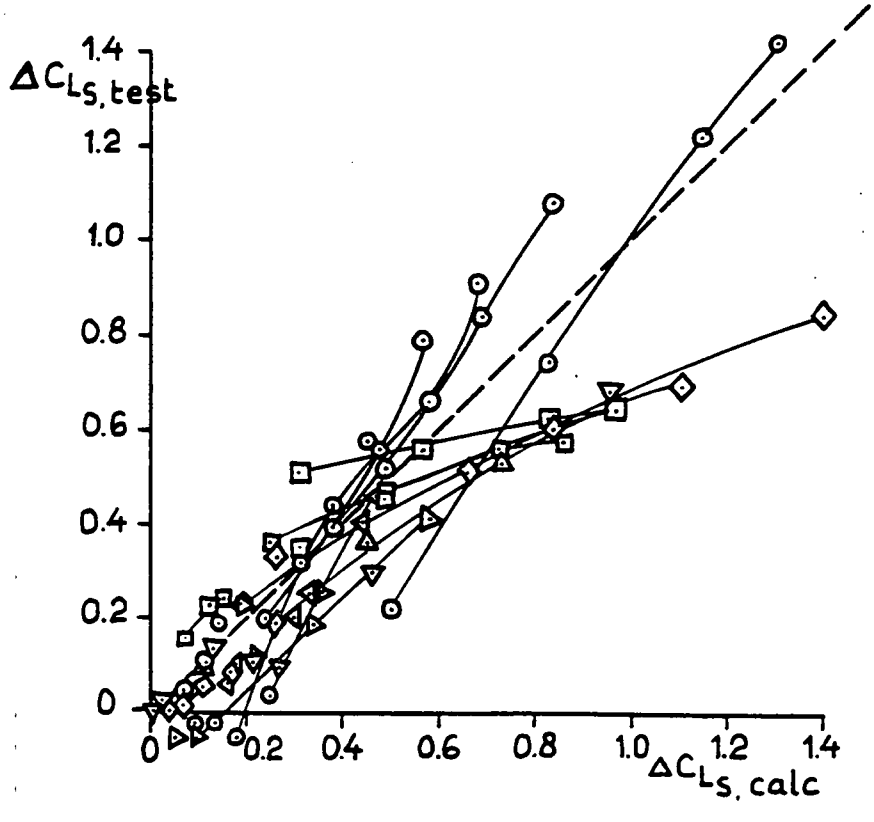

Figure 7 - Increase in wing lift due to slipstream. A comparison between calculated and windtunnel test data. Flaps retracted.

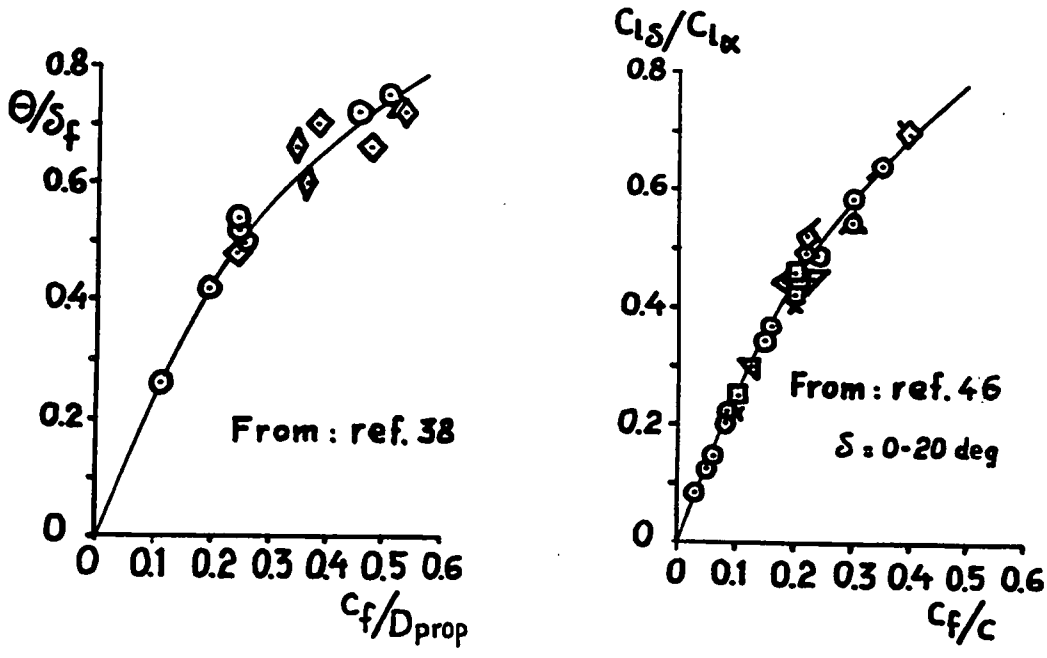

Figure 8 a. slipstream turning angle per degree flap angle versus the flap-chord-to-propeller diameter ratio.

b. $C_{l\delta}/C_{l\alpha}$ versus flap-chord-to-wing-section-chord ratio.

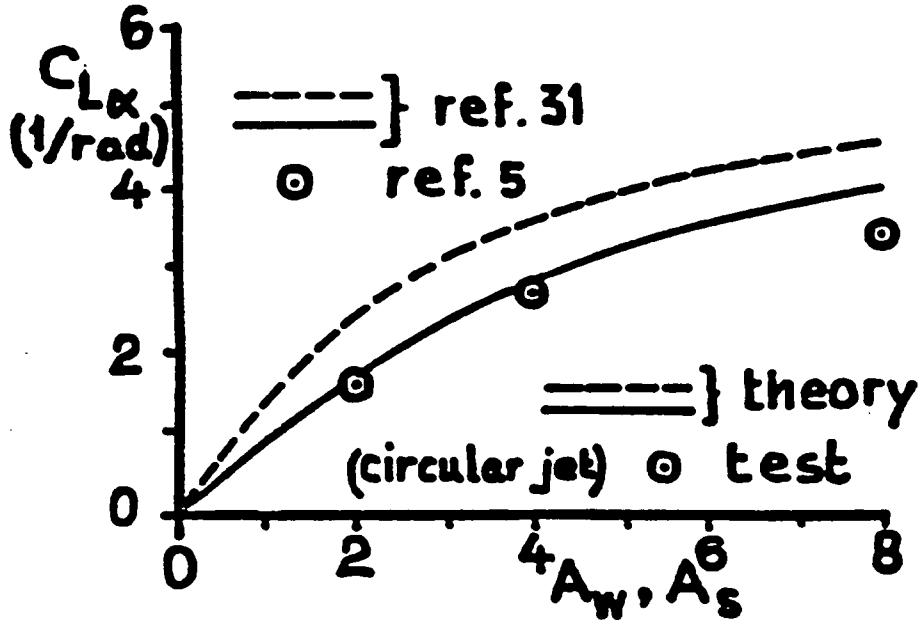

Figure 9 - The lift curve slope of a wing in free air and in a free jet.

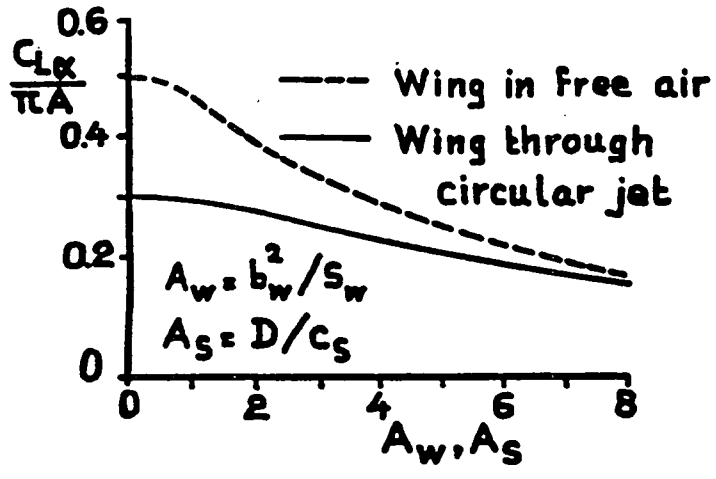

Figure 10 - The lift curve slope $C_{L\alpha}$ devided by π A for a wing in free air and in a free jet.

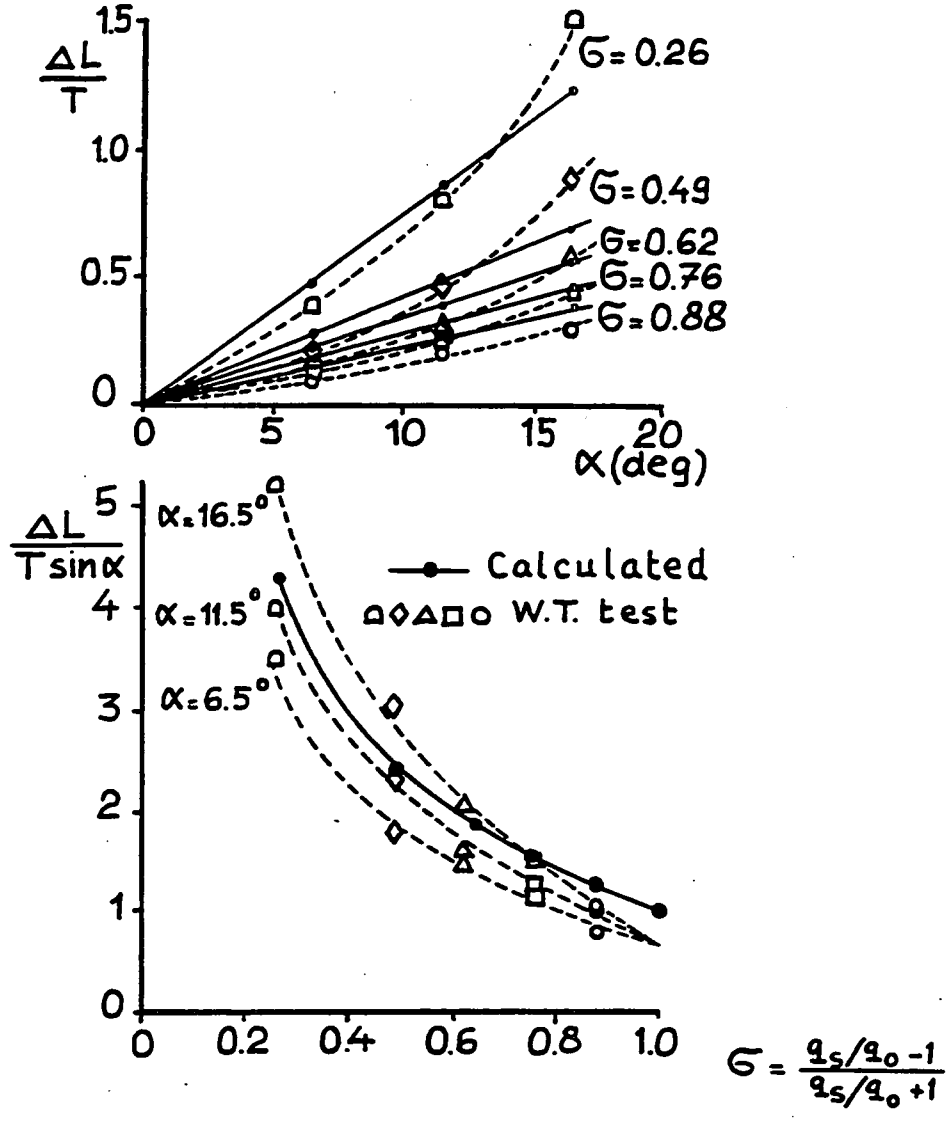

Figure 11 - The lift due to slipstream as a function of the dynamic pressure ratio of slipstream and free flow.

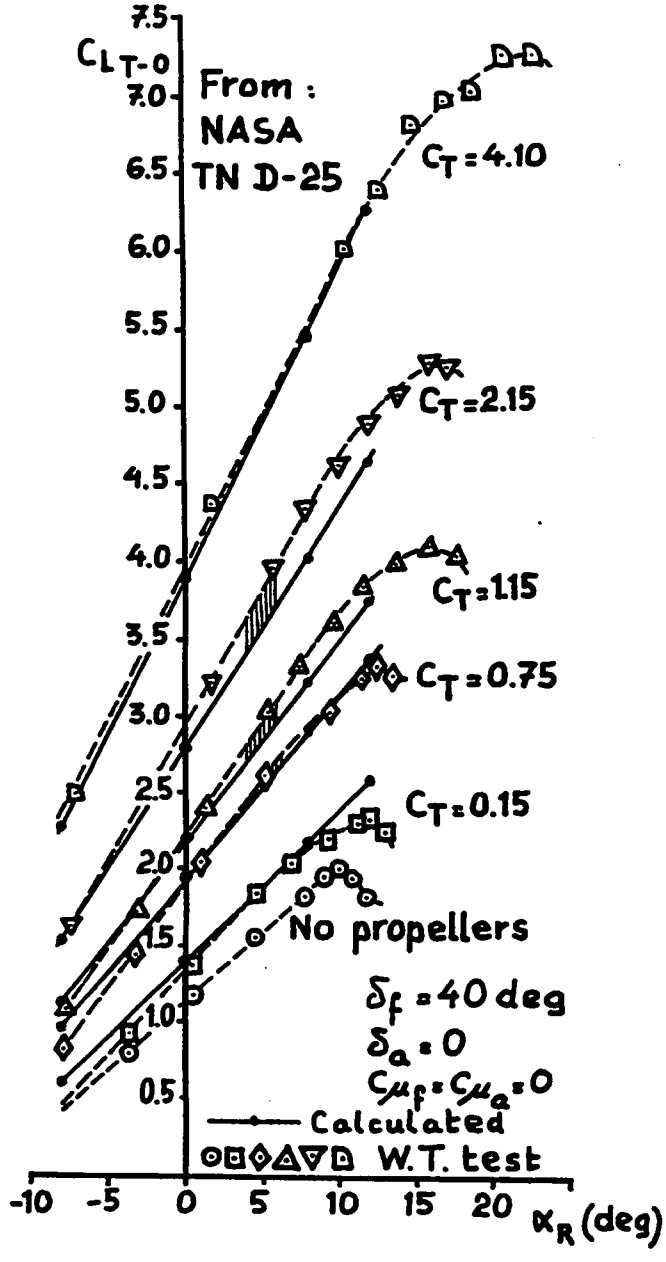

Figure 12 - Lift curves. Configuration of ref. 36 with flaps deflected 40 deg.

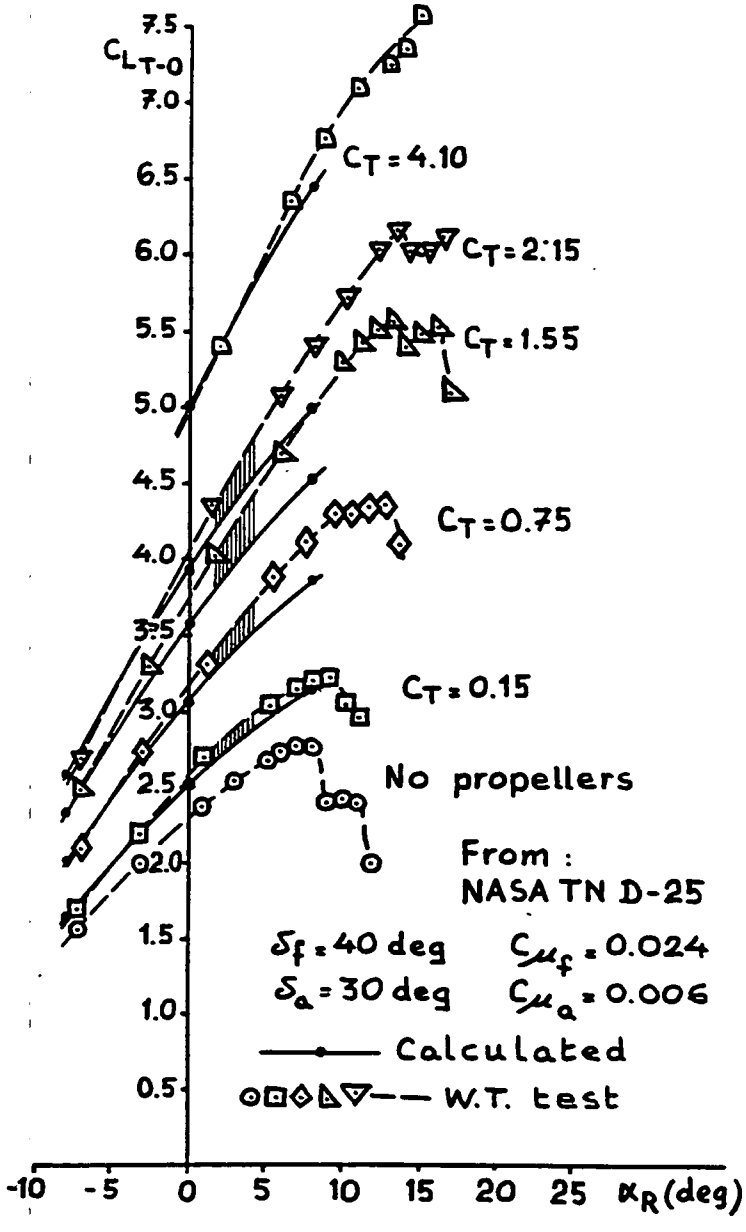

Figure 13 - Lift curves. Configuration of ref. 36 with flaps deflected 40 deg and ailerons 30 deg.

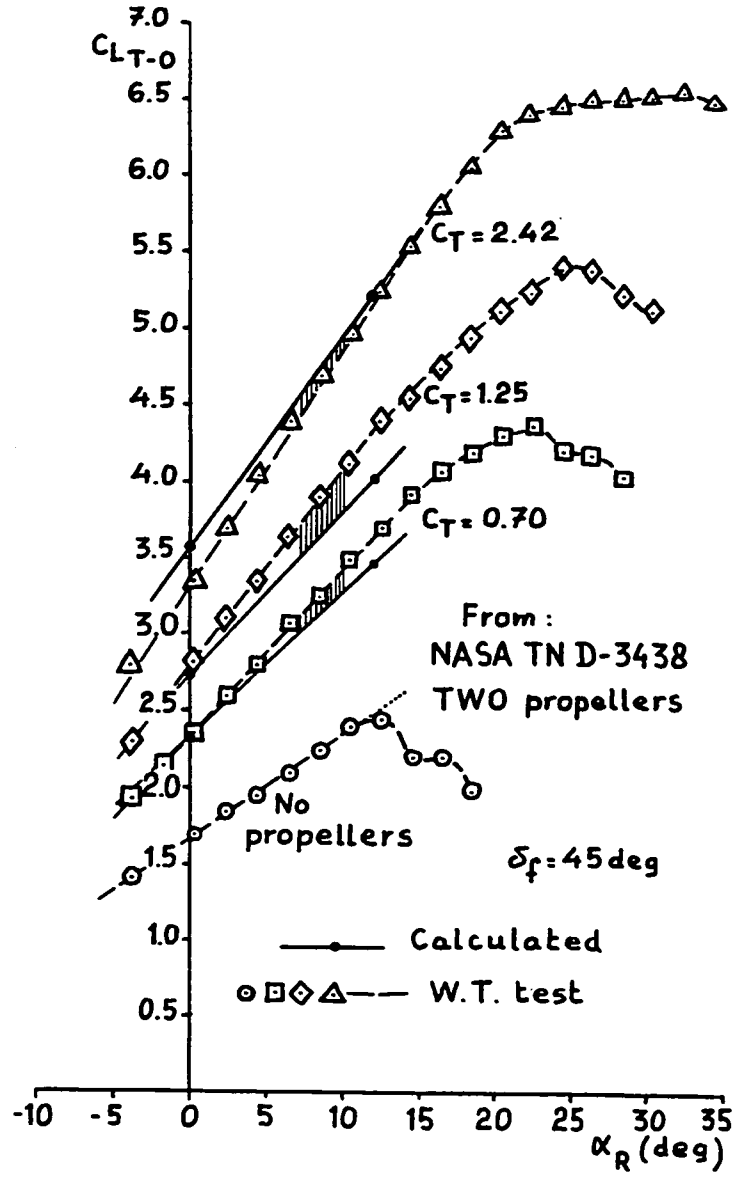

Figure 14 - Lift curves. Configuration of ref. 21 with flaps deflected 45 deg.

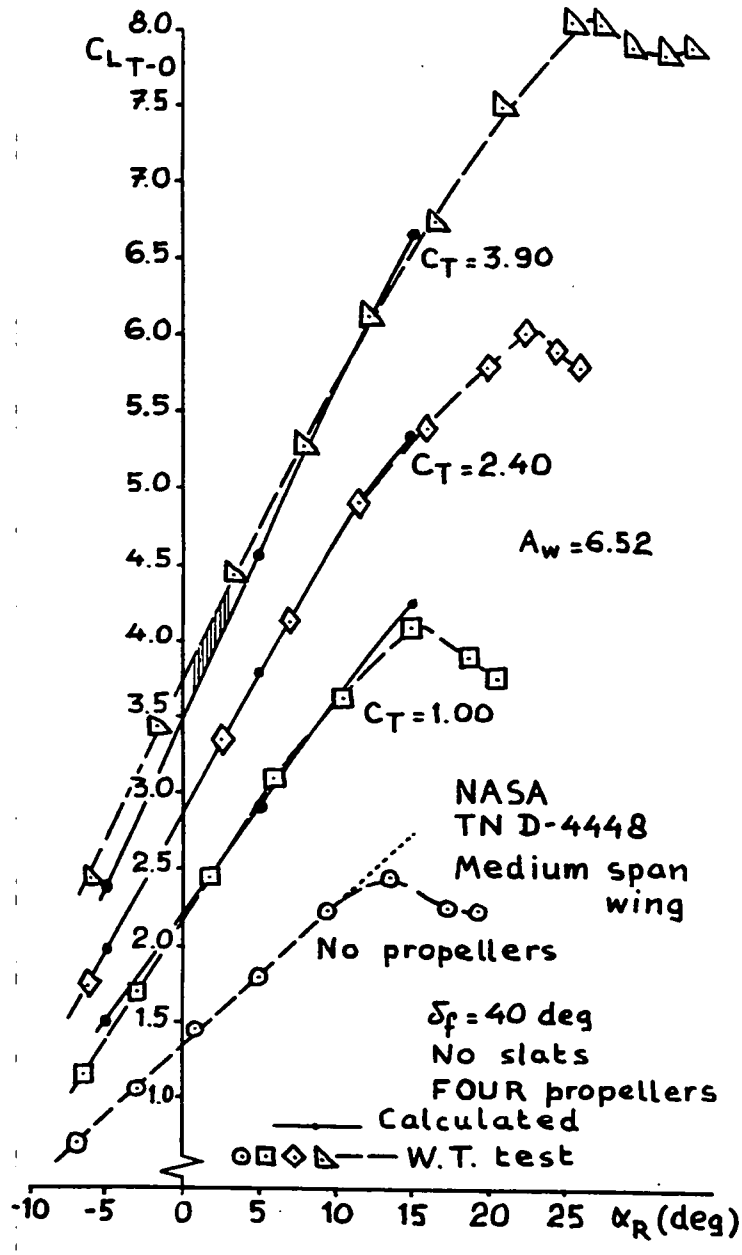

Figure 15 - Lift curves. Configuration of ref. 22 with flaps deflected 40 deg.

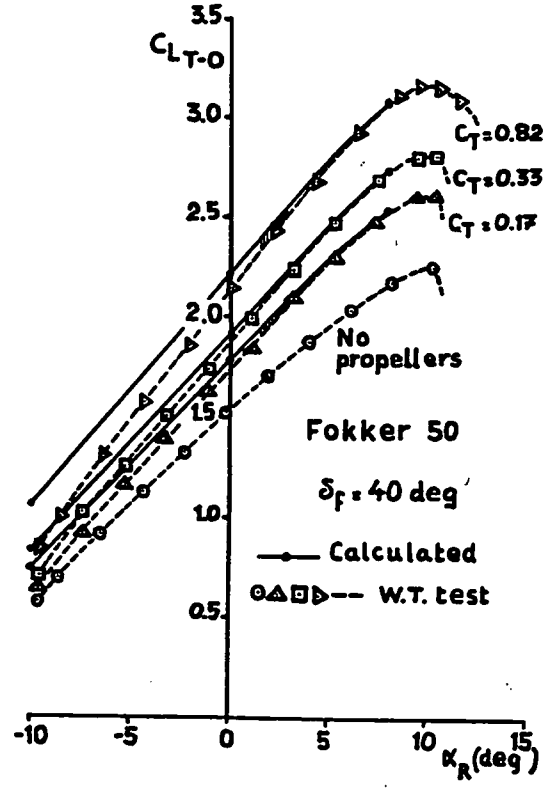

Figure 16 - Lift curves of Fokker 50. Flaps deflected 40 deg.

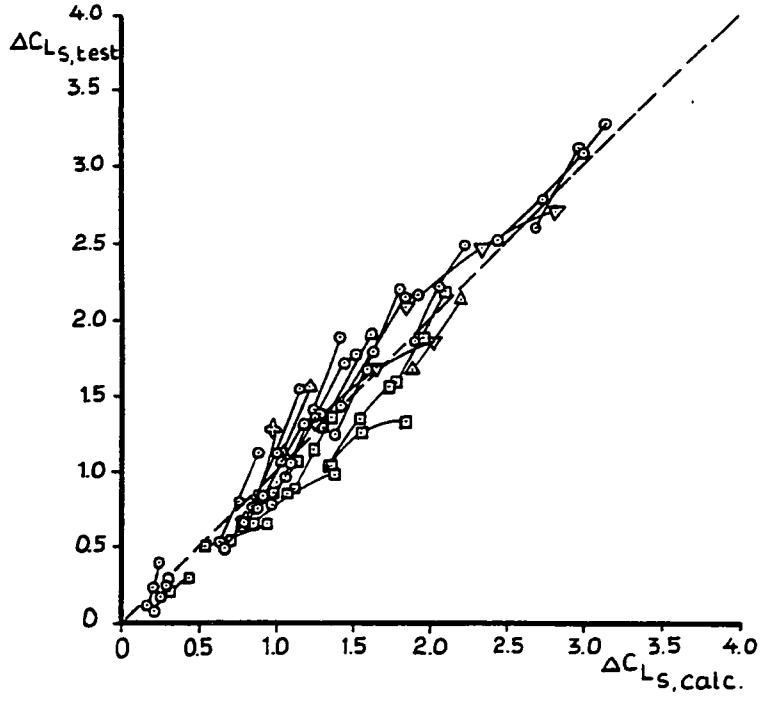

Figure 17 - Increase in wing lift due to slipstream. A comparison between calculated and wintunnel test data. Flaps extended.

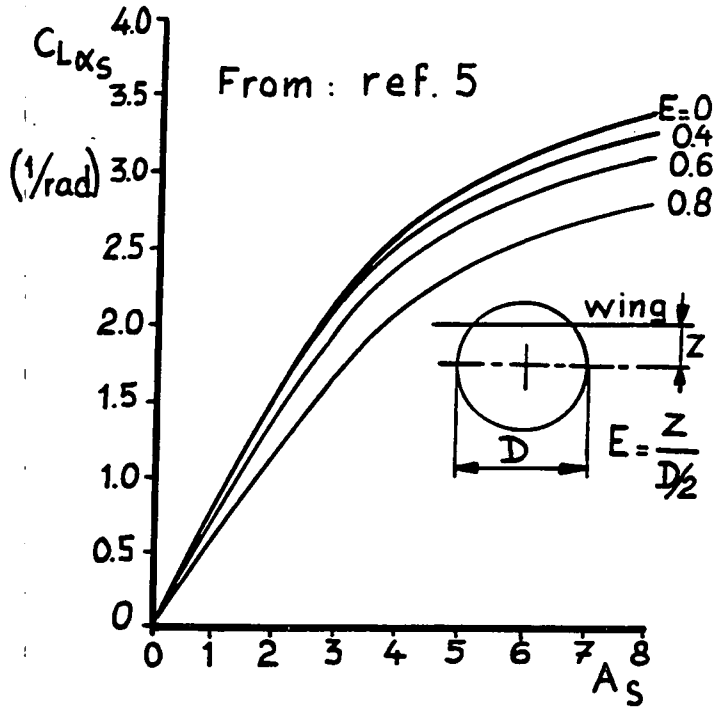

Figure 18 - Effect of the relative jet position on the lift of a wing in a free jet.

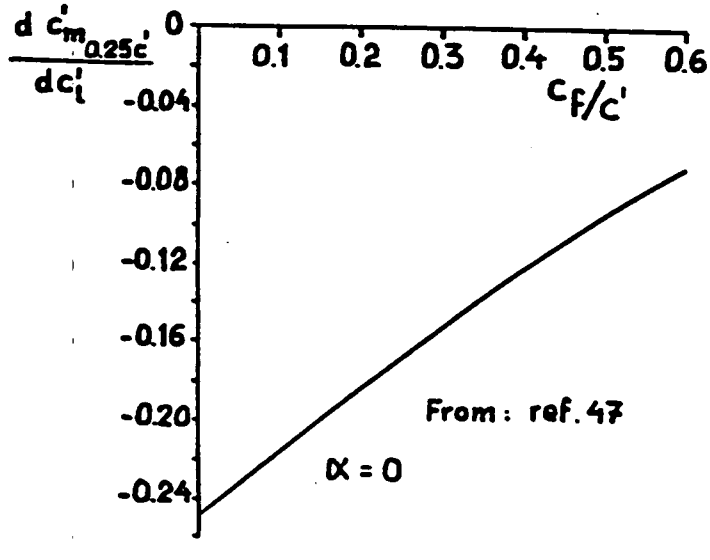

Figure 19 - The effect of the flap-chord-to-airfoil-section-chord ratio on the pitching moment due to flap deflection.
a. From Glauert's theory.

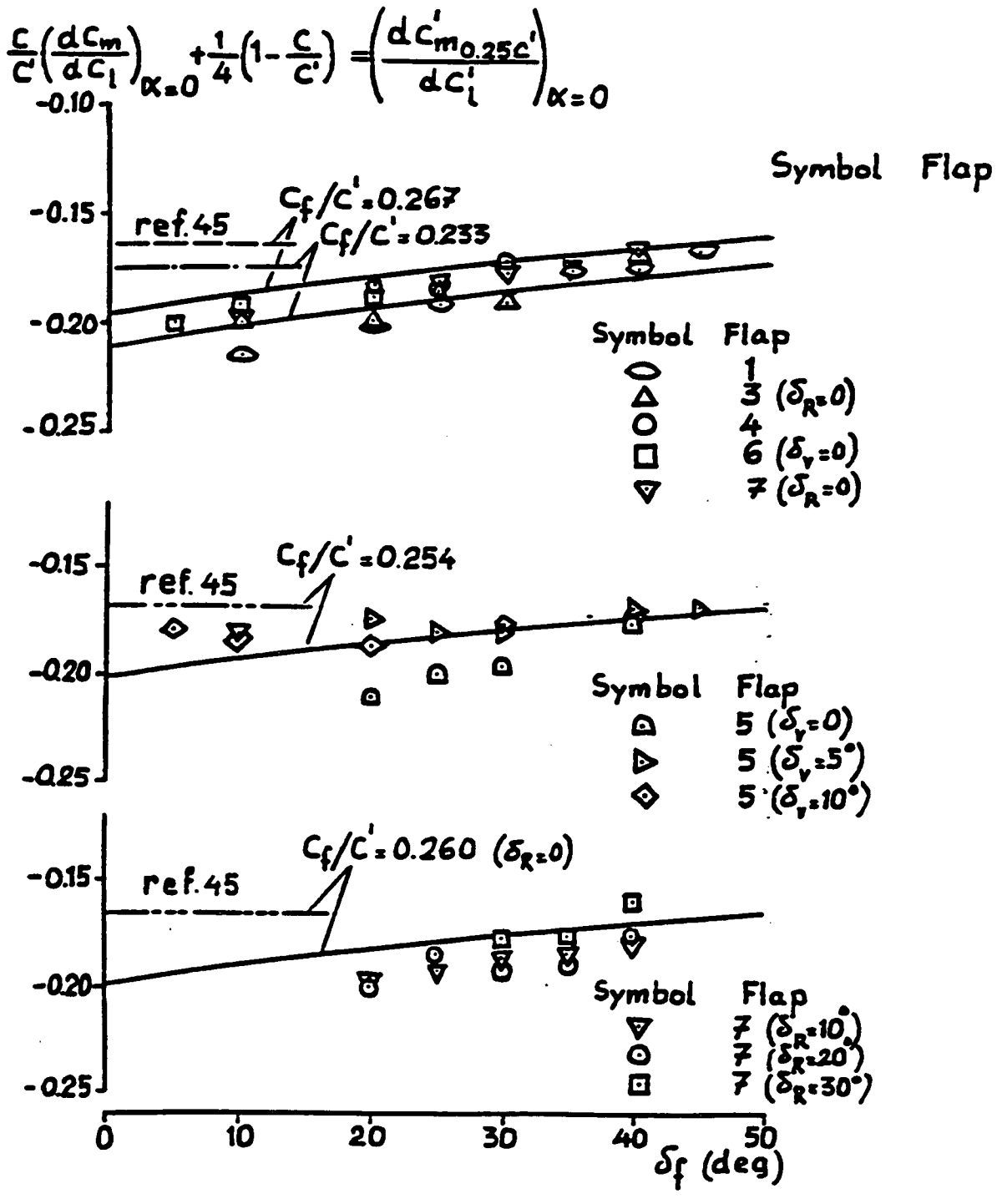

Figure 19 - The effect of the flap-chord-to-airfoil-section-chord ratio on the pitching moment due to flap deflection.

b. Windtunnel test data.

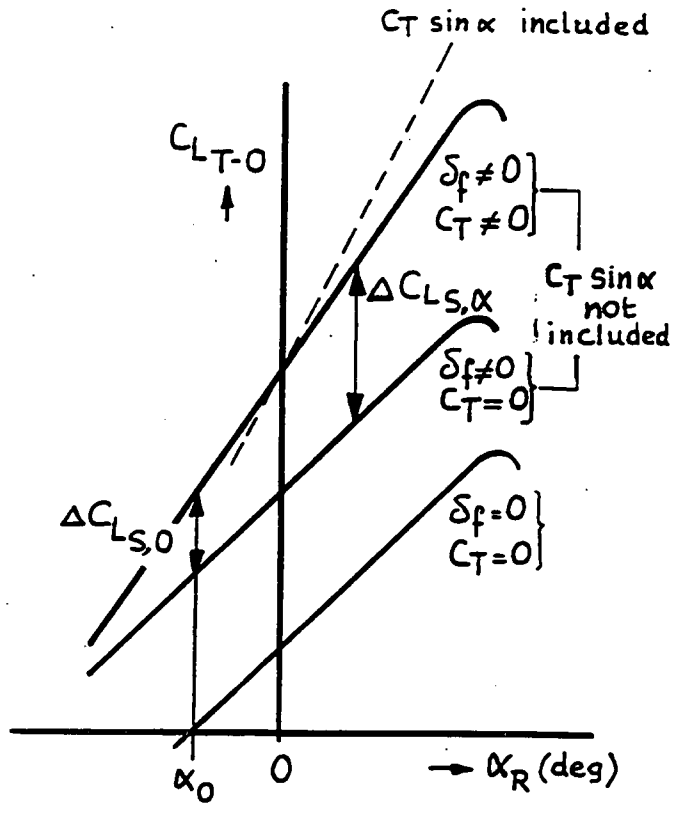

Figure 20 - Definition of $\Delta C_{L_{s,o}}$ and $\Delta C_{L_{s,\alpha}}$ and α_0 (3-dim).

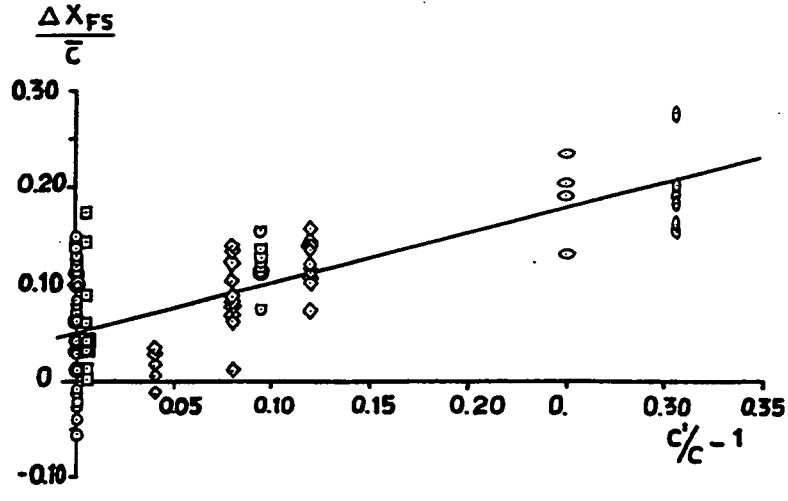

Figure 21 - Assumed shift in point of application of lift due to slipstream to improve the correlation between calculated and measured pitching moment changes due to propeller slipstream.

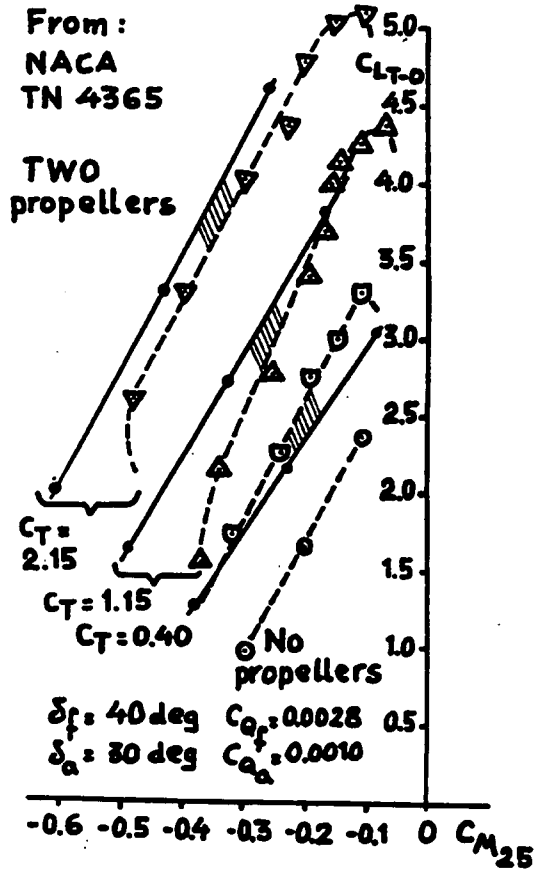

Figure 22 - Tail-off pitching moment curves.
Configuration of refs. 34 and 35. Flaps deflected 40 deg and ailerons 30 deg.

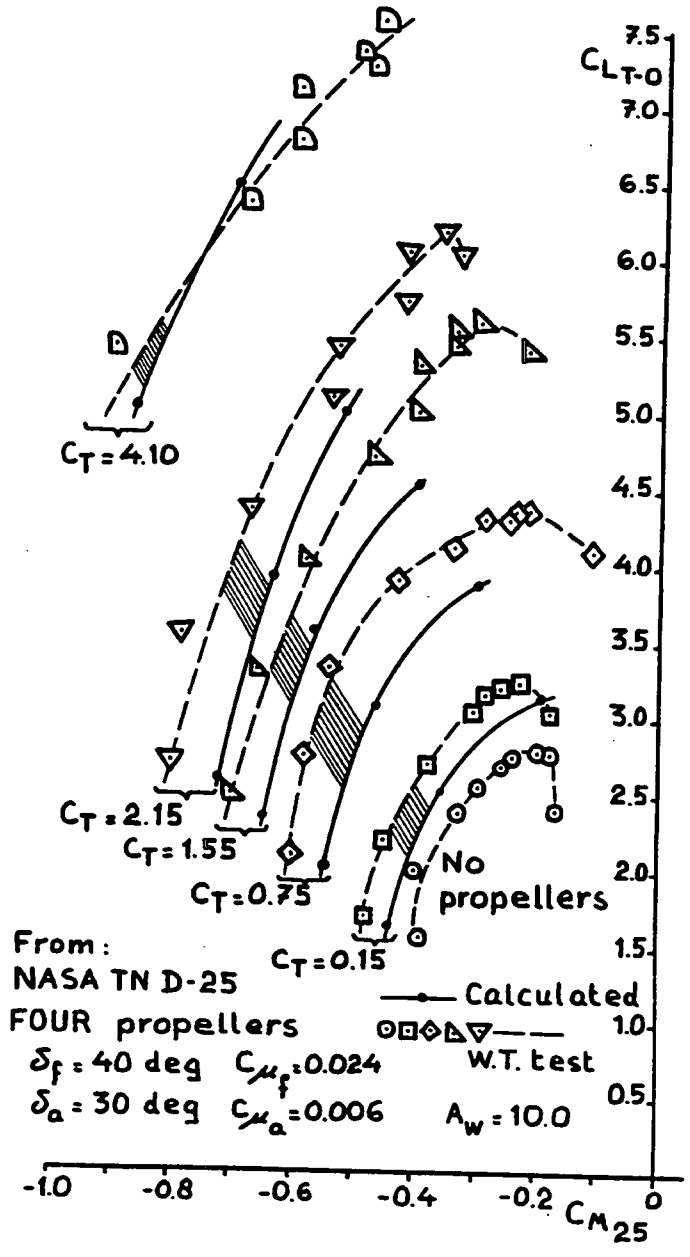

Figure 23 - Tail-off pitching moment curves.
Configuration of ref. 36. Flaps deflected 40 deg. and ailerons 30 deg.

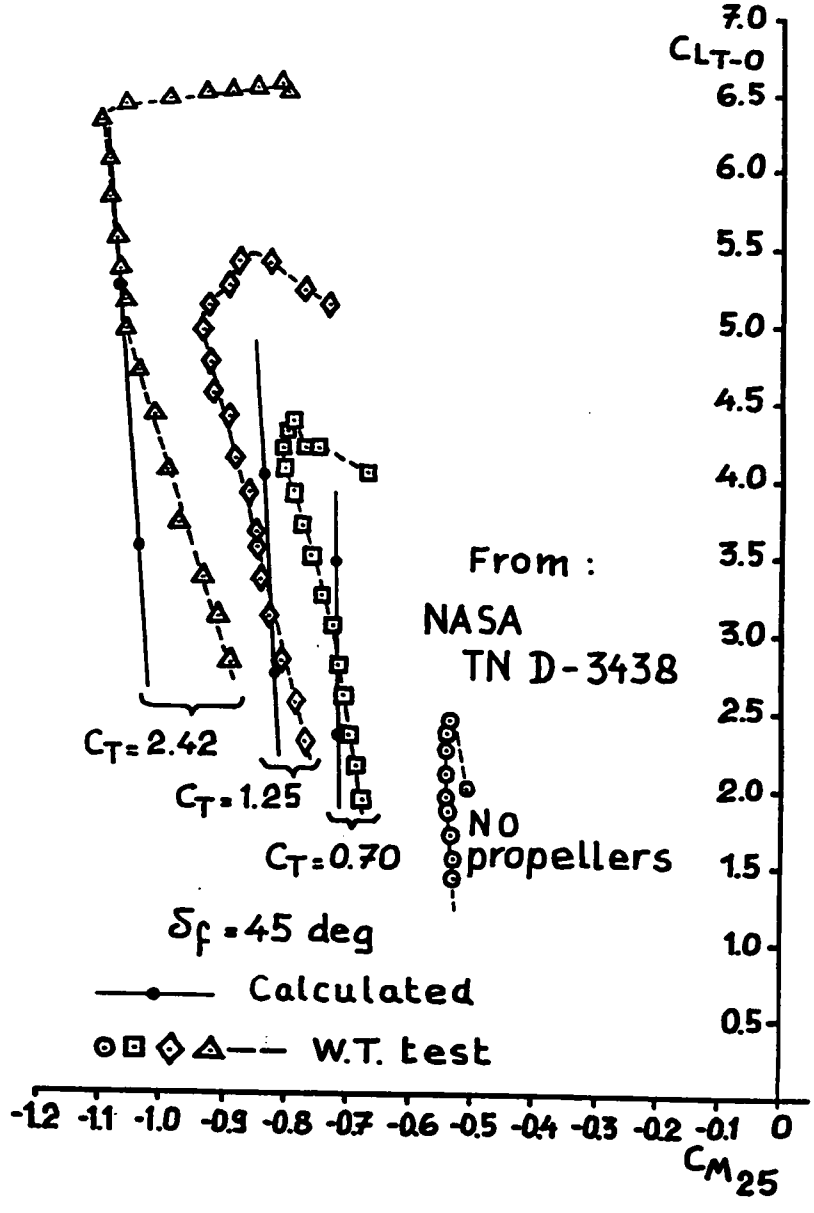

Figure 24 - Tail-off pitching moment curves.
Configuration of ref. 21. Flaps deflected 45 deg.

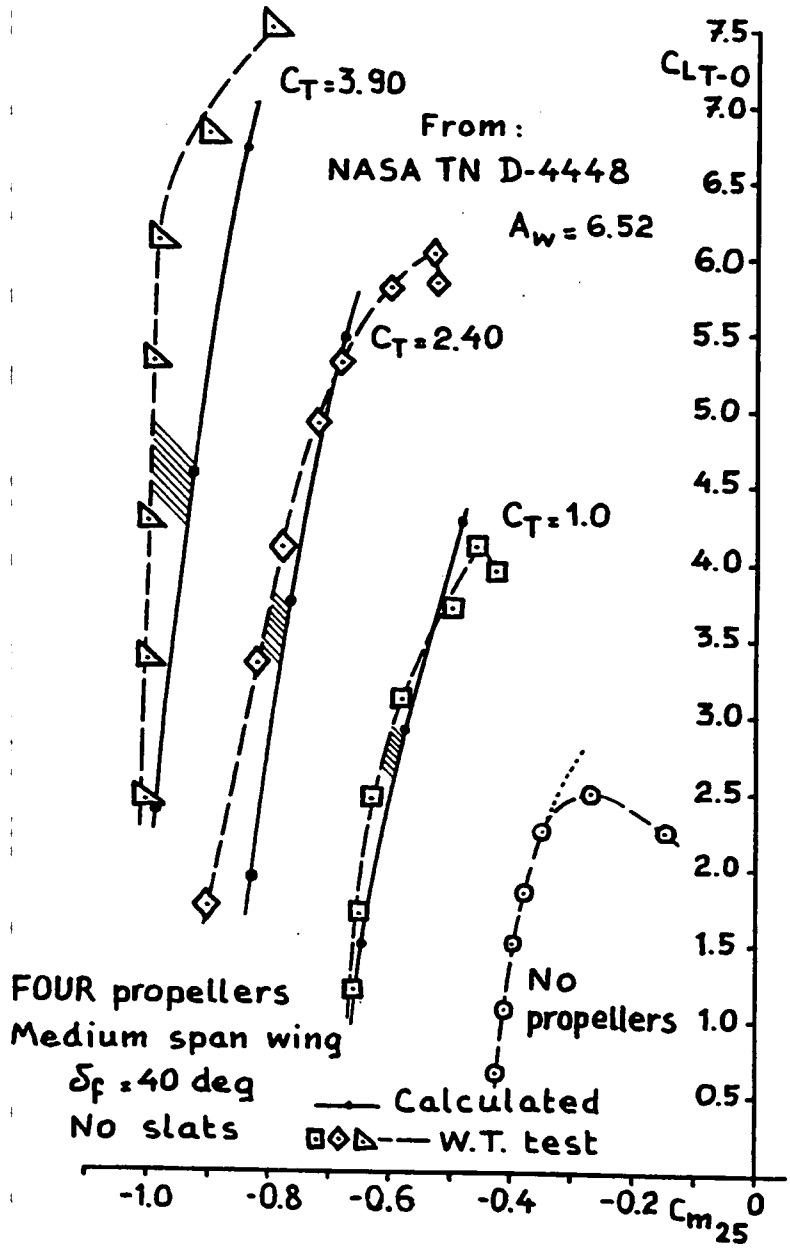

Figure 25 - Tail-off pitching moment curves.
Configuration of ref. 22. Flaps deflected 40 deg.

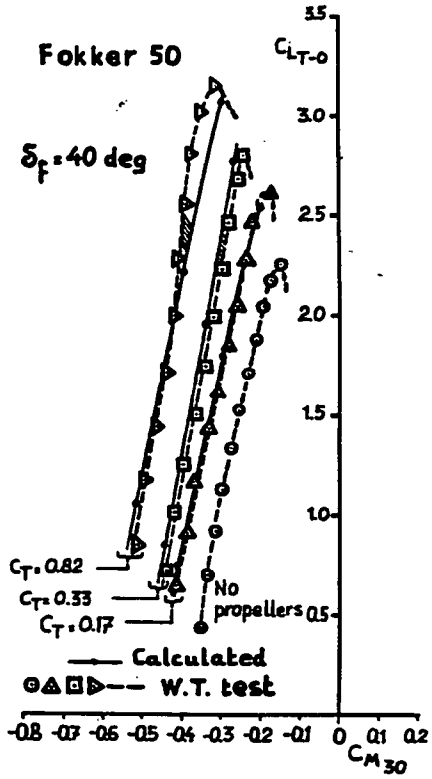

Figure 26 - Tail-off pitching moment curves. Fokker 50. Flaps deflected 40 deg.

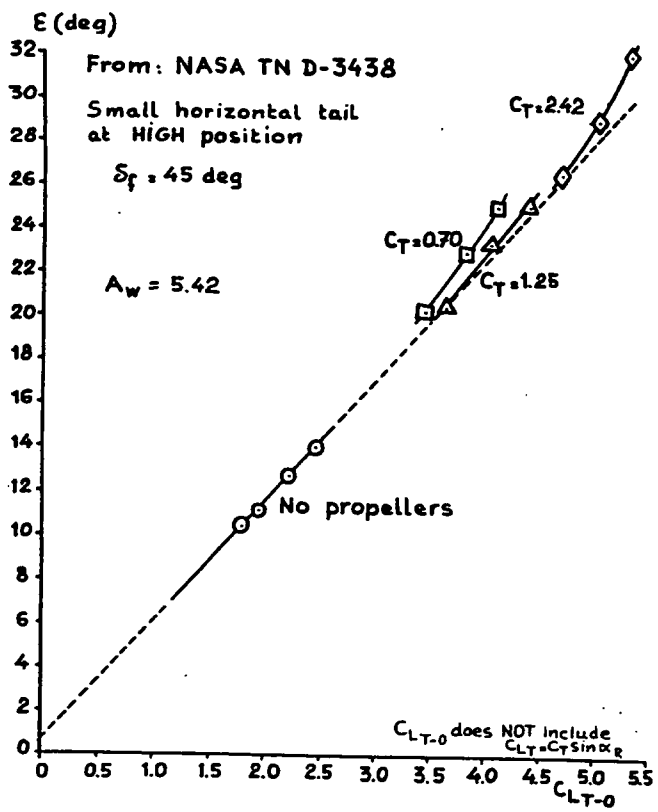

Figure 27 - Downwash angle-versus-lift. Configuration of ref. 21. Flaps deflected 45 deg.

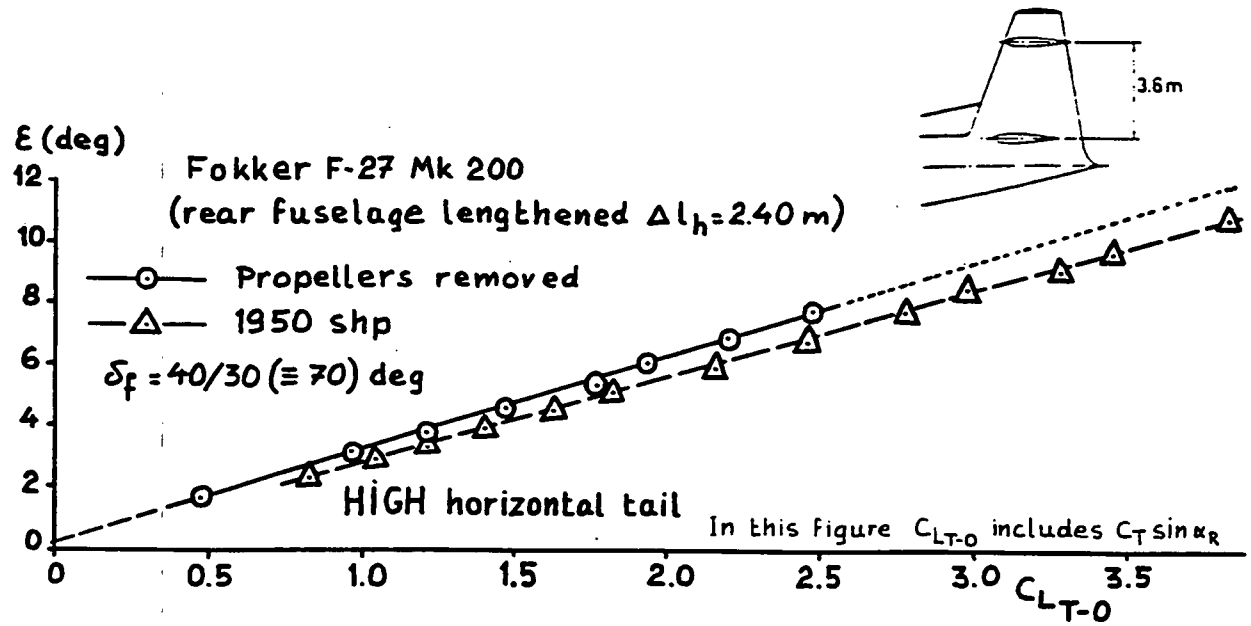

Figure 28 - Downwash angle-versus lift. Fokker F-27 model with high tail. Double-slotted flap deflected 70 deg.

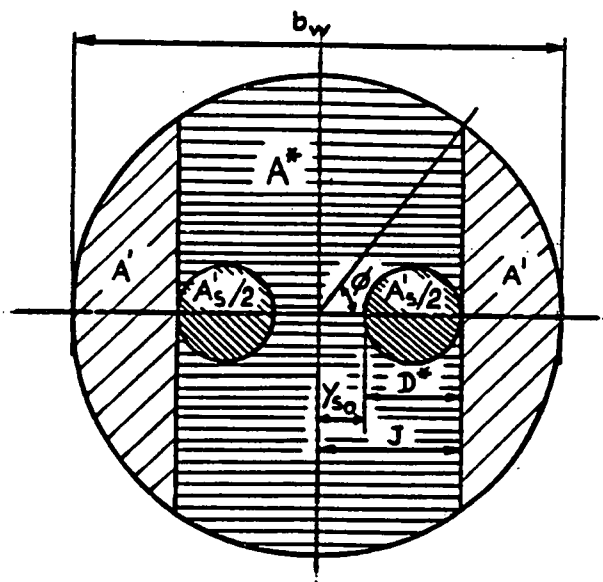

Figure 29 - Idealised cross section of flow over a wing with propeller slipstream.

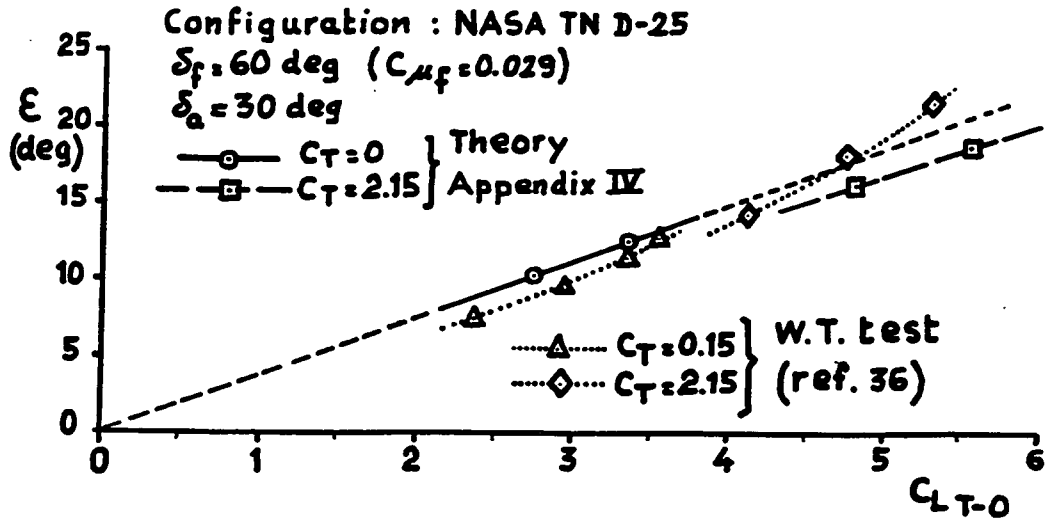

Figure 30 - Effect of propeller slipstream on downwash. Comparison between theory and experiment.

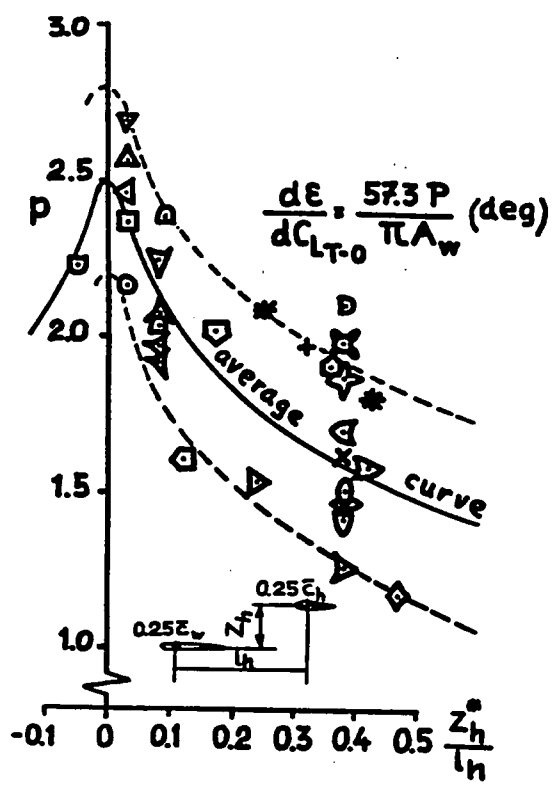

Figure 31 - Effect of tailplane height above the wing plane on downwash gradient.

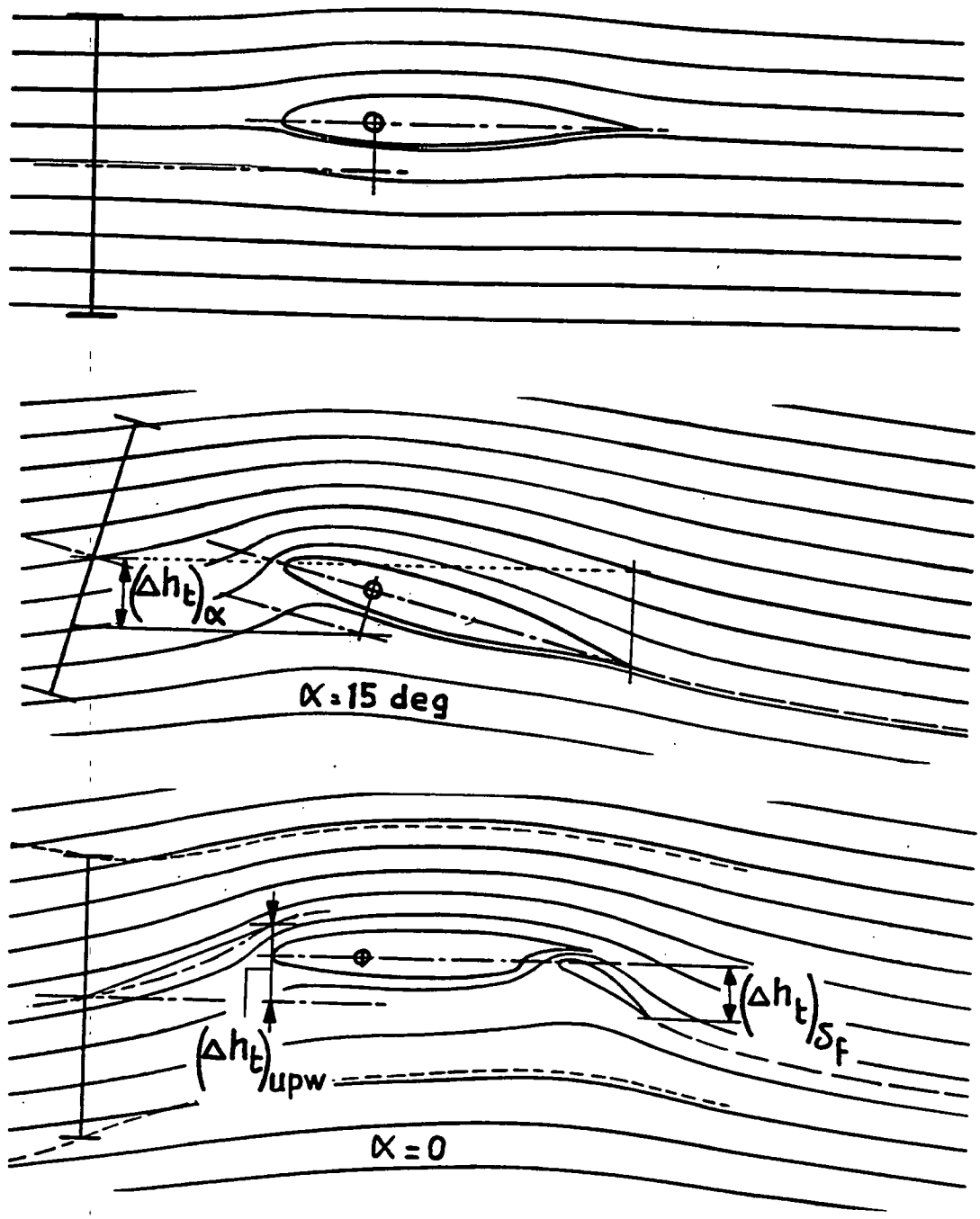

Figure 33 - The vertical displacement of the slipstream centre line due to angle-of-attack and flap deflection.

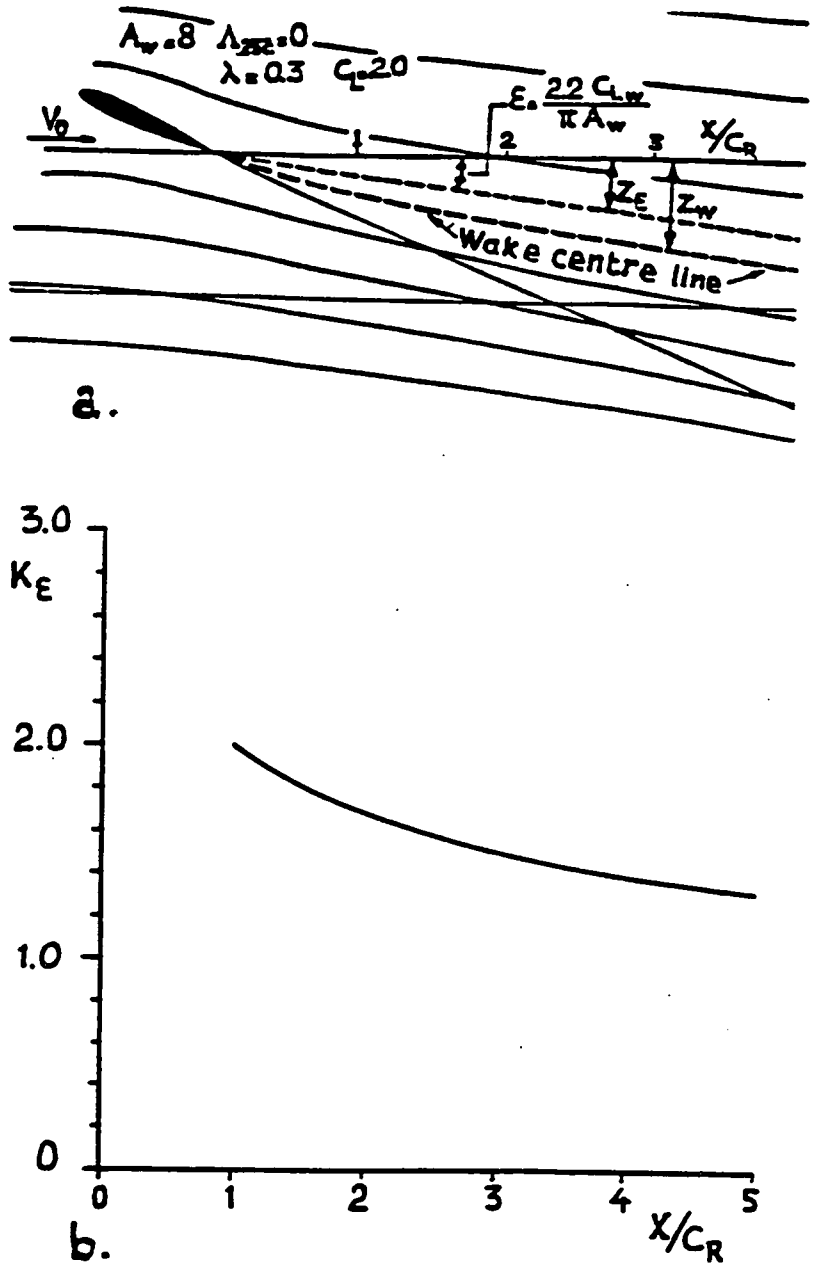

Figure 32 - Shape and position of wing wake.
a. Typical example of flow condition.
b. Kε versus distance behind the wing trailing edge.

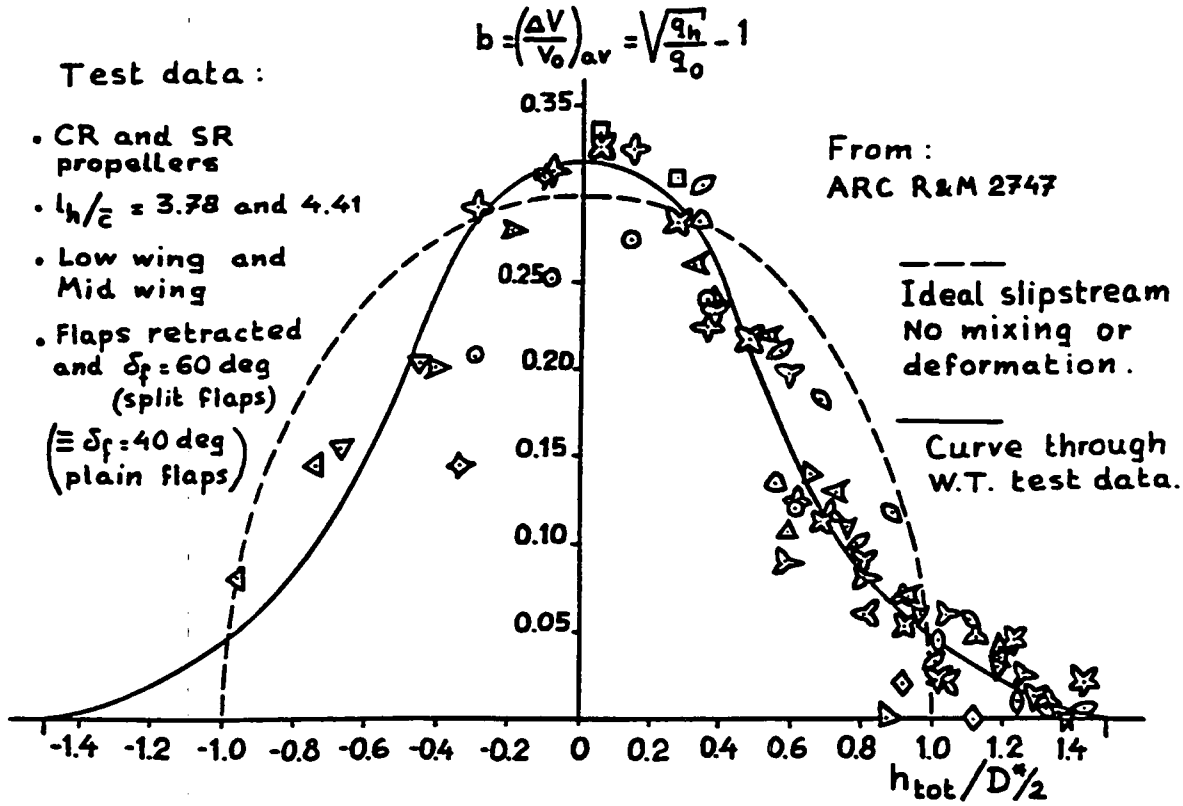

Figure 34 - Effect of slipstream position on average dynamic pressure at the horizontal tailplane. Comparison between theory and experiment.

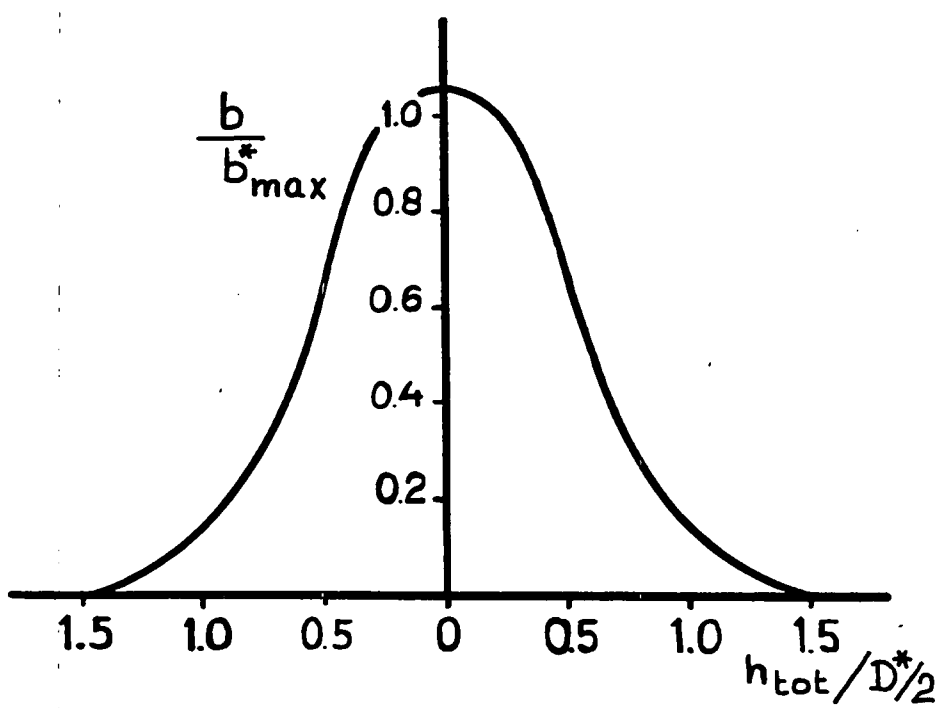

Figure 35 - Effect of slipstream position on average dynamic pressure at the tailplane. Generalized curve.

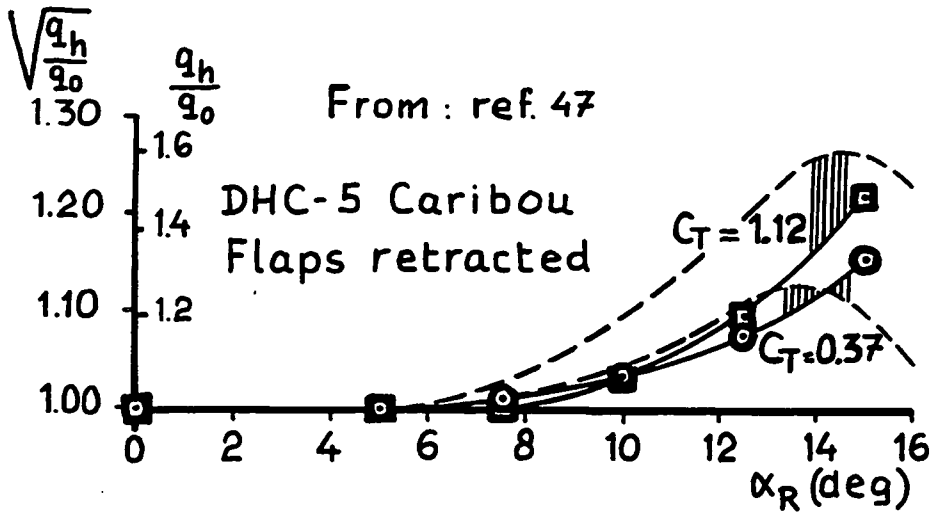

Figure 36 - Average dynamic pressure at the horizontal tail on the DHC-5 Caribou.

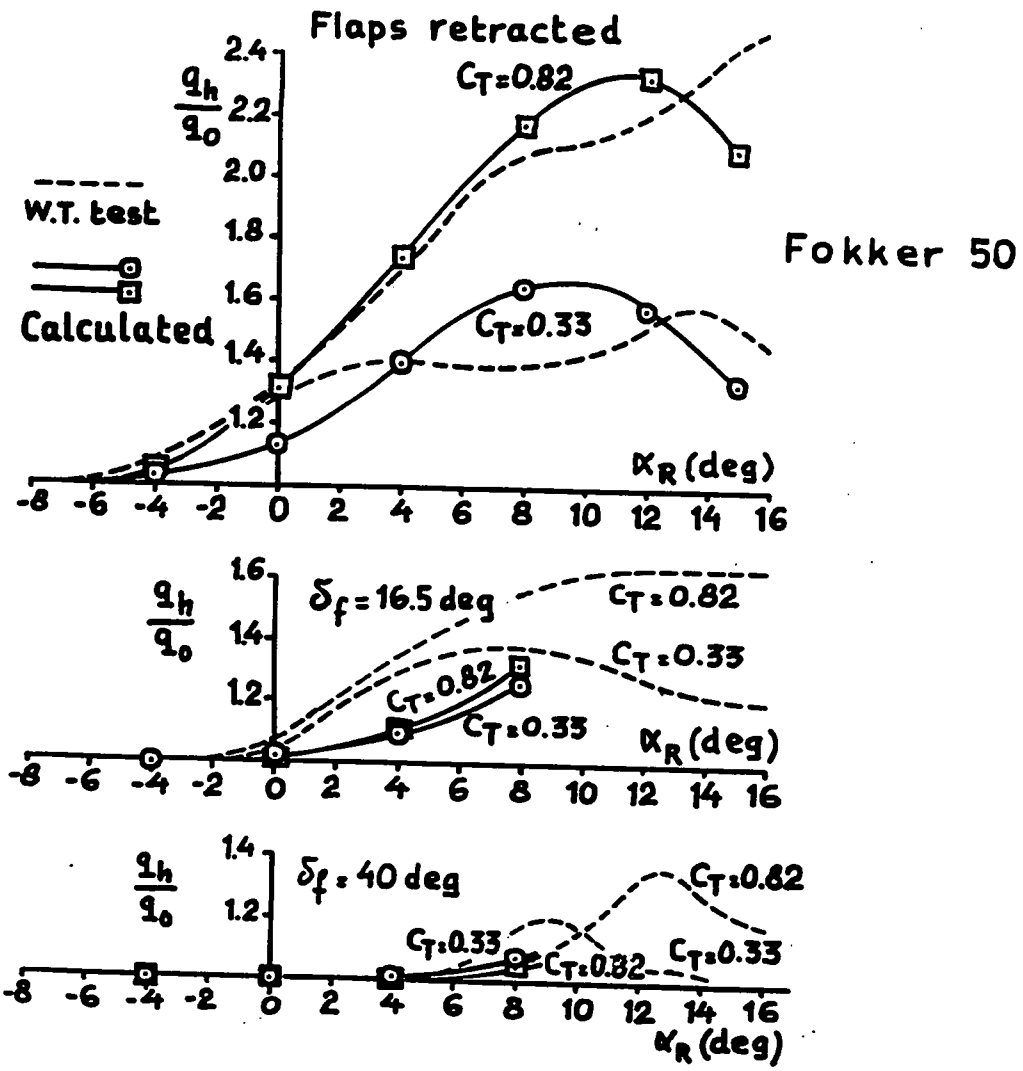

Figure 37 - Average dynamic pressure at the horizontal tail on the Fokker 50.

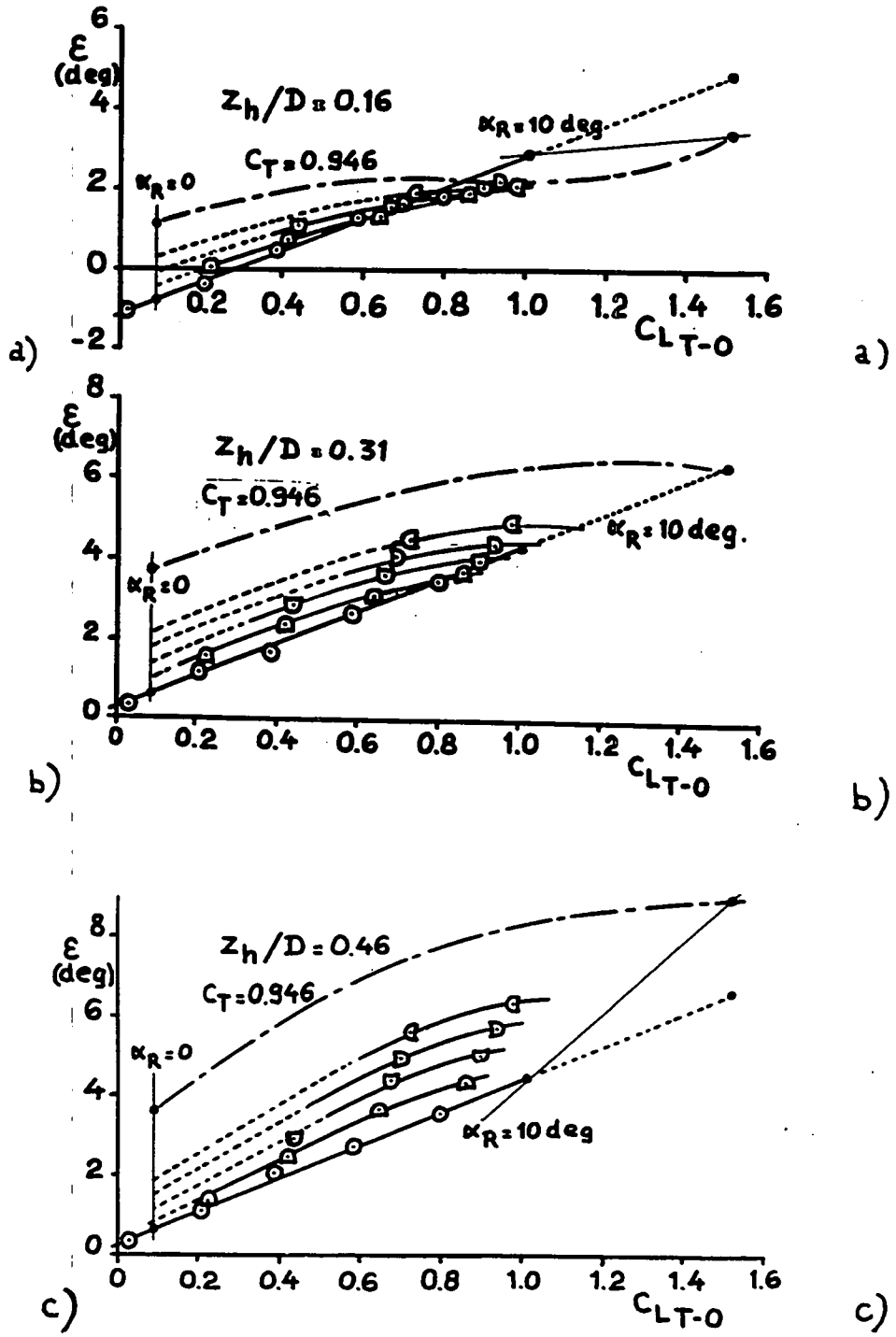

Figure 38 - Effect of the slipstream position on the average downwash angle at the horizontal tailplane. (I)

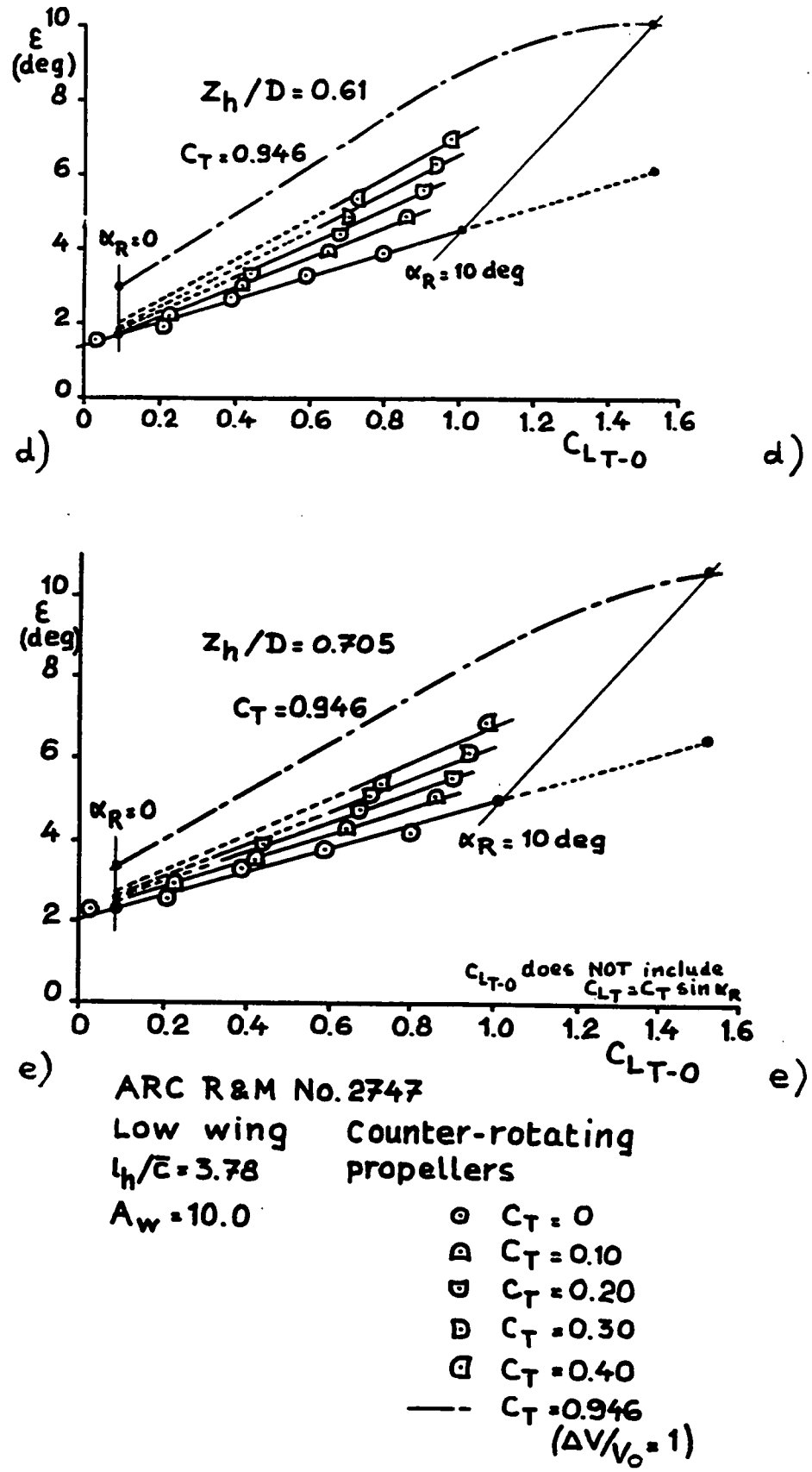

Figure 38 - Increase in downwash at the tailplane due to inflow into the slipstream. (II)

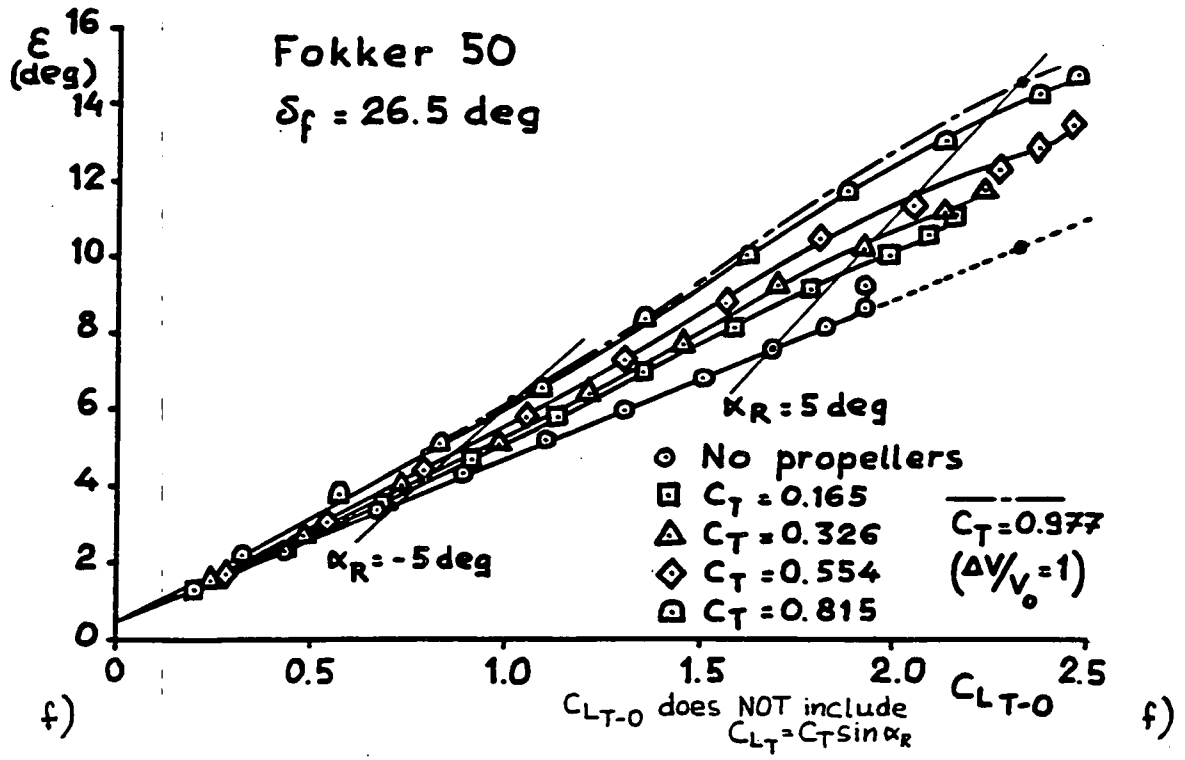

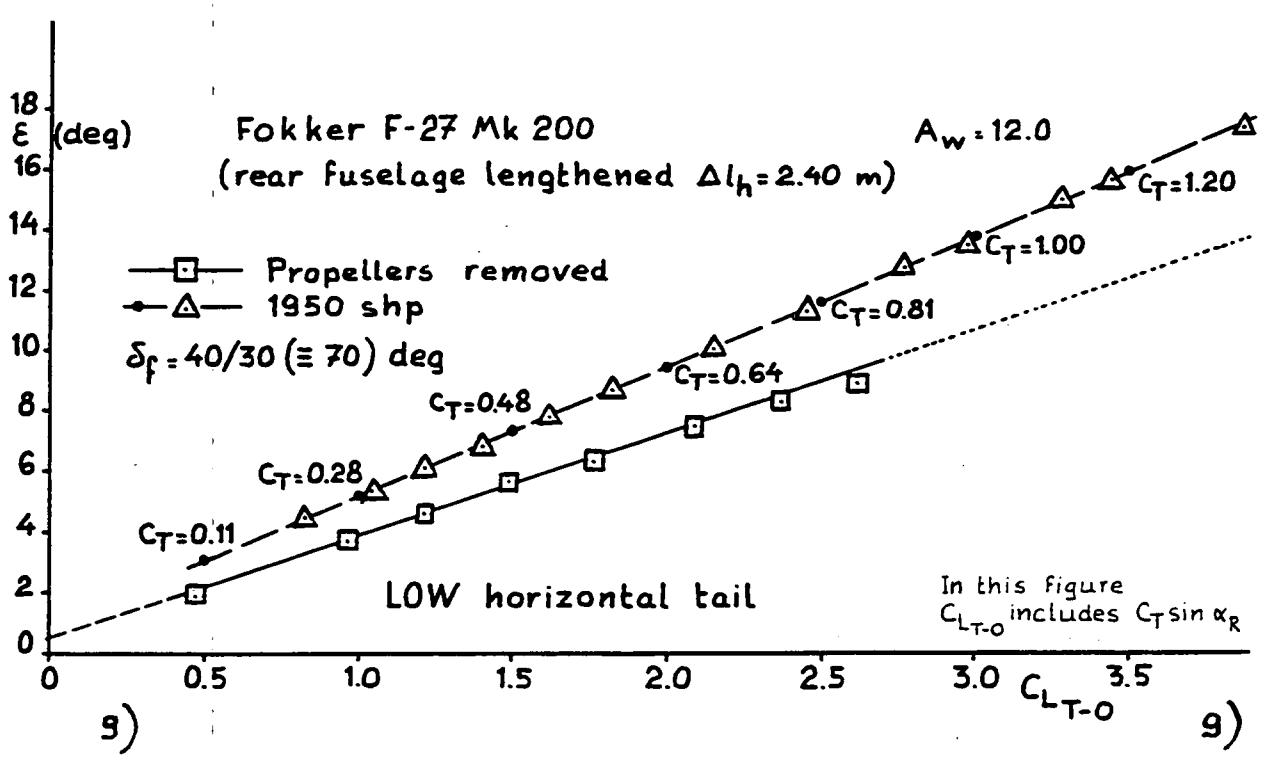

Figure 38 - Effect of the slipstream position on the average downwash angle at the horizontal tailplane. (III)

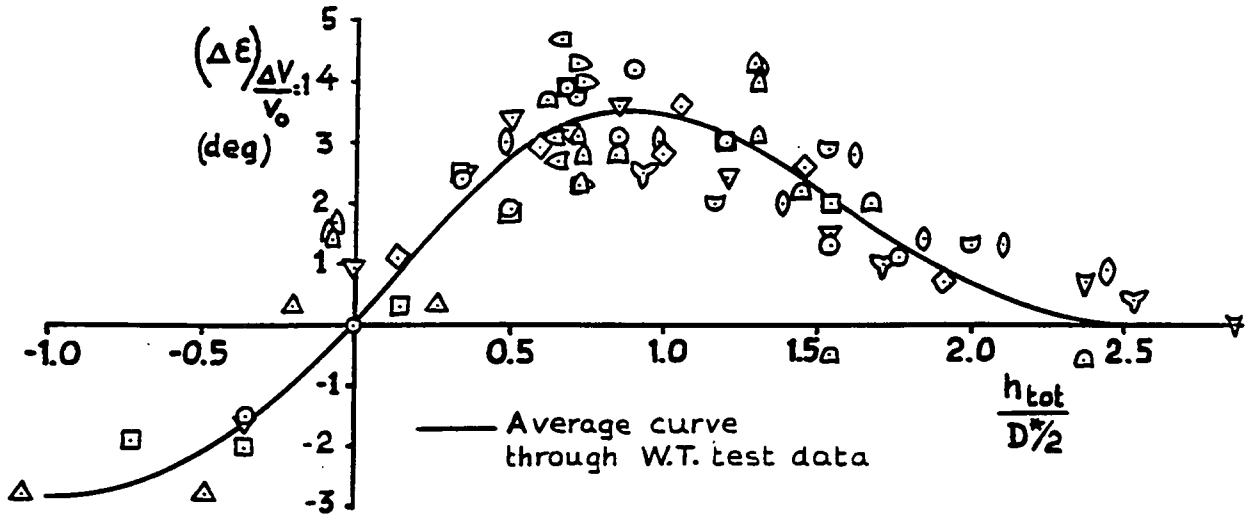

Figure 39 - Increase in downwash at the tailplane due to inflow into the slipstream.

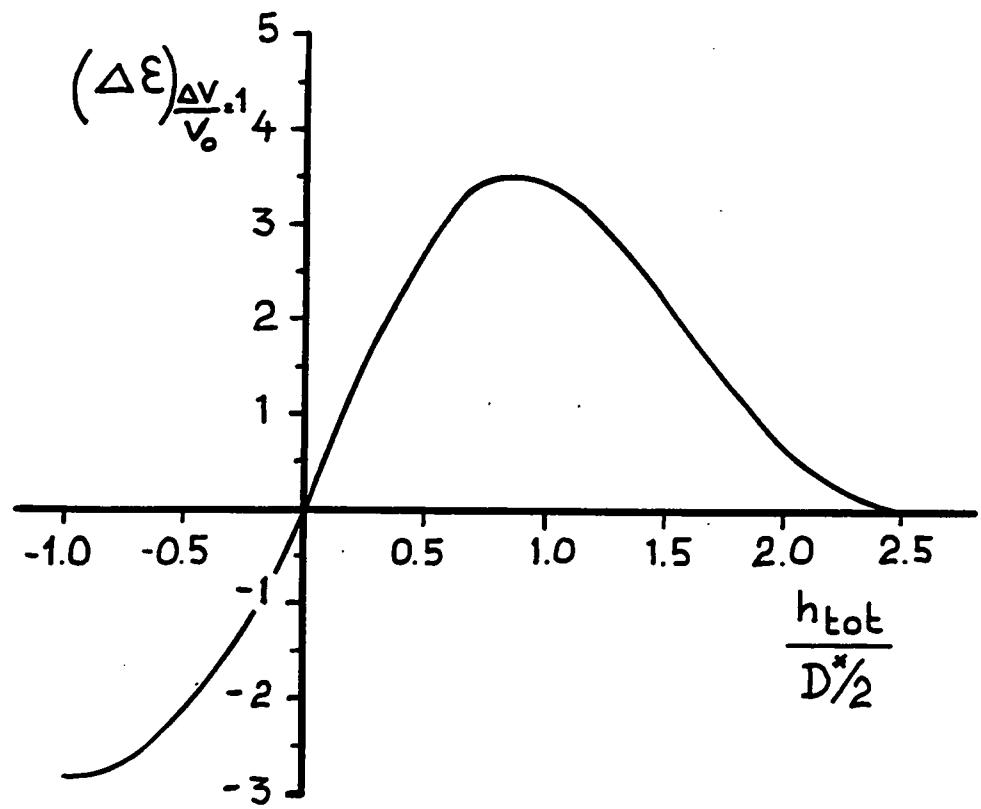

Figure 40 - Increase in downwash at the tailplane due to inflow into the slipstream. - Generalized curve.

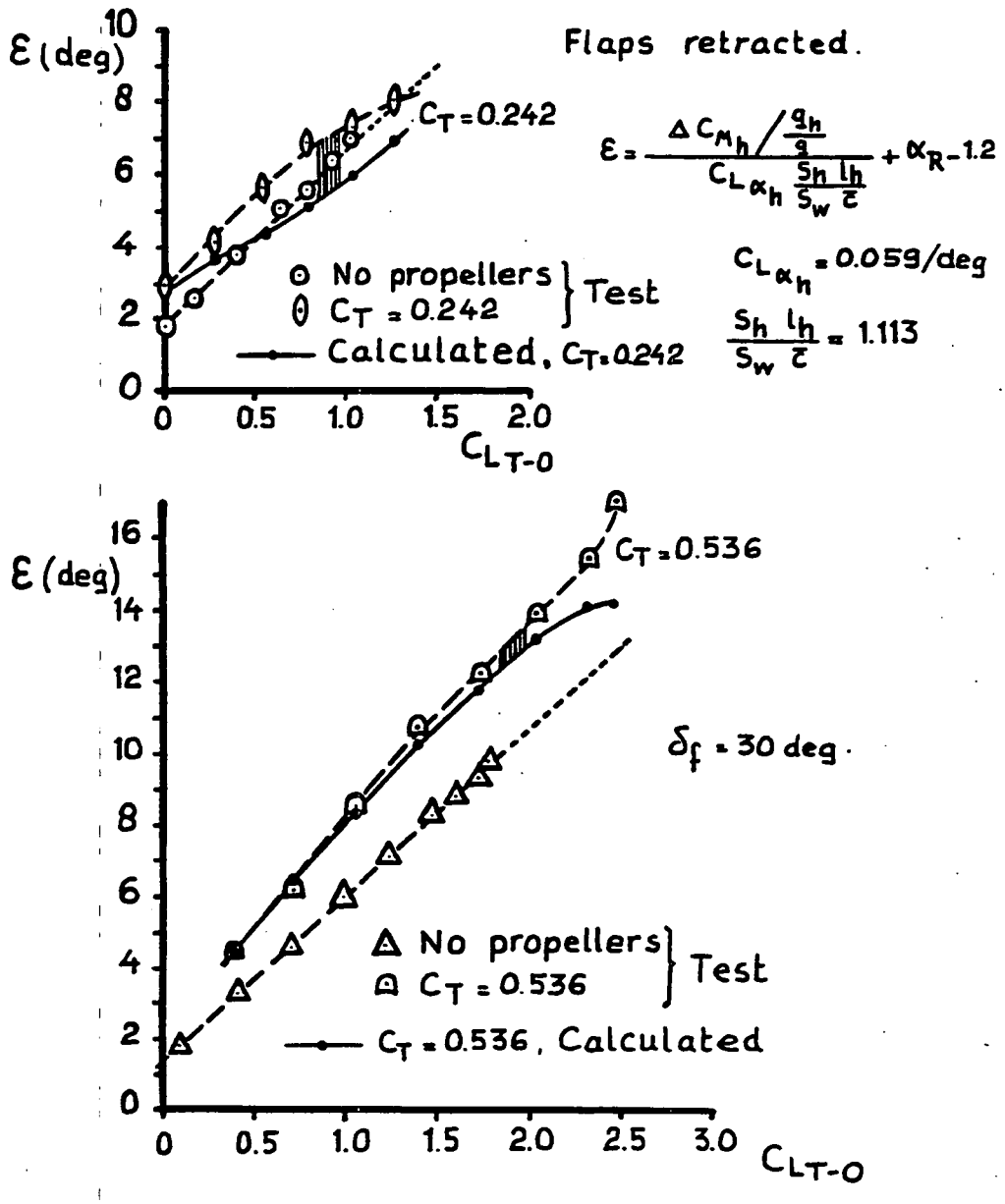

Figure 41 - Effect of propeller slipstream on the average downwash angle at the tailplane on the C-160 Transall. Comparison between theory and experiment. (I)

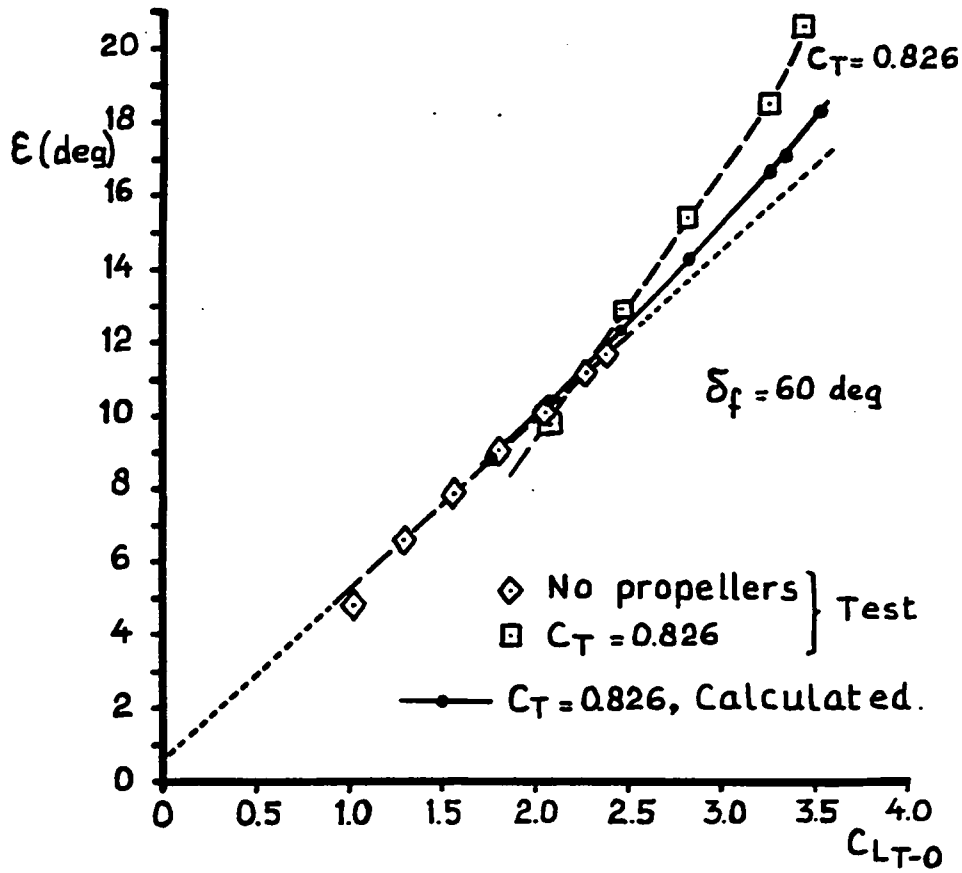

Figure 41 - Effect of propeller slipstream on the average downwash angle at the tailplane on the C-160 Transall. Comparison between theory and experiment. (II)

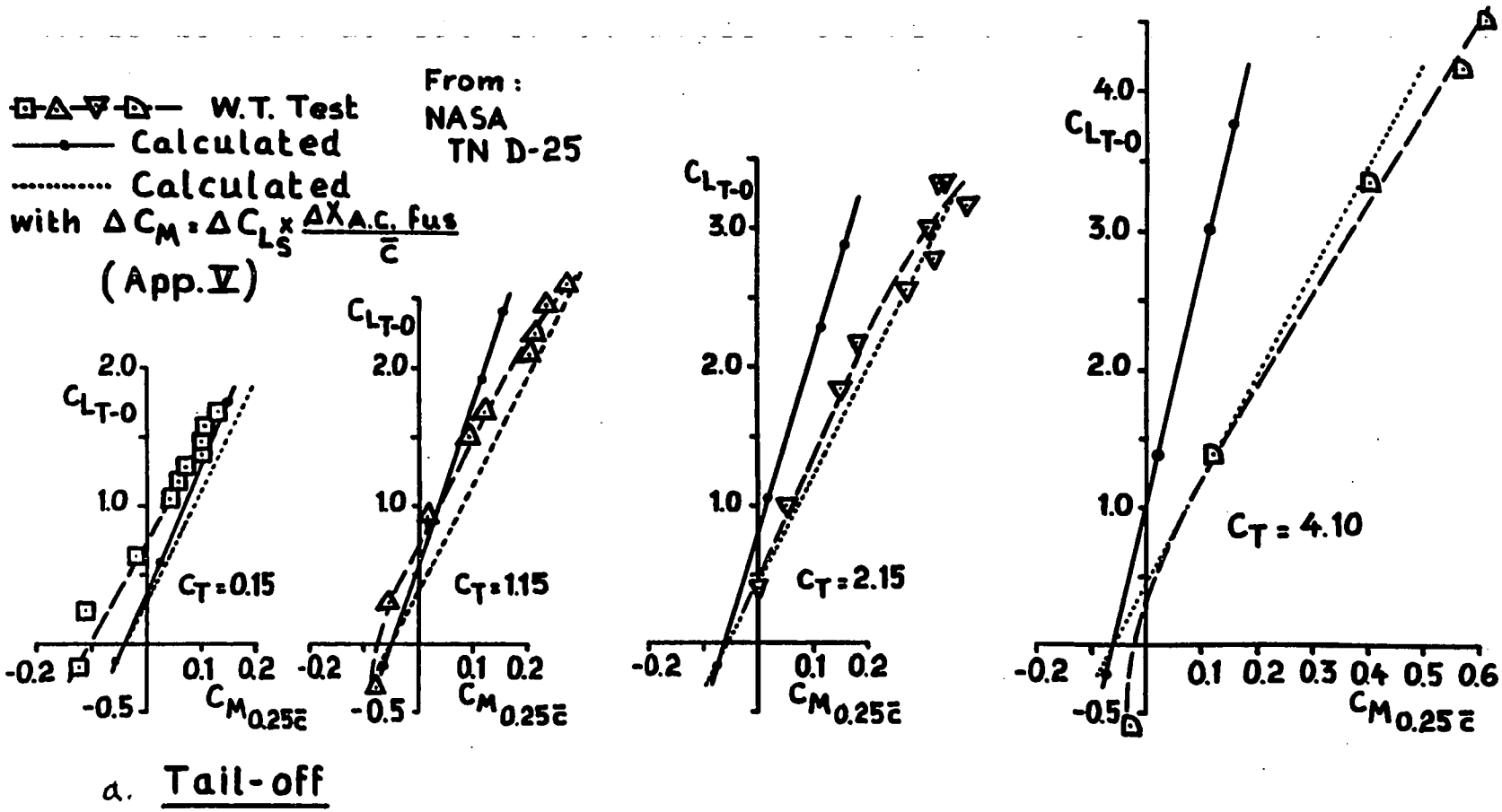

Figure 42 - Tail-off and tail-on pitching moment curves with flaps retracted. Comparison between theory and experiment. (I)

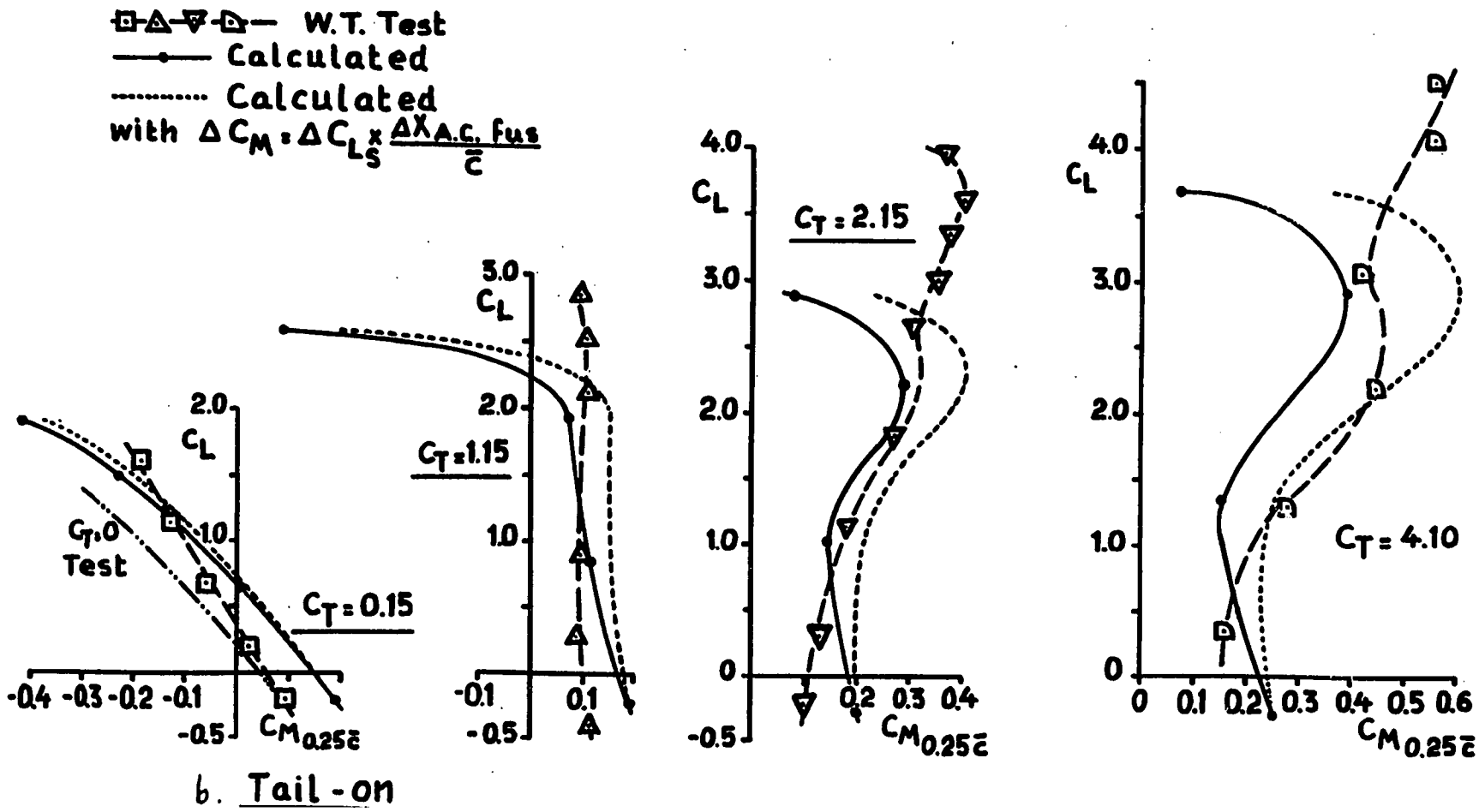

Figure 42 - Tail-off and tail-on pitching moment curves with flaps retracted. Comparison between theory and experiment. (II)

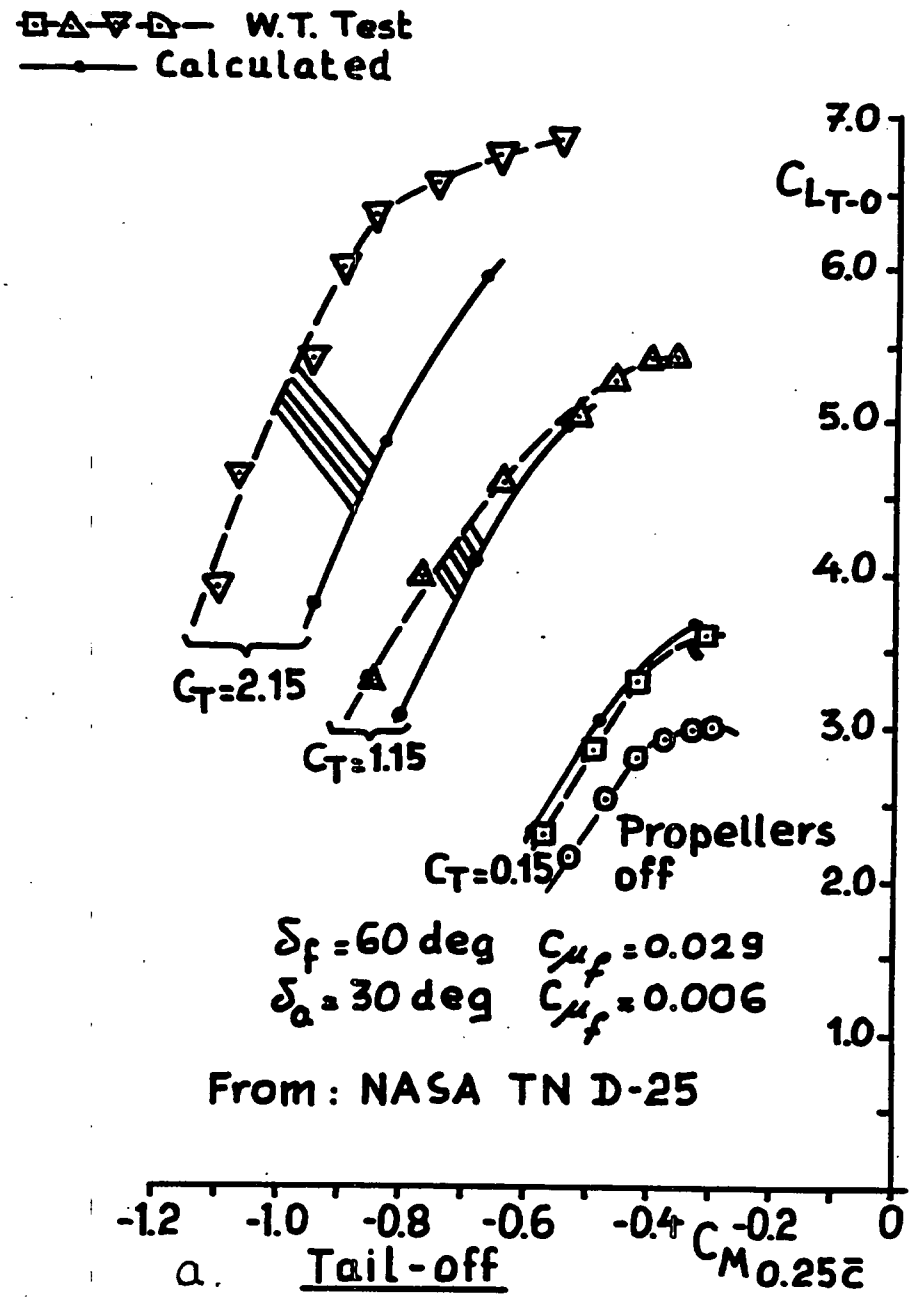

Figure 43 - Tail-off and tail-on pitching moment curves with flaps extended. Comparison between theory and experiment. (I)

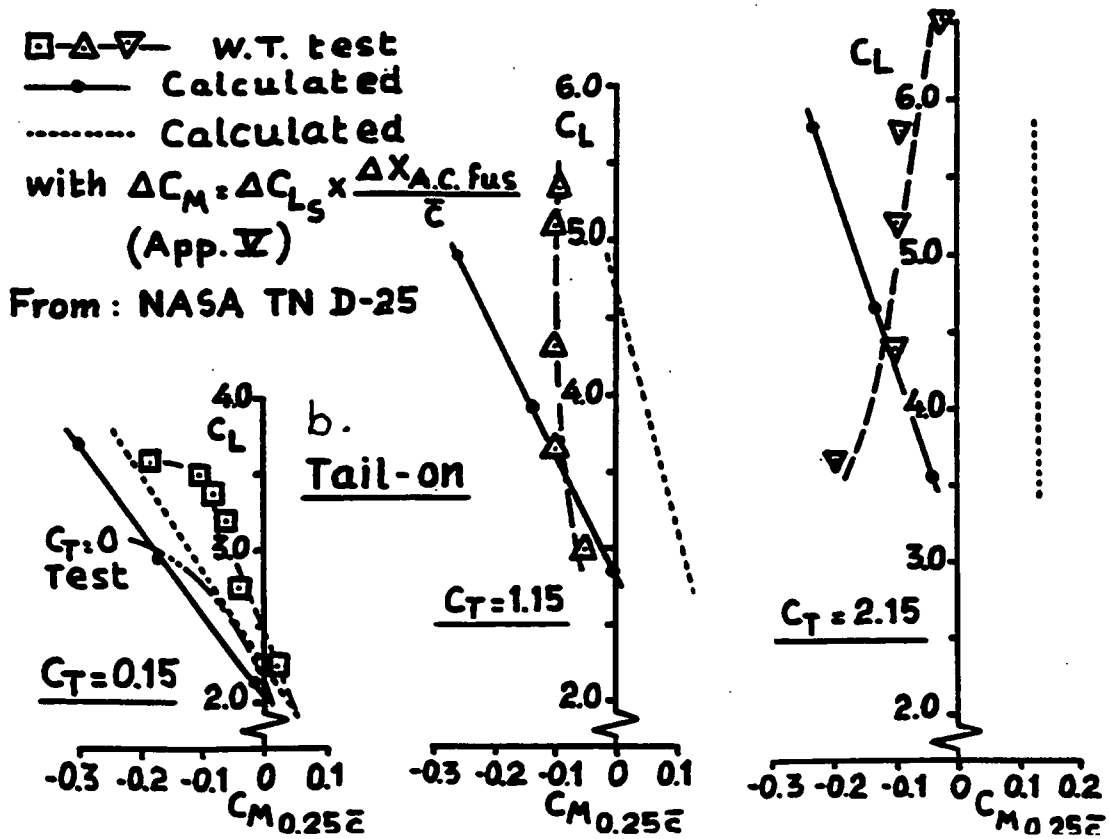

Figure 43 - Tail-off and tail-on pitching moment curves with flaps extended. Comparison between theory and experiment. (II)

Appendix I

The total lift on a lifting surface with running propellers

According to lifting line theory the lift on a wing with elliptic lift distribution can be written as:

$$L_W = \overset{\circ}{m}_o \, V_o \sin \varepsilon = \rho \frac{\pi}{4} b_w^2 \, V_o^2 \sin \varepsilon$$

where ε is the average downwash of the flow over the wing infinitely far behind the wing. The flow can thus be considered as s stream tube with circular cross section and diameter b_w which is deflected downward over an angle ε. This model is now assumed to apply to any conventional wing shape.
The lift due to slipstream is also considered to be equal to the momentum resulting from the downward deflection over an angle ε_s of each slipstream tube with fully contracted diameter D^*.
where:

$$D^* = D \sqrt{\frac{V_o + \Delta V/2}{V_o + \Delta V}}$$

The lift due to slipstream can then be written as:

$$L_s = n_e \overset{\circ}{m}_s \, (V_o + \Delta V) \sin \varepsilon_s = n_e \rho \frac{\pi}{4} D^* \, (V_o + \Delta V)^2 \sin \varepsilon_s$$

On a lifting wing with slipstream present the cross-sectional area from the slipstream tubes has to be subtracted from the cross-sectional area of the stream tube describing the outer flow (see fig. 1). The total wing lift then becomes:

$$L_{W+S} = \rho \, V_o^2 \left[\frac{\pi}{4} b_w^2 - n_e \frac{\pi}{4} D^{*2}\right] \sin \varepsilon + \rho \, [V_o + \Delta V]^2 n_e \frac{\pi}{4} D^{*2} \sin \varepsilon_s$$

and:

$$C_{L_{W+S}} = \frac{L_{W+S}}{\frac{1}{2}\rho V_o^2 S_W} = \frac{2}{S_W} \left(\frac{\pi}{4} b_w^2 - n_e \frac{\pi}{4} D^{*2}\right) \sin \varepsilon + \frac{F}{T} n_e \frac{\pi D^{*2}}{2 S_w} \frac{(V_o + \Delta V)^2}{V_o^2} \sin \varepsilon_s$$

where the factor $\frac{F}{T}$ is discussed at the end of this appendix.

When the propeller thrust is parallel to the fuselage reference line the total propeller thrust can be written as: (see fig. Ia).

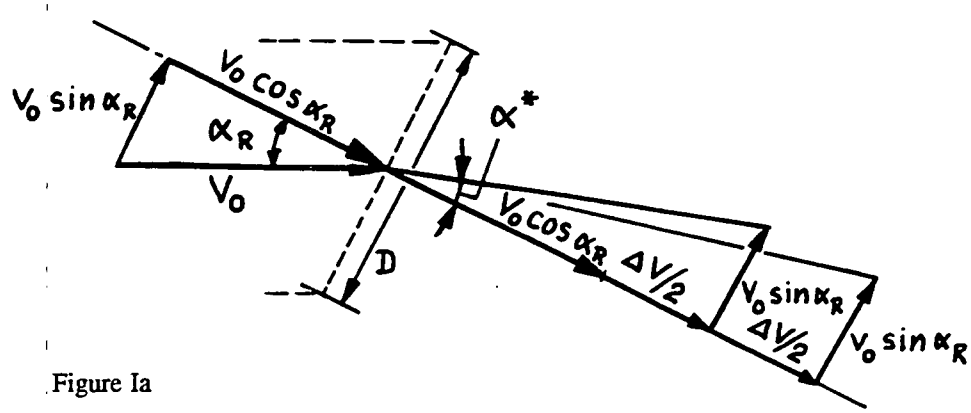

Figure Ia

$$T = C_T \frac{1}{2} \rho \, V_o^2 \, S_w = \dot{m}_s \, \Delta V = \rho \left[V_o \cos \alpha_R + \frac{\Delta V}{2} \right] \frac{\pi}{4} D^2 \cos \alpha_R \, \Delta V$$

and the downwash angle far behind the propeller: $\varepsilon_p = \alpha_R - \alpha^*$,

where $\alpha^* = arctg \dfrac{V_o \sin \alpha_R}{V_o \cos \alpha_R + \Delta V}$

An extensive comparison between calculated and measured increase in lift due to slipstream showed a much better correlation when α^* was written as:

$$\alpha^* = arctg \frac{V_o \sin \alpha_R}{V_o \cos \alpha_R + \Delta V/2}$$

This means the downwash behind the propeller is considered at the propeller disc. This definition of α^* is used in all further calculations.

For the wing part covered by the slipstream the average effective angle-of- attack relative to the fuselage reference line is equal to α^*.
However the aerodynamic angle-of-attack measured from the zero-lift line is:

$$\alpha_s = \alpha^* + i_{c_s} - \alpha_o - \Delta\alpha_{o,f}$$

where: i_{c_s} = angle of incidence of the local wing chord relative to the fuselage reference line.
α_o = zero-lift angle-of-attack relative to the chord line of the airfoil section at the propeller axis location.
$\Delta\alpha_{o,f}$ = change in zero-lift angle-of-attack due to flap deflection

$$\Delta\alpha_{o,f} = - \frac{dc_l/d\delta}{dc_l/d\alpha} \times \delta_{f_{eff}}$$

As discussed in the main text the lift due to slipstream is considered to be equal to the lift on a wing with aspect ratio $A_{s,eff}$ in a free stream with velocity $V = V_o + \Delta V$.

$$\sin \varepsilon_s = \frac{2 \, C_{L_{s,eff}}}{\pi \, A_{s,eff}} \sin \alpha_s$$

If $A_{s,eff} \leq 1.5$ then $A_{s,eff} \approx \pi/2 \, A_s$ and $\sin \varepsilon_s = \sin \alpha_s$

Note that strictly speaking C_{L_s} should be determined as indicated in fig. Ib.

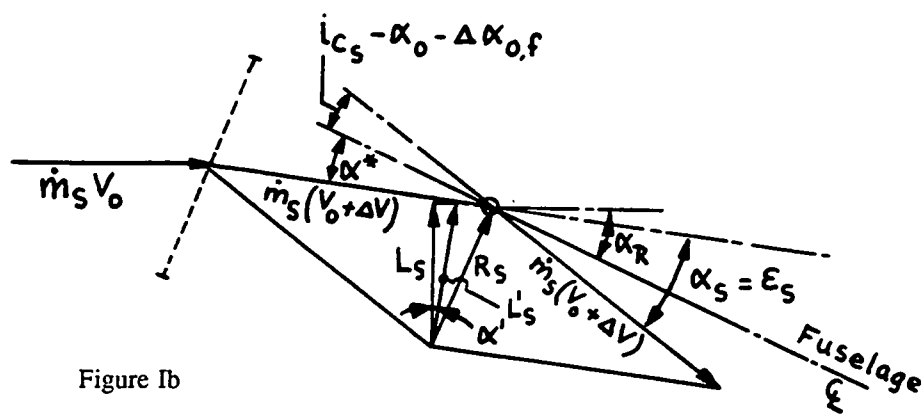

Figure Ib

However for small values of $\alpha' = (\alpha - \alpha_s + \varepsilon_s/2)$ the difference between R_S and L_S can be neglected. In the examples presented in this paper and ref. 49 this difference has consistently been neglected. At very large angles-of-attack and very high C_T-values this may no longer be acceptable.

Kuhn has shown that at large flap deflections momentum losses occur in the slipstream, possibly due to viscous effects. Fig. Ic shows the curves adopted in the present method for the factor F/T as a function of flap setting for various flap types to account for these momentum losses.

For the total increase in lift due to running propellers the vertical thrust component

$$L_T = C_T \frac{1}{2} \rho V_0^2 S_W \sin \alpha_R$$

and the total propeller normal force

$$L_P = C_{L_P} \frac{1}{2} \rho V_0^2 S_W$$

has to be added to the total wing lift. C_{L_P} is determined according to the method presented in ref. 24.

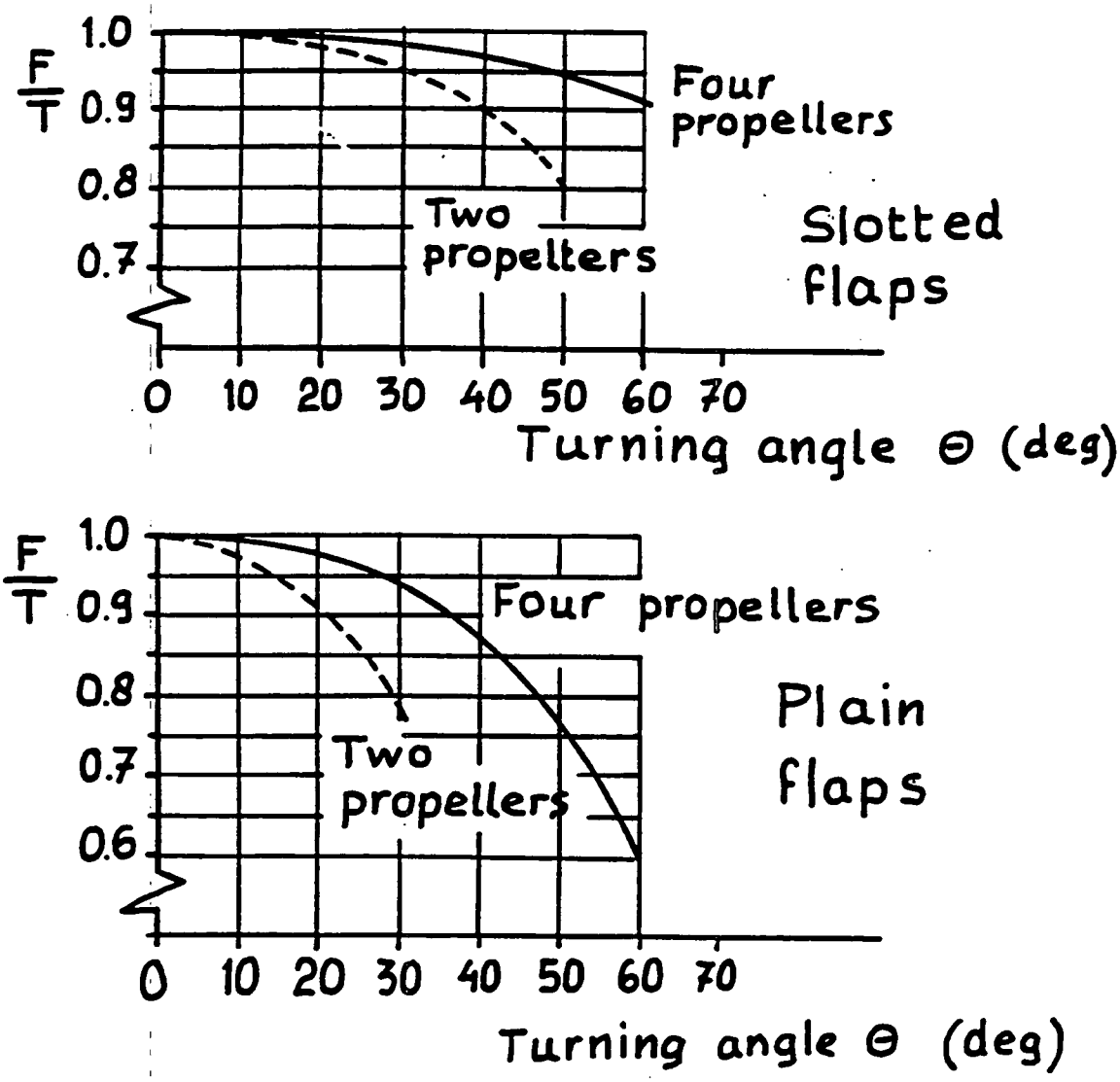

Figure IC

Appendix II

Estimation of the lift due to slipstream for the configuration analysed in ref. 28. (UTIA TN No 11)

In report UTIA TN No 11 a parameter σ was defined:

$$\sigma = \frac{\bar{q}_{jet}/q_o - 1}{\bar{q}_{jet}/q_o + 1} \quad where\ jet = slipstream$$

This can also be written as:

$$\frac{\bar{q}_{jet}}{q_o} = \frac{1+\sigma}{1-\sigma}$$

For $\Delta V/V_0 = 0$ the total lift can be written as $L_{tot} = L_W + L_S$.

$$Then: \quad \Delta L_S = [L_W + L_S]_{\frac{\Delta V}{V_o}=0} - [L_W]_{\frac{\Delta V}{V_o}=0}$$

With the equations from Appendix I this can be written as:

$$\Delta L_S = \rho\,[V_o + \Delta V]^2\ \frac{\pi}{4} D^{*2} \sin \varepsilon_s - \rho V_o^2\ \frac{\pi}{4} D^{*2} \sin \varepsilon$$

The thrust $T = \rho \frac{\pi}{4} D^{*2} [V_o + \Delta V]\ \Delta V$ and $\frac{\Delta L_S}{T} = \frac{[V_o+\Delta V]^2 \sin \varepsilon_s - V_o^2 \sin \varepsilon}{(V_o+\Delta V)\ \Delta V}$

As the model under consideration is a 2-dim. model $\varepsilon = 0$.

$$So: \quad \frac{\Delta L_S}{T} = \frac{(V_o+\Delta V)^2 \sin \varepsilon_s}{(V_o+\Delta V)\ \Delta V} = \left[\frac{V_o}{\Delta V} + 1\right] \sin \varepsilon_s$$

As D = 8 in, c = 8 in, b = 32 in it is assumed again that $\varepsilon_s = \alpha_s$. and as the propeller is not attached to the model and fixed in the tunnel $\alpha_s = \alpha$.

So: $\frac{\Delta L_s}{T} = \left[\frac{V_o}{\Delta V} + 1\right] \sin \alpha$ and $\left[\frac{V_o}{\Delta V} + 1\right] = \frac{\Delta L_S}{T \sin \alpha}$

As $\frac{1+\sigma}{1-\sigma} = \frac{q_j}{q_o} = \left[1 + \frac{\Delta V}{V_o}\right]^2$ a unique relation exists between σ, $V_o/\Delta V$ and $\frac{\Delta L_S}{T \sin \alpha}$
In the following table some numerical values are presented

σ	$V_o/\Delta V$	$\frac{\Delta L_S}{T \sin}$
1.00	0	1.00
0.88	0.338	1.338
0.76	0.586	1.586
0.62	0.947	1.947
0.49	1.410	2.410
0.26	3.289	4.289

A comparison between these calculated data and windtunnel test results is presented in figs. 11a, b.

Appendix III

The theoretical average dynamic pressure at the horizontal tail of multi-engined propeller aircraft

The effect of propeller slipstream on the theoretical average dynamic pressure at the tail q_h, is considered under the following assumptions:

1. The slipstream is fully contracted at the tail location.

2. The slipstream cross-section is circular with diameter D^*.
No mixing on the slipstream boundary occurs nor any deformation of the cross-section. The average dynamic pressure in the slipstream is:

$$q_s = \frac{1}{2}\rho V_o^2 \left[1 + \frac{\Delta V}{V_o}\right]^2$$

The average dynamic pressure at the tailplane location is:

$$q_h = \frac{1}{2}\rho V_o^2 \left[1 + \left(\frac{\Delta V}{V_o}\right)_{av}\right]^2 = \frac{1}{2}\rho V_o^2 \ (1+b)^2$$

According to fig. III a the width of the tailplane part covered by the slipstream of a single propeller is:

$$b_s = 2\sqrt{\left[\frac{D^*}{2}\right]^2 - h_{tot}^2}$$

or:

$$b_s = D^*\sqrt{1 - \left[\frac{h_{tot}}{D^*/2}\right]^2}$$

The tail area covered by the slipstream of two propellers is:

$$S_s = 2 \times b_s \times c_s$$

The average dynamic pressure at the tail is then:

$$\frac{1}{2}\rho\,(1+b)^2\,V_o^2 = \frac{1}{2}\rho\left[1 + \frac{\Delta V}{V_o}\right]^2 V_o^2\,S_s + V_o^2\,[S_h - S_s]$$

or:

$$(1+b)^2 = \left[1 + \frac{\Delta V}{V_o}\right]^2 \frac{S_s}{S_h} + \frac{S_h - S_s}{S_h}$$

Then:

$$b = \sqrt{\left[1 + \frac{\Delta V}{V_o}\right]^2 \frac{S_s}{S_h} + \frac{S_h - S_s}{S_h}} - 1$$

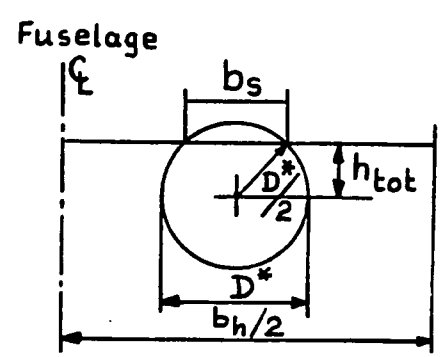

Figure IIIa

and

$$b_{max} = \sqrt{\left[1 + \frac{\Delta V}{V_o}\right]^2 \frac{2 \times D^* \times c_s}{S_h} + \frac{S_h - 2 \times D^* \times c_s}{S_h}} - 1$$

For the configuration from report ARC R&M No 2747 (ref. 16) b has been calculated as a function of $h_{tot}/D^*/2$ for $C_T = 0.40$.

$\frac{\Delta V}{V_o}$=0.506; D^*=9.12 ; S_h=197.3 sq. ; c_s=5.80

The result is shown as the broken curve in fig. 34. This figure illustrates that the estimated location of the slipstream centre line is correct. Slipstream spread and deformation does occur however. The curve for b to be used in the method described in the present report is also indicated in fig. 34.

Appendix IV

The theoretical average downwash angle at the horizontal tailplane behind a wing with running propellers

It is assumed that the average downwash angle at the tail of a multi-engined propeller aircraft is determined by the combined effects of lift due to wing angle-of-attack and due to slipstream.

As before, the lift of a wing with slipstream is considered to be equivalent to the sum of the vertical components of the outgoing momentum of a stream tube determined by the wing span and of the stream tubes determined by the fully contracted propeller slipstream.

The cross-sectional area of the basic wing lift stream tube is then devided in a central part with area A^* determined by the outer edges of the two inboard fully contracted slipstream diameters and the two outerparts with total cross-sectional area 2A.

These area's can be written as

$$2A = 2\left[\frac{\varphi}{2}\,\frac{b_w^2}{4} - \frac{b_w}{2}\cos\varphi \times J\right]$$

or

$$2A = 2\,\frac{b_w^2}{4}\left[\frac{\varphi}{2} - \cos\varphi\left[Y_{s_o} + D^*/2\right]\right]$$

then

$$A = \varphi \times \frac{b_w^2}{4} - \frac{b_w}{2}\cos\varphi\;\frac{Y_{s_o}+D^*/2}{b_w/2}$$

or

$$A = \frac{b_w^2}{4}\left[\varphi - \sin\varphi\cos\varphi\right]$$

and

$$\varphi = \arccos\frac{Y_{s_o}+D^*/2}{b_w/2}$$

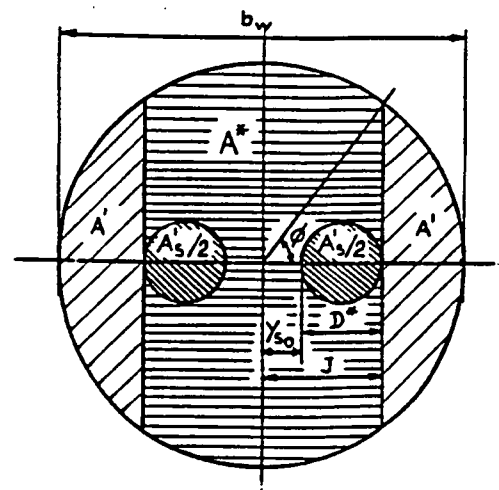

Figure IV a

The slipstream cross sectional area is: $A_S' = n_e\frac{\pi}{4}D^{*2} = 2\times\frac{\pi}{4}D^{*2}$

Then: $A^* = \frac{\pi}{4}b_w^2 - \frac{b_w^2}{4}(\varphi - \sin\varphi\cos\varphi) - \frac{\pi}{2}D^{*2}$

It is now assumed that the mutual interference between slipstream and outer flow results in the same average downwash angle for both slipstream and the central part of the outer flow with area A^* determined by the addition of both the vertical components of the outgoing momentum and of the mass flow of the three stream tubes with cross sectional area's A^* and $A_{.S}$.
So,

$$\sin\varepsilon' = \frac{\rho V_O^2 A^*\sin\varepsilon + \rho\,(V_o+\Delta V)^2 A_s'\sin\varepsilon_s}{\rho V_O^2 A^* + \rho\,(V_o+\Delta V)^2 A_S'}$$

For the configuration from report NASA TN D-25 (ref. 36) with flaps deflected to 60 deg and ailerons to 30 deg the average downwash angle ε' was determined for both power-off conditions and for C_T = 2.15. With

$D^*/2 = 0.60$ m , $b_w/2 = 6.86$ m , $Y_{so} = 3.09$ m, then $\phi = 57.46$ deg.
ϕ
The lift was calculated according to the method described in the main body of this paper. This lead to the following results:

	$C_T = 0$	$C_T = 2.35$
$\alpha_R = 0$	: $C_L = 2.75$; $\varepsilon = 10.2$ deg	$C_L = 4.81$; $\varepsilon' = 16.0$ deg
$\alpha_R = 8$ deg	: $C_L = 3.35$; $\varepsilon = 12.5$ deg	$C_L = 5.58$; $\varepsilon' = 18.9$ deg

In fig. 30 a comparison is shown between calculated and actual test data.
The assumption that slipstream and outer flow have identical average downwash angles seems to hold.

Note that the decrease in average downwash at the horizontal tail location which occurs when the tail is moved further away from the wing-wake/slipstream centre line remains. This account for the difference in actual downwash angle obtained from theory and windtunnel tests.

Appendix V

NOTES

1. When the direct thrust contribution to the pitching moment ΔC_{D_T} is considered not the thrust coefficient C_T but the effective thrust coefficient $C_{T_{eff}}$ has to be taken. $C_{T_{eff}}$ is defined as

   $C_{T_{eff}} = C_T - \Delta C_T$ where ΔC_T is a measure for the increase in wing drag due to slipstream. On the basis of the data presented in refs. 33-37 and under the assumption that $\Delta C_T = \Delta C_D$ due to slipstream figure Va was prepared.

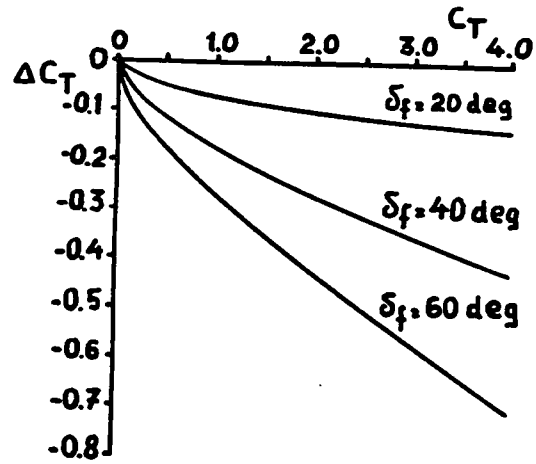

Figure Va

2. When figures 42 and 43 were prepared it was noticed that better agreement between calculated and test data was obtained when the pitching moment contribution from the fuselage due to the upwash in front of the wing was extended to the increase in lift due to slipstream. Then, at a given angle-of-attack the following pitching moment contribution has to be added to the pitching moment calculated with the formulae given in the main part of this paper:

$$\Delta C_M = \Delta C_{L_a} \times \Delta \frac{X_{ac.fus}}{\bar{c}}$$

where $\Delta \frac{X_{ac.fus}}{\bar{c}}$ is the forward shift in aerodynamic centre due to the presence of the fuselage.

This subject is analysed in more detail in Appendix XV.

Appendix VI

Geometric characteristics

Table I contains all geometry data of the various aircraft configurations analysed as required for the calculation of lift, pitching moment, downwash and dynamic pressure at the tail.

On pages VIII-4 to VIII-17 plan vieuws or three-vieuw drawings are presented of all configurations analysed.

Table I Geometric Characteristics

No	Conf.	ref.	b_w	S_w	A_w	C_s	δ_f (deg)	C_f/C	C'/C	no of props	D_{prop}	$\frac{\pi}{4} b_w^2$	$n_e \frac{\pi}{4} D_{prop}^2$	ι_{C_s} (deg)	α_o (deg)	$\frac{C_{l\delta}}{C_{l\alpha}}$	$\Delta\alpha_{\delta_f}$ (deg)	$\frac{F}{T}$	di-mensions
			①	②	③	④	⑤	⑥	⑦	⑧	⑨	⑩	⑪	⑫	⑬	⑭	⑮	⑯	⑰
1	NASA TN D-25	36	13.72	19.09	9.86	1.62	0	—	—	4	1.454	147.84	6.65	7.5	-1.0	—	0	1.00	m
							40	0.250	1.00	4						0.52	-20.8	0.99	"
							40/30	0.250	1.00	4						0.52	-20.8	0.99	"
							60/50	0.250	1.00	4	1.454	147.84	6.65	7.5	-1.0	0.52	-31.2	0.98	m
2	NASA Memo 12-3-58A	35	13.72	19.09	9.86	1.62	0	—	—	2	2.057	147.84	6.64	7.5	-1.0	—	0	1.00	m
							20	0.250	1.00	2	2.057	147.84	6.64	7.5	-1.0	0.52	-10.4	0.99	m
3	NACA TN 4365	34	13.72	19.09	9.86	1.62	40	0.250	1.00	2	2.057	147.84	6.64	7.5	-1.0	0.52	-20.8	0.95	m
							40/30	0.250	1.00	2	2.057	147.84	6.64	7.5	-1.0	0.52	-20.8	0.95	m
							60/50	0.250	1.00	2	2.057	147.84	6.64	7.5	-1.0	0.52	-31.2	0.92	m
4	ARC R&M No 2747	16	100	996.5	10	11.07	0	—	—	4	10.0	7854	314.2	0	-0.9	—	0	1.00	in
5	NACA TN 3304	—	6.832	10.250	4.55	1.568	0	—	—	2	2.00	36.659	6.28	0	0	—	0	1.00	ft
6	NASA TN D-3938	21	2.130	0.840	5.42	0.394	0	—	—	2	0.610	3.563	0.584	0	-4.0	—	0	1.00	m
							45	0.481	1.314	2	0.610	3.563	0.584	0	-4.0	0.66	-29.7	0.95	m
7	NASA TN D-4448	22	42.94	352.8	6.52	7.40	0	—	—	4	9.30	1805	271.7	0	-2.5	—	0	1.00	ft
							40	0.383	1.095	4	9.30	1805	271.7	0	-2.5	(0.57)	-18.0	0.97	ft
8	NASA TN D-6393	23	43.34	329.0	5.71	7.80	0	—	—	2	9.30	1475.3	135.8	0	-2.5	—	0	1.00	ft
9	NAE Rep. LR-501	—	84.70	1520	4.72	18.0	0	—	—	2	24.0	5634.5	904.8	0	-4.0	—	0	1.00	in
							30	0.30	1.00	2	24.0	5634.5	904.8	0	-4.0	0.59	-17.2	0.89	in
10	NLR TR 77081C	—	2.100	0.630	7.00	0.300	0	—	—	4	0.200	3.464	0.127	0	-5.5	—	0	1.00	m
							30	0.250	1.25	4	0.200	3.464	0.127	0	-5.5	0.44	-13.2	0.97	m
11	Fokker F-27	—	1.933	0.3111	12.0	0.180	40	0.30	1.12	2	0.244	2.935	0.0935	3.4	-3.0	0.56	-22.4	0.95	m
						(11)	70	0.33	1.15	2	0.244	2.935	0.0935	3.4	-3.0	0.56	-30.0	0.92	m
12	Fokker F-27 (Fokker 50)	—	29.00	70.00	12.0	2.80	0	—	—	2	3.81	660.52	22.80	3.5	-2.7	—	0	1.00	m
						(11.7)	16.5	0.32	1.04	2	3.81	660.52	22.80	3.5	-2.7	0.56	-7.7	1.00	m
						(12.1)	26.5	0.32	1.08	2	3.81	660.52	22.80	3.5	-2.7	0.56	-12.4	0.98	m
						(12)	40	0.32	1.12	2	3.81	660.52	22.80	3.5	-2.7	0.56	-17.9	0.97	m
13	C-160 Transall	—	2.105	0.4435	10.0	0.254	0	—	—	2	0.289	3.480	0.131	2.0	-1.0	—	0	1.00	m
							30	0.33	1.08	2	0.289	3.480	0.131	2.0	-1.0	0.56	-16.8	0.98	m
							60	0.33	1.15	2	0.289	3.480	0.131	2.0	-1.0	0.56	-33.6	0.92	m
14	Breguet Atlantique	—	38.00	120.00	12.0	4.00	50	0.33	1.18	2	4.88	1137.7	37.4	3.0	-3.0	0.57	-28.5	0.93	m

Table I Geometric Characteristics (Concluded)

No	Conf.	ref.	b_w	S_w	A_w	C_s	δ_f (deg)	C_f/C	C'/C	no of props	D_{prop}	$\frac{\pi}{4} b_w^2$	$n_e \frac{\pi}{4} D_{prop}^2$	i_{c_s} (deg)	α_0 (deg)	$\frac{C_{l_\delta}}{C_{l_\alpha}}$	$\Delta\alpha_{\delta_f}$ (deg)	$\frac{F}{T}$	dimensions
			(1)	(2)	(3)	(4)	(5)	(6)	(7)	(8)	(9)	(10)	(11)	(12)	(13)	(14)	(15)	(16)	(17)
15	ARC R&M No 2310	–	72.0	767.5	6.75	12.8	0	0	–	2	12.0	4072.5	226.2	0	-1.7	0	0	1.00	in in
16	DHC-5 Caribou	47	29.15	84.72	10.03	3.55	0	0	–	2	3.99	667.3	24.99	3.0	-3.0	0	0	1.00	m m

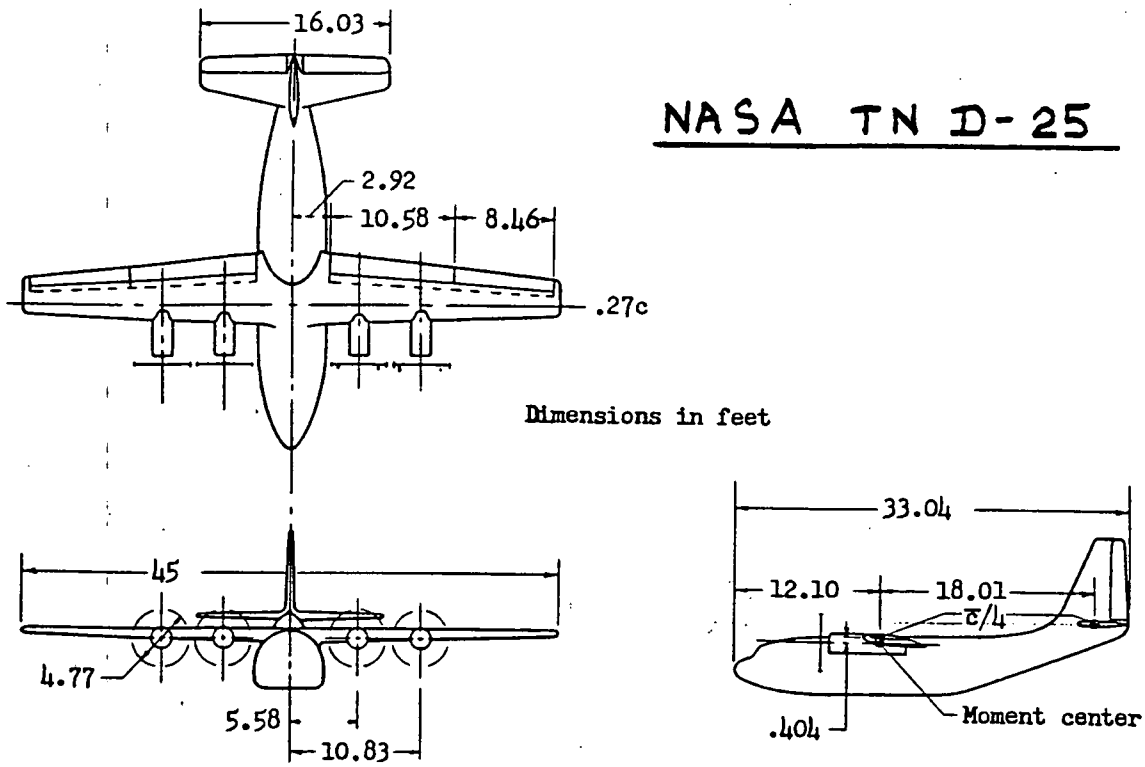

NASA TN D-25

Dimensions in feet

Geometry of the model.

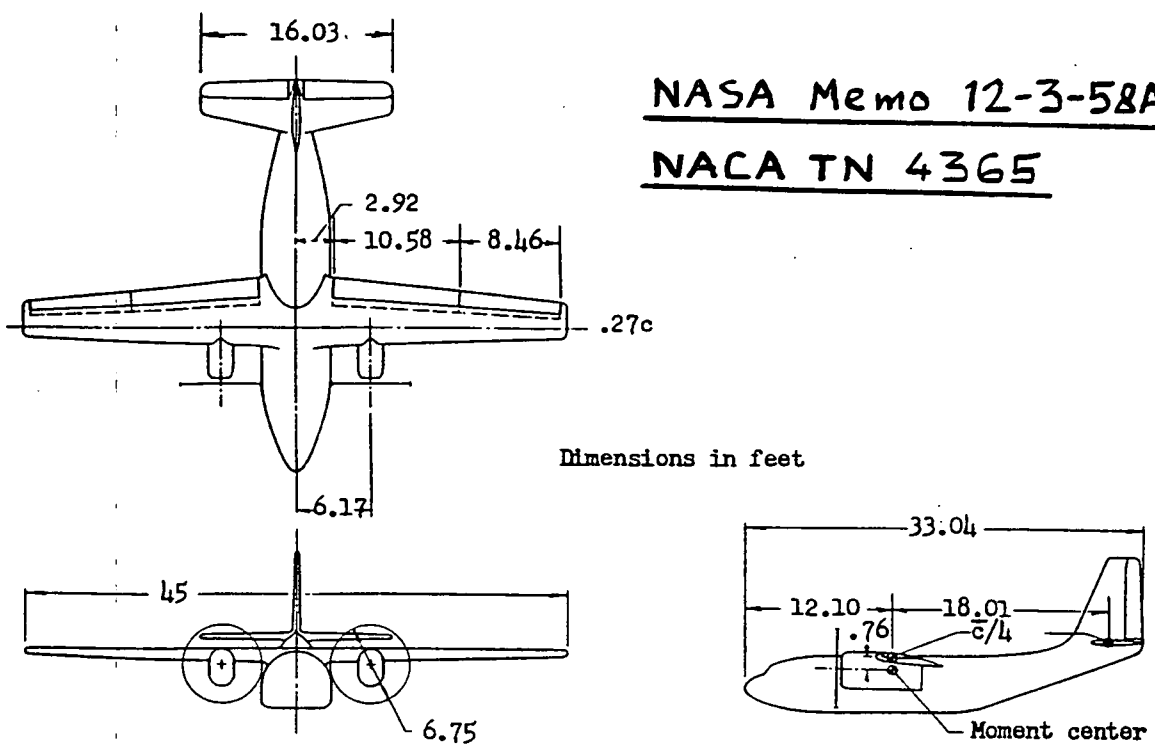

NASA Memo 12-3-58A

NACA TN 4365

Dimensions in feet

- Geometry of the model.

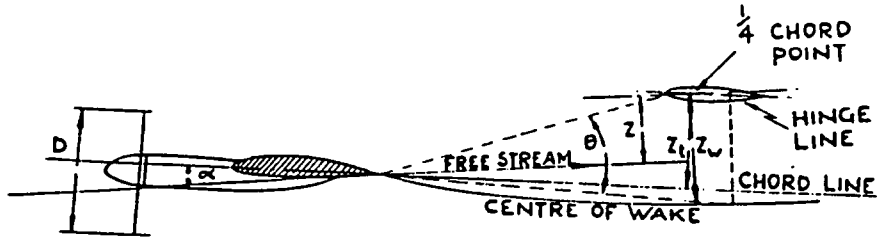

Notation.

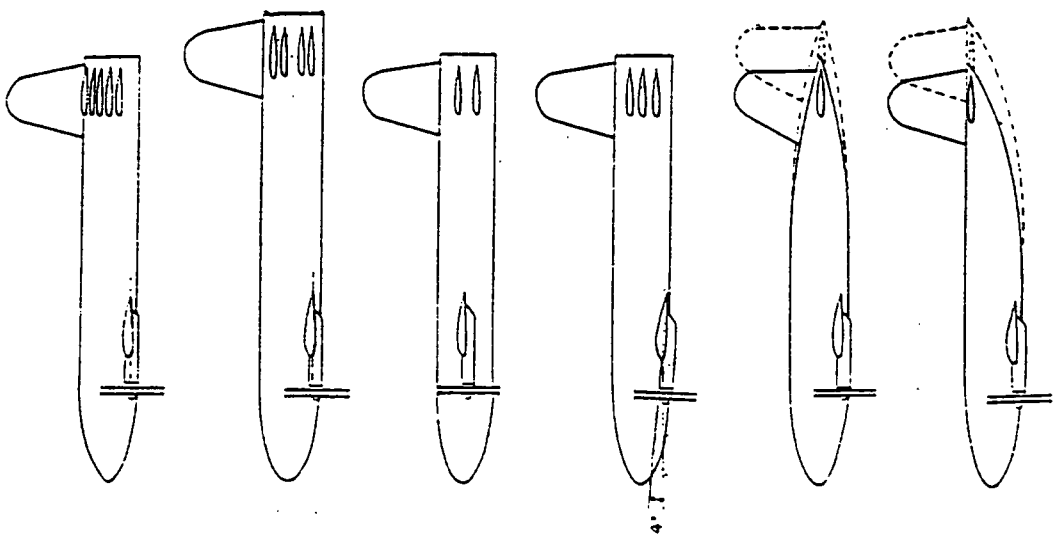

Wing-body arrangements and tailplane heights. Flaps up.

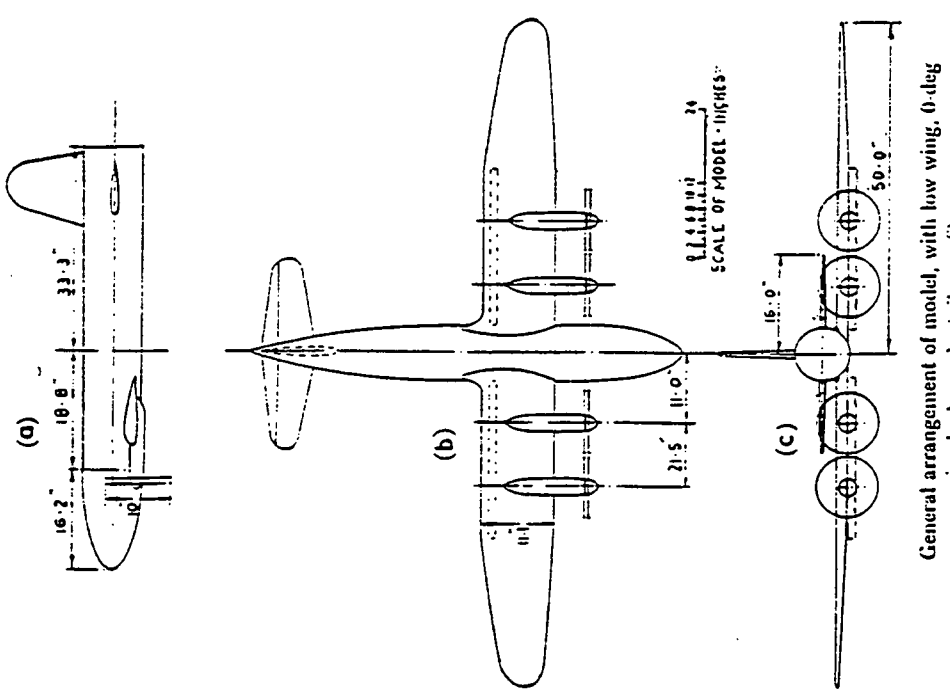

General arrangement of model, with low wing, 0-deg wing-body angle, tail arm (l).

ARC R & M No 2747

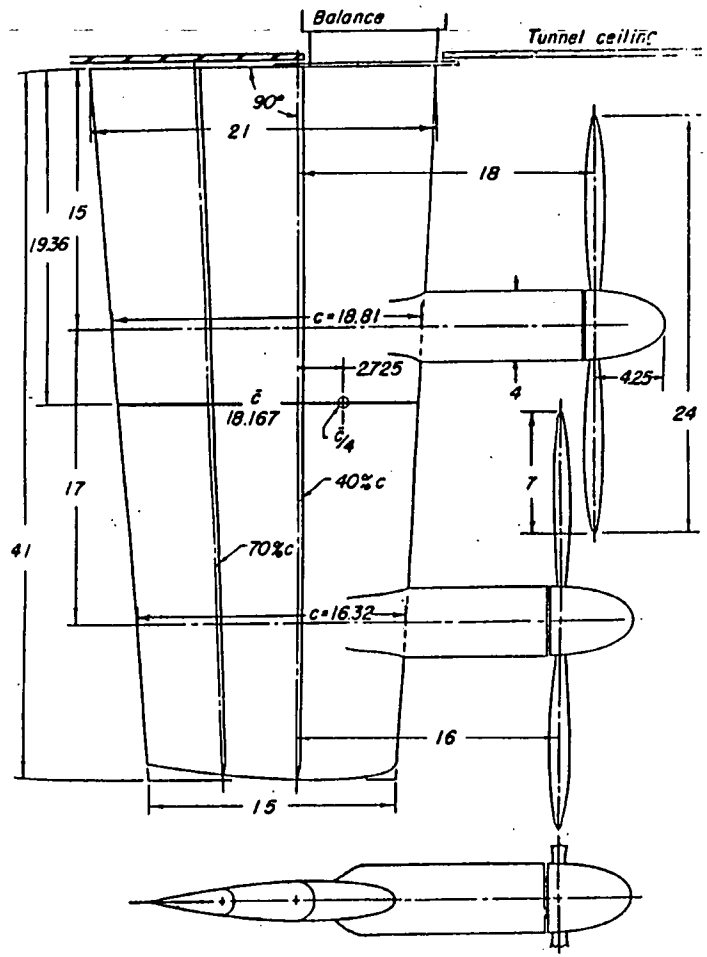

Plan and cross-sectional views of model. (All dimensions in inches.)

NAE Rep. LR-501

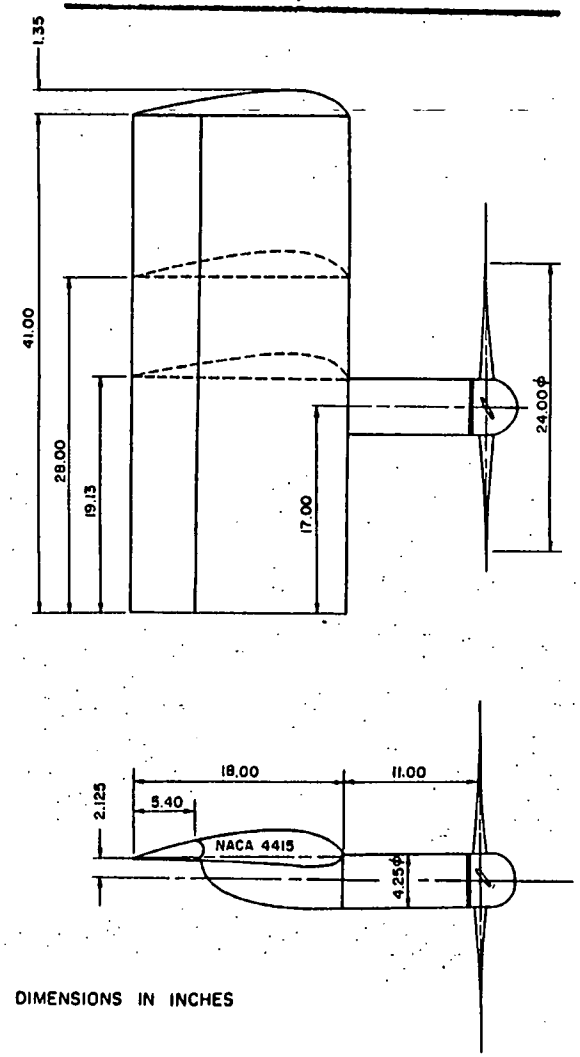

ALL DIMENSIONS IN INCHES

PLAN AND CROSS-SECTIONAL VIEW OF MODEL

NASA TN D-3438

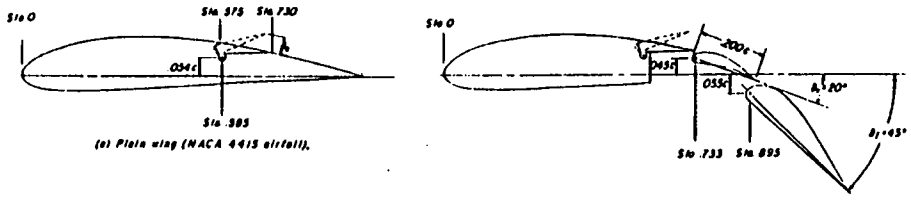

(a) Plain wing (NACA 4415 airfoil).

(c) Flap deflected 45°.

Wing:			
Airfoil section			NACA 4415
Chord, ft (m)			1.29 (.39)
Area, ft² (m²)			9.04 (.84)
Span, ft (m)			7.00 (2.13)
Aspect ratio			5.42
Horizontal tail		**Large tail**	**Small tail**
Area, ft² (m²)		3.86 (.36)	2.88 (.27)
Span, ft (m)		3.48 (1.06)	3.00 (.91)
Chord, ft (m)		1.11 (.34)	.96 (.29)
Aspect ratio		3.13	3.13
l_t/wing chord	High position	2.70	2.67
	Low position	2.44	2.41
h_t/wing chord	High position	.94	.94
	Low position	.15	.15
Propellers:			
Diameter, ft (m)			2.00 (.61)
Nacelle diameter, ft (m)			.33 (.10)
Number of blades (each)			3

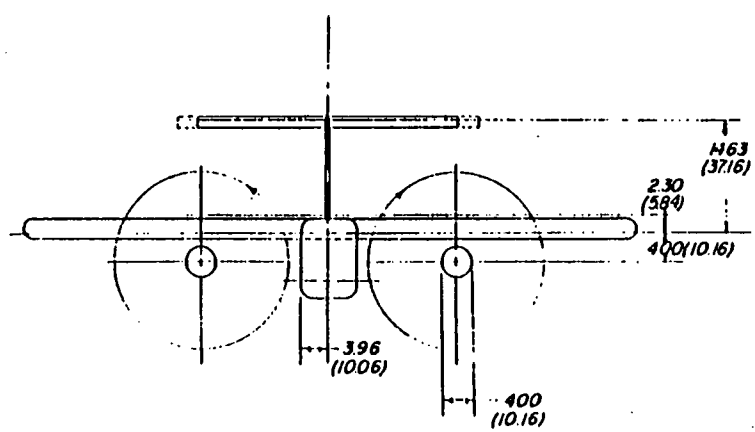

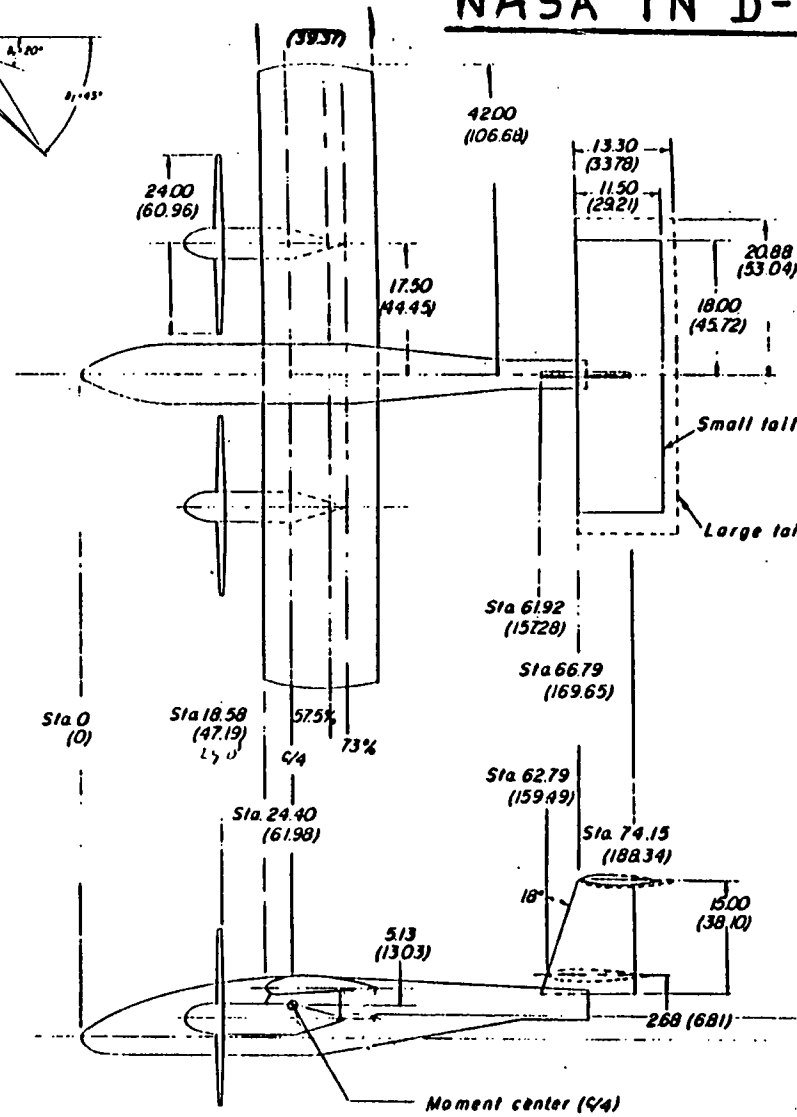

Three-view drawing of 1/5-scale model and table of geometric characteristics. All dimensions are in inches (centimeters) unless otherwise noted.

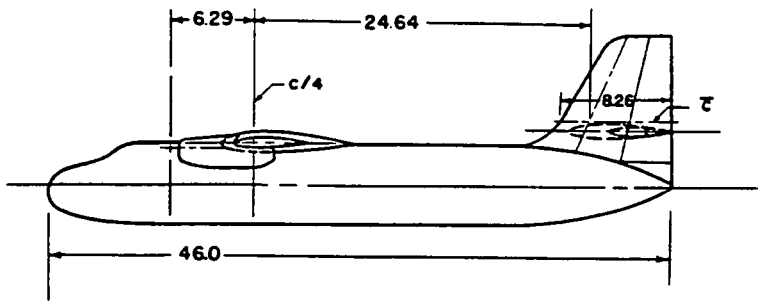

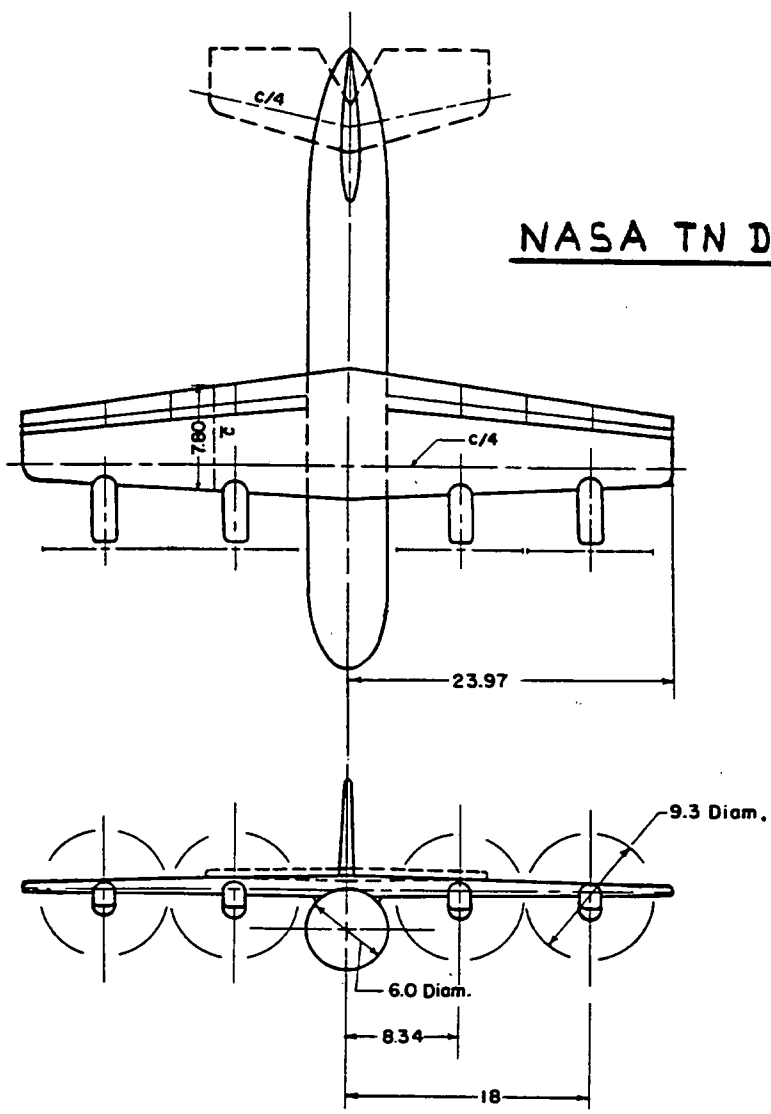

NASA TN D-4448

Three views of model; dimensions in feet.

Model geometry.

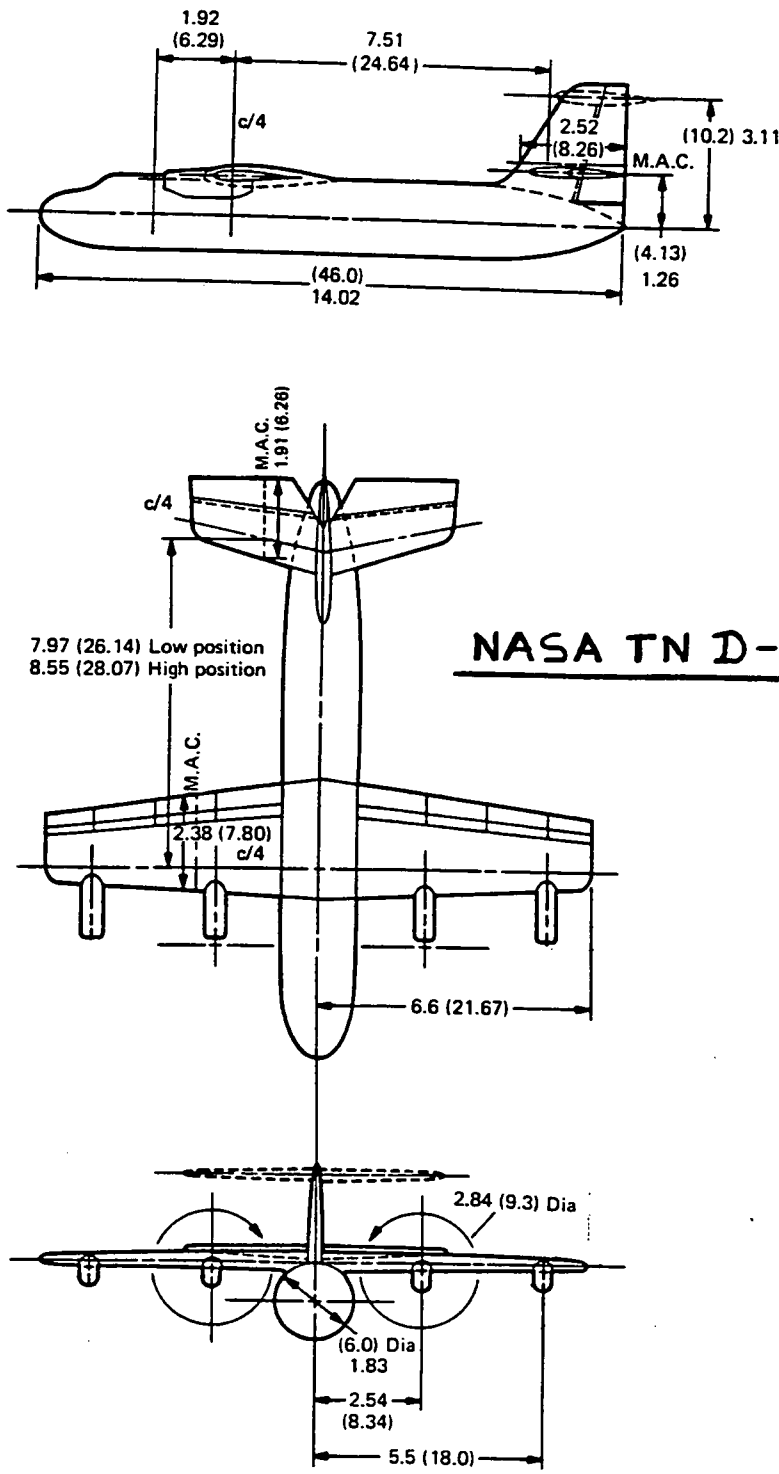

NASA TN D-6393

Three-view drawing; dimensions, m (ft).

Figure 2.- Model geometry.

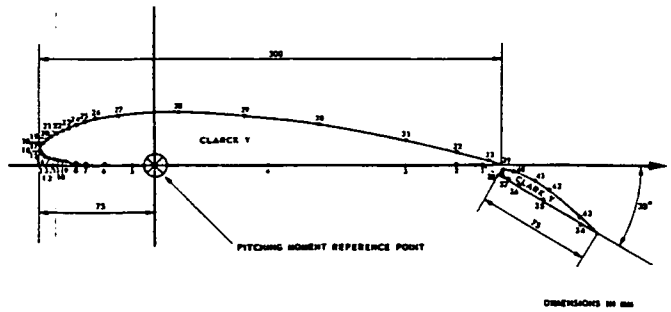

Cross-sectional view of wing-flap combination with indication of pressure hole locations

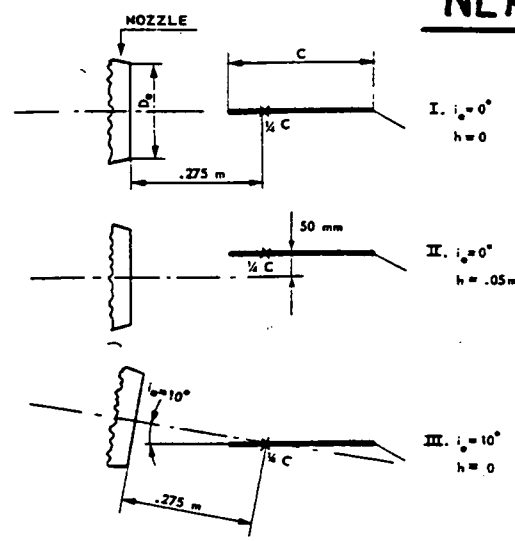

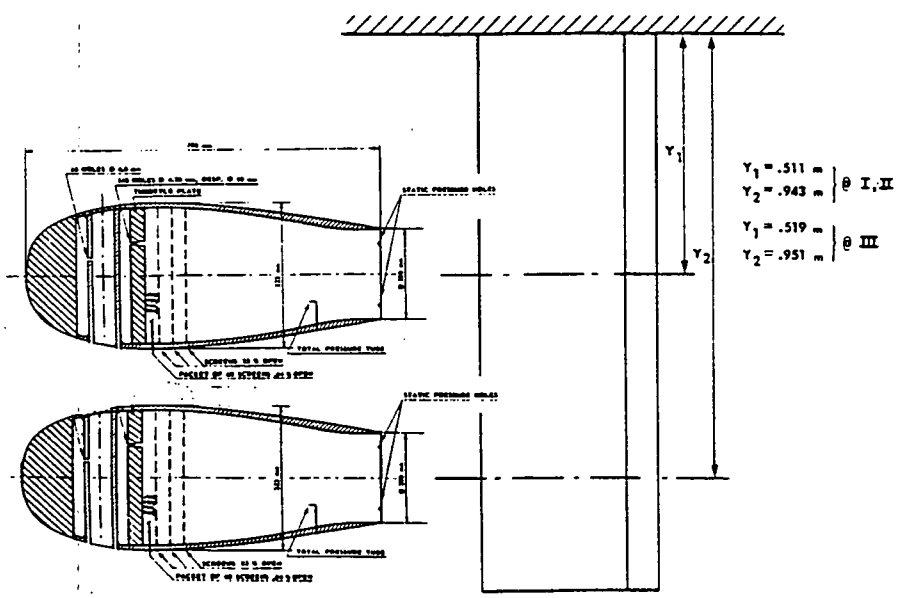

Nacelle positions relative to the wing model

Fokker F-27 Mk 200

Three-viewdrawing of the model with F 3 fuselage (Δ 0).

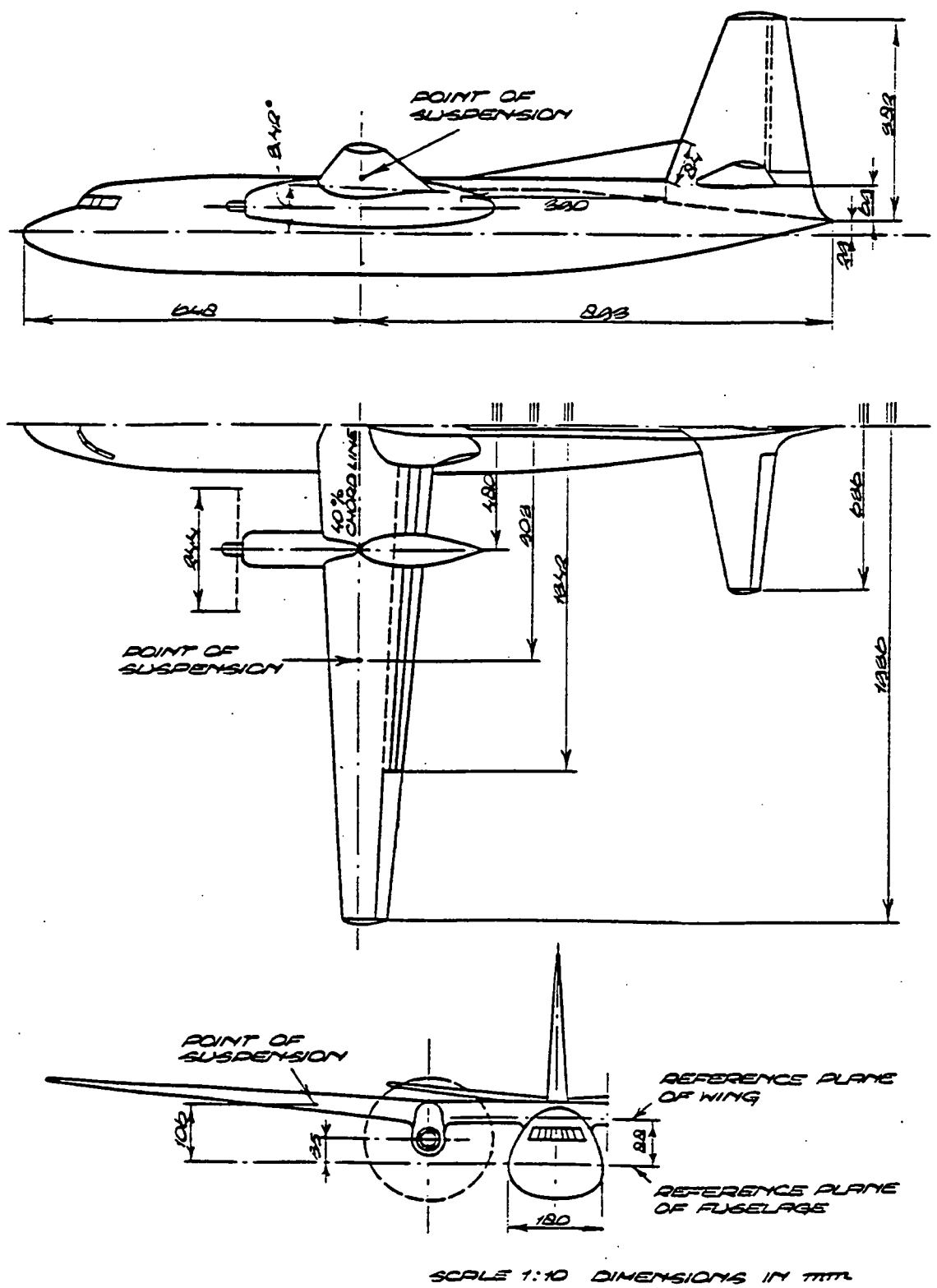

Fokker F-27 development model

Side view of the model with stretched fuselage (Δ 190) and position of the three horizontal tails F 5, h 120 and h 240.

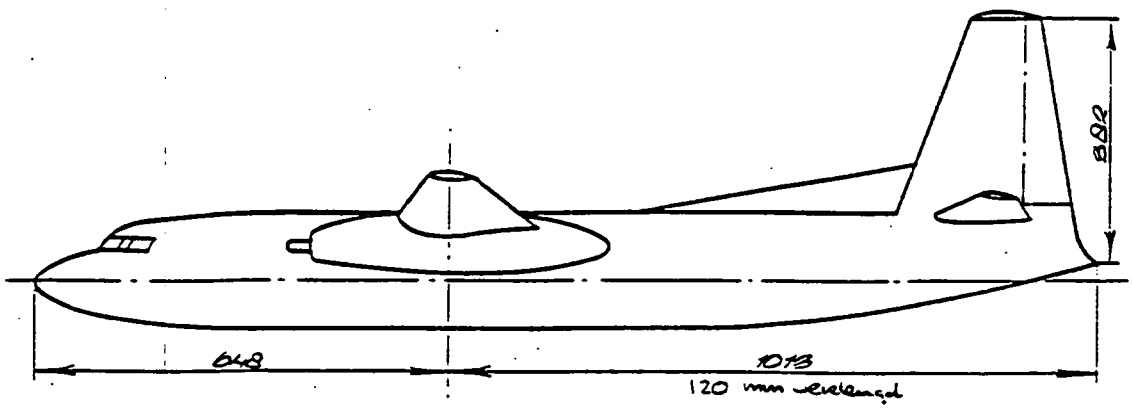

Scale 1:10

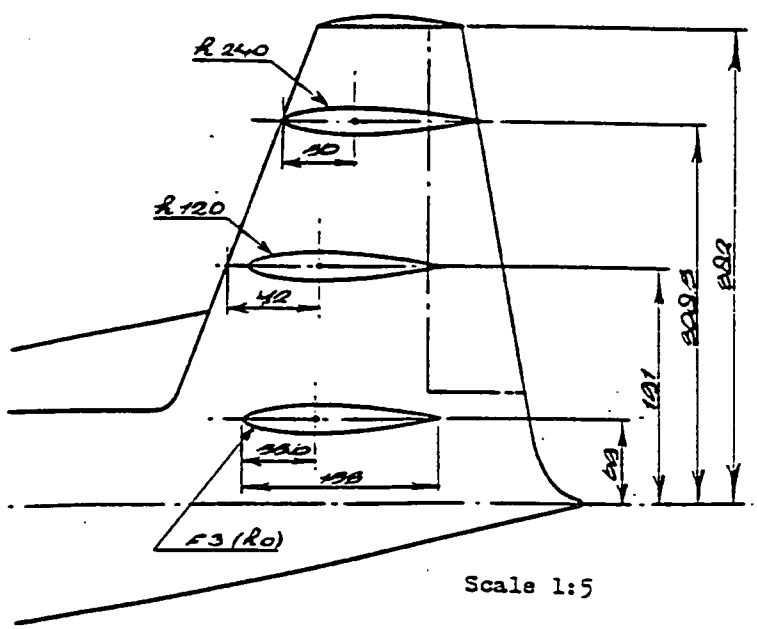

Scale 1:5

Dimensions in mm

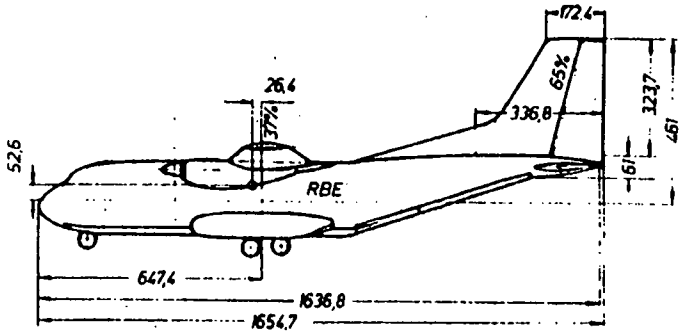

● = Momentenbezugspunkt

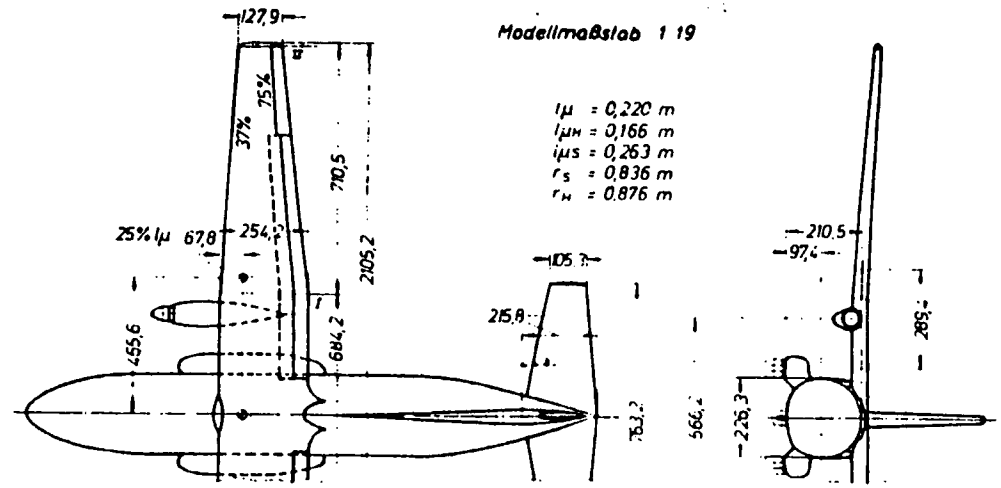

Modellmaßstab 1 19

l_μ = 0,220 m
$l_{\mu H}$ = 0,166 m
$l_{\mu S}$ = 0,263 m
r_S = 0,836 m
r_H = 0,876 m

Messung mit Turbulenzsieb

Symbol	η_K [°]	HLW	c_S	Re·10^6
○	0	ohne	-	0,69
□	30		-	0,69
△	60		-	0,69
●	0		0,2419	0,50
■	30		0,5369	0,37
▲	60	ohne	0,8260	0,43

geometrische Daten:

Flügel
(bis Schnitt I: NACA 63_2A218)
(Schnitt II: NACA 63_2A314)

F = 0,4435 (m^2)
Λ = 10
l_μ = 0,220 (m)
ε_F = 2° (Schnitt I)
ε_F = -1° (Schnitt II)
ν = 3,5° (Trapezteil)

Höhenleitwerk
(NACA 23012, negative Wölbung)

F = 0,1213 (m^2), mit Rumpfanteil
F = 0,1114 (m^2) ohne Rumpfanteil
l_μ = 0,166 (m)
Λ = 4,8
ε_H = -12°

Bericht: Einfluß des Schraubenstrahles auf Abwind und Staudruck am Ort des HLW und auf die HLW-Wirksamkeit der TRANSALL C-160

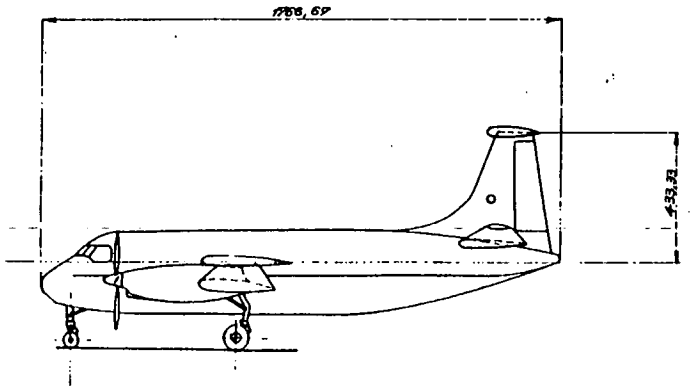

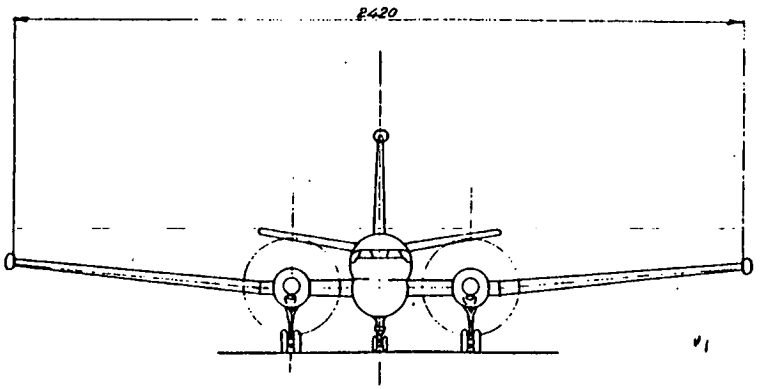

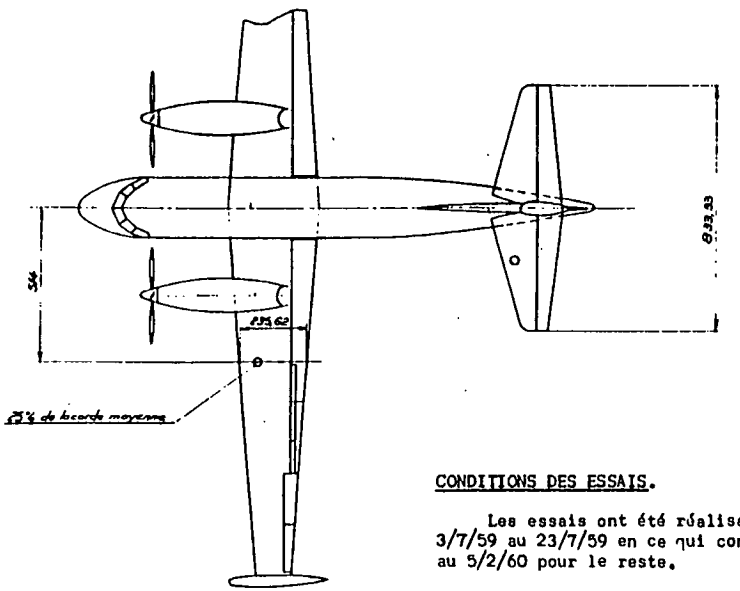

DÉFINITION DES SYMBOLES UTILISÉS POUR LE TRAIN D'ATTERRISSAGE

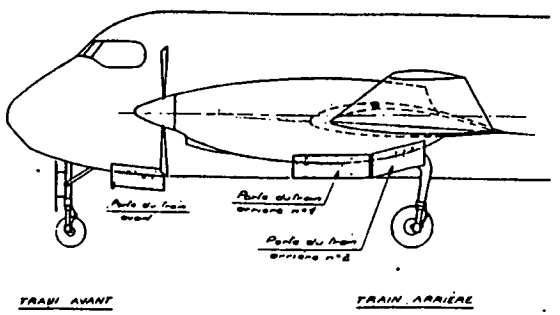

TRAIN AVANT

TRAIN ARRIÈRE

CONDITIONS DES ESSAIS.

Les essais ont été réalisés à la soufflerie BREGUET de Vélizy du 3/7/59 au 23/7/59 en ce qui concerne la première partie et du 16/12/59 au 5/2/60 pour le reste.

La première partie des essais a été faite sur balance à mât central 5 composantes (strain-gages) du type Lilienthal. Centrage de la maquette X = 25,7 % Z = 9,35 % au-dessus du BA de la corde du plan central. En ce qui concerne la deuxième partie des essais une balance 2 mâts à 5 composantes (strain-gages) du type Eiffel a été spécialement conçu.

Centrage de la maquette : X = 25 % Z = 11 % au-dessus du BA de la corde du plan central.

ATELIERS D'AVIATION LOUIS BREGUET

BREGUET 1150

ENSEMBLE 3 VUES

LE 14.4.59 Ech. 1/15

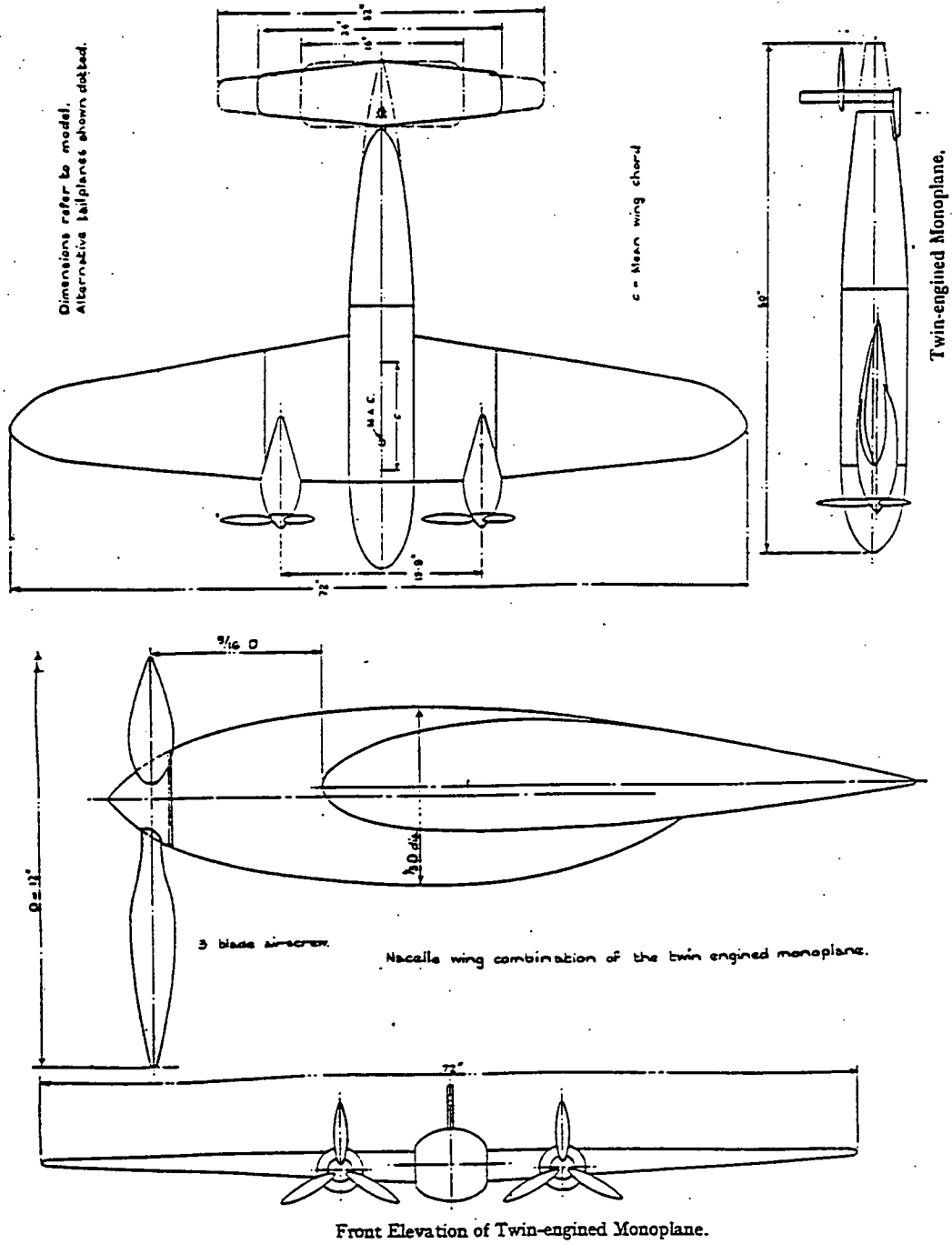

Front Elevation of Twin-engined Monoplane.

Report ARC R & M No 2310

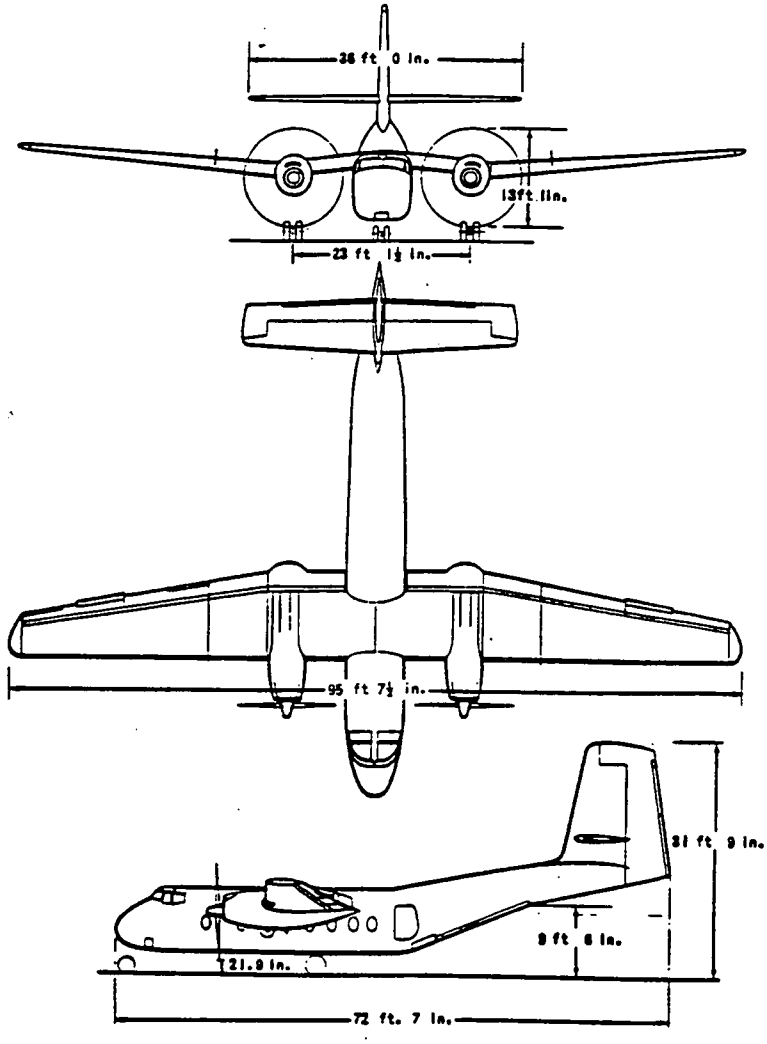

De Havilland DHC-4 Caribou

From: ARC R&M No. 1735

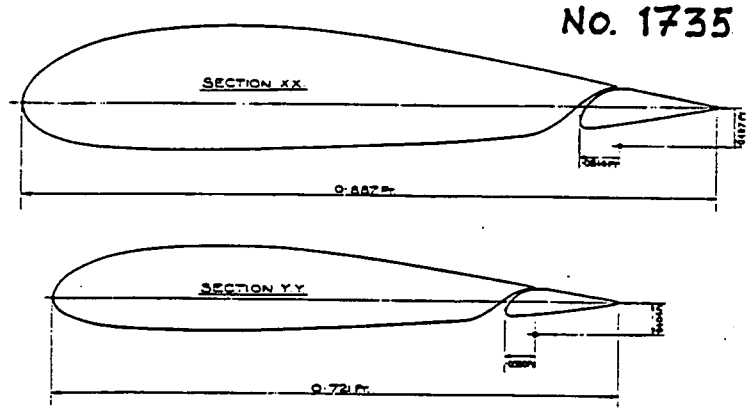

FIG. 2.

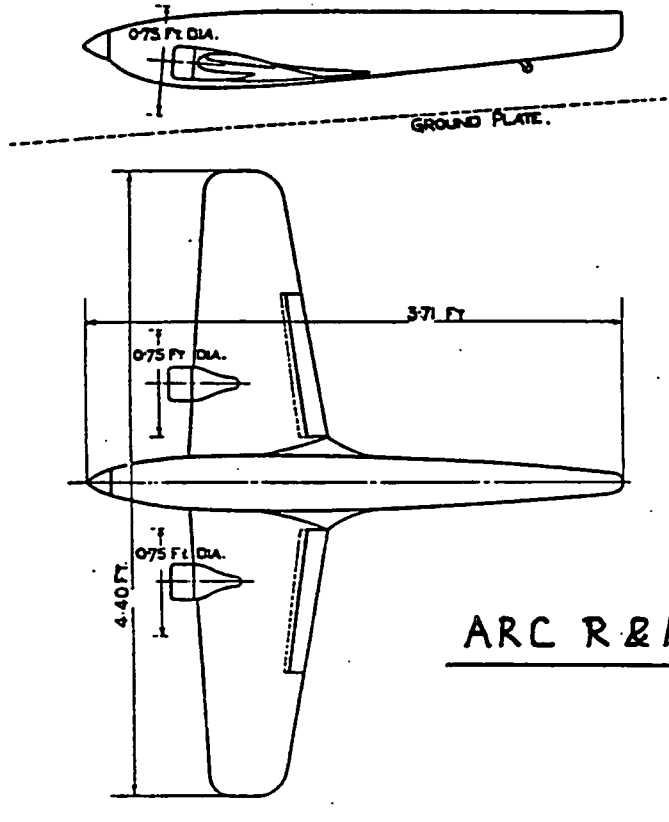

ARC R&M No. 1797

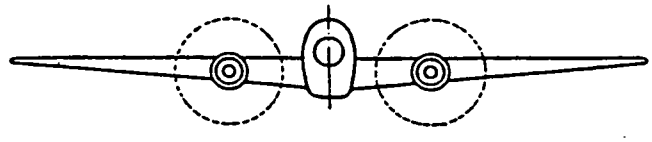

FIG. 1.—Twin-Engined Model.

Appendix VII

Total Propeller Normal-Force Coefficient

The propeller normal force is determined according to the method presented in the USAF Datcom and in ref. 24.

In the present analysis non-linear effects due to cos $\alpha = 1$ and sin $\alpha = \alpha$ are neglected.

Thus, the total propeller normal-force coefficient is:

$$C_{L_p} = K \times C'_{N_{\alpha_{in}}} \left[\frac{d\alpha_{in}}{d\alpha} \left(\alpha_R - \alpha_{C_L=0} \right) + \alpha_{C_L=0} + i_{prop} \right] \frac{n_e \frac{\pi}{4} D^2_{prop}}{S_w} \frac{1}{57.3} \tag{37}$$

where:

$$C'_{N_{\alpha_{in}}} = \frac{4.25\sigma_e}{1+2\sigma_e} \sin(\beta+8) \left(1 + \frac{3T'_c}{8\sqrt{1+\frac{2}{3}T'_c}} \right) \text{per rad.} \tag{25}$$

for single-rotation propellers, and

$$C_{N_{\alpha_{in}}} = \frac{3.86\sigma_e}{1+\sigma_e} \sin(\beta+14) \left(1 + \frac{3T'_c}{8\sqrt{1+\frac{2}{3}T'_c}} \right) \text{per rad.}$$

for counter-rotating propellers.

Furthermore:

The local angle-of-attack gradient is:

$$\frac{d\alpha_{in}}{d\alpha} = 1 + \frac{2A_W}{9A_W+10} \left(\frac{\frac{1}{X_{L.75}}}{c_r} + \frac{1}{10} + \frac{\frac{1}{X_{R.75}}}{c_r} \frac{1}{10} \right) + \frac{1}{2} \left[\left(\frac{R_{fus}}{Y_{L.75}} \right)^2 + \left(\frac{R_{fus}}{Y_{R.75}} \right)^2 \right] \tag{35}$$

$$\alpha_{prop} = \frac{d\alpha_{in}}{d\alpha} \left(\alpha_R - \alpha_{C_{L=0}} \right) + \alpha_{C_{L=0}} + i_{prop} \tag{36}$$

Notation

C'_N normal-force coefficient based on free-stream velocity and propeller disk area, $\frac{N}{q_\infty S_p}$

i_{prop} angle between propeller thrustline and fuselage reference line

c_r	wing root chord, ft
D	propeller diameter, ft
N	propeller normal force, lb
n_e	number of propellers
q_∞	free-stream dynamic pressure, lb/sq ft
R	propeller radius, ft
R_{fus}	maximum fuselage radius forward of propeller plane
r	radial distance to blade element, ft
S_p	propeller disk area, $\frac{\pi}{4}D^2$, sq ft
T	propeller thrust, lb
T_C'	thrust coefficient based on free-stream velocity and propeller disk area $\frac{T}{q_\infty S_p}$
x	longitudinal coordinate measured positive forward from wing leading edge, ft
y	lateral coordinate measured positive to right of plane of symmetry, ft.
Δ_y	lateral distance from thrust axis of one propeller blade to element of another, ft
α	wing angle of attack measured from zero lift, deg
α_{in}	inflow angle at propeller disk, deg
β	blade angle at .75R blade station, deg
σ	propeller solidity, ratio of blade element area to annulus area at .75R
σ_e	effective propeller solidity (propeller solidity based on average blade chord)

Subscripts

α_{in}	differentiation with respect to inflow angle, α_{in}
$L_{.75}$	left blade position at three-quarters radius point
$R_{.75}$	right blade position at three-quarters radius point
fus	fuselage

$$K = \frac{C'_N(\alpha, J\cos\alpha)}{C'_{N_\alpha}(\alpha_O, J\cos\alpha)\times(\alpha_R - \alpha_{C_L=0})}$$

For all configurations considered in the present report it has been assumed that K = 1 (α_{prop} < 30 deg).

The actual values of the various parameters can be found in the columns in the tables with the encircled number (XY).

C_{Lp}	(37)	T'_C	(24)
$C'_{N_{\alpha_{in}}}$	(25)	A_W	(3)
$\frac{d\alpha_{in}}{d\alpha}$	(35)	$\frac{X_L}{C_r} = \frac{X_{in}}{C_r}$	(27) (29)
α_R	(19)	$\frac{X_R}{C_r} = \frac{X_{out}}{C_r}$	(28) (30)
$\alpha_{C_L=0}$	(18)	$\frac{R_{fus}}{y_L} = \frac{R_{fus}}{y_{in}}$	(31) (33)
i_{prop}	(20)	$\frac{R_{fus}}{y_R} = \frac{R_{fus}}{y_{out}}$	(32) (34)
N_e	(8)	α_{prop}	(36)
D_{prop}	(9)		
S_W	(2)		
σ_e	(22)		
β	(23)		

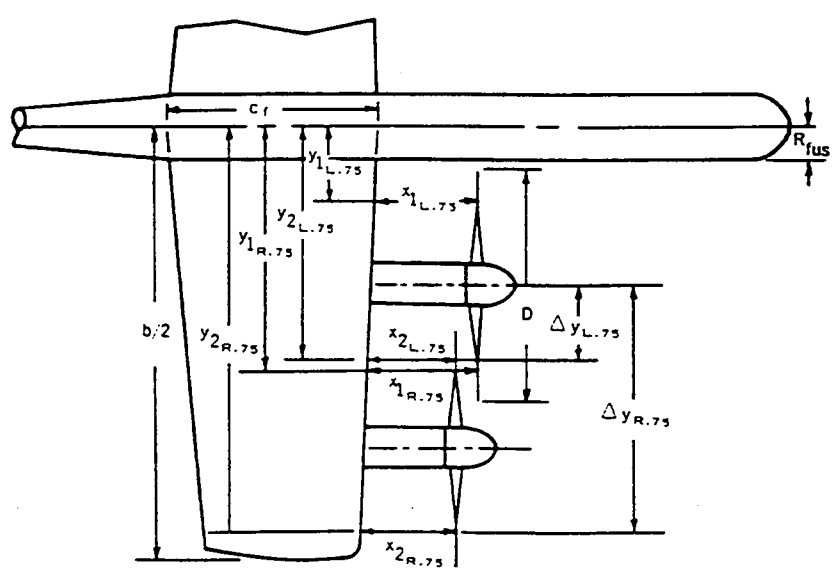

Table II Total Propeller Normal Force Coefficient C_{LP}

No	Conf.	ref.	S_w	A_w	δ_f (deg)	$\alpha_{C_{LT}=0}$ (deg)	α_R (deg)	i_{prop} (deg)	no of props	D_{prop}	no of blades	σ_e	$\beta_{0.7}$ (deg)	$T_c' = \frac{T}{\rho n^2 D^4}$	$C_{N^i_{K_{in}}}$	C_T
			(2)	(3)	(5)	(18)	(19)	(20)	(8)	(9)	(21)	(22)	(23)	(24)	(25)	(26)
1	NASA TN D-25	36	19.09	9.86	0	-7.0	-8.0	0	4	1.454	3	0.107	22	0.431	0.214	0.15
							0									
							8.0									
					0		12.0	0	4	1.454	3	0.107	22	0.431	0.214	0.15
					0		-8.0	0	4	1.454	3	0.107	22	2.153	0.285	0.75
							0									
							8.0									
					0		12.0	0	4	1.454	3	0.107	22	2.153	0.285	0.75
					0		-8.0	0	4	1.454	3	0.107	22	3.301	0.317	1.15
							0									
							8.0									
					0		12.0	0	4	1.454	3	0.107	22	3.301	0.317	1.15
					0		-8.0	0	4	1.454	3	0.107	22	4.450	0.344	1.55
							0									
							8.0									
					0		12.0	0	4	1.454	3	0.107	22	4.450	0.344	1.55
					0		-8.0	0	4	1.454	3	0.107	22	6.172	0.379	2.15
							0									
							8.0									
					0		12.0	0	4	1.454	3	0.107	22	6.172	0.379	2.15
					0		-8.0	0	4	1.454	3	0.107	22	11.720	0.466	4.10
							0									
							8.0									
			19.09	9.86	0	-7.0	12.0	0	4	1.454	3	0.107	22	11.720	0.466	4.10
1	NASA TN D-25	36	19.09	9.86	40	-12.5	-8.0	0	4	1.454	3	0.107	22	0.431	0.214	0.15
							0									
							8.0									
					40		12.0	0	4	1.454	3	0.107	22	0.431	0.214	0.15
														153	0.285	0.75
														153	0.285	0.75
					40		-8.0	0	4	1.454	3	0.107	22	3.301	0.317	1.15
							0									
							8.0									
			19.09	9.86	40	-12.5	12.0	0	4	1.454	3	0.107	22	3.301	0.317	1.15

Example of calculating procedure

Table II Total Propeller Normal Force Coefficient (Concluded)

No	Conf	$\frac{x_{in}}{c_R}$ Inboard Eng.	$\frac{x_{out}}{c_R}$ Inboard Eng.	$\frac{x_{in}}{c_R}$ Outboard Engine	$\frac{x_{out}}{c_R}$ Outboard Engine	$\frac{R_f}{y_{in}}$ Inboard Engine	$\frac{R_f}{y_{out}}$ Inboard Engine	$\frac{R_f}{y_{in}}$ Outboard Engine	$\frac{R_f}{y_{out}}$ Outboard Engine	$\frac{d\alpha_{in}}{d\alpha}$	α_{prop} (deg)	C_{L_p}	C_T	α_R (deg)	δ_f (deg)
		(27)	(28)	(29)	(30)	(31)	(32)	(33)	(34)	(35)	(36)	(37)	(26)	(19)	(5)
1	NASA TN D-25	0.59	0.61	0.61	0.63	0.71	0.38	0.32	0.23	Inboard: 1.633	-8.5	-0.0111	0.15	-8.0	0
										Outboard: 1.309	3.3	0.0043		0	
		0.59	0.61	0.61	0.63	0.71	0.38	0.32	0.23	Average: 1.471	15.1	0.0197		8.0	
											20.9	0.0273	0.15	12.0	
		0.59	0.61	0.61	0.63	0.71	0.38	0.32	0.23	1.471	-8.5	-0.0147	0.75	-8.0	
											3.3	0.0057		0	
											15.1	0.0262		8.0	
		0.59	0.61	0.61	0.63	0.71	0.38	0.32	0.23	1.471	20.9	0.0364	0.75	12.0	
		0.59	0.61	0.61	0.63	0.71	0.38	0.32	0.23	1.471	-8.5	-0.0164	1.15	-8.0	
											3.3	0.0063		0	
											15.1	0.0292		8.0	
		0.59	0.61	0.61	0.63	0.71	0.38	0.32	0.23	1.471	20.9	0.0404	1.15	12.0	
		0.59	0.61	0.61	0.63	0.71	0.38	0.32	0.23	1.471	-8.5	-0.0178	1.55	-8.0	
											3.3	0.0069		0	
											15.1	0.0317		8.0	
		0.59	0.61	0.61	0.63	0.71	0.38	0.32	0.23	1.471	20.9	0.0439	1.55	12.0	
		0.59	0.61	0.61	0.63	0.71	0.38	0.32	0.23	1.471	-8.5	-0.0196	2.15	-8.0	
											3.3	0.0076		0	
											15.1	0.0349		8.0	
		0.59	0.61	0.61	0.63	0.71	0.38	0.32	0.23	1.471	20.9	0.0484	2.15	12.0	
		0.59	0.61	0.61	0.63	0.71	0.38	0.32	0.23	1.471	-8.5	-0.0241	4.10	-8.0	
											3.3	0.0094		0	
											15.1	0.0429		8.0	
		0.59	0.61	0.61	0.63	0.71	0.38	0.32	0.23	1.471	20.9	0.0595	4.10	12.0	0
1	NASA TN D-25	0.59	0.61	0.61	0.63	0.71	0.38	0.32	0.23	1.471	-5.9	-0.0077	0.15	-8.0	40
											5.9	+0.0077		0	
											17.7	0.0231		8.0	
		0.59	0.61	0.61	0.63	0.71	0.38	0.32	0.23	1.471	23.5	0.0307	0.15	12.0	
		0.59	0.61	0.61	0.63	0.71	0.38	0.32	0.23	1.471	-5.9	-0.0103	0.75	-8.0	
											5.9	+0.0103		0	
											17.7	0.0308		8.0	
		0.59	0.61	0.61	0.63	0.71	0.38	0.32	0.23	1.471	23.5	0.0409	0.75	12.0	
		0.59	0.61	0.61	0.63	0.71	0.38	0.32	0.23	1.471	-5.9	-0.0114	1.15	-8.0	
											5.9	0.0114		0	
											17.7	0.0342		8.0	
		0.59	0.61	0.61	0.63	0.71	0.38	0.32	0.23	1.471	23.5	0.0454	1.15	12.0	40

Appendix VIII

Total tail-off lift coefficient

The following equations were used:

$$C_{L_{TOT}} = C_{L_W} + C_{L_S} + C_{L_T} + C_{L_P} \qquad (57)$$

where:

$$NOTE: \Delta C_{L_S} = C_{L_{TOT}} - C_{L_{P-O}} - C_{L_T} - C_{L_P} \qquad (58) \quad (59)$$

$$C_{L_W} = \frac{2}{S_W}\left(\frac{\pi}{4} b_W^2 - n_e \frac{\pi}{4} D^{*2}\right) \sin\varepsilon \qquad (53)$$

$$C_{L_S} = \frac{F}{T} n_e \frac{\pi}{2} D^{*2} \left(\frac{V_O + \Delta V}{V_O}\right)^2 \frac{1}{S_W} \sin\varepsilon_s \qquad (54)$$

or:

$$C_{L_W} = A \sin\varepsilon \text{ with } A = \frac{2}{S_W}\left(\frac{\pi}{4} b_W^2 - n_e \frac{\pi}{4} D^{*2}\right) \qquad (51)$$

$$C_{L_S} = B \sin\varepsilon_s \text{ with } B = \frac{F}{T} n_e \frac{\pi}{2} D^{*2} \left(\frac{V_O + \Delta V}{V_O}\right)^2 \qquad (52)$$

$$C_{L_T} = C_T \sin\alpha \qquad (55)$$

$$C_{L_P} \qquad (56) \equiv (37)$$

$$\sin\varepsilon = \frac{2 C_L}{\pi A_W} \qquad (50)$$

$$\sin\varepsilon_S = \frac{2 C_{L_{\alpha_{S,eff}}}}{\pi A_{S,eff}} \times 57.3 \times \sin\alpha_S \qquad (49)$$

$$A_{S_{eff}} = A_S + (A_W - A_S)\left(\frac{V_O}{V_O + \Delta V}\right)(A_W - A_S) \qquad (44)$$

$$A_S = \frac{D^*}{C_S} \tag{43}$$

$$\alpha_S = \alpha^* + i_{c_s} - \alpha_o - \Delta\alpha_{o,f}$$

$$\alpha^* = arctg \frac{V_o \sin\alpha}{\frac{\Delta V}{2} + V_o \cos\alpha} \tag{47}$$

$$\frac{\Delta V}{V_o} = \sqrt{1 + C_T \frac{S_W}{n_e \frac{\pi}{4} D^2}} - 1 \tag{40}$$

$$D^* = D \sqrt{\frac{V_o + \Delta V/2}{V_o + \Delta V}} \tag{42}$$

With :

b_w	(1)	$C_{L_{\alpha_s}}$, $C_{L_{\alpha_s,eff}}$	(48)
		$\Delta\alpha_{o,f}$	(15)
S_w	(2)	(From tests or with $\Delta\alpha_{o,f} = \frac{C_{l_\delta}}{C_{l_\alpha}} \times \delta_f$)	(5)/(14)
A_w	(3)		
C_s	(4)		
$D = D_{prop}$	(9)		
$\frac{\pi}{4} b_W^2$	(10)	F/T	(16)
i_{c_s}	(12)	C_T	(26)
α_o	(13)	$C_{L_{p-o}}$	(38)
N_e	(8)		

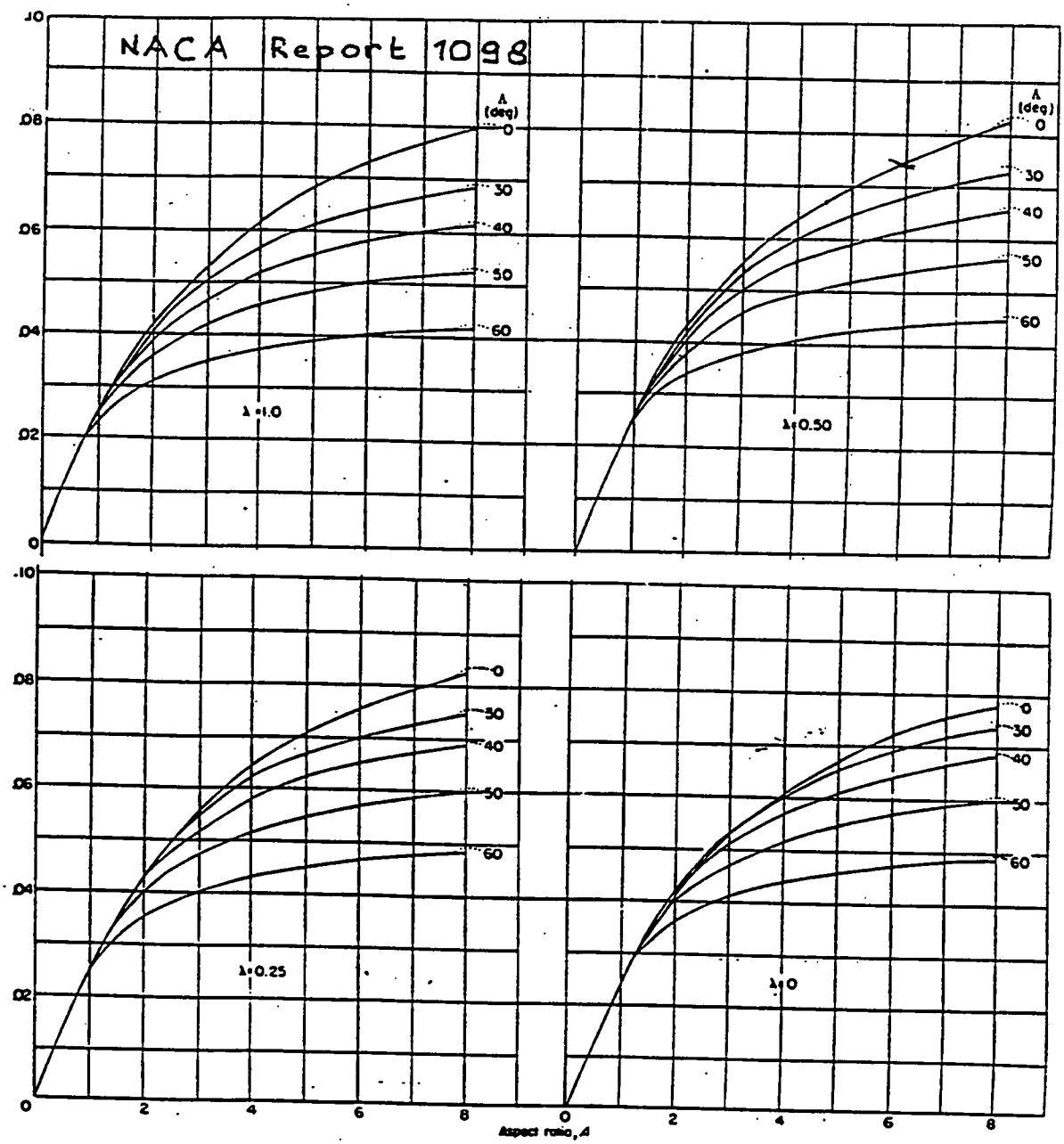

Variation of lift-curve slope with aspect ratio, taper ratio, and sweepback for the case of subsonic incompressible flow. $\alpha_0 = 0.11$.

For the determination of $C_{L_{\alpha_{S,eff}}}$ (eq. (49))
use upper left figure. ($\lambda = 1.0$)

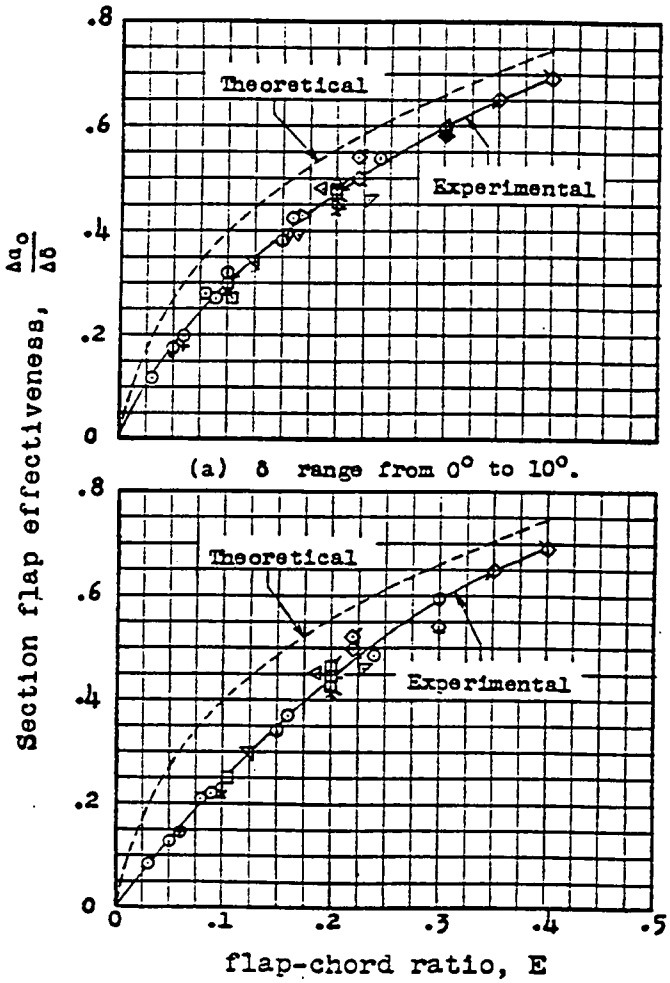

(b) δ range from 0° to 20°.

Variation of section flap effectiveness with flap chord ratio for true-airfoil-contour flaps without exposed overhang balance on a number of airfoil sections; gaps sealed; $c_t = 0$.

From: NASA Memo 1-16-59A

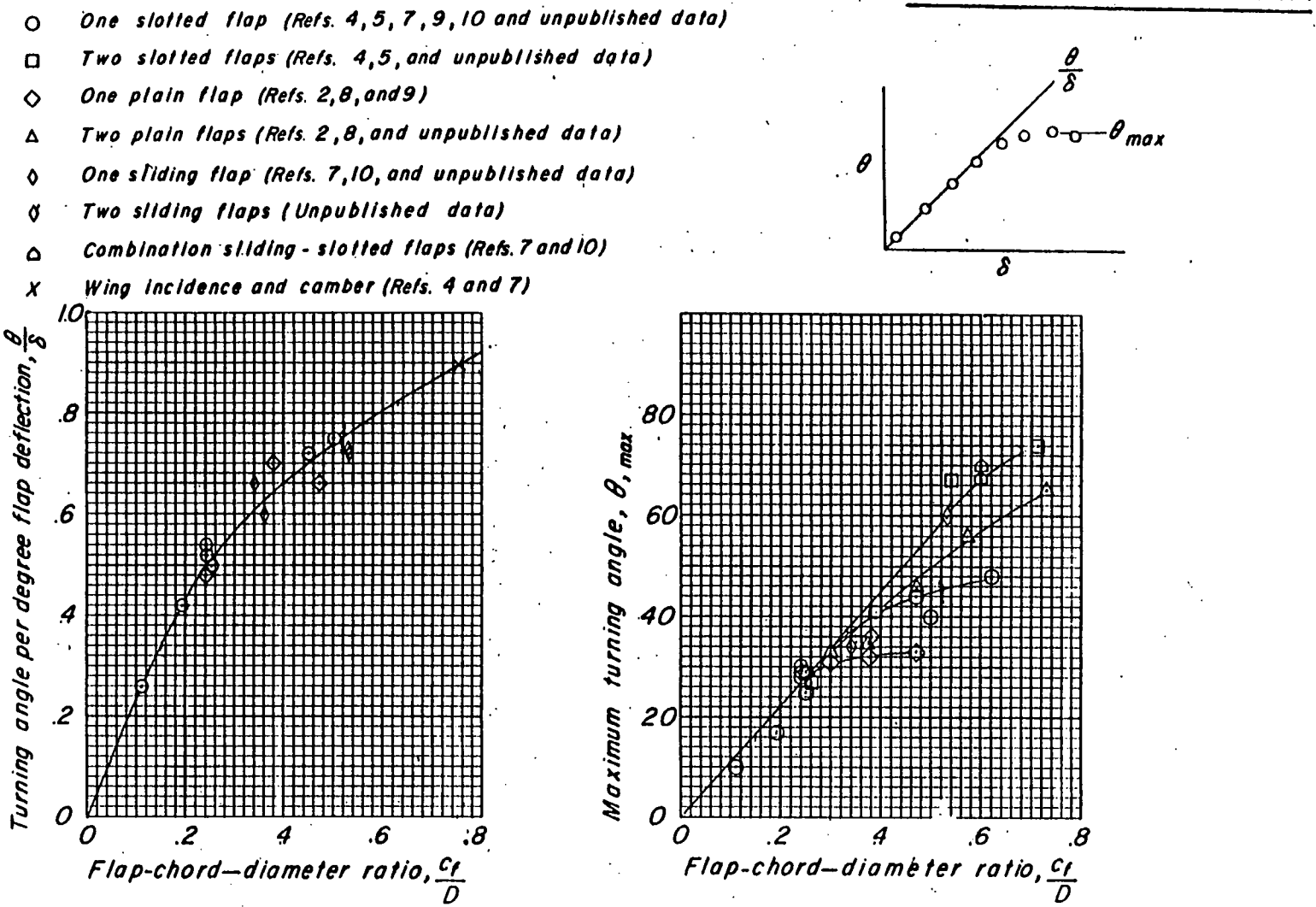

Variation of turning angle with the ratio of total flap chord to propeller diameter for various flap configurations in hovering out of ground-effect region.

From : NASA Memo 1-16-59A

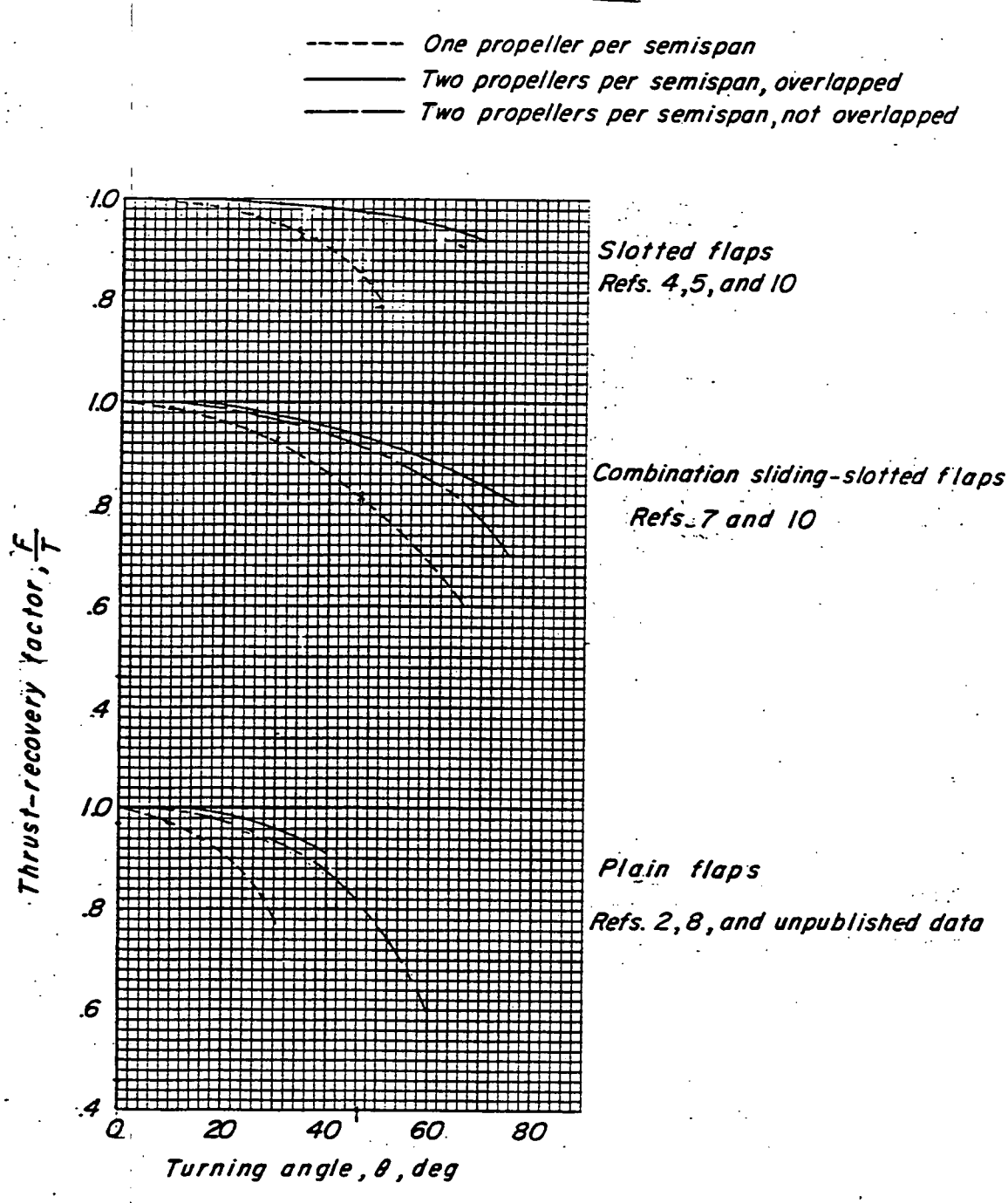

Variation of the average thrust-recovery factor F/T for various flap and propeller configurations in hovering out of ground-effect region.

Table III Total Lift Coefficient (Tail-off)

No	Conf.	δ_f (deg)	T_c	T_c'	C_T	α_R (deg)	$C_{L_{P-0}}$ (TEST)	$C_{L_{TOT}}$ (TEST)		$\frac{\Delta V}{V_0}$	ΔV (m/s; V_0=10 m/s)	D^*	A_S	$A_{S_{eff}}$	$\sin\alpha_R$	$\cos\alpha_R$	α^* deg	$C_{L_{\alpha_S}}$ (1/deg)
		(5)	(60)	(24)	(26)	(19)	(38)	(39)		(40)	(41)	(42)	(43)	(44)	(45)	(46)	(47)	(48)
1	NASA TN D-25	0	–	–	0.15	-8.0	-0.12	-0.17		0.196	1.96	1.393	0.860	2.66	-0.1392	0.9903	-7.29	0.049
			–	–		0	0.55	0.60							0	1.0000	0	
			–	–		8.0	1.25	1.40							0.1392	0.9903	7.29	
		0	–	–	0.15	12.0	1.55	1.80		0.196	1.96	1.393	0.860	2.66	0.2079	0.9781	10.93	0.049
		0	–	–	0.75	-8.0	-0.12	-0.26		0.777	7.77	1.285	0.793	0.842	-0.1392	0.9903	-5.77	0.0274 + $\frac{\Delta S_{eff}}{S}$
			–	–		0	0.55	0.76							0	1.0000	0	
			–	–		8.0	1.25	1.77							0.1392	0.9903	5.77	
		0	–	–	0.75	12.0	1.55	2.32		0.777	7.77	1.285	0.793	0.842	0.2079	0.9781	8.65	
		0	–	–	1.15	-8.0	-0.12	-0.32		1.074	10.74	1.252	0.773	0.785	-0.1392	0.9903	-5.20	
			–	–		0	0.55	0.88							0	1.0000	0	
			–	–		8.0	1.25	2.00							0.1392	0.9903	5.20	
		0	–	–	1.15	12.0	1.55	2.62		1.074	10.74	1.252	0.773	0.785	0.2079	0.9781	7.81	
		0	–	–	1.55	-8.0	-0.12	-0.40		1.336	13.36	1.229	0.759	0.763	-0.1392	0.9903	-4.80	
			–	–		0	0.55	0.90							0	1.0000	0	
			–	–		8.0	1.25	2.16							0.1392	0.9903	4.80	
		0	–	–	1.55	12.0	1.55	2.83		1.336	13.36	1.229	0.759	0.763	0.2079	0.9781	7.20	
		0	–	–	2.15	-8.0	-0.12	-0.40		1.678	16.78	1.205	0.744	0.745	-0.1392	0.9903	-4.35	
			–	–		0	0.55	1.08							0	1.000	0	
			–	–		8.0	1.25	2.42							0.1392	0.9903	4.35	
		0	–	–	2.15	12.0	1.55	3.12		1.678	16.78	1.205	0.744	0.745	0.2079	0.9781	6.53	
		0	–	–	4.10	-8.0	-0.12	-0.50		2.576	25.76	1.163	0.718	0.718	-0.1392	0.9903	-3.50	0.0275 + $\frac{\Delta S_{eff}}{S}$
			–	–		0	0.55	1.30							0	1.0000	0	
			–	–		8.0	1.25	3.08							0.1392	0.9903	3.50	
		0	–	–	4.10	12.0	1.55	3.88		2.576	25.76	1.163	0.718	0.718	0.2079	0.9781	5.25	
1	NASA TN D-25	40	–	–	0.15	-8.0	+0.42	0.47		0.196	1.96	1.393	0.860	2.66	-0.1392	0.9903	-7.29	0.049
			–	–		0	1.15	1.34							0	1.0000	0	
			–	–		8.0	1.85	2.14							0.1392	0.9903	7.29	
		40	–	–	0.15	12.0	2.22	2.58		0.196	1.96	1.393	0.860	2.66	0.2079	0.9781	10.93	0.049
		40													.1392	0.9903	-5.77	0.0274 + $\frac{\Delta S_{eff}}{S}$
															.0	1.0000	0	
		40													.1392	0.9903	5.77	
															2079	0.9781	8.65	
		40													.1392	0.9903	-5.20	
															0	1.0000	0	
		40	–	–	1.15	8.0	1.85	3.36							0.1392	0.9903	5.20	0.0275 + $\frac{\Delta S_{eff}}{S}$
			–	–		12.0	2.22	3.86		1.074	10.74	1.252	0.773	0.785	0.2079	0.9781	7.81	

Example of calculating procedure

Table III Total Lift Coefficient (Tail-off) Concluded.

No	δ_f (deg)	C_T	α_R (deg)	$\sin\varepsilon_s$	$\sin\varepsilon$	A	B	C_{L_W}	C_{L_S}	C_{L_T}	C_{L_P}	$C_{L_{Tot}}$ CALC	$C_{L_{TEST}}$	ΔC_{L_S} calc	ΔC_{L_S} Test	Remarks
	(5)	(26)	(19)	(49)	(50)	(51)	(52)	(53)	(54)	(55)	(56)=(37)	(57)	(39)	(58)	(59)	
1	0	0.15	-8.0	0.0142	-0.0077	14.849	0.914	-0.115	0.013	-0.021	-0.011	-0.138	-0.17	±0.018	-0.02	
			0	0.0393	0.0355			0.527	0.091	0	0.004	0.622	0.60	0.068	0.05	
			8.0	0.1828	0.0807			1.198	0.167	0.021	0.020	1.406	1.40	0.115	0.11	
	0	0.15	12.0	0.2236	0.1000	14.849	0.914	1.485	0.204	0.031	0.027	1.747	1.80	0.139	0.19	
	0	0.75	-8.0	0.0476	-0.0077	14.945	1.716	-0.115	0.082	-0.104	-0.015	-0.152	-0.26	0.087	-0.02	
			0	0.1478	0.0355			0.531	0.254	0	0.006	0.791	0.76	0.235	0.20	
			8.0	0.2465	0.0807			1.206	0.423	0.104	0.026	1.759	1.77	0.379	0.39	
	0	0.75	12.0	0.2949	0.1000	14.945	1.716	1.495	0.506	0.156	0.036	2.193	2.32	0.451	0.58	
	0	1.15	-8.0	0.0576	-0.0077	14.973	2.219	-0.115	0.128	-0.160	-0.016	-0.163	-0.32	0.133	-0.02	
			0	0.1478	0.0355			0.532	0.328	0	0.006	0.866	0.88	0.310	0.32	
			8.0	0.2368	0.0807			1.208	0.525	0.160	0.029	1.922	2.00	0.483	0.56	
	0	1.15	12.0	0.2808	0.1000	14.973	2.219	1.497	0.623	0.239	0.040	2.399	2.62	0.570	0.79	
	0	1.55	-8.0	0.0645	-0.0077	14.992	2.710	-0.115	0.175	-0.216	-0.018	-0.174	-0.40	0.180	-0.05	
			0	0.1478	0.0355			0.532	0.401	0	0.007	0.940	0.90	0.383	0.44	
			8.0	0.2300	0.0807			1.210	0.623	0.216	0.032	2.081	2.16	0.583	0.66	
	0	1.55	12.0	0.2706	0.1000	14.992	2.710	1.499	0.733	0.322	0.044	2.598	2.83	0.682	0.91	
	0	2.15	-8.0	0.0724	-0.0077	15.011	3.426	-0.116	0.248	-0.299	-0.020	-0.187	-0.40	0.252	0.04	
			0	0.1478	0.0355			0.533	0.506	0	0.008	1.047	1.08	0.489	0.52	
			8.0	0.2139	0.0807			1.211	0.733	0.299	0.035	2.278	2.42	0.694	0.84	
	0	2.15	12.0	0.2593	0.1000	15.011	3.426	1.503	0.888	0.447	0.048	2.886	3.12	0.841	1.08	
	0	4.10	-8.0	0.0872	-0.0077	15.044	5.696	-0.116	0.497	-0.571	-0.024	-0.214	-0.50	0.501	0.22	
			0	0.1478	0.0355			0.534	0.842	0	0.009	1.385	1.30	0.826	0.74	
			8.0	0.2029	0.0807			1.214	1.184	0.571	0.043	3.012	3.08	1.148	1.22	
	0	4.10	12.0	0.2327	0.1000	15.044	5.696	1.504	1.354	0.852	0.060	3.720	3.88	1.308	1.42	
1	40	0.15	-8.0	0.2519	0.0271	14.849	0.905	0.402	0.228	-0.021	-0.008	0.601	0.47	0.210	0.08	
			0	0.3289	0.0743			1.103	0.298	0	0.008	1.409	1.34	0.251	0.18	
			8.0	0.4005	0.1194			1.773	0.362	0.021	0.023	2.179	2.14	0.285	0.25	
	40	0.15	12.0	0.4340	0.1433	14.849	0.905	2.128	0.393	0.031	0.031	2.583	2.58	0.301	0.30	
	40	0.75	-8.0	0.3984	0.0271	14.945	1.699	0.405	0.677	-0.104	-0.010	0.968	0.80	0.662	0.49	
			0	0.4894	0.0743			1.110	0.831	0	0.010	1.951	1.92	0.791	0.76	
			8.0	0.5253	0.1194			1.784	0.972	0.104	0.031	2.896	2.92	0.911	0.94	
	40	0.75	12.0	0.6150	0.1433	14.945	1.699	2.142	1.045	0.156	0.041	3.384	3.30	0.967	0.88	
	40	1.15	-8.0	0.4083	0.0271	14.973	2.197	0.406	0.897	-0.160	-0.011	1.132	1.00	0.883	0.75	
			0	0.4894	0.0743			1.112	1.075	0	0.011	2.198	2.23	1.037	1.07	
			8.0	0.5664	0.1194			1.788	1.244	0.160	0.034	3.226	3.36	1.182	1.32	
	40	1.15	12.0	0.6033	0.1433	14.973	2.197	2.146	1.325	0.239	0.045	3.755	3.86	1.251	1.36	

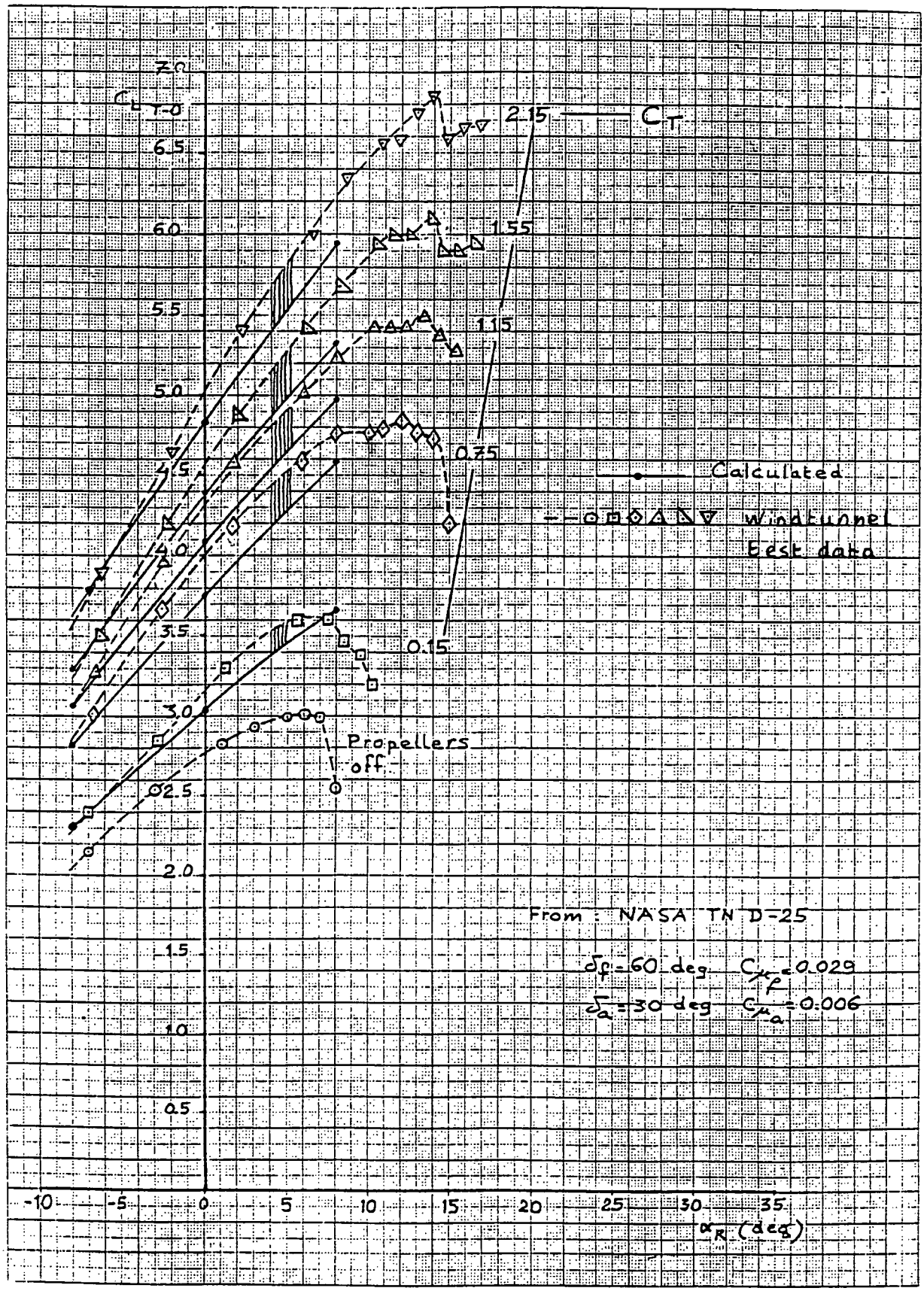
C_L
7.0
6.5
6.0
5.5
5.0
4.5
4.0
3.5
3.0
2.5
2.0
1.5
1.0
0.5
2.15
1.55
1.15
0.75
0.15
C_T
Calculated
Windtunnel test data
Propellers off
From : NASA TN D-25
δ_f = 60 deg C_{μ_f} = 0.029
δ_a = 30 deg C_{μ_a} = 0.006
-10
-5
0
5
10
15
20
25
30
35
α_R (deg)

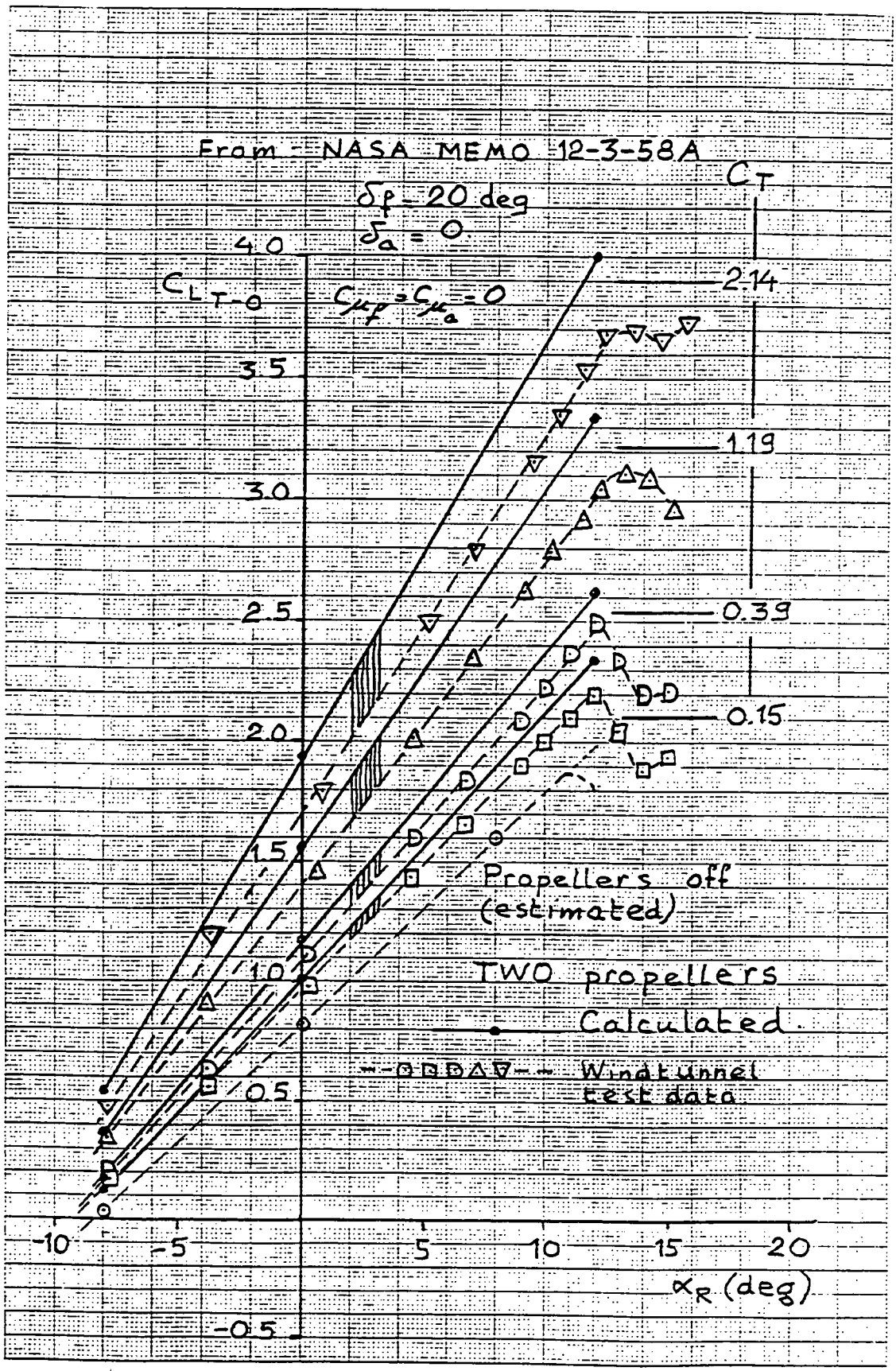
From - NASA MEMO 12-3-58A
δ_f = 20 deg
δ_a = 0
$C_{L_{T-0}}$
$C_{\mu_f} = C_{\mu_a} = 0$
C_T
2.14
1.19
0.39
0.15
4.0
3.5
3.0
2.5
2.0
1.5
1.0
0.5
-0.5
-10
-5
5
10
15
20
α_R (deg)
Propellers off (estimated)
TWO propellers
Calculated
Wind tunnel test data

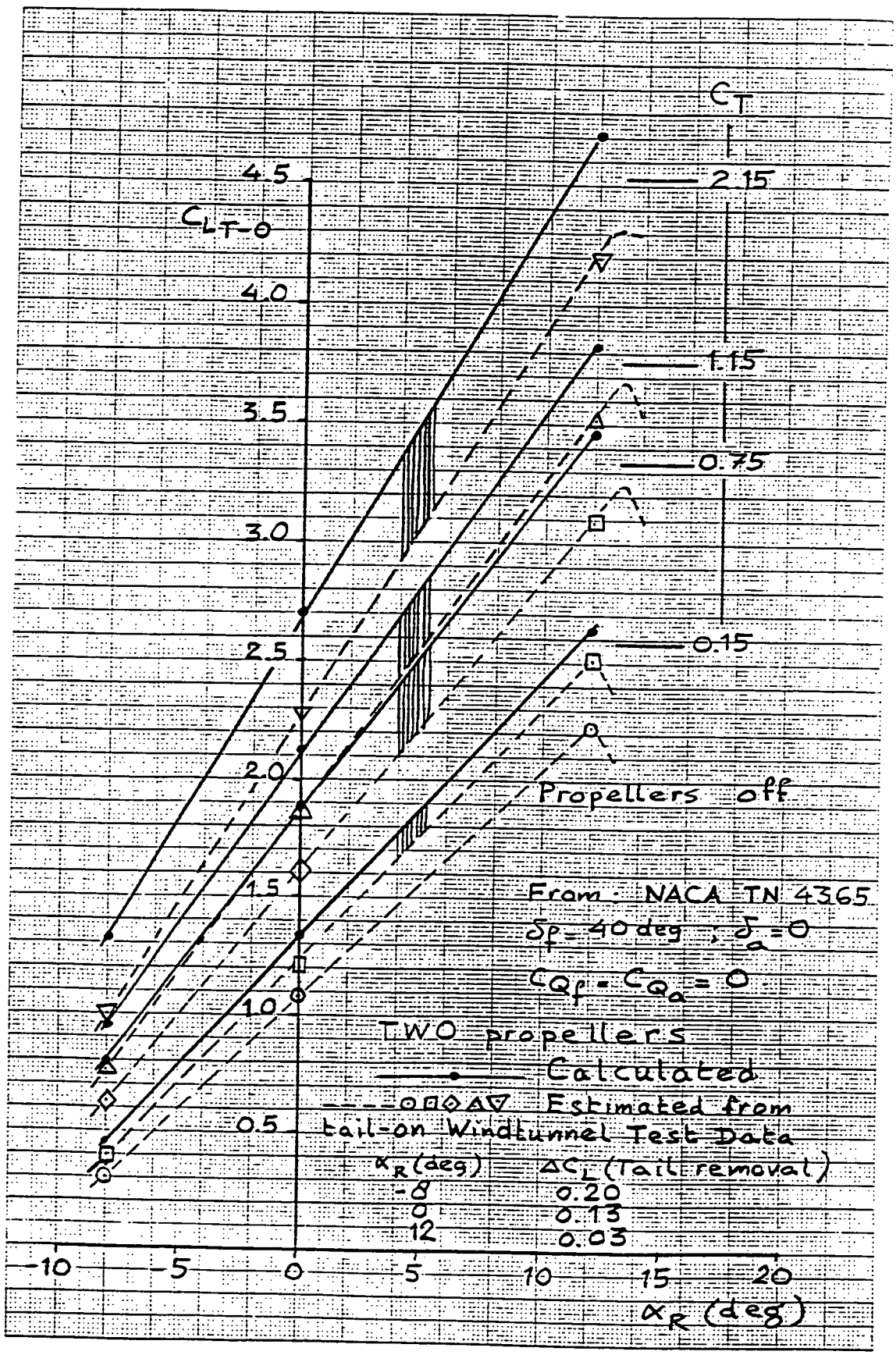
C_T
2.15
1.15
0.75
0.15
$C_{L_{T-0}}$
4.5
4.0
3.5
3.0
2.5
2.0
1.5
1.0
0.5
Propellers off
From: NACA TN 4365
$\delta_f = 40$ deg ; $\delta_a = 0$
$C_{Q_f} - C_{Q_a} = 0$
TWO propellers
Calculated
Estimated from tail-on Windtunnel Test Data
α_R (deg) ΔC_L (Tail removal)
-8 0.20
0 0.13
12 0.03
-10 -5 0 5 10 15 20
α_R (deg)

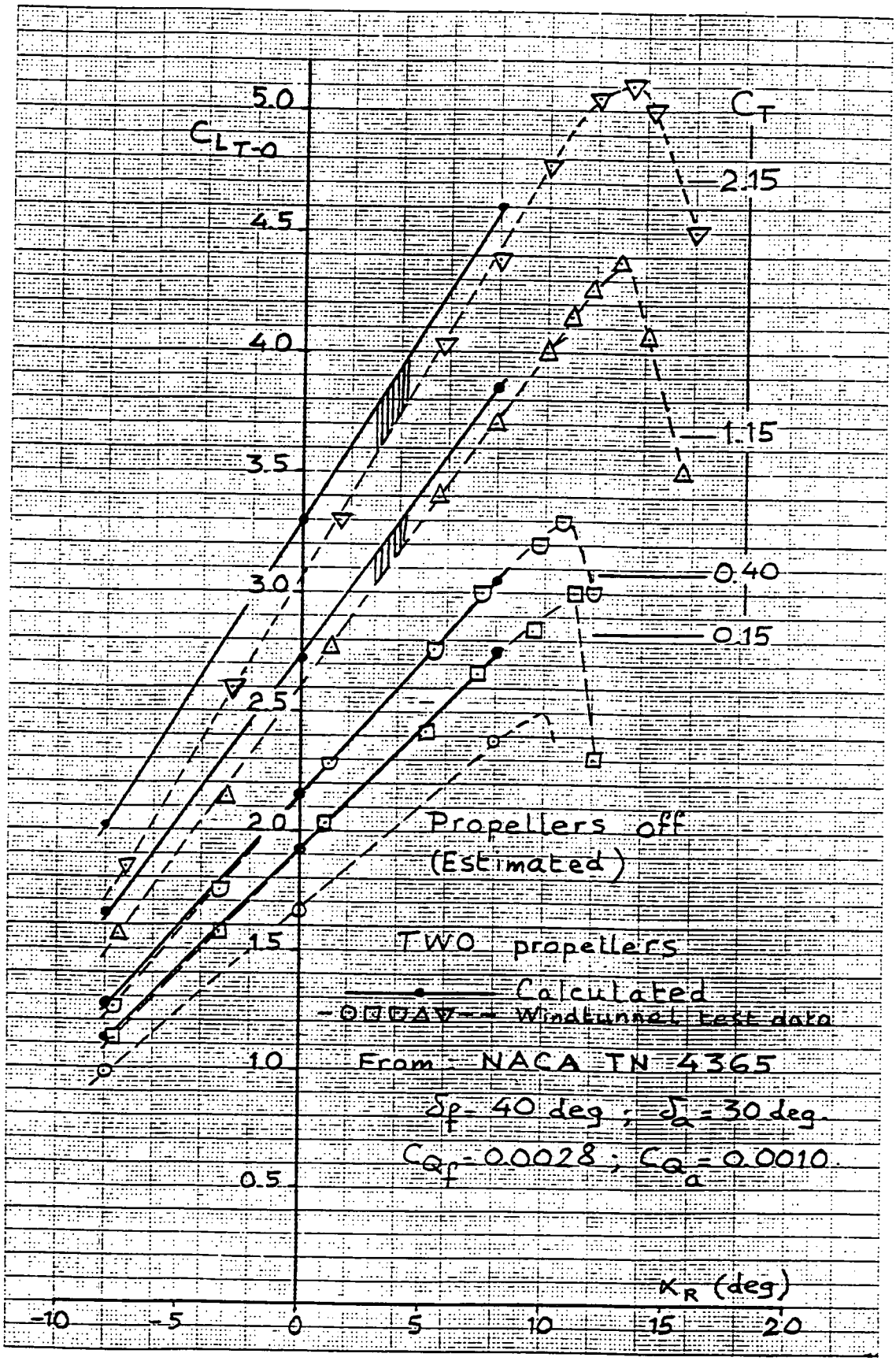
$C_{L_{T=0}}$
5.0
4.5
4.0
3.5
3.0
2.5
2.0
1.5
1.0
0.5
C_T
2.15
1.15
0.40
0.15
Propellers off
(Estimated)
TWO propellers
Calculated
Windtunnel test data
From - NACA TN 4365
δ_f - 40 deg ; δ_a = 30 deg.
C_{Q_f} = 0.0028 ; C_{Q_a} = 0.0010
α_R (deg)
-10
-5
0
5
10
15
20

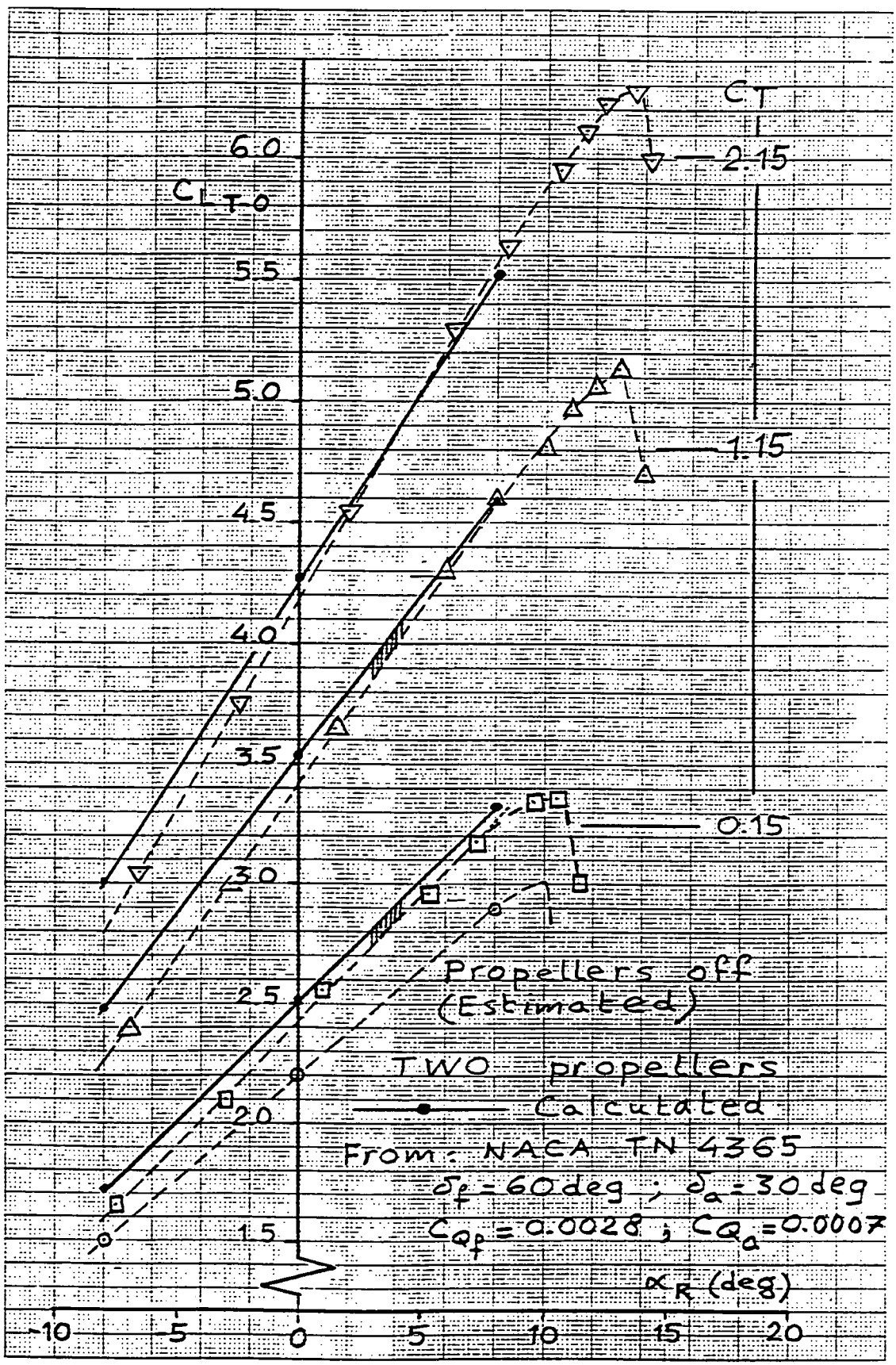
C_T
2.15
1.15
0.15
$C_{L_{T-O}}$
6.0
5.5
5.0
4.5
4.0
3.5
3.0
2.5
2.0
1.5
Propellers off
(Estimated)
TWO propellers
Calculated
From: NACA TN 4365
$\delta_f = 60$ deg ; $\delta_a = 30$ deg
$C_{Q_f} = 0.0028$; $C_{Q_a} = 0.0007$
α_R (deg)
-10
-5
0
5
10
15
20

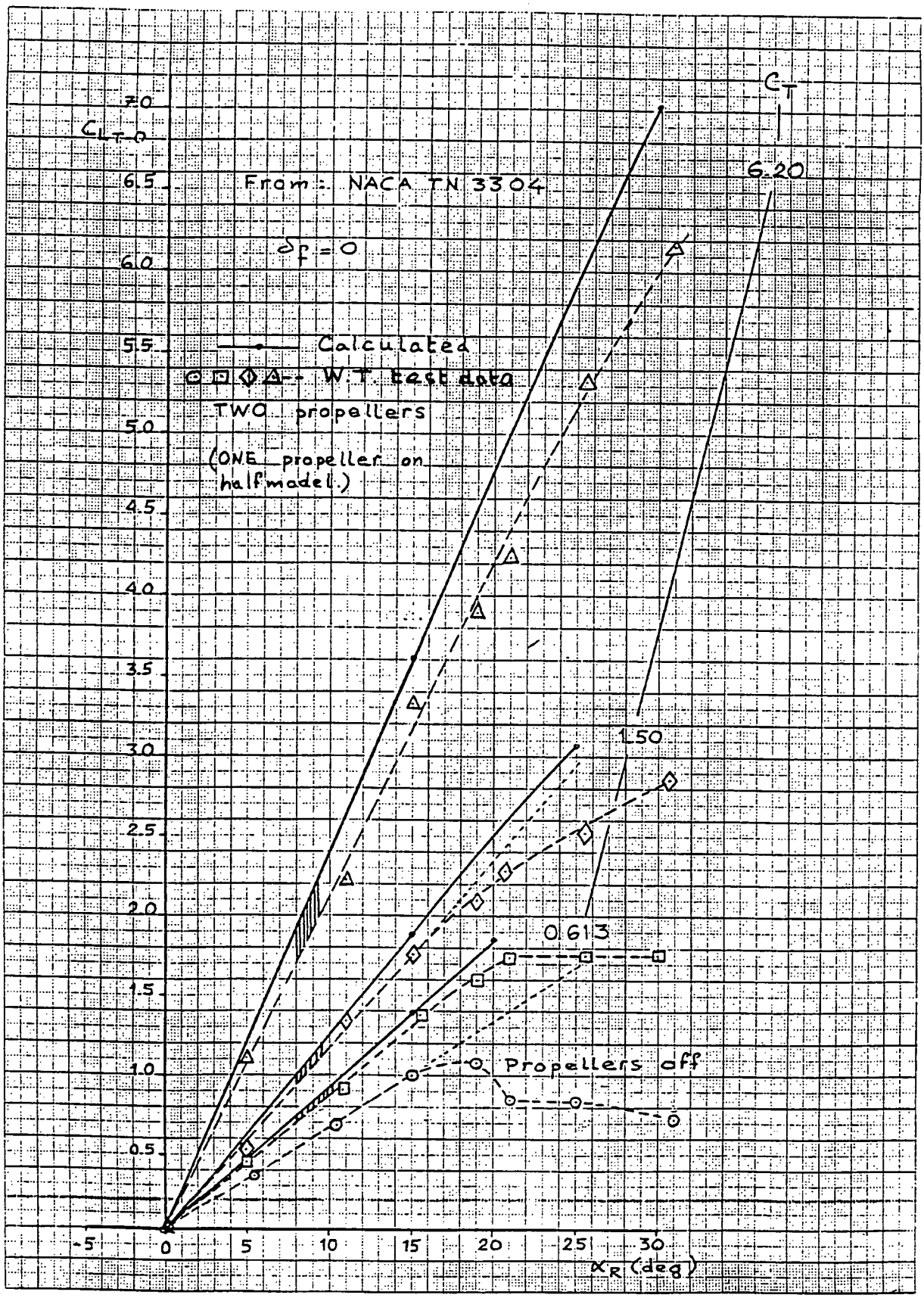
$C_{L_{T-O}}$
From: NACA TN 3304
$\delta_f = 0$
Calculated
W.T. test data
TWO propellers
(ONE propeller on half model.)
C_T
6.20
1.50
0.613
Propellers off
α_R (deg)
7.0
6.5
6.0
5.5
5.0
4.5
4.0
3.5
3.0
2.5
2.0
1.5
1.0
0.5
-5
0
5
10
15
20
25
30

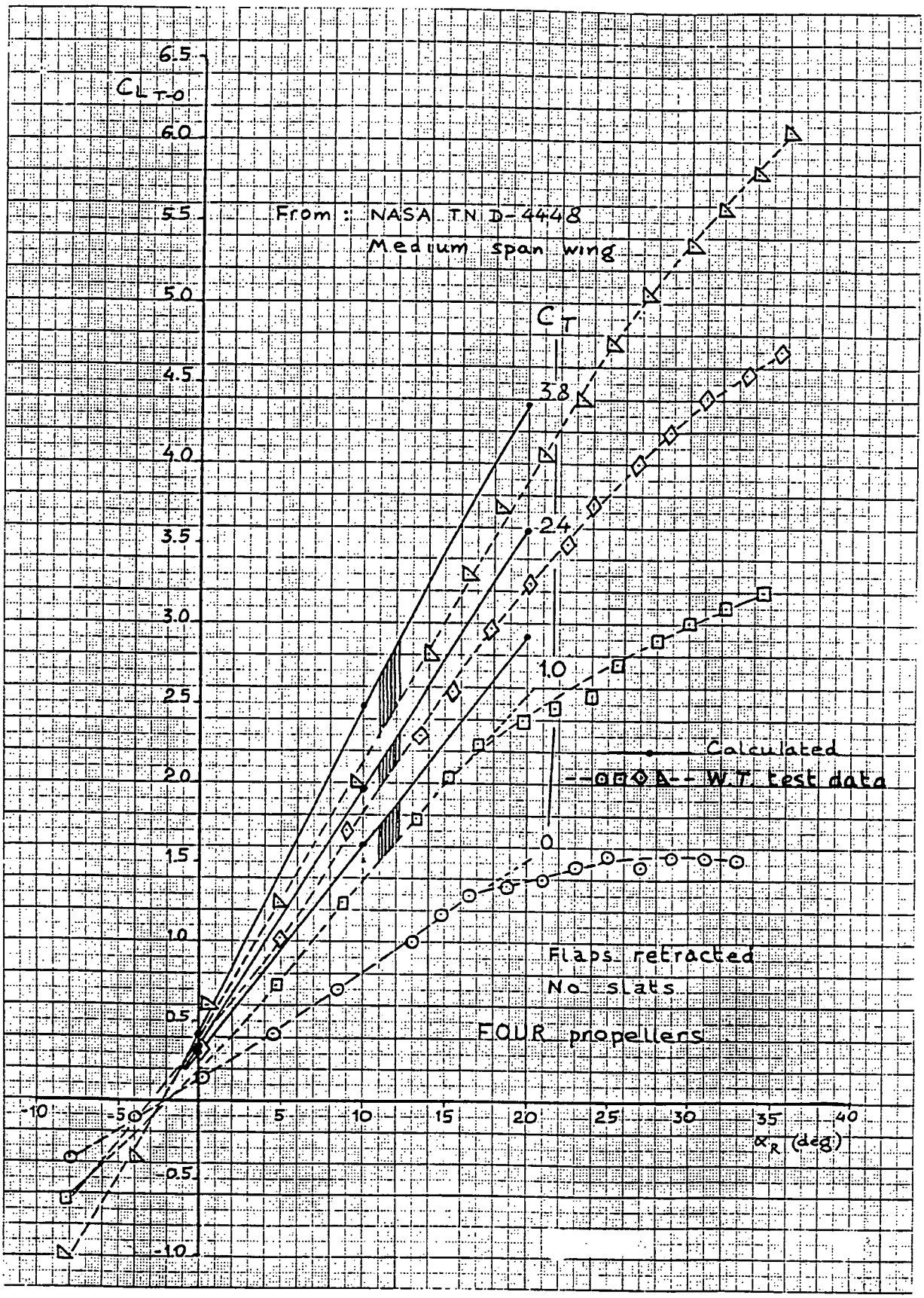
$C_{L\,T-O}$
6.5
6.0
5.5
5.0
4.5
4.0
3.5
3.0
2.5
2.0
1.5
1.0
0.5
-0.5
-1.0
From : NASA TN D-4448
Medium span wing
C_T
3.8
2.4
1.0
0
Calculated
W.T. test data
Flaps retracted
No slats
FOUR propellers
-10
-5
5
10
15
20
25
30
35
40
α_R (deg)

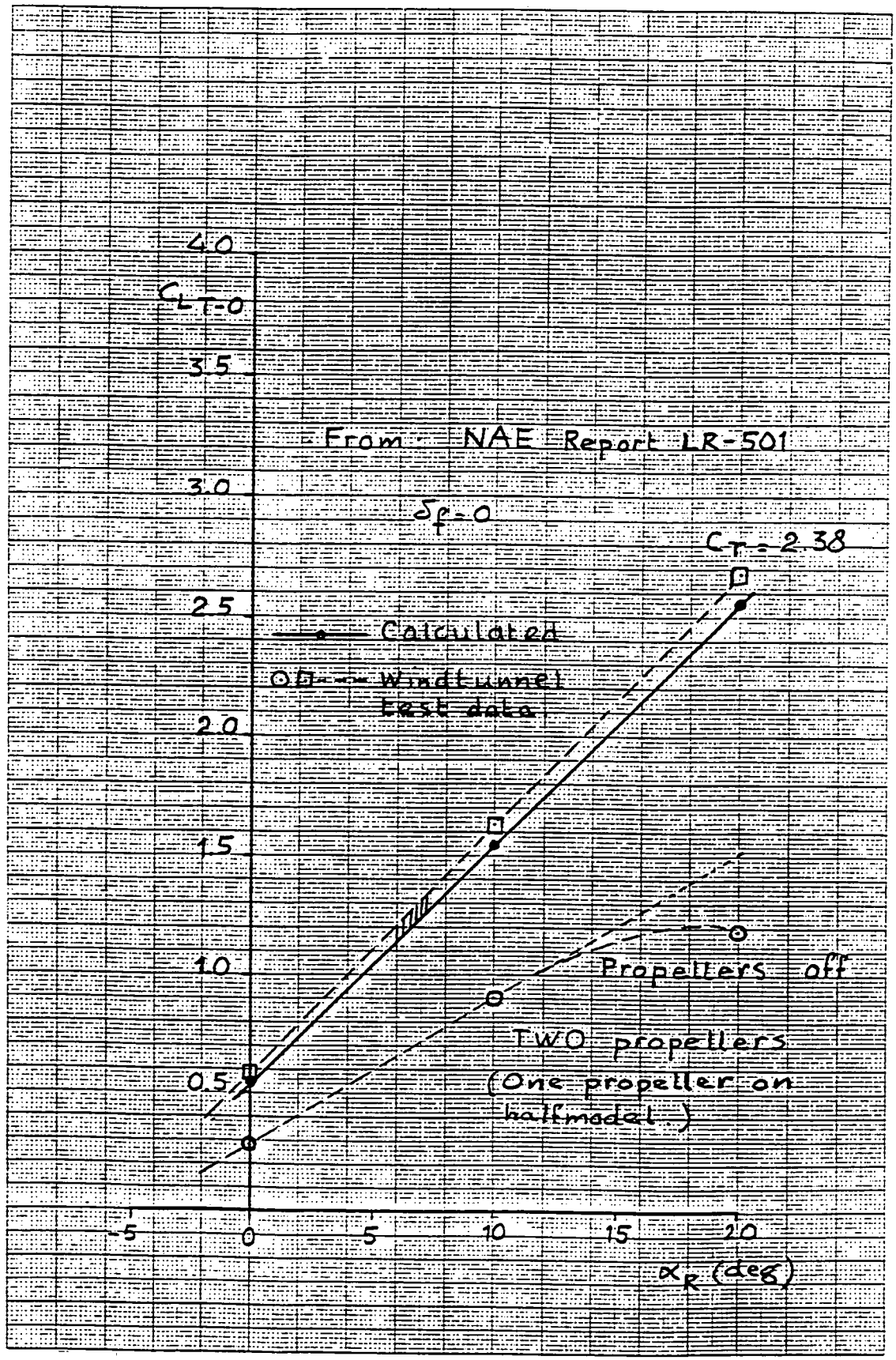
4.0
$C_{LT=0}$
3.5
From - NAE Report LR-501
3.0
$\delta_f = 0$
$C_T = 2.38$
2.5
Calculated
Windtunnel test data
2.0
1.5
1.0
Propellers off
TWO propellers (One propeller on halfmodel)
0.5
-5
0
5
10
15
20
α_R (deg)

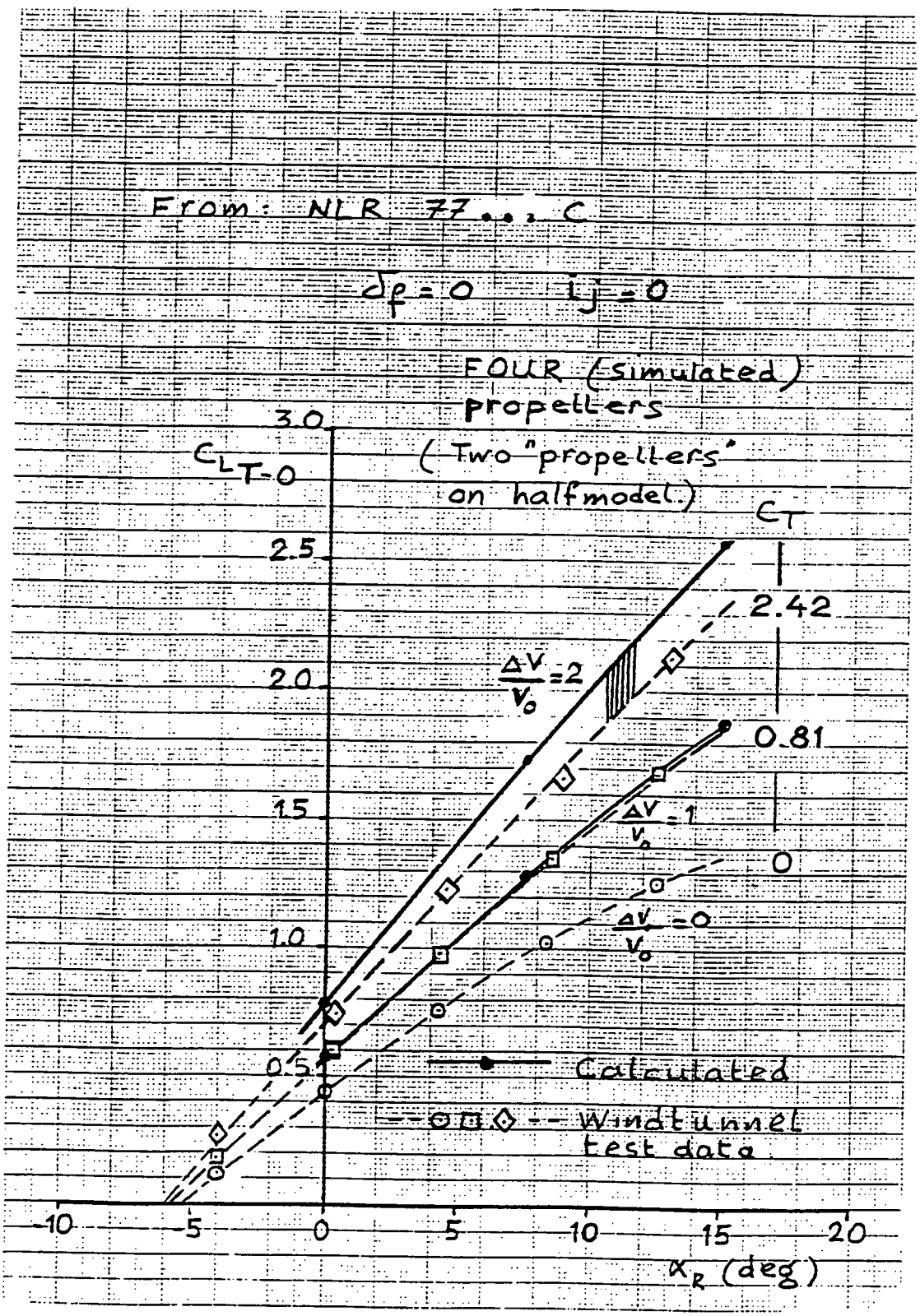
From: NLR 77...C
df = 0 ij = 0
FOUR (simulated) propellers
(Two "propellers" on halfmodel)
$C_{LT=0}$
C_T
2.42
0.81
0
$\frac{\Delta V}{V_0}$=2
$\frac{\Delta V}{V_0}$=1
$\frac{\Delta V}{V_0}$=0
3.0
2.5
2.0
1.5
1.0
0.5
Calculated
Windtunnel test data
-10
-5
0
5
10
15
20
α_R (deg)

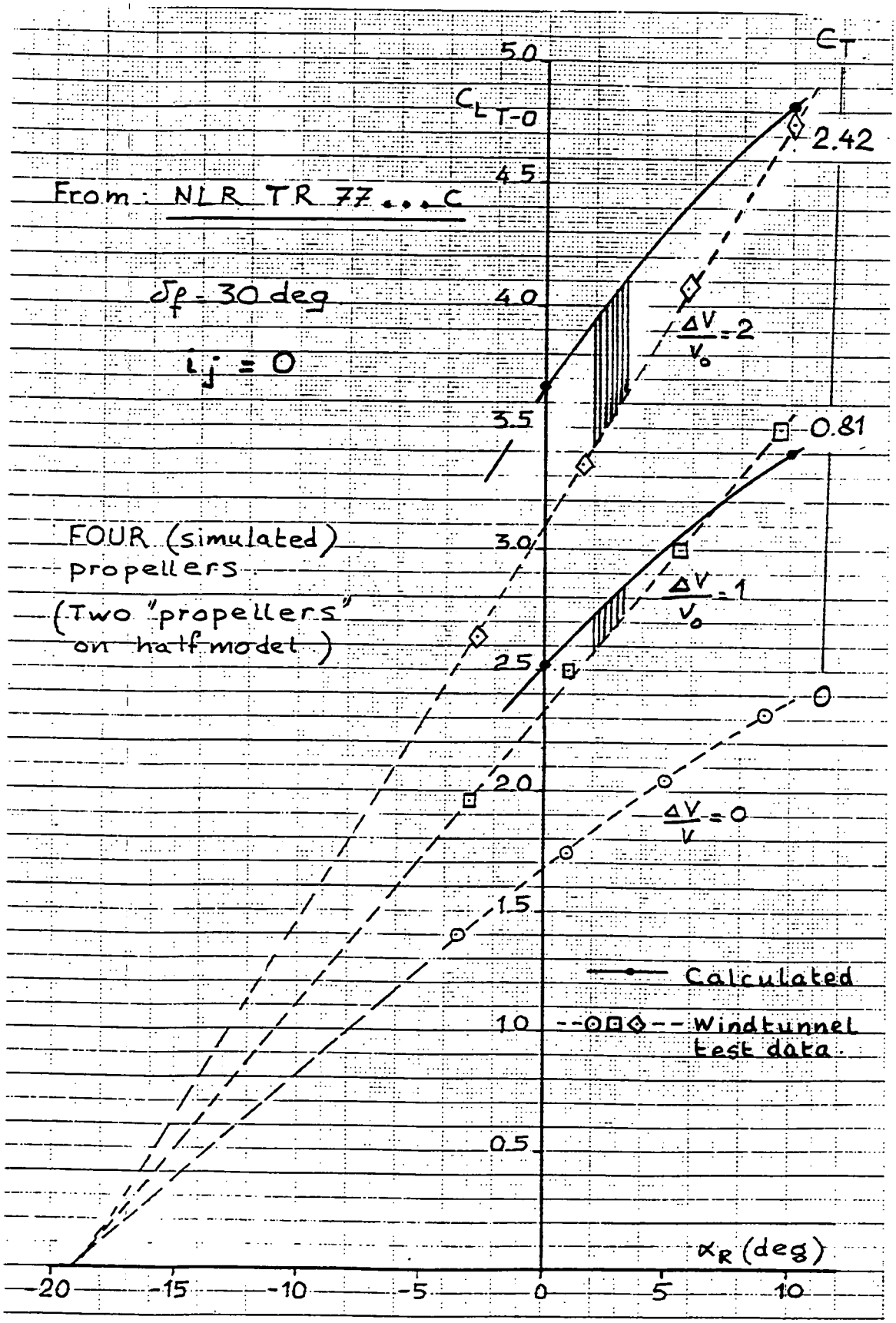
C_T
$C_{L_{T-0}}$
5.0
4.5
4.0
3.5
3.0
2.5
2.0
1.5
1.0
0.5
From: NLR TR 77 ... C
δ_f = 30 deg
i_j = 0
FOUR (simulated) propellers
(Two "propellers" on half model)
2.42
0.81
$\frac{\Delta V}{V_0}$ = 2
$\frac{\Delta V}{V_0}$ = 1
$\frac{\Delta V}{V}$ = 0
Calculated
Windtunnel test data
α_R (deg)
-20
-15
-10
-5
0
5
10

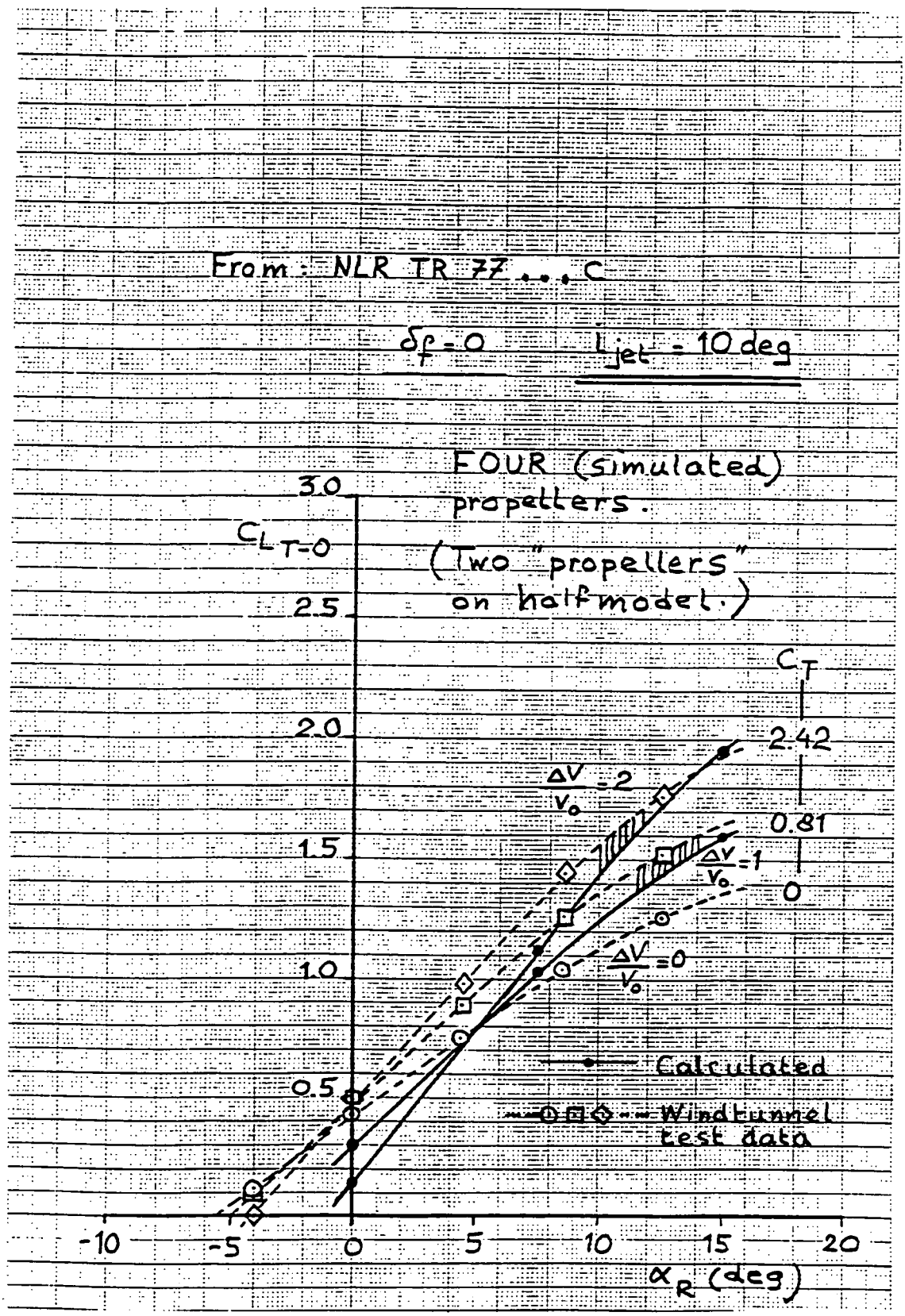
From: NLR TR 77 ... C
$\delta_f = 0$
$i_{jet} = 10$ deg
FOUR (simulated) propellers.
(Two "propellers" on halfmodel.)
$C_{L_{T=0}}$
3.0
2.5
2.0
1.5
1.0
0.5
C_T
2.42
0.81
0
$\frac{\Delta V}{V_o} = 2$
$\frac{\Delta V}{V_o} = 1$
$\frac{\Delta V}{V_o} = 0$
Calculated
Windtunnel test data
-10
-5
0
5
10
15
20
α_R (deg)

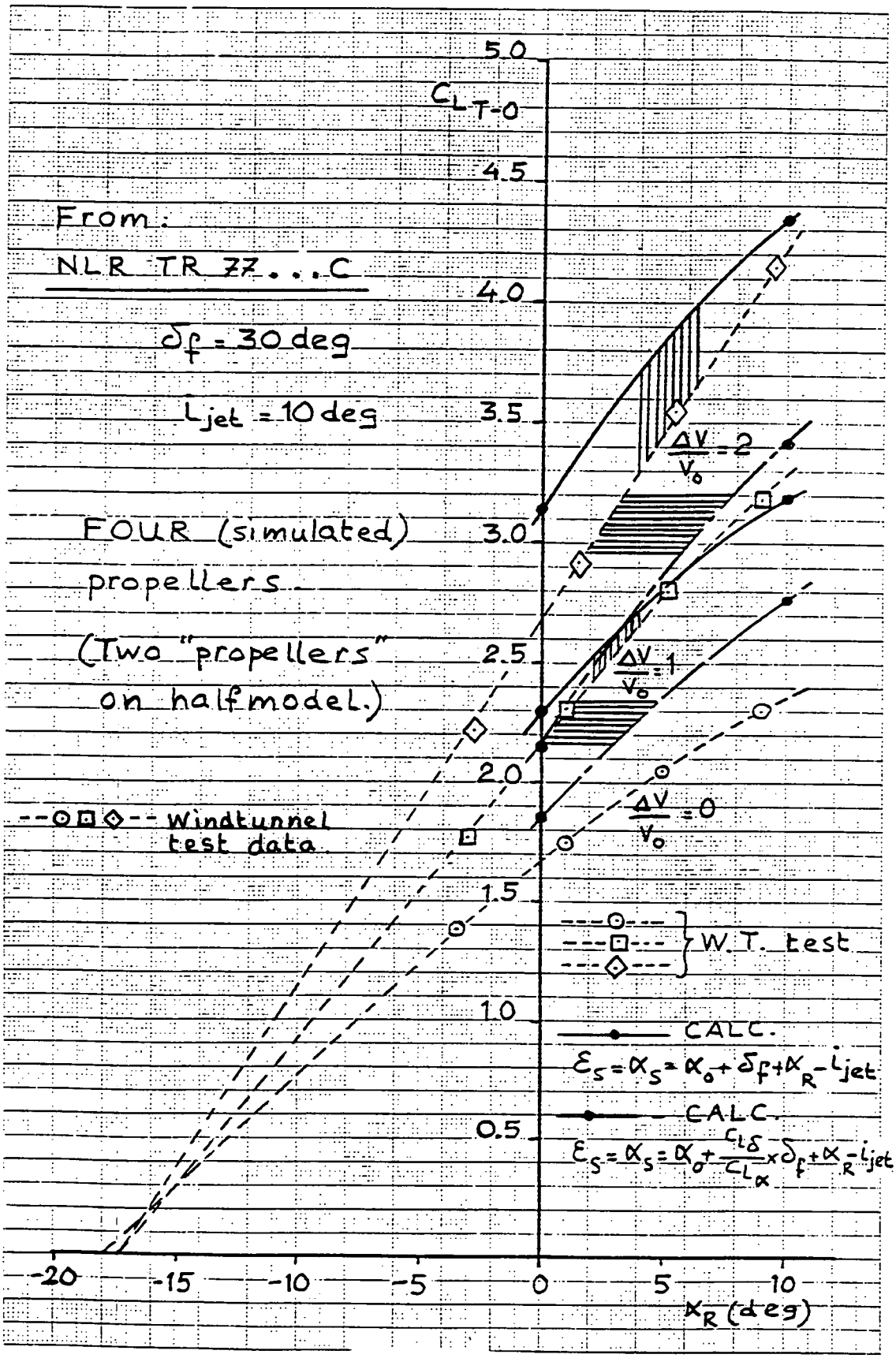
From:
NLR TR 77...C
δ_f = 30 deg
i_{jet} = 10 deg
FOUR (simulated) propellers
(Two "propellers" on halfmodel.)
--○□◇-- Windtunnel test data
$C_{L_{T-O}}$
5.0
4.5
4.0
3.5
3.0
2.5
2.0
1.5
1.0
0.5
$\frac{\Delta V}{V_o}$ = 2
$\frac{\Delta V}{V_o}$ = 1
$\frac{\Delta V}{V_o}$ = 0
W.T. test
CALC.
$\varepsilon_s = \alpha_s = \alpha_o + \delta_f + \alpha_R - i_{jet}$
CALC.
$\varepsilon_s = \alpha_s = \alpha_o + \frac{C_{L\delta}}{C_{L\alpha}} \times \delta_f + \alpha_R - i_{jet}$
-20
-15
-10
-5
0
5
10
α_R (deg)

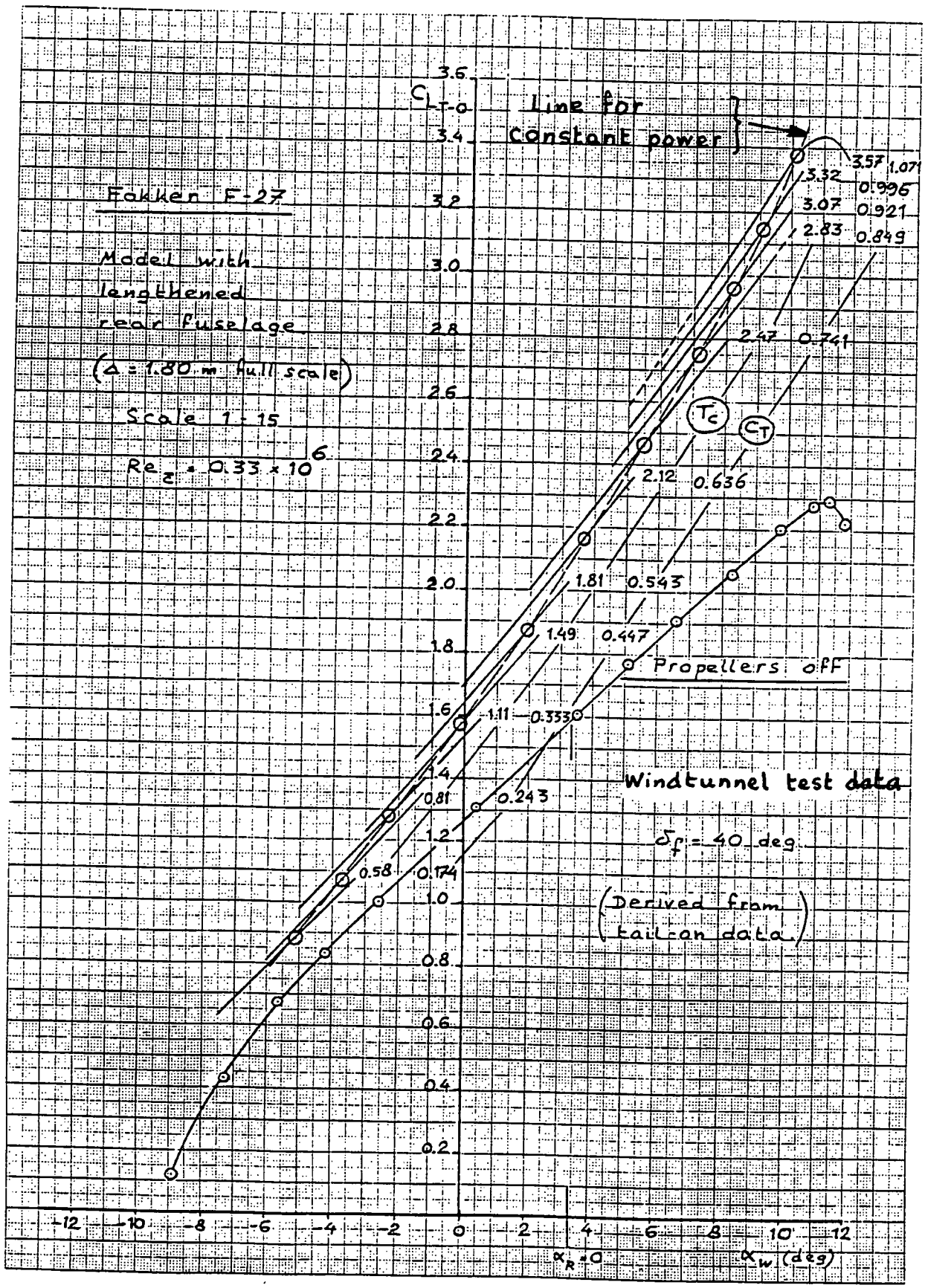
Fokker F-27
Model with lengthened rear fuselage
(Δ = 1.80 m full scale)
Scale 1 : 15
Re = 0.33 × 10^6
C_L T-O
Line for constant power
Propellers off
Windtunnel test data
δf = 40 deg
(Derived from tail-on data)
Tc
CT
3.57 1.071
3.32 0.996
3.07 0.921
2.83 0.849
2.47 0.741
2.12 0.636
1.81 0.543
1.49 0.447
1.11 0.333
0.81 0.243
0.58 0.174
3.6
3.4
3.2
3.0
2.8
2.6
2.4
2.2
2.0
1.8
1.6
1.4
1.2
1.0
0.8
0.6
0.4
0.2
-12 -10 -8 -6 -4 -2 0 2 4 6 8 10 12
αR = 0
αw (deg)

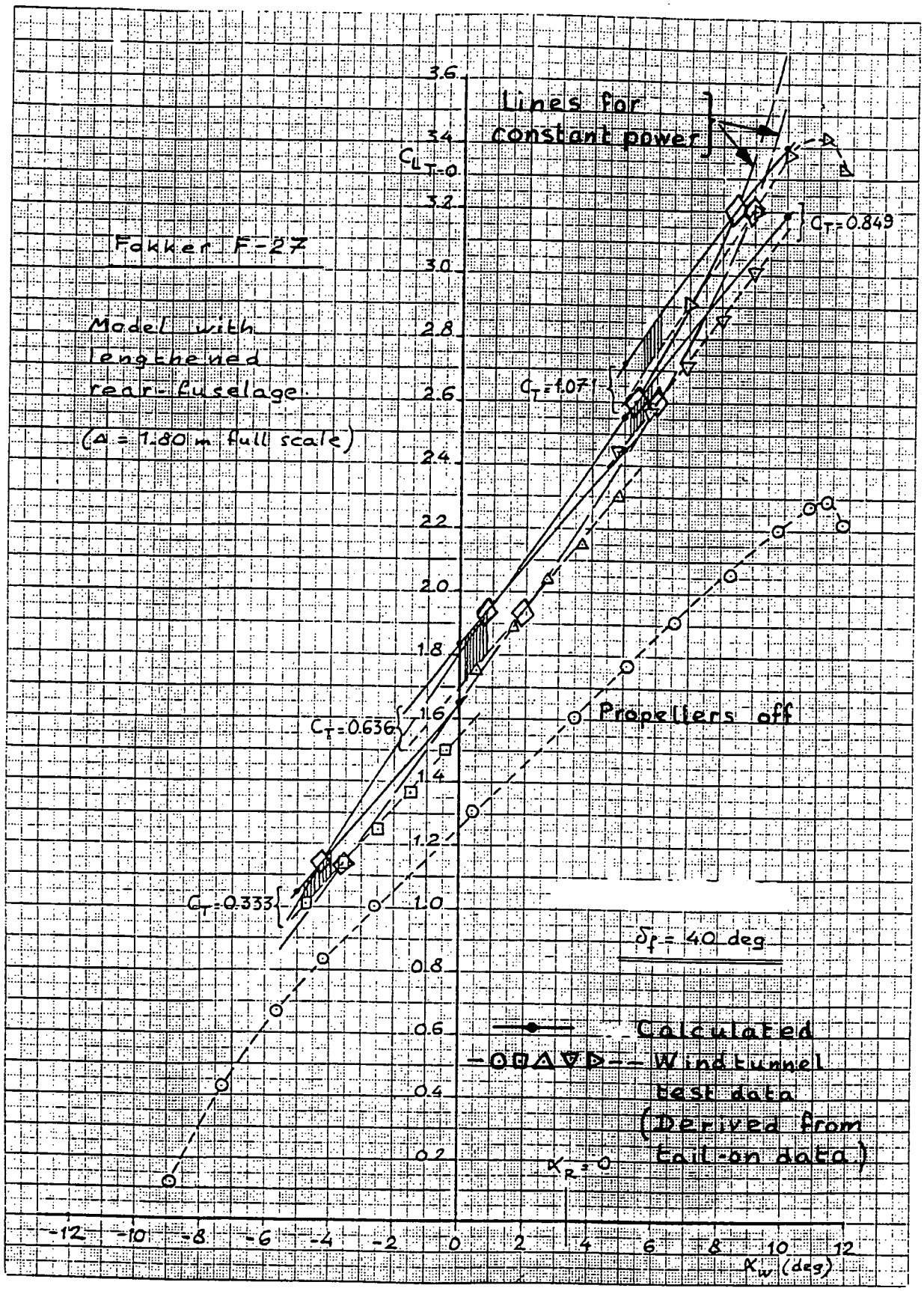
Fokker F-27
Model with lengthened rear-fuselage
(Δ = 1.80 m full scale)
Lines for constant power
C_T = 0.849
C_T = 1.071
C_T = 0.636
C_T = 0.333
Propellers off
δ_f = 40 deg
Calculated
Wind tunnel test data (Derived from tail-on data)
i_R = 0
$C_{L_{T=0}}$
α_w (deg)
3.6
3.4
3.2
3.0
2.8
2.6
2.4
2.2
2.0
1.8
1.6
1.4
1.2
1.0
0.8
0.6
0.4
0.2
-12
-10
-8
-6
-4
-2
0
2
4
6
8
10
12

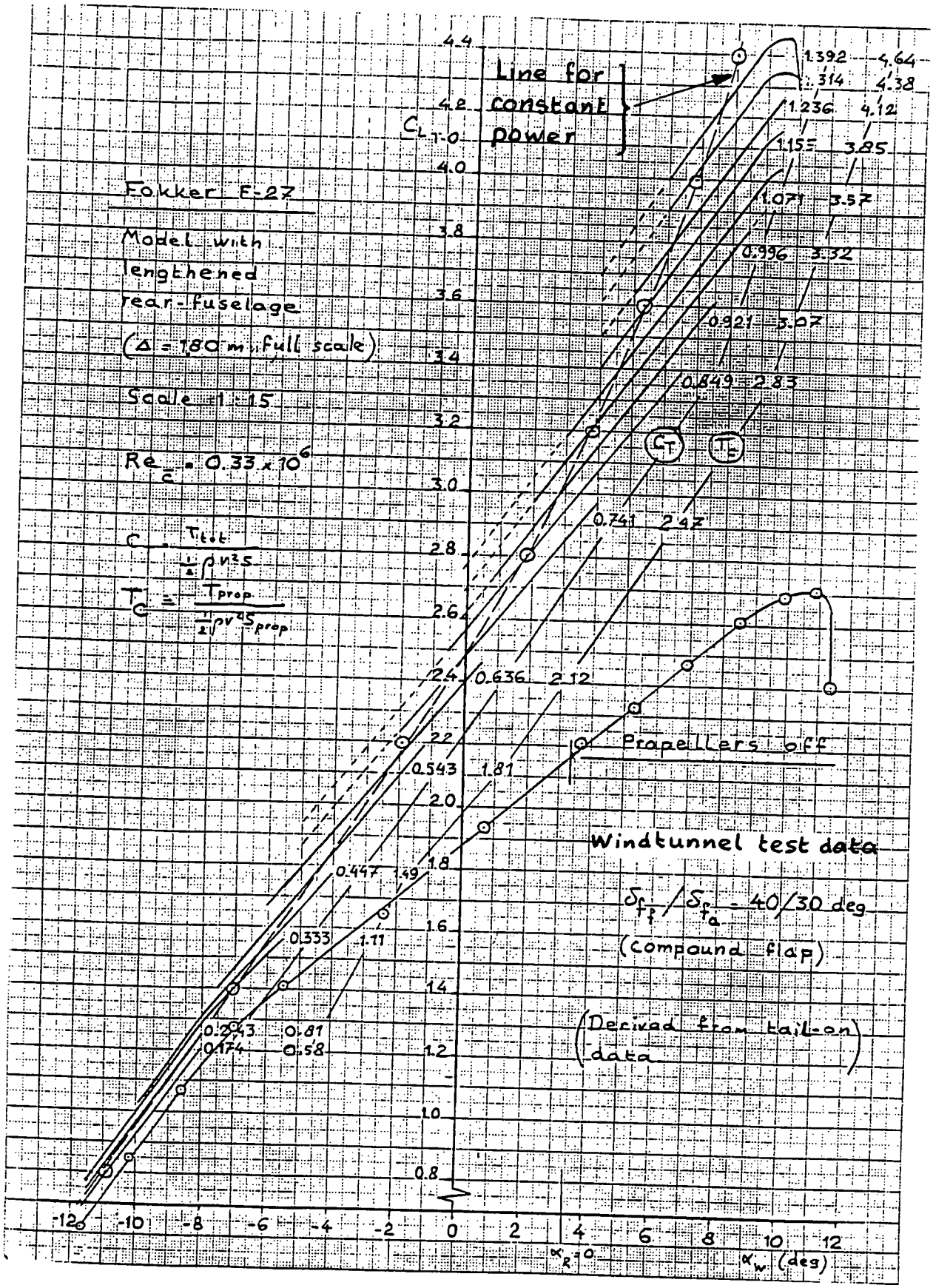
Line for constant power
Fokker F-27
Model with lengthened rear-fuselage
(Δ = 180 m, full scale)
Scale 1 : 15
$Re_{\bar{c}} = 0.33 \times 10^6$
$C_T = \frac{T_{tot}}{\frac{1}{2}\rho V^2 S}$
$T_C = \frac{T_{prop}}{\frac{1}{2}\rho V^2 S_{prop}}$
C_L
C_T
T_C
1.392 4.64
1.314 4.38
1.236 4.12
1.15 3.85
1.071 3.57
0.996 3.32
0.921 3.07
0.849 2.83
0.741 2.47
0.636 2.12
0.543 1.81
0.447 1.49
0.333 1.11
0.243 0.81
0.174 0.58
Propellers off
Windtunnel test data
$\delta_{f_f} / \delta_{f_a}$ = 40/30 deg
(compound flap)
(Derived from tail-on data)
$\alpha_{R=0}$
α_w (deg)

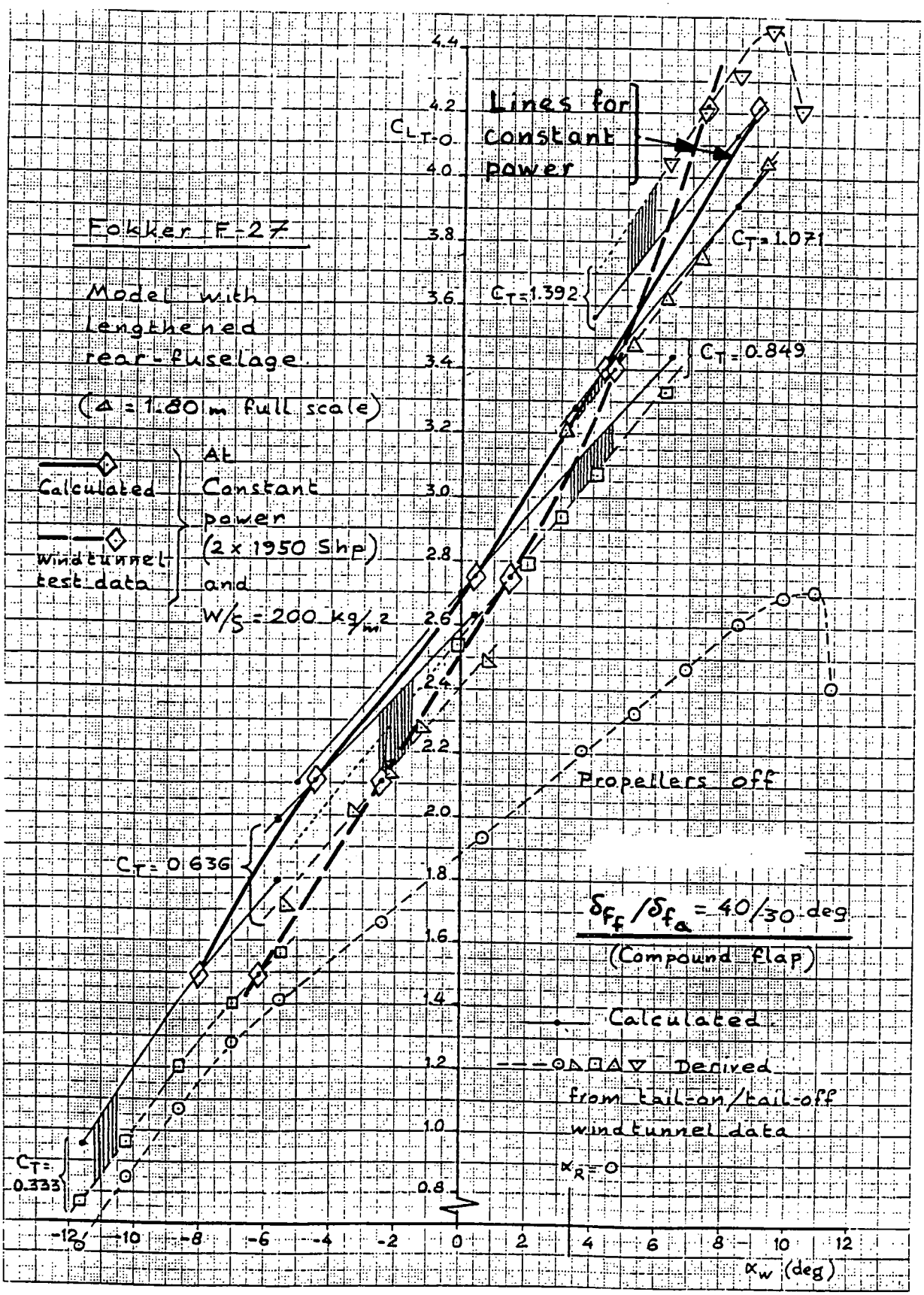
Lines for constant power
Fokker F-27
Model with lengthened rear-fuselage
(Δ = 1.80 m full scale)
At Constant power (2 x 1950 shp) and W/S = 200 kg/m²
Calculated
Windtunnel test data
$C_{L_{T-O}}$
C_T=1.392
C_T=1.071
C_T=0.849
C_T=0.636
C_T=0.333
Propellers off
$\delta_{f_f}/\delta_{f_a}$ = 40/30 deg
(Compound flap)
Calculated
Derived from tail-on/tail-off windtunnel data
α_R=0
α_w (deg)

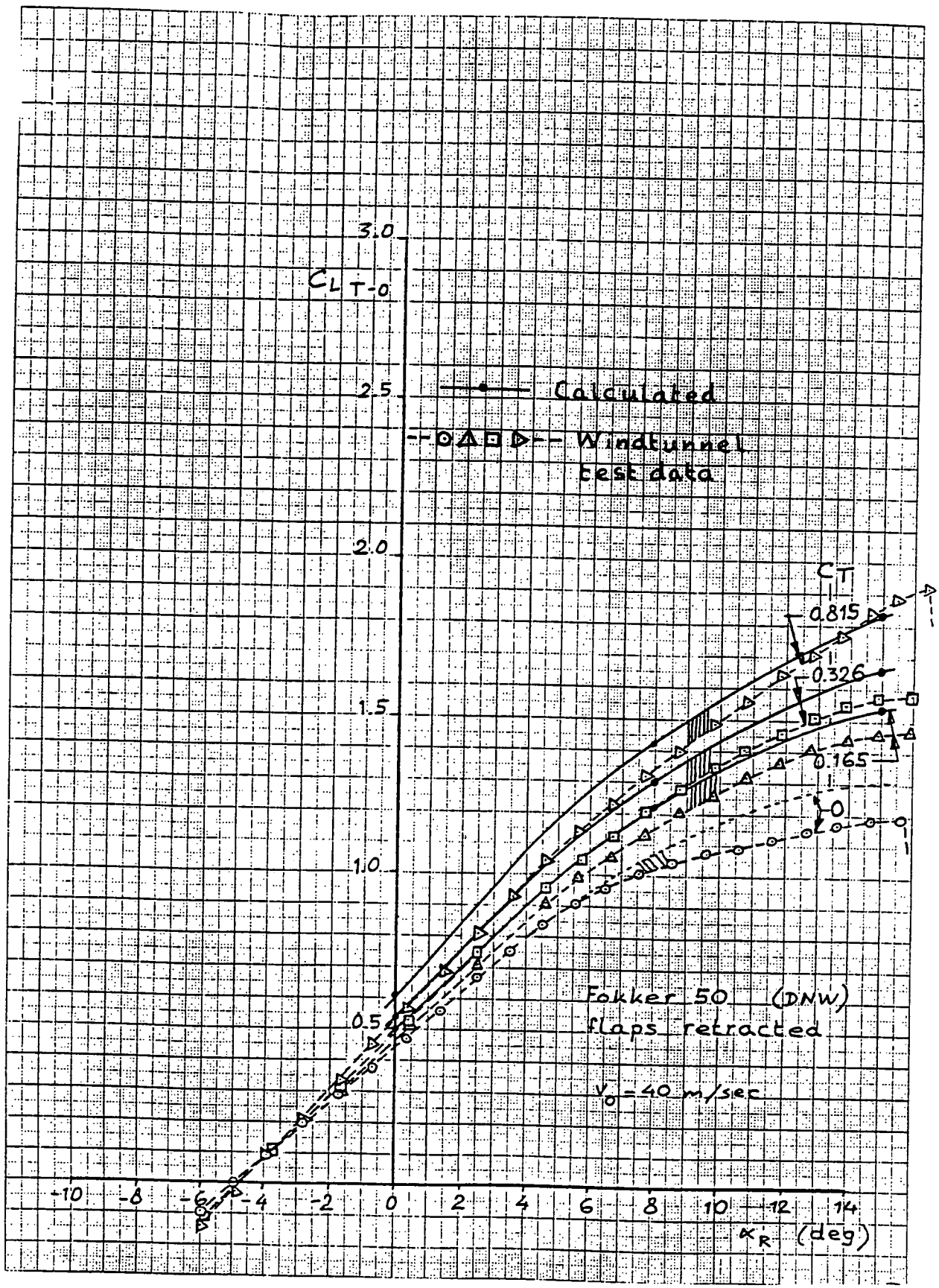
3.0
$C_{L\,T-0}$
2.5
Calculated
Windtunnel test data
2.0
C_T
0.815
0.326
0.165
0
1.5
1.0
0.5
Fokker 50 (DNW)
flaps retracted
V_0 = 40 m/sec
-10
-8
-6
-4
-2
0
2
4
6
8
10
12
14
α_R (deg)

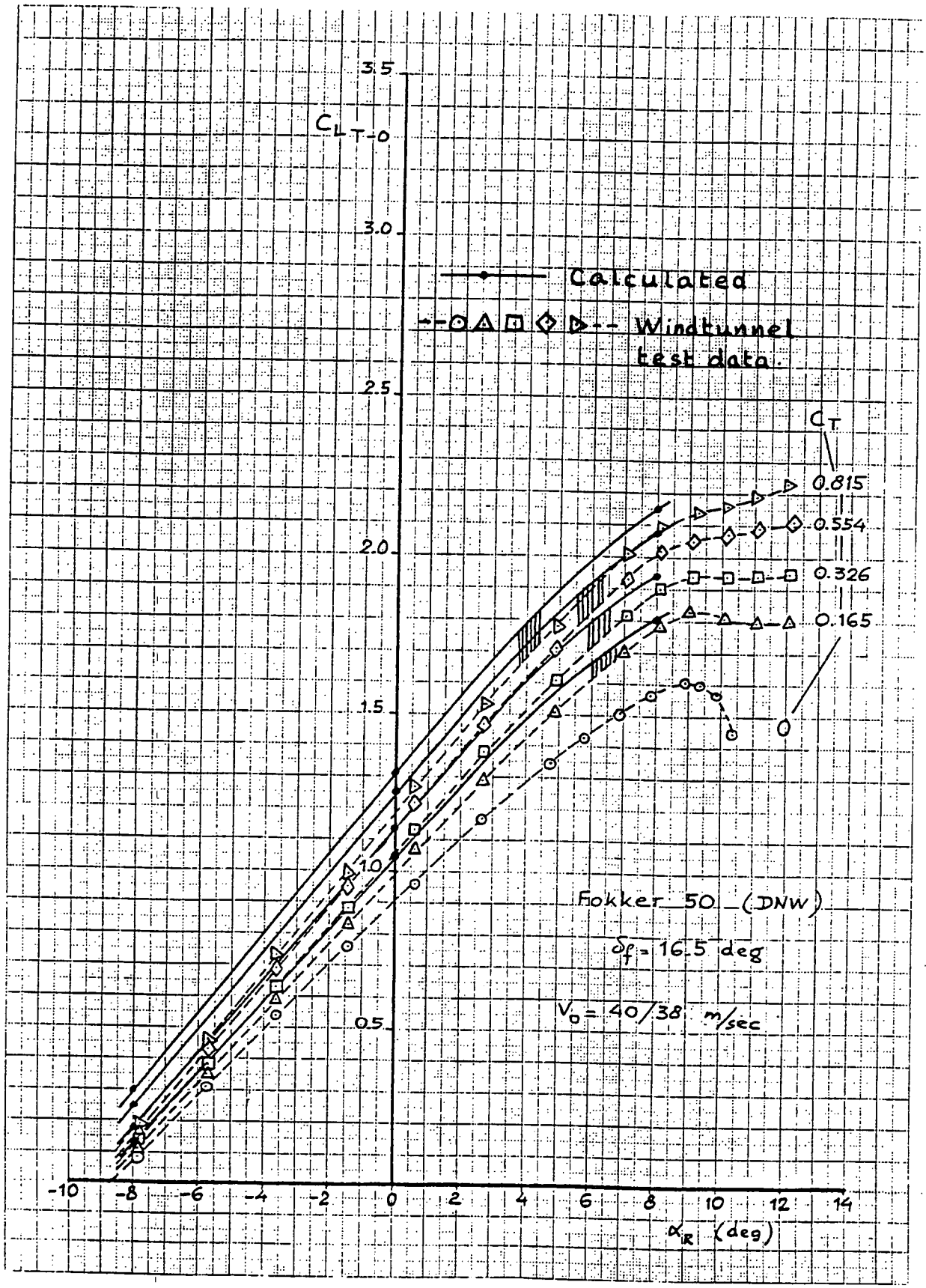
$C_{L_{T=0}}$
3.5
3.0
2.5
2.0
1.5
1.0
0.5
Calculated
Windtunnel test data.
C_T
0.815
0.554
0.326
0.165
0
Fokker 50 (DNW)
δ_f = 16.5 deg
V_0 = 40/38 m/sec
-10
-8
-6
-4
-2
0
2
4
6
8
10
12
14
α_R (deg)

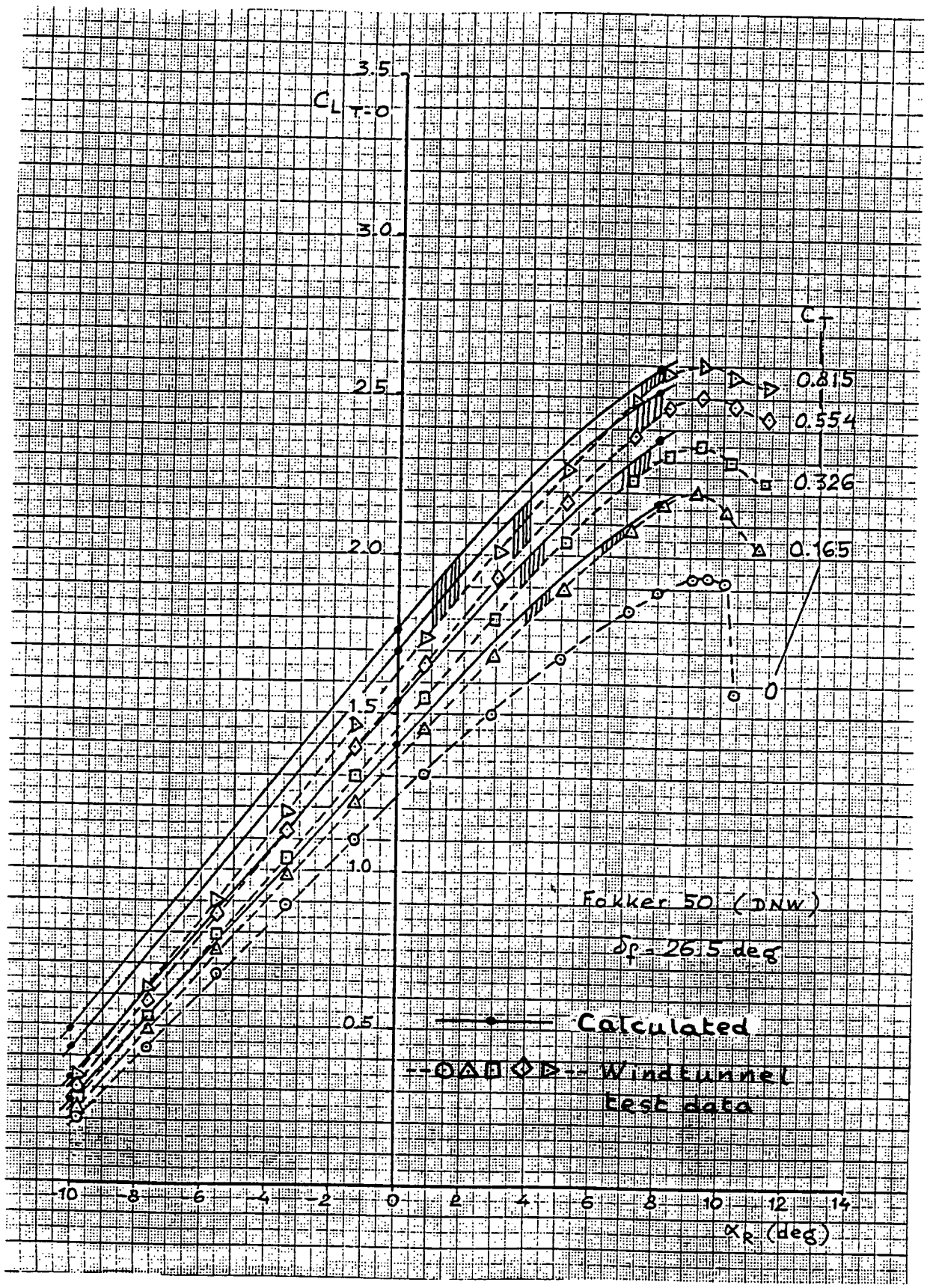
$C_{L_{T=0}}$
3.5
3.0
2.5
2.0
1.5
1.0
0.5
C_T
0.815
0.554
0.326
0.165
0
Fokker 50 (DNW)
δ_f = 26.5 deg
Calculated
Windtunnel test data
-10
-8
-6
-4
-2
0
2
4
6
8
10
12
14
α_R (deg)

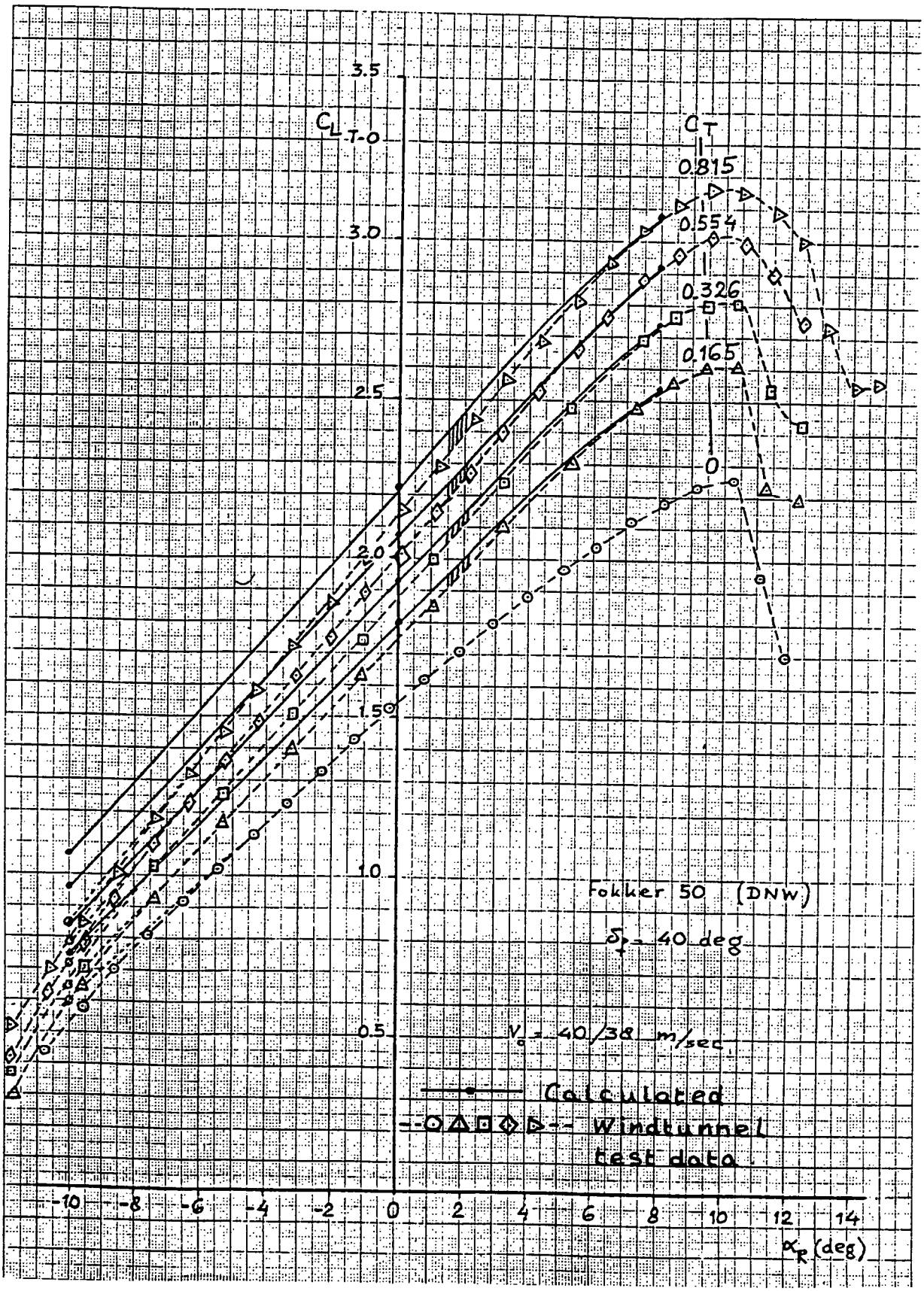
$C_{L\_T\text{-}O}$
C_T
0.815
0.554
0.326
0.165
0
3.5
3.0
2.5
2.0
1.5
1.0
0.5
-10
-8
-6
-4
-2
0
2
4
6
8
10
12
14
α_R (deg)
Fokker 50 (DNW)
δ_f = 40 deg
V_o = 40/38 m/sec
Calculated
Windtunnel test data

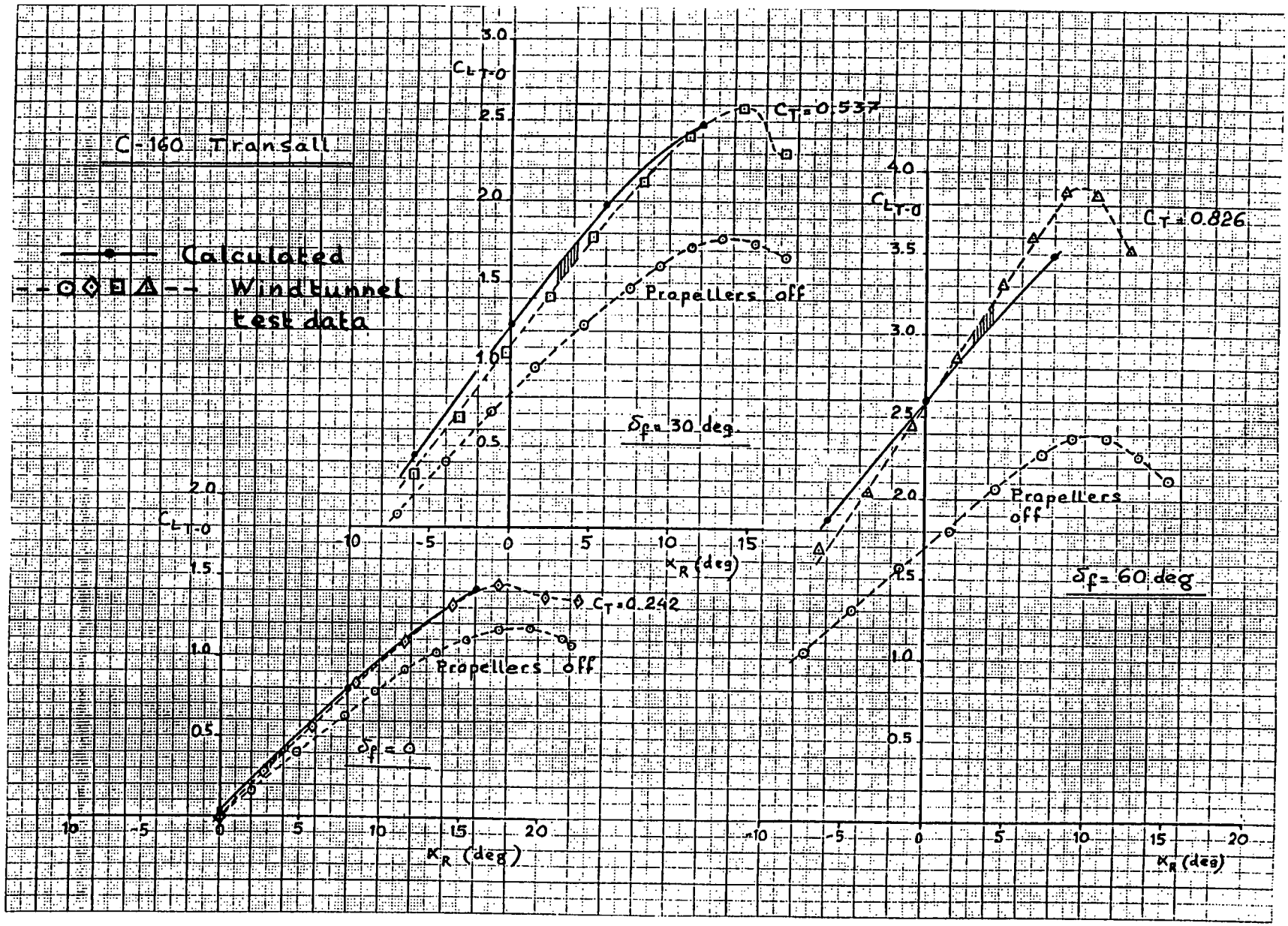
C-160 Transall
Calculated
Windtunnel test data
$C_{L_{T-O}}$
$C_T = 0.537$
$C_T = 0.826$
$C_T = 0.242$
Propellers off
$\delta_f = 30$ deg
$\delta_f = 60$ deg
$\delta_f = 0$
κ_R (deg)

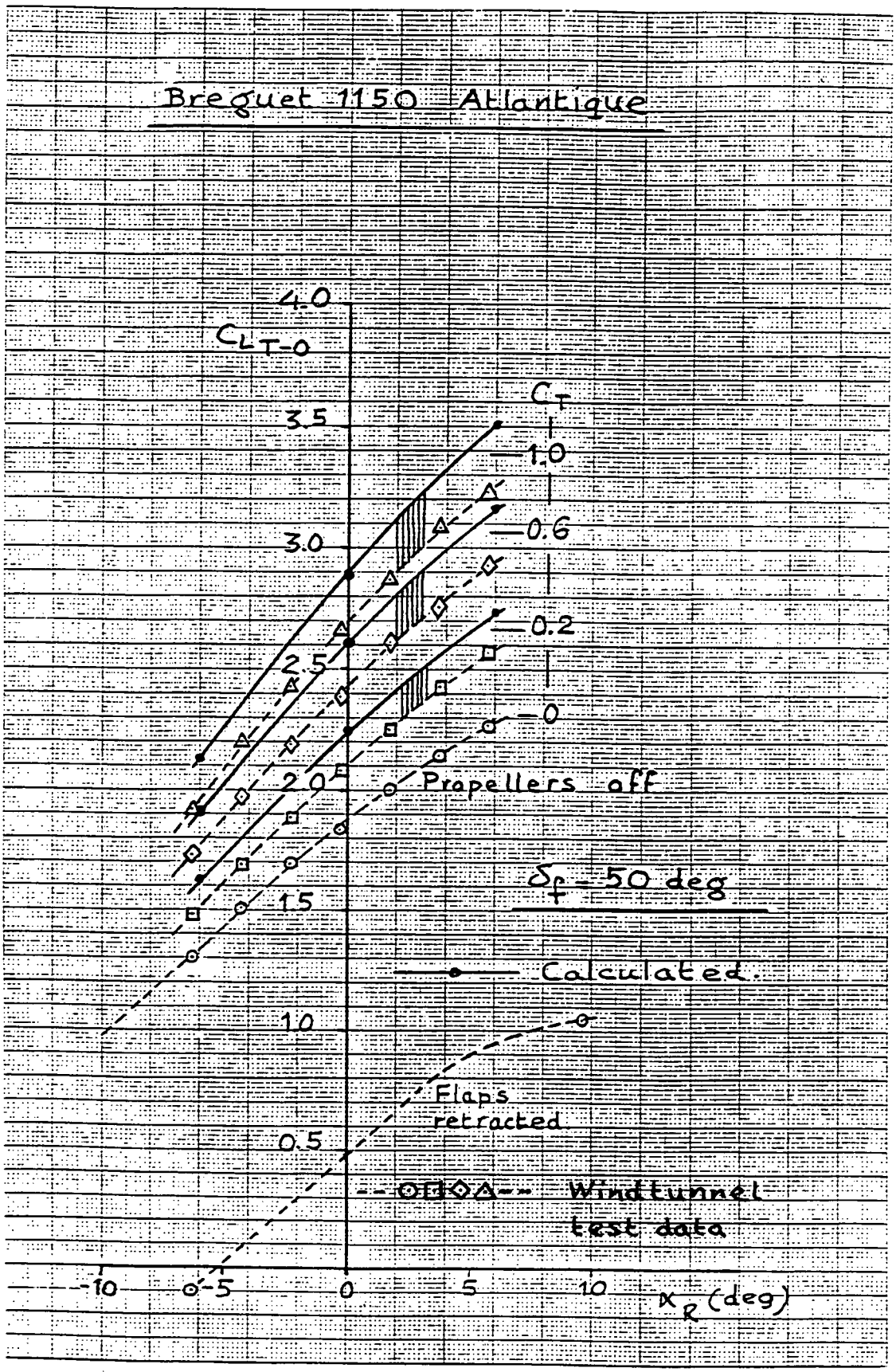
Breguet 1150 Atlantique
4.0
$C_{L_{T-O}}$
3.5
3.0
2.5
2.0
1.5
1.0
0.5
C_T
1.0
0.6
0.2
0
Propellers off
$\delta_f = 50$ deg
Calculated.
Flaps retracted
Windtunnel test data
-10
-5
0
5
10
α_R (deg)

Appendix IX

Tail-off Pitching Moment Coefficient ($\delta_f \neq 0$)

The following equations were used:

$$(C_{M_s} = \Delta C_{M_s})$$

$$C_{M_s} = \frac{C'}{\bar{C}}\left(-0.25 + 0.32\,\frac{Cf}{C'}\right)\left[1 + 0.2\left(1 - \sqrt{2}\,\sin\delta_f\right)\right]\Delta C_{L_{s,o}} +$$

$$+\left[-0.25\left(\frac{C'}{\bar{C}} - 1\right) + \frac{X_{CG} - X_{0.25CS}}{\bar{C}}\right] x\,\Delta C_{L_{s,\alpha}} +$$

$$+\frac{X_{CG} - X_{prop}}{\bar{C}}\,C_{L_p} - \frac{Z_T - Z_{CG}}{\bar{C}}\,C_T$$

$$-\left[0.05 + 0.5\left(\frac{C'}{\bar{C}} - 1\right)\right]\Delta C_{L_{s,\alpha}} \qquad (74)$$

Or:

$$C_{M_s} = E \times \Delta C\text{-}L_{S,\alpha} + F \times \Delta C_{L_{s,\alpha}} + G \times C_{L_p}$$

with:

$$E:\ \frac{C'}{\bar{C}}\left(-0.25 + 0.32\,\frac{C_f}{C'}\right)\left[1 + 0.2\left(1 - \sqrt{2}\,\sin\delta_f\right)\right] \qquad (62)$$

$$F = \left[-0.25\left(\frac{C'}{\bar{C}} - 1\right) + \frac{X_{CG} - 0.25}{\bar{C}}\right] \qquad (67)$$

$$G = \frac{X_{CG} - X_{prop}}{\bar{C}} \qquad (68)$$

$$H = \frac{Z_T - Z_{CG}}{\bar{C}} \qquad (69)$$

$$C_M = (C_M)_{C_{T=0}} + C_{M_S} \qquad (C_{M_S} = \Delta C_{M_S}) \qquad (78)$$

at constant α

$(C_M)_{C_{T=0}}$	(76)
$\frac{C'}{C}$	(7)
$\frac{C_f}{C'}$	(61)
δ_f	(5)
$\Delta C_{L_{s,o}}$	(64)
$\Delta C_{L_{s,\alpha}}$	(65)
$X_{CG}/\overline{C}$	(66)
C_{L_p}	(37)
C_T	(26)

Encircled numbers (X Y) denote columns in tables where actual values are presented.

Comparison of five different single slotted flaps.
The lift and pitching moment increments at $\alpha = 0$.

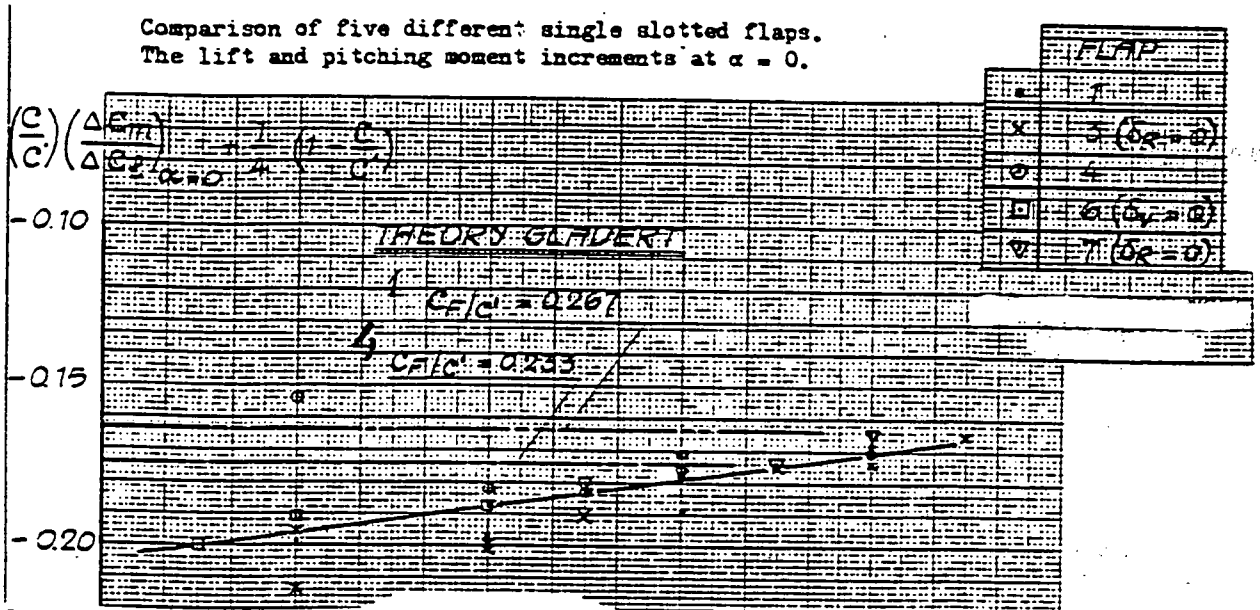

Influence of the rear flap deflection of flap 3 on the lift and the pitching moment increment at $\alpha = 0$.

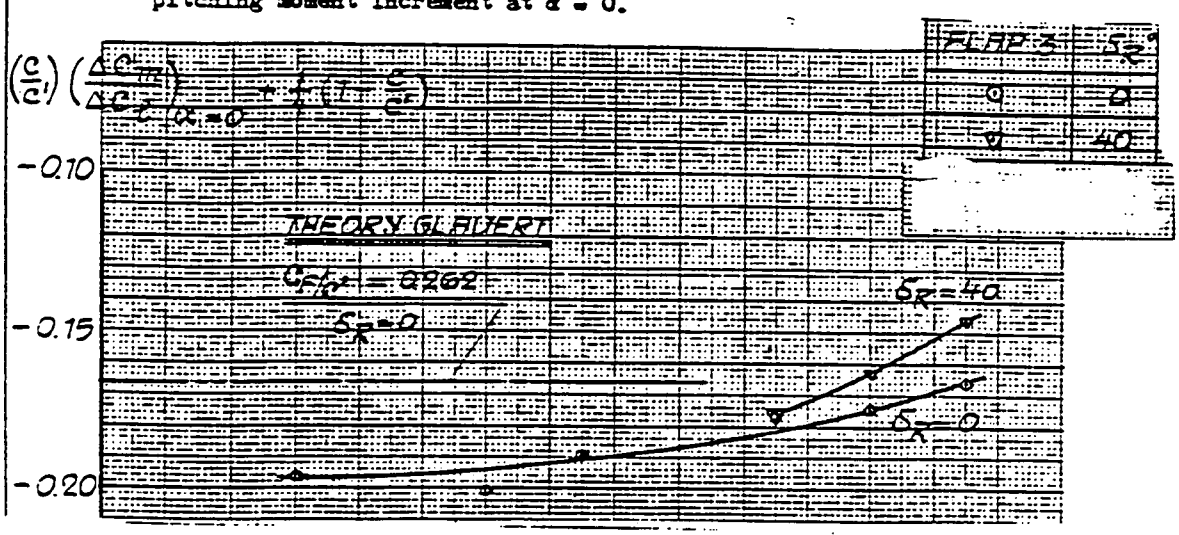

The influence of the vane angle (δ_V) of flap 5 on the lift and the pitching moment increments at $\alpha = 0$.

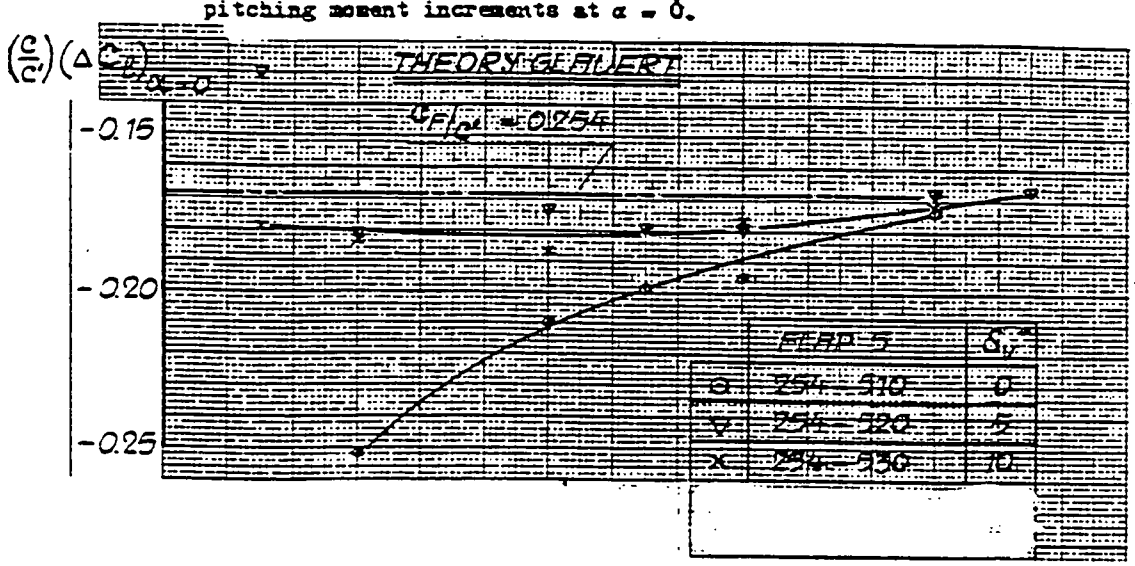

The influence of the vane deflection of flap 6 on the lift and the pitching moment increments at $\alpha = 0$.

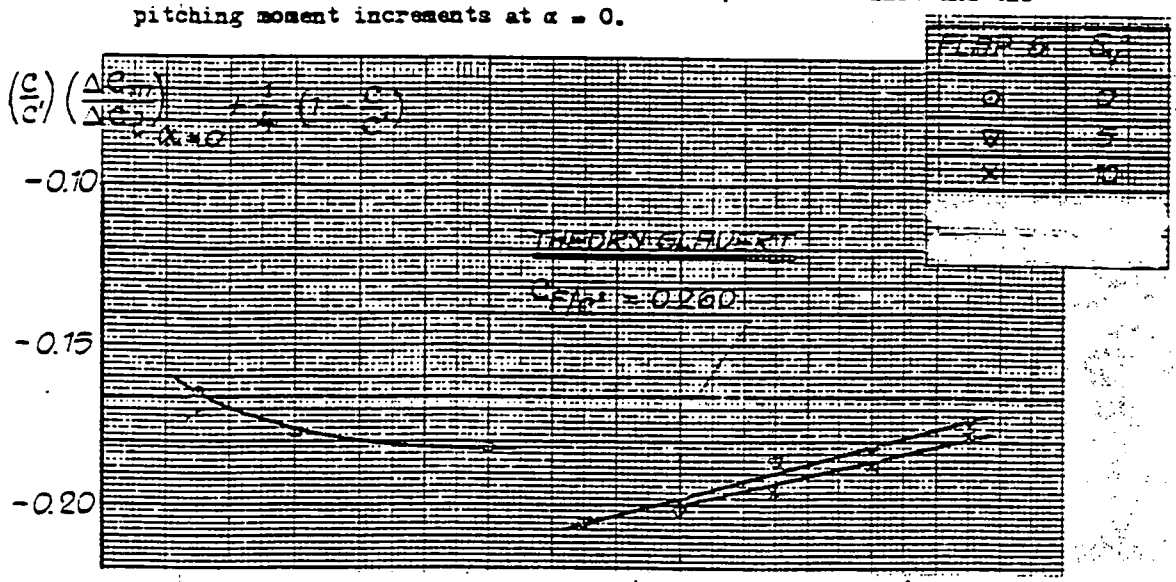

The influence of the rear flap deflection of flap 7 on the lift and the pitching moment increments at $\alpha = 0$.

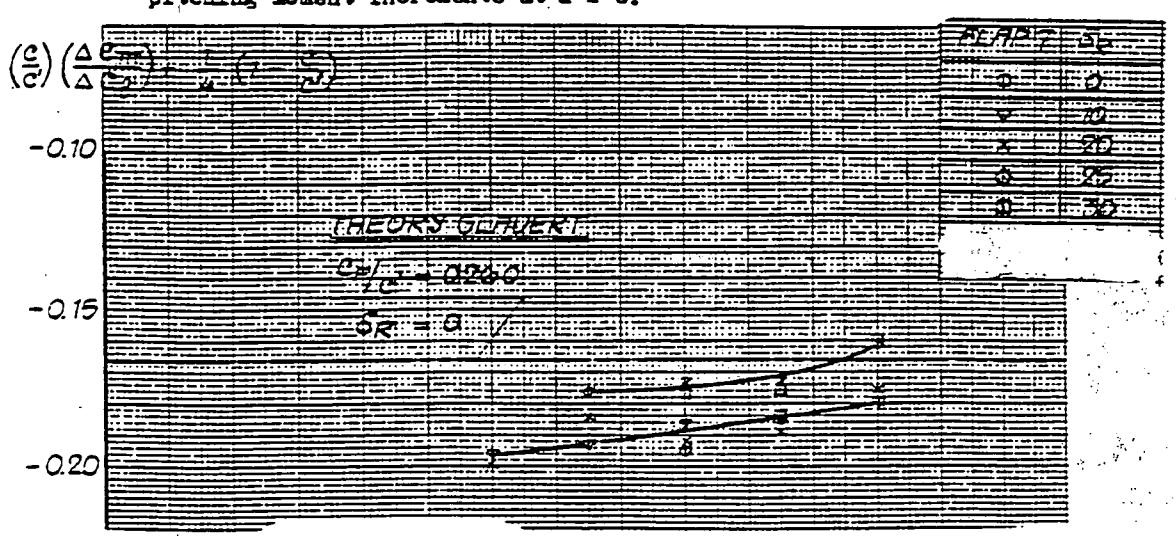

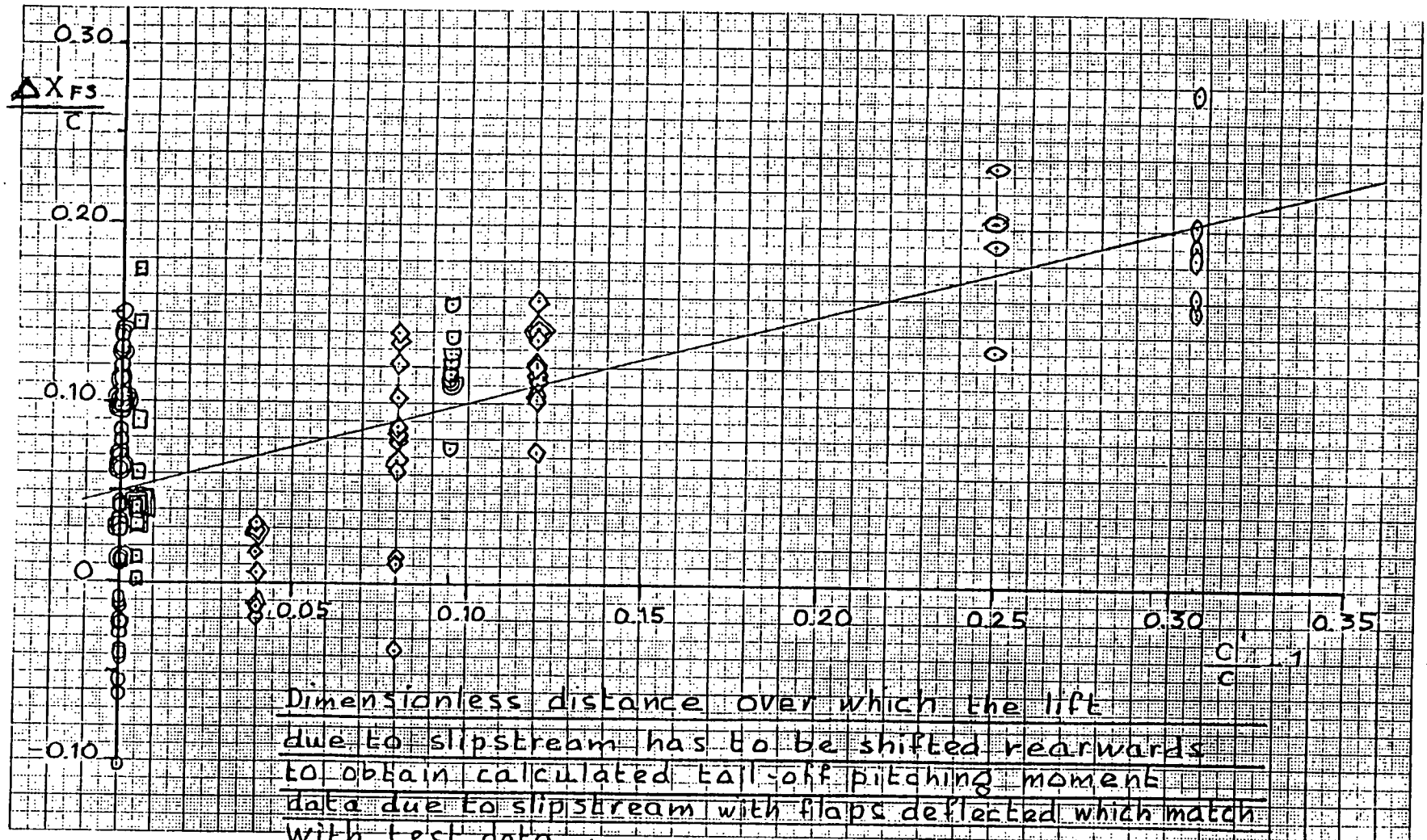

Dimensionless distance over which the lift due to slipstream has to be shifted rearwards to obtain calculated tail off pitching moment data due to slipstream with flaps deflected which match with test data.

Table IV Pitching Moment Coefficient

No.	Conf	C_T (26)	$\frac{C'}{C}$ (7)	$\frac{C_f}{C}$ (6)	$\frac{C_f}{C'}$ (61)	δ_f (deg) (5)	E (62)	α_R (deg) (13)	α_{000} (deg) (63)	$\Delta C_{L_{\delta 0}}$ (at α_{000}) (64)	$\Delta C_{L_{\delta,\alpha}}$ (65)	$\frac{X_{CG}}{\bar{C}}$ (66)	F (67)	$\frac{X_{CG}-X_p}{\bar{C}} = G$ (68)	C_{L_p} (37)	$\frac{Z_T - Z_{CG}}{\bar{C}} = H$ (69)
1	NASA TN D-25	0.15	1.00	0.25	0.25	40	-0.1731	-8.0	-6.5	0.218	0.210	0.250	0	0.92	-0.008	0
								0			0.251				0.008	
								8.0			0.285				0.023	
		0.15	1.00	0.25	0.25	40	-0.1731	12.0	-6.5	0.218	0.301	0.250	0	0.92	0.031	0
		0.75	1.00	0.25	0.25	40	-0.1731	-8.0	-6.5	0.686	0.662	0.250	0	0.92	-0.010	0
								0			0.791				0.010	
								8.0			0.911				0.031	
		0.75	1.00	0.25	0.25	40	-0.1731	12.0	-6.5	0.686	0.967	0.250	0	0.92	0.041	0
		1.15	1.00	0.25	0.25	40	-0.1731	-8.0	-6.5	0.912	0.883	0.250	0	0.92	-0.011	0
								0			1.037				0.011	
								8.0			1.182				0.034	
		1.15	1.00	0.25	0.25	40	-0.1731	12.0	-6.5	0.912	1.251	0.250	0	0.92	0.045	0
		1.55	1.00	0.25	0.25	40	-0.1731	-8.0	-6.5	1.132	1.099	0.250	0	0.92	-0.012	0
								0			1.277				0.012	
								8.0			1.444				0.037	
		1.55	1.00	0.25	0.25	40	-0.1731	12.0	-6.5	1.132	1.524	0.250	0	0.92	0.049	0
		2.15	1.00	0.25	0.25	40	-0.1731	-8.0	-6.5	1.460	1.421	0.250	0	0.92	-0.014	0
								0			1.629				0.014	
								8.0			1.824				0.041	
		2.15	1.00	0.25	0.25	40	-0.1731	12.0	-6.5	1.460	1.921	0.250	0	0.92	0.054	0
		3.10	1.00	0.25	0.25	40	-0.1731	-8.0	-6.5	2.496	2.442	0.250	0	0.92	-0.017	0
								0			2.728				0.017	
								8.0			3.001				0.050	
		3.10	1.00	0.25	0.25	40	-0.1731	12.0	-6.5	2.496	3.133	0.250	0	0.92	0.067	0
1	NASA TN D-25	0.15	1.00	0.25	0.25	$40/\sqrt{30}$	-0.1731	-8.0	-6.5	0.172	0.165	0.250	0	0.92	-0.002	0
								0			0.203				0.014	
		0.15	1.00	0.25	0.25	$40/\sqrt{30}$	-0.1731	8.0	-6.5	0.172	0.244	0.250	0	0.92	0.029	0
		0.3													-0.002	0
		0.3													0.018	
		1.1													0.039	0
															-0.002	0
		1.15	1.00	0.25	0.25	$40/\sqrt{30}$	-0.1731	8.0	-6.5	0.875	1.149	0.250	0	0.92	0.021	
															0.043	0

Example of calculating procedure

Table IV Pitching Moment Coefficient (Concluded)

No	Conf	δ_f (deg) (5)	α_R (deg) (19)	C_T (26)	$\Delta C'_{m_S}$ (70)	$\left(\frac{\Delta x_{FS}}{\bar{c}}\right)^*_{TEST}$ (71)	$\frac{\Delta x_{FS}}{\bar{c}}_{CALC.}$ (72)	$\Delta C_{m_{FS}}$ CALC. (73)	C_{m_S} calc. (74)	C_{m_S} TEST (75)	C_m $C_{T=0}$ TEST (76)	C_L $C_{T=0}$ TEST (38)	C_m TEST (77)	C_L TEST (39)	C_m calc (78)	C_L calc (57)
1	NASA TN D-25	40	-8.0	0.15	-0.045	(-0.452)	0.050	-0.011	-0.056	+0.05	-0.26	0.42	-0.21	0.47	-0.316	0.601
			0		-0.030	(-0.398)		-0.013	-0.043	+0.07	-0.17	1.15	-0.10	1.34	-0.213	1.409
			8.0		-0.017	(-0.235)		-0.014	-0.031	+0.05	-0.05	1.85	0	2.14	-0.081	2.179
		40	12.0	0.15	-0.009	(-0.096)	0.050	-0.015	-0.024	+0.02	+0.04	2.22	+0.06	2.58	+0.016	2.583
		40	-8.0	0.75	-0.128	-0.102	0.050	-0.033	-0.161	-0.06	-0.26	0.42	-0.32	0.80	-0.421	0.968
			0		-0.110	+0.013		-0.040	-0.150	-0.12	-0.17	1.15	-0.29	1.92	-0.320	1.951
			8.0		-0.090	+0.011		-0.046	-0.136	-0.10	-0.05	1.85	-0.15	2.92	-0.186	2.896
		40	12.0	0.75	-0.081	-0.022	0.050	-0.048	-0.129	-0.06	+0.04	2.22	-0.02	3.30	-0.089	3.384
		40	-8.0	1.15	-0.168	-0.054	0.050	-0.044	-0.212	-0.12	-0.26	0.42	-0.38	1.00	-0.472	1.132
			0		-0.148	-0.008		-0.052	-0.200	-0.14	-0.17	1.15	-0.31	2.23	-0.370	2.198
			8.0		-0.126	-0.039		-0.059	-0.185	-0.08	-0.05	1.85	-0.13	3.36	-0.235	3.226
		40	12.0	1.15	-0.116	-0.061	0.050	-0.063	-0.179	-0.04	+0.04	2.22	0	3.86	-0.139	3.755
		40	-8.0	1.55	-0.207	+0.012	0.050	-0.055	-0.262	-0.22	-0.26	0.42	-0.48	1.25	-0.522	1.291
			0		-0.185	+0.043		-0.064	-0.249	-0.24	-0.17	1.15	-0.41	2.55	-0.419	2.439
			8.0		-0.162	-0.022		-0.072	-0.234	-0.13	-0.05	1.85	-0.18	3.82	-0.284	3.546
		40	12.0	1.55	-0.151	-0.027	0.050	-0.076	-0.227	-0.11	+0.04	2.22	-0.07	4.37	-0.187	4.115
		40	-8.0	2.15	-0.268	-0.013	0.050	-0.071	-0.339	-0.25	-0.26	0.42	-0.51	1.55	-0.599	1.528
			0		-0.237	+0.014		-0.081	-0.318	-0.26	-0.17	1.15	-0.43	2.95	-0.488	2.792
			8.0		-0.215	-0.036		-0.091	-0.306	-0.15	-0.05	1.85	-0.20	4.34	-0.356	4.027
		40	12.0	2.15	-0.203	-0.043	0.050	-0.096	-0.299	-0.12	+0.04	2.22	-0.08	4.88	-0.259	4.642
		40	-8.0	4.10	-0.448	+0.079	0.050	-0.122	-0.570	-0.64	-0.26	0.42	-0.90	2.35	-0.830	2.274
			0		-0.416	+0.063		-0.136	-0.552	-0.59	-0.17	1.15	-0.76	3.95	-0.722	3.894
			8.0		-0.386	+0.045		-0.150	-0.536	-0.52	-0.05	1.85	-0.57	5.55	-0.586	5.472
		40	12.0	4.10	-0.370	+0.029	0.050	-0.157	-0.527	-0.46	+0.04	2.22	-0.42	6.30	-0.487	6.272
1	NASA TN D-25	40/$\frac{\delta_f}{130}$	-8.0	0.15	-0.032	(0.353)	0.050	-0.008	-0.040	-0.09	-0.40	1.50	-0.49	1.60	-0.440	1.642
			0		-0.017	(0.262)		-0.010	-0.027	-0.07	-0.33	2.30	-0.40	2.55	-0.357	2.517
		40/$\frac{\delta_f}{130}$	8.0	0.15	-0.003	(0.192)	0.050	-0.012	-0.015	-0.05	-0.18	2.85	-0.23	3.30	-0.195	3.144
		40/$\frac{\delta_f}{130}$	-8.0	0.75	-0.114	0.138	0.050	-0.031	-0.145	-0.20	-0.40	1.50	-0.60	1.92	-0.545	2.019
			0		-0.096	0.139		-0.038	-0.134	-0.20	-0.33	2.30	-0.53	3.12	-0.464	3.068
		40/$\frac{\delta_f}{130}$	8.0	0.75	-0.076	0.130	0.050	-0.044	-0.120	-0.19	-0.18	2.85	-0.37	4.12	-0.300	3.870
		40/$\frac{\delta_f}{130}$	-8.0	1.15	-0.153	0.150	0.050	-0.042	-0.195	-0.28	-0.40	1.50	-0.68	2.10	-0.595	2.184
			0		-0.132	0.128		-0.050	-0.182	-0.26	-0.33	2.30	-0.59	3.45	-0.512	3.319
		40/$\frac{\delta_f}{130}$	8.0	1.15	-0.112	0.103	0.050	-0.057	-0.169	-0.23	-0.18	2.85	-0.41	4.60	-0.349	4.202

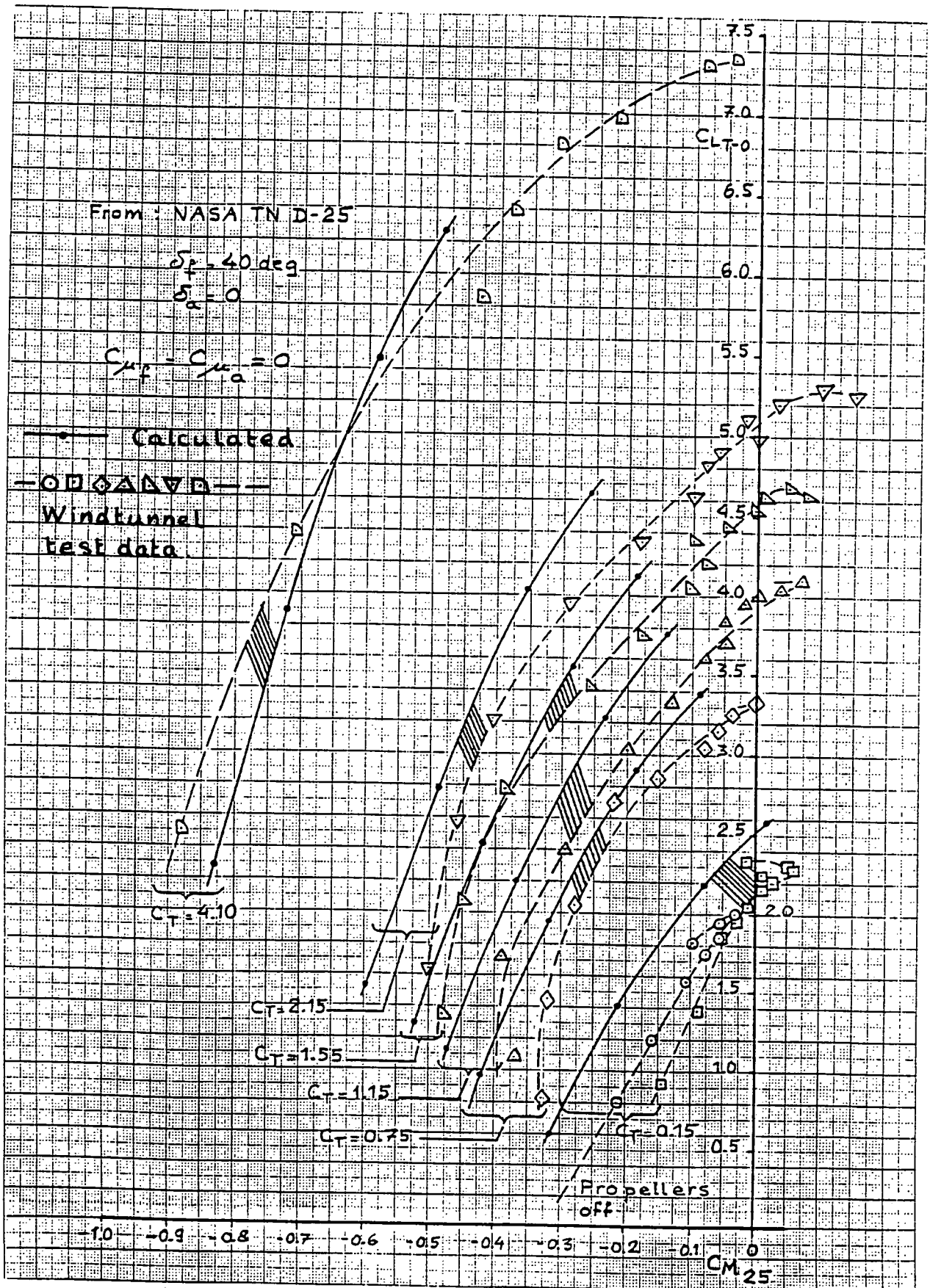
From : NASA TN D-25
δ_f = 40 deg
δ_a = 0
$C_{\mu_f} - C_{\mu_a} = 0$
Calculated
Windtunnel test data
$C_{L_{T=0}}$
C_T = 4.10
C_T = 2.15
C_T = 1.55
C_T = 1.15
C_T = 0.75
C_T = 0.15
Propellers off
$C_{M_{.25}}$
7.5
7.0
6.5
6.0
5.5
5.0
4.5
4.0
3.5
3.0
2.5
2.0
1.5
1.0
0.5
-1.0
-0.9
-0.8
-0.7
-0.6
-0.5
-0.4
-0.3
-0.2
-0.1
0

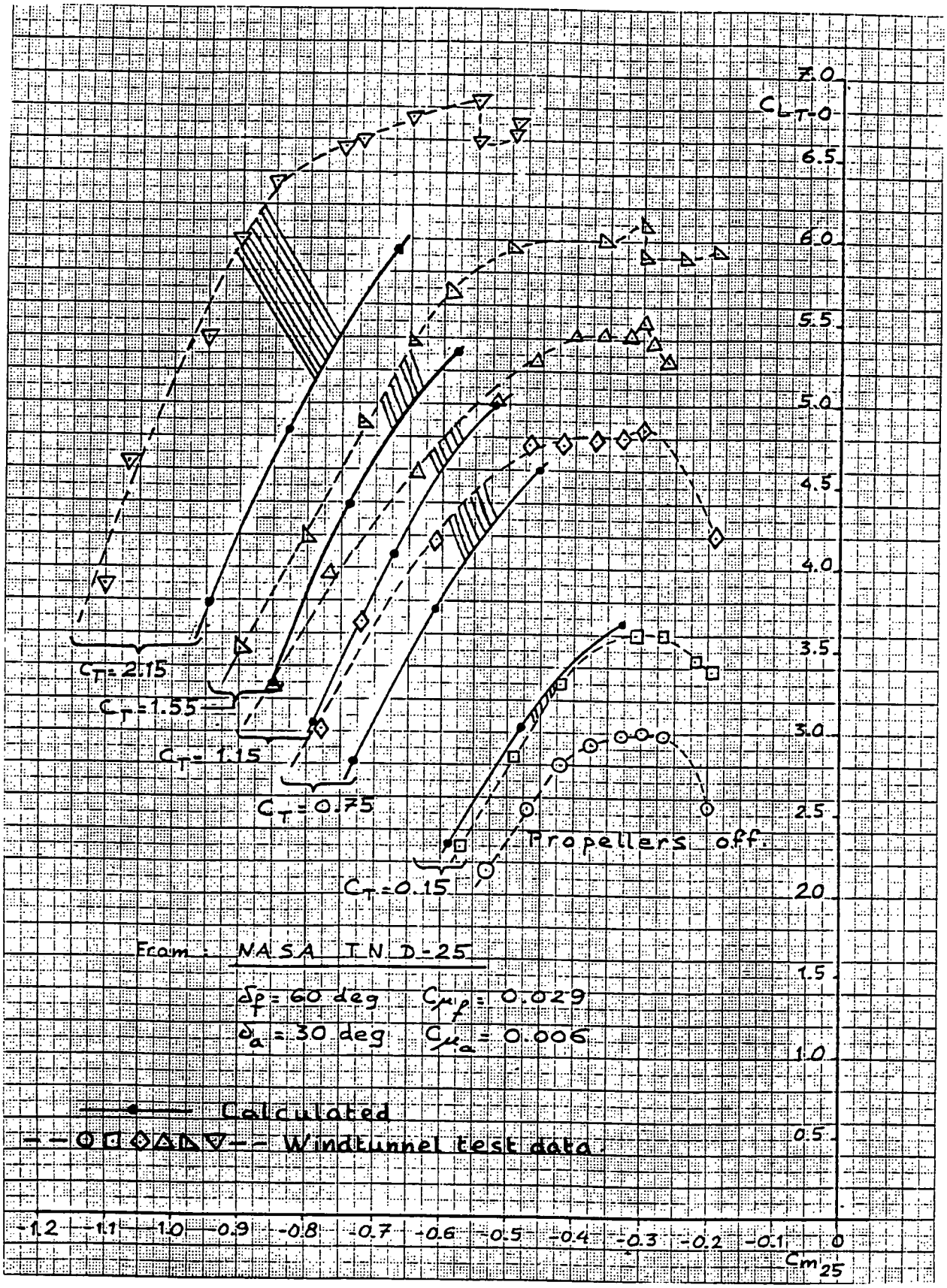
7.0
C_{L_T}-0
6.5
6.0
5.5
5.0
4.5
4.0
3.5
3.0
2.5
2.0
1.5
1.0
0.5
C_T=2.15
C_T=1.55
C_T=1.15
C_T=0.75
C_T=0.15
Propellers off.
From: NASA TND-25
δ_f = 60 deg C_{μ_f} = 0.029
δ_a = 30 deg C_{μ_a} = 0.006
Calculated
Windtunnel test data.
-1.2 -1.1 -1.0 -0.9 -0.8 -0.7 -0.6 -0.5 -0.4 -0.3 -0.2 -0.1 0
$C_{m_{25}}$

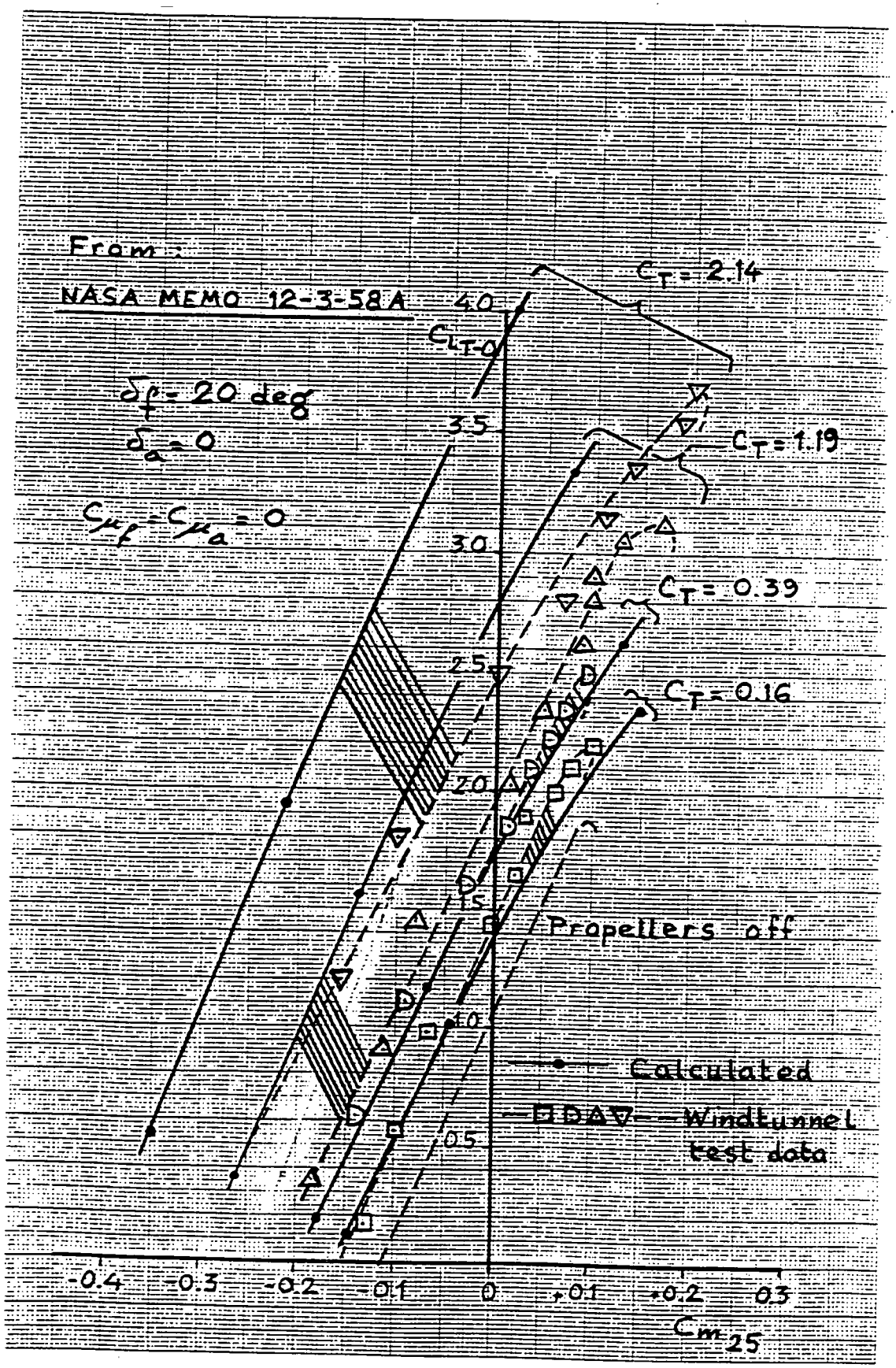
From:
NASA MEMO 12-3-58A
δ_f = 20 deg
δ_a = 0
$C_{\mu_f} = C_{\mu_a} = 0$
$C_{L_{T=0}}$
C_T = 2.14
C_T = 1.19
C_T = 0.39
C_T = 0.16
4.0
3.5
3.0
2.5
2.0
1.5
1.0
0.5
Propellers off
Calculated
Windtunnel test data
-0.4
-0.3
-0.2
-0.1
0
+0.1
+0.2
0.3
$C_{m_{25}}$

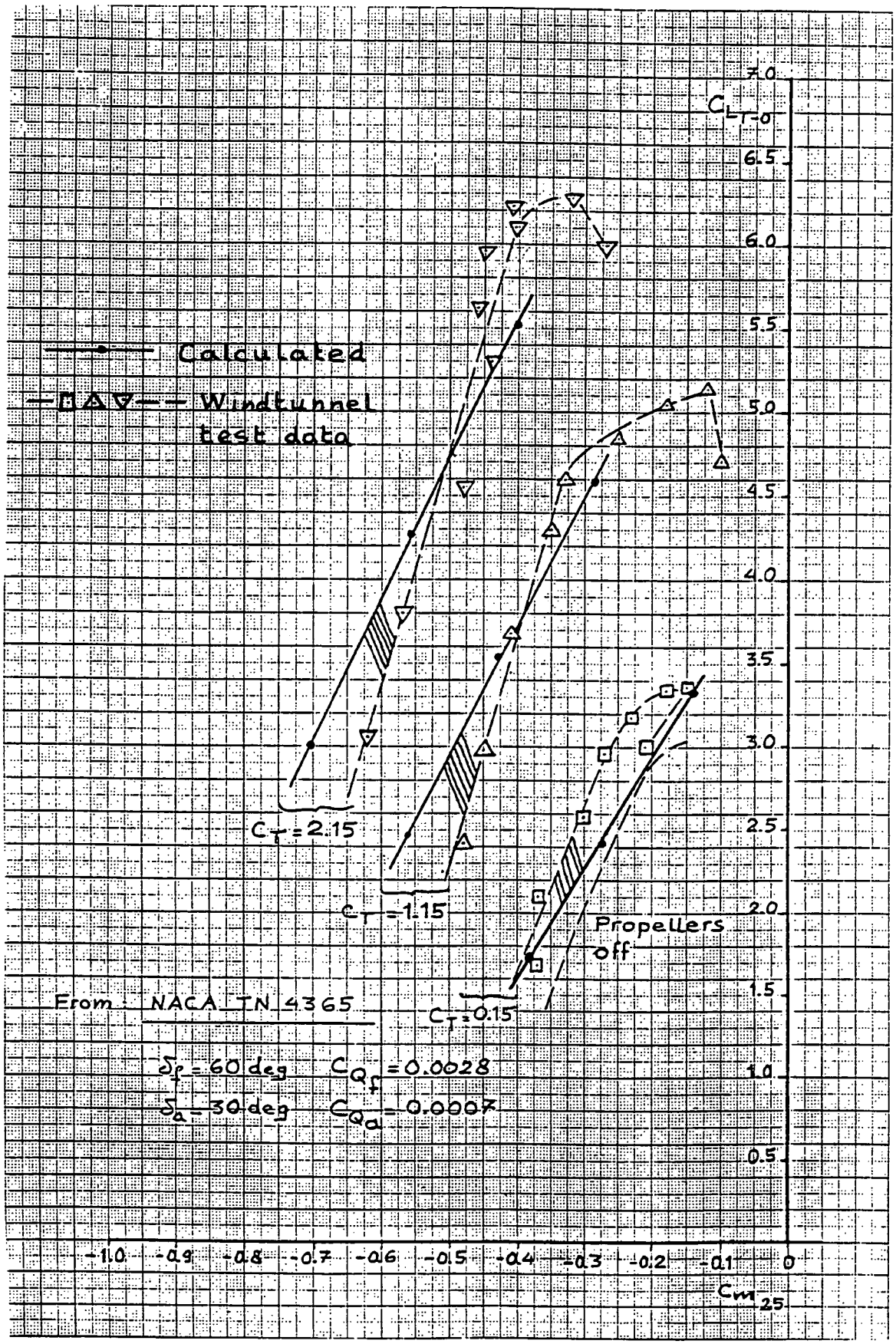
Calculated
Windtunnel test data
$C_{L_{T-0}}$
7.0
6.5
6.0
5.5
5.0
4.5
4.0
3.5
3.0
2.5
2.0
1.5
1.0
0.5
$C_T = 2.15$
$C_T = 1.15$
$C_T = 0.15$
Propellers off
From: NACA TN 4365
$\delta_f = 60$ deg $C_{Q_f} = 0.0028$
$\delta_a = 30$ deg $C_{Q_a} = 0.0007$
-1.0 -0.9 -0.8 -0.7 -0.6 -0.5 -0.4 -0.3 -0.2 -0.1 0
$C_{m_{.25}}$

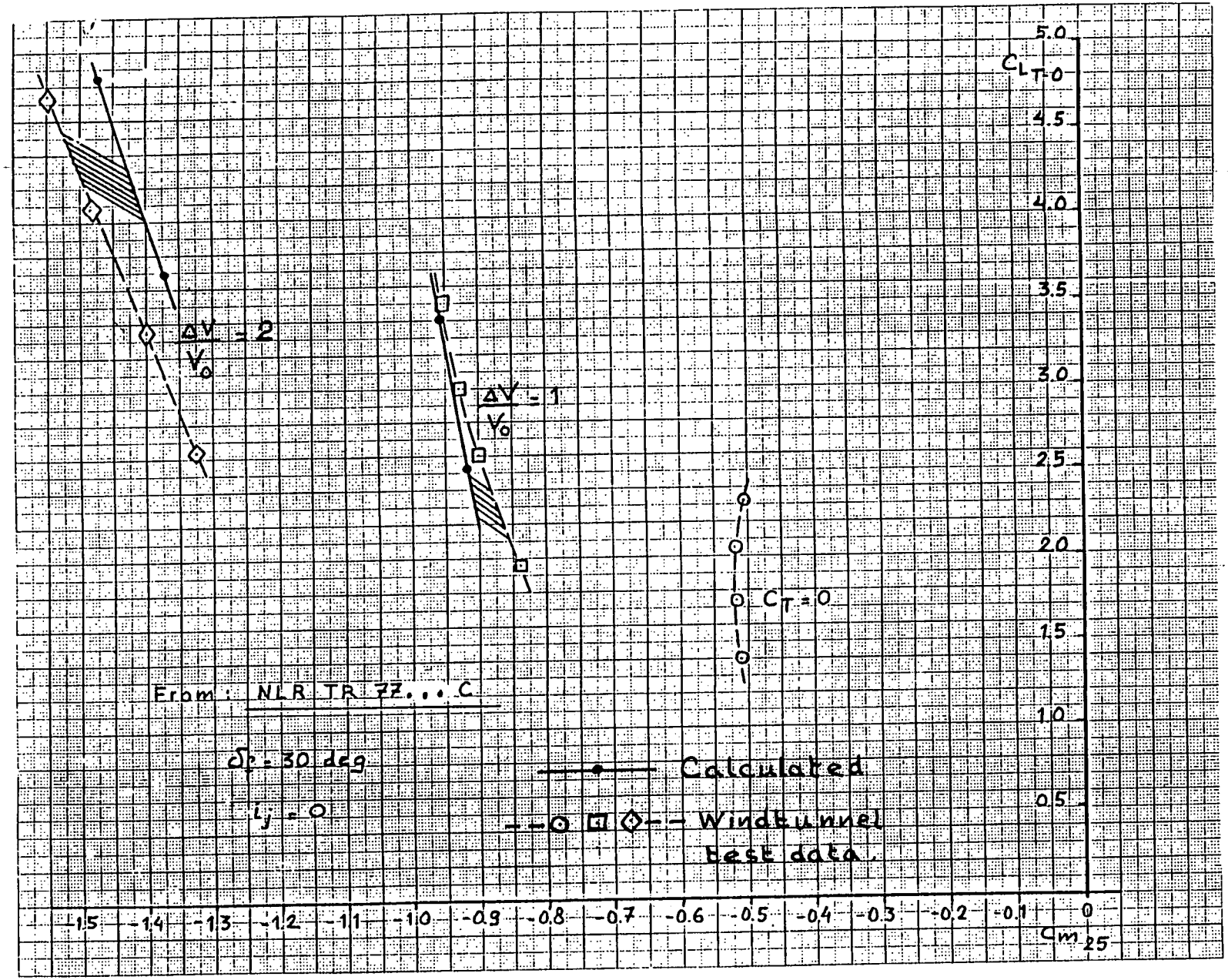
5.0
$C_{L_{T=0}}$
4.5
4.0
3.5
3.0
2.5
2.0
1.5
1.0
0.5
$\frac{\Delta V}{V_0} = 2$
$\frac{\Delta V}{V_0} = 1$
$C_T = 0$
From: NLR TR 77... C
$\delta_f = 30$ deg
$i_j = 0$
Calculated
Windtunnel test data.
-1.5 -1.4 -1.3 -1.2 -1.1 -1.0 -0.9 -0.8 -0.7 -0.6 -0.5 -0.4 -0.3 -0.2 -0.1 0
$C_{m_{25}}$

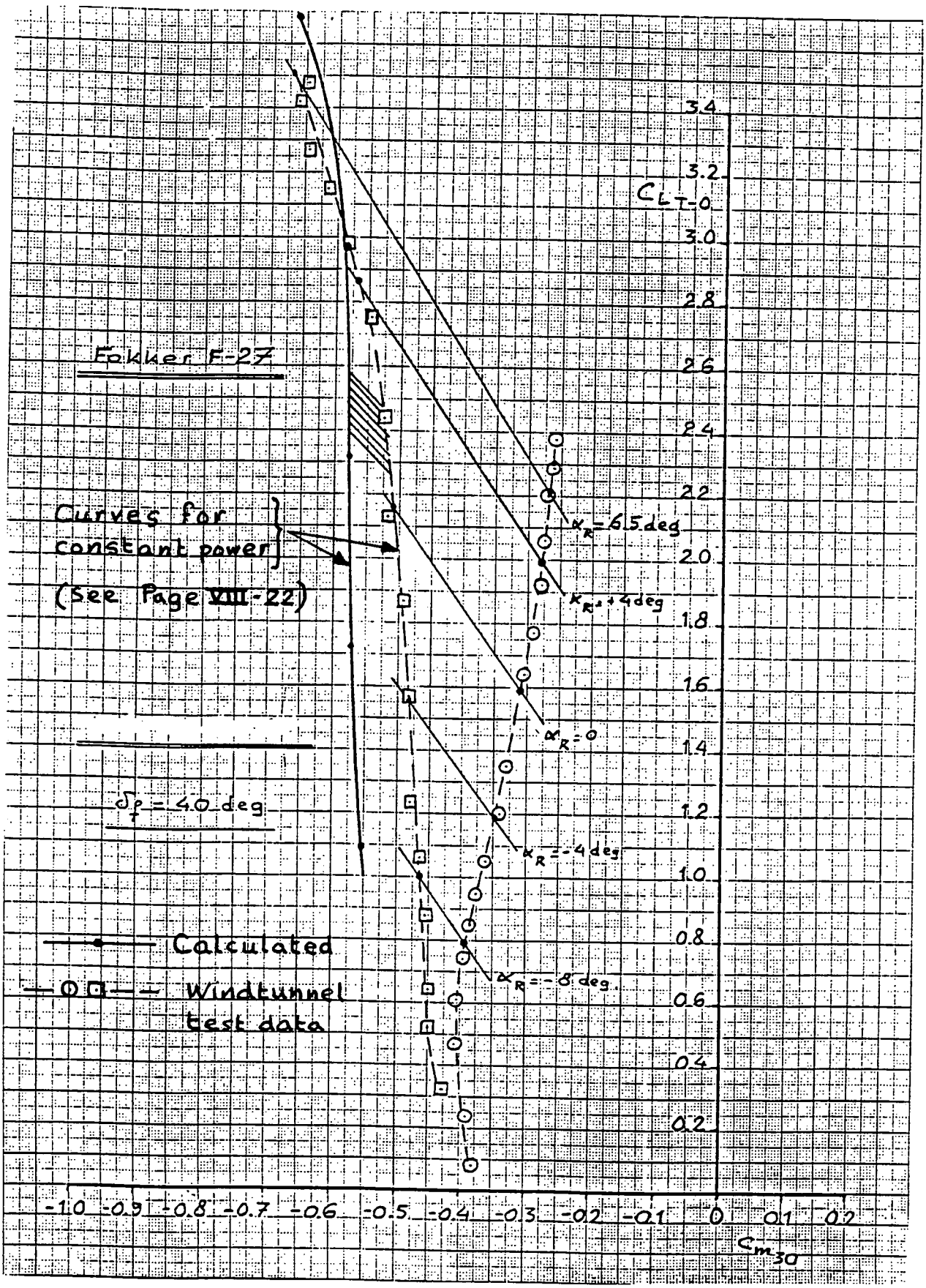
Fokker F-27
Curves for constant power
(See Page VIII-22)
δ_f = 40 deg
Calculated
Windtunnel test data
α_R = 6.5 deg
α_R = 4 deg
α_R = 0
α_R = -4 deg
α_R = -8 deg
$C_{L_{T-O}}$
3.4
3.2
3.0
2.8
2.6
2.4
2.2
2.0
1.8
1.6
1.4
1.2
1.0
0.8
0.6
0.4
0.2
-1.0 -0.9 -0.8 -0.7 -0.6 -0.5 -0.4 -0.3 -0.2 -0.1 0 0.1 0.2
$C_{m_{30}}$

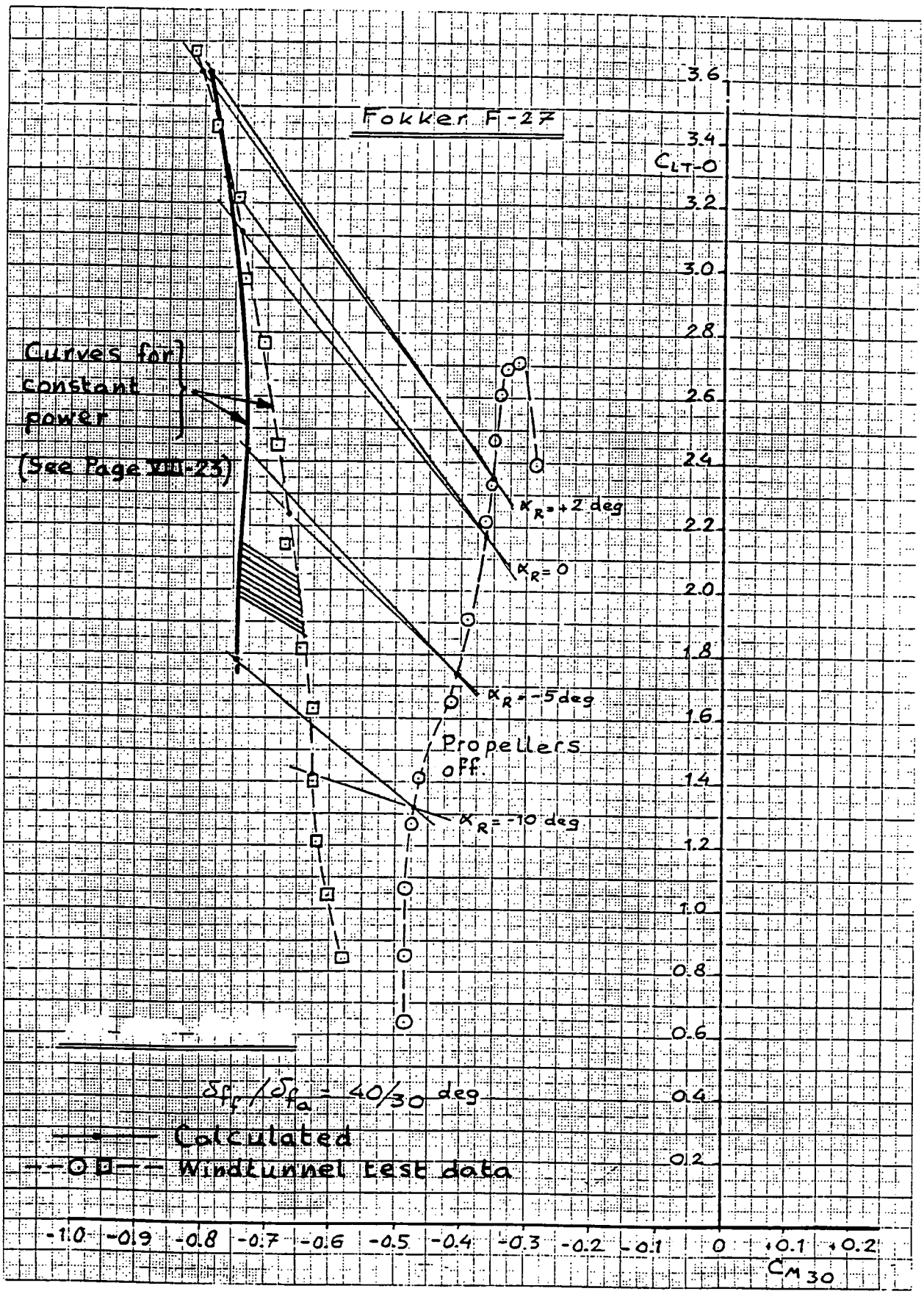
Fokker F-27
C_{LT-O}
3.6
3.4
3.2
3.0
2.8
2.6
2.4
2.2
2.0
1.8
1.6
1.4
1.2
1.0
0.8
0.6
0.4
0.2
Curves for constant power
(See Page IX-23)
$\alpha_R = +2$ deg
$\alpha_R = 0$
$\alpha_R = -5$ deg
Propellers off.
$\alpha_R = -10$ deg
$\delta f_f / \delta f_a = 40/30$ deg
Calculated
Windtunnel test data
-1.0 -0.9 -0.8 -0.7 -0.6 -0.5 -0.4 -0.3 -0.2 -0.1 0 +0.1 +0.2
C_{M30}

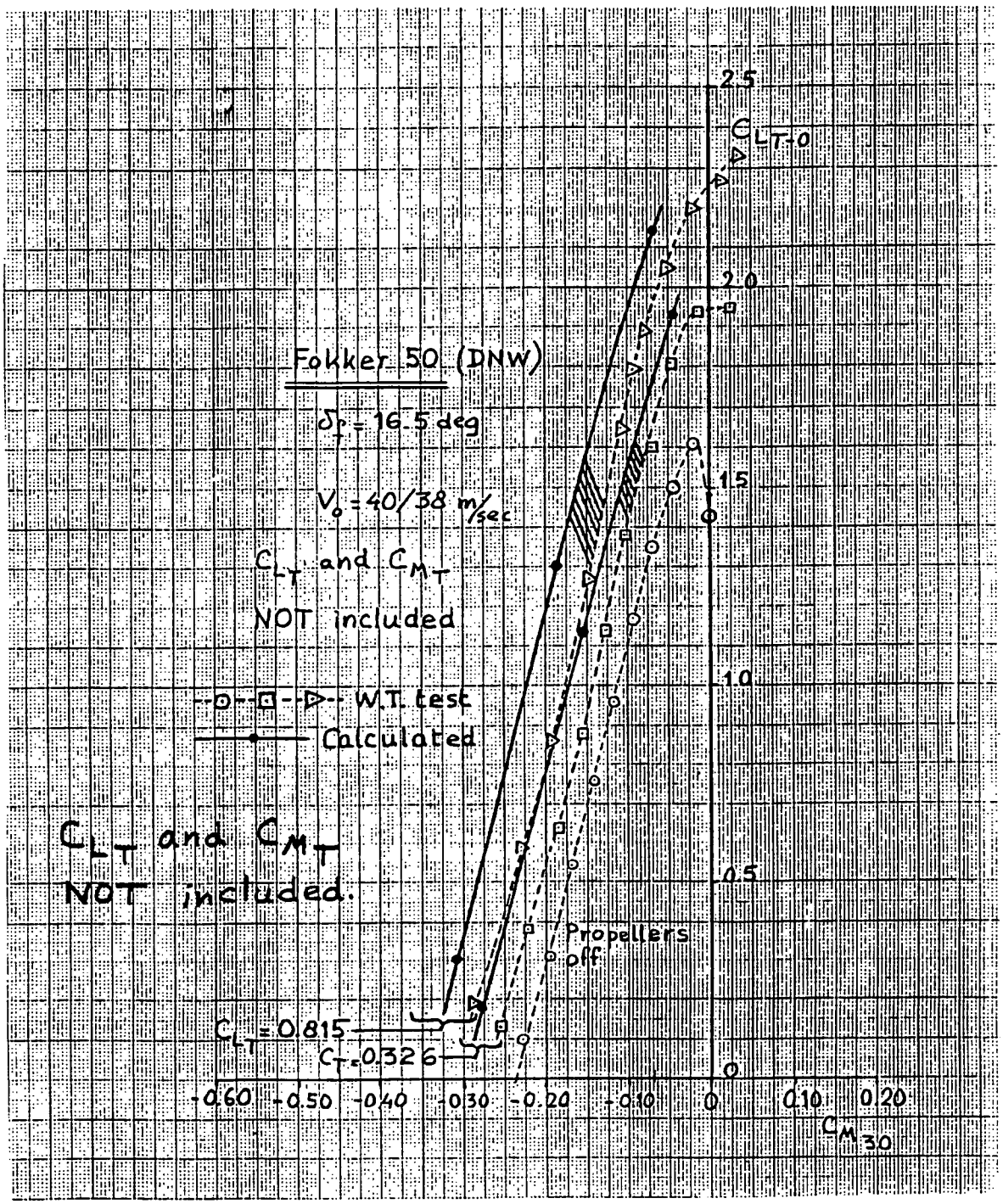
Fokker 50 (DNW)
δ_T = 16.5 deg
V_o = 40/38 m/sec
C_{LT} and C_{MT} NOT included
W.T. test
Calculated
C_{LT} and C_{MT} NOT included.
Propellers off
C_{LT} = 0.815
C_T = 0.326
$C_{LT=0}$
2.5
2.0
1.5
1.0
0.5
0
-0.60
-0.50
-0.40
-0.30
-0.20
-0.10
0
0.10
0.20
$C_{M_{30}}$

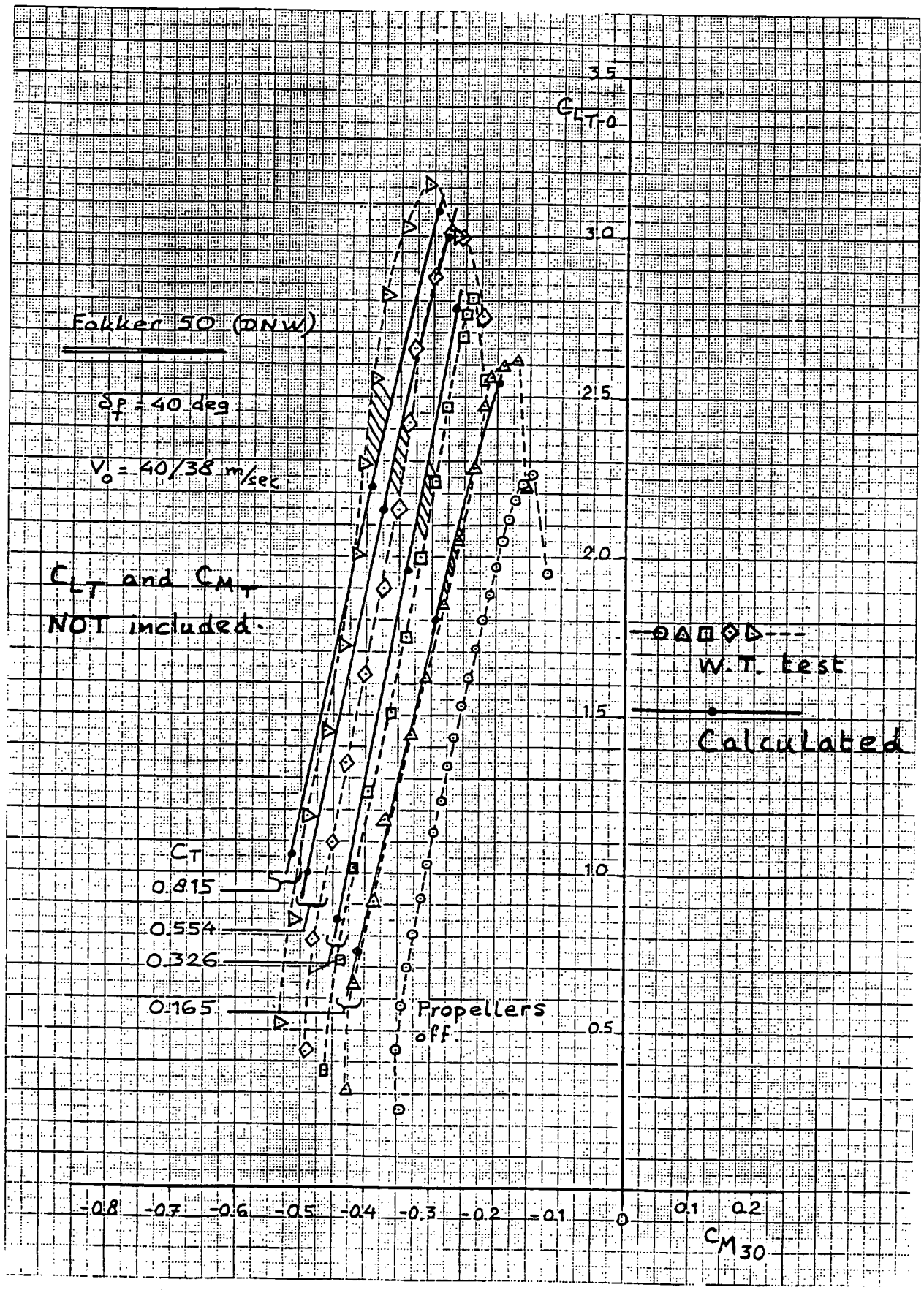
Fokker 50 (DNW)
δ_f = 40 deg
V_o = 40/38 m/sec
C_{L_T} and C_{M_T}
NOT included.
$C_{L_{T-O}}$
3.5
3.0
2.5
2.0
1.5
1.0
0.5
W.T. test
Calculated
C_T
0.815
0.554
0.326
0.165
Propellers off.
-0.8 -0.7 -0.6 -0.5 -0.4 -0.3 -0.2 -0.1 0 0.1 0.2
$C_{M_{30}}$

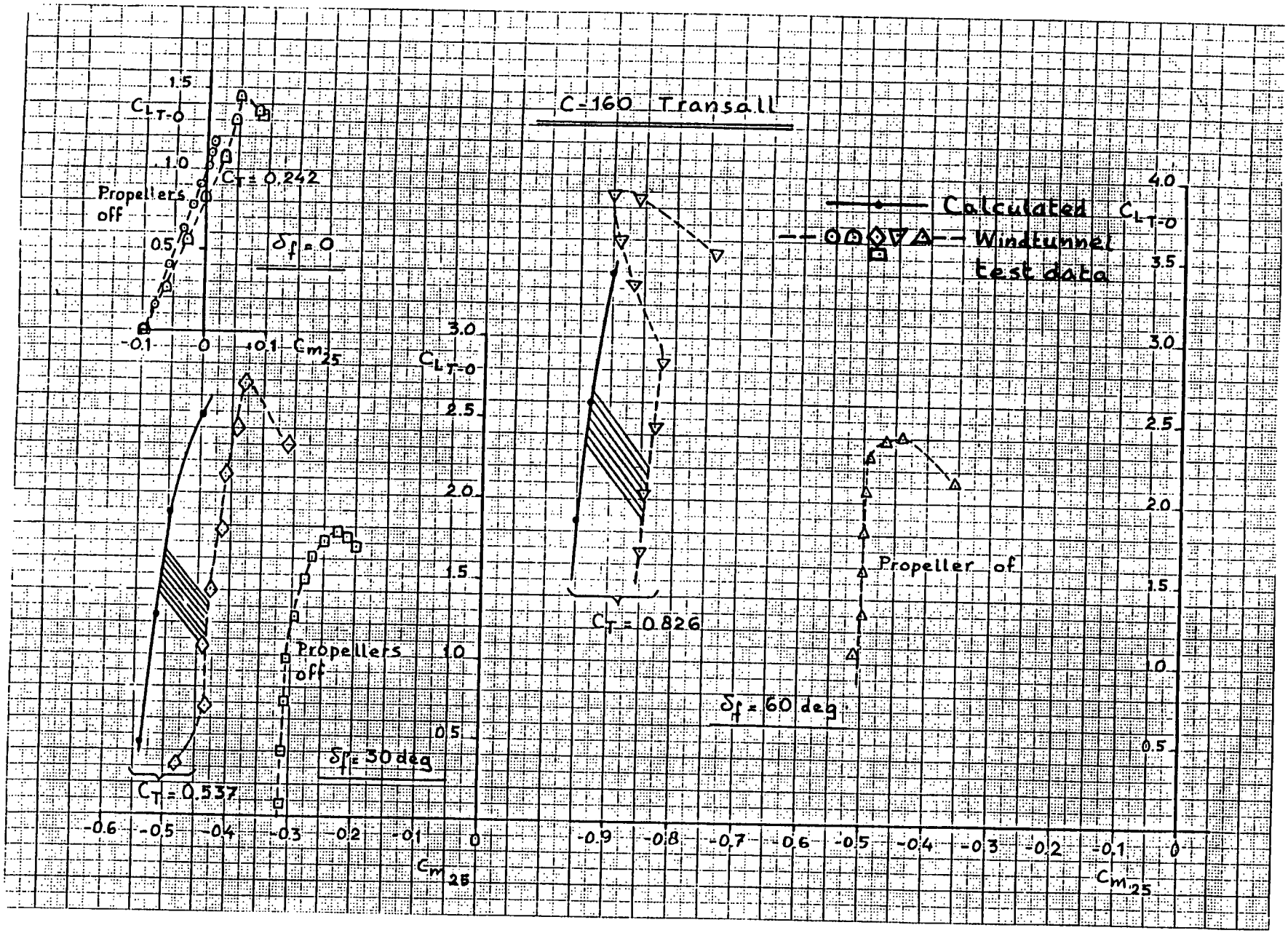
C-160 Transall
Calculated $C_{L_{T-0}}$
Windtunnel test data
$C_{L_{T-0}}$
$C_{m_{25}}$
Propellers off
$C_T = 0.242$
$\delta_f = 0$
$C_T = 0.537$
$\delta_f = 30$ deg
$C_T = 0.826$
$\delta_f = 60$ deg
Propeller of

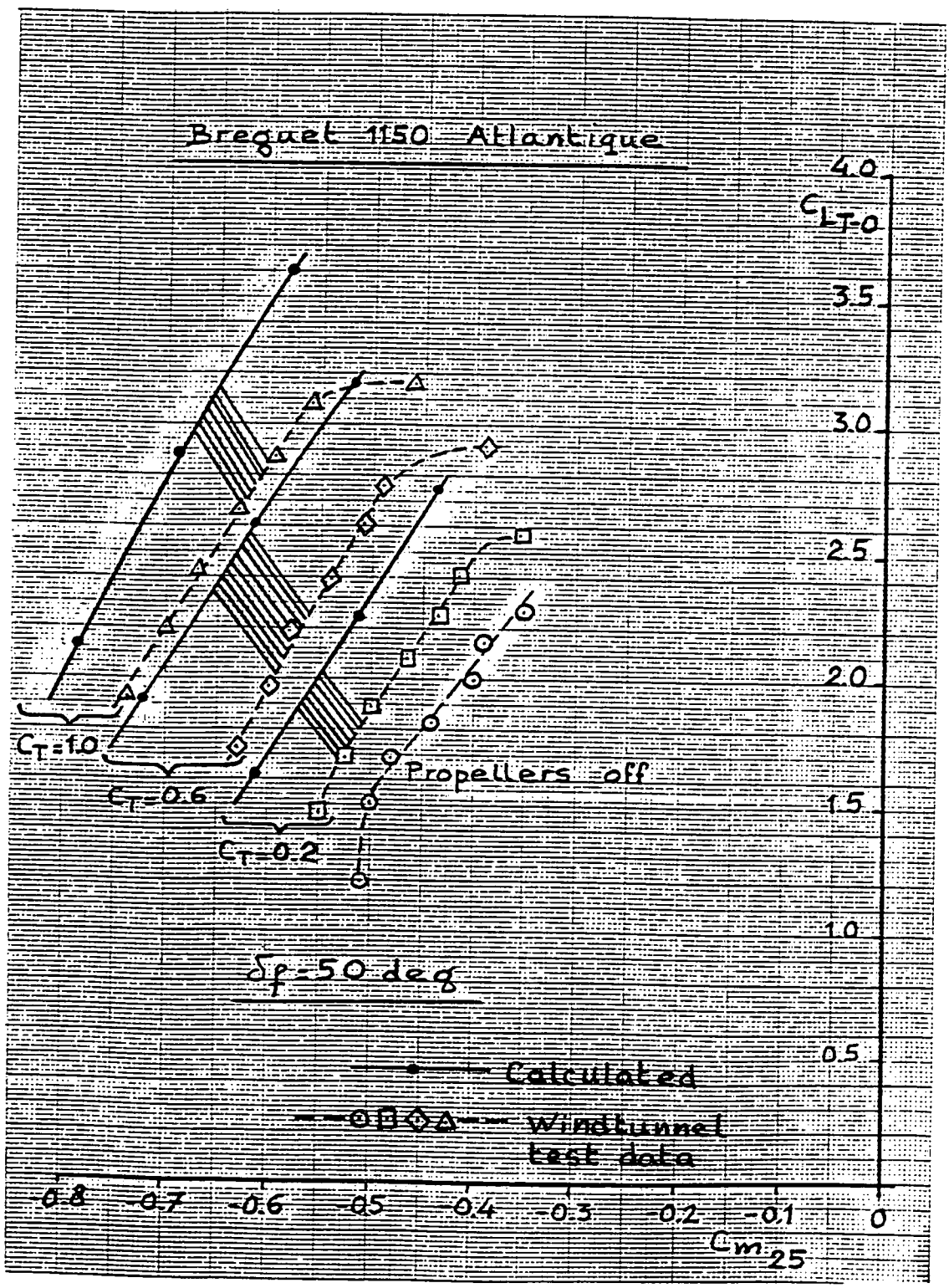
Breguet 1150 Atlantique
4.0
$C_{L_{T-O}}$
3.5
3.0
2.5
2.0
1.5
1.0
0.5
C_T=1.0
C_T=0.6
C_T=0.2
Propellers off
δ_f=50 deg
Calculated
Windtunnel test data
-0.8
-0.7
-0.6
-0.5
-0.4
-0.3
-0.2
-0.1
0
$C_{m_{25}}$

Appendix X

Downwash characteristics (I)

The vertical position of the slipstream centre-line at the tailplane location.

The following equations are used:

$$h_{tot} = h_t + l_h^* \, tg \left[K\varepsilon \frac{d\varepsilon}{dC_L} \frac{dC_L}{d\alpha} \alpha_R + K_\varepsilon \frac{d\varepsilon}{dC_L} \Delta C_{L_s} + K_\varepsilon \varepsilon_{\alpha=o} \right]$$

$$- l_h \, tg \, \alpha_R - \left[X_{0.25c_s} - X_{prop} \right] \sin \alpha_R$$

$$+ C_f \sin \delta_f - 0.25 \left(X_{0.25c_s} - X_{prop} \right) \sin \Delta \alpha_{o,f}$$

or :

$$h_{tot} = h_t + P - l_h \, tg \, \alpha_R + (\Delta h_t)_\alpha + (\Delta h_t)_{\delta_f}$$

$$+ (\Delta h_t)_{upw} \qquad (109)$$

where :

$$P = l_h^* \, tg \, [M + N + O] \qquad (108)$$

with:

$$M = K_\varepsilon \frac{d\varepsilon}{dC_L} \frac{dC_L}{d\alpha} \alpha_R \qquad (105)$$

$$N = K_\varepsilon \frac{d\varepsilon}{dC_L} \Delta C_{L_s} \qquad (106)$$

$$O = K_\varepsilon \cdot \varepsilon_{\alpha=o} \qquad (107)$$

$$(\Delta h_t)_{\alpha} = - (X_{0.25C_s} - X_{prop}) \sin \alpha_R \qquad (98)$$

$$(\Delta h_t)_{\delta_f} = + C_f . \sin \delta_f \qquad (83)$$

$$(\Delta h_t)_{upw} = - 0.25 (X_{0.25C_s} - X_{prop}) \sin \Delta\alpha_{o,f} \qquad (99)$$

with :

h_t	(95)	$\varepsilon_{\alpha=0}$	(104)
l_h	(94)	$(X_{0.25C_s} - X_{prop})$	(96)
α_R	(82)	C_f	(93)
L_h*	(97)	δ_f	(81)
Kε	(101)	$C_f \sin \delta_f$	(83)
$\frac{d\varepsilon}{dC_L}$	(100)	$\Delta\alpha_{o,f}$	(84) ≡ (15)
$\left(\frac{dC_L}{d\alpha}\right)_{C_T=0}$	(102)		
ΔC_{Ls}	(103 = (58)	Encircled numbers (X Y Z) denote columns in tables where actual values are presented.	

Note :

$h_t = z_h - z_t$ where z_t is the height of the propeller thrust line <u>above</u> the airfoil section chord at the thrust line location.

The equation for h_{tot} as presented at the beginning of this appendix has been applied to the majority of the configurations tested and presented in report R&M No. 2747 (ref. 16) for CT = 0.40 and ΔV/Vo = 0.506 for

α_R = 0 and α_R = 10 deg	(i_w = 0 , δ_f = 0)
α_R = -4 deg α_R = + 6 deg	(i_w = 4 deg, δ_f = 0)
α_R = 0 and α_R = + 8 deg	(i_w = 0, δ_f = 60 deg)

The results are presented as h_{tot} and $h_{tot}/D^*/2$ in columns (109) and (111).

For comparison with windtunnel test data the figures on pages X-8 to X-11 show the interpolated values for $h_{tot}/D^*/2$ for the angles-of-attack at which the windtunnel data were obtained.

Under the assumption that no slipstream deformation occurs the increase in average dynamic pressure at the tailplane can be calculated with the formulae derived in Appendix III.

With the equations from Appendix III

$$b_{s_h} = D^* \sqrt{1 - \left(\frac{h_{tot}}{D^*/2}\right)^2}$$

$$s_{s_h} = 2 \times b_{s_h} \times c_{s_h}$$

$$b = \sqrt{\frac{qh}{q}} - 1 = \sqrt{\left(1 + \frac{\Delta V}{V_o}\right)^2 \frac{S_{s_h}}{S_h} + \frac{S_h - S_{h_h}}{S_h}} - 1$$

b_{s_h}, S_{s_h} and b were determined for the various angles-of-attack and the associated values for htot/D*/2. The various data are presented in columns (112), (114) and (121) of Tables Va and Vb and in the figures on pages X-12 and X-13.

The actual windtunnel test values for

$$\sqrt{q_h/q} - 1$$

as reported in report R&M No 2747 are presented on page X-14.

As mentioned in the main part of this report the location of the slipstream centre line seems to be correctly determined with the equations as presented.

Table V Downwash Characteristics (I)

No.	Conf.	$\frac{h}{c}$	i_w (deg)	$\frac{z_h}{D}$	δ_f (deg)	α_R (deg)	$C_f \sin\delta_f$	$\Delta\alpha_{o.f}$ (deg)	C_T	$\frac{\Delta V}{V_o}$	$C_{L_{FP-0}}$	ΔC_{L_S} TEST	C_L^*	D_{prop}	D^*	C_S	C_f	Remarks
		(78)	(79)	(80)	(81)	(82)	(83)	(84)	(85)	(86)	(87)	(88)	(89)	(90)	(91)	(92)	(93)	
4	ARC R&M No 2747	3.78	0	0.16	0	0	0	0	0.40	0.506	0.09	0	0.09	10.0	9.12	11.1	2.20	LW, CR
		3.78	0	0.16	0	10.0	0	0	0.40	0.506	1.01	0.23	1.24	10.0	9.12	11.1	2.20	
		3.78	0	0.31	0	0	0	0	0.40	0.506	0.09	0	0.09	10.0	9.12	11.1	2.20	
		3.78	0	0.31	0	10.0	0	0	0.40	0.506	1.01	0.23	1.24	10.0	9.12	11.1	2.20	
		3.78	0	0.46	0	0	0	0	0.40	0.506	0.09	0	0.09	10.0	9.12	11.1	2.20	
		3.78	0	0.46	0	10.0	0	0	0.40	0.506	1.01	0.23	1.24	10.0	9.12	11.1	2.20	
		3.78	0	0.61	0	0	0	0	0.40	0.506	0.09	0	0.09	10.0	9.12	11.1	2.20	
		3.78	0	0.61	0	10.0	0	0	0.40	0.506	1.01	0.23	1.24	10.0	9.12	11.1	2.20	
		3.78	0	0.705	0	0	0	0	0.40	0.506	0.09	0	0.09	10.0	9.12	11.1	2.20	
		3.78	0	0.705	0	10.0	0	0	0.40	0.506	1.01	0.23	1.24	10.0	9.12	11.1	2.20	LW, CR
4	ARC R&M No 2747	4.41	0	0.01	0	0	0	0	0.40	0.506	0.09	0	0.09	10.0	9.12	11.1	2.20	LW, CR
		4.41	0	0.01	0	10.0	0	0	0.40	0.506	1.01	0.23	1.24	10.0	9.12	11.1	2.20	
		4.41	0	0.16	0	0	0	0	0.40	0.506	0.09	0	0.09	10.0	9.12	11.1	2.20	
		4.41	0	0.16	0	10.0	0	0	0.40	0.506	1.01	0.23	1.24	10.0	9.12	11.1	2.20	
		4.41	0	0.46	0	0	0	0	0.40	0.506	0.09	0	0.09	10.0	9.12	11.1	2.20	
		4.41	0	0.46	0	10.0	0	0	0.40	0.506	1.01	0.23	1.24	10.0	9.12	11.1	2.20	
		4.41	0	0.61	0	0	0	0	0.40	0.506	0.09	0	0.09	10.0	9.12	11.1	2.20	
		4.41	0	0.61	0	10.0	0	0	0.40	0.506	1.01	0.23	1.24	10.0	9.12	11.1	2.20	LW, CR
4	ARC R&M No 2747	3.78	0	-0.15	0	0	0	0	0.40	0.506	0.11	0	0.11	10.0	9.12	11.1	2.20	MW, CR
		3.78	0	-0.15	0	10.0	0	0	0.40	0.506	1.03	0.23	1.26	10.0	9.12	11.1	2.20	
		3.78	0	0.10	0	0	0	0	0.40	0.506	0.11	0	0.11	10.0	9.12	11.1	2.20	
		3.78	0	0.10	0	10.0	0	0	0.40	0.506	1.03	0.23	1.26	10.0	9.12	11.1	2.20	MW, CR
4	ARC R&M No 2747	3.78	4														2.20	LW, CR
		3.78	4														2.20	
		3.78	4														2.20	
		3.78	4														2.20	
		3.78	4.0	0.55	0	-4.0	0	0	0.40	0.506	0.09	0	0.09	10.0	9.12	11.1	2.20	
		3.78	4.0	0.55	0	6.0	0	0	0.40	0.506	1.01	0.23	1.24	10.0	9.12	11.1	2.20	LW, CR

Example of calculating procedure

Table V Downwash Characteristics (1) (Continued)

No	Conf	l_h	h_t	$x_{cg}-x_{pr}$	l_h^*	$(\Delta h_t)_\alpha$	$(\Delta h_t)_{upw.}$	$\frac{d\varepsilon}{dC_L}$	K_ε	$\left(\frac{dC_L}{d\alpha/r\cdot 0}\right)_{C_T=0}$ (1/deg)	ΔC_{L_s}	$\varepsilon_{\alpha=0}$	M	N	O	P	α_R (deg)	dim.
		(94)	(95)	(96)	(97)	(98)	(99)	(100)	(101)	(102)	(103)	(104)	(105)	(106)	(107)	(108)	(82)	
4	ARC R&M No 2747 LW, CR	37.6	2.18	8.88	28.5	0	0	4.05	1.5	0.095	0	0	0	0	0	0	0	in
		37.6	2.18	8.88	28.5	-1.54	0	4.05	1.5	0.095	0.23	0	5.77	1.40	0	3.59	10.0	in
		37.6	3.68	8.88	28.5	0	0	4.05	1.5	0.095	0	0	0	0	0	0	0	in
		37.6	3.68	8.88	28.5	-1.54	0	4.05	1.5	0.095	0.23	0	5.77	1.40	0	3.59	10.0	in
		37.6	5.18	8.88	28.5	0	0	4.05	1.5	0.095	0	0	0	0	0	0	0	in
		37.6	5.18	8.88	28.5	-1.54	0	4.05	1.5	0.095	0.23	0	5.77	1.40	0	3.59	10.0	in
		37.6	6.68	8.88	28.5	0	0	4.05	1.5	0.095	0	0	0	0	0	0	0	in
		37.6	6.68	8.88	28.5	-1.54	0	4.05	1.5	0.095	0.23	0	5.77	1.40	0	3.59	10.0	in
		37.6	7.63	8.88	28.5	0	0	4.05	1.5	0.095	0	0	0	0	0	0	0	in
		37.6	7.63	8.88	28.5	-1.54	0	4.05	1.5	0.095	0.23	0	5.77	1.40	0	3.59	10.0	in
4	ARC R&M No 2747 LW, CR	43.9	0.59	8.88	35.5	0	0	4.05	1.5	0.095	0	0	0	0	0	0	0	in
		43.9	0.59	8.88	35.5	-1.54	0	4.05	1.5	0.095	0.23	0	5.77	1.40	0	4.47	10.0	in
		43.9	2.18	8.88	35.5	0	0	4.05	1.5	0.095	0	0	0	0	0	0	0	in
		43.9	2.18	8.88	35.5	-1.54	0	4.05	1.5	0.095	0.23	0	5.77	1.40	0	4.47	10.0	in
		43.9	5.18	8.88	35.5	0	0	4.05	1.5	0.095	0	0	0	0	0	0	0	in
		43.9	5.18	8.88	35.5	-1.54	0	4.05	1.5	0.095	0.23	0	5.77	1.40	0	4.47	10.0	in
		43.9	6.68	8.88	35.5	0	0	4.05	1.5	0.095	0	0	0	0	0	0	0	in
		43.9	6.68	8.88	35.5	-1.54	0	4.05	1.5	0.095	0.23	0	5.77	1.40	0	4.47	10.0	in
4	ARC R&M No 2747 MW, CR	37.6	-0.92	8.88	28.5	0	0	4.05	1.5	0.095	0	0	0	0	0	0	0	in
		37.6	-0.92	8.88	28.5	-1.54	0	4.05	1.5	0.095	0.23	0	5.77	1.40	0	3.59	10.0	in
		37.6	1.58	8.88	28.5	0	0	4.05	1.5	0.095	0	0	0	0	0	0	0	in
		37.6	1.58	8.88	28.5	-1.54	0	4.05	1.5	0.095	0.23	0	5.77	1.40	0	3.59	10.0	in
4	ARC R&M No 2747 LW, CR	37.6	1.65	8.88	28.5	+0.62	0	4.05	1.5	0.095	0	1.5	-2.31	0	2.25	-0.03	-4.0	in
		37.6	1.65	8.88	28.5	-0.93	0	4.05	1.5	0.095	0.23	1.5	3.46	1.40	2.25	3.55	6.0	in
		37.6	3.65	8.88	28.5	+0.62	0	4.05	1.5	0.095	0	1.5	-2.31	0	2.25	-0.03	-4.0	in
		37.6	3.65	8.88	28.5	-0.93	0	4.05	1.5	0.095	0.23	1.5	3.46	1.40	2.25	3.55	6.0	in
		37.6	5.65	8.88	28.5	+0.62	0	4.05	1.5	0.095	0	1.5	-2.31	0	2.25	-0.03	-4.0	in
		37.6	5.65	8.88	28.5	-0.93	0	4.05	1.5	0.095	0.23	1.5	3.46	1.40	2.25	3.55	6.0	in

Table V Downwash Characteristics(I)(Concluded)

No	Conf	δ_f (deg) (81)	α_R (deg) (82)	h_{tot} (103)	h_{tot} TEST (110)	$\frac{h_{tot}}{D^*/2}$ (111)	b_{s_h} (112)	c_{s_h} (113)	s_{s_h} (114)	S_h (115)	$\frac{q_s}{q}$ (116)	b_{max} (117)	$b = \frac{(\Delta V)_{av}}{(V_0)_{av}}$ TEST (118)	$\frac{q_h}{q}$ (119)	$\frac{q_h}{q}$ TEST (120)	b CALC. (121)
4	ARC R&M No 2747 LW, CR	0	0	2.18	—	0.48	7.98	5.80	92.8	197.3	2.268	0.298	—	1.602	—	0.266
		0	10.0	-2.40	—	-0.53	7.72	5.80	89.6	197.3	2.268	0.298	—	1.580	—	0.257
		0	0	3.68	—	0.81	5.25	5.80	60.9	197.3	2.268	0.298	—	1.388	—	0.178
		0	10.0	-0.90	—	-0.20	8.92	5.80	103.5	197.3	2.268	0.298	—	1.677	—	0.295
		0	0	5.18	—	1.14	0	5.80	0	197.3	2.268	0.298	—	1.000	—	0
		0	10.0	0.60	—	0.13	9.04	5.80	104.9	197.3	2.268	0.298	—	1.682	—	0.297
		0	0	6.68	—	1.46	0	5.80	0	197.3	2.268	0.298	—	1.000	—	0
		0	10.0	2.10	—	0.45	8.12	5.80	94.2	197.3	2.268	0.298	—	1.615	—	0.271
		0	0	7.63	—	1.67	0	5.80	0	197.3	2.268	0.298	—	1.000	—	0
		0	10.0	3.05	—	0.67	6.75	5.80	78.3	197.3	2.268	0.298	—	1.506	—	0.227
4	ARC R&M No 2747 LW, CR	0	0	0.59	—	0.13	9.05	5.80	105.0	197.3	2.268	0.298	—	1.682	—	0.297
		0	10.0	-4.22	—	-0.93	3.35	5.80	38.9	197.3	2.268	0.298	—	1.248	—	0.117
		0	0	2.18	—	0.48	7.98	5.80	92.6	197.3	2.268	0.298	—	1.603	—	0.266
		0	10.0	-2.63	—	-0.58	7.40	5.80	85.8	197.3	2.268	0.298	—	1.555	—	0.247
		0	0	5.18	—	1.14	0	5.80	0	197.3	2.268	0.298	—	1.000	—	0
		0	10.0	0.37	—	0.08	9.10	5.80	105.6	197.3	2.268	0.298	—	1.682	—	0.297
		0	0	6.68	—	1.46	0	5.80	0	197.3	2.268	0.298	—	1.000	—	0
		0	10.0	1.87	—	0.41	8.30	5.80	96.3	197.3	2.268	0.298	—	1.628	—	0.276
4	ARC R&M No 2747 MW, CR	0	0	-0.92	—	-0.20	8.92	5.80	103.5	197.3	2.268	0.298	—	1.677	—	0.295
		0	10.0	-5.50	—	-1.21	0	5.80	0	197.3	2.268	0.298	—	1.000	—	0
		0	0	1.58	—	0.35	8.52	5.80	98.8	197.3	2.268	0.298	—	1.649	—	0.284
		0	10.0	-3.00	—	-0.66	6.85	5.80	79.5	197.3	2.268	0.298	—	1.508	—	0.228
4	ARC R&M No 2747 LW, CR	0	-4.0	4.87	—	1.07	0	5.80	0	197.3	2.268	0.298	—	1.000	—	0
		0	6.0	0.32	—	0.07	9.10	5.80	105.6	197.3	2.268	0.298	—	1.685	—	0.298
		0	-4.0	6.87	—	1.51	0	5.80	0	197.3	2.268	0.298	—	1.000	—	0
		0	6.0	2.32	—	0.51	7.83	5.80	90.8	197.3	2.268	0.298	—	1.590	—	0.261
		0	-4.0	8.87	—	1.95	0	5.80	0	197.3	2.268	0.298	—	1.000	—	0
		0	6.0	4.32	—	0.95	2.90	5.80	33.6	197.3	2.268	0.298	—	1.210	—	0.100

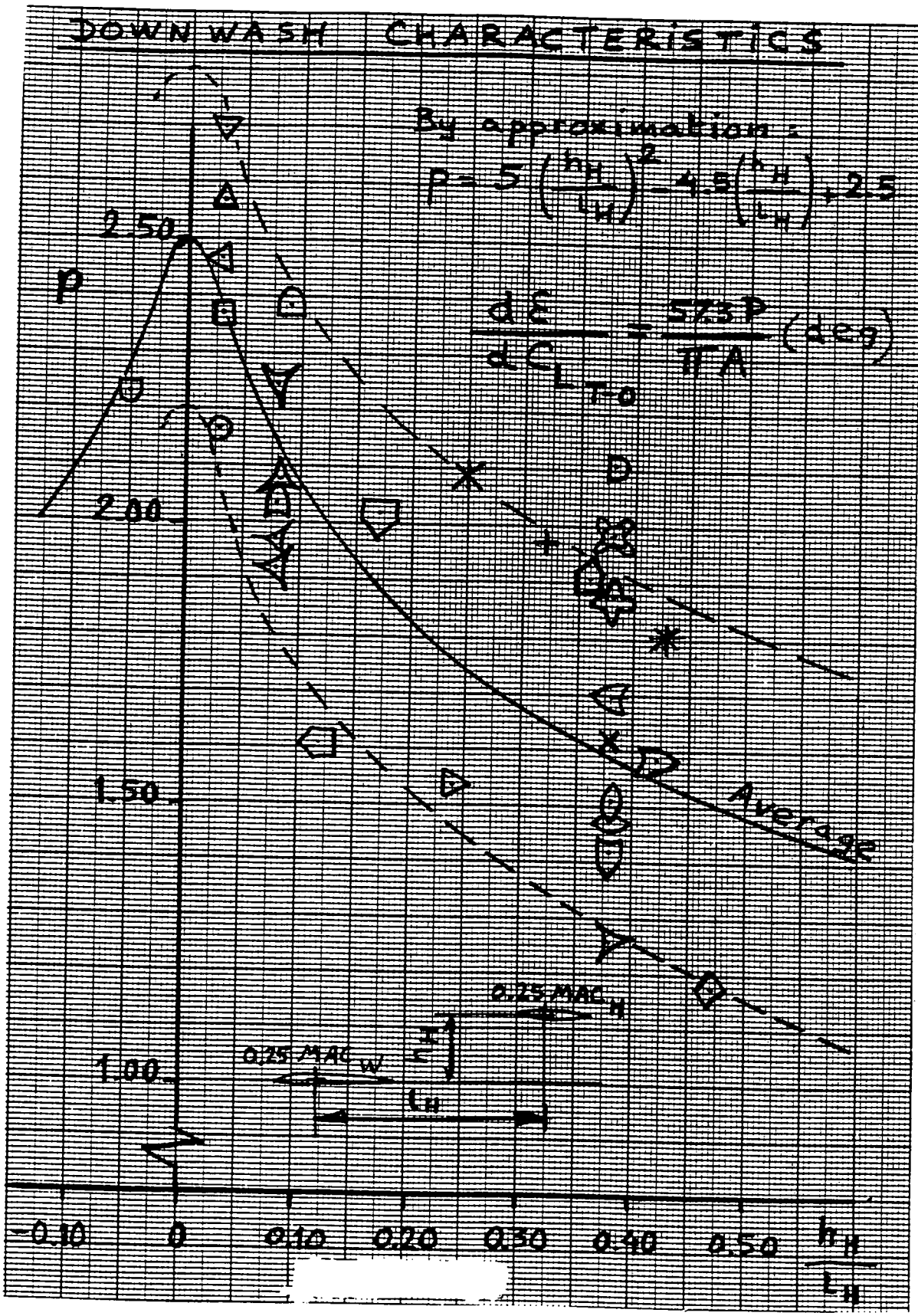
DOWNWASH CHARACTERISTICS
By approximation :
$P = 5\left(\frac{h_H}{L_H}\right)^2 - 4.5\left(\frac{h_H}{L_H}\right) + 2.5$
$\frac{d\varepsilon}{d C_{L_{T-O}}} = \frac{57.3\,P}{\pi A}\,(deg)$
P
2.50
2.00
1.50
1.00
-0.10
0
0.10
0.20
0.30
0.40
0.50
$\frac{h_H}{L_H}$
Average
0.25 MAC W
0.25 MAC H
L_H

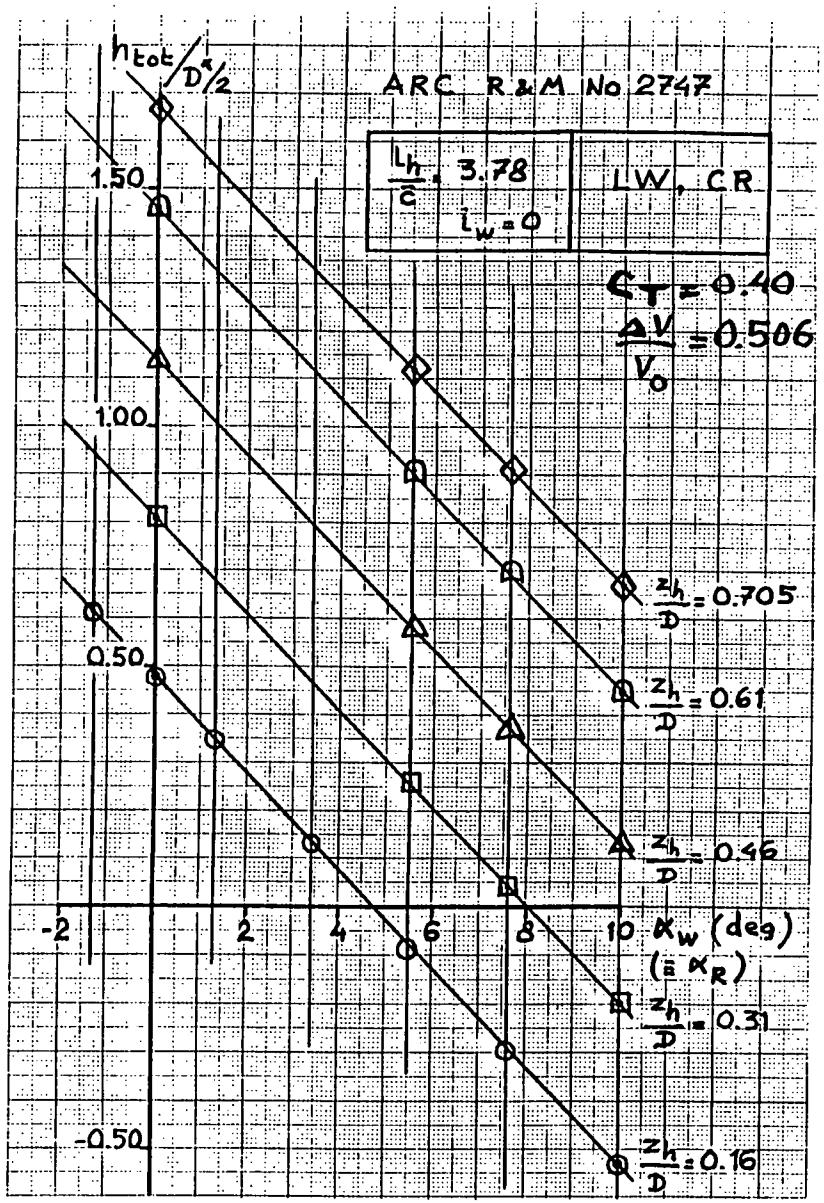
ARC R&M No 2747
$h_{tot}/D^*/2$
$\frac{l_h}{c}$ = 3.78 i_w = 0
LW, CR
C_T = 0.40
$\frac{\Delta V}{V_0}$ = 0.506
1.50
1.00
0.50
-0.50
-2
2
4
6
8
10
α_w (deg) (≡ α_R)
$\frac{z_h}{D}$ = 0.705
$\frac{z_h}{D}$ = 0.61
$\frac{z_h}{D}$ = 0.46
$\frac{z_h}{D}$ = 0.31
$\frac{z_h}{D}$ = 0.16

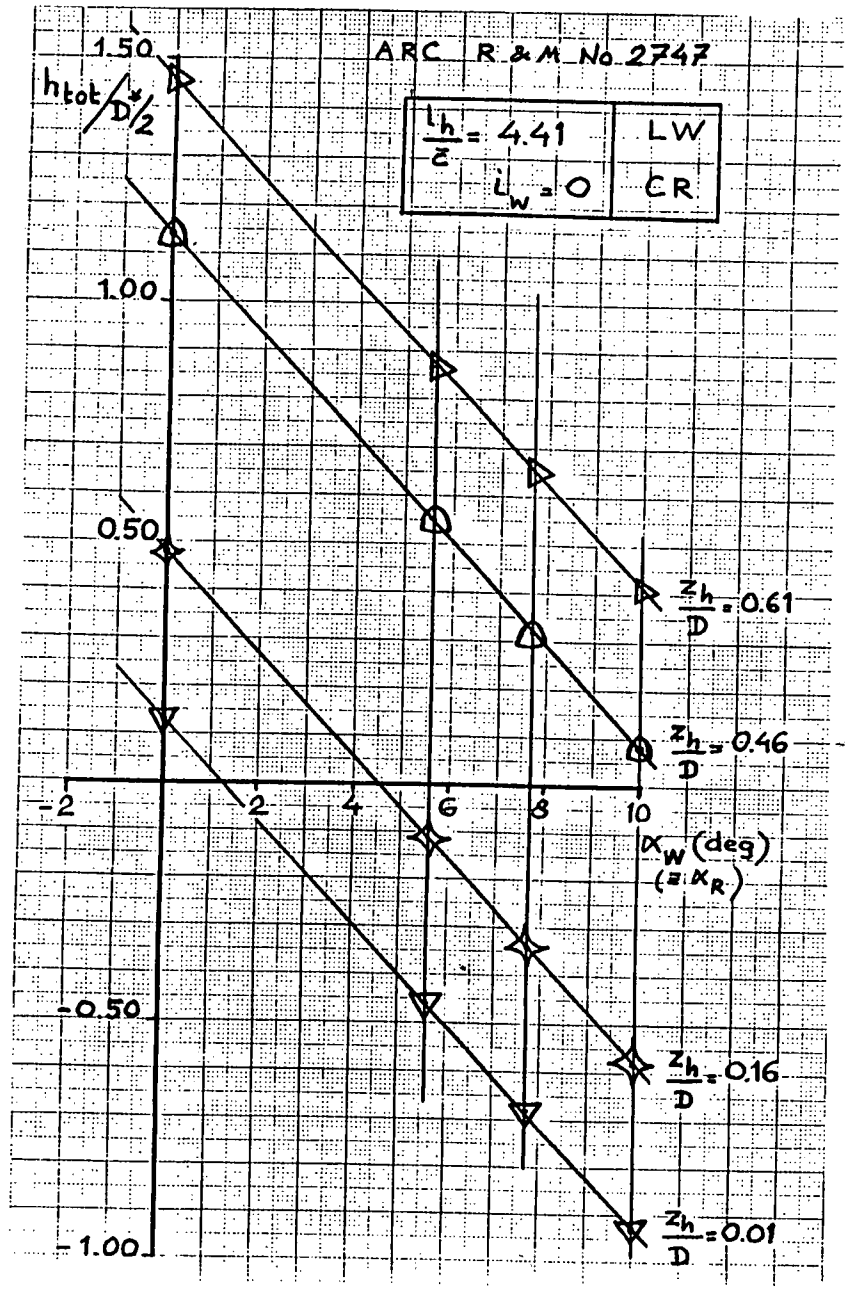
ARC R&M No 2747
$h_{tot}/D^*/2$
$\frac{l_h}{c}$ = 4.41 i_w = 0
LW
CR
1.50
1.00
0.50
-0.50
-1.00
-2
2
4
6
8
10
α_w (deg) (≡ α_R)
$\frac{z_h}{D}$ = 0.61
$\frac{z_h}{D}$ = 0.46
$\frac{z_h}{D}$ = 0.16
$\frac{z_h}{D}$ = 0.01

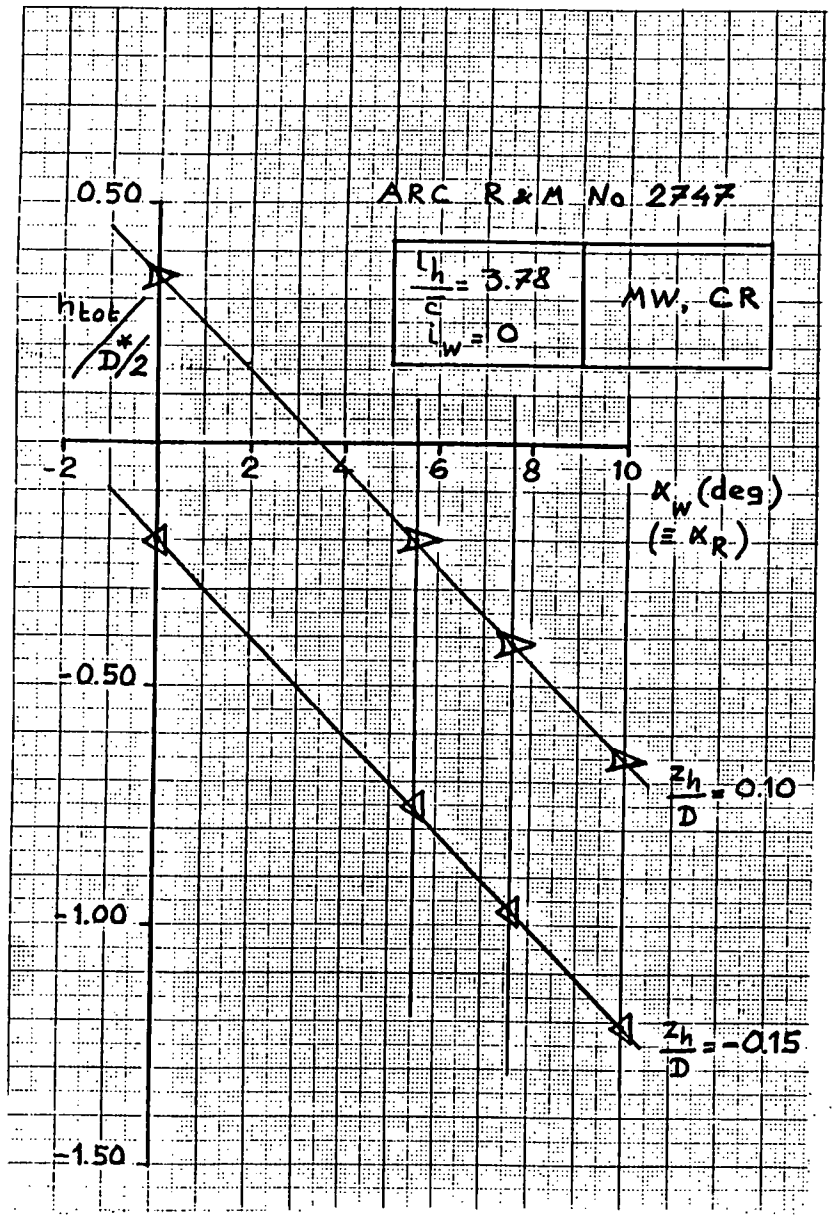
ARC R&M No 2747
$\frac{l_h}{c} = 3.78$
$i_w = 0$
MW, CR
$h_{tot}/D^*/2$
0.50
-0.50
-1.00
-1.50
-2
2
4
6
8
10
α_w (deg)
$(\equiv \alpha_R)$
$\frac{z_h}{D} = 0.10$
$\frac{z_h}{D} = -0.15$

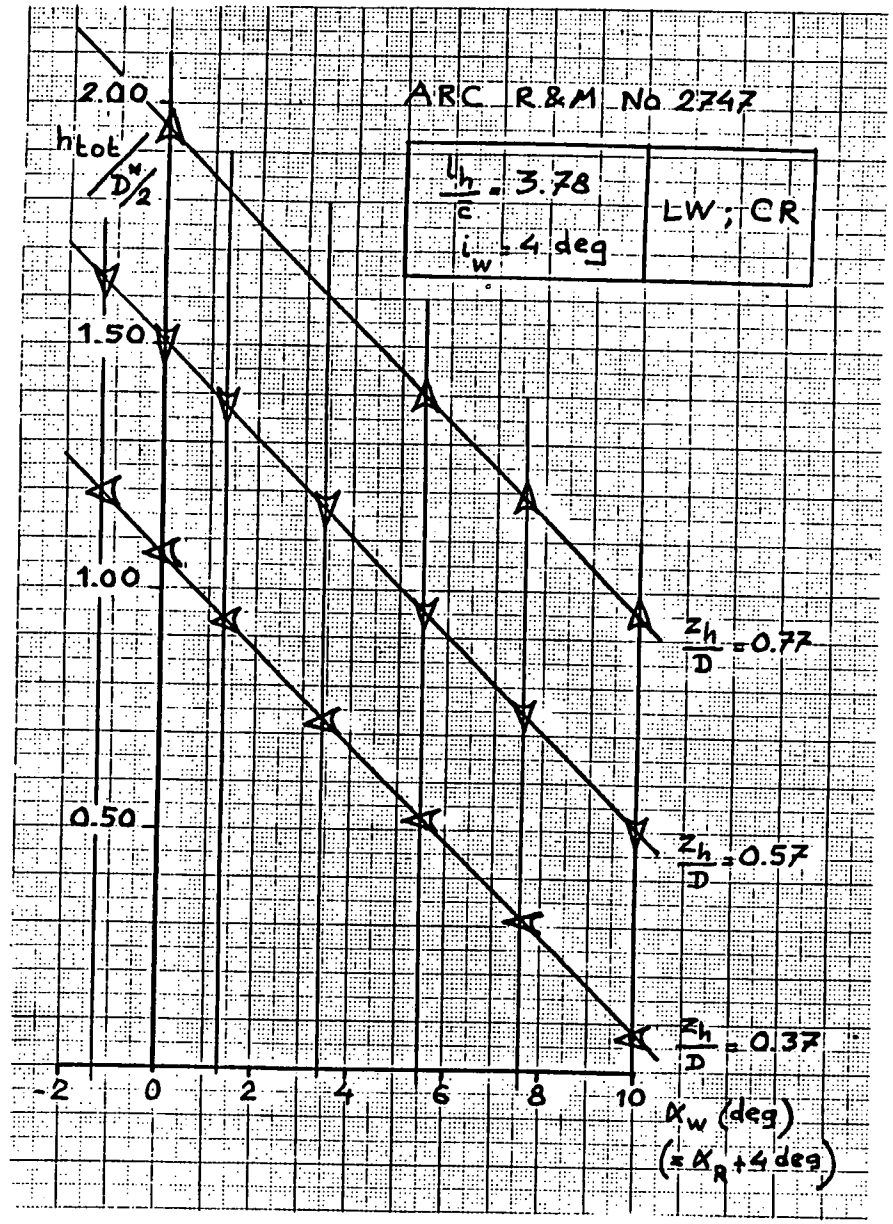
ARC R&M No 2747
$\frac{l_h}{c} = 3.78$
$i_w = 4$ deg
LW; CR
$h_{tot}/D^*/2$
2.00
1.50
1.00
0.50
-2
0
2
4
6
8
10
α_w (deg)
$(\equiv \alpha_R + 4$ deg$)$
$\frac{z_h}{D} = 0.77$
$\frac{z_h}{D} = 0.57$
$\frac{z_h}{D} = 0.37$

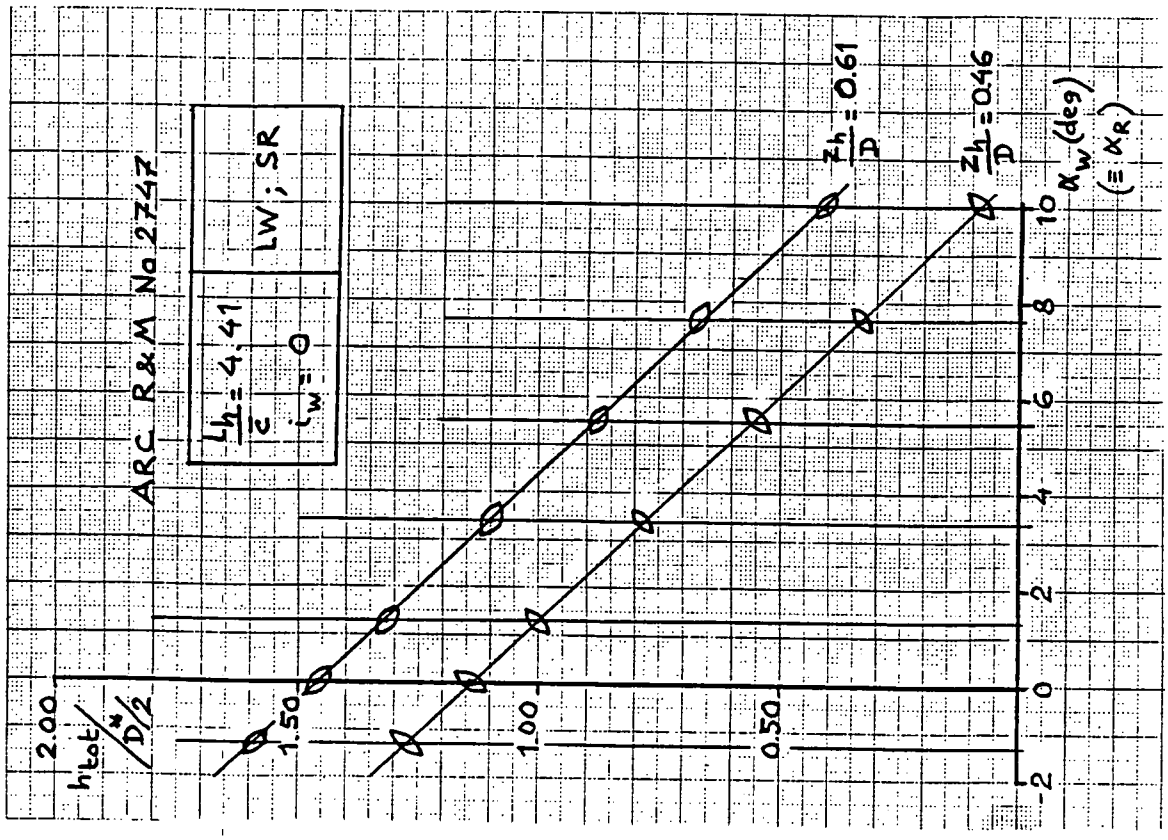
ARC R&M No 2747
$\frac{L_h}{c}$ = 4.41
i_w = 0
LW; SR
$\frac{h_{tot}}{D/2}$
2.00
1.50
1.00
0.50
$\frac{z_h}{D}$ = 0.61
$\frac{z_h}{D}$ = 0.46
α_w (deg)
($\equiv \alpha_R$)
10
8
6
4
2
0
-2

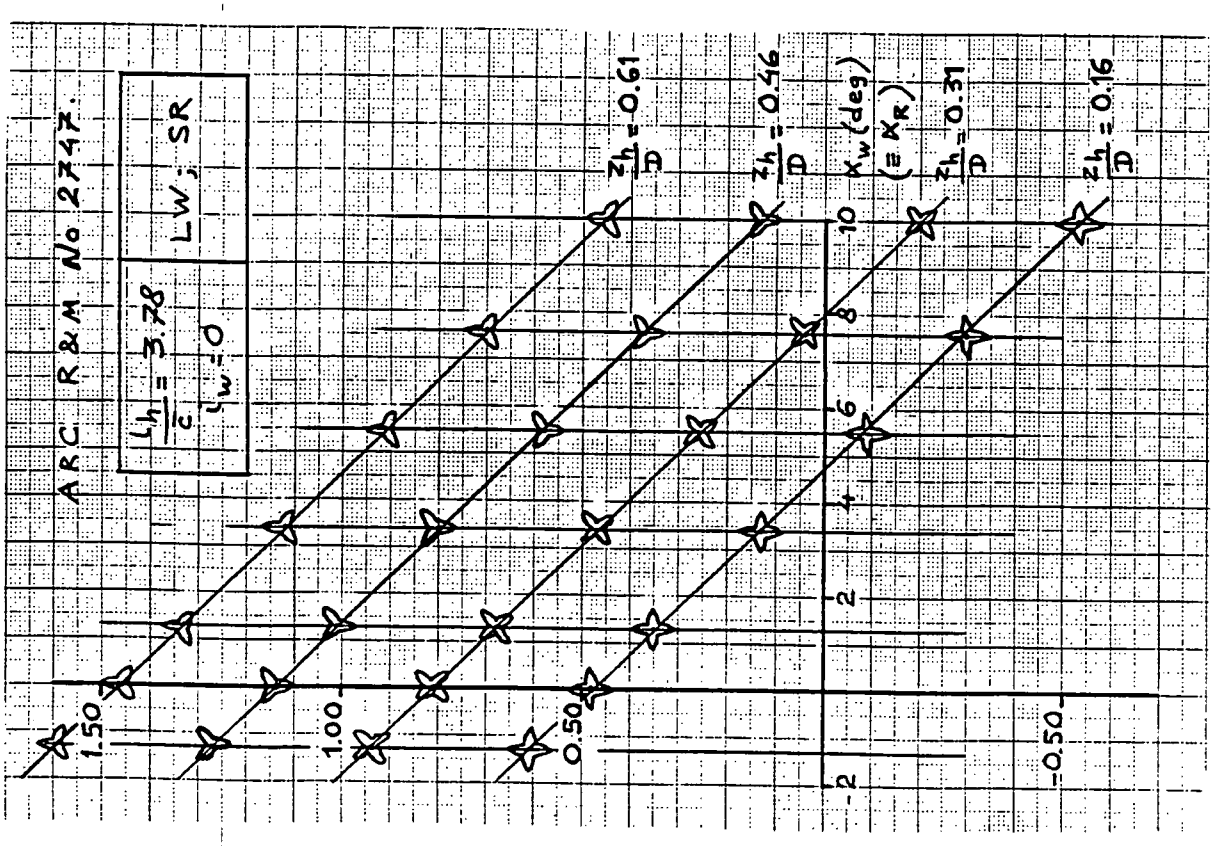
ARC R&M No 2747.
$\frac{L_h}{c}$ = 3.78
i_w = 0
LW; SR
1.50
1.00
0.50
$\frac{z_h}{D}$ = 0.61
$\frac{z_h}{D}$ = 0.46
$\frac{z_h}{D}$ = 0.31
$\frac{z_h}{D}$ = 0.16
α_w (deg)
($\equiv \alpha_R$)
10
8
6
4
2
-2
-0.50

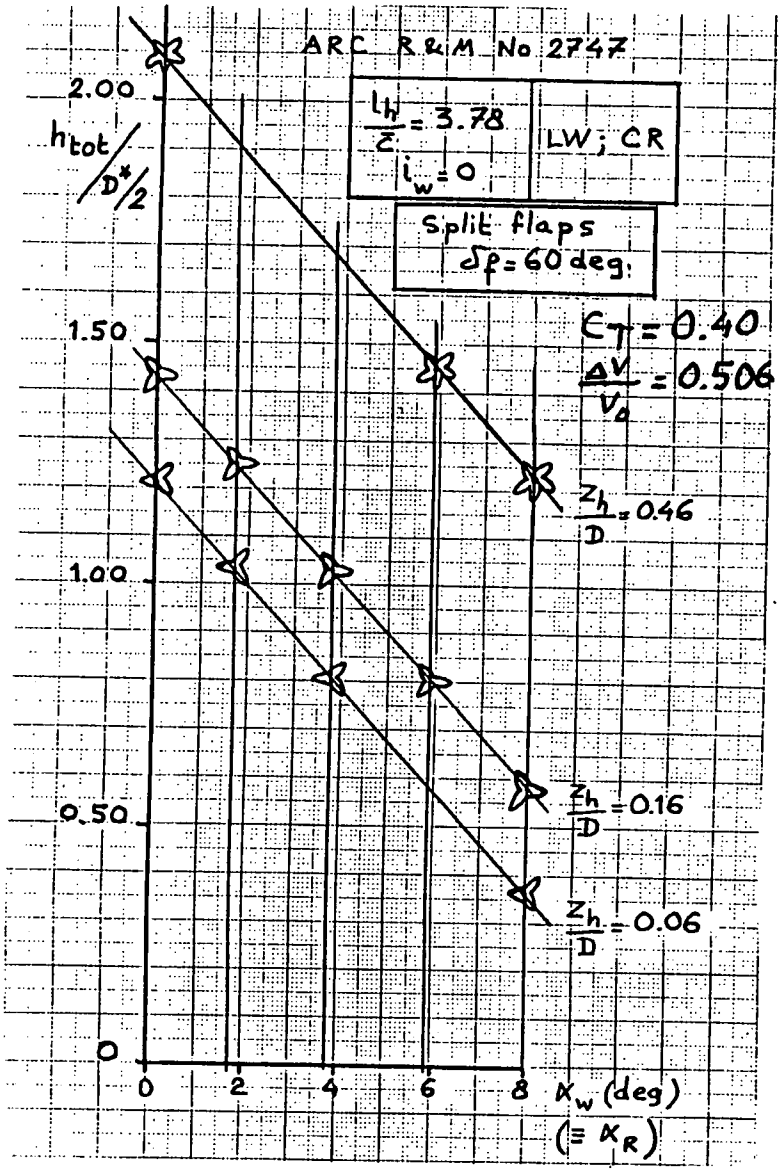
ARC R&M No 2747
$\frac{l_h}{c} = 3.78$ LW; CR
$i_w = 0$
Split flaps
$\delta_f = 60$ deg.
$C_T = 0.40$
$\frac{\Delta V}{V_0} = 0.506$
$\frac{z_h}{D} = 0.46$
$\frac{z_h}{D} = 0.16$
$\frac{z_h}{D} = 0.06$
$h_{tot}/D^*/2$
2.00
1.50
1.00
0.50
0
0
2
4
6
8
α_w (deg)
($\equiv \alpha_R$)

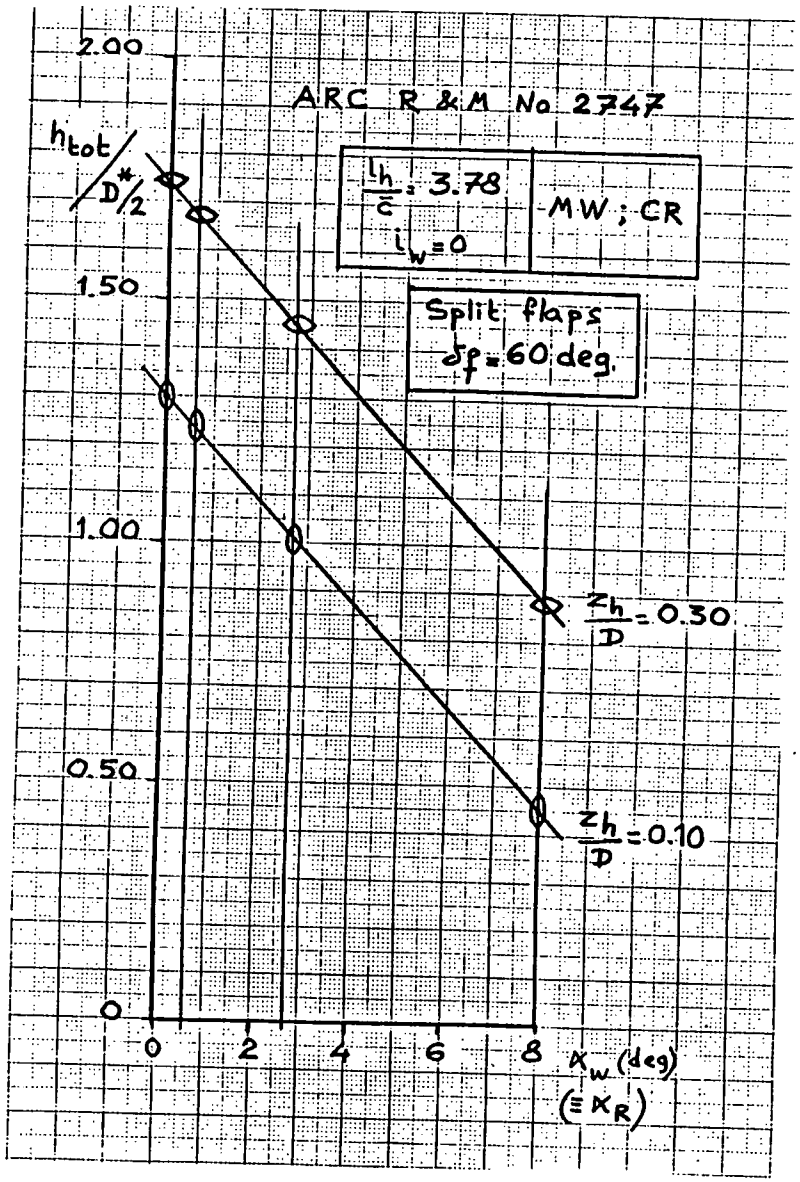
ARC R&M No 2747
$\frac{l_h}{c} = 3.78$ MW; CR
$i_w = 0$
Split flaps
$\delta_f = 60$ deg.
$\frac{z_h}{D} = 0.30$
$\frac{z_h}{D} = 0.10$
$h_{tot}/D^*/2$
2.00
1.50
1.00
0.50
0
0
2
4
6
8
α_w (deg)
($\equiv \alpha_R$)

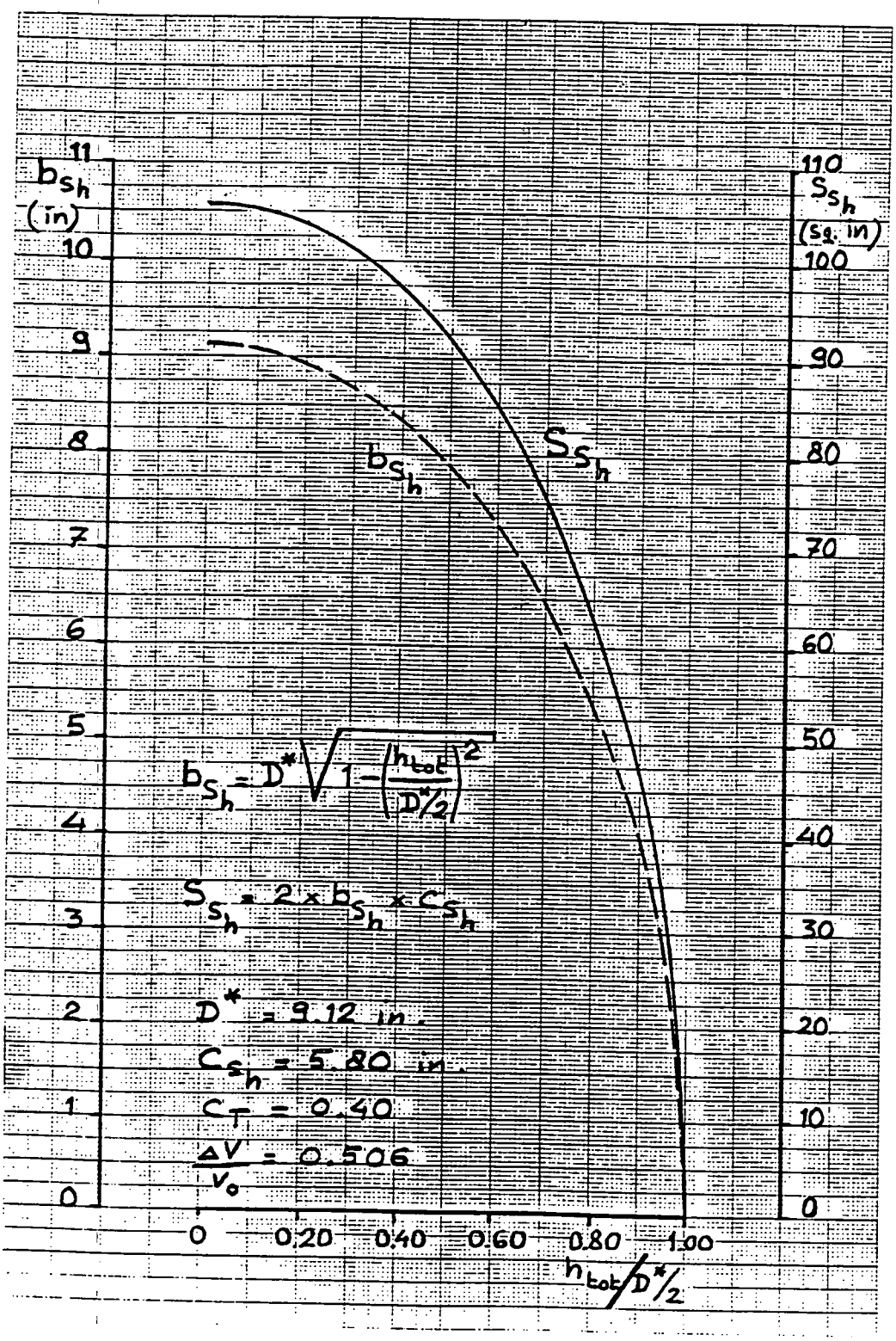
b_{S_h} (in)
S_{S_h} (sq. in)
b_{S_h}
S_{S_h}
$b_{S_h} = D^* \sqrt{1 - \left(\frac{h_{tot}}{D^*/2}\right)^2}$
$S_{S_h} = 2 \times b_{S_h} \times C_{S_h}$
$D^* = 9.12$ in.
$C_{S_h} = 5.80$ in.
$C_T = 0.40$
$\frac{\Delta V}{V_o} = 0.506$
$h_{tot}/D^*/2$

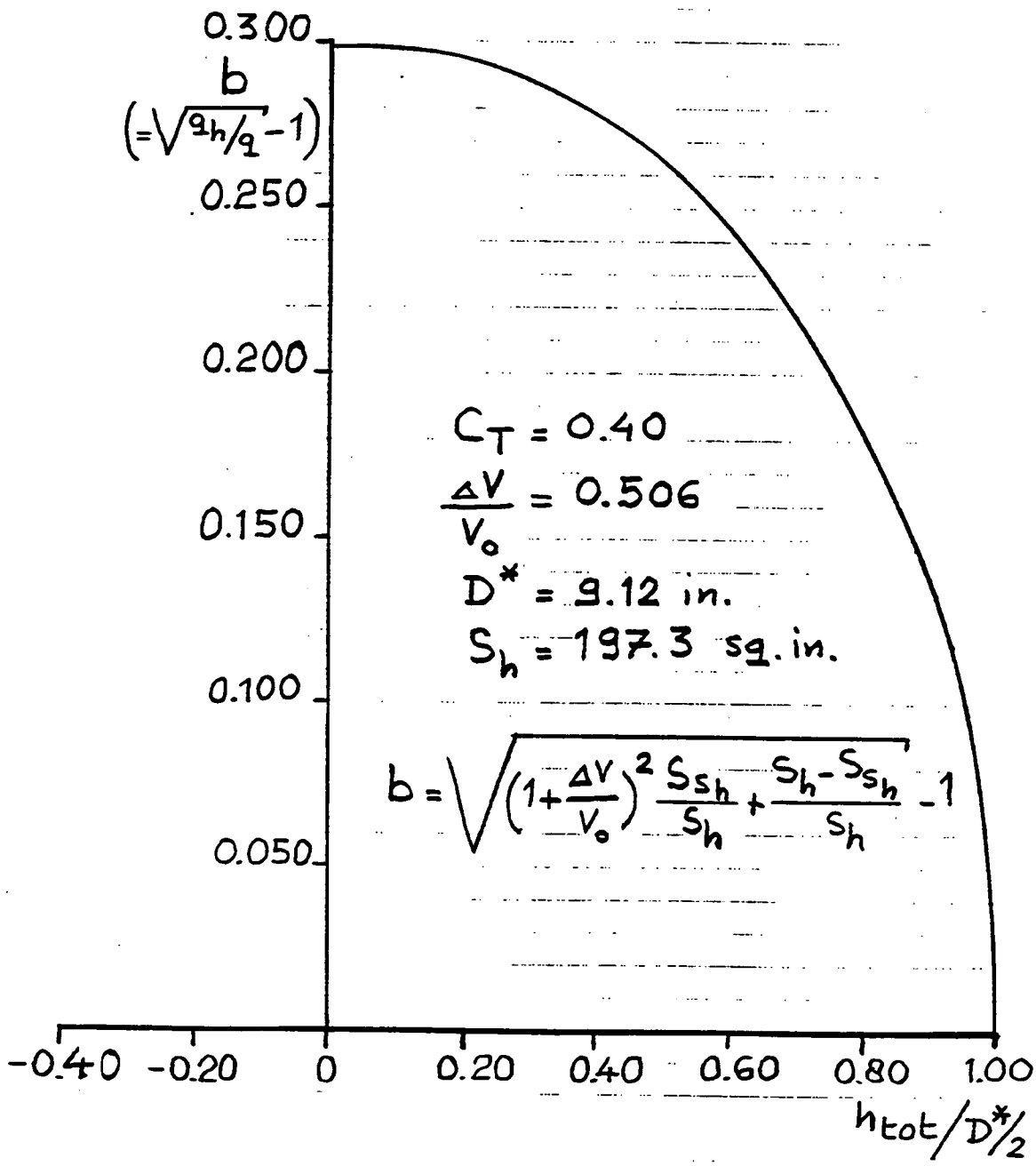
0.300
b
$(=\sqrt{q_h/q}-1)$
0.250
0.200
0.150
0.100
0.050
$C_T = 0.40$
$\frac{\Delta V}{V_o} = 0.506$
$D^* = 9.12$ in.
$S_h = 197.3$ sq. in.
$b = \sqrt{\left(1+\frac{\Delta V}{V_o}\right)^2 \frac{S_{s_h}}{S_h} + \frac{S_h - S_{s_h}}{S_h}} - 1$
-0.40
-0.20
0
0.20
0.40
0.60
0.80
1.00
$h_{tot}/D^*/2$

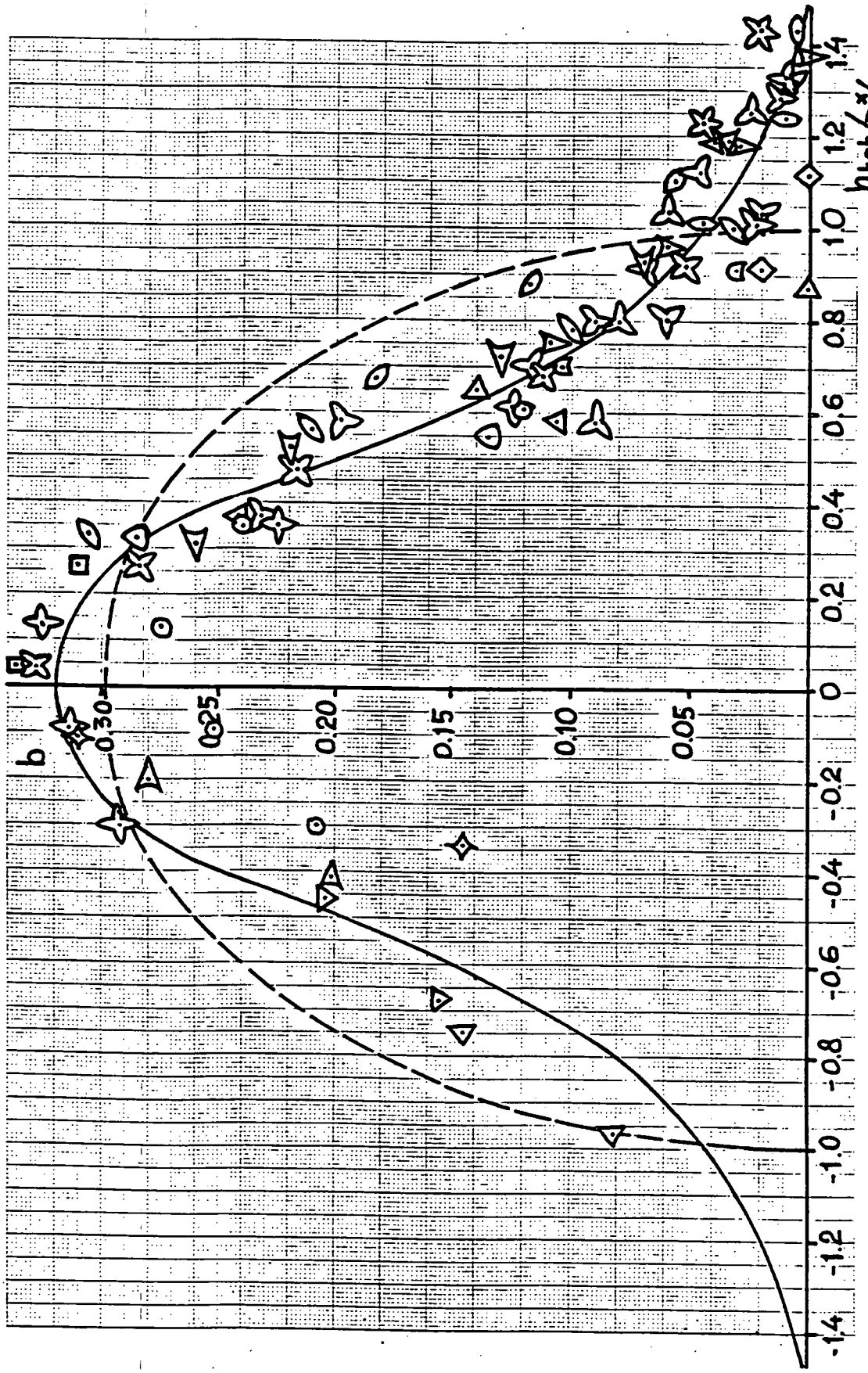
b
0.30
0.25
0.20
0.15
0.10
0.05
0
0.2
0.4
0.6
0.8
1.0
1.2
1.4
-0.2
-0.4
-0.6
-0.8
-1.0
-1.2
-1.4
htot/D*/2

Appendix XI

Downwash characteristics (II)

A comparison of the vertical distance h_{tot} between the slipstream centre line and the horizontal tailplane as calculated and as derived from windtunnel tests on a Fokker F-27 model.

On pages XI-5 to XI-8 dynamic pressure surveys are presented as measured in a vertical plane through the quarter chord line of the horizontal tailplane on a development windtunnel model of the F27 with lengthened rear fuselage. The figures show data for four of the six flap configurations investigated.

Under the assumption based on the data from Appendix X and in particular on figure X-8 on page X-14 that the dynamic pressure ratio q_h/q starts deviating from $q_h/q = 1$ when $h_{tot}/D^*/2 < 1.5$ the distance h_{tot} can be estimated for each data point.

This distance h_{tot} as derived from the windtunnel tests on the F-27 model is presented in column (110) in Table VI.

With the equations from Appendix X h_{tot} has been calculated for the same configurations and α_R and C_T as used in the windtunnel tests.

The calculated values of h_{tot} are presented in column (109) of Table VI.

A comparison of calculated and test data is also presented in the figures on pages XI-9 and XI-10.

Table VI Downwash Characteristics (II)

No	Conf.	l_h/c	i_w (deg)	z_h/D	δ_f (deg)	α_R (deg)	$C_f \sin\delta_f$	$\Delta\alpha_{0,f}$ (deg)	C_T	$\Delta V/V_0$	$C_{l_{P-0}}$	ΔC_{L_S} TEST.	C_L^*	D_{prop}	D^*	C_S	C_f	
		(78)	(79)	(80)	(81)	(82)	(83)	(84) = (15)	(85)	(86)	(82) + (84)	(89) = (87) + (88)		(90) = (9)	(91) = (92)	(92) = (4)	(93)	
11	Fokker F-27	5.01	3.4	0.136	0	-1.0	0	0	0.078	0.125	0.50	0.02	0.52	0.244	0.237	0.197	0.063	
						+1.4			0.156	0.233	0.74	0.06	0.80		0.232			
						+4.7			0.333	0.452	1.00	0.19	1.19		0.224			
		5.01	3.4	0.136	0	+8.1	0	0	0.447	0.578	1.14	0.38	1.52	0.244	0.221	0.197	0.063	
11	Fokker F-27	5.01	3.4	0.136	40/25/40	3.2	0.031	-8.6	0.741	0.862	1.90	0.58	2.48	0.244	0.214	0.197	0.063	$\delta_{f_{eff}} = 29$ deg
						6.3			0.921	1.017	2.17	0.81	2.98		0.211			
						7.2			0.996	1.078	2.26	0.88	3.14		0.210			
		5.01	3.4	0.136	40/25/40	7.8	0.031	-8.6	1.071	1.137	2.32	1.02	3.34	0.244	0.209	0.197	0.063	
11	Fokker F-27	5.01	3.4	0.136	40	7.6	0.034	-9.6	1.155	1.202	2.38	1.17	3.55	0.244	0.208	0.197	0.063	$\delta_{f_{eff}} = 33$ deg
		5.01	3.4	0.136	40	8.2	0.034	-9.6	1.200	1.235	2.43	1.21	3.64	0.244	0.207	0.197	0.063	
11	Fokker F-27	5.01	3.4	0.136	60/25/60	-3.0	0.034	-12.0	0.543	0.676	1.60	0.27	1.87	0.244	0.218	0.197	0.063	$\delta_{f_{eff}} = 32.5$ deg
						-1.3			0.636	0.766	1.79	0.35	2.14		0.216			
						-1.0			0.636	0.766	1.82	0.35	2.17		0.216			
						+2.3			0.849	0.956	2.12	0.61	2.73		0.212			
						4.7			0.996	1.077	2.30	0.89	3.19		0.210			
		5.01	3.4	0.136	60/25/60	+6.5	0.034	-12.0	1.155	1.202	2.50	1.11	3.61	0.244	0.207	0.197	0.063	
11	Fokker F-27	5.01	3.4	0.136	70/25/40	-5.2	0.035	-13.0	0.447	0.578	1.38	0.18	1.56	0.244	0.220	0.197	0.063	
						-2.5			0.636	0.766	1.74	0.38	2.12		0.216			
						-2.1			0.636	0.766	1.77	0.42	2.19		0.216			$\delta_{f_{eff}} = 33.5$ deg
						1.7			0.849	0.956	2.07	0.73	2.80		0.212			
						4.0			0.996	1.077	2.34	0.86	3.20		0.210			
		5.01	3.4	0.136	70/25/40	5.5	0.035	-13.0	1.155	1.202	2.47	1.15	3.62	0.244	0.207	0.197	0.063	
11	Fokker F-27	5.01	3.4	0.136	70	-5.9	0.042	-15.0	0.636	0.766	1.66	0.43	2.09	0.244	0.216	0.197	0.063	
						-3.8			0.741	0.862	1.84	0.69	2.55		0.214			
						-1.1			0.921	1.017	2.08	0.85	2.93		0.211			$\delta_{f_{eff}} =$ 42 deg
						-0.7			0.921	1.017	2.11	0.87	2.98		0.211			
						1.3			1.071	1.137	2.28	1.13	3.41		0.209			
		5.01	3.4	0.136	70	4.3	0.042	-15.0	1.392	1.374	2.54	1.71	4.25	0.244	0.206	0.197	0.063	

Example of calculating procedure

Table VI

Downwash Characteristics (II) (Continued)

No	Conf	l_h	h_t	$x_{0.25} - x_{pr}$	l_h^*	$(\Delta h_t)_{/\alpha}$	$(\Delta h_t)_{upw.}$	$\frac{d\varepsilon}{dC_L}$	K_ε	$\left(\frac{dC_L}{d\,K/T\cdot 0}\right)_{(1/deg)\,C_T=0}$	ΔC_{L_S} $\frac{T\&S\,T}{(53)}$	$\varepsilon_{\alpha=0}$	M	N	O	P	K_R (deg)	dim.
		(94)	(95)	(96)	(97)	(98)	(99)	(100)	(101)	(102)	(88)	(104)	(105)	(106)	(107)	(108)	(82)	
11	Fokker F-27	0.858	0.065	0.215	0.710	0.004	0	3.60	1.5	0.099	0.02	2.5	-0.54	0.11	3.75	0.041	-1.0	m
						-0.005	0				0.06		0.75	0.32		0.060	1.4	m
						-0.018	0				0.19		2.51	1.03		0.091	4.7	m
		0.858	0.065	0.215	0.710	-0.030	0	3.60	1.5	0.099	0.38	2.5	4.33	2.05	3.75	0.122	8.1	m
11	Fokker F-27	0.858	0.065	0.215	0.710	-0.012	-0.008	3.60	1.5	0.099	0.58	6.1	1.71	3.13	9.15	0.177	3.2	m
						-0.024	-0.008				0.81		3.37	4.37		0.216	6.3	m
						-0.027	-0.008				0.88		3.85	4.75		0.227	7.2	m
		0.858	0.065	0.215	0.710	-0.029	-0.008	3.60	1.5	0.099	1.02	6.1	4.17	5.51	9.15	0.242	7.8	m
11	Fokker F-27	0.858	0.065	0.215	0.710	-0.028	-0.009	3.60	1.5	0.096	1.17	6.6	3.94	6.32	9.90	0.261	7.6	m
		0.858	0.065	0.215	0.710	-0.031	-0.009	3.60	1.5	0.096	1.21	6.6	4.25	6.53	9.90	0.268	8.2	m
11	Fokker F-27	0.858	0.065	0.215	0.710	0.011	-0.011	3.60	1.5	0.095	0.27	6.1	-1.54	1.46	9.15	0.113	-3.0	m
						0.005					0.35		-0.67	1.89		0.130	-1.3	m
						0.004					0.35		-0.51	1.89		0.132	-1.0	m
						-0.009					0.61		1.18	3.29		0.122	2.3	m
						-0.018					0.89		2.41	4.81		0.209	4.7	m
		0.858	0.065	0.215	0.710	-0.024	-0.011	3.60	1.5	0.095	1.11	6.1	3.33	5.99	9.15	0.232	6.5	m
11	Fokker F-27	0.858	0.065	0.215	0.710	+0.019	-0.012	3.60	1.5	0.094	0.18	6.3	-2.64	0.97	9.45	0.097	-5.2	m
						0.009					0.38		-1.22	2.05		0.128	-2.5	m
						0.008					0.42		-1.07	2.27		0.134	-2.1	m
						-0.006					0.73		0.86	3.94		0.180	1.7	m
						-0.015					0.86		2.03	4.64		0.205	4.0	m
		0.858	0.065	0.215	0.710	-0.021	-0.012	3.60	1.5	0.094	1.15	6.3	2.29	6.21	9.45	0.237	5.5	m
11	Fokker F-27	0.858	0.065	0.215	0.710	0.022	-0.014	3.60	1.5	0.0827	0.43	7.7	-2.72	2.32	11.55	0.139	-5.9	m
						0.014					0.69		-1.79	3.23		0.120	-3.8	m
						0.004					0.85		-0.52	4.59		0.119	-1.1	m
						0.003					0.87		-0.33	4.70		0.203	-0.7	m
						-0.005					1.13		0.61	6.10		0.234	1.3	m
		0.858	0.065	0.215	0.710	-0.016	-0.014	3.60	1.5	0.0827	1.71	7.7	2.02	9.23	11.55	0.218	4.3	m

Table VI Downwash Characteristics (II) (Concluded)

No	Conf	δ_f (deg)	α_R (deg)	h_{tot} CALC.	h_{tot} TEST	$\frac{h_{tot}}{D^*/2}$	b_{s_h}	c_{s_h}	s_{s_h}	s_h	$\frac{q_s}{q}$	ψ_{max}	$b = \left(\frac{\Delta v}{v_0}\right)_{\Delta v}$	$\frac{q_h}{q}$	$\frac{q_h}{q}_{TEST}$
		(81)	(82)	(109)	(110)										
11	Fokker F-27	0	-1.0	0.125	0.191										
			1.4	0.099	0.159										
			4.7	0.067	0.121										
		0	8.1	0.040	0.100										
11	Fokker F-27	40/25/40	3.2	0.205	0.207										
			6.3	0.185	0.189										
			7.2	0.180	0.176										
		40/25/40	7.8	0.183	0.180										
11	Fokker F-27	40	7.6	0.209	0.175										
		40	8.2	0.203	0.179										
11	Fokker F-27	60/25/60	-3.0	0.257	0.263										
			-1.3	0.242	0.251										
			-1.0	0.239	0.251										
			2.3	0.217	0.223										
			4.7	0.208	0.218										
		60/25/60	6.5	0.203	0.208										
11	Fokker F-27	70/25/70	-5.2	0.282	-										
			-2.5	0.262	0.262										
			-2.1	0.261	0.237										
			1.7	0.236	0.225										
			4.0	0.218	0.218										
		70/25/70	5.5	0.221	0.221										
11	Fokker F-27	70	-5.9	0.343	0.262										
			-3.8	0.334	0.253										
			-1.1	0.312	0.234										
			-0.7	0.309	0.234										
			1.3	0.303	0.229										
		70	4.3	0.310	0.221										

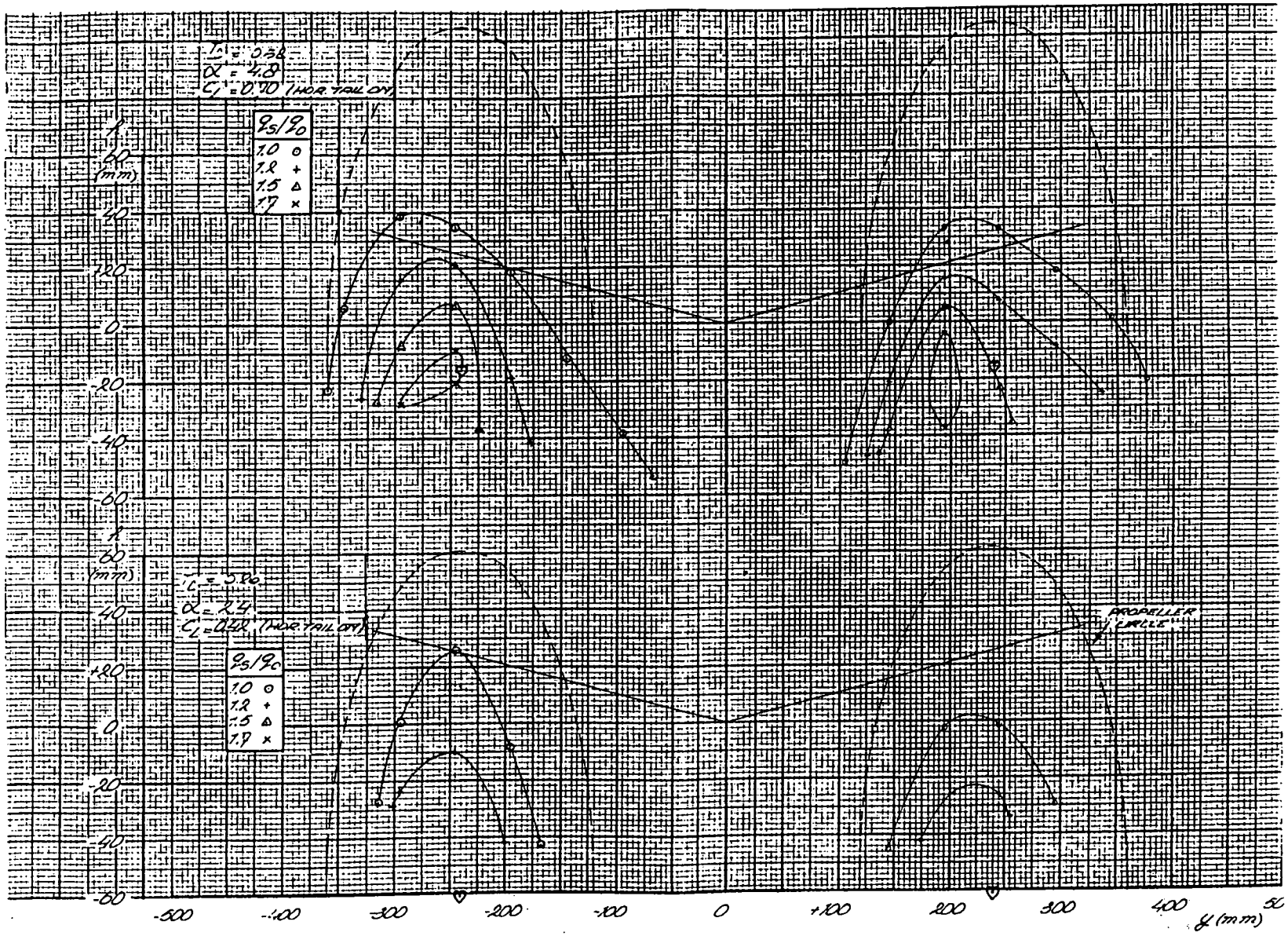

Dynamic-pressure contours in the hor.tail region.

Δ 180; constant power (1950 s.h.p.); δ_f = 0

Dynamic-pressure contours in the hor.tail region.

Δ 180; constant power (1950 s.h.p.); δ_f = 40-25-40

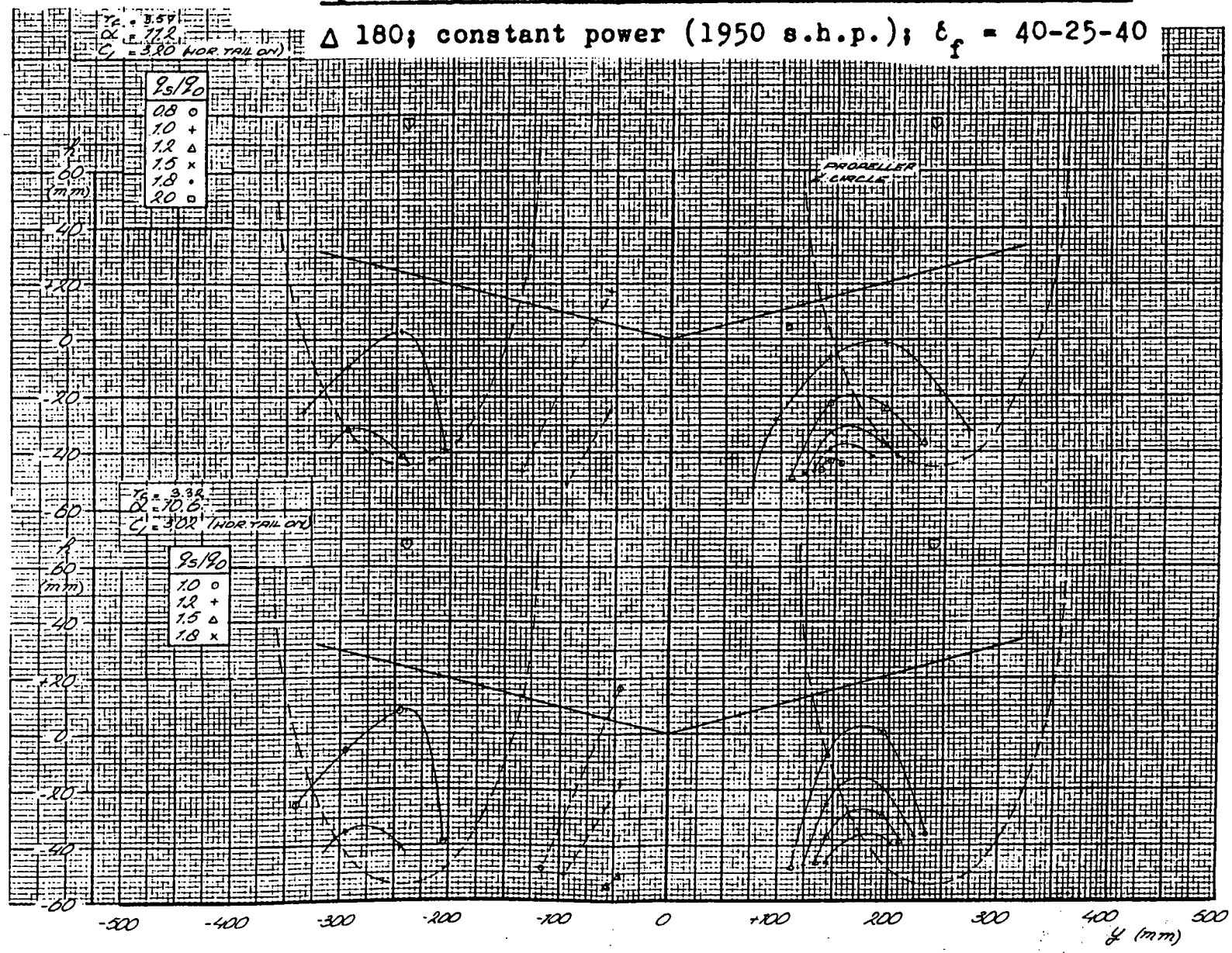

Dynamic-pressure contours in the hor.tail region.

Δ 180; constant power (1950 s.h.p.); δ_f = 70-25-70

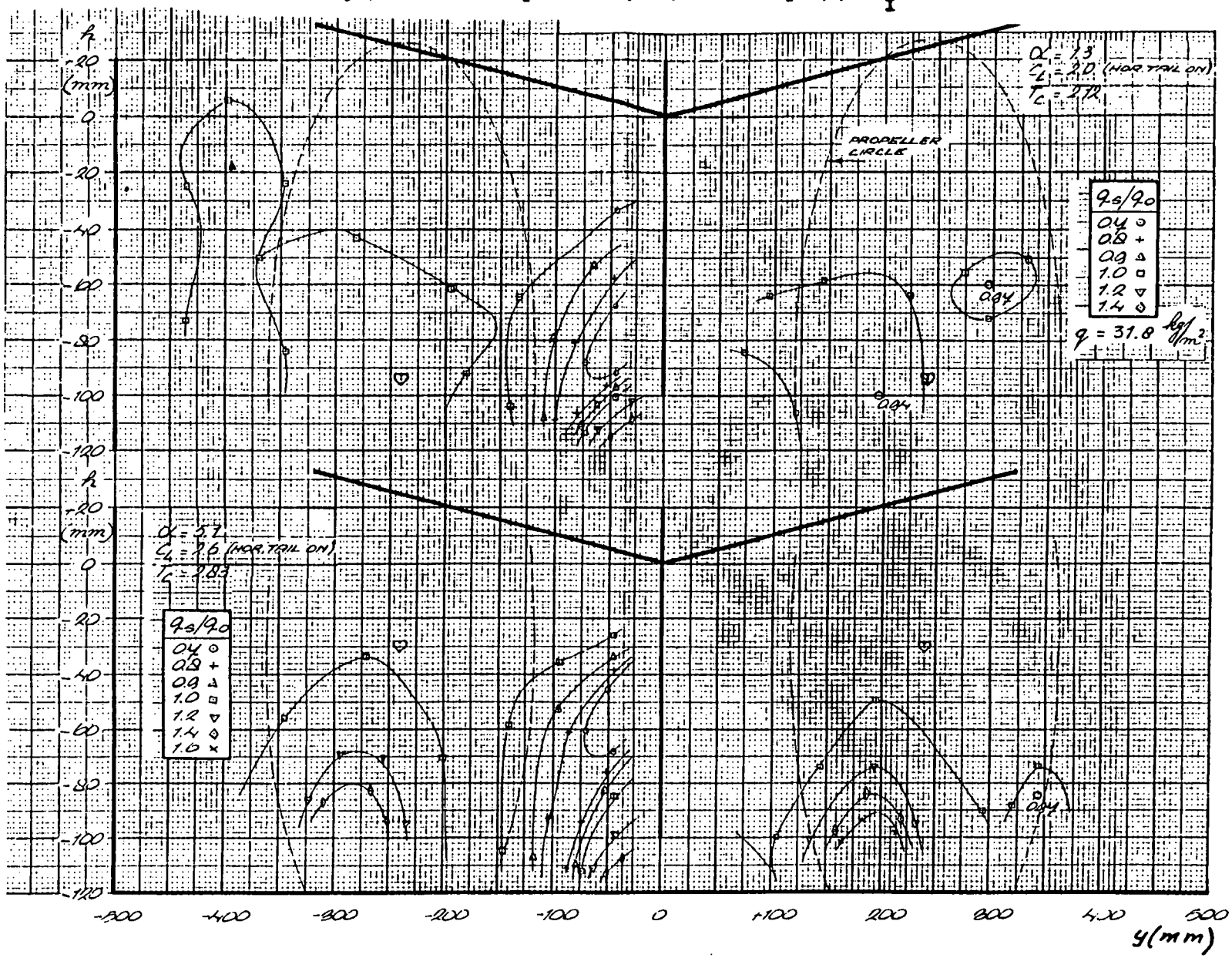

Dynamic-pressure contours in the hor.tail region.

Δ 180; constant power (1950 s.h.p.); δ_f = 70

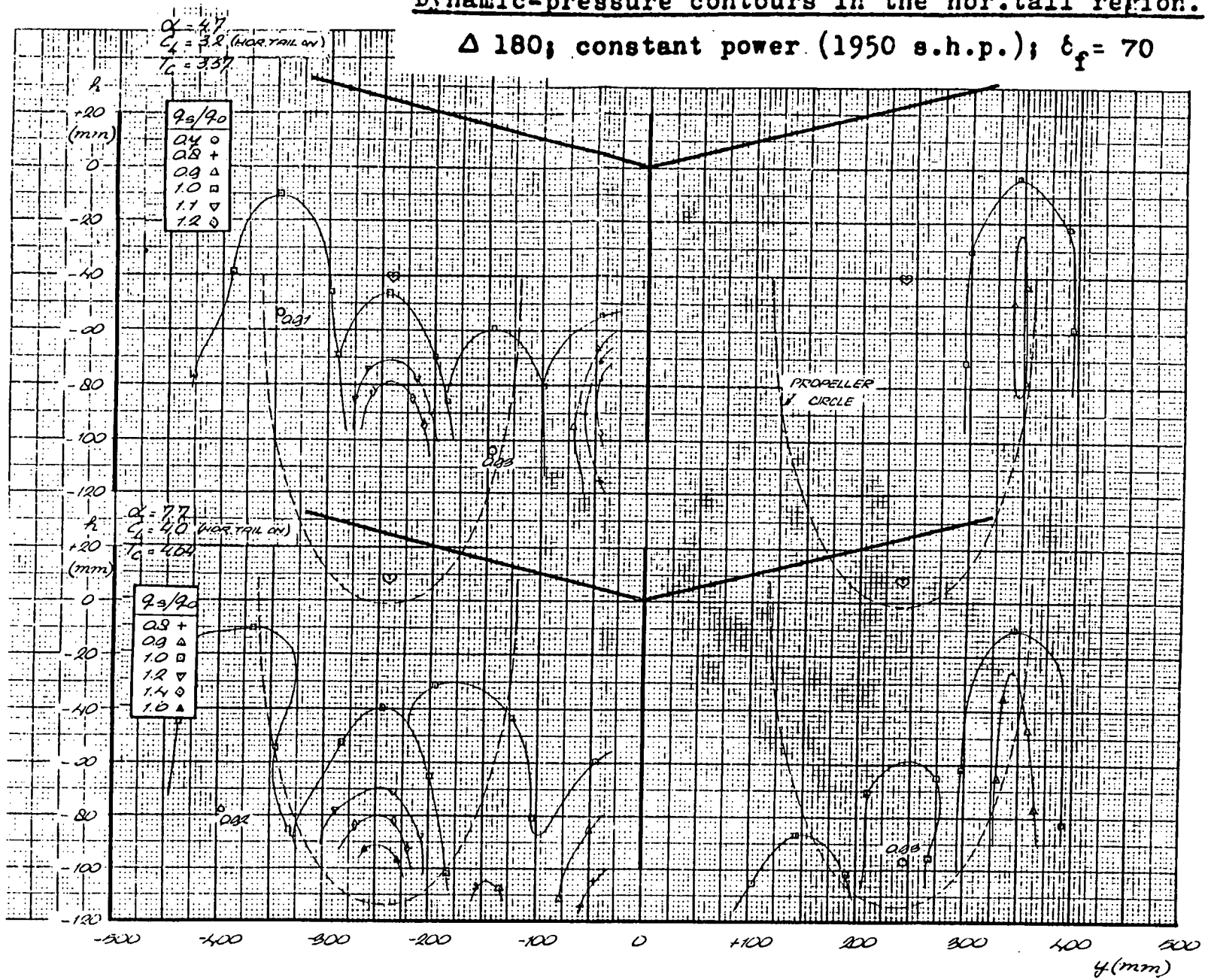

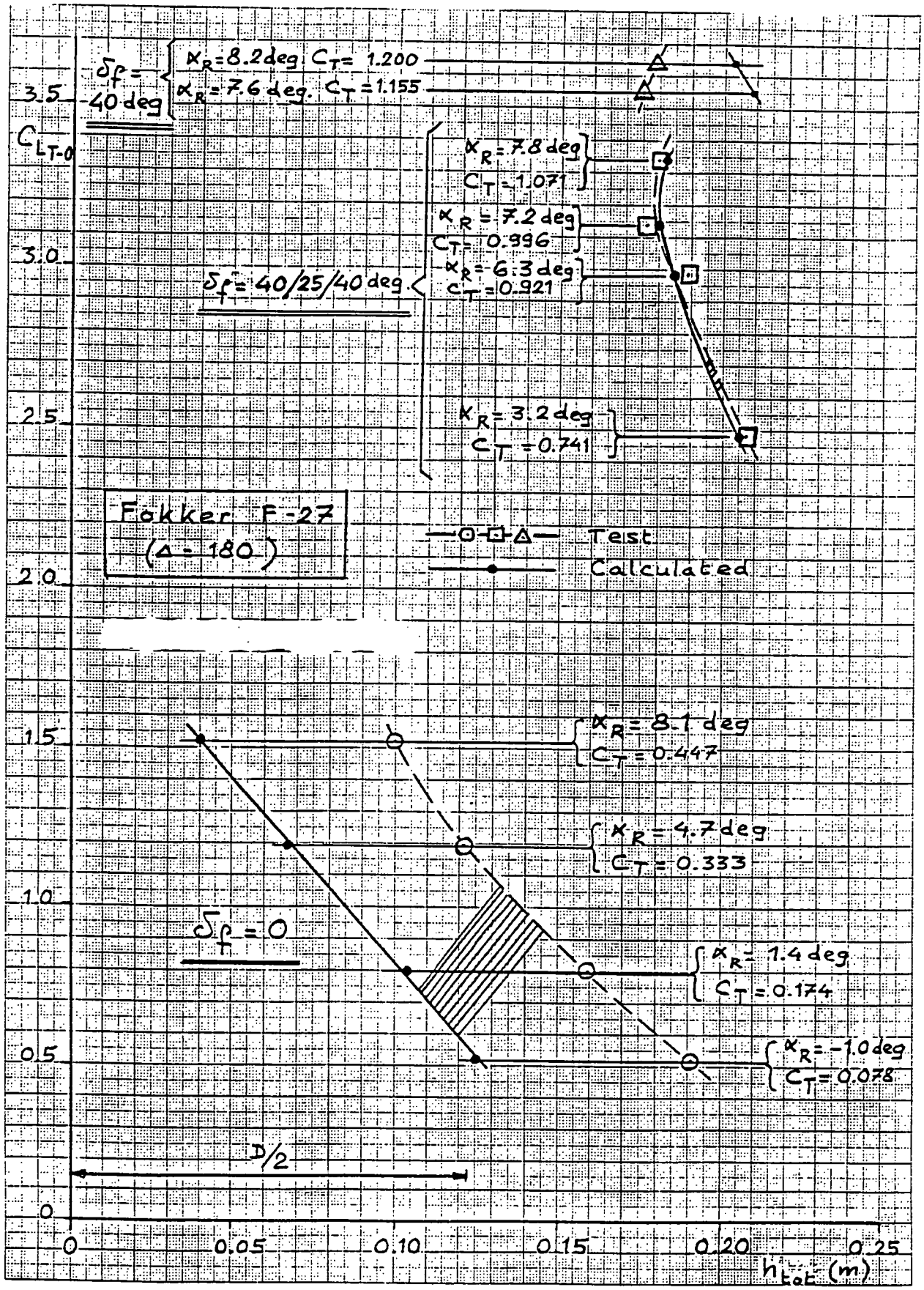
δ_f = 40 deg
α_R = 8.2 deg C_T = 1.200
α_R = 7.6 deg. C_T = 1.155
C_{LT-0}
3.5
3.0
2.5
2.0
1.5
1.0
0.5
0
α_R = 7.8 deg
C_T = 1.071
α_R = 7.2 deg
C_T = 0.996
α_R = 6.3 deg
C_T = 0.921
δ_f = 40/25/40 deg
α_R = 3.2 deg
C_T = 0.741
Fokker F-27
(Δ = 180)
Test
Calculated
α_R = 8.1 deg
C_T = 0.447
α_R = 4.7 deg
C_T = 0.333
δ_f = 0
α_R = 1.4 deg
C_T = 0.174
α_R = -1.0 deg
C_T = 0.078
D/2
0
0.05
0.10
0.15
0.20
0.25
h_{tot} (m)

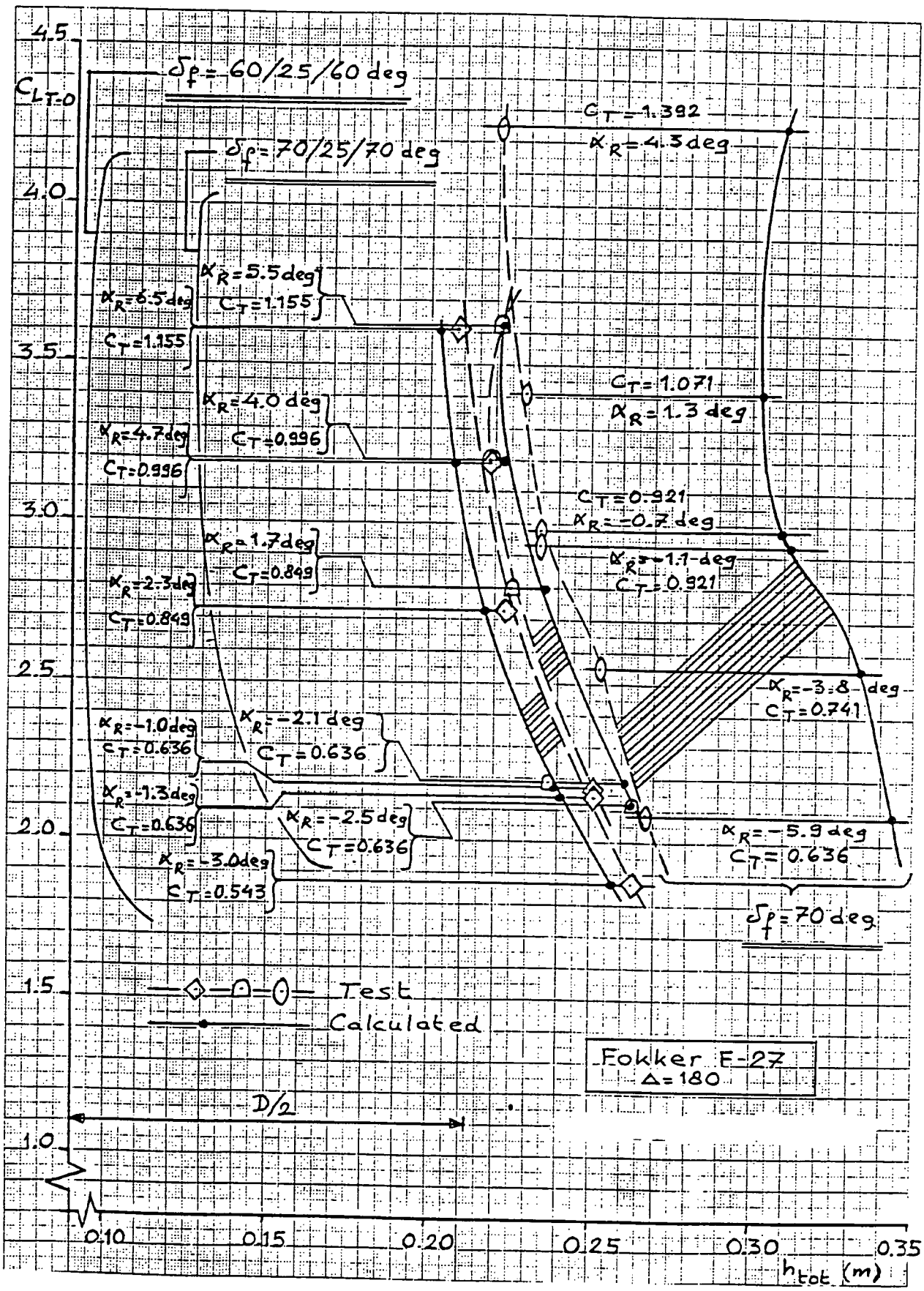
$C_{L_{T=0}}$
4.5
4.0
3.5
3.0
2.5
2.0
1.5
1.0
δ_f = 60/25/60 deg
δ_f = 70/25/70 deg
C_T = 1.392
α_R = 4.3 deg
α_R = 5.5 deg
C_T = 1.155
α_R = 6.5 deg
C_T = 1.155
C_T = 1.071
α_R = 1.3 deg
α_R = 4.0 deg
C_T = 0.996
α_R = 4.7 deg
C_T = 0.996
C_T = 0.921
α_R = -0.7 deg
α_R = 1.7 deg
C_T = 0.849
α_R = -1.1 deg
C_T = 0.921
α_R = 2.3 deg
C_T = 0.849
α_R = -3.8 deg
C_T = 0.741
α_R = -1.0 deg
C_T = 0.636
α_R = -2.1 deg
C_T = 0.636
α_R = -1.3 deg
C_T = 0.636
α_R = -2.5 deg
C_T = 0.636
α_R = -5.9 deg
C_T = 0.636
α_R = -3.0 deg
C_T = 0.543
δ_f = 70 deg
Test
Calculated
Fokker F-27
Δ = 180
D/2
0.10
0.15
0.20
0.25
0.30
0.35
h_{tot} (m)

Appendix XII

Downwash characteristics (III)

The increase in the average downwash at the horizontal tailplane due to propeller slipstream

As described in chapters 6.3 and 6.4 of the main text and in Appendix IV the average downwash at the wing wake centre line can be estimated using simple momentum considerations from lifting line theory. This downwash angle only depends on the wing lift coefficient independent from whether lift is generated entirely by free flow conditions or partly by propeller slipstream.
This also applies when, with slipstream present, the downwash is considered sufficiently far away from the slipstream.

The rate of change of the downwash due to lift coefficient in these cases $d\varepsilon/dC_L$ is given on page X-7.

Between the slipstream centre line and a distance $Z = 1.25\ D^*$ from the slipstream centre line an additional change in downwash occurs which suggests an in flow into the slipstream from the external flow.
This is illustrated in the following figure:

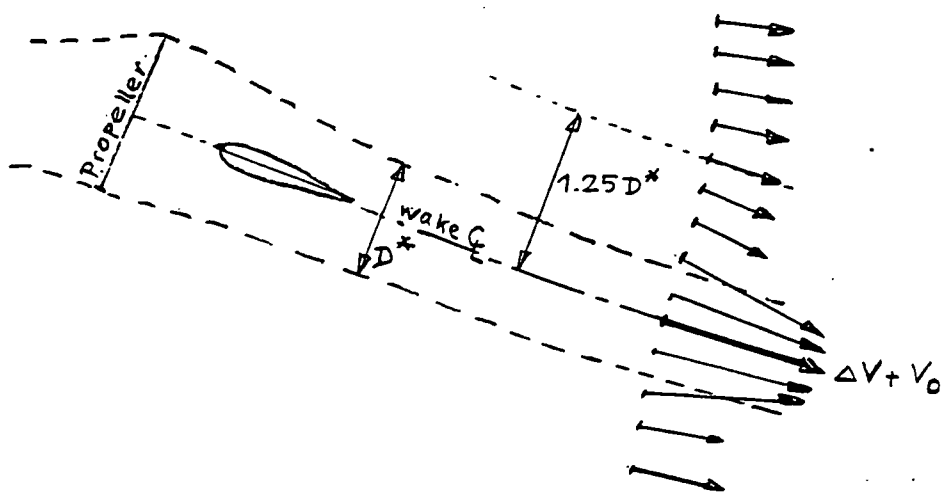

Based on windtunnel tests it is assumed that $\Delta\varepsilon$ is proportional to $\Delta V/V_o$

$$so: \Delta\varepsilon = (\Delta\varepsilon)_{\frac{\Delta V}{V_o}=1} \times \frac{\Delta V}{V_o}$$

On page XII -5 to XII -37 all available test data on downwash with propeller slipstream present is shown. Based on this information the generalized curve for $(\Delta\varepsilon)_{\Delta V/V_O = 1} = f\,(h_{tot}/D^*/2)$ as presented on pages XII -38 and XII -39 was determined.

The calculation procedure followed for the determination of the distance between slipstream centre line and horizontal tail surface is presented on pages XII -2 to XII -4.

On pages XII -40 to XII -47 some additional dowwash data, mainly from tests on an early F-27 model, are presented.

Table VII

Downwash Characteristics (III)

No.	Conf.	l_h/c (78)	i_w (deg) (79)	z_h/D (80)	δ_f (deg) (81)	α_R (deg) (82)	$C_f \sin\delta_f$ (83)	$\Delta\alpha_{0,f}$ (deg) (94) ≡ (15)	C_T $\frac{\Delta V}{V_0}=1$ (111)	$C_{L_{P=0}}$ (87) ≡ (88)	ΔC_{L_S} $\frac{\Delta V}{V_0}=1$ TEST (112)	C_L^* $\frac{\Delta V}{V_0}=1$ TEST (113) = (97)+(112)	$\Delta\varepsilon$ $\frac{\Delta V}{V_0}=1$ (deg) (114)	D_{prop} (30) ≡ (9)	D^* $\frac{\Delta V}{V_0}=1$ (91) ≡ (42)	C_S (92) ≡ (4)	C_f (93)	
1	NASA TN D-25	3.76	8.3	0.32	0	-8.0	0	0	1.04	-0.10	0	-0.10	0.4	1.454	1.26	1.62	0.405	
		3.76	8.3	0.32	0	0	0	0	1.04	0.53	0.32	0.85	1.0					
		3.76	8.3	0.32	0	8.0	0	0	1.04	1.26	0.64	1.90	2.5	1.454	1.26	1.62	0.405	
		3.76	8.3	0.32	60/10 δ_f	-8.0	0.260	-31.2	1.04	2.05	1.17	3.22	0	1.454	1.26	1.62	0.405	
		3.76	8.3	0.32		0	0.260	-31.2		2.25	1.46	4.21	0					
		3.76	8.3	0.32	60/10 δ_f	8.0	0.260	-31.2	1.04	3.35	1.62	4.87	0	1.454	1.26	1.62	0.405	
4	ARC R&M No 2747	3.78	0	0.06	0	0	0	0	0.946	0.09	0	0.09	-	10.0	8.66	11.1	2.20	LW, CR
		3.78	0	0.06	0	10.0	0	0	0.946	1.01	0.51	1.52	-	10.0	8.66	11.1	2.20	
		3.78	0	0.16	0	0	0	0	0.946	0.09	0	0.09	1.9	10.0	8.66	11.1	2.20	
		3.78	0	0.16	0	10.0	0	0	0.946	1.01	0.51	1.52	-1.5	10.0	8.66	11.1	2.20	
		3.78	0	0.31	0	0	0	0	0.946	0.09	0	0.09	3.1	10.0	8.66	11.1	2.20	
		3.78	0	0.31	0	10.0	0	0	0.946	1.01	0.51	1.52	0	10.0	8.66	11.1	2.20	
		3.28	0	0.46	0	0	0	0	0.946	0.09	0	0.09	3.0	10.0	8.66	11.1	2.20	
		3.28	0	0.46	0	10.0	0	0	0.946	1.01	0.51	1.52	2.4	10.0	8.66	11.1	2.20	
		3.28	0	0.61	0	0	0	0	0.946	0.09	0	0.09	1.3	10.0	8.66	11.1	2.20	
		3.28	0	0.61	0	10.0	0	0	0.946	1.01	0.51	1.52	3.9	10.0	8.66	11.1	2.20	
		3.78	0	0.705	0	0	0	0	0.946	0.09	0	0.09	1.1	10.0	8.66	11.1	2.20	
		3.78	0	0.705	0	10.0	0	0	0.946	1.01	0.51	1.52	4.2	10.0	8.66	11.1	2.20	LW, CR
4	ARC R&M No 2747	4.41	0	0.01	0	0	0	0	0.946	0.09	0	0.09	0.3	10.0	8.66	11.1	2.20	LW, CR
		4.41	0	0.01	0	10.0	0	0	0.946	1.01	0.51	1.52	-1.9	10.0	8.66	11.1	2.20	
		4.41	0	0.16	0	0	0	0	0.946	0.09	0	0.09	1.8	10.0	8.66	11.1	2.20	
		4.41	0	0.16	0	10.0	0	0	0.946	1.01	0.51	1.52	-2.0	10.0	8.66	11.1	2.20	
		4.41	0	0.46	0	0	0	0	0.946	0.09	0	0.09	3.0	10.0	8.66	11.1	2.20	
		4.41															2.20	
		4.41															2.20	
		4.41															2.20	
		4.41															2.20	LW, CR
4	ARC R&M No 2747	3.78	0	-0.15	0	0	0	0	0.946	0.11	0	0.11	0.3	10.0	8.66	11.1	2.20	MW, CR
		3.78	0	-0.15	0	10.0	0	0	0.946	1.03	0.51	1.54	-2.8	10.0	8.66	11.1	2.20	MW, CR

Example of calculating procedure

Table VII

Downwash Characteristics (III) (Continued)

No	Conf	l_h	h_t	$x_{0.25\bar{c}} - x_{pr.}$	l_h''	$(\Delta h_t)_\alpha$	$(\Delta h_t)_{upw.}$	$\frac{d\varepsilon}{dC_L}$	K_ε	$\frac{(dC_L)}{2K/1\cdot0}$ (1/deg) $C_T = 0$	ΔC_{L_S} $\frac{\Delta V}{V} = -1$ TEST	$\varepsilon_{K=0}$	M	N	O	P	K_R	dim.
		(94)	(95)	(96)	(97)	(98)	(99)	(100)	(101)	(102)	(112)	(104)	(105)	(106)	(107)	(108)	(82)	
1	NASA	5.55	0.575	1.45	4.41	+0.202	0	4.10	1.5	0.082	0	3.0	-4.03	0	+4.50	0.04	-8.0	m
	TN D-25	5.55				0	0				0.32	3.0	0	+1.97	+4.50	0.50	0	m
		5.55	0.575	1.45	4.41	-0.202	0	4.10	1.5	0.082	0.64	3.0	4.03	+4.09	+4.50	0.99	8.0	m
		5.55	0.575	1.45	4.41	+0.202	-0.188	4.10	1.5	0.065	1.17	8.7	-3.20	7.20	13.05	1.35	-8.0	m
		5.55				0	-0.188				1.46	8.7	0	8.98	13.05	1.78	0	m
		5.55	0.575	1.45	4.41	-0.202	-0.188	4.10	1.5	0.065	1.62	8.7	3.20	9.96	13.05	2.17	8.0	m
4	ARC R&M	37.6	1.18	8.88	28.5	0	0	4.05	1.5	0.095	0	0	0	0	0	0	0	in
	No 2747	37.6	1.18	8.88	28.5	-1.54	0	4.05	1.5	0.095	0.51	0	5.77	+3.10	0	4.45	10.0	in
		37.6	2.18	8.88	28.5	0	0	4.05	1.5	0.095	0	0	0	0	0	0	0	in
		37.6	2.18	8.88	28.5	-1.54	0	4.05	1.5	0.095	0.51	0	5.77	+3.10	0	4.45	10.0	in
		37.6	3.68	8.88	28.5	0	0	4.05	1.5	0.095	0	0	0	0	0	0	0	in
		37.6	3.68	8.88	28.5	-1.54	0	4.05	1.5	0.095	0.51	0	5.77	+3.10	0	4.45	10.0	in
		37.6	5.18	8.88	28.5	0	0	4.05	1.5	0.095	0	0	0	0	0	0	0	in
		37.6	5.18	8.88	28.5	-1.54	0	4.05	1.5	0.095	0.51	0	5.77	+3.10	0	4.45	10.0	in
		37.6	6.68	8.88	28.5	0	0	4.05	1.5	0.095	0	0	0	0	0	0	0	in
		37.6	6.68	8.88	28.5	-1.54	0	4.05	1.5	0.095	0.51	0	5.77	3.10	0	4.45	10.0	in
		37.6	7.63	8.88	28.5	0	0	4.05	1.5	0.095	0	0	0	0	0	0	0	in
		37.6	7.63	8.88	28.5	-1.54	0	4.05	1.5	0.095	0.51	0	5.77	3.10	0	4.45	10.0	in
4	ARC R&M	43.9	0.59	8.88	35.5	0	0	4.05	1.5	0.095	0	0	0	0	0	0	0	in
	No 2747	43.9	0.59	8.88	35.5	-1.54	0	4.05	1.5	0.095	0.51	0	5.77	3.10	0	5.54	10.0	in
		43.9	2.18	8.88	35.5	0	0	4.05	1.5	0.095	0	0	0	0	0	0	0	in
		43.9	2.18	8.88	35.5	-1.54	0	4.05	1.5	0.095	0.51	0	5.77	3.10	0	5.54	10.0	in
		43.9	5.18	8.88	35.5	0	0	4.05	1.5	0.095	0	0	0	0	0	0	0	in
		43.9	5.18	8.88	35.5	-1.54	0	4.05	1.5	0.095	0.51	0	5.77	3.10	0	5.54	10.0	in
		43.9	6.68	8.88	35.5	0	0	4.05	1.5	0.095	0	0	0	0	0	0	0	in
		43.9	6.68	8.88	35.5	-1.54	0	4.05	1.5	0.095	0.51	0	5.77	3.10	0	5.54	10.0	in
4	ARC R&M	37.6	-0.92	8.88	28.5	0	0	4.05	1.5	0.095	0	0	0	0	0	0	0	in
	No 2747	37.6	-0.92	8.88	28.5	-1.54	0	4.05	1.5	0.095	0.51	0	5.77	3.10	0	4.45	10.0	in

Table VII Downwash Characteristics (III) (Concluded)

No	Conf	δ_f (deg) (81)	α_R (deg) (82)	h_{tot} $\frac{\Delta V}{V_o}=1$ (109)	h_{tot} TEST	$\frac{h_{tot}}{D/2}$ $\frac{\Delta V}{V_o}=1$ (111)	b_{s_h}	c_{s_h}	s_{s_h}	S_h	$\frac{q_s}{q}$	b_{max}	$b=\left(\frac{\Delta V}{V_o}\right)_{\Delta V}$	$\frac{q_h}{q}$	$\frac{q_h}{q}$ TEST	
1	NASA TN D-25	0	-8.0	1.60	—	2.53										
		0	0	1.08	—	1.71										
		0	8.0	0.58	—	0.93										
		60/c/20	-8.0	2.98	—	4.73										
		60/c/20	0	2.43	—	3.85										
		60/c/20	8.0	1.84	—	2.91										
4	ARC R&M No 2747	0	0	1.18	—	0.27										
		0	10.0	-2.54	—	-0.59										
		8	0	2.18	—	0.50										
		8	10.0	-1.54	—	-0.36										
		0	0	3.68	—	0.85										
		0	10.0	-0.04	—	-0.01										
		0	0	5.18	—	1.20										
		0	10.0	1.46	—	0.34										
		0	0	6.68	—	1.54										
		0	10.0	2.96	—	0.68										
		0	0	7.63	—	1.76										
		0	10.0	3.91	—	0.90										
4	ARC R&M No 2747	0	0	0.59	—	0.14										
		0	10.0	-3.15	—	-0.73										
		0	0	2.18	—	0.50										
		0	10.0	-1.56	—	-0.36										
		0	0	5.18	—	1.20										
		0	10.0	1.44	—	0.33										
		0	0	6.68	—	1.54										
		0	10.0	2.94	—	0.68										
4	ARC R&M No 2747	0	0	-0.92	—	-0.21										
		0	10.0	-3.29	—	-1.08										

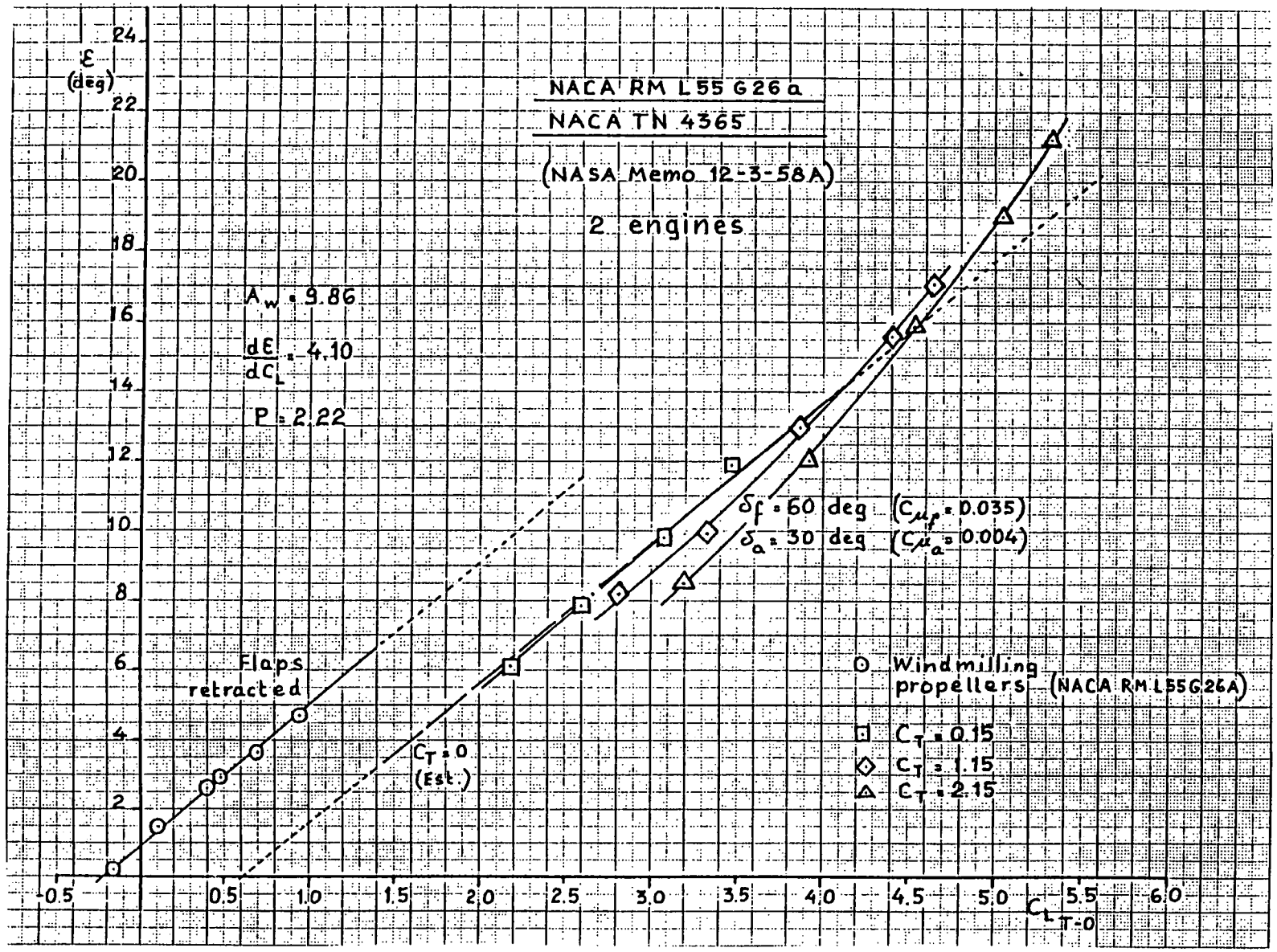
NACA RM L55 G26a
NACA TN 4365
(NASA Memo 12-3-58A)
2 engines
$A_w = 9.86$
$\frac{d\varepsilon}{dC_L} = 4.10$
$P = 2.22$
$\delta_f = 60$ deg ($C_{\mu_f} = 0.035$)
$\delta_a = 30$ deg ($C_{\mu_a} = 0.004$)
Flaps retracted
$C_T = 0$ (Est.)
Windmilling propellers (NACA RM L55G26A)
$C_T = 0.15$
$C_T = 1.15$
$C_T = 2.15$
ε (deg)
$C_{L_{T=0}}$

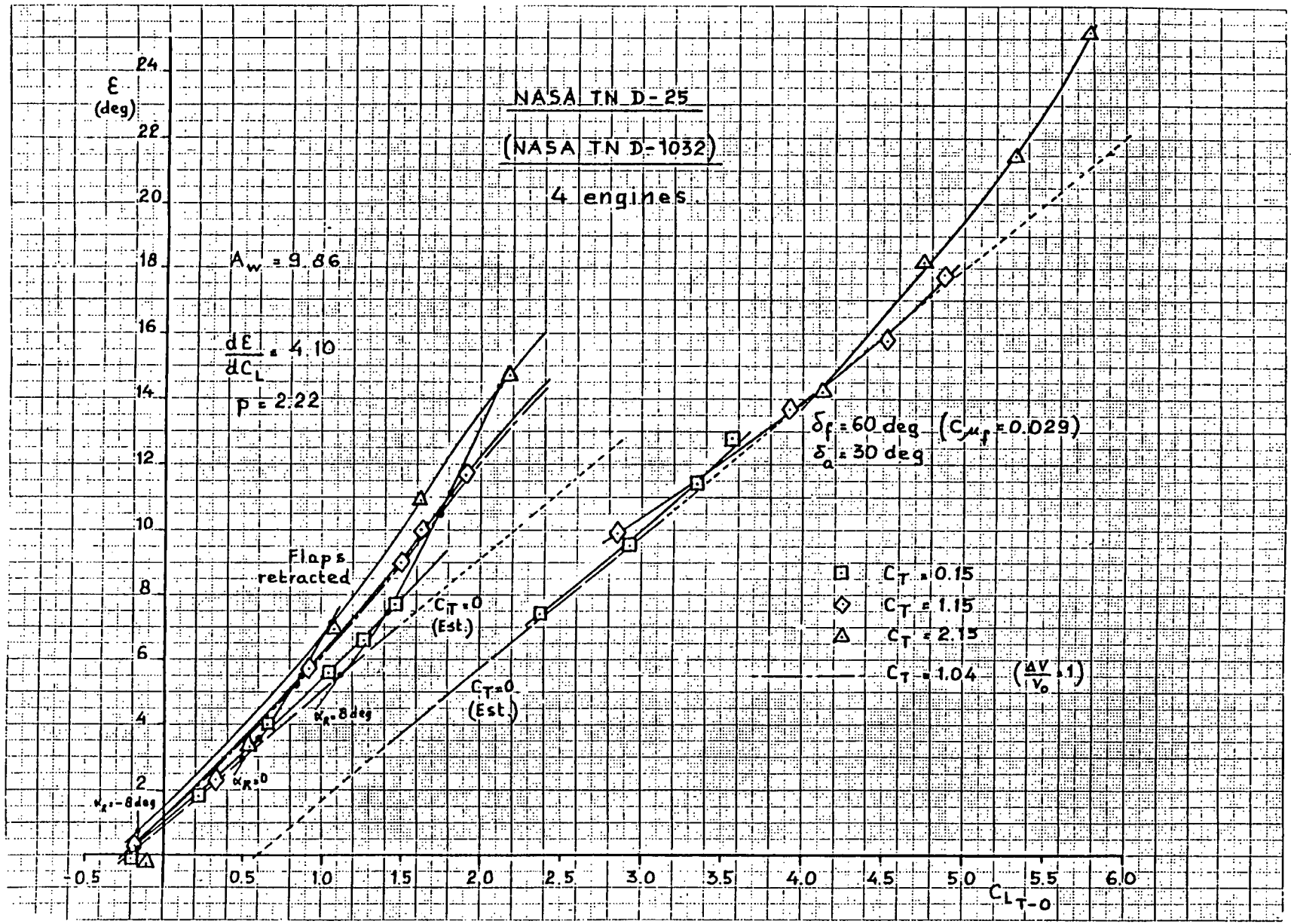
NASA TN D-25
(NASA TN D-1032)
4 engines
ε (deg)
$A_w = 9.86$
$\frac{d\varepsilon}{dC_L} = 4.10$
$p = 2.22$
$\delta_f = 60$ deg ($C_{\mu_f} = 0.029$)
$\delta_a = 30$ deg
Flaps retracted
$C_T = 0.15$
$C_T = 1.15$
$C_T = 2.15$
$C_T = 1.04$ ($\frac{\Delta V}{V_0} = .1$)
$C_{T=0}$ (Est.)
$C_{T=0}$ (Est.)
$\alpha_R = 8$ deg
$\alpha_R = 0$
$\alpha_R = -8$ deg
$C_{L_{T-0}}$

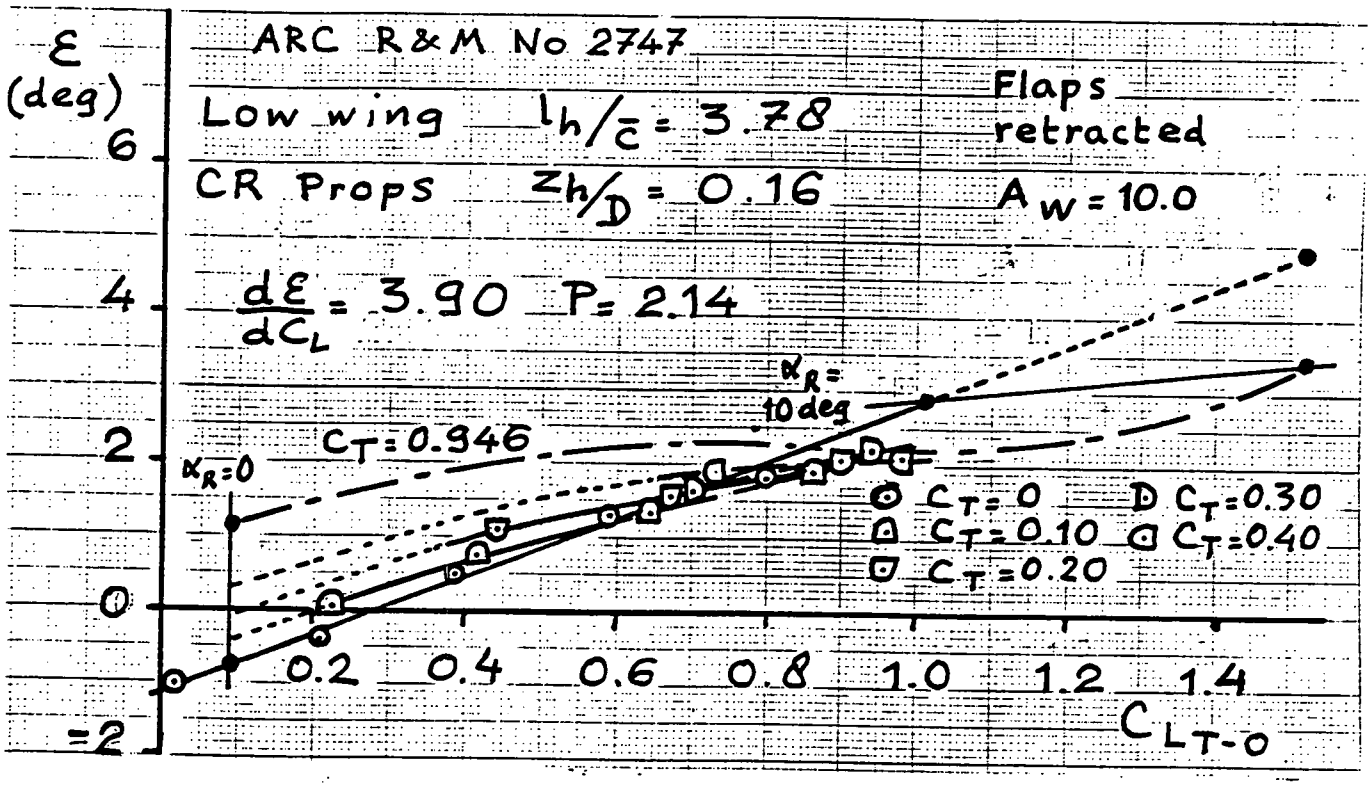
ε (deg)
ARC R&M No 2747
Low wing $l_h/\bar{c}$ = 3.78
CR Props z_h/D = 0.16
Flaps retracted
A_W = 10.0
$\frac{d\varepsilon}{dC_L}$ = 3.90 P = 2.14
α_R = 10 deg
C_T = 0.946
α_R = 0
C_T = 0
C_T = 0.10
C_T = 0.20
C_T = 0.30
C_T = 0.40
6
4
2
0
=2
0.2
0.4
0.6
0.8
1.0
1.2
1.4
C_{LT-O}

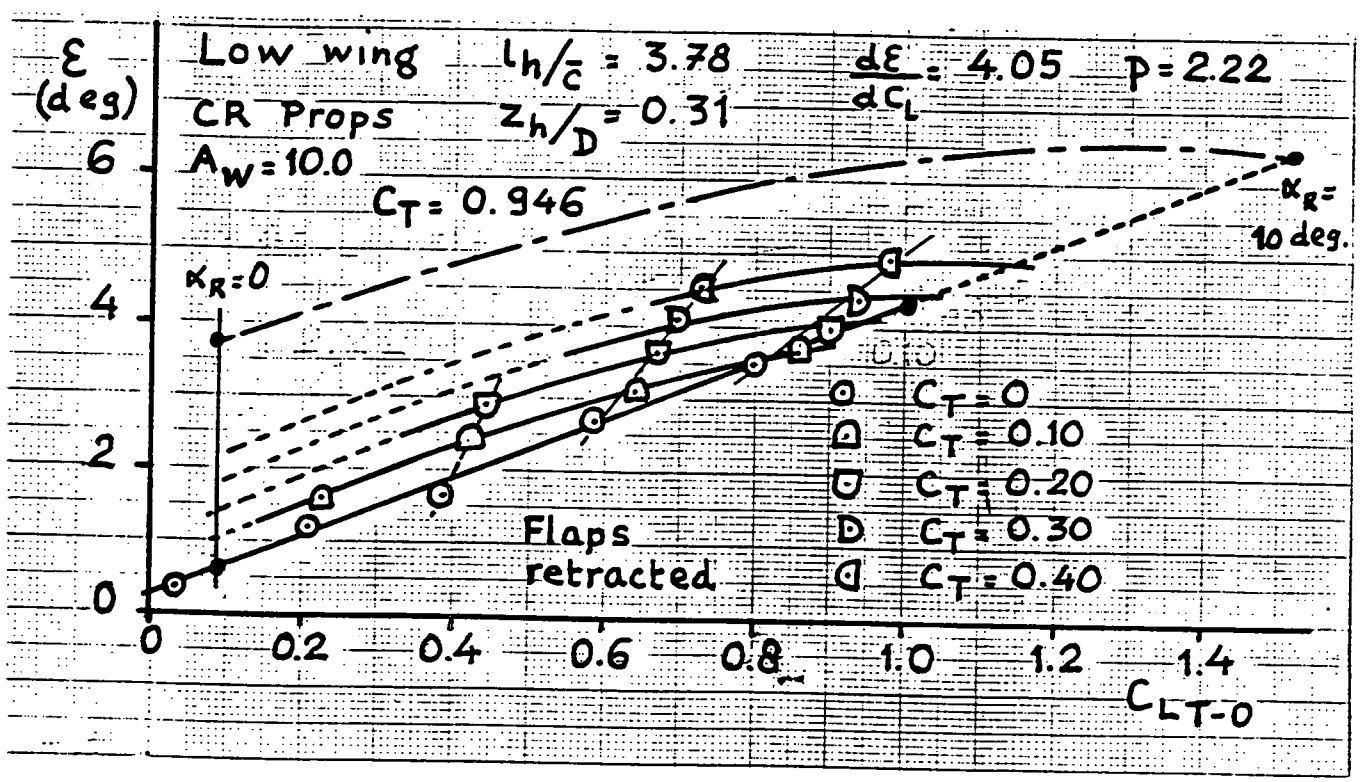
ε (deg)
Low wing $l_h/\bar{c}$ = 3.78
CR Props z_h/D = 0.31
A_W = 10.0
$\frac{d\varepsilon}{dC_L}$ = 4.05 P = 2.22
C_T = 0.946
α_R = 10 deg.
α_R = 0
C_T = 0
C_T = 0.10
C_T = 0.20
C_T = 0.30
C_T = 0.40
Flaps retracted
6
4
2
0
0.2
0.4
0.6
0.8
1.0
1.2
1.4
C_{LT-O}

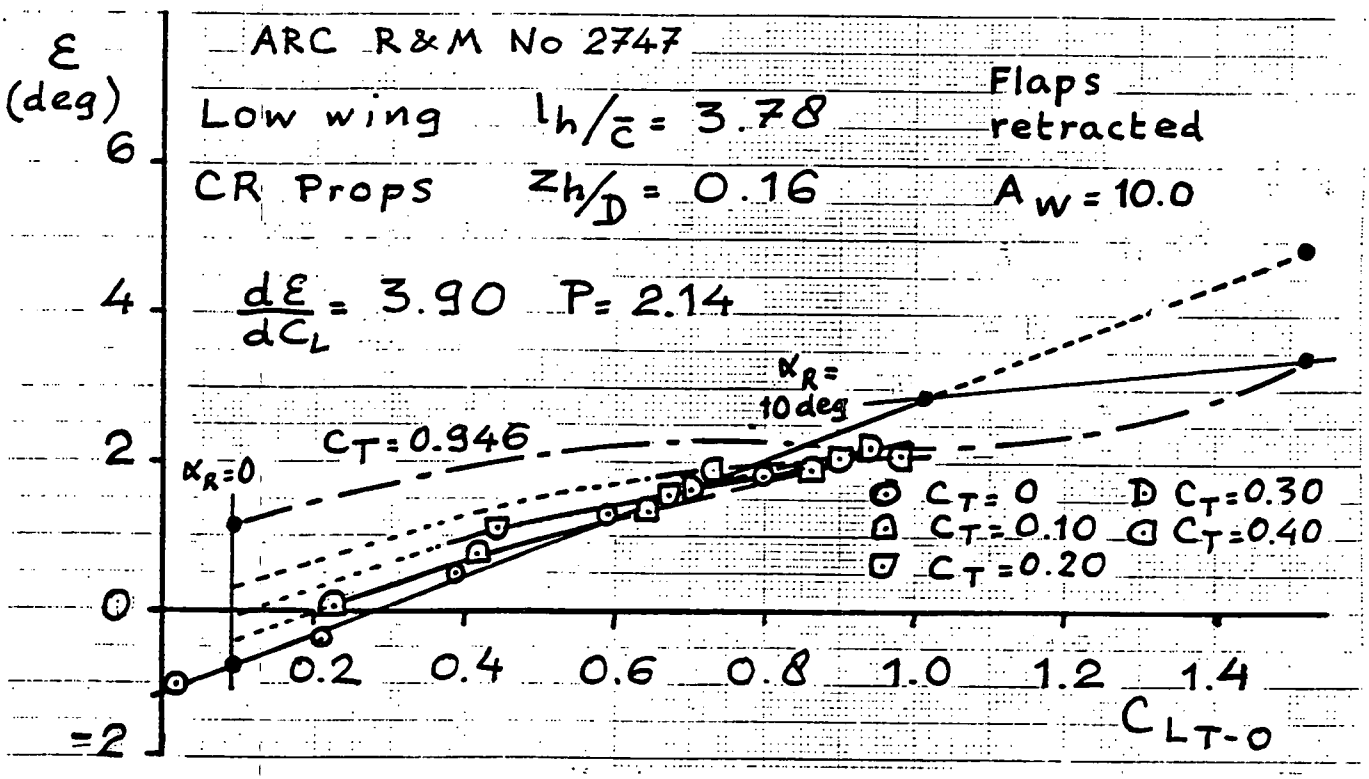
ε (deg)
ARC R&M No 2747
Low wing
CR Props
$l_h/c = 3.78$
$z_h/D = 0.16$
Flaps retracted
$A_w = 10.0$
$\frac{d\varepsilon}{dC_L} = 3.90$
P = 2.14
α_R = 10 deg
$C_T = 0.946$
$\alpha_R = 0$
$C_T = 0$
$C_T = 0.10$
$C_T = 0.20$
$C_T = 0.30$
$C_T = 0.40$
6
4
2
0
=2
0.2
0.4
0.6
0.8
1.0
1.2
1.4
$C_{L_{T-0}}$

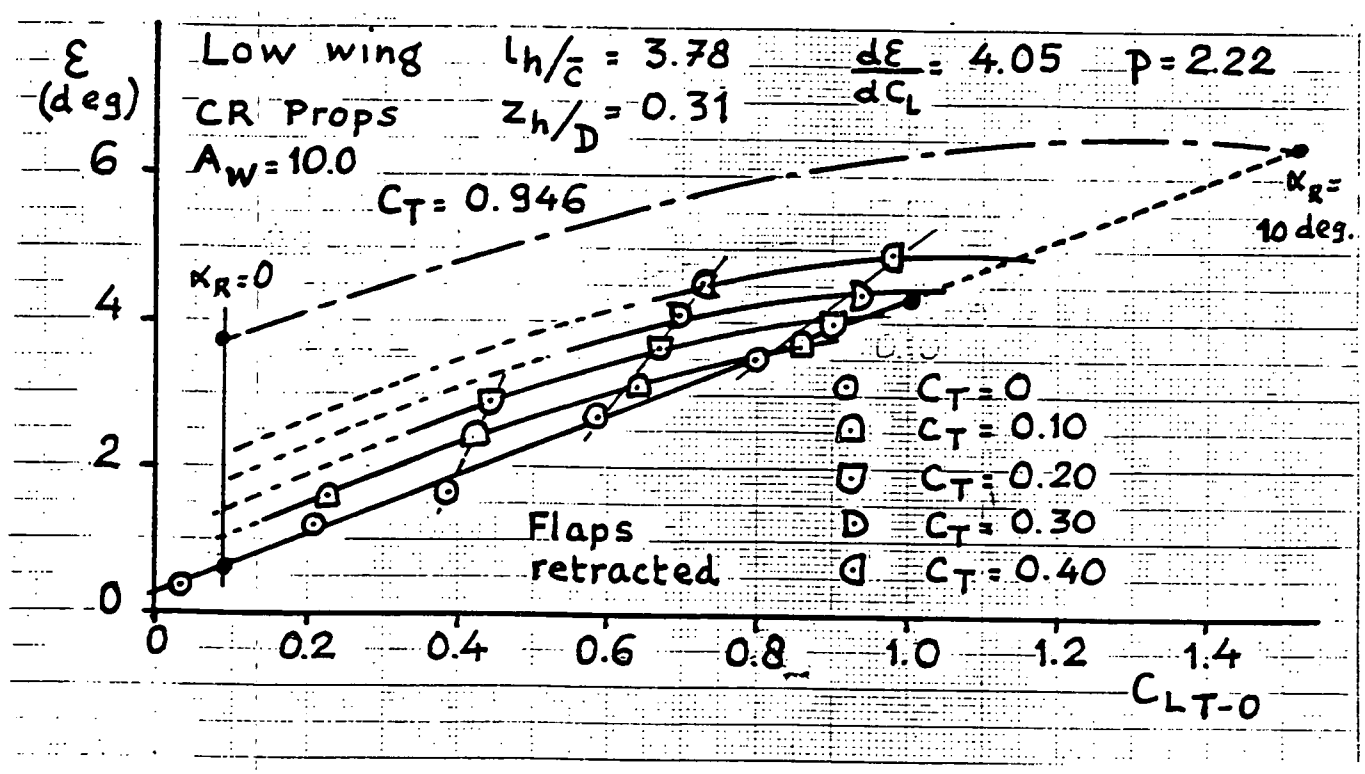
ε (deg)
Low wing
CR Props
$A_w = 10.0$
$l_h/c = 3.78$
$z_h/D = 0.31$
$\frac{d\varepsilon}{dC_L} = 4.05$
P = 2.22
$C_T = 0.946$
α_R = 10 deg.
$\alpha_R = 0$
$C_T = 0$
$C_T = 0.10$
$C_T = 0.20$
$C_T = 0.30$
$C_T = 0.40$
Flaps retracted
6
4
2
0
0.2
0.4
0.6
0.8
1.0
1.2
1.4
$C_{L_{T-0}}$

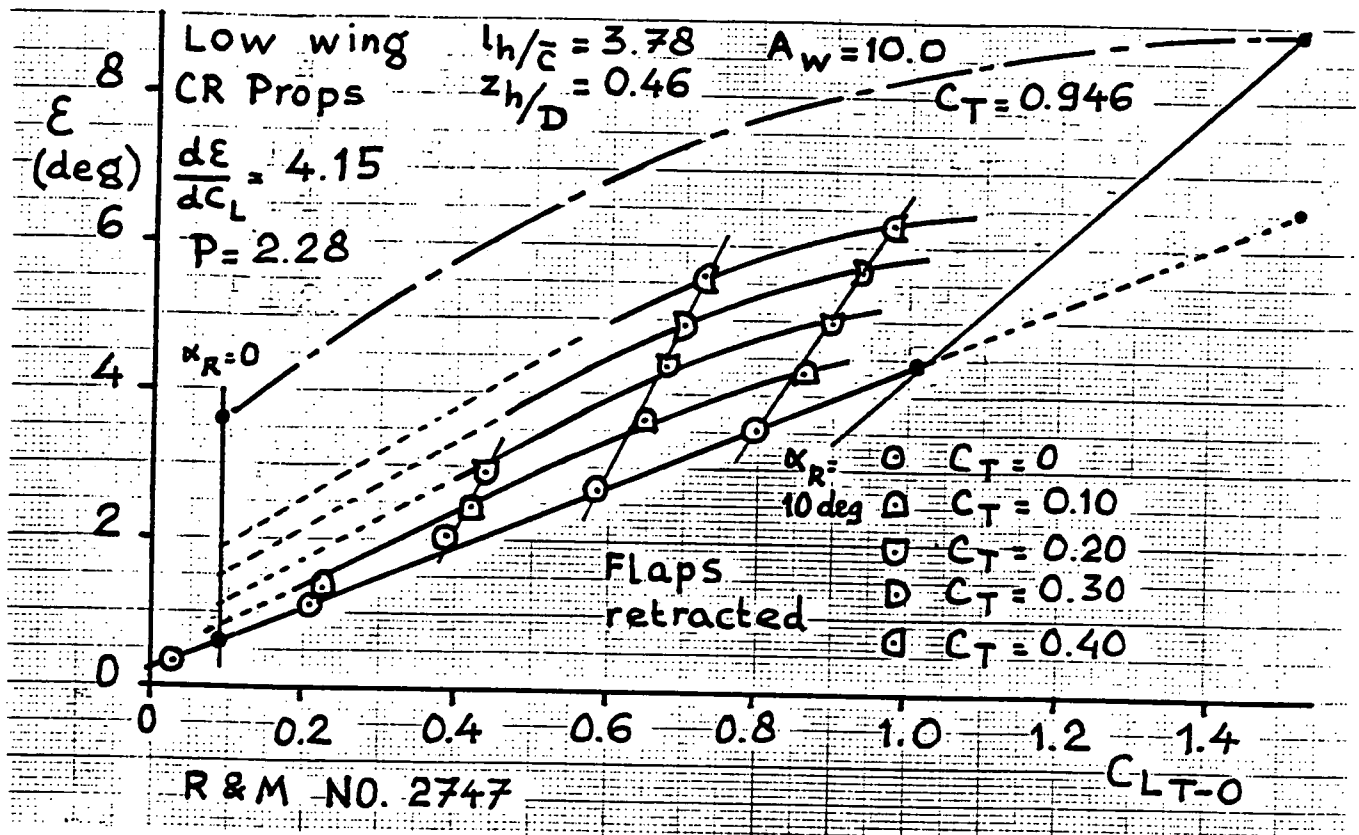
Low wing
CR Props
$l_h/\bar{c} = 3.78$
$z_h/D = 0.46$
$A_w = 10.0$
$C_T = 0.946$
$\frac{d\varepsilon}{dC_L} = 4.15$
P = 2.28
ε (deg)
$\alpha_R = 0$
α_R = 10 deg
$C_T = 0$
$C_T = 0.10$
$C_T = 0.20$
$C_T = 0.30$
$C_T = 0.40$
Flaps retracted
C_{LT-O}
R & M NO. 2747

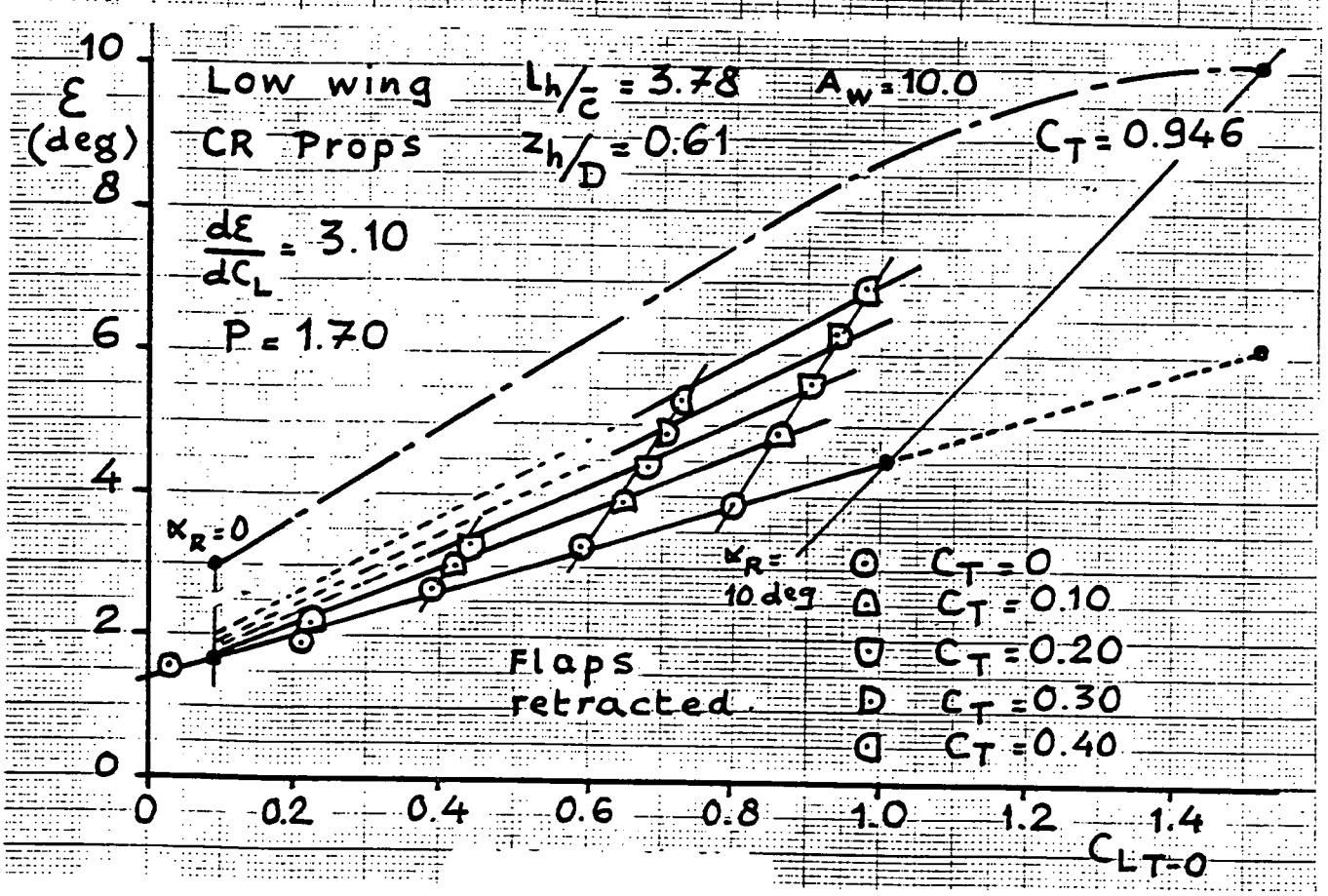
Low wing
CR Props
$l_h/\bar{c} = 3.78$
$z_h/D = 0.61$
$A_w = 10.0$
$C_T = 0.946$
$\frac{d\varepsilon}{dC_L} = 3.10$
P = 1.70
ε (deg)
$\alpha_R = 0$
α_R = 10 deg
$C_T = 0$
$C_T = 0.10$
$C_T = 0.20$
$C_T = 0.30$
$C_T = 0.40$
Flaps retracted
C_{LT-O}

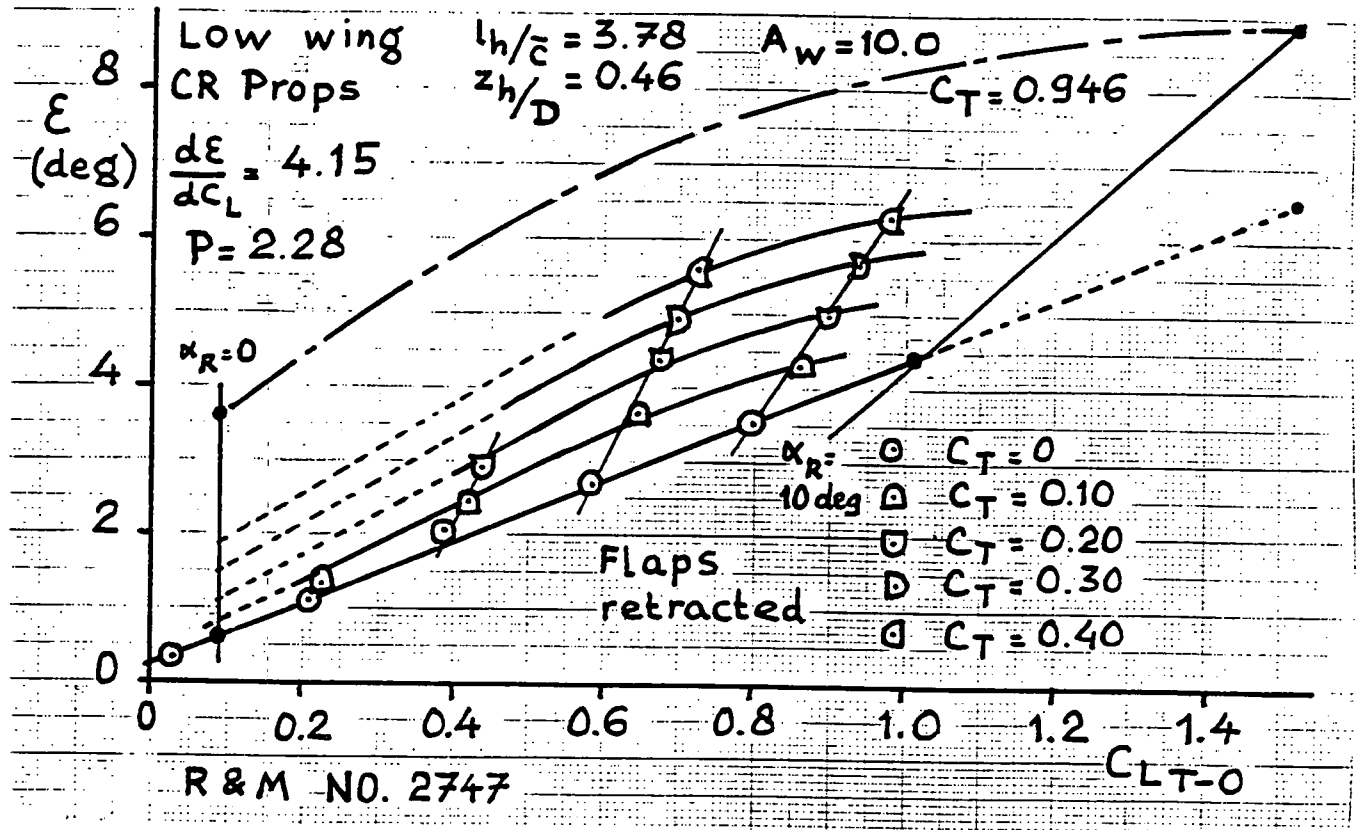
Low wing
CR Props
$\frac{d\varepsilon}{dC_L}$ = 4.15
P = 2.28
$l_h/\bar{c}$ = 3.78
z_h/D = 0.46
A_w = 10.0
C_T = 0.946
ε (deg)
α_R=0
α_R= 10 deg
C_T = 0
C_T = 0.10
C_T = 0.20
C_T = 0.30
C_T = 0.40
Flaps retracted
C_{LT-O}

R & M NO. 2747

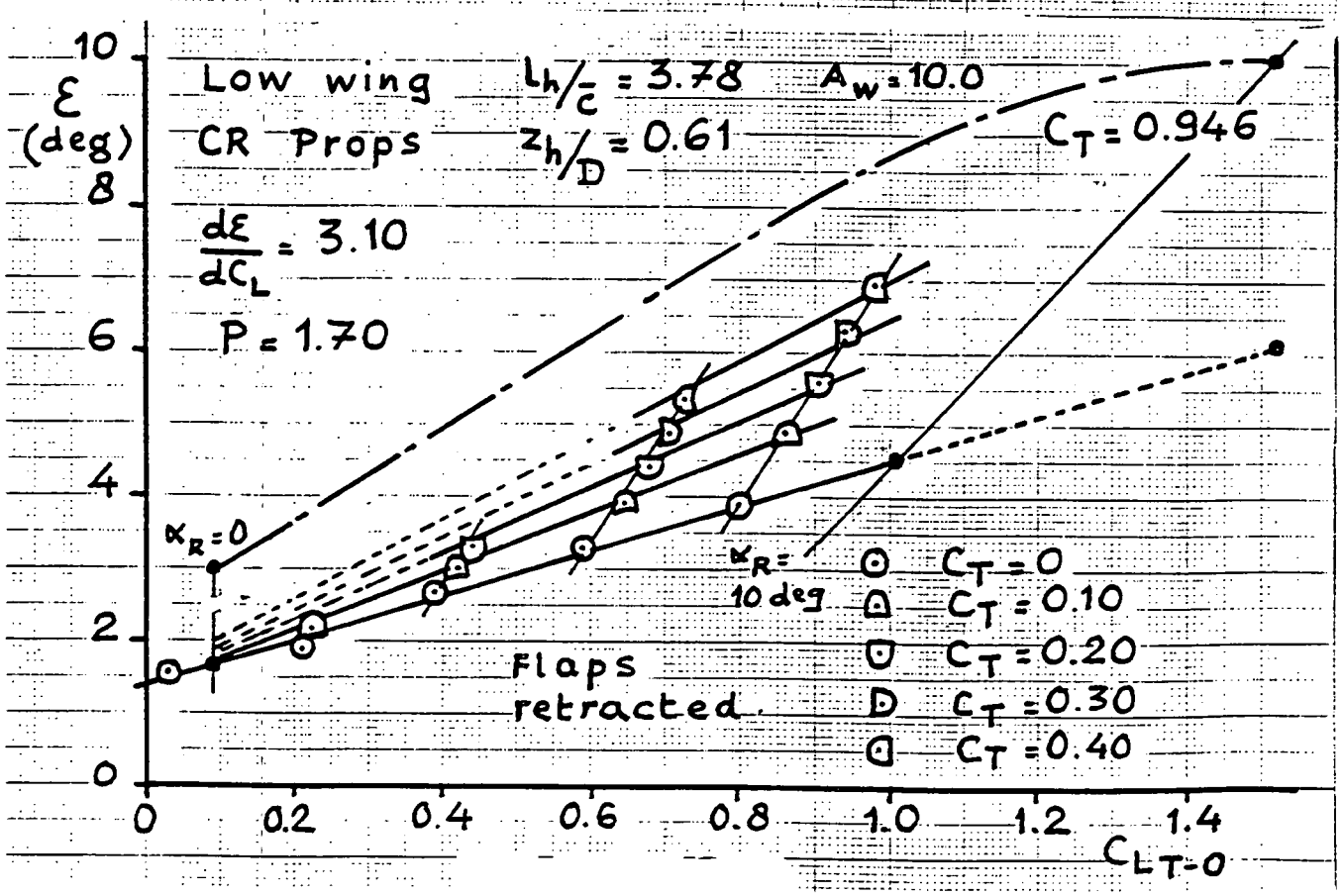
Low wing
CR Props
$\frac{d\varepsilon}{dC_L}$ = 3.10
P = 1.70
$l_h/\bar{c}$ = 3.78
z_h/D = 0.61
A_w = 10.0
C_T = 0.946
ε (deg)
α_R=0
α_R= 10 deg
C_T = 0
C_T = 0.10
C_T = 0.20
C_T = 0.30
C_T = 0.40
Flaps retracted
C_{LT-O}

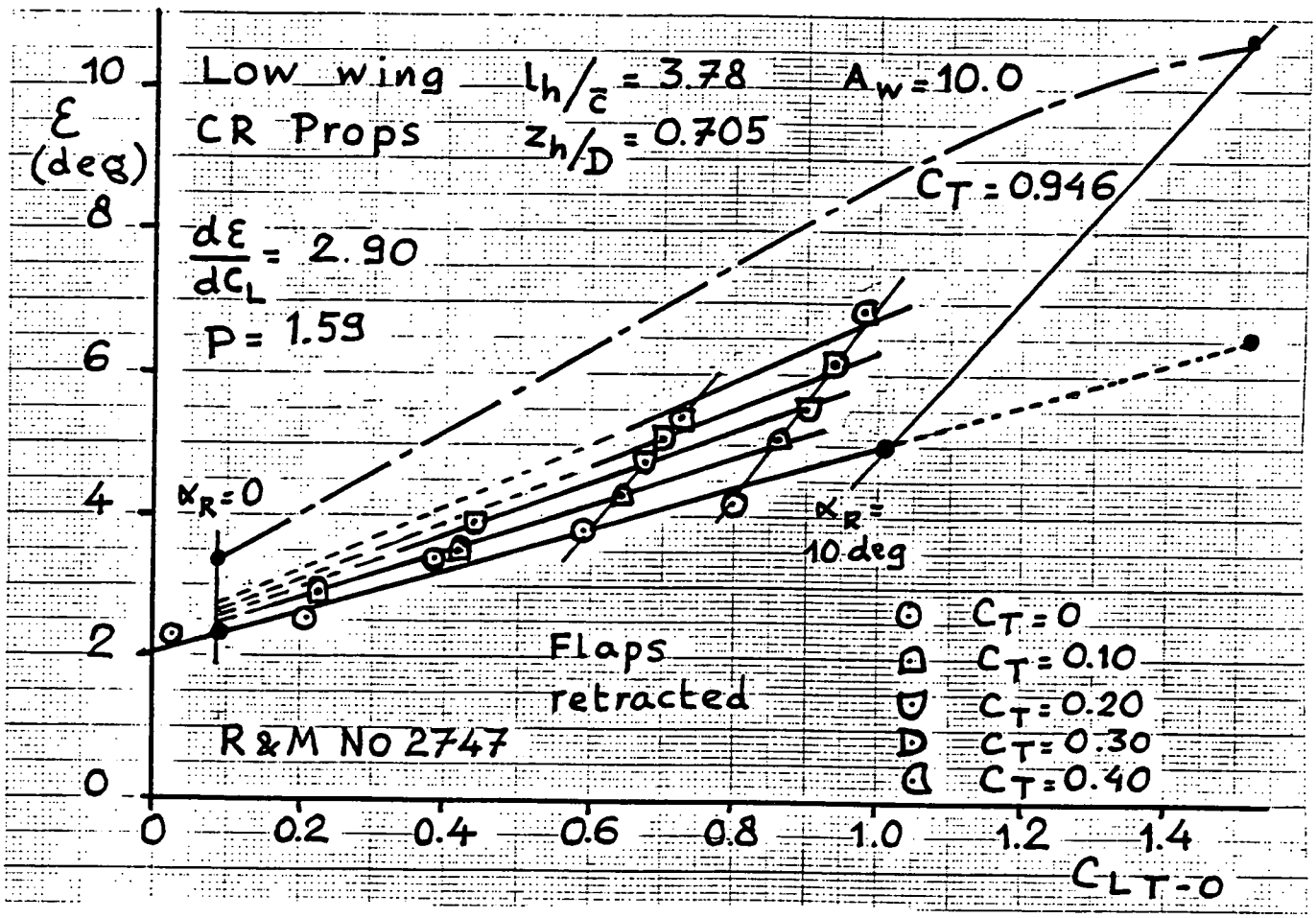
Low wing $l_h/\bar{c} = 3.78$ $A_w = 10.0$
CR Props $z_h/D = 0.705$
$C_T = 0.946$
$\frac{d\varepsilon}{dC_L} = 2.90$
$P = 1.59$
$\alpha_R = 0$
$\alpha_R = 10$ deg
Flaps retracted
R & M No 2747
$C_T = 0$
$C_T = 0.10$
$C_T = 0.20$
$C_T = 0.30$
$C_T = 0.40$
ε (deg)
10
8
6
4
2
0
0
0.2
0.4
0.6
0.8
1.0
1.2
1.4
C_{LT-0}

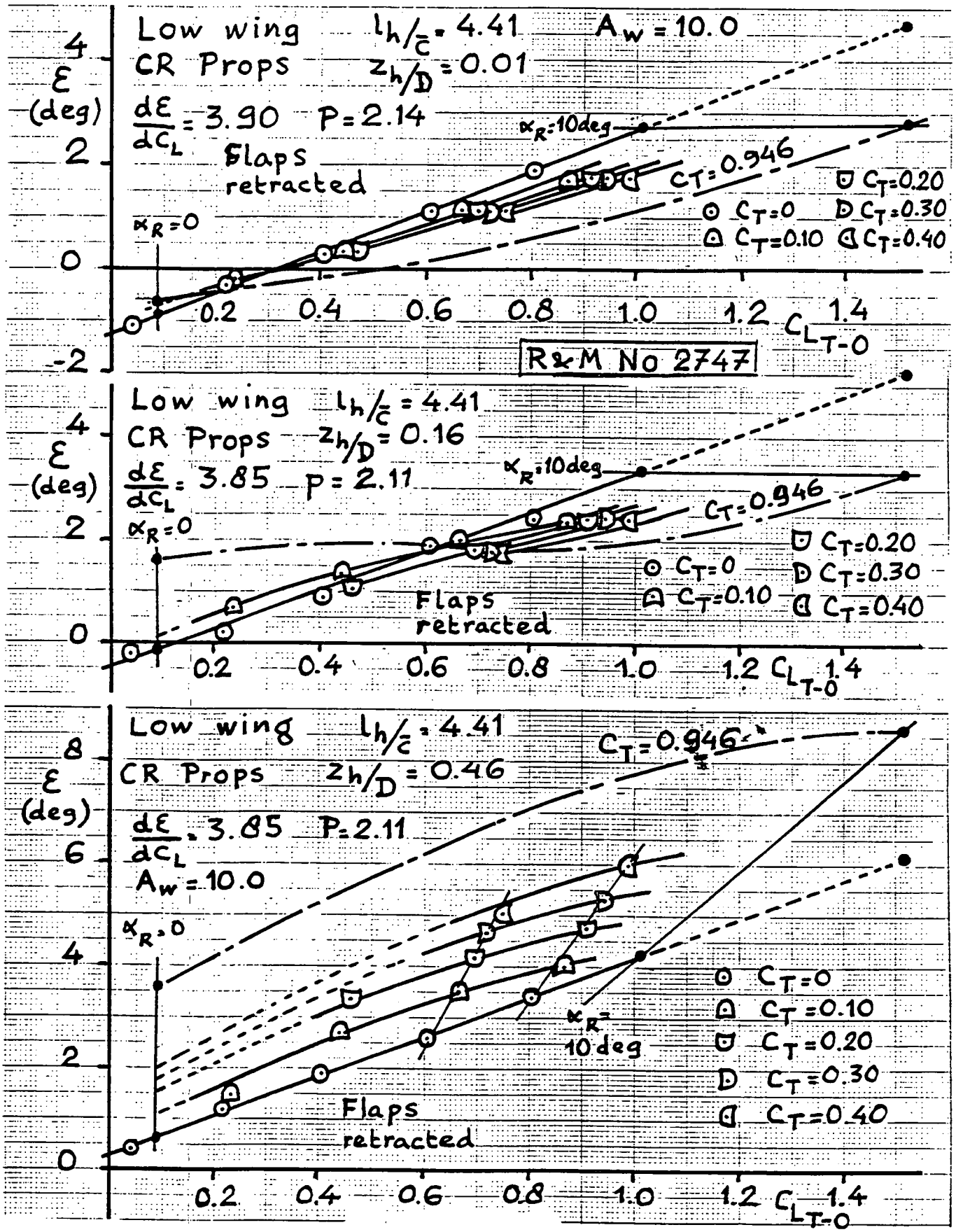
Low wing $l_h/c = 4.41$ $A_w = 10.0$
CR Props $z_h/D = 0.01$
$\frac{d\varepsilon}{dC_L} = 3.90$ $P = 2.14$
Flaps retracted
$\alpha_R = 10$deg
$\alpha_R = 0$
$C_T = 0.946$
$C_T = 0$
$C_T = 0.10$
$C_T = 0.20$
$C_T = 0.30$
$C_T = 0.40$
ε (deg)
$C_{L_{T-0}}$
R & M No 2747
Low wing $l_h/c = 4.41$
CR Props $z_h/D = 0.16$
$\frac{d\varepsilon}{dC_L} = 3.85$ $P = 2.11$
Flaps retracted
Low wing $l_h/c = 4.41$
CR Props $z_h/D = 0.46$
$\frac{d\varepsilon}{dC_L} = 3.85$ $P = 2.11$
$A_w = 10.0$
$\alpha_R = 10$ deg

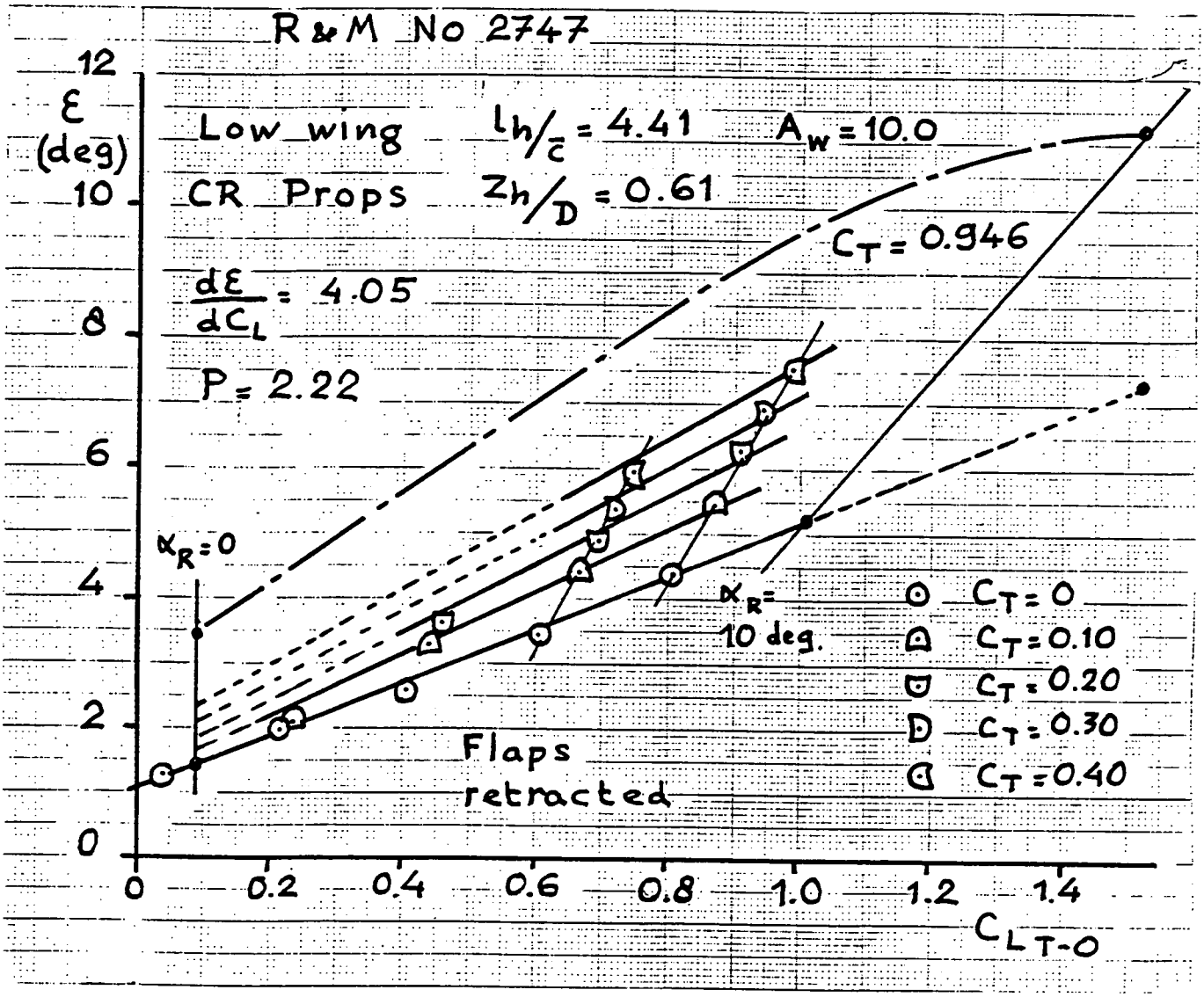
R & M No 2747
ε (deg)
12
10
8
6
4
2
0
Low wing
CR Props
$l_h/c = 4.41$
$A_w = 10.0$
$z_h/D = 0.61$
$C_T = 0.946$
$\frac{d\varepsilon}{dC_L} = 4.05$
P = 2.22
$\alpha_R = 0$
$\alpha_R =$ 10 deg.
Flaps retracted
○ $C_T = 0$
◎ $C_T = 0.10$
◎ $C_T = 0.20$
D $C_T = 0.30$
◎ $C_T = 0.40$
0
0.2
0.4
0.6
0.8
1.0
1.2
1.4
$C_{L\,T-O}$

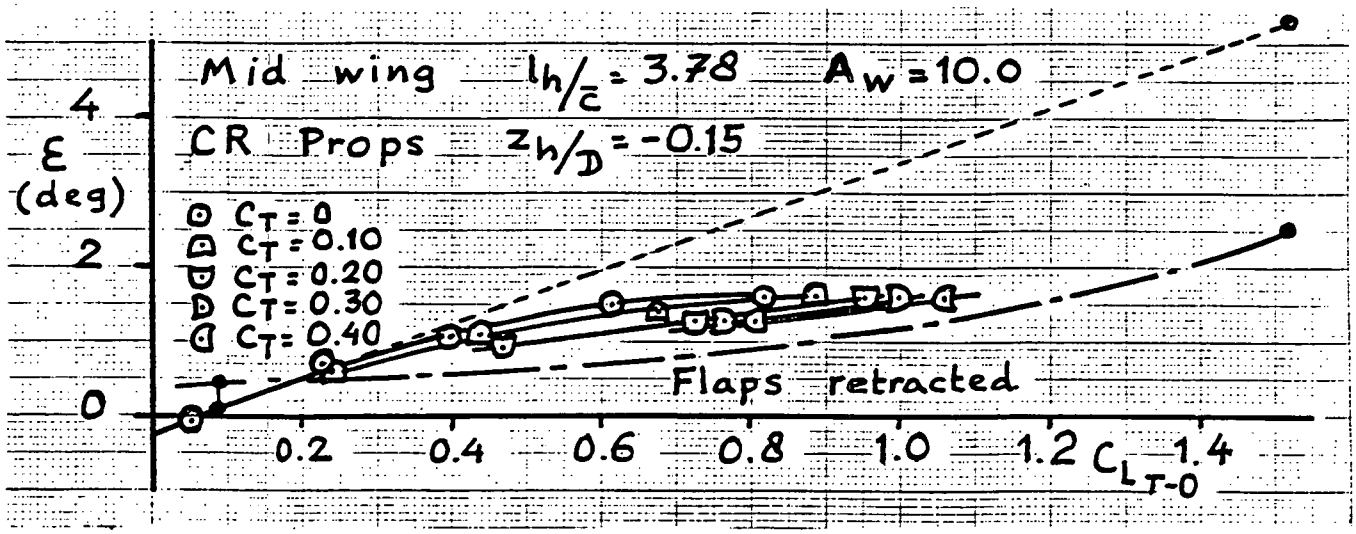
Mid wing $l_h/c = 3.78$ $A_w = 10.0$
CR Props $z_h/D = -0.15$
ε (deg)
$C_T = 0$
$C_T = 0.10$
$C_T = 0.20$
$C_T = 0.30$
$C_T = 0.40$
Flaps retracted
4
2
0
0.2
0.4
0.6
0.8
1.0
1.2
1.4
$C_{L_{T-0}}$

R & M No 2747

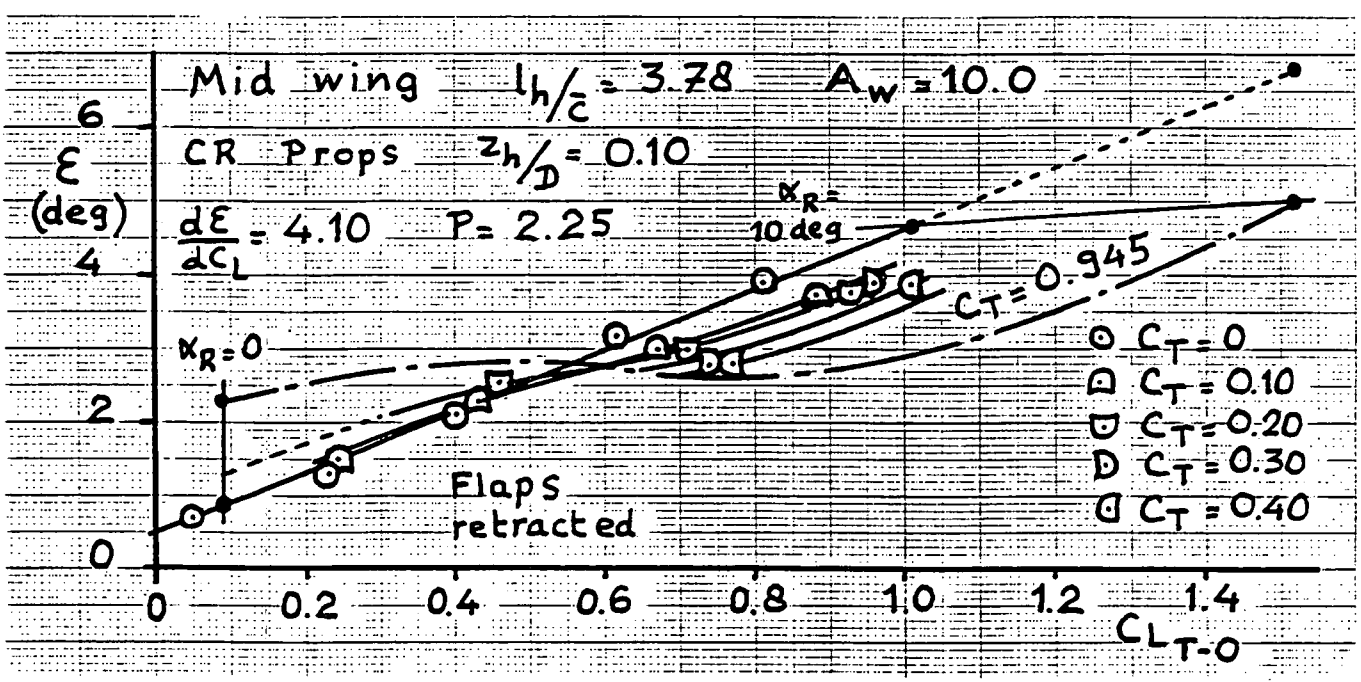
Mid wing $l_h/c = 3.78$ $A_w = 10.0$
CR Props $z_h/D = 0.10$
ε (deg)
$\frac{d\varepsilon}{dC_L} = 4.10$ $P = 2.25$
$\alpha_R = 10$ deg
$C_T = 0.945$
$\alpha_R = 0$
Flaps retracted
$C_T = 0$
$C_T = 0.10$
$C_T = 0.20$
$C_T = 0.30$
$C_T = 0.40$
6
4
2
0
0
0.2
0.4
0.6
0.8
1.0
1.2
1.4
$C_{L_{T-0}}$

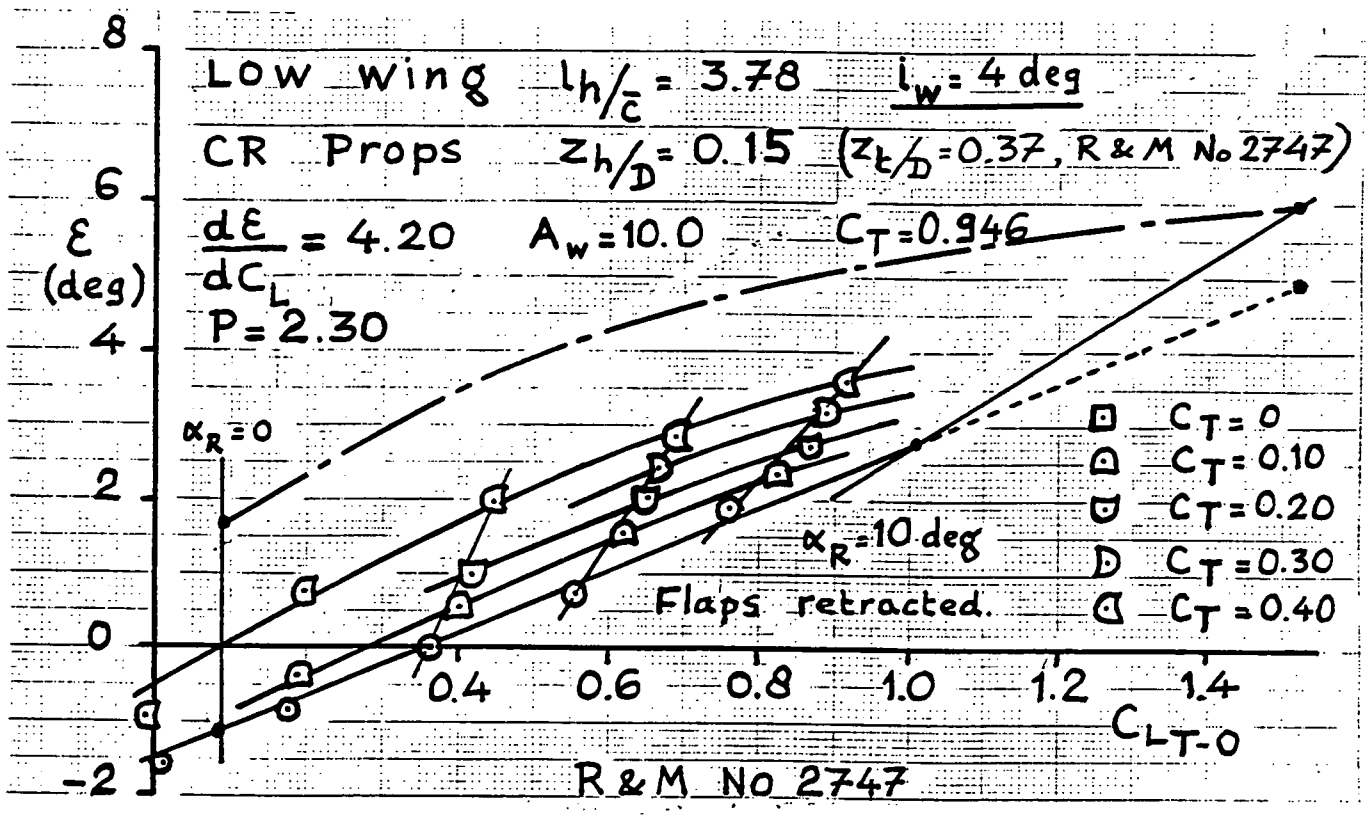
Low wing $l_h/\bar{c} = 3.78$ $i_w = 4$ deg
CR Props $z_h/D = 0.15$ ($z_t/D = 0.37$, R & M No 2747)
$\frac{d\varepsilon}{dC_L} = 4.20$ $A_w = 10.0$ $C_T = 0.946$
P = 2.30
ε (deg)
$\alpha_R = 0$
$\alpha_R = 10$ deg
Flaps retracted.
$C_T = 0$
$C_T = 0.10$
$C_T = 0.20$
$C_T = 0.30$
$C_T = 0.40$
C_{LT-0}
R & M No 2747

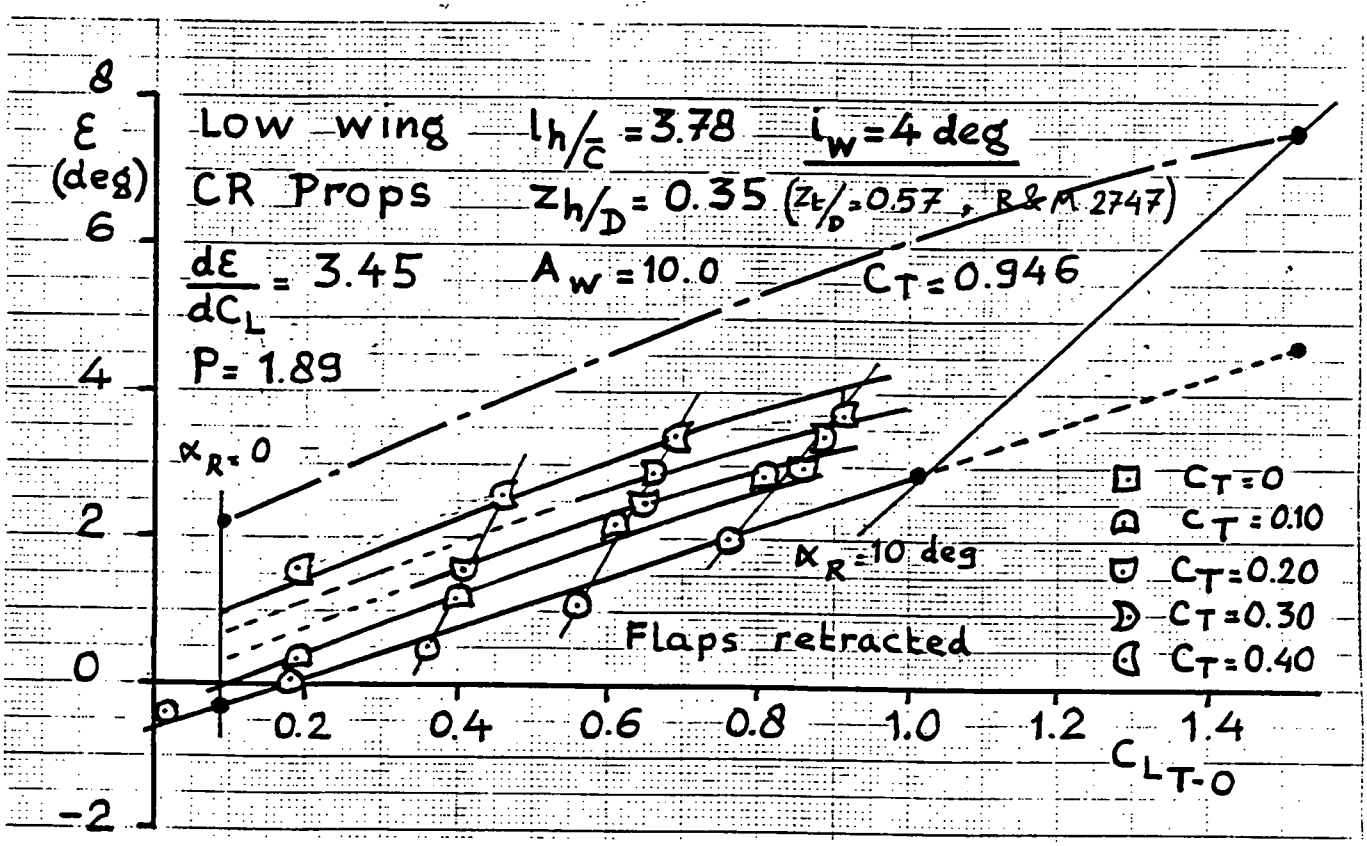
Low wing $l_h/\bar{c} = 3.78$ $i_w = 4$ deg
CR Props $z_h/D = 0.35$ ($z_t/D = 0.57$, R & M 2747)
$\frac{d\varepsilon}{dC_L} = 3.45$ $A_w = 10.0$ $C_T = 0.946$
P = 1.89
ε (deg)
$\alpha_R = 0$
$\alpha_R = 10$ deg
Flaps retracted
$C_T = 0$
$C_T = 0.10$
$C_T = 0.20$
$C_T = 0.30$
$C_T = 0.40$
C_{LT-0}

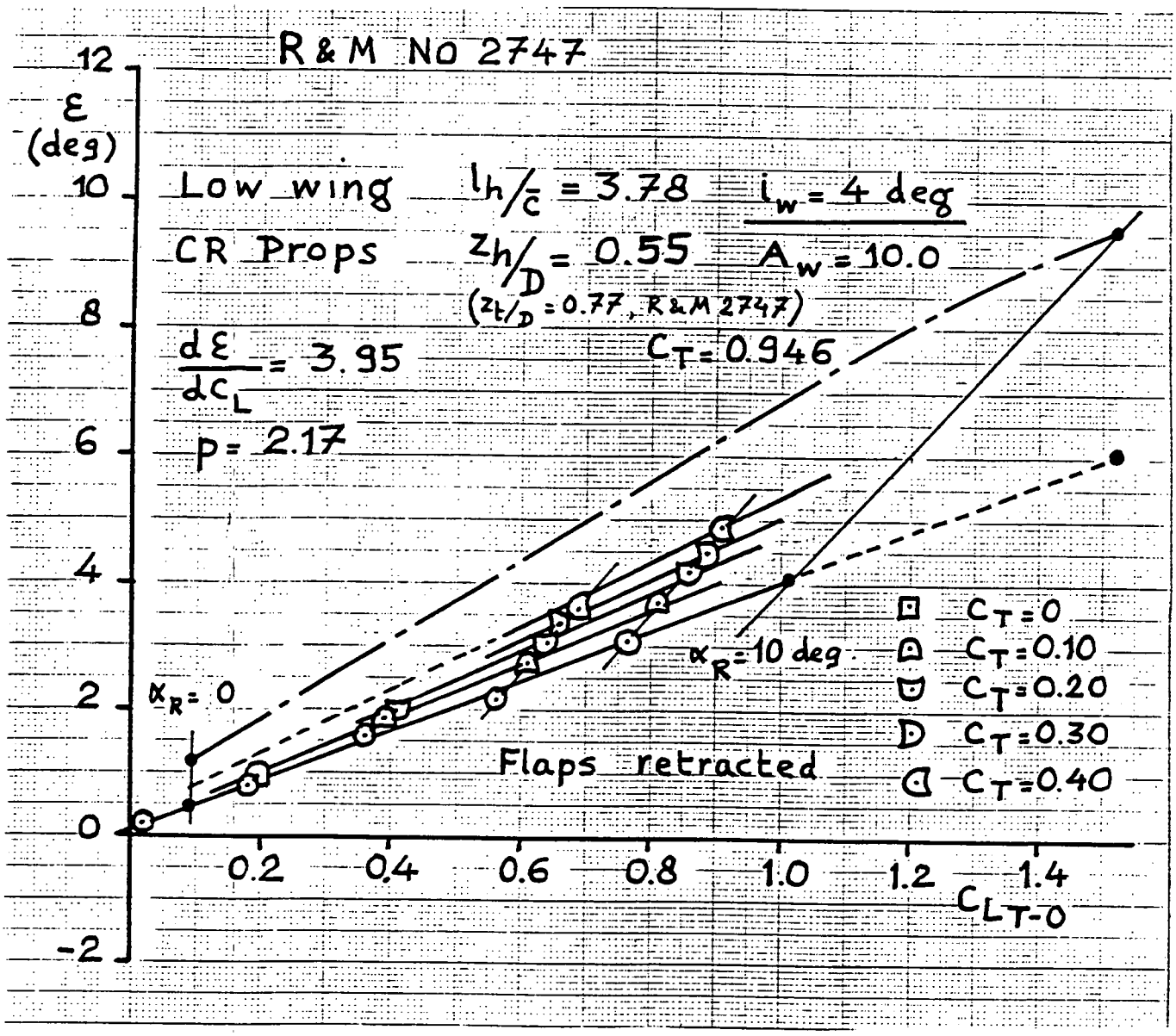
R & M No 2747
ε (deg)
12
10
8
6
4
2
0
-2
Low wing
CR Props
$l_h/c = 3.78$
$i_w = 4$ deg
$z_h/D = 0.55$
$A_w = 10.0$
($z_t/D = 0.77$, R&M 2747)
$C_T = 0.946$
$\frac{d\varepsilon}{dC_L} = 3.95$
$p = 2.17$
$\alpha_R = 0$
$\alpha_R = 10$ deg
Flaps retracted
$C_T = 0$
$C_T = 0.10$
$C_T = 0.20$
$C_T = 0.30$
$C_T = 0.40$
0.2
0.4
0.6
0.8
1.0
1.2
1.4
$C_{L_{T-0}}$

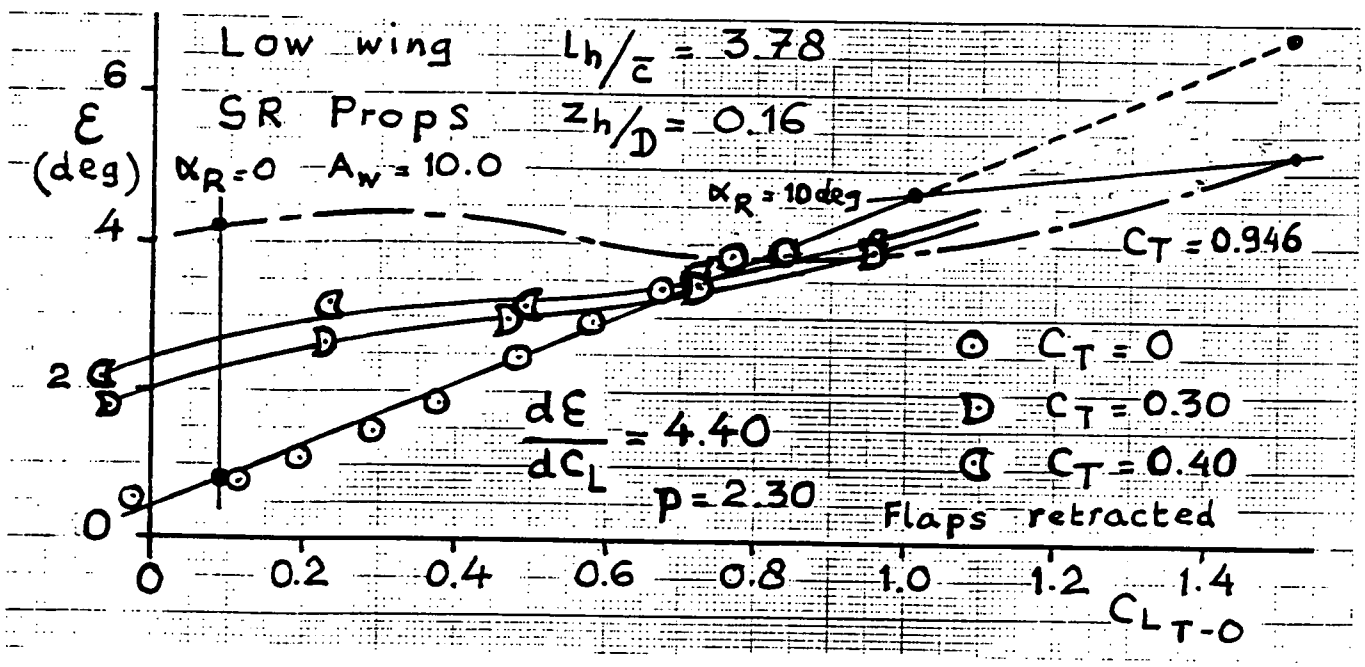
Low wing $l_h/\bar{c} = 3.78$
SR Props $z_h/D = 0.16$
$\alpha_R = 0$ $A_w = 10.0$
$\alpha_R = 10$ deg
$C_T = 0.946$
$C_T = 0$
$C_T = 0.30$
$C_T = 0.40$
$\frac{d\varepsilon}{dC_L} = 4.40$
$p = 2.30$
Flaps retracted
ε (deg)
$C_{L_{T-0}}$

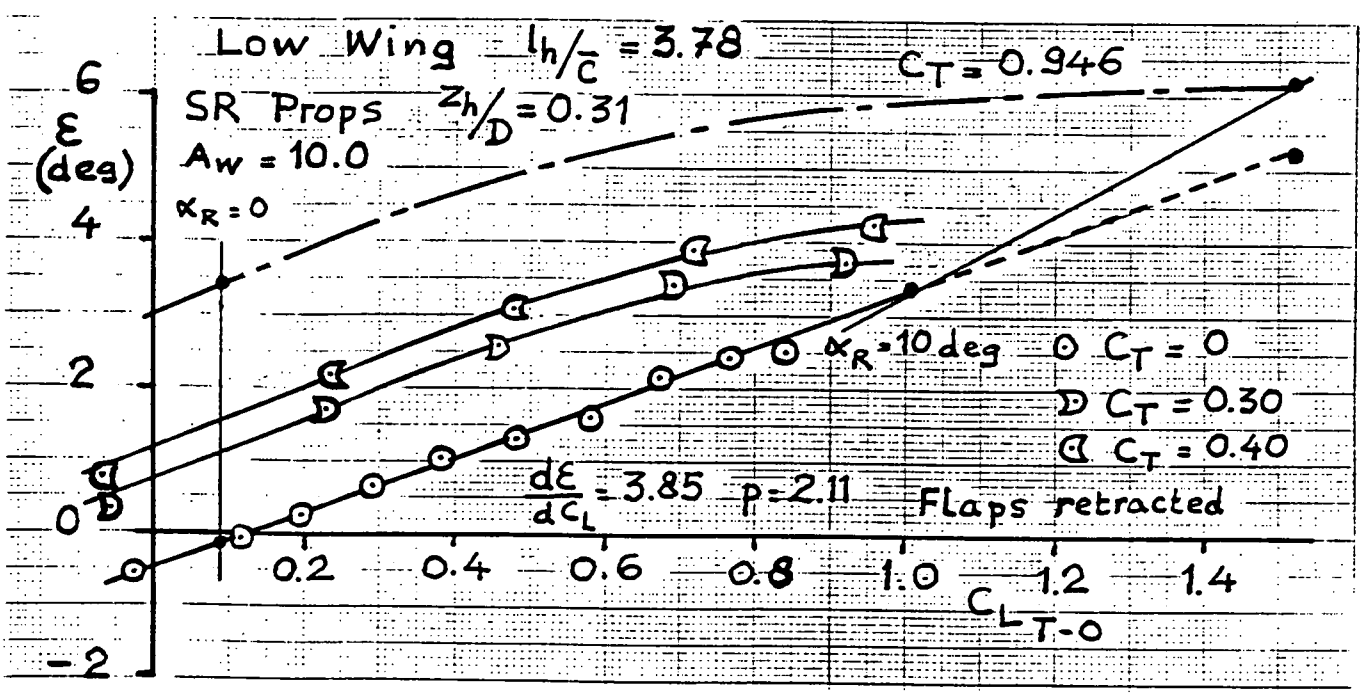
Low Wing $l_h/\bar{c} = 3.78$
SR Props $z_h/D = 0.31$
$A_w = 10.0$
$\alpha_R = 0$
$C_T = 0.946$
$\alpha_R = 10$ deg
$C_T = 0$
$C_T = 0.30$
$C_T = 0.40$
$\frac{d\varepsilon}{dC_L} = 3.85$
$p = 2.11$
Flaps retracted
ε (deg)
$C_{L_{T-0}}$

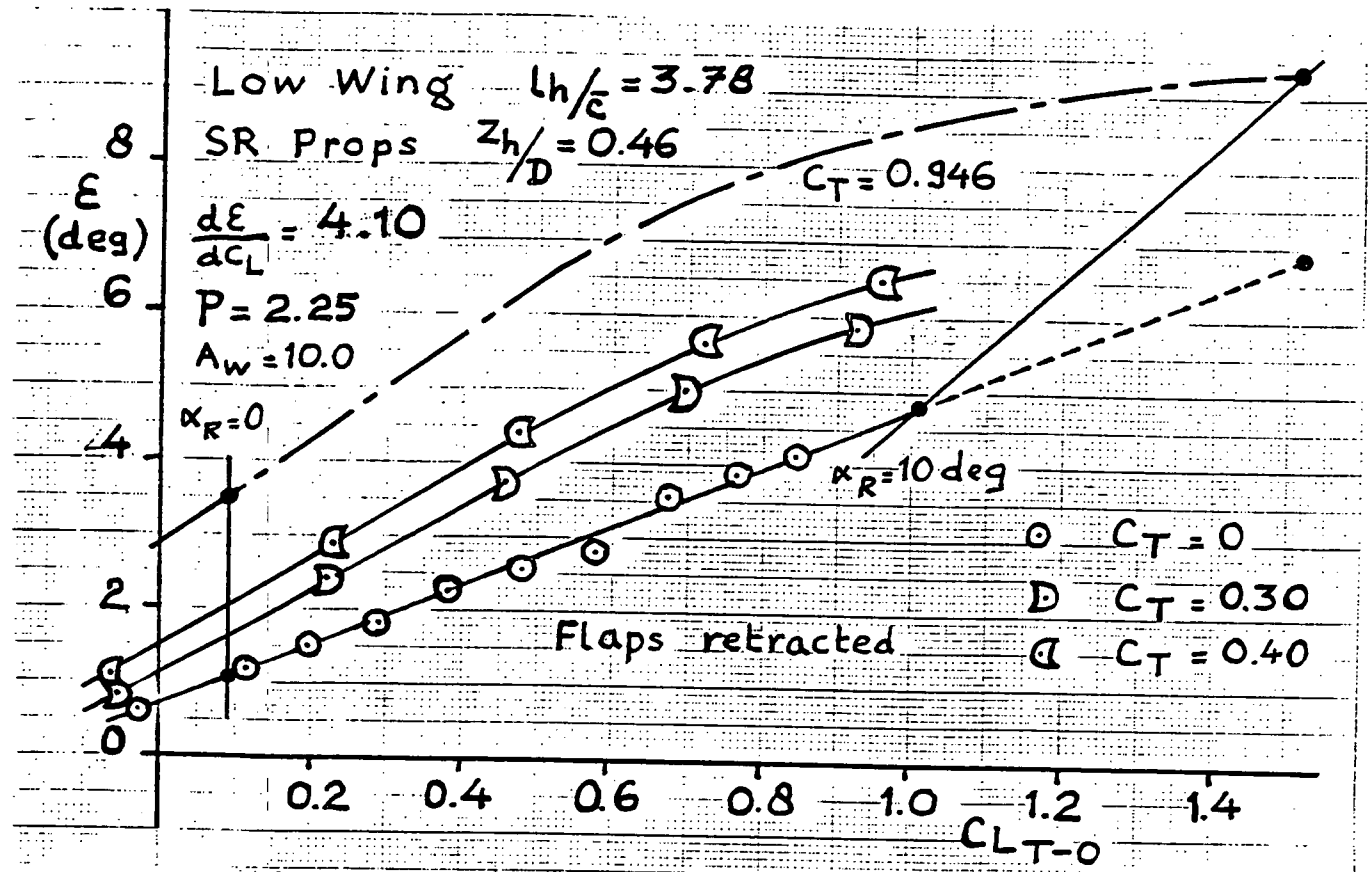
Low Wing $l_h/\bar{c} = 3.78$
SR Props $z_h/D = 0.46$
$\frac{d\varepsilon}{dC_L} = 4.10$
P = 2.25
$A_w = 10.0$
$\alpha_R = 0$
$\alpha_R = 10$ deg
$C_T = 0.946$
○ $C_T = 0$
D $C_T = 0.30$
◁ $C_T = 0.40$
Flaps retracted
ε (deg)
8
6
4
2
0
0.2
0.4
0.6
0.8
1.0
1.2
1.4
$C_{L_{T-O}}$

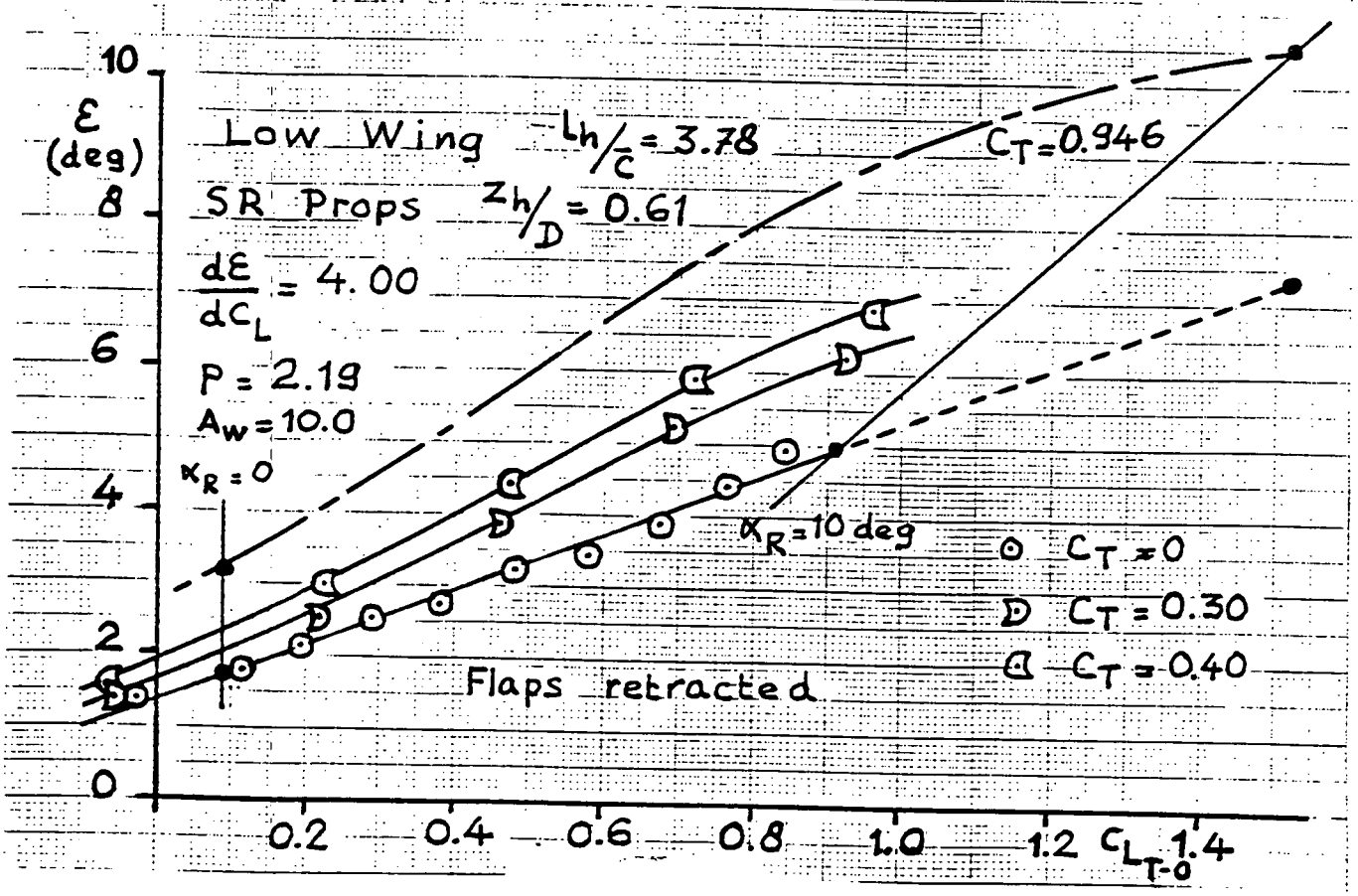
Low Wing $l_h/\bar{c} = 3.78$
SR Props $z_h/D = 0.61$
$\frac{d\varepsilon}{dC_L} = 4.00$
P = 2.19
$A_w = 10.0$
$\alpha_R = 0$
$\alpha_R = 10$ deg
$C_T = 0.946$
○ $C_T = 0$
D $C_T = 0.30$
◁ $C_T = 0.40$
Flaps retracted
ε (deg)
10
8
6
4
2
0
0.2
0.4
0.6
0.8
1.0
1.2
1.4
$C_{L_{T-O}}$

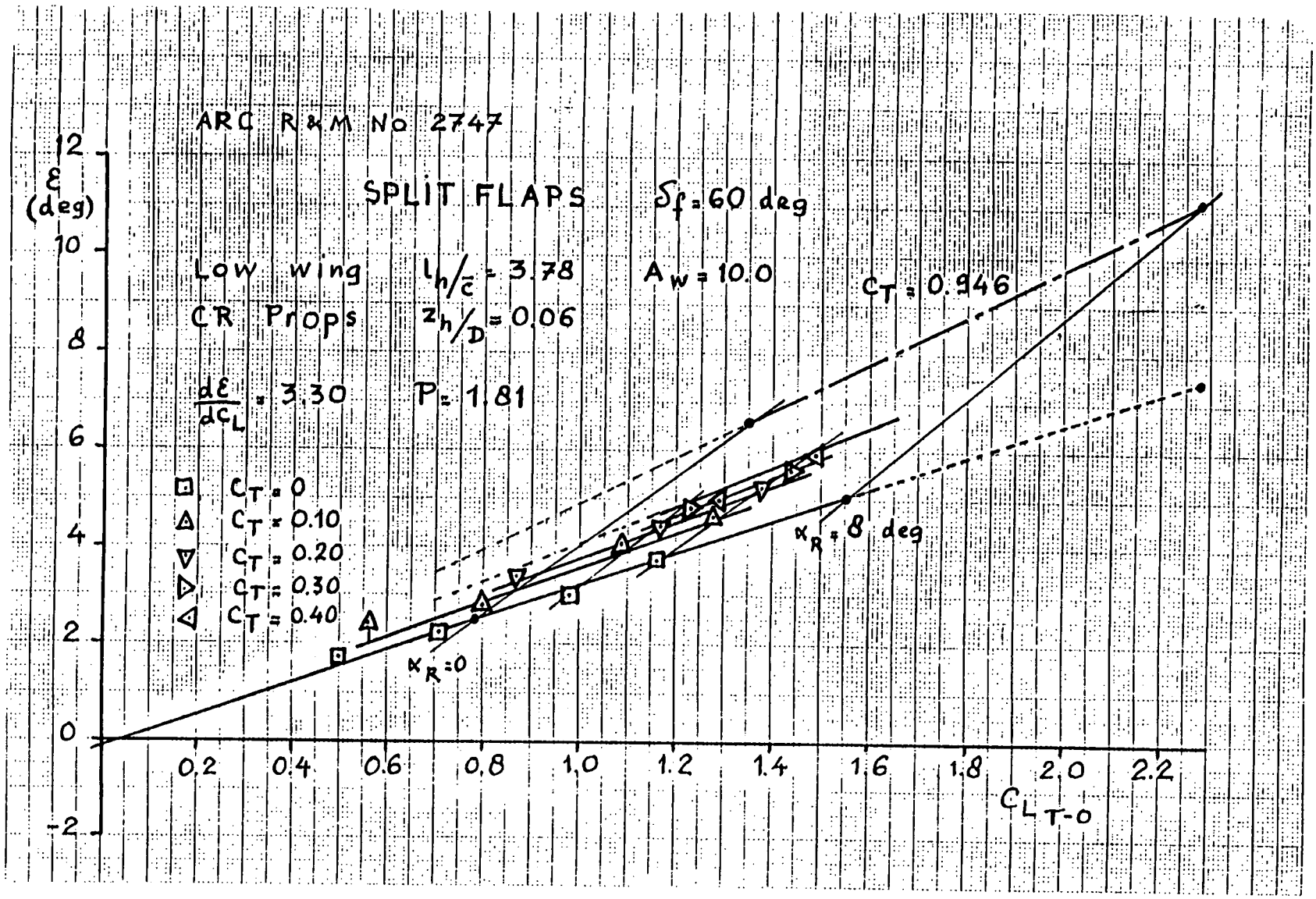
ARC R & M No 2747
SPLIT FLAPS $\delta_f = 60$ deg
Low wing $l_h/\bar{c} = 3.78$ $A_w = 10.0$
CR Props $z_h/D = 0.06$
$\frac{d\varepsilon}{dC_L} = 3.30$ $P = 1.81$
$C_T = 0$
$C_T = 0.10$
$C_T = 0.20$
$C_T = 0.30$
$C_T = 0.40$
$C_T = 0.946$
$\alpha_R = 0$
$\alpha_R = 8$ deg
ε (deg)
$C_{L\,T-O}$
12
10
8
6
4
2
0
-2
0.2
0.4
0.6
0.8
1.0
1.2
1.4
1.6
1.8
2.0
2.2

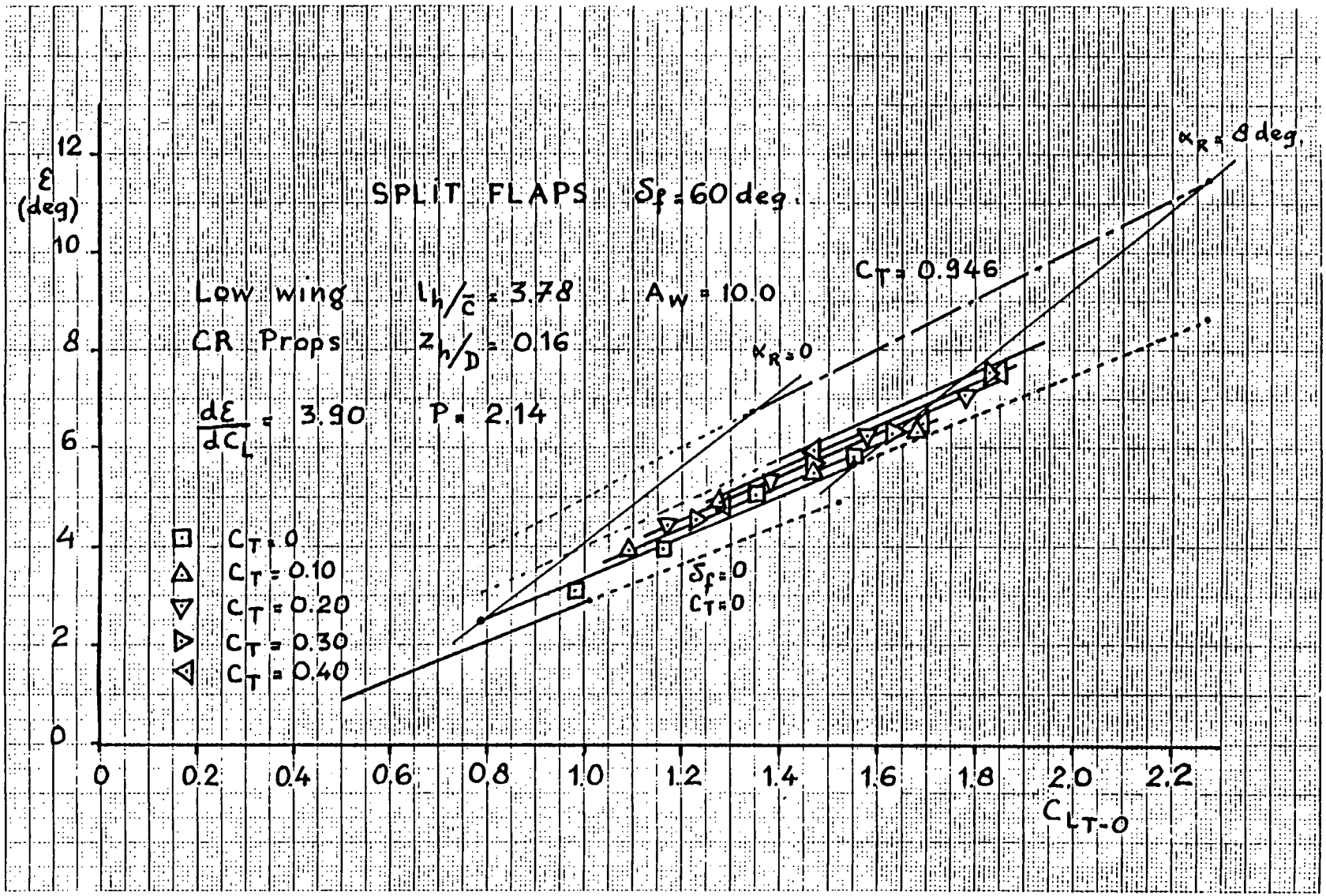
SPLIT FLAPS $\delta_f = 60$ deg.
Low wing $l_h/\bar{c} = 3.78$ $A_W = 10.0$
CR Props $z_{h/D} = 0.16$
$\frac{d\varepsilon}{dC_L} = 3.90$ $P = 2.14$
$C_T = 0$
$C_T = 0.10$
$C_T = 0.20$
$C_T = 0.30$
$C_T = 0.40$
$C_T = 0.946$
$\alpha_R = 8$ deg.
$\alpha_R = 0$
$\delta_f = 0$
$C_T = 0$
ε (deg)
$C_{L_{T-O}}$
0
2
4
6
8
10
12
0.2
0.4
0.6
0.8
1.0
1.2
1.4
1.6
1.8
2.0
2.2

SPLIT FLAPS δ_f = 60 deg
Low wing A_w = 10.0
CR Props $l_h/\bar{c}$ = 3.78
$\frac{d\varepsilon}{dC_L}$ = 4.15 z_h/D = 0.46
P = 2.28
C_T = 0.946
C_T = 0 C_T = 0.10 C_T = 0.20 C_T = 0.30 C_T = 0.40
δ_f = 0
C_T = 0
ε (deg)
C_L-o

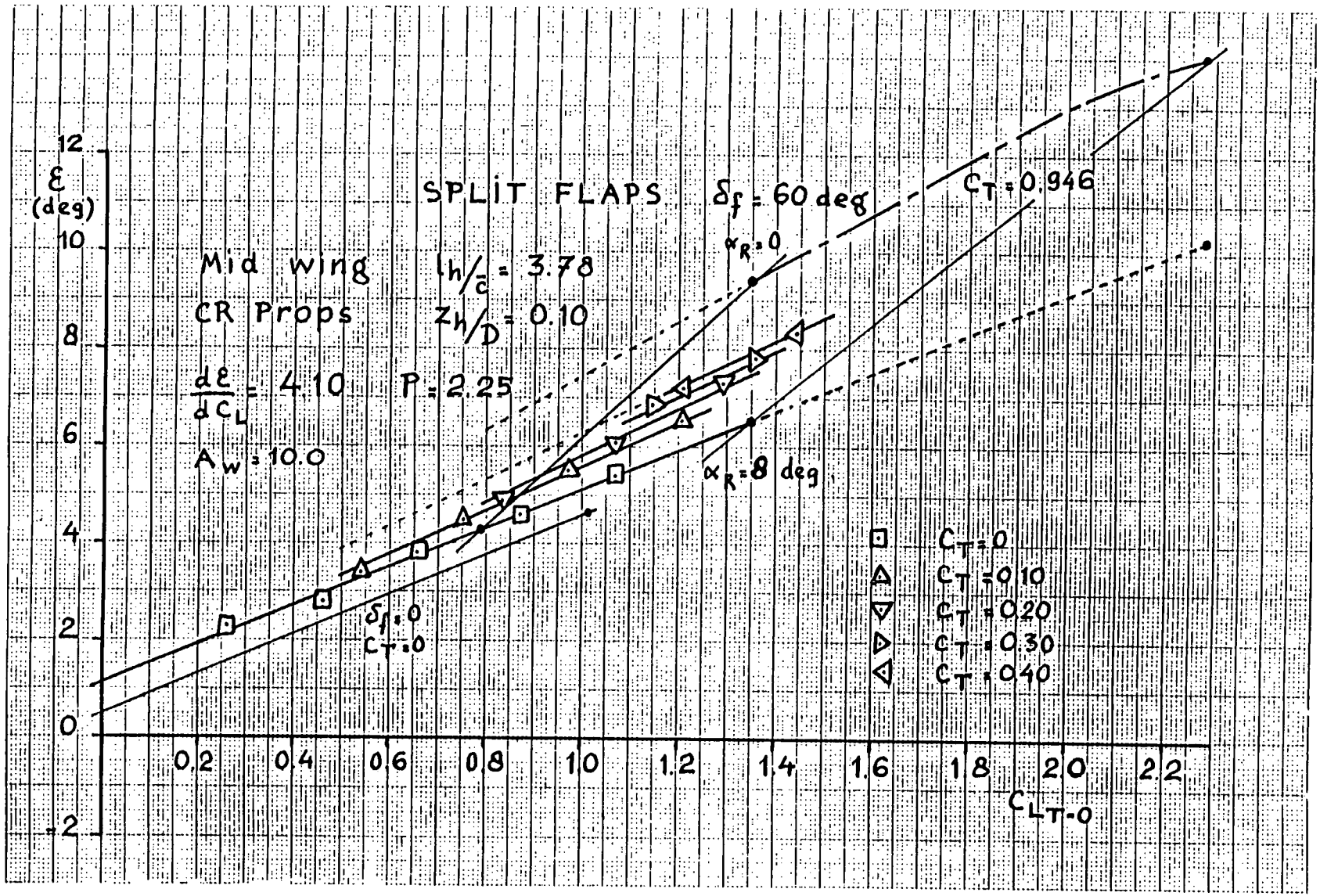
SPLIT FLAPS δ_f = 60 deg
Mid wing h/c = 3.78
CR Props z_h/D = 0.10
$\frac{d\varepsilon}{dC_L}$ = 4.10 P = 2.25
Aw = 10.0
C_T = 0.946
α_R = 0
α_R = 8 deg
δ_f = 0
C_T = 0
C_T = 0
C_T = 0.10
C_T = 0.20
C_T = 0.30
C_T = 0.40
ε (deg)
C_{LT-0}

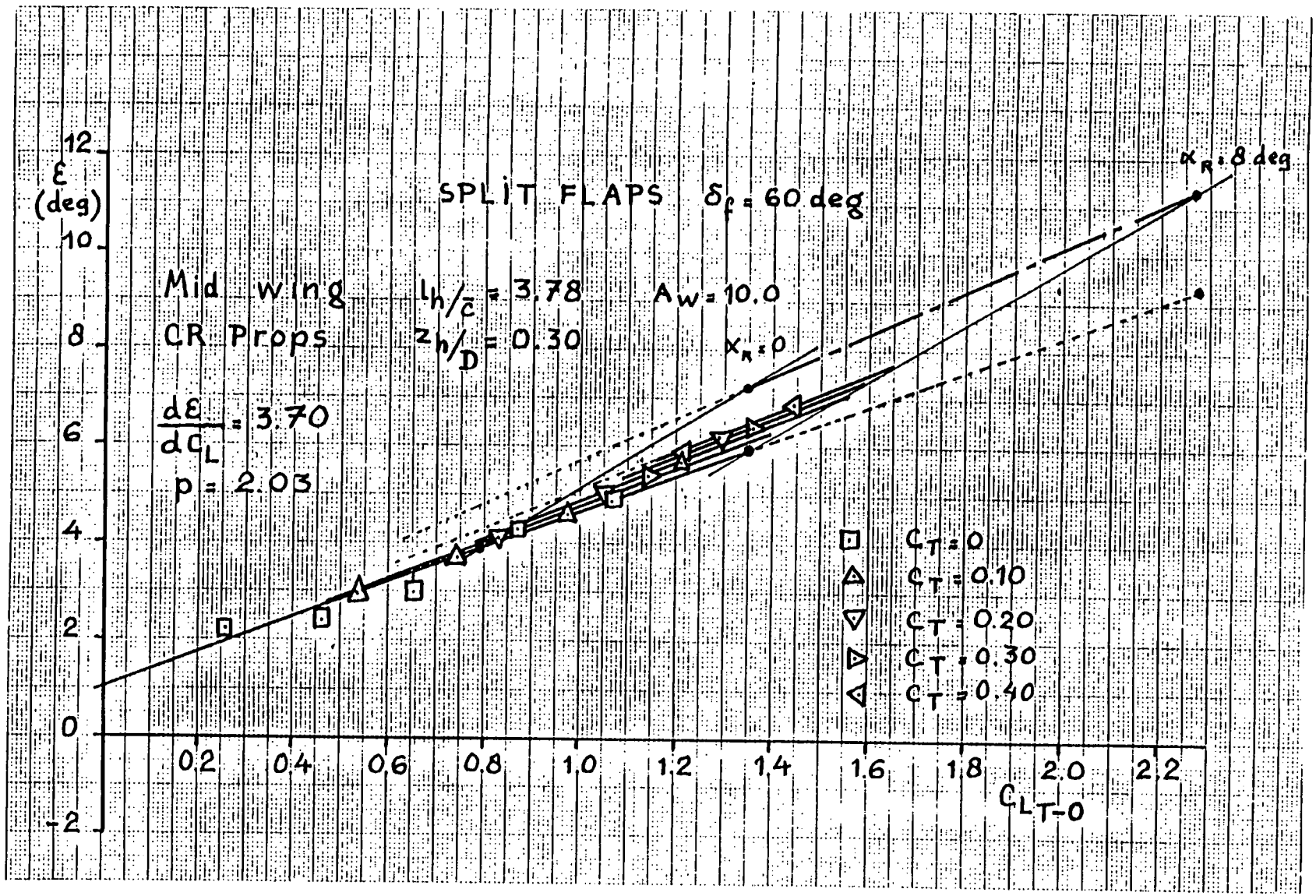
SPLIT FLAPS δ_f = 60 deg
Mid wing $l_h/\bar{c}$ = 3.78 A_w = 10.0
CR Props z_h/D = 0.30
$\frac{d\varepsilon}{dC_L}$ = 3.70
p = 2.03
α_R = 8 deg
α_R = 0
C_T = 0
C_T = 0.10
C_T = 0.20
C_T = 0.30
C_T = 0.40
ε (deg)
C_{LT-0}

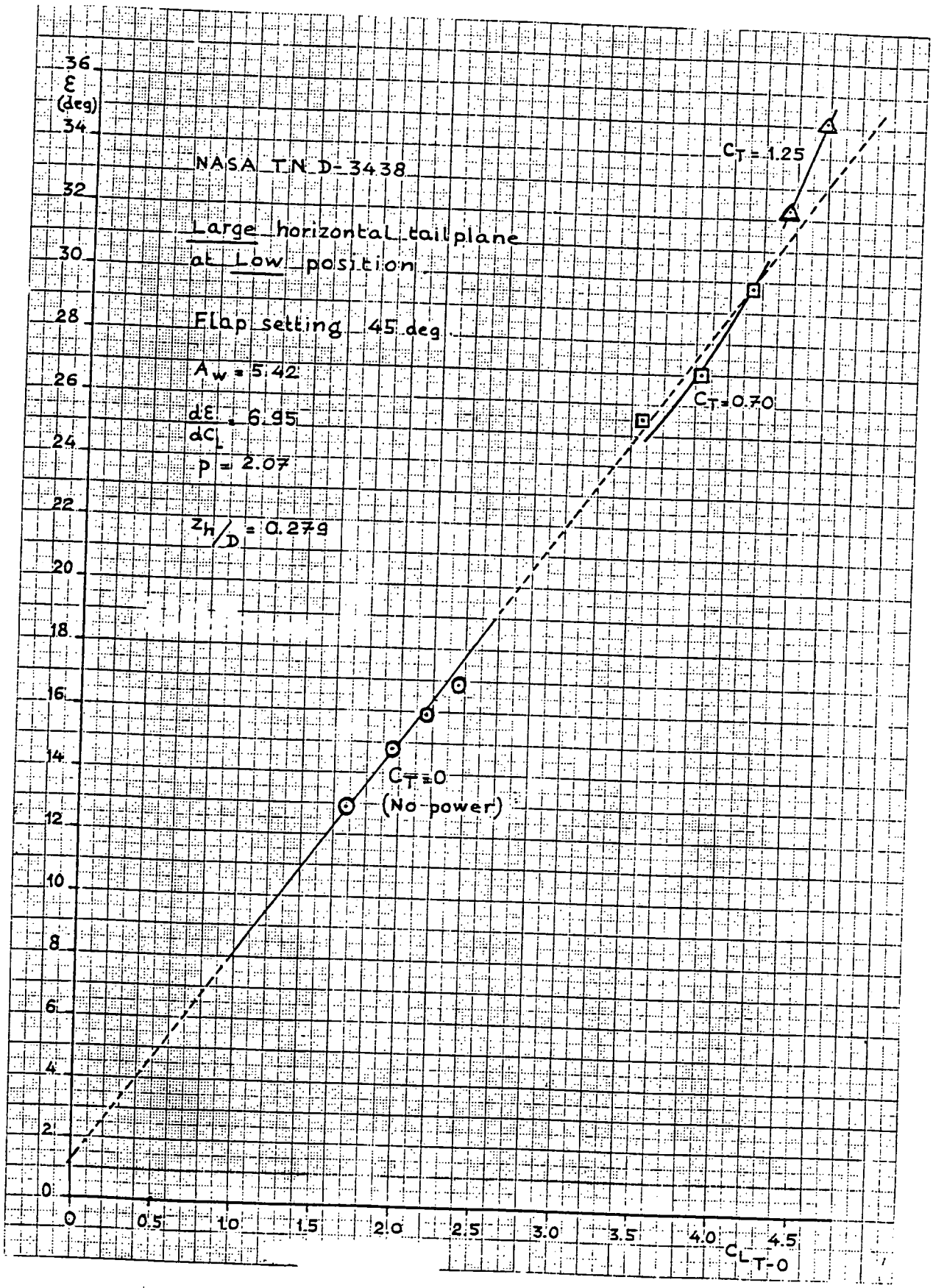
ε (deg)
36
34
32
30
28
26
24
22
20
18
16
14
12
10
8
6
4
2
0
0
0.5
1.0
1.5
2.0
2.5
3.0
3.5
4.0
4.5
$C_{L_{T=0}}$
NASA TN D-3438
Large horizontal tailplane at Low position
Flap setting 45 deg
$A_w = 5.42$
$\frac{d\varepsilon}{dC_L} = 6.95$
$P = 2.07$
$z_h/D = 0.279$
$C_T = 1.25$
$C_T = 0.70$
$C_T = 0$
(No-power)

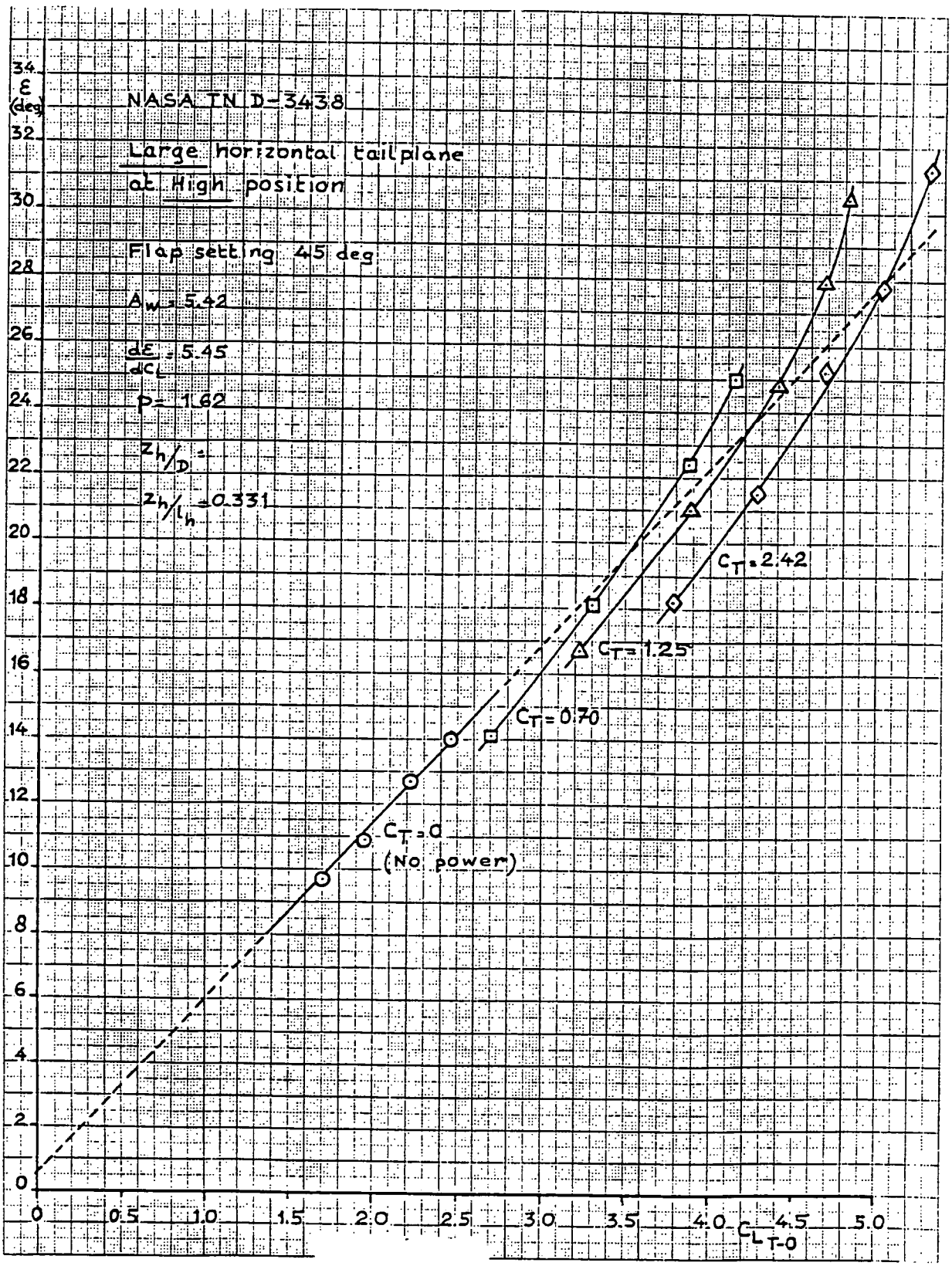
ε (deg)
NASA TN D-3438
Large horizontal tailplane at High position
Flap setting 45 deg
A_w = 5.42
$\frac{d\varepsilon}{dC_L}$ = 5.45
P = 1.62
z_h/D =
z_h/l_h = 0.331
C_T = 2.42
C_T = 1.25
C_T = 0.70
C_T = 0
(No power)
$C_{L_{T-0}}$

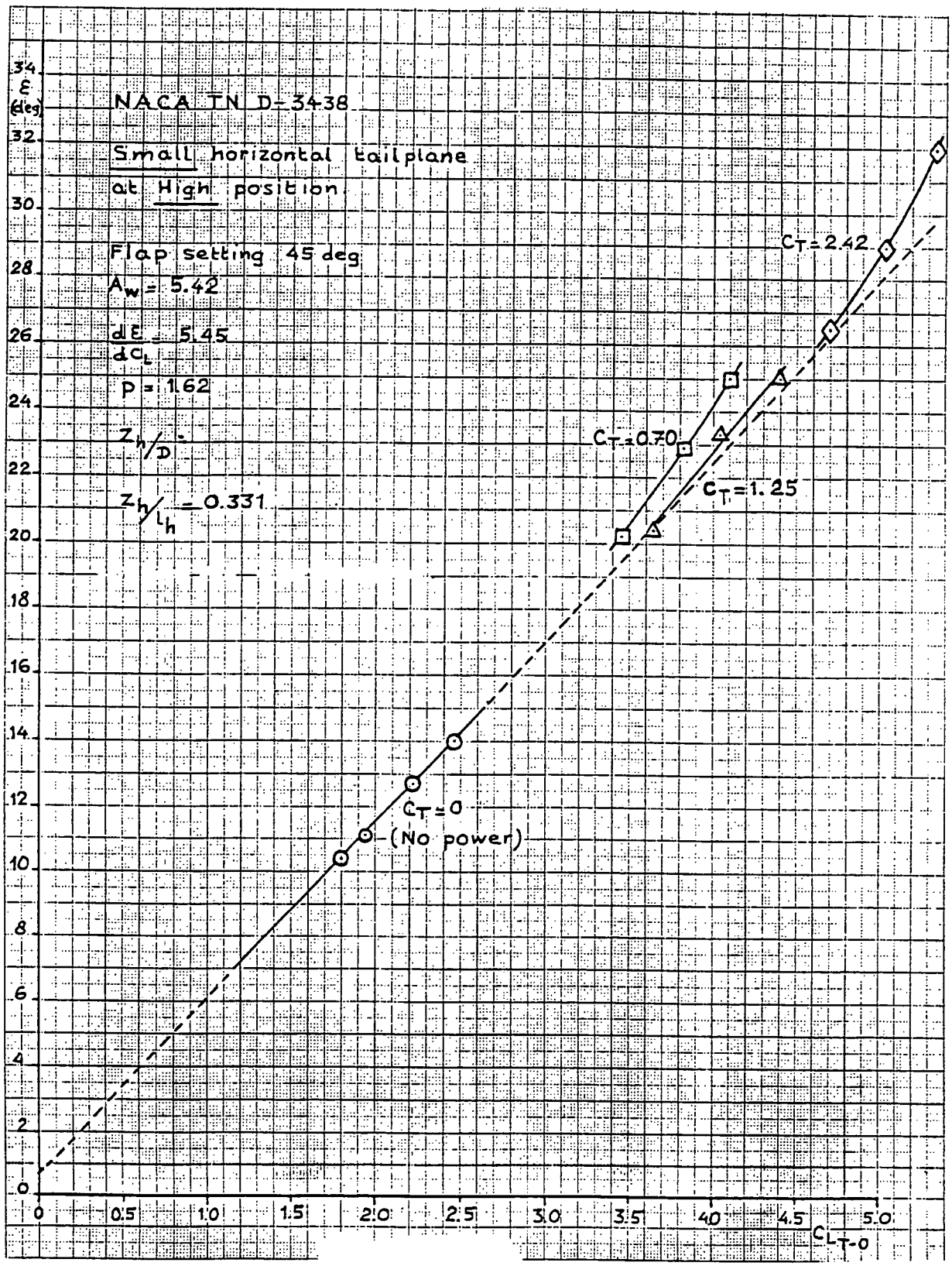
NACA TN D-3438
Small horizontal tailplane
at High position
Flap setting 45 deg
$A_w = 5.42$
$\frac{d\varepsilon}{dC_L} = 5.45$
$P = 1.62$
Z_h/D -
$Z_h/l_h = 0.331$
$C_T = 2.42$
$C_T = 0.70$
$C_T = 1.25$
$C_T = 0$
(No power)
ε (deg)
$C_{L_{T-0}}$

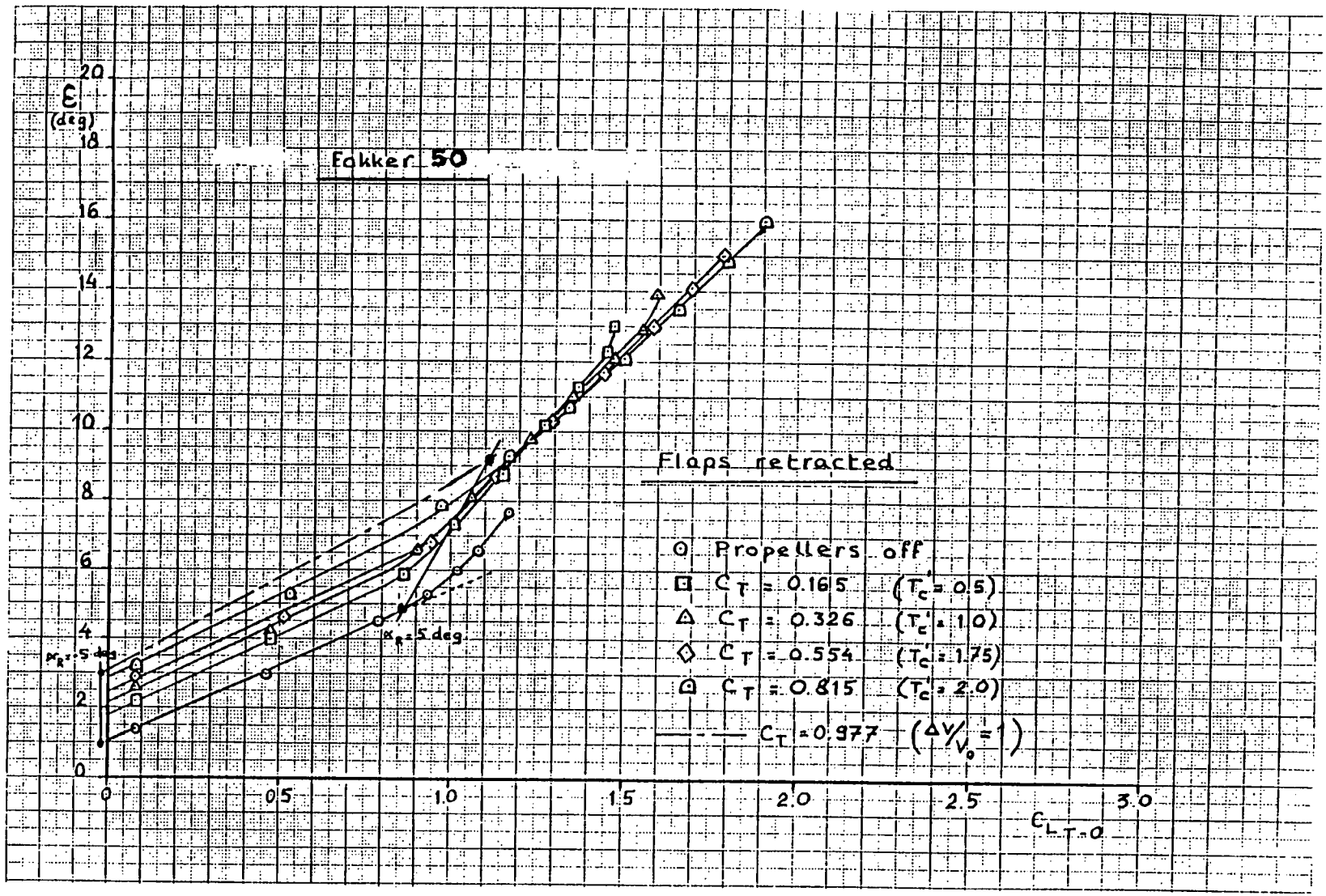
Fokker 50
ε (deg)
20
18
16
14
12
10
8
6
4
2
0
α_R = -5 deg
α_R = 5 deg
0
0.5
1.0
1.5
2.0
2.5
3.0
$C_{L_{T-O}}$
Flaps retracted
Propellers off
C_T = 0.165 (T_c' = 0.5)
C_T = 0.326 (T_c' = 1.0)
C_T = 0.554 (T_c' = 1.75)
C_T = 0.815 (T_c' = 2.0)
C_T = 0.977 ($\Delta V/V_0$ = 1)

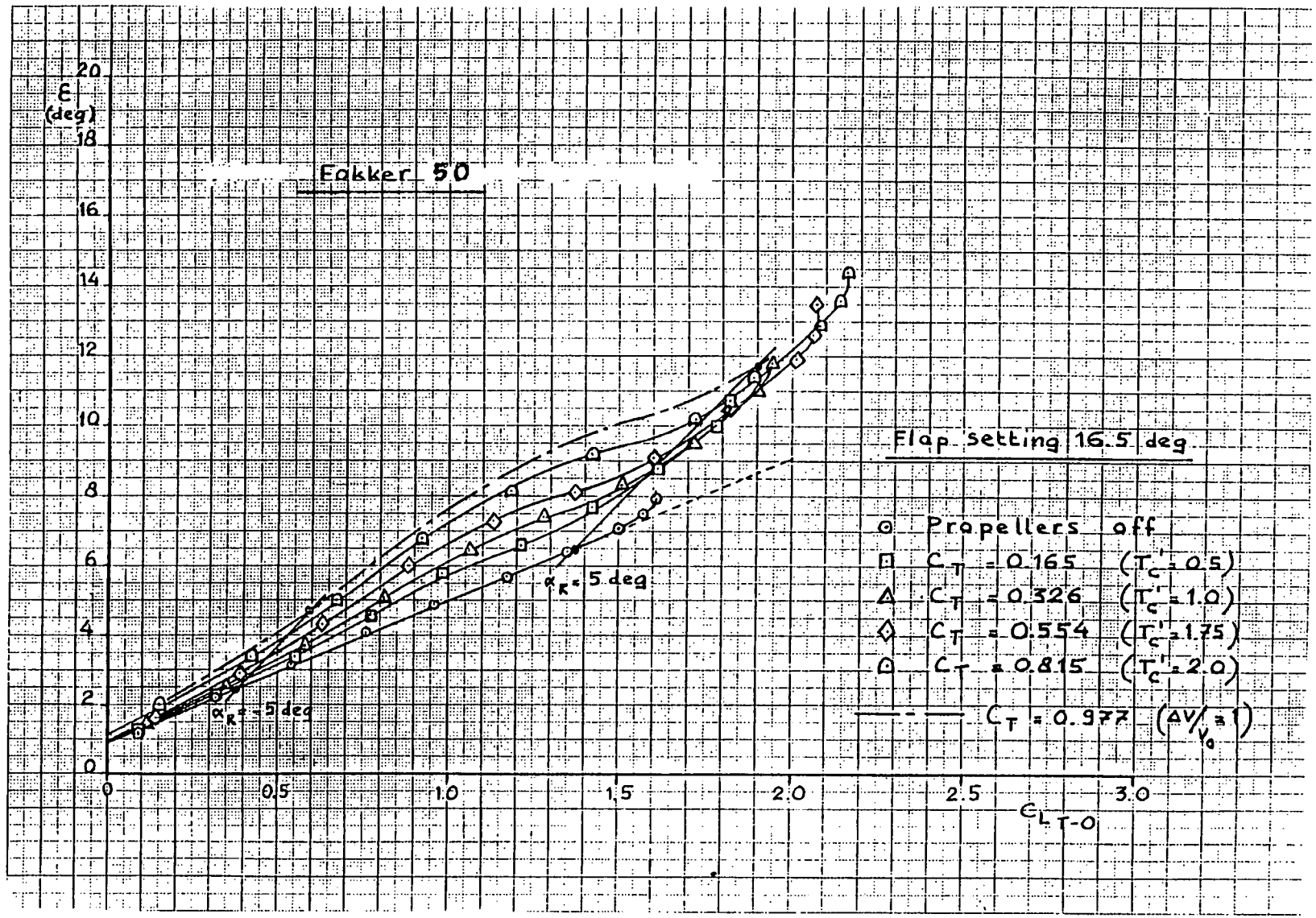
Fokker 50
ε (deg)
20
18
16
14
12
10
8
6
4
2
0
0
0.5
1.0
1.5
2.0
2.5
3.0
$C_{L_{T-O}}$
$\alpha_R = -5$ deg
$\alpha_R = 5$ deg
Flap setting 16.5 deg
Propellers off
$C_T = 0.165$ $(T_c' = 0.5)$
$C_T = 0.326$ $(T_c' = 1.0)$
$C_T = 0.554$ $(T_c' = 1.75)$
$C_T = 0.815$ $(T_c' = 2.0)$
$C_T = 0.977$ $(\Delta V/V_0 = 1)$

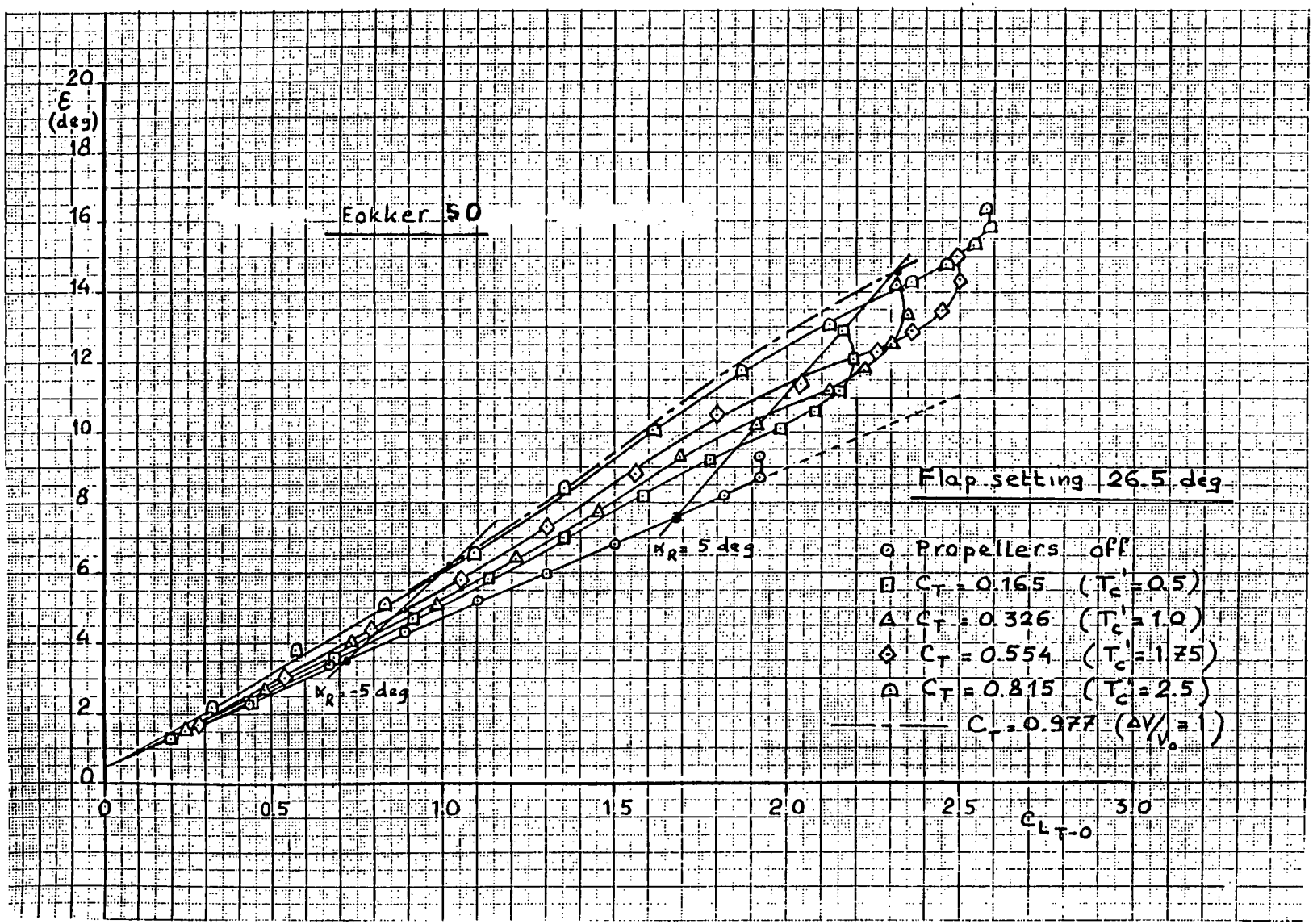
Fokker 50
ε (deg)
20
18
16
14
12
10
8
6
4
2
0
0
0.5
1.0
1.5
2.0
2.5
3.0
$C_{L_{T-O}}$
α_R=5 deg.
α_R=5 deg
Flap setting 26.5 deg
Propellers off
C_T = 0.165 (T_c'=0.5)
C_T = 0.326 (T_c'=1.0)
C_T = 0.554 (T_c'=1.75)
C_T = 0.815 (T_c'=2.5)
C_T = 0.977 ($\Delta V/V_o$ = 1)

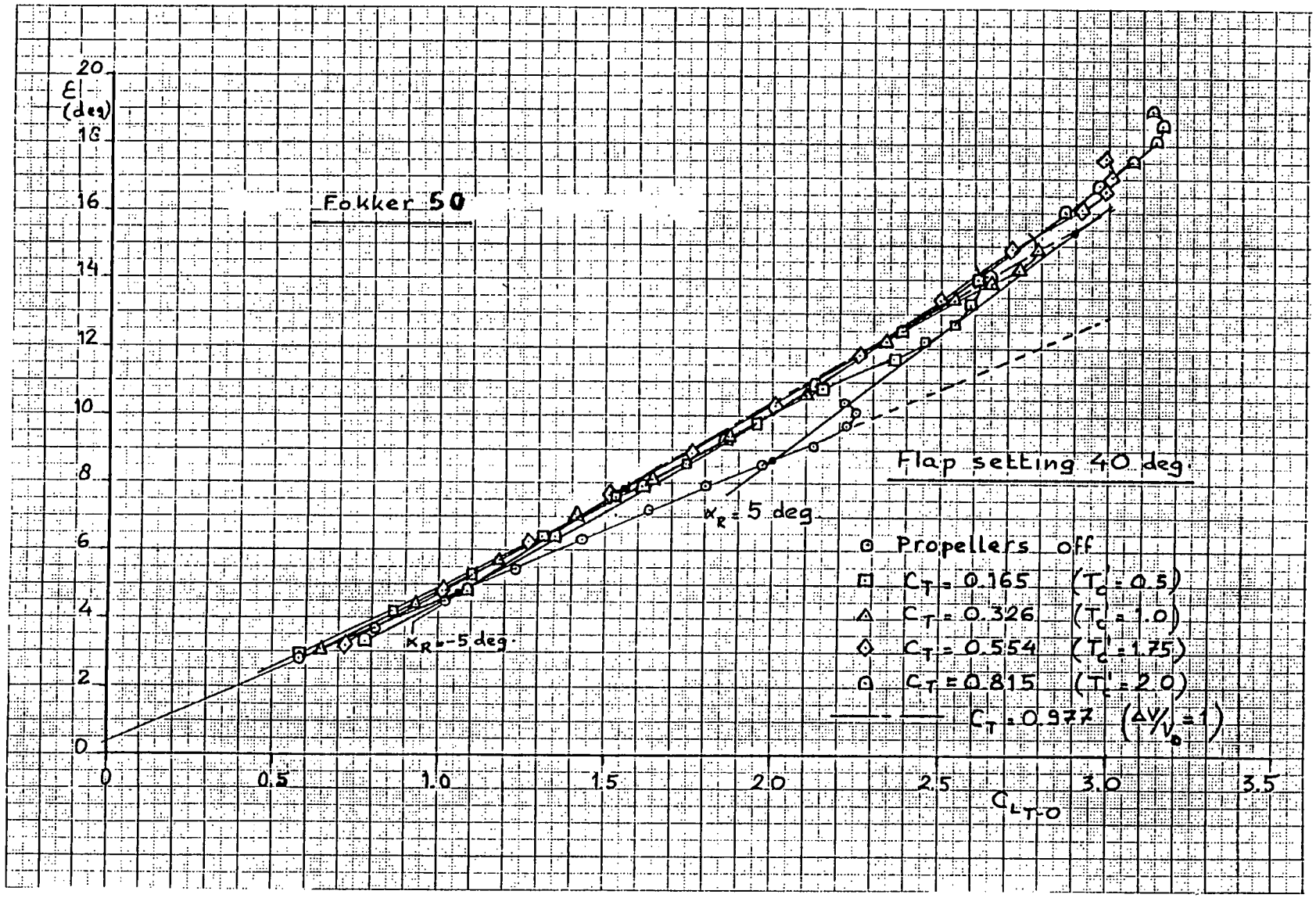
Fokker 50
ε (deg)
20
18
16
14
12
10
8
6
4
2
0
0
0.5
1.0
1.5
2.0
2.5
3.0
3.5
$C_{LT=0}$
Flap setting 40 deg.
κ_R = 5 deg
κ_R = -5 deg
Propellers off
C_T = 0.165 (T_c' = 0.5)
C_T = 0.326 (T_c' = 1.0)
C_T = 0.554 (T_c' = 1.75)
C_T = 0.815 (T_c' = 2.0)
C_T = 0.977 ($\Delta V/V_0$ = 1)

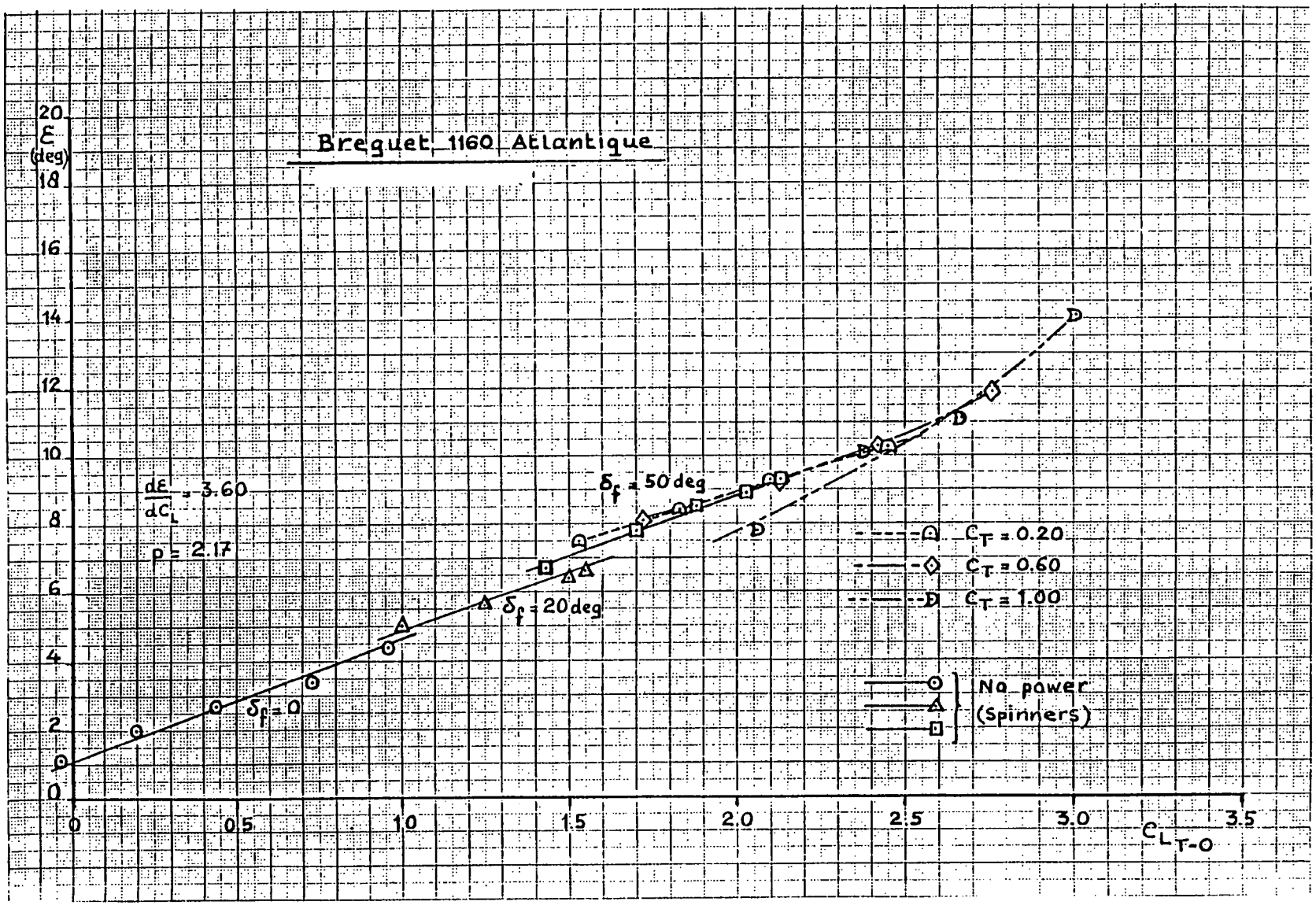
Breguet 1160 Atlantique
ε (deg)
20
18
16
14
12
10
8
6
4
2
0
0
0.5
1.0
1.5
2.0
2.5
3.0
3.5
$C_{L_{T-O}}$
$\frac{d\varepsilon}{dC_L} = 3.60$
$\rho = 2.17$
$\delta_f = 0$
$\delta_f = 20$ deg
$\delta_f = 50$ deg
$C_T = 0.20$
$C_T = 0.60$
$C_T = 1.00$
No power
(Spinners)

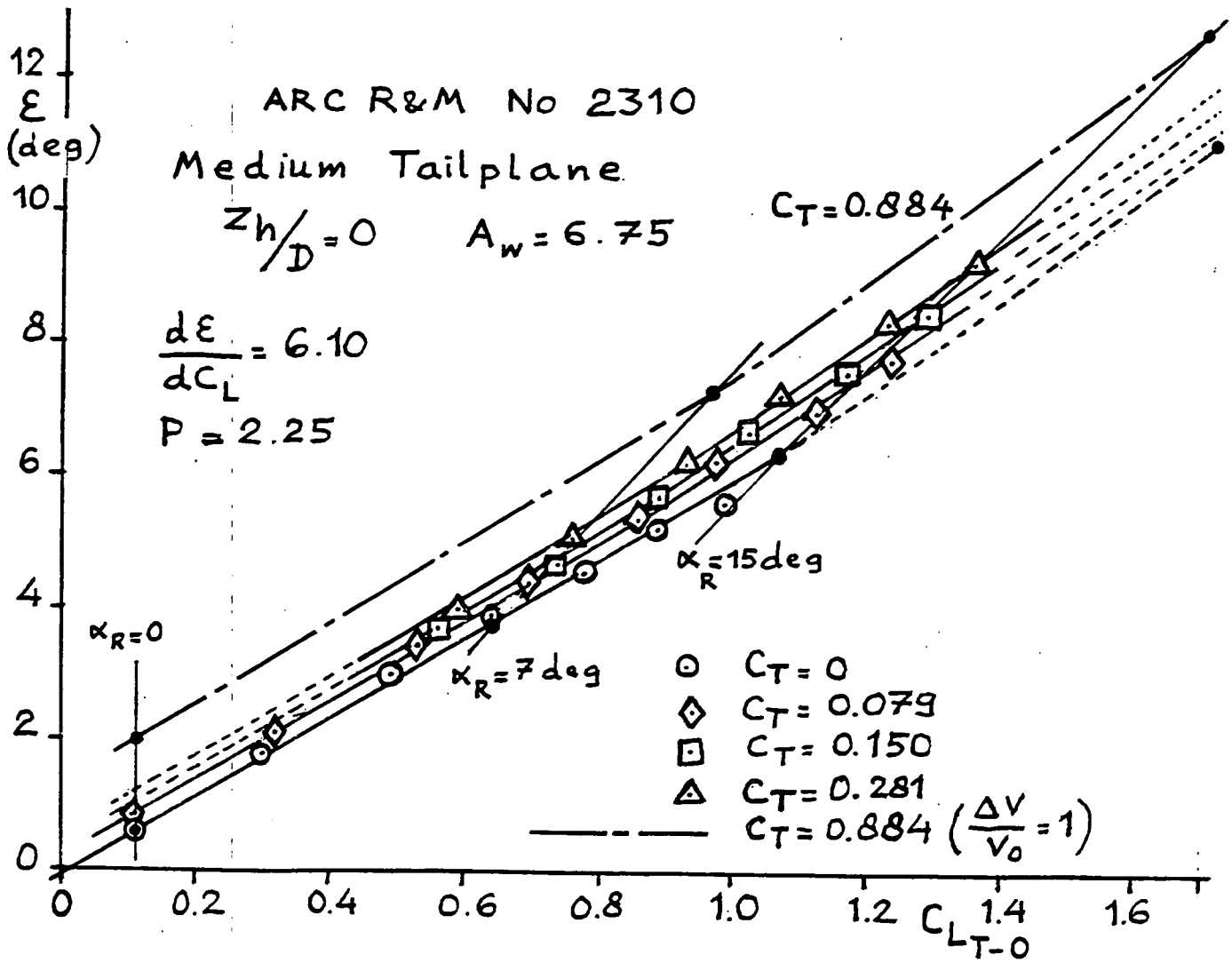
ARC R&M No 2310
Medium Tailplane
$z_{h/D} = 0$
$A_w = 6.75$
$\frac{d\varepsilon}{dC_L} = 6.10$
$P = 2.25$
$C_T = 0.884$
$\alpha_R = 0$
$\alpha_R = 7\,deg$
$\alpha_R = 15\,deg$
$C_T = 0$
$C_T = 0.079$
$C_T = 0.150$
$C_T = 0.281$
$C_T = 0.884$ $(\frac{\Delta V}{V_0} = 1)$
ε (deg)
$C_{L_{T-0}}$
0
2
4
6
8
10
12
0.2
0.4
0.6
0.8
1.0
1.2
1.4
1.6

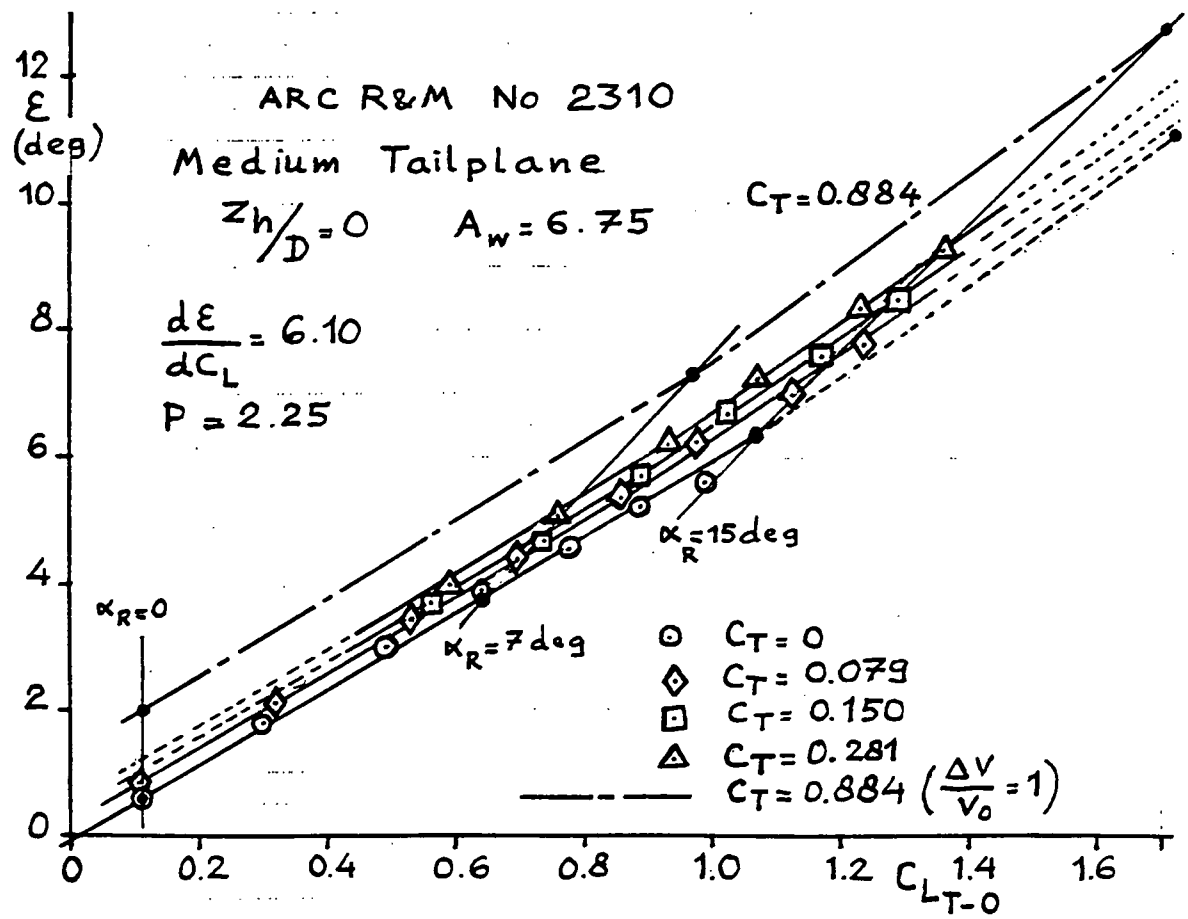
ARC R&M No 2310
Medium Tailplane
$z_h/D = 0$
$A_w = 6.75$
$\frac{d\varepsilon}{dC_L} = 6.10$
$P = 2.25$
$C_T = 0.884$
$\alpha_R = 0$
$\alpha_R = 7$ deg
$\alpha_R = 15$ deg
$C_T = 0$
$C_T = 0.079$
$C_T = 0.150$
$C_T = 0.281$
$C_T = 0.884$ $\left(\frac{\Delta V}{V_0} = 1\right)$
ε (deg)
$C_{L_{T-0}}$
0
2
4
6
8
10
12
0.2
0.4
0.6
0.8
1.0
1.2
1.4
1.6

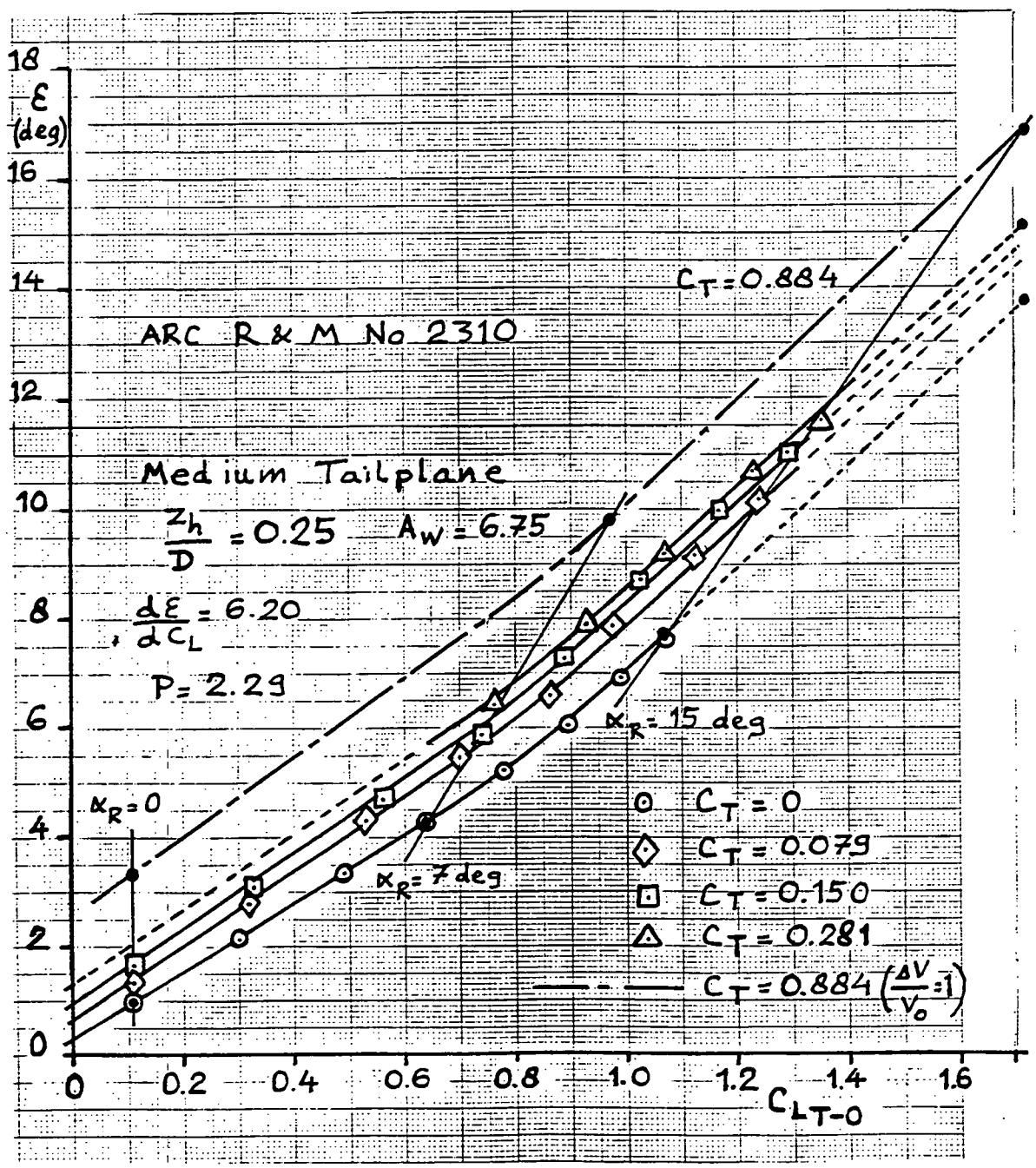
ε (deg)
18
16
14
12
10
8
6
4
2
0
0
0.2
0.4
0.6
0.8
1.0
1.2
1.4
1.6
C_{LT-0}
ARC R & M No 2310
Medium Tailplane
$\frac{z_h}{D} = 0.25$
$A_W = 6.75$
$\frac{d\varepsilon}{dC_L} = 6.20$
P = 2.29
$C_T = 0.884$
$\alpha_R = 15$ deg
$\alpha_R = 7$ deg
$\alpha_R = 0$
$C_T = 0$
$C_T = 0.079$
$C_T = 0.150$
$C_T = 0.281$
$C_T = 0.884 \left(\frac{\Delta V}{V_o} = 1\right)$

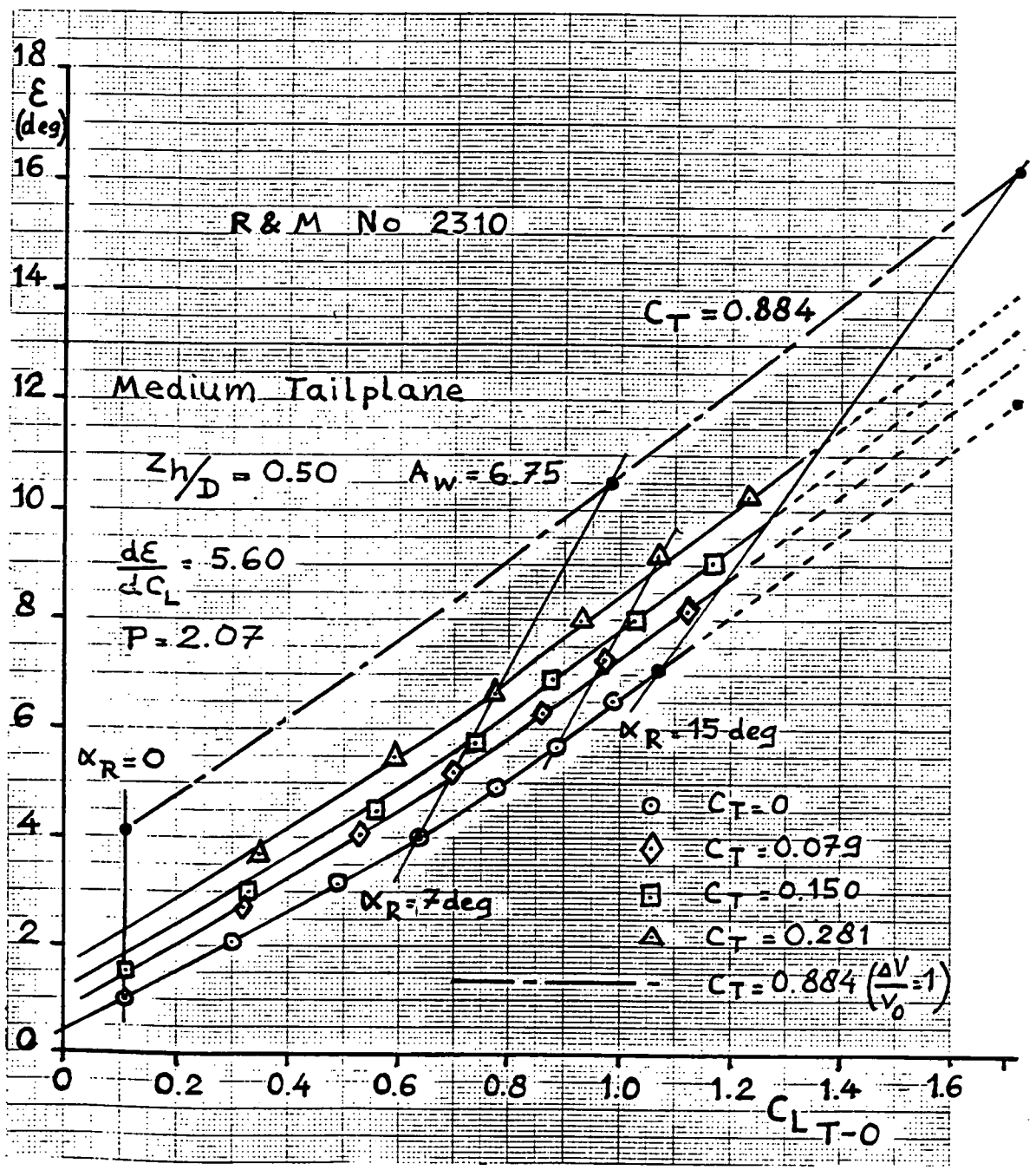
ε (deg)
R & M No 2310
Medium Tailplane
$z_h/D = 0.50$
$A_w = 6.75$
$\frac{d\varepsilon}{dC_L} = 5.60$
P = 2.07
$C_T = 0.884$
$\alpha_R = 0$
$\alpha_R = 7$ deg
$\alpha_R = 15$ deg
$C_T = 0$
$C_T = 0.079$
$C_T = 0.150$
$C_T = 0.281$
$C_T = 0.884 \left(\frac{\Delta V}{V_0} = 1\right)$
$C_{L_{T-0}}$
0
2
4
6
8
10
12
14
16
18
0.2
0.4
0.6
0.8
1.0
1.2
1.4
1.6

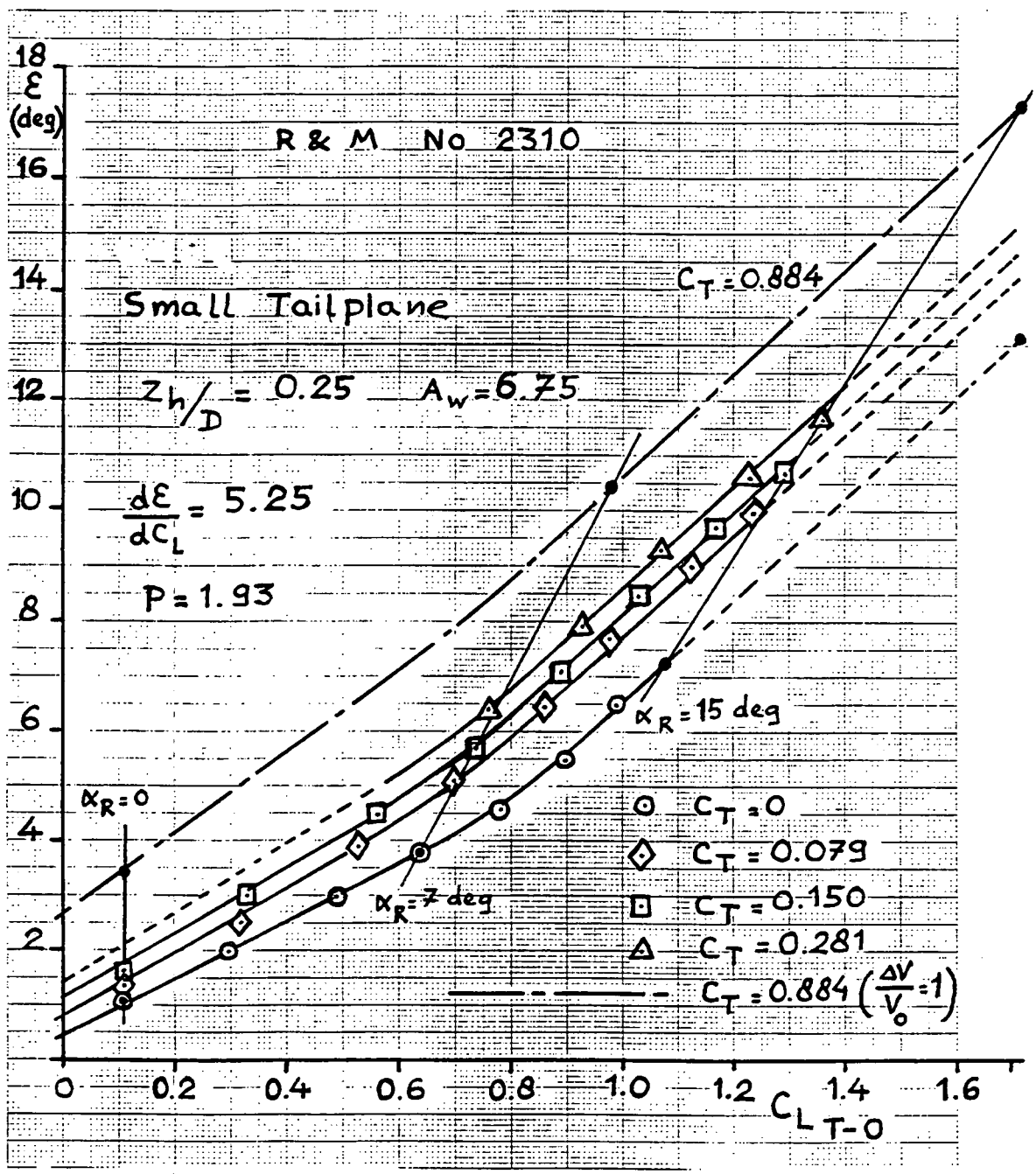
R & M No 2310
Small Tailplane
$z_h/D = 0.25$ $A_w = 6.75$
$\frac{d\varepsilon}{dC_L} = 5.25$
P = 1.93
$C_T = 0.884$
$\alpha_R = 15$ deg
$\alpha_R = 7$ deg
$\alpha_R = 0$
$C_T = 0$
$C_T = 0.079$
$C_T = 0.150$
$C_T = 0.281$
$C_T = 0.884 \left(\frac{\Delta V}{V_o} = 1\right)$
ε (deg)
18
16
14
12
10
8
6
4
2
0
0.2
0.4
0.6
0.8
1.0
1.2
1.4
1.6
$C_{L\,T-0}$

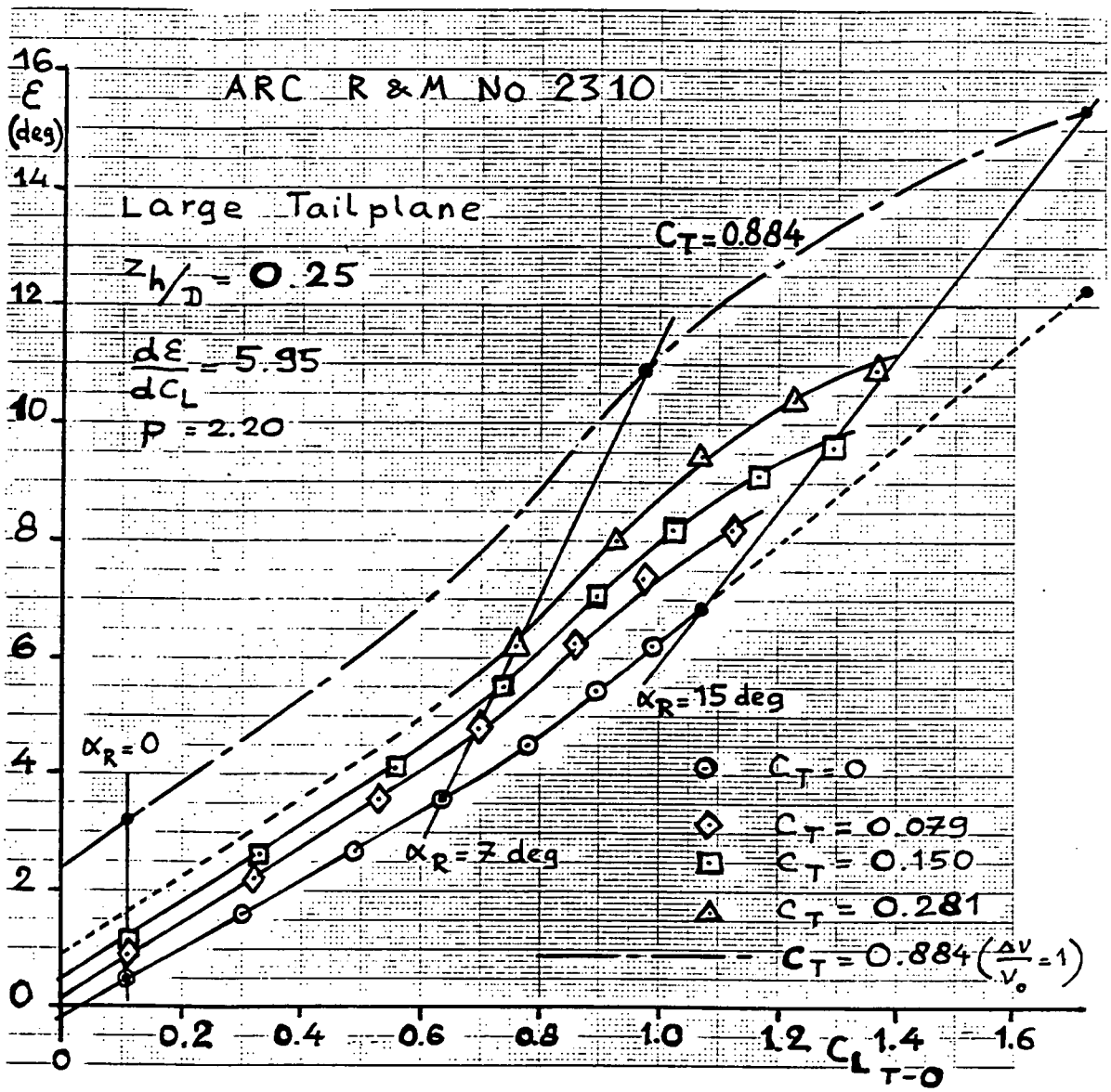
ARC R & M No 2310
Large Tailplane
$z_{h/D} = 0.25$
$\frac{d\varepsilon}{dC_L} = 5.95$
$P = 2.20$
$C_T = 0.884$
$\alpha_R = 15$ deg
$\alpha_R = 7$ deg
$\alpha_R = 0$
$C_T = 0$
$C_T = 0.079$
$C_T = 0.150$
$C_T = 0.281$
$C_T = 0.884 \left(\frac{\Delta V}{V_o} = 1\right)$
ε (deg)
C_L T-O
0
2
4
6
8
10
12
14
16
0.2
0.4
0.6
0.8
1.0
1.2
1.4
1.6

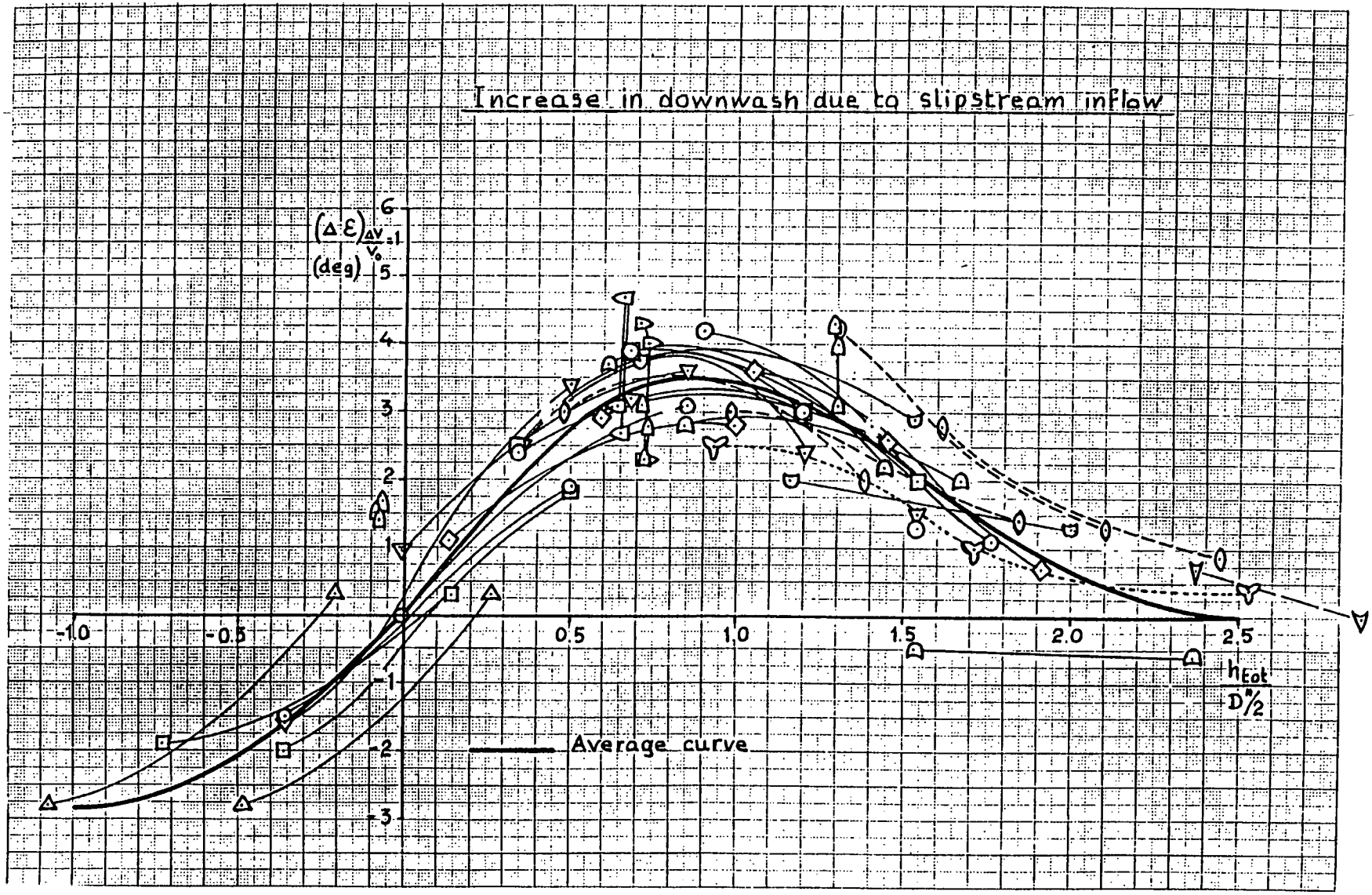
Increase in downwash due to slipstream inflow
$(\Delta\varepsilon)_{\frac{\Delta V}{V_0}=1}$ (deg)
6
5
4
3
2
1
-1
-2
-3
-1.0
-0.5
0.5
1.0
1.5
2.0
2.5
$\frac{h_{tot}}{D/2}$
Average curve

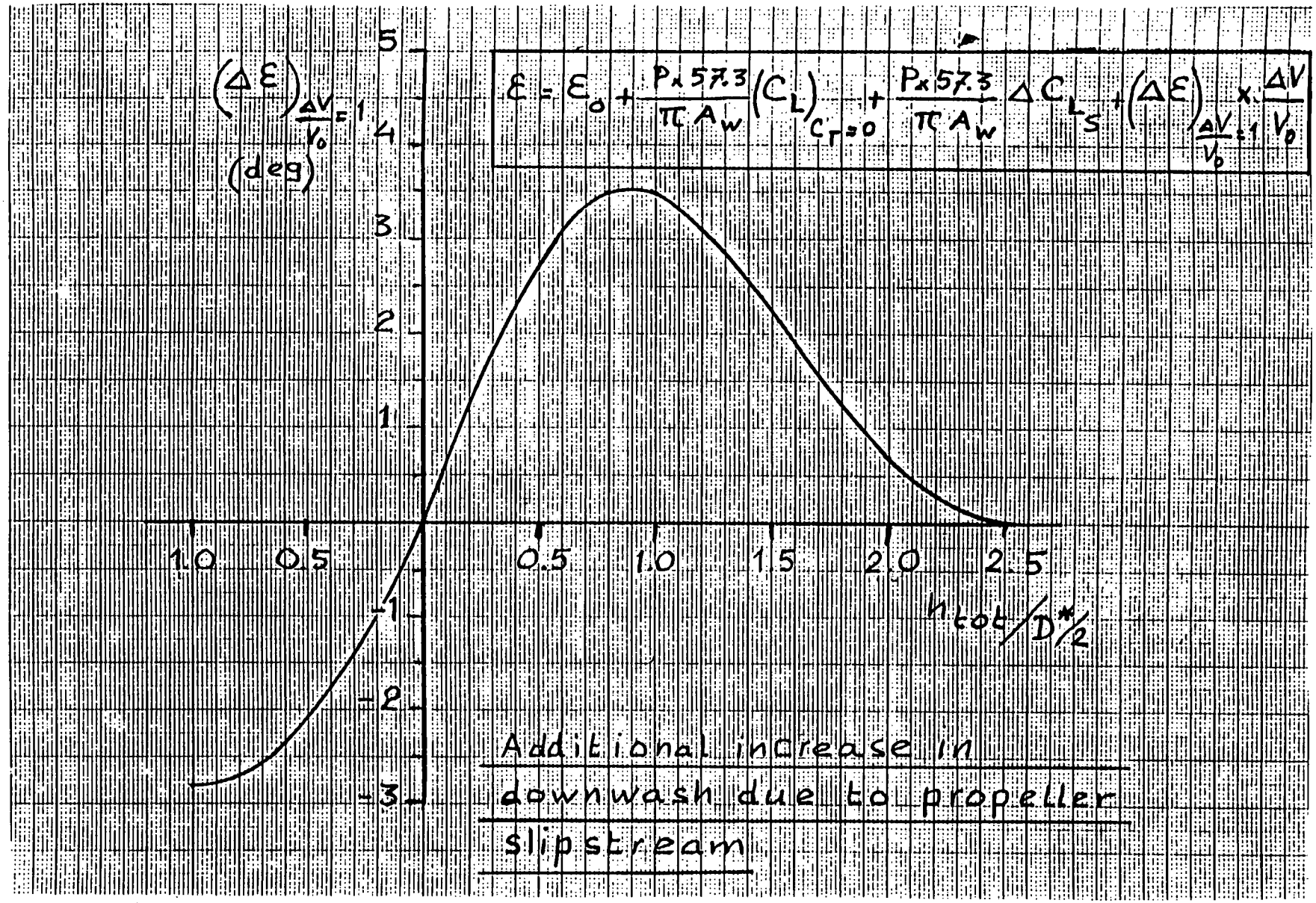
$\varepsilon = \varepsilon_0 + \frac{P \times 57.3}{\pi A_w}(C_L)_{C_T=0} + \frac{P \times 57.3}{\pi A_w}\Delta C_{L_S} + \left(\Delta\varepsilon\right)_{\frac{\Delta V}{V_0}=1} \times \frac{\Delta V}{V_0}$
$\left(\Delta\varepsilon\right)_{\frac{\Delta V}{V_0}=1}$ (deg)
5
4
3
2
1
-1
-2
-3
1.0
0.5
0.5
1.0
1.5
2.0
2.5
$h_{tot}/D^*/2$
Additional increase in downwash due to propeller slipstream

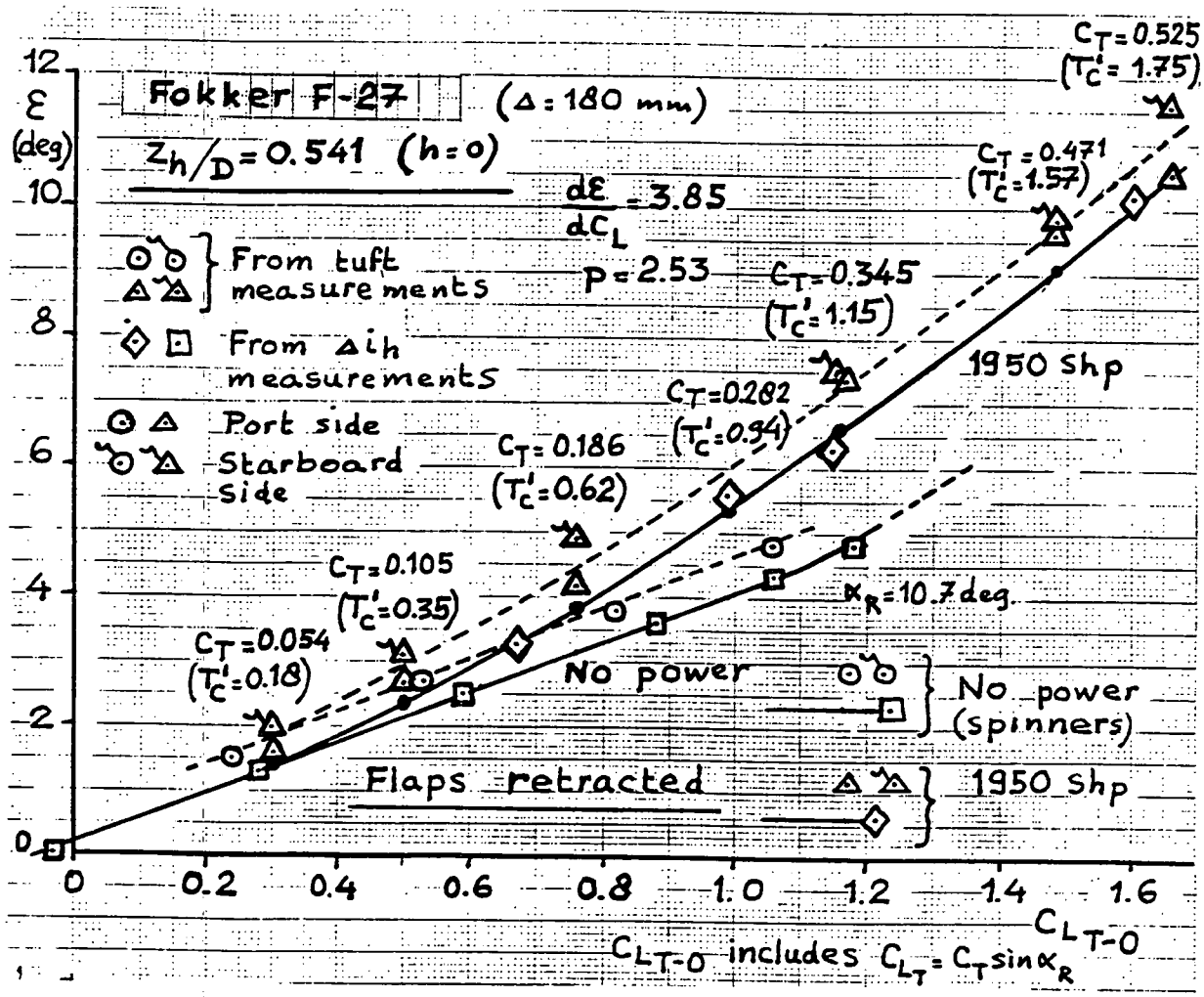
Fokker F-27
(Δ = 180 mm)
$Z_h/D = 0.541$ (h = 0)
$\frac{d\varepsilon}{dC_L} = 3.85$
P = 2.53
From tuft measurements
From Δih measurements
Port side
Starboard side
$C_T = 0.525$ ($T_C' = 1.75$)
$C_T = 0.471$ ($T_C' = 1.57$)
$C_T = 0.345$ ($T_C' = 1.15$)
$C_T = 0.282$ ($T_C' = 0.94$)
$C_T = 0.186$ ($T_C' = 0.62$)
$C_T = 0.105$ ($T_C' = 0.35$)
$C_T = 0.054$ ($T_C' = 0.18$)
1950 shp
$\alpha_R = 10.7$ deg
No power
No power (spinners)
Flaps retracted
1950 shp
ε (deg)
12
10
8
6
4
2
0
0
0.2
0.4
0.6
0.8
1.0
1.2
1.4
1.6
$C_{L_{T-0}}$
$C_{L_{T-0}}$ includes $C_{L_T} = C_T \sin \alpha_R$

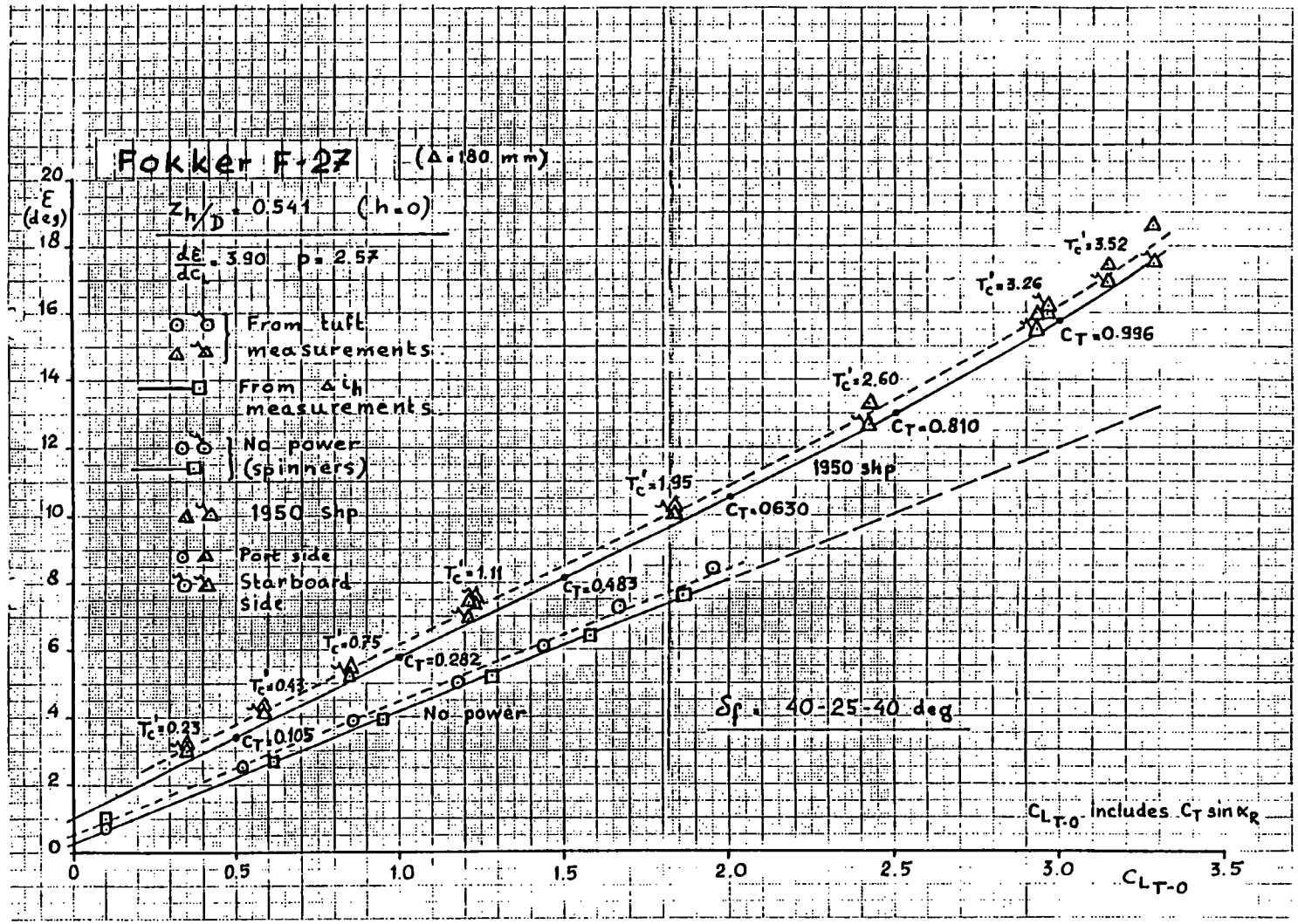
Fokker F-27
(Δ = 180 mm)
z_h/D = 0.541 (h = 0)
$\frac{d\varepsilon}{dC_L}$ = 3.90 p = 2.57
From tuft measurements
From Δi_h measurements
No power (spinners)
1950 shp
Port side
Starboard side
T_c' = 0.23
C_T = 0.105
T_c' = 0.43
T_c' = 0.75
C_T = 0.282
T_c' = 1.11
C_T = 0.483
T_c' = 1.95
C_T = 0630
T_c' = 2.60
C_T = 0.810
T_c' = 3.26
C_T = 0.996
T_c' = 3.52
No power
1950 shp
δ_f = 40-25-40 deg
$C_{L_{T-0}}$ includes $C_T \sin \alpha_R$
ε (deg)
$C_{L_{T-0}}$
0
0.5
1.0
1.5
2.0
2.5
3.0
3.5
2
4
6
8
10
12
14
16
18
20

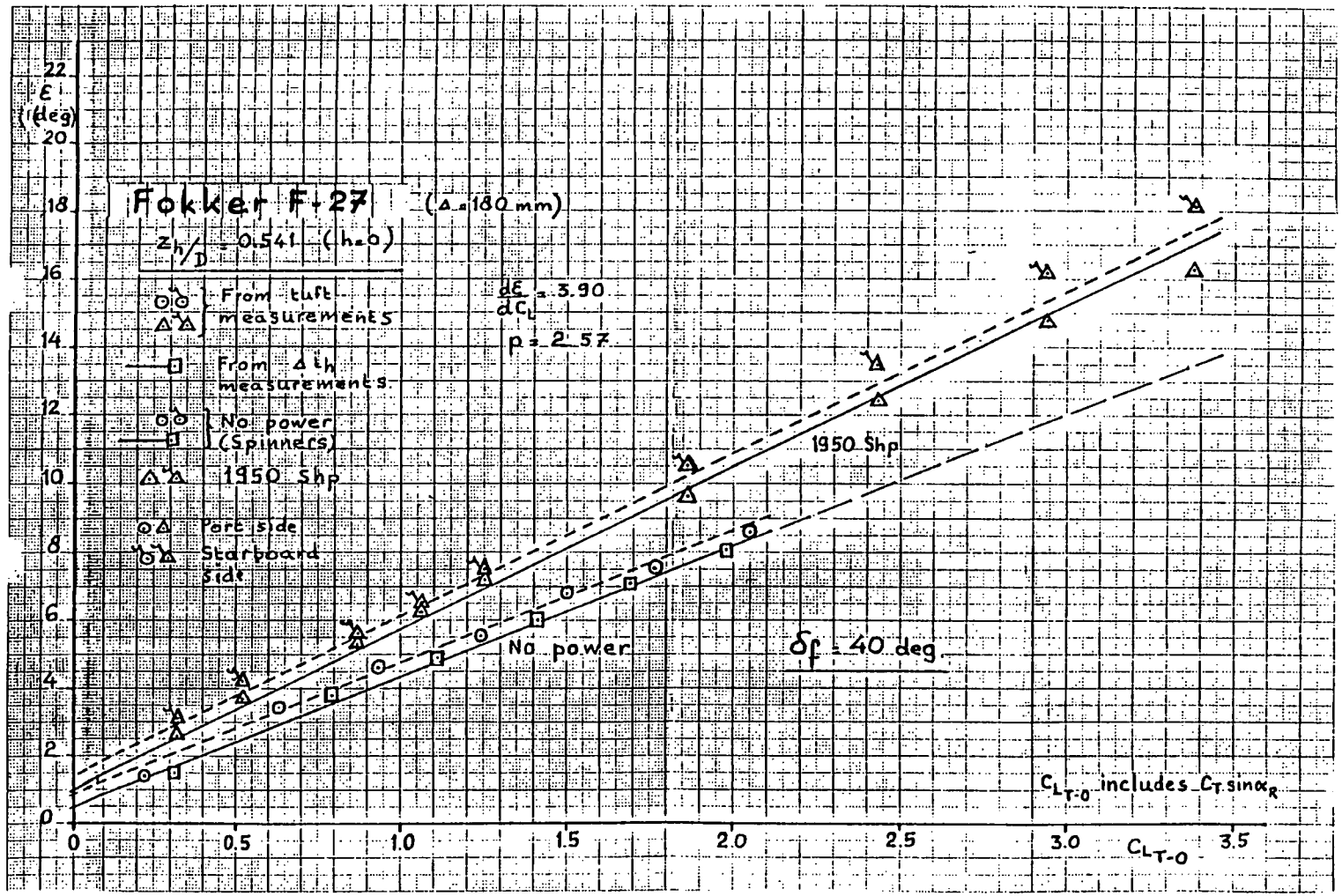
Fokker F-27 (Δ = 180 mm)
z_h/D = 0.541 (h=0)
From tuft measurements
From Δ th measurements
No power (Spinners)
1950 Shp
Port side
Starboard side
$\frac{d\varepsilon}{dC_L}$ = 3.90
p = 2.57
1950 Shp
No power
δ_f = 40 deg
$C_{L_{T-0}}$ includes $C_T \sin\alpha_R$
ε (deg)
$C_{L_{T-0}}$
0
0.5
1.0
1.5
2.0
2.5
3.0
3.5
2
4
6
8
10
12
14
16
18
20
22

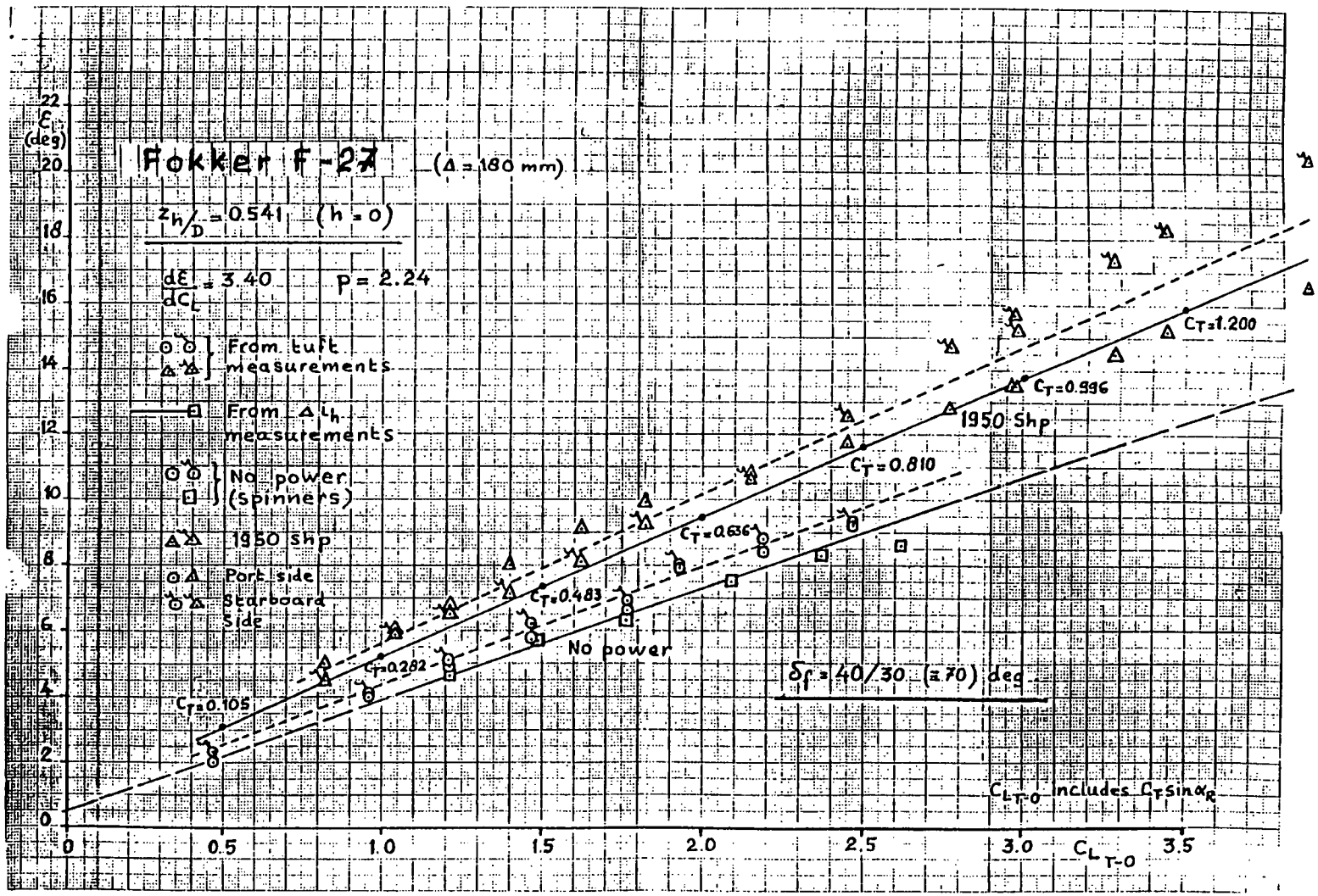
Fokker F-27 (Δ = 180 mm)
$z_{h/D}$ = 0.541 (h = 0)
$\frac{d\varepsilon}{dC_L}$ = 3.40 P = 2.24
From tuft measurements
From Δ_h measurements
No power (spinners)
1950 shp
Port side
Starboard side
C_T = 0.105
C_T = 0.282
C_T = 0.483
C_T = 0.636
C_T = 0.810
C_T = 0.996
C_T = 1.200
1950 Shp
No power
δ_f = 40/30 (=70) deg
$C_{L_{T=0}}$ includes $C_T \sin\alpha_R$
ε_L (deg)
$C_{L_{T=0}}$

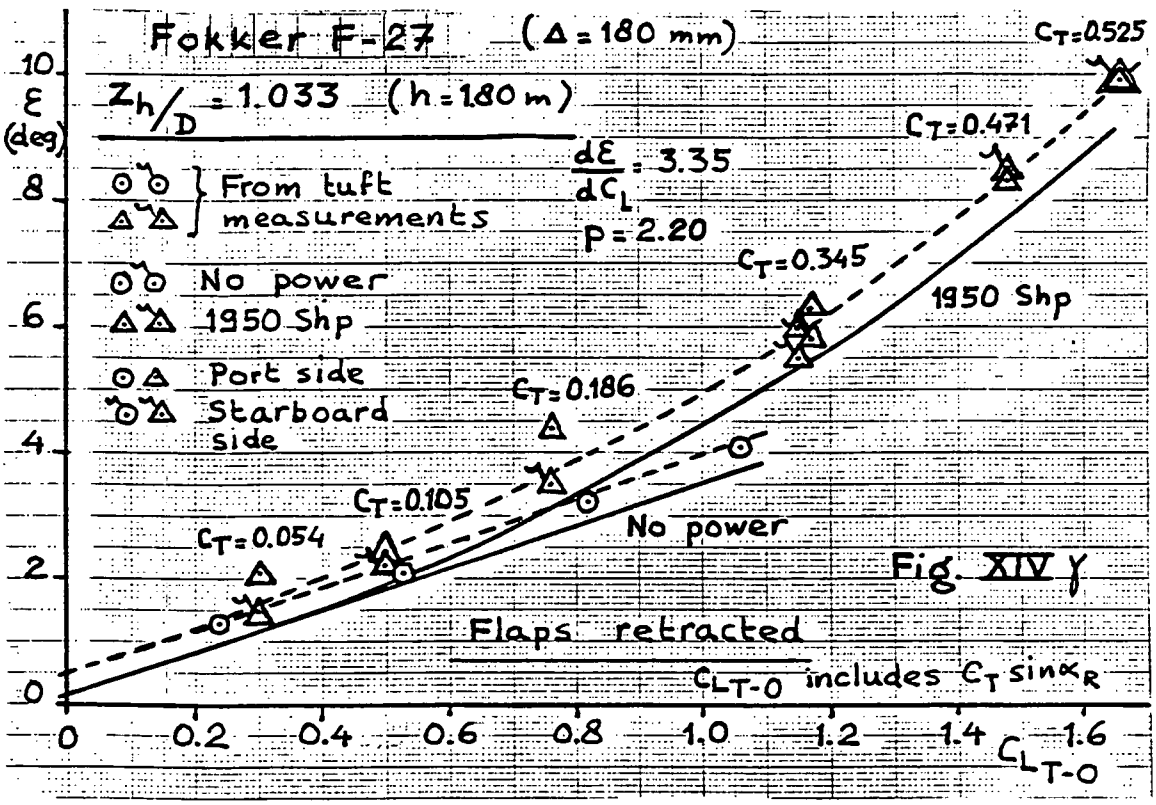

Fig. XIV γ

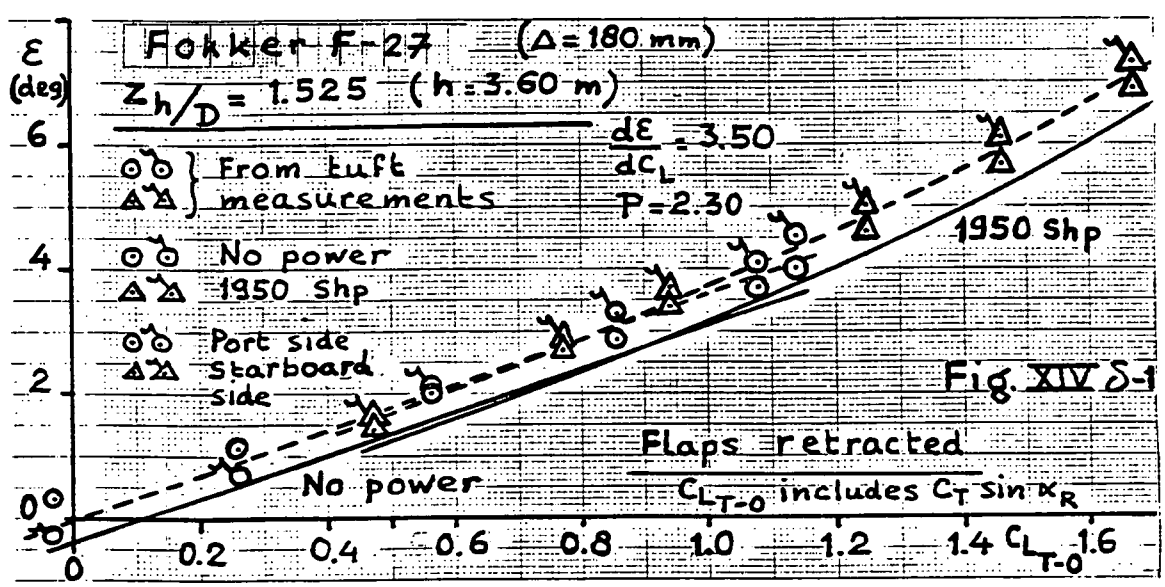

Fig. XIV δ-1

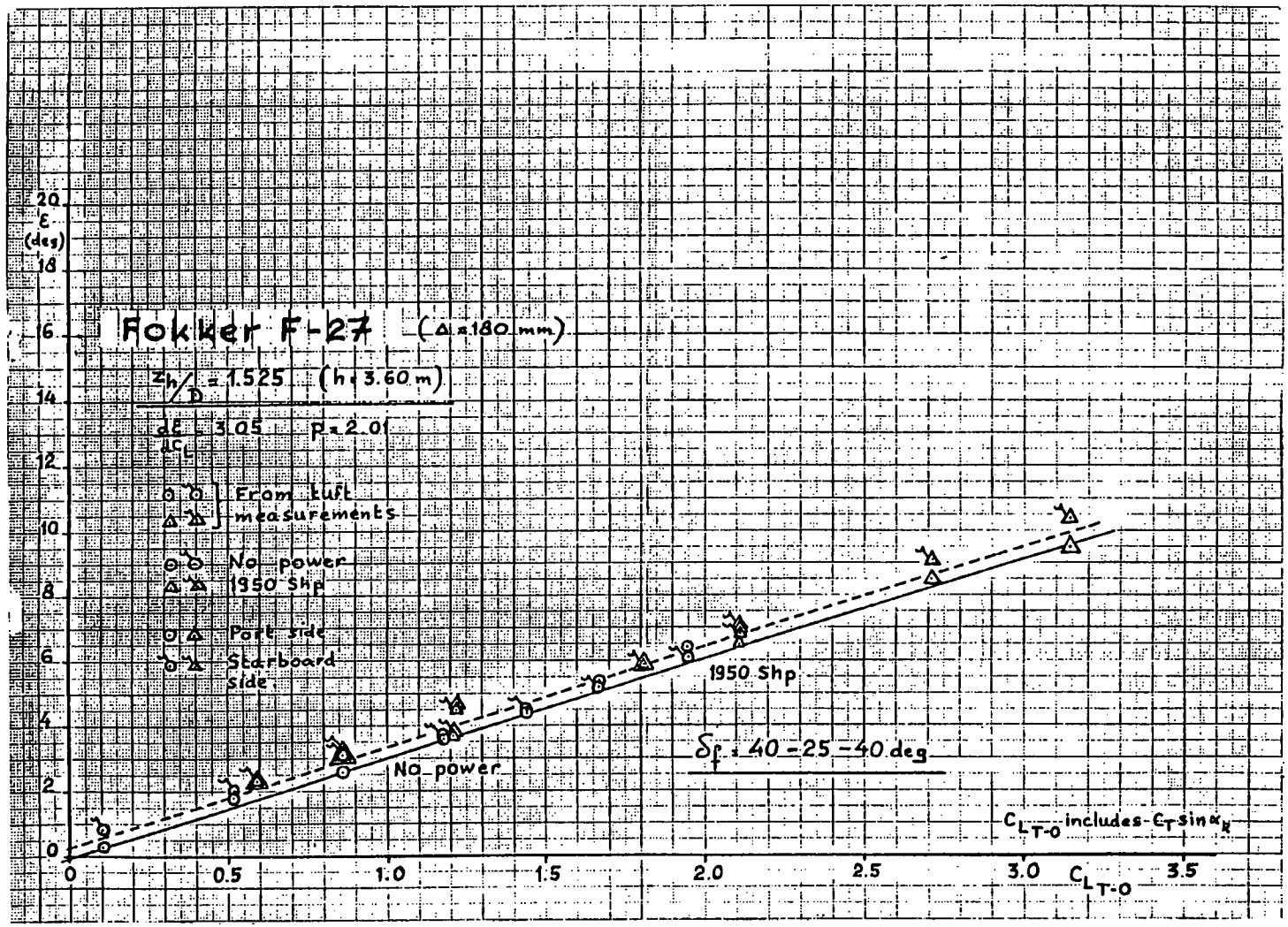
Fokker F-27 (Δ=180 mm)
z_h/D = 1.525 (h = 3.60 m)
$\frac{dε}{dC_L}$ = 3.05 p = 2.0
From luft measurements
No power
1950 Shp
Port side
Starboard side
1950 Shp
No-power
δ_f = 40 - 25 - 40 deg
$C_{L_{T-O}}$ includes $-C_T \sin \alpha_R$
ε (deg)
$C_{L_{T-O}}$
0
0.5
1.0
1.5
2.0
2.5
3.0
3.5
2
4
6
8
10
12
14
16
18
20

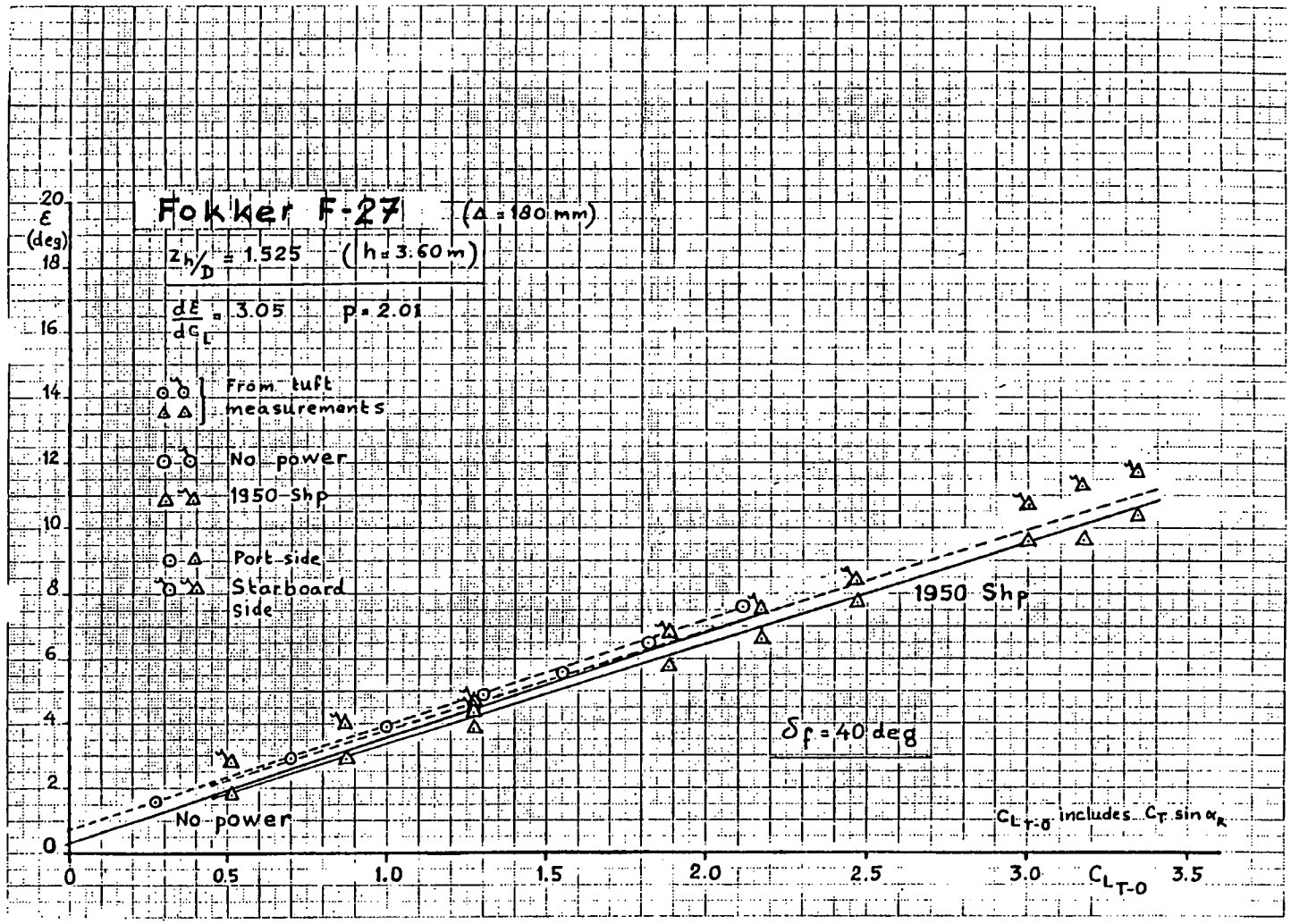
Fokker F-27
(Δ = 180 mm)
z_h/D = 1.525 (h = 3.60 m)
$\frac{d\varepsilon}{dC_L}$ = 3.05 p = 2.01
From tuft measurements
No power
1950-Shp
Port-side
Starboard side
1950 Shp
No power
δ_f = 40 deg
$C_{L_{T-O}}$ includes $C_T \sin \alpha_R$
ε (deg)
$C_{L_{T-O}}$
0
0.5
1.0
1.5
2.0
2.5
3.0
3.5
2
4
6
8
10
12
14
16
18
20

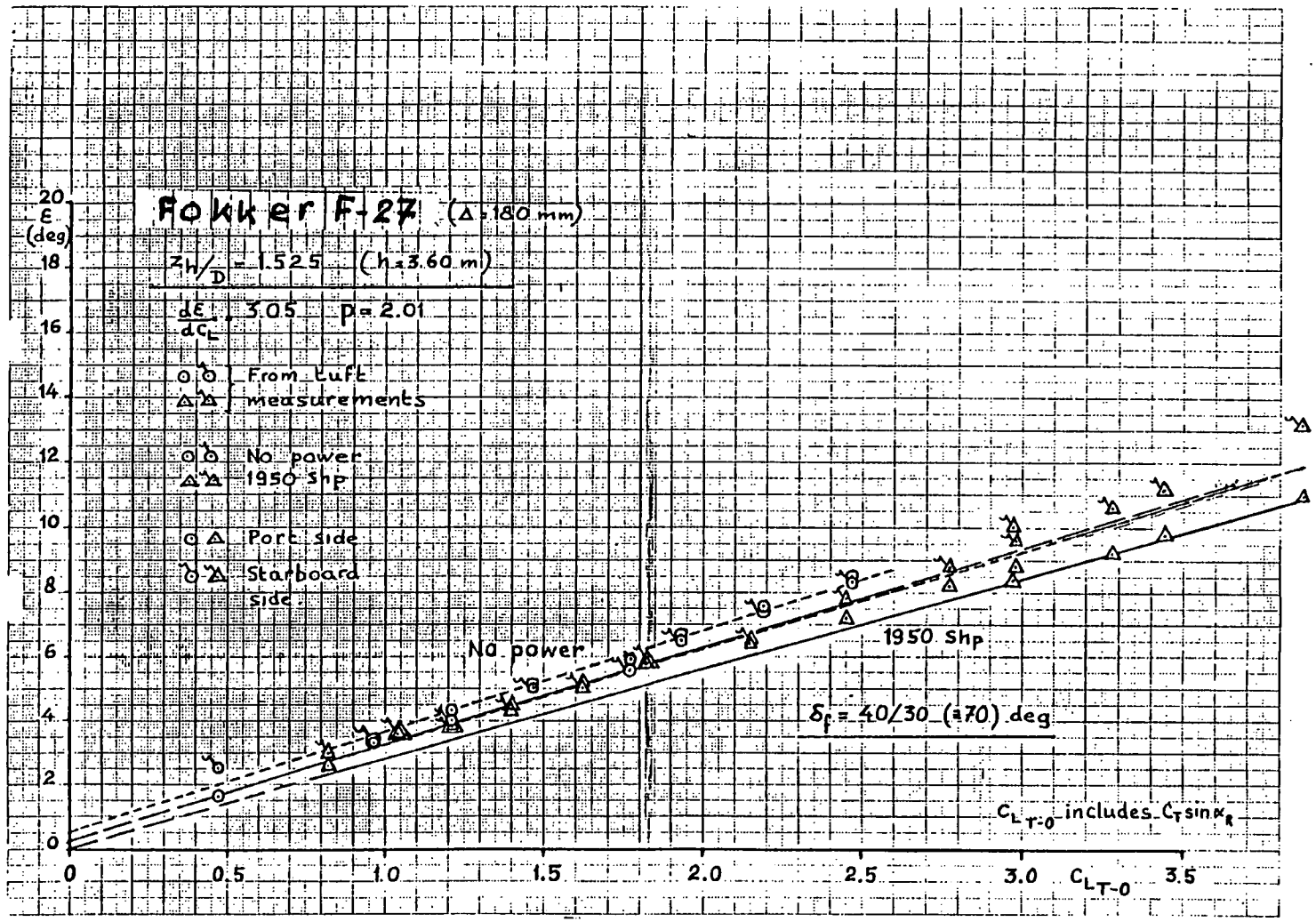
Fokker F-27 (Δ=180 mm)
$z_{H/D}$ = 1.525 (h=3.60 m)
$\frac{d\varepsilon}{dC_L}$ = 3.05 p = 2.01
From tuft measurements
No power
1950 shp
Port side
Starboard side
No power
1950 shp
δ_f = 40/30 (=70) deg
$C_{L_{T=0}}$ includes $C_T \sin\alpha_s$
ε (deg)
$C_{L_{T-0}}$
0
0.5
1.0
1.5
2.0
2.5
3.0
3.5
2
4
6
8
10
12
14
16
18
20

Appendix XIII

A comparison between the calculated increase in average dynamic pressure at the tailplane and windtunnel test data.

In chapter 6.4 of the main text the process is described through which the average dynamic pressure at the horizontal tailplane can be determined.
In figures 36 and 37 calculated and measured data for two aircraft are compared.

This appendix presents the calculations.

Table VIII(a) Downwash Characteristics (IV)

No.	Conf.	l_h/c	i_w (deg)	z_h/D	δ_f (deg)	α_R (deg)	$C_f \sin\delta_f$	$\Delta\alpha_{\alpha_f}$ (deg)	ϵ_T	$\Delta V/V_0$	$C_{L_{P.0}}$ TEST	ΔC_{L_S} TEST	C_L^*	D_{prop}	D^*	C_S	C_f
		(78)	(79)	(80)	(81)	(82)	(83)	(84) ≡ (15)	(85)	(86)	(87) ≡ (38)	(88) ≡ (57)	(89) = (87)+(88)	(90) ≡ (9)	(91) ≡ (42)	(92) ≡ (4)	(93)
12	Fokker 50	4.53	3.4	0.131	0	-4.0	0	0	0.326	0.414	0.07	0	0.07	3.81	3.52	2.95	0.95
						0					0.43	0.06	0.49				
						4.0					0.79	0.11	0.90				
						8.0					(1.06)	0.16	1.22				
						12.0					(1.25)	0.22	1.47				
		4.53	3.4	0.131	0	15.0	0	0	0.326	0.414	(1.31)	0.27	1.58	3.81	3.52	2.95	0.95
		4.53	3.4	0.131	0	-4.0	0	0	0.815	0.892	0.07	0	0.07	3.81	3.34	2.95	0.95
						0					0.43	0.10	0.53				
						4.0					0.79	0.20	0.99				
						8.0					(1.06)	0.30	1.36				
						12.0					(1.15)	0.40	1.55				
		4.53	3.4	0.131	0	15.0	0	0	0.815	0.892	(1.31)	0.48	1.79	3.81	3.34	2.95	0.95
12	Fokker 50	4.53	3.4	0.131	16.5	-4.0	0.225	-4.0	0.326	0.414	0.49	0.16	0.65	3.81	3.52	2.95	0.95
						0					0.90	0.24	1.14				
						4.0					1.28	0.32	1.60				
						8.0					1.57	0.40	1.97				
		4.53	3.4	0.131	16.5	10.0	0.225	-4.0	0.326	0.414	—	—	—	3.81	3.52	2.95	0.95
		4.53	3.4	0.131	16.5	-4.0	0.225	-4.0	0.815	0.892	0.49	0.28	0.77	3.81	3.34	2.95	0.95
						0					0.90	0.40	1.30				
						4.0					1.28	0.52	1.80				
						8.0					1.57	0.65	2.22				
		4.53	3.4	0.131	16.5	10.0	0.225	-4.0	0.815	0.892	—	—	—	3.81	3.34	2.95	0.95
12	Fokker 50	4.53	3.4	0.131	40	-4.0	0.503	-11.5	0.326	0.414	1.16	0.23	1.39	3.81	3.52	2.95	0.95
						0					1.55	0.31	1.86				
						4.0					1.88	0.40	2.28				
						8.0					2.25	0.48	2.73				
		4.53	3.4	0.131	40	12.0	0.503	-11.5	0.326	0.414	—	—	—	3.81	3.52	2.95	0.95
		4.53	3.4	0.131	40	-4.0	0.503	-11.5	0.815	0.892	1.16	0.43	1.59	3.81	3.34	2.95	0.95
						0					1.55	0.56	2.11				
						4.0					1.88	0.68	2.56				
						8.0					2.25	0.81	3.06				
		4.53	3.4	0.131	40	12.0	0.503	-11.5	0.815	0.892	—	—	—	3.81	3.34	2.95	0.95

Example of calculating procedure

Table VIII (a) Downwash Characteristics (III) (Continued)

No	Conf	l_h	h_t	$x_{cg}-x_{pr}$	l_h^*	$(\Delta h_t)_\alpha$	$(\Delta h_t)_{upw.}$	$\frac{d\varepsilon}{dC_L}$	K_ε	$\left(\frac{dC_L}{d\alpha_{T\text{-}O}}\right)_{C_T=0}$ (1/deg)	ΔC_{L_S} rest.	$\varepsilon_{\alpha=0}$	M	N	O	P	α_R (deg)	dim
		(94)	(95)	(96)	(97)	(98)	(99)	(100)	(101)	(102)	(88) = (59)	(104)	(105)	(106)	(107)	(108)	(82)	
12	Fokker 50	11.18	0.76	3.32	8.85	0.23	0	3.90	1.5	0.090	0	2.9	-2.11	0	4.35	0.35	-4.0	m
						0					0.06		0	0.35		0.73	0	
						-0.23					0.11		2.11	0.64		1.10	4.0	
						-0.46					0.16		4.21	0.94		1.48	8.0	
						-0.69					0.22		6.32	1.29		1.87	12.0	
		11.18	0.76	3.32	8.85	-0.86	0	3.90	1.5	0.090	0.27	2.9	7.90	1.58	4.35	2.18	15.0	m
		11.18	0.76	3.32	8.85	0.23	0	3.90	1.5	0.090	0	2.9	-2.11	0	4.35	0.35	-4.0	m
						0					0.10		0	0.59		0.76	0	
						-0.23					0.20		2.11	1.17		1.19	4.0	
						-0.46					0.30		4.21	1.76		1.61	8.0	
						-0.69					0.40		6.32	2.34		2.04	12.0	
		11.18	0.76	3.32	8.85	-0.86	0	3.90	1.5	0.090	0.48	2.9	7.90	2.81	4.35	2.38	15.0	m
12	Fokker 50	11.18	0.76	3.32	8.85	0.23	-0.06	3.90	1.5	0.100	0.16	4.7	-2.34	0.94	7.05	0.88	-4.0	m
						0					0.24		0	1.40		1.31	0	
						-0.23					0.32		2.34	1.87		1.76	4.0	
						-0.46					0.40		4.68	2.34	7.05	2.22	8.0	
		11.18	0.76	3.32	8.85	—	-0.06	3.90	1.5	0.100	—	4.7	—	—	—	—	12.0	m
		11.18	0.76	3.32	8.85	0.23	-0.06	3.90	1.5	0.100	0.28	4.7	-2.34	1.64	7.05	0.98	-4.0	m
						0					0.40		0	2.34		1.46	0	
						-0.23					0.52		2.34	3.04		1.95	4.0	
						-0.46					0.65		4.68	3.80	7.05	2.46	8.0	
		11.18	0.76	3.32	8.85	—	-0.06	3.90	1.5	0.100	—	4.7	—	—	—	—	12.0	m
12	Fokker 50	11.18	0.76	3.32	8.85	0.23	-0.17	3.90	1.5	0.088	0.23	6.8	-2.06	1.35	10.2	1.48	-4.0	m
1						0					0.31		0	1.81		1.88	0	
						-0.23					0.40		2.06	2.34		2.31	4.0	
						-0.46					0.48		4.12	2.81	10.2	2.73	8.0	
		11.18	0.76	3.32	8.85	—	-0.17	3.90	1.5	0.088	—	6.8	—	—	—	—	12.0	m
		11.18	0.76	3.32	8.85	0.23	-0.17	3.90	1.5	0.088	0.43	6.8	-2.06	2.52	10.2	1.67	-4.0	m
						0					0.56		0	3.28		2.12	0	
						-0.23					0.68		2.06	3.98		2.58	4.0	
						-0.46					0.81		4.12	4.74	10.2	3.06	8.0	
		11.18	0.76	3.32	8.85	—	-0.17	3.90	1.5	0.088	—	6.8	—	—	—	—	12.0	m

Table VIII(a) Downwash Characteristics (IV) (Concluded)

No	Conf	δ_f (deg) (81)	α_R (deg) (82)	h_{tot} CALC (109)	h_{tot} TEST (110)	$\frac{h_{tot}}{D^*/2}$ CALC (111)	b_{s_h} (112)	c_{s_h} (113)	s_{s_h} (114)	s_h (115)	$\frac{q_s}{q}$ CALC (116)	b_{max} CALC (117)	$\frac{b_a}{b_{AV}} = \left(\frac{V}{V_0}\right)_{AV}$ CALC (122)	$\frac{q_h}{q}$ CALC (123)	$\frac{q_h}{q}$ TEST (120)	$\frac{b}{b_{max}}$ CALC (124)	$\left(\frac{q_h}{q}\right)_{max}$ CALC (125)
12	Fokker 50	0	-4.0	2.12	—	1.21		1.35		16.0	2.000	0.262	0.013	1.026	1.04	0.05	1.594
			0	1.49	—	0.85							0.063	1.130	1.28	0.24	
			4.0	0.85	—	0.48							0.183	1.400	1.40	0.70	
			8.0	0.21	—	0.12							0.283	1.646	1.40	1.08	
			12.0	-0.44	—	-0.25							0.257	1.579	1.53	0.98	
		0	15.0	-0.92	—	-0.52		1.35		16.0	2.000	0.262	0.160	1.345	1.53	0.61	1.594
		0	-4.0	2.12	—	1.27		1.35		16.0	3.580	0.567	0.023	1.046	1.09	0.04	2.454
			0	1.52	—	0.91							0.147	1.317	1.34	0.26	
			4.0	0.94	—	0.56							0.318	1.736	1.20	0.56	
			8.0	0.34	—	0.20							0.476	2.179	2.07	0.84	
			12.0	-0.27	—	-0.16							0.522	2.333	2.21	0.93	
		0	15.0	-0.72	—	-0.43		1.35		16.0	3.580	0.567	0.948	2.097	2.42	0.79	2.454
12	Fokker 50	16.5	-4.0	2.82	—	1.60		1.35		16.0	2.000	0.262	0	1.000	1.00	0	1.594
			0	2.24	—	1.27							0.010	1.020	1.04	0.04	
			4.0	1.67	—	0.95							0.045	1.091	1.28	0.17	
			8.0	1.11	—	0.63							0.123	1.261	1.32	0.47	
		16.5	12.0	—				1.35		16.0	2.000	0.262	—	—	—	—	1.594
		16.5	-4.0	2.92	—	1.75		1.35		16.0	3.580	0.567	0	1.000	1.00	0	2.454
			0	2.39	—	1.43							0.006	1.012	1.10	0.01	
			4.0	1.86	—	1.12							0.051	1.105	1.35	0.09	
			8.0	1.35	—	0.81							0.147	1.317	1.56	0.26	
		16.5	12.0	—		—		1.35		16.0	3.580	0.567	—	—	—	—	2.454
12	Fokker 50	40	-4.0	3.58	—	2.04		1.35		16.0	2.000	0.262	0	1.000	1.00	0	1.594
			0	2.97	—	1.78							0	1.000	1.00	0	
			4.0	2.39	—	1.36							0.005	1.010	1.00	0.02	
			8.0	1.79	—	1.02							0.037	1.075	1.15	0.14	
		40	12.0	—		—		1.35		16.0	2.000	0.262	—	—	—	—	1.594
		40	-4.0	4.47	—	2.68		1.35		16.0	3.580	0.567	0	1.000	1.00	0	2.454
			0	3.44	—	2.06							0	1.000	1.00	0	
			4.0	2.68	—	1.61							0	1.000	1.00	0	
			8.0	2.12	—	1.27							0.023	1.046	1.06	0.04	
		40	12.0	—		—		1.35		16.0	3.580	0.567	—	—	—	—	2.454

Table VIII(b) Downwash Characteristics (IV)

No	Conf.	l_h/c (78)	i_w (deg) (79)	z_h/D (80)	δ_f (deg) (81)	α_R (deg) (82)	$C_f \sin\delta_f$ (83)	$\Delta\alpha_{0,f}$ (deg) (84) = (15)	C_T (85)	$\frac{\Delta V}{V_0}$ (86)	$C_{l_{P.0}}$ TEST (87) = (38)	ΔC_{L_S} TEST (88) = (59)	C_L^* (89) = (83)+(88)	D_{prop} (90) = (9)	D^* (91) = (42)	C_S (92) = (4)	C_f (93)	
16	DHC-5 Caribou		3.0		0	0	0	0	0.37	0.501	0.40			3.99	3.643	3.55	—	
						5.0					0.85						—	
						7.5					1.08	0.19					—	
						10.0					1.30	0.23					—	
						12.5					1.53	0.26					—	
			3.0		0	15.0	0	0	0.32	0.501	(1.75)	0.29		3.99	3.643	3.55	—	
			3.0		0	0	0	0	1.12	1.190	0.40			3.99	3.405	3.55	—	ΔC_{L_S} Calculated
						5.0					0.85						—	
						7.5					1.08	0.35					—	
						10.0					1.30	0.40					—	
						12.5					1.53	0.45					—	
			3.5		0	15.0	0	0	1.12	1.190	(1.75)	0.50		3.99	3.405	3.55	—	

No	Conf	l_h (94)	h_t (95)	$x_{cg}-x_{pr}$ (96)	l_h^* (97)	$(\Delta h_t)_\alpha$ (98)	$(\Delta h_t)_{upw.}$ (99)	$\frac{d\varepsilon}{dC_L}$ (100)	K_ε (101)	$\left(\frac{dC_L}{d\alpha}\right)_{T.0}$ (1/deg) $C_T \geq 0$ (102)	ΔC_{L_S} (88) = (59)	$\varepsilon_{\alpha,0}$ (104)	M (105)	N (106)	O (107)	P (108)	α_R (deg) (82)	dim
16	DHC-5 Caribou	12.19	3.11	2.78	9.40	0	0	4.01	1.5	0.090		1.6	0		2.4		0	m
						-0.24							2.707				5.0	
						-0.36					0.19		4.060	1.143		1.25	7.5	
						-0.48					0.23		5.414	1.383		1.52	10.0	
						-0.60					0.26		6.767	1.564		1.78	12.5	
		12.19	3.11	2.78	9.40	-0.72	0	4.01	1.5	0.090	0.29	1.6	8.120	1.744	2.4	2.04	15.0	m
		12.19	3.11	2.78	9.40	0	0	4.01	1.5	0.090		1.6	0		2.4		0	m
						-0.24							2.707				5.0	
						-0.36					0.35		4.060	2.105		1.42	7.5	
						-0.48					0.40		5.414	2.406		1.69	10.0	
						-0.60					0.45		6.767	2.707		1.98	12.5	
		12.19	3.11	2.78	9.40	-0.72	0	4.01	1.5	0.090	0.50	1.6	8.120	3.008	2.4	2.26	15.0	m

XIII-5

Table VIII (b) Downwash Characteristics (IV) (Concluded)

No	Conf	δ_f (deg) (81)	α_R (deg) (82)	h_{tot} CALC (109)	h_{tot} TEST (110)	$\frac{h_{tot}}{D/2}$ CALC (111)	b_{s_h} (112)	C_{s_h} (113)	S_{s_h} (114)	S_h (115)	$\frac{q_s}{q}$ CALC. (116)	$\bar{v}_{max}$ CALC. (117)	$b = \left(\frac{\Delta V}{V_{0_{av}}}\right)_{av}$ CALC (122)	$\frac{q_h}{q}$ CALC. (123)	$\frac{q_h}{q}$ TEST (120)	$\frac{b}{b_{max}}$ CALC (124)	$\left(\frac{q_h}{q}\right)_{MAX}$ CALC (125)
16	DHC-5 Caribou	0	0	—	—	—		1.82		20.61	2.25	0.342	0.000	1.000	1.000	0	1.80
			5.0	—	—	—							0.000	1.000	1.000	0	
			7.5	2.40	—	1.32							0.010	1.021	1.021	0.03	
			10.0	2.00	—	1.10							0.034	1.069	1.092	0.10	
			12.5	1.59	—	0.87							0.075	1.156	1.212	0.22	
		0	15.0	1.16	—	0.64		1.82		20.61	2.25	0.342	0.154	1.331	1.210	0.45	1.80
		0	0	—	—	—		1.82		20.61	4.80	0.809	0.000	1.000	1.000	0	3.27
			5.0	—	—	—							0.000	1.000	1.000	0	
			7.5	2.56	—	1.51							0.000	1.000	1.061	0.00	
			10.0	2.17	—	1.28							0.032	1.066	1.199	0.04	
			12.5	1.79	—	1.05							0.092	1.203	1.392	0.12	
		0	15.0	1.38	—	0.81		1.82		20.61	4.80	0.809	0.218	1.485	1.525	0.27	3.27

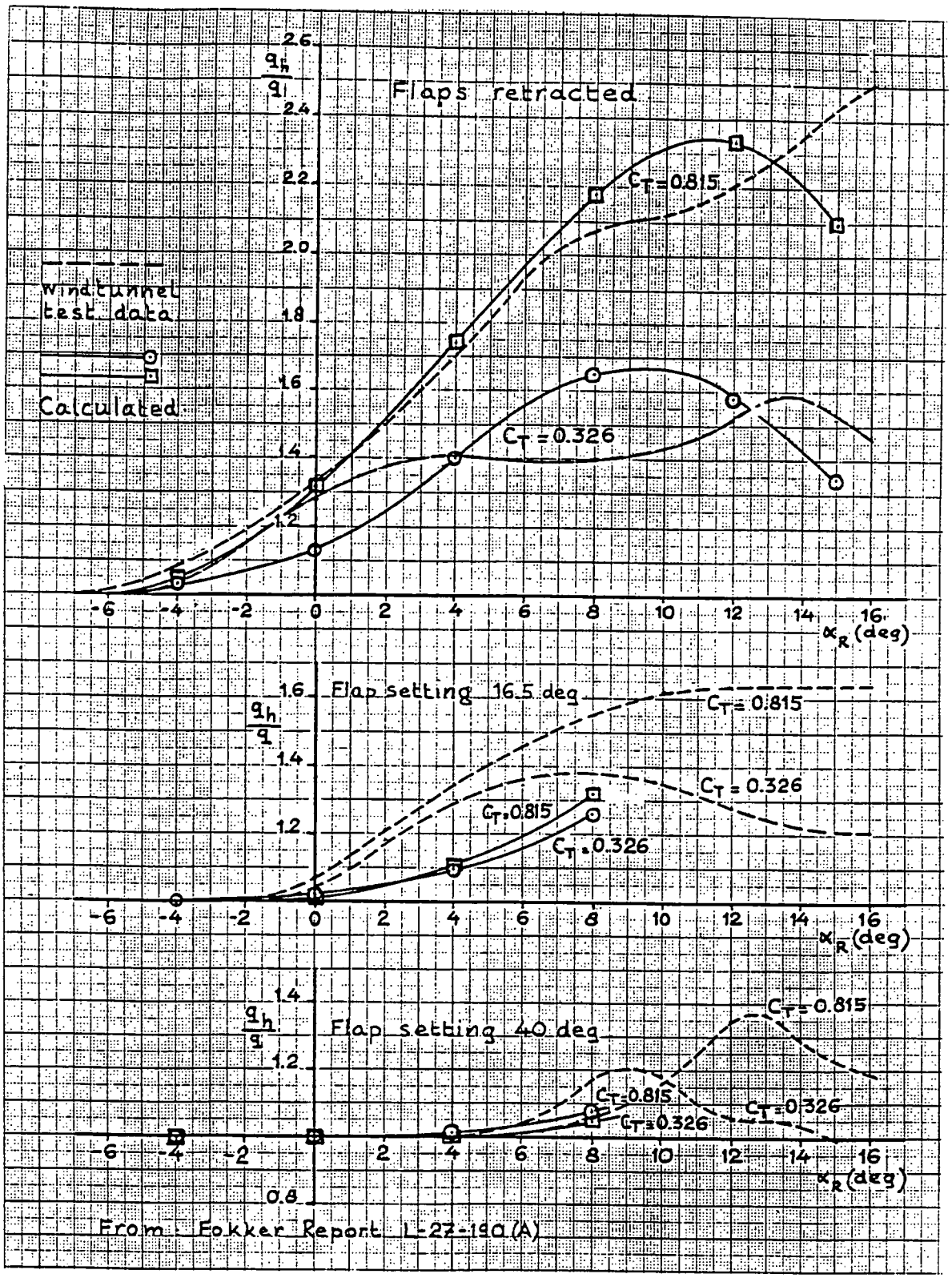
Flaps retracted
$\frac{q_h}{q}$
2.6
2.4
2.2
2.0
1.8
1.6
1.4
1.2
C_T=0.815
C_T=0.326
Windtunnel test data
Calculated
-6 -4 -2 0 2 4 6 8 10 12 14 16
α_R (deg)
Flap setting 16.5 deg
C_T=0.815
C_T=0.326
C_T=0.815
C_T=0.326
Flap setting 40 deg
C_T=0.815
C_T=0.326
C_T=0.815
C_T=0.326
0.8
From : Fokker Report L-27-190 (A)

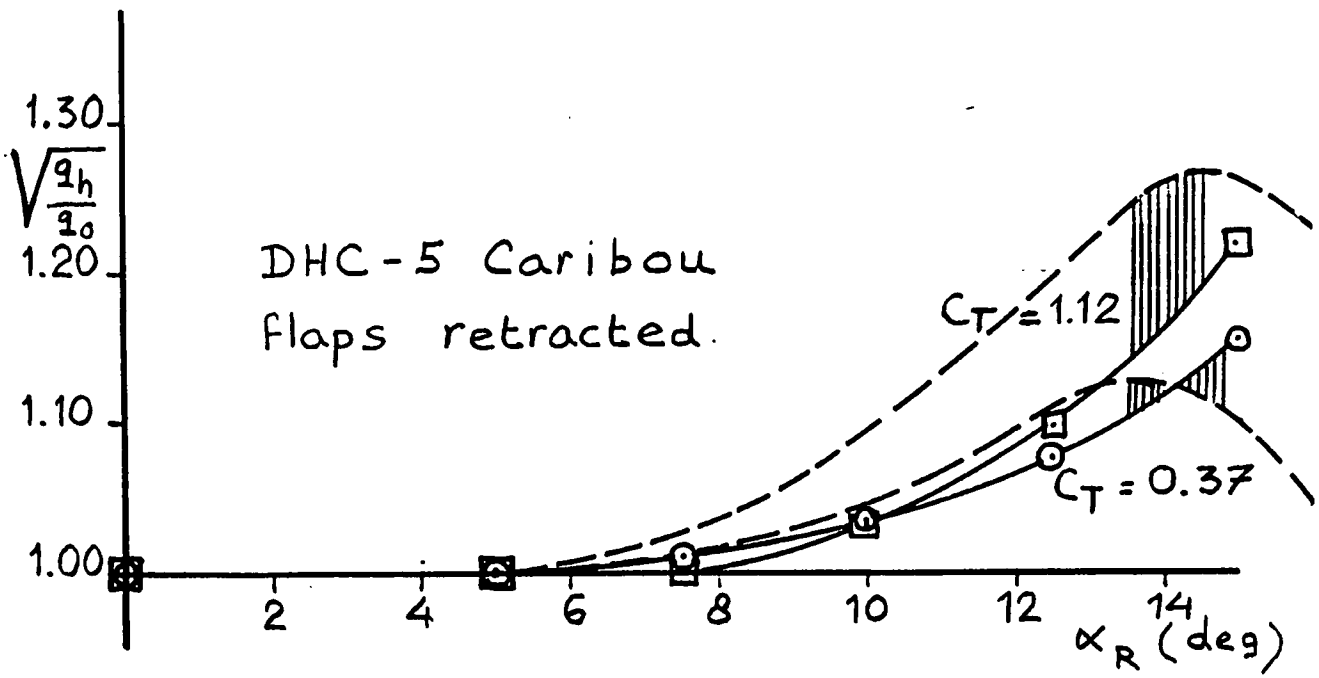
1.30
$\sqrt{\frac{q_h}{q_0}}$
1.20
1.10
1.00
DHC-5 Caribou
Flaps retracted
$C_T = 1.12$
$C_T = 0.37$
2
4
6
8
10
12
14
α_R (deg)

Appendix XIV

Downwash characteristics (IV)

Downwash of three aircraft configurations with and without propeller slipstream

For most of the aircraft configurations analysed in the present report downwash data were directly available.
For three configurations the downwash had to be determined separately.
This is presented in this appendix.

1. Model configuration analysed in report NASA TN D-3438.

At constant α_R :

$$(\Delta C_M)_H = C_{M_{Tail\text{-}on}} - C_{M_{Tail\text{-}off}}$$

$$\alpha_H = \frac{(\Delta C_M)_H}{C_{L_{\alpha_H}} \times \bar{V}_H \times \frac{q_H}{q}}$$

When $(\Delta C_M)_H = 0$. then $\alpha_H = 0$

$\varepsilon = \alpha_R - \alpha_H + i_h$,

So, when $\Delta C_M = 0$, then

$$\boxed{\varepsilon = \alpha_R + i_h}$$

$A_H = 3.13$

Small tail : $\bar{V}_H = 0.85$

Large tail (high) : $\bar{V}_H = 1.15$

Large tail (low) : $\bar{V}_H = 1.04$

$C_{L_{\alpha_H}} = 0.054/\text{deg}$.

$i_h = 0$

$\delta_f = 45$ deg

$(\alpha_H)_{C_{L_H}=0} = +3.0$ deg.

Handed propellers

For the three tail configurations tested i_h for $(\Delta C_M)_H = 0$ has been determined for a number of angles-of-attack α_R and thrust coefficients C_T on pages XIV-3 to XIV-4, XIV-6 to XIV-7, XIV-9 to XIV-10. ε versus $C_{L_{T\text{-}O}}$ is presented on pages XIV-5, XIV-8 and XIV-11.

Note that the tail surfaces had inverted NACA 4415 camber lines. Thus, in an aerodynamic sense $i_h = -3$deg when nominally $i_h = 0$. Therefore, all downwash data in the figures has to be decreased by 3 deg.

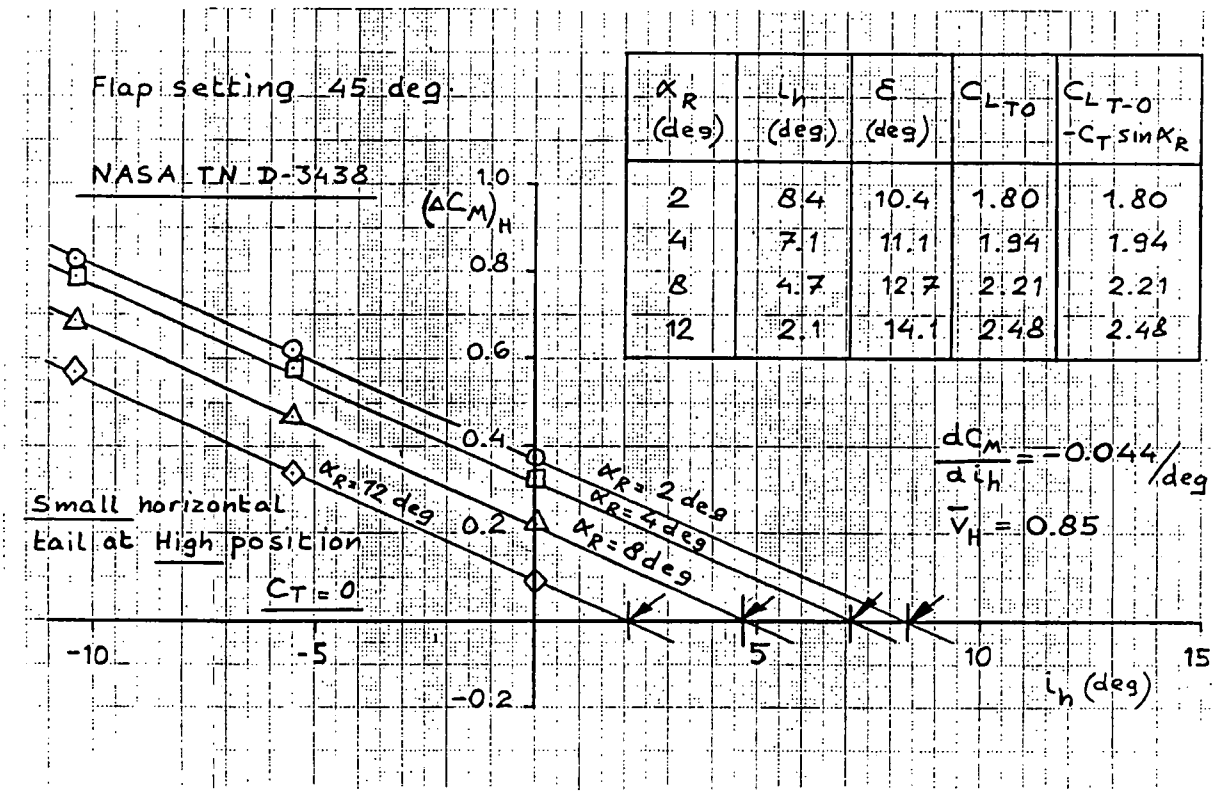

α_R (deg)	i_h (deg)	ε (deg)	$C_{L_{T-O}}$	$C_{L_{T-O}} - C_T \sin\alpha_R$
2	8.4	10.4	1.80	1.80
4	7.1	11.1	1.94	1.94
8	4.7	12.7	2.21	2.21
12	2.1	14.1	2.48	2.48

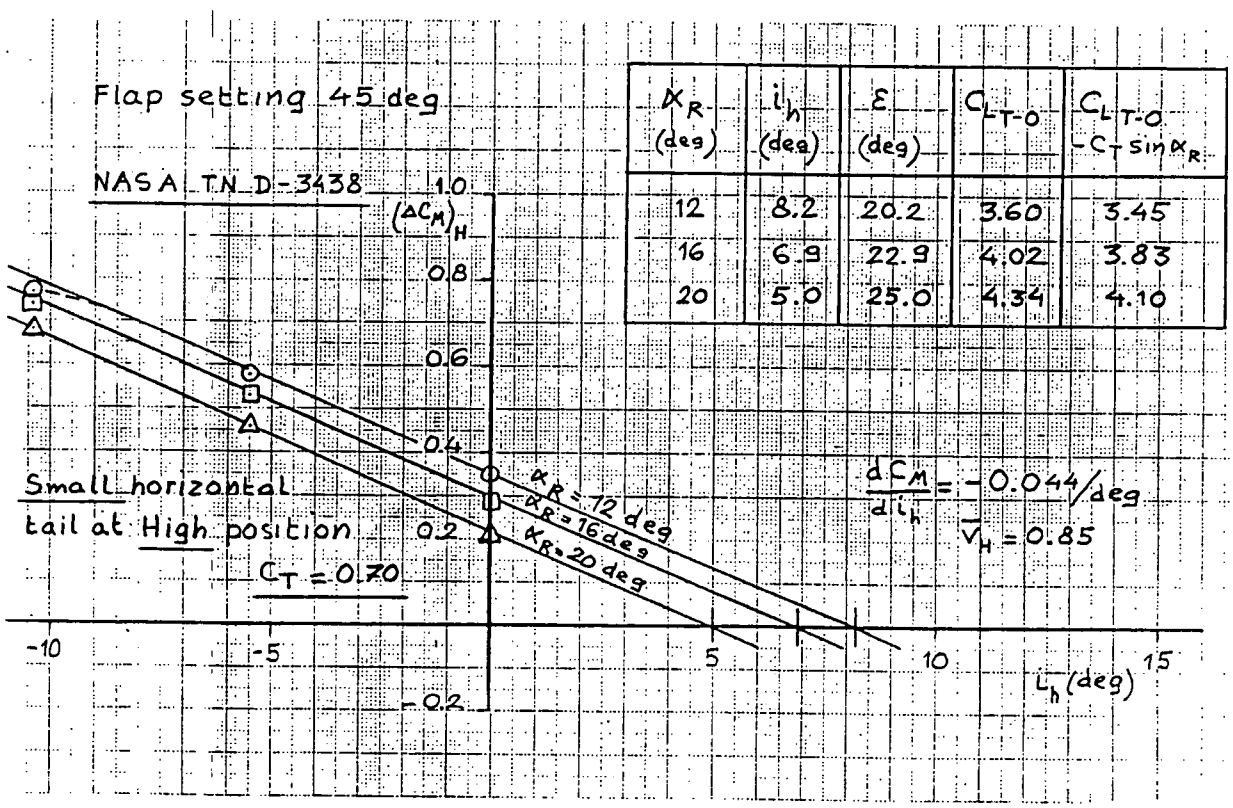

α_R (deg)	i_h (deg)	ε (deg)	$C_{L_{T-O}}$	$C_{L_{T-O}} - C_T \sin\alpha_R$
12	8.2	20.2	3.60	3.45
16	6.9	22.9	4.02	3.83
20	5.0	25.0	4.34	4.10

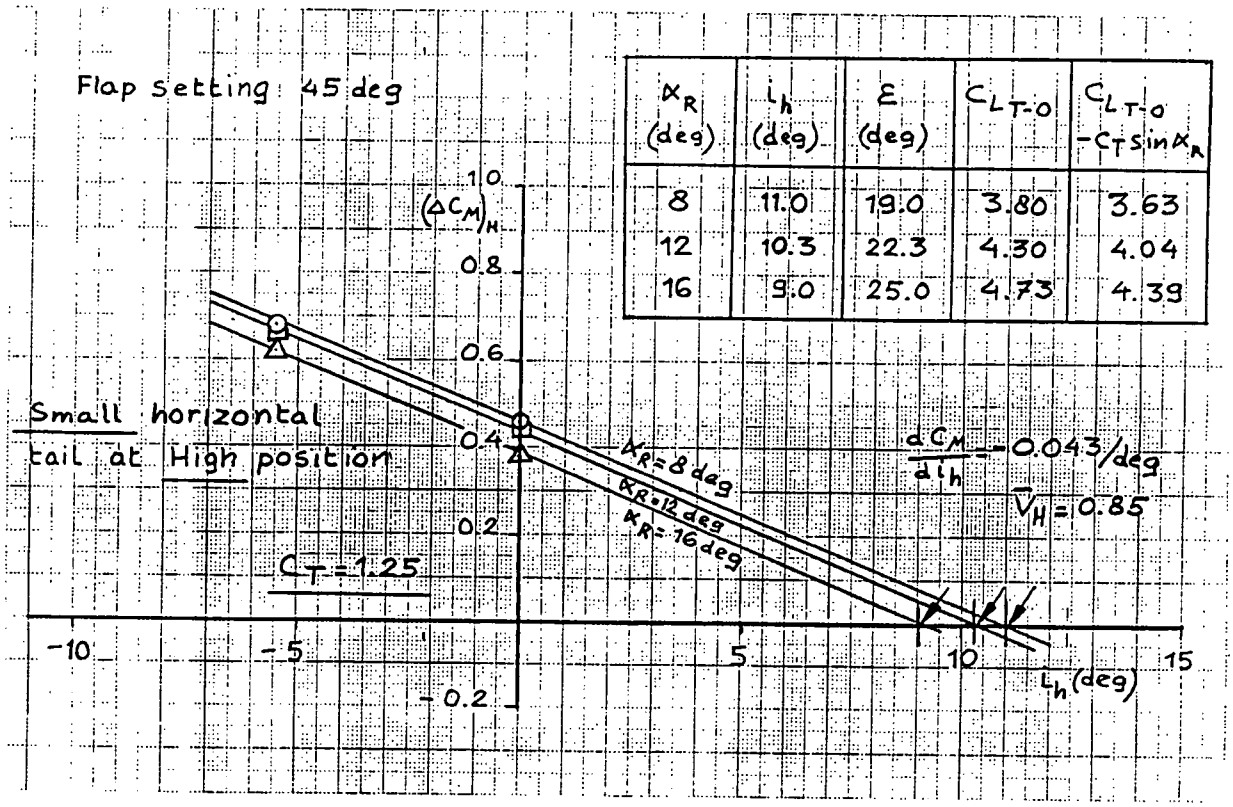

α_R (deg)	i_h (deg)	ε (deg)	$C_{L_{T-O}}$	$C_{L_{T-O}} - C_T \sin\alpha_R$
8	11.0	19.0	3.80	3.63
12	10.3	22.3	4.30	4.04
16	9.0	25.0	4.73	4.39

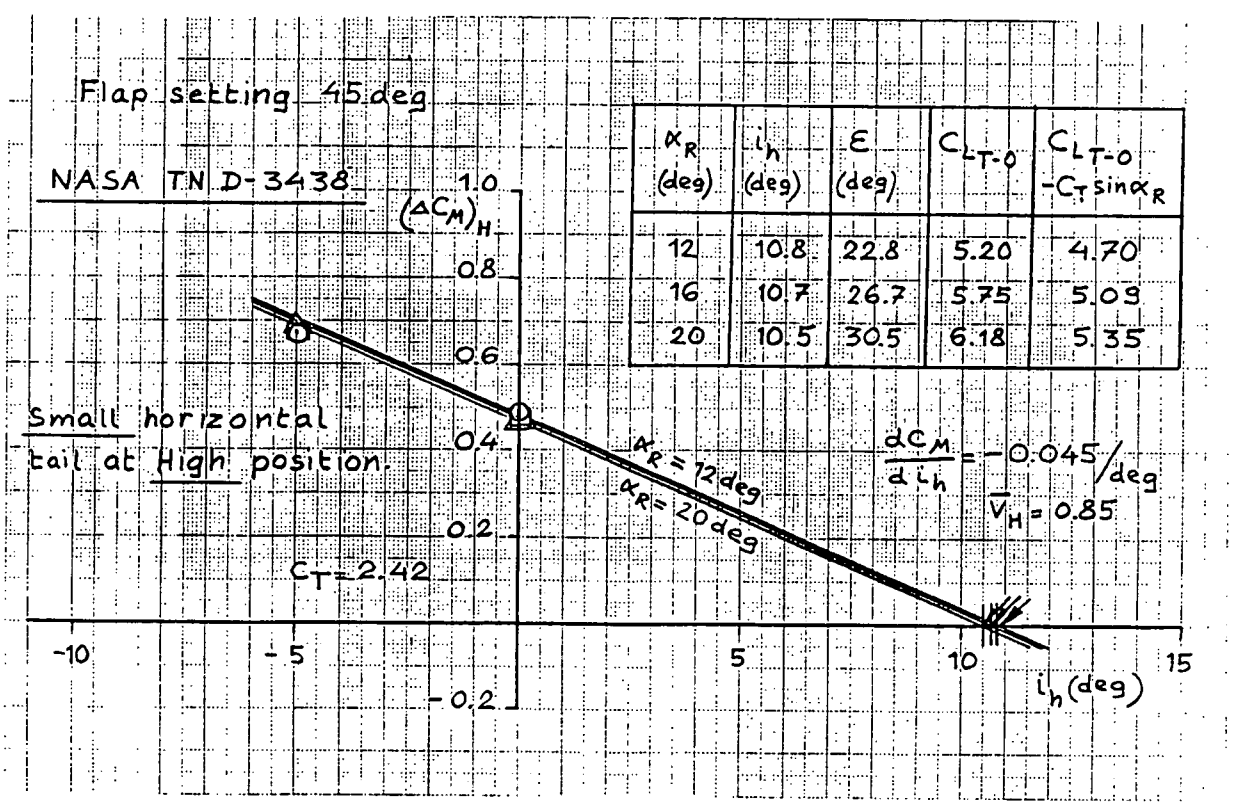

α_R (deg)	i_h (deg)	ε (deg)	$C_{L_{T-O}}$	$C_{L_{T-O}} - C_T \sin\alpha_R$
12	10.8	22.8	5.20	4.70
16	10.7	26.7	5.75	5.09
20	10.5	30.5	6.18	5.35

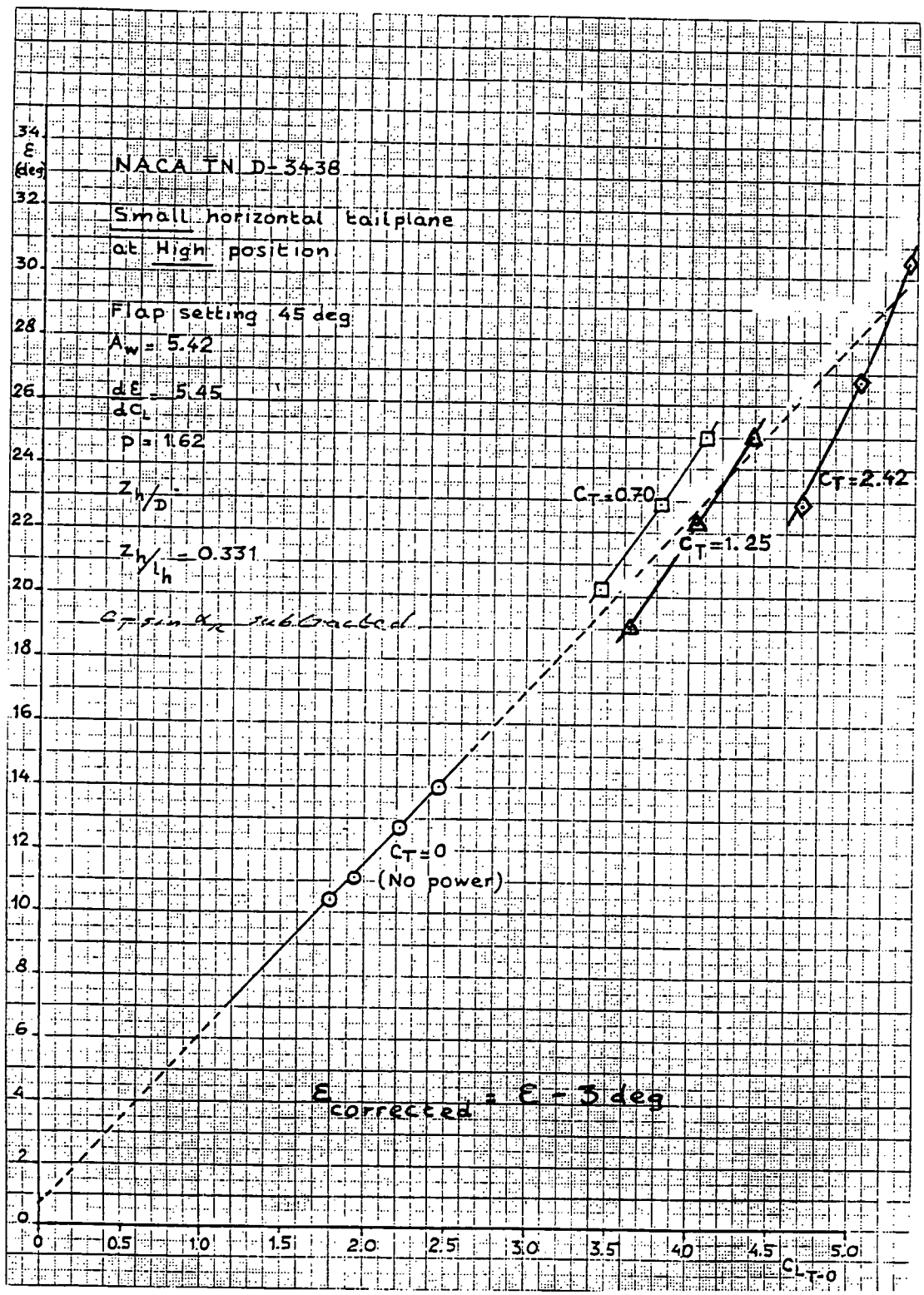
ε (deg)
NACA TN D-3438
Small horizontal tailplane
at High position
Flap setting 45 deg
A_w = 5.42
$\frac{d\varepsilon}{dC_L}$ = 5.45
P = 1.62
z_h/D -
z_h/l_h = 0.331
$\varepsilon_{corrected} = \varepsilon - 3$ deg
C_T = 0.70
C_T = 1.25
C_T = 2.42
C_T = 0
(No power)
$C_{L_{T=0}}$

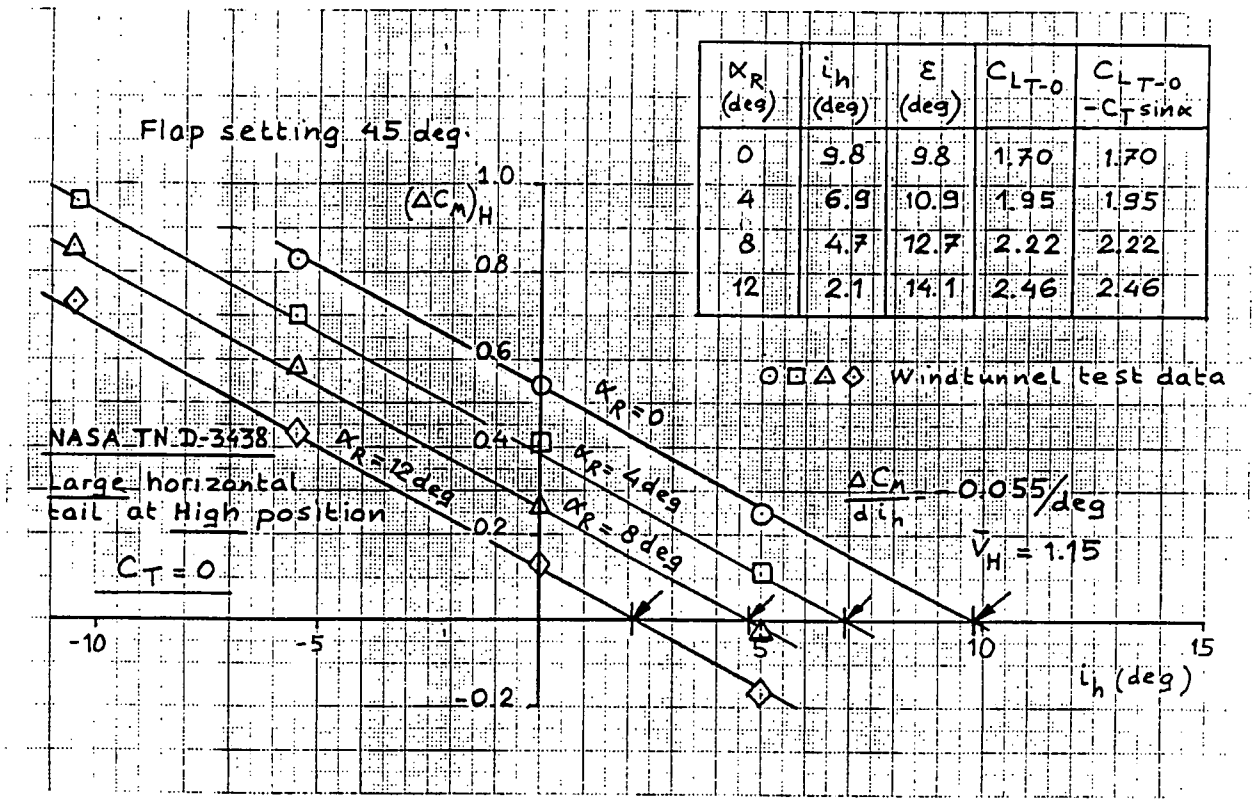

α_R (deg)	i_h (deg)	ε (deg)	$C_{L_{T-0}}$	$C_{L_{T-0}} - C_T \sin\alpha$
0	9.8	9.8	1.70	1.70
4	6.9	10.9	1.95	1.95
8	4.7	12.7	2.22	2.22
12	2.1	14.1	2.46	2.46

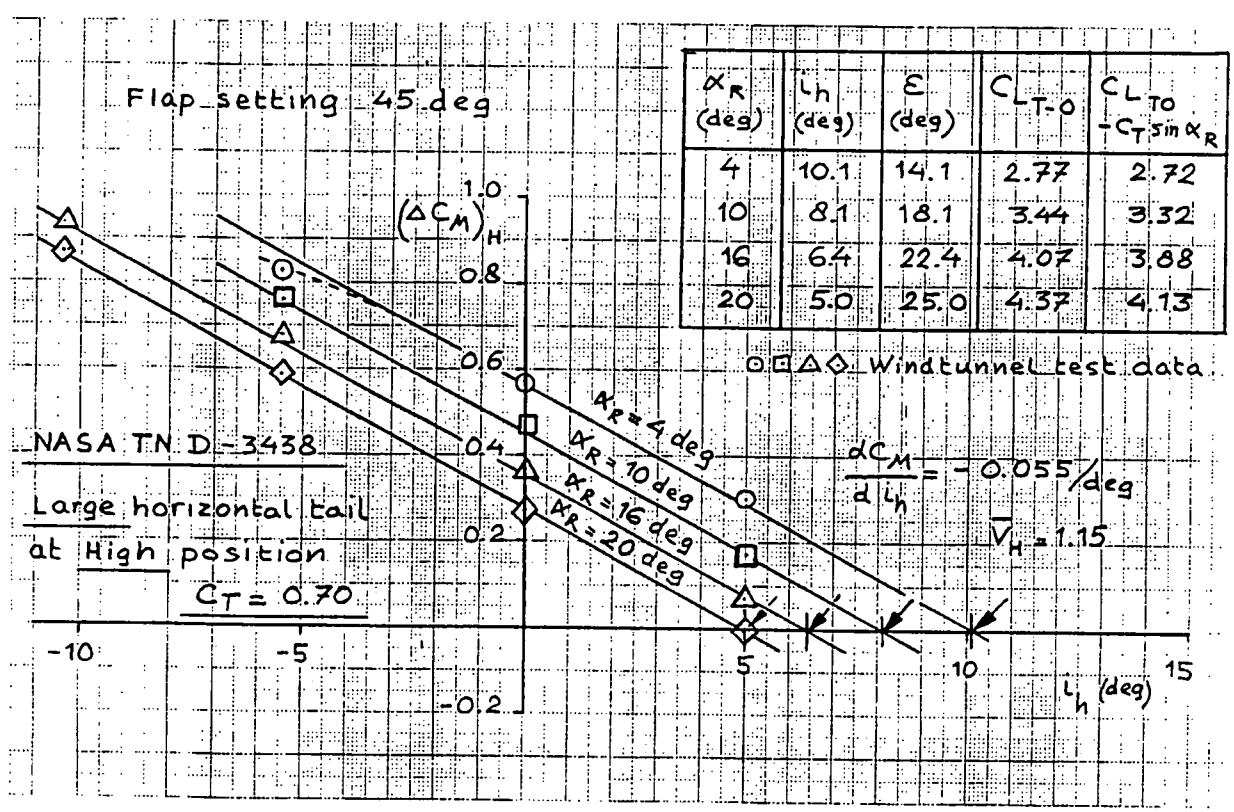

α_R (deg)	i_h (deg)	ε (deg)	$C_{L_{T-0}}$	$C_{L_{TO}} - C_T \sin\alpha_R$
4	10.1	14.1	2.77	2.72
10	8.1	18.1	3.44	3.32
16	6.4	22.4	4.07	3.88
20	5.0	25.0	4.37	4.13

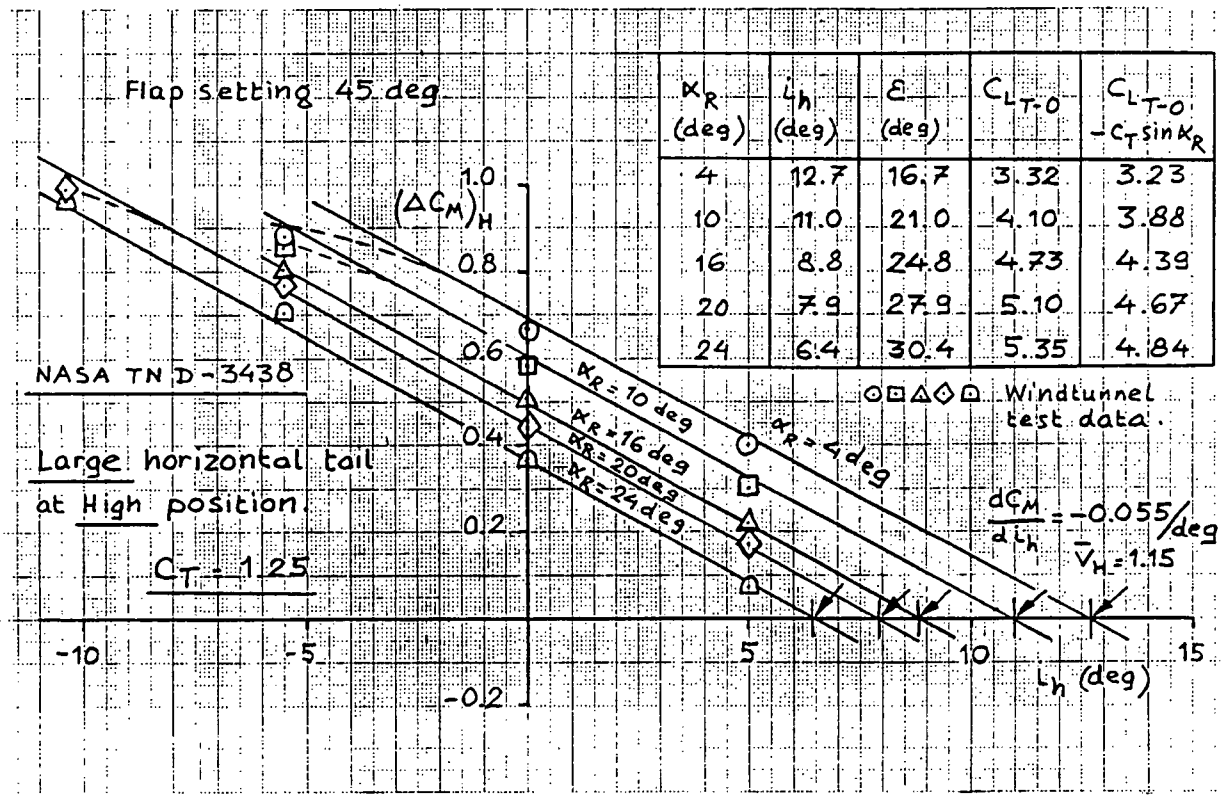

α_R (deg)	i_h (deg)	ε (deg)	$C_{L_{T-0}}$	$C_{L_{T-0}} - C_T \sin\alpha_R$
4	12.7	16.7	3.32	3.23
10	11.0	21.0	4.10	3.88
16	8.8	24.8	4.73	4.39
20	7.9	27.9	5.10	4.67
24	6.4	30.4	5.35	4.84

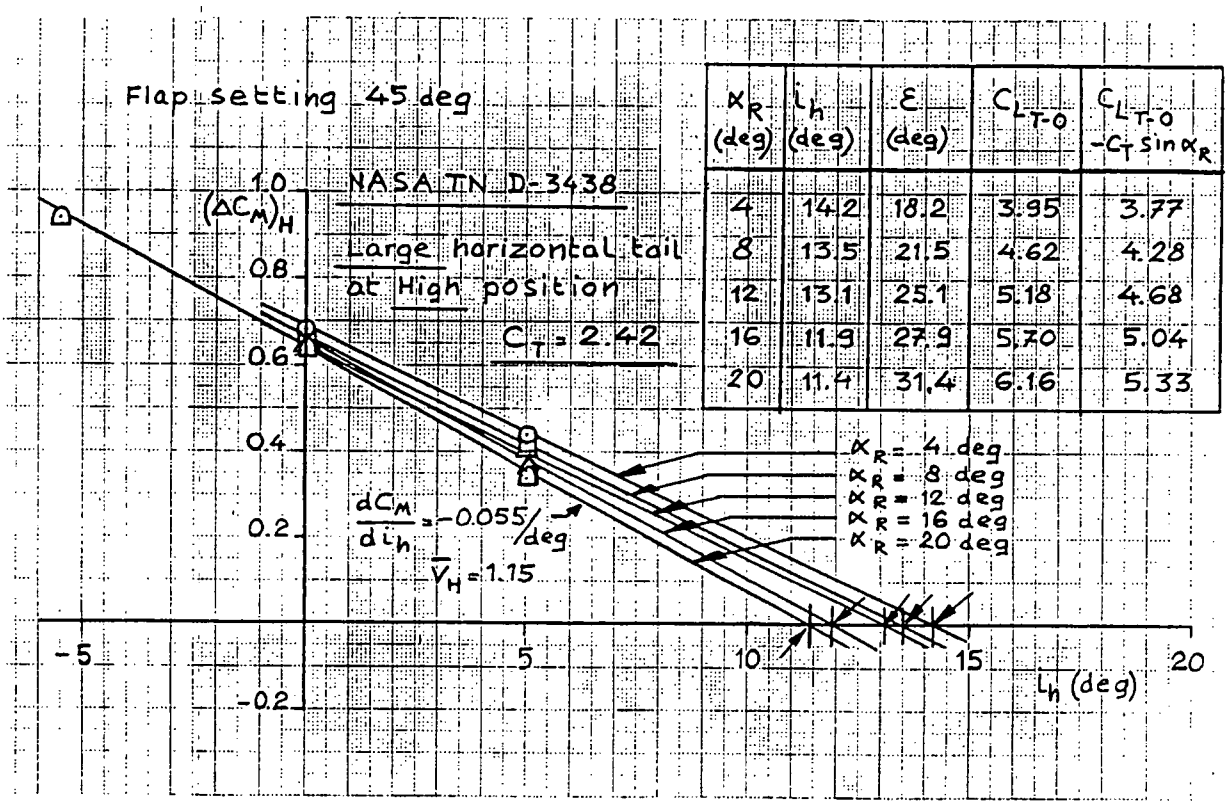

α_R (deg)	i_h (deg)	ε (deg)	$C_{L_{T-0}}$	$C_{L_{T-0}} - C_T \sin\alpha_R$
4	14.2	18.2	3.95	3.77
8	13.5	21.5	4.62	4.28
12	13.1	25.1	5.18	4.68
16	11.9	27.9	5.70	5.04
20	11.4	31.4	6.16	5.33

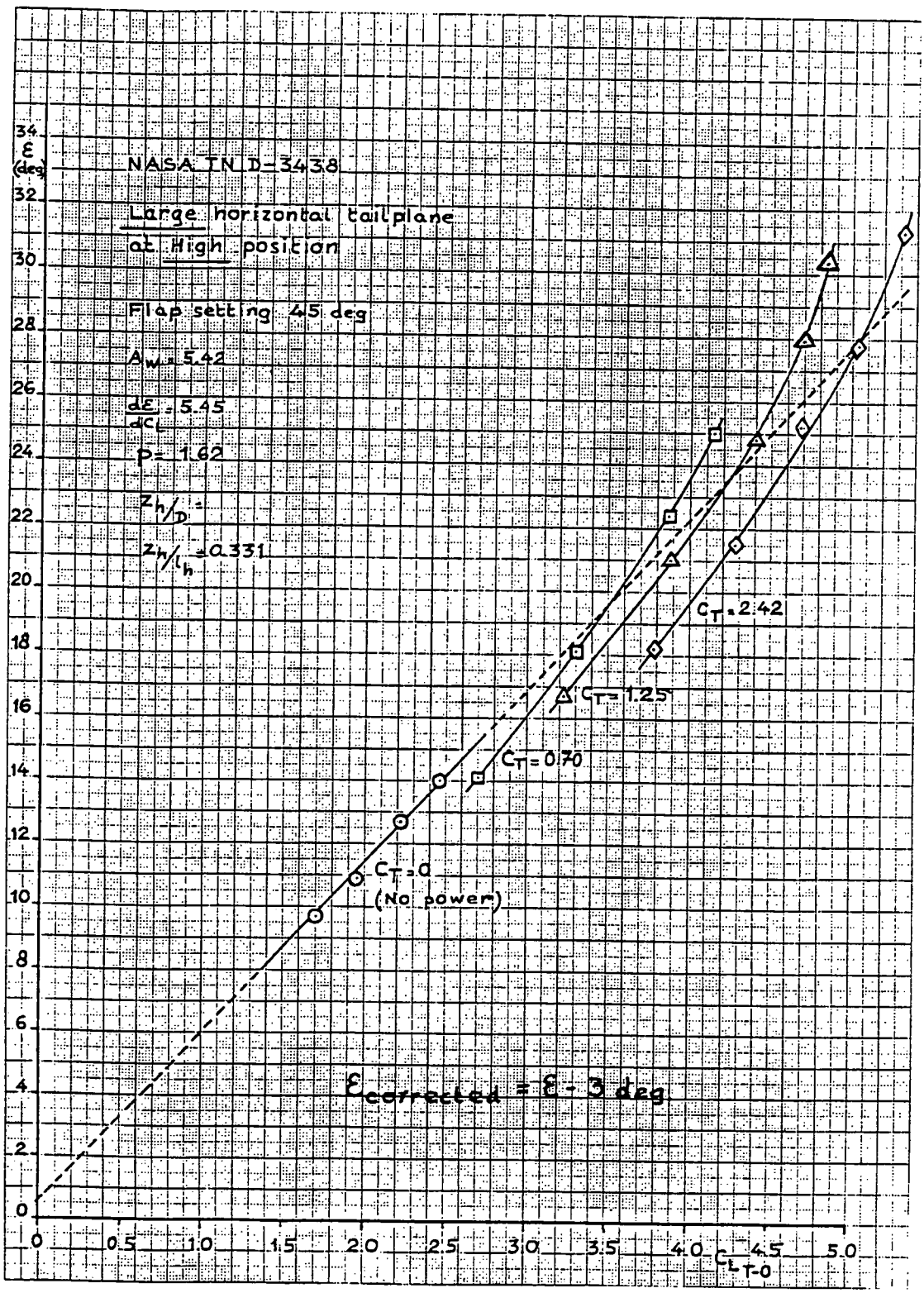
ε (deg)
NASA TN D-3438
Large horizontal tailplane at High position
Flap setting 45 deg
$A_w = 5.42$
$\frac{d\varepsilon}{dC_L} = 5.45$
P = 1.62
$z_h/D =$
$z_h/l_h = 0.331$
$C_T = 2.42$
$C_T = 1.25$
$C_T = 0.70$
$C_T = 0$
(No power)
$\varepsilon_{corrected} = \varepsilon - 3$ deg
$C_{L_{T=0}}$

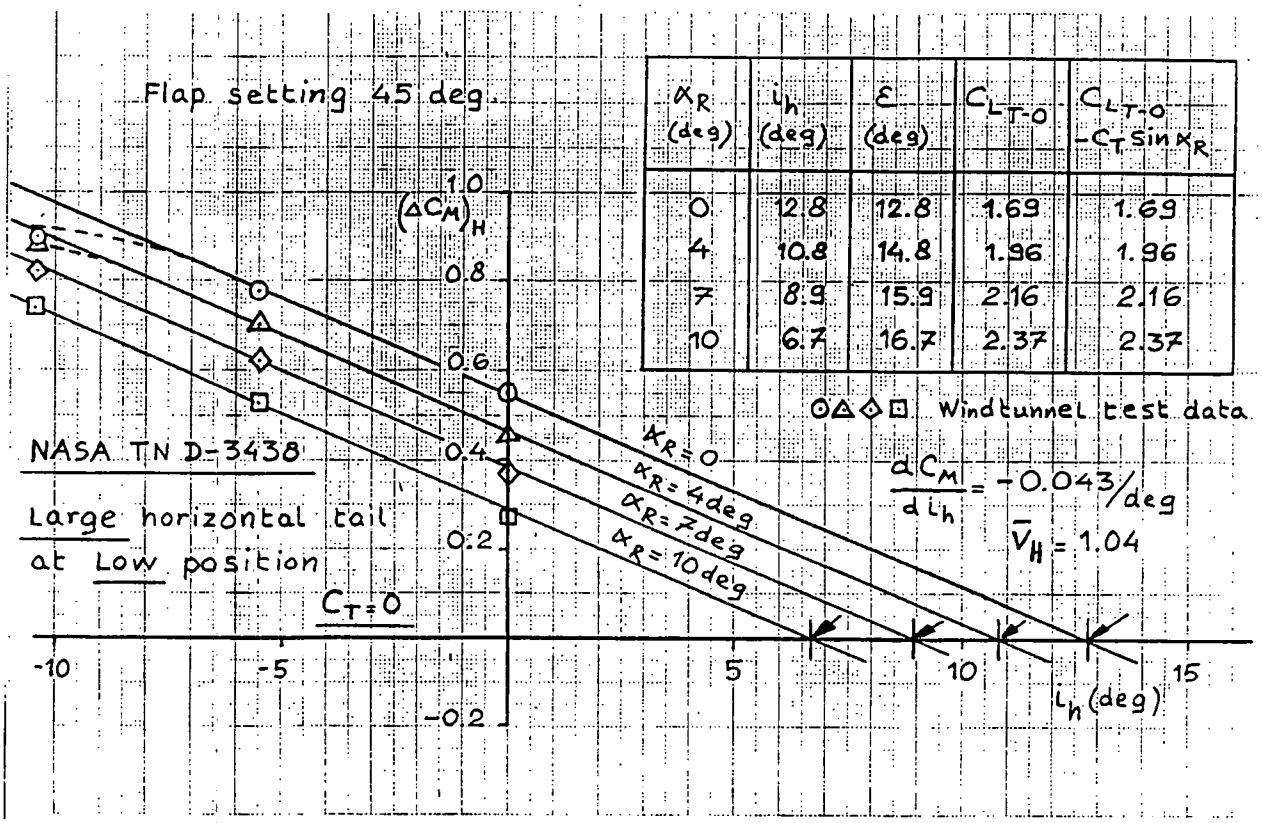

α_R (deg)	i_h (deg)	ε (deg)	$C_{L_{T-0}}$	$C_{L_{T-0}} - C_T \sin\alpha_R$
0	12.8	12.8	1.69	1.69
4	10.8	14.8	1.96	1.96
7	8.9	15.9	2.16	2.16
10	6.7	16.7	2.37	2.37

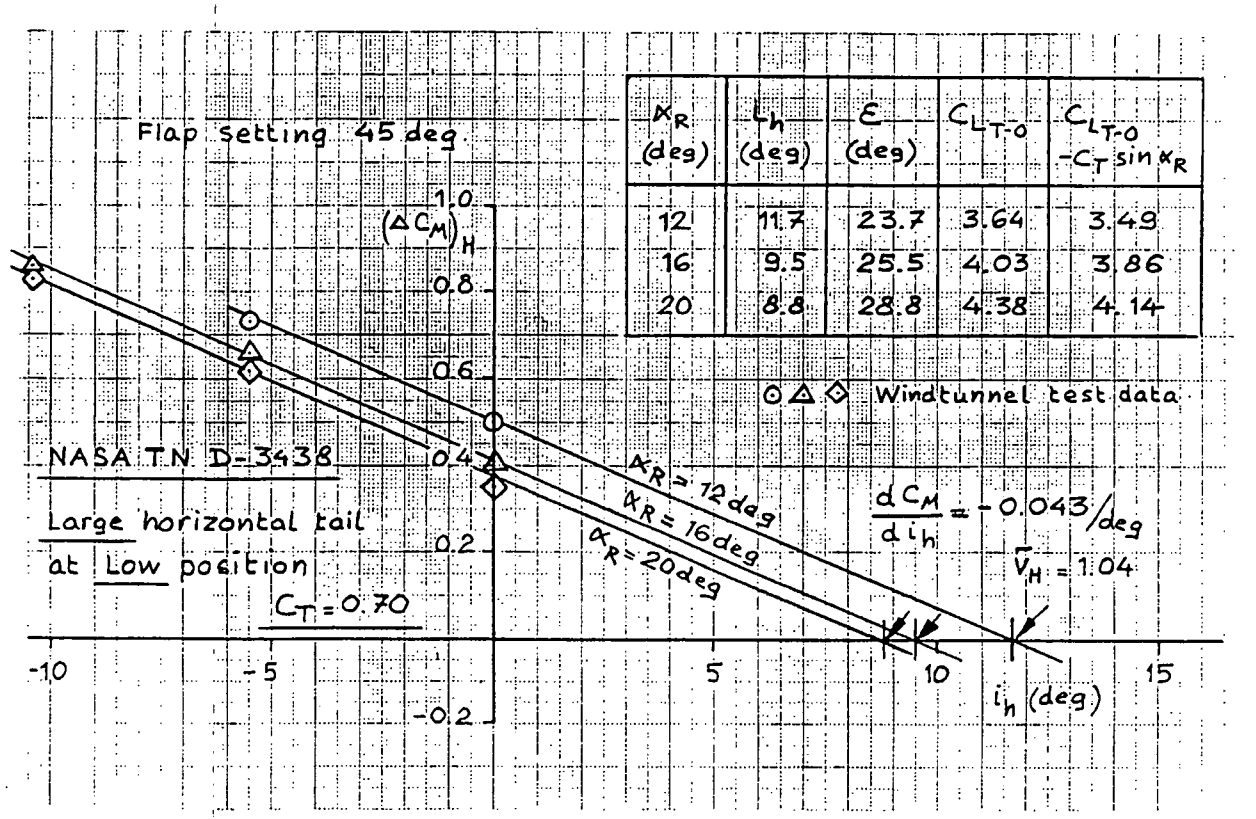

α_R (deg)	i_h (deg)	ε (deg)	$C_{L_{T-0}}$	$C_{L_{T-0}} - C_T \sin\alpha_R$
12	11.7	23.7	3.64	3.49
16	9.5	25.5	4.03	3.86
20	8.8	28.8	4.38	4.14

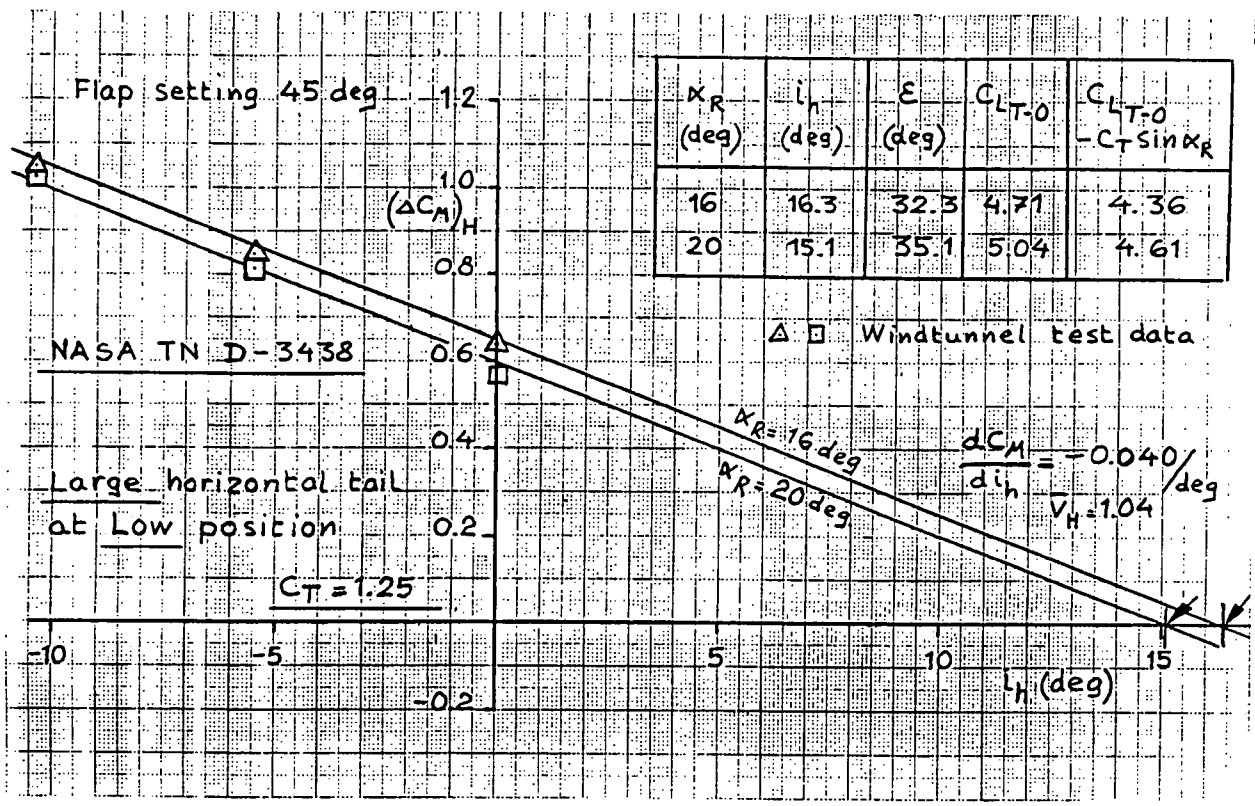

α_R (deg)	i_h (deg)	ε (deg)	$C_{L_{T-0}}$	$C_{L_{T-0}} - C_T \sin\alpha_R$
16	16.3	32.3	4.71	4.36
20	15.1	35.1	5.04	4.61

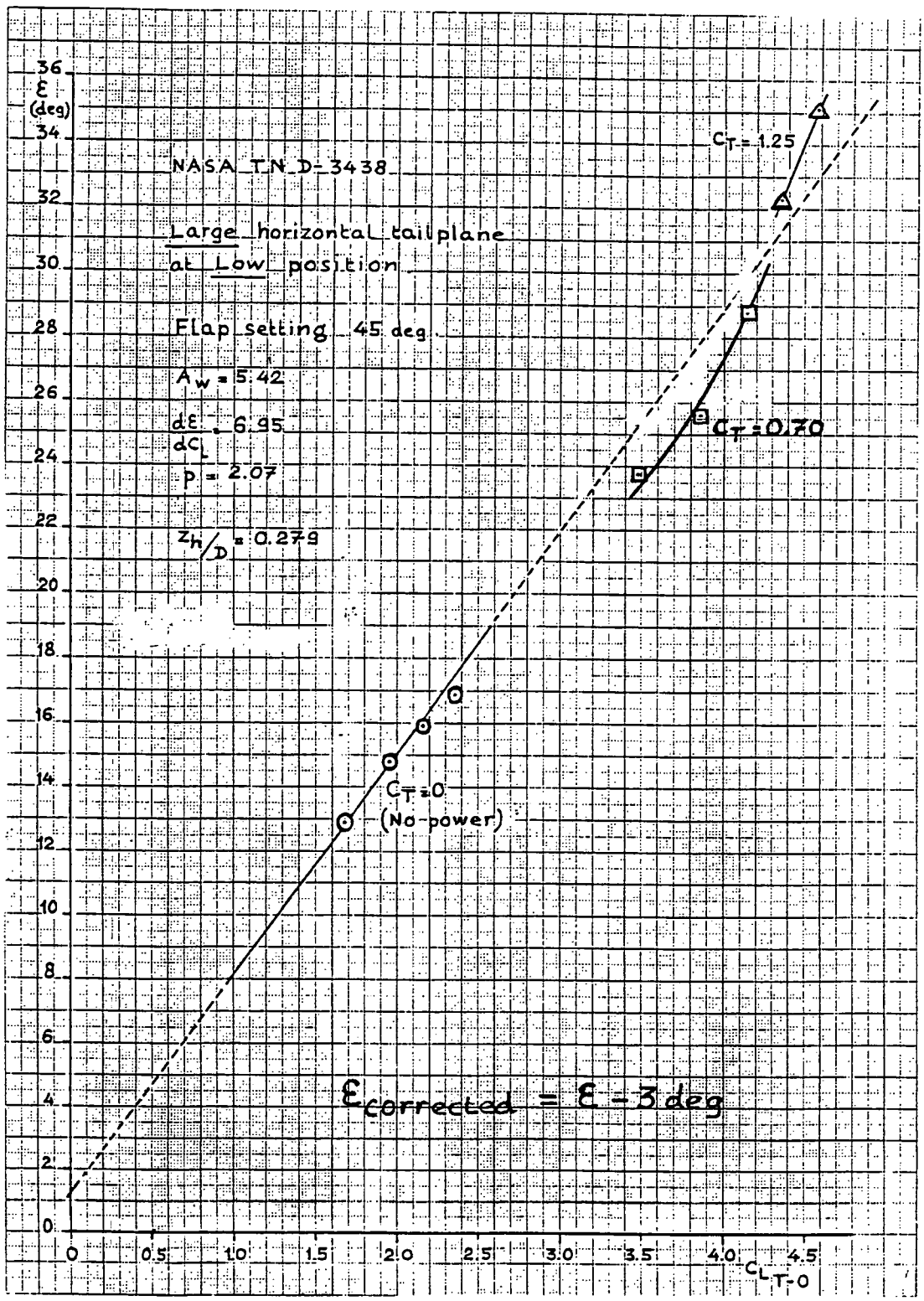
ε (deg)
NASA TN D-3438
Large horizontal tailplane at Low position
Flap setting 45 deg
$A_w = 5.42$
$\frac{d\varepsilon}{dC_L} = 6.95$
$P = 2.07$
$z_h/D = 0.279$
$C_T = 1.25$
$C_T = 0.70$
$C_T = 0$
(No-power)
$\varepsilon_{corrected} = \varepsilon - 3$ deg
$C_{L_{T=0}}$

2. Transall C-160

At constant α_R:

$$(\Delta C_M)_H = C_{M_{Tail\text{-}on}} - C_{M_{Tail\text{-}off}}$$

$$\alpha_H = \frac{(\Delta C_M)_H}{C_{L_{\alpha_H}} \times \bar{V}_H \times \frac{q_H}{q}}$$

$$\varepsilon = \alpha_R - \alpha_H + i_h$$

$i_h = -1.2$ deg

$A_H = 4.8$

$C_{L_{\alpha_H}} = 0.059/\text{deg}$

$\bar{V}_H = 1.113$

$\delta_f = 0$

	$C_T = 0$			$C_T = 0.242$			
α_R (deg)	$(C_M)_{i_h=-1.2}$	$C_{M_{T-O}}$	$C_{L_{T-O}}$	$(C_M)_{i_h=-1.2°}$	$C_{M_{T-O}}$	$C_{L_{T-O}}$	α_R (deg)
0	0.105	-0.095	0	0.290	-0.095	0	0
2.0	0.040	-0.080	0.16	0.190	-0.060	0.28	2.8
4.8	-0.050	-0.060	0.40	0.080	-0.030	0.56	5.8
7.8	-0.140	-0.040	0.63	-0.050	0	0.83	8.6
9.7	-0.210	-0.020	0.78	-0.210	+0.030	1.08	11.6
11.6	-0.275	-0.015	0.91	-0.330	+0.045	1.32	14.5
13.6	-0.350	0	1.02	-0.420	+0.050	1.45	17.4
15.5	-0.440	+0.005	1.10				
17.5	-0.520	+0.015	1.16				

$C_T = 0$ $\quad q_h/q = 1.00$

α_R (deg)	$C_{L_{T-O}}$	ΔC_{M_H}	α_H (deg)	ε (deg)
0	0	0.200	-3.0	+1.8
2.0	0.160	0.120	-1.8	+2.6
4.8	0.400	0.010	-0.2	+3.8
7.8	0.630	-0.100	+1.5	+5.1
9.7	0.780	-0.190	+2.9	+5.6
11.6	0.910	-0.260	+4.0	+6.4
13.6	1.020	-0.350	+5.3	+7.1
15.5	1.100	-0.450	+6.8	(+7.5)
17.5	1.160	-0.540	+8.2	(+8.1)

C-160 $\delta_f = 0$

$C_T = 0.241$ $\Delta V/V_0 = 0.349$ $b_{max} = 0.213$

α_R (deg)	$C^*_{L_{T-0}} = C_{L_{T-0}} - C_T \sin\alpha_R$	ΔC_{M_H}	$\frac{h_{tot}}{D^*/2}$	b	$\frac{q_h}{q}$	α_h (deg)	ε (deg)	$\Delta\varepsilon$ (deg) CALC.	ε (deg) CALC.
0	0	0.385	0.40	0.179	1.390	-4.2	3.0	0.8	2.7
2.8	0.27	0.250	0.15	0.219	1.487	-2.6	4.2	0.3	3.5
5.8	0.54	0.110	-0.11	0.222	1.492	-1.1	5.7	-0.2	4.3
8.6	0.79	-0.050	-0.36	0.196	1.430	+0.5	6.9	-0.6	5.1
11.6	1.03	-0.240	-0.63	0.094	1.197	+3.1	7.3	-0.8	6.0
14.5	1.26	-0.375	-0.88	0.047	1.096	+5.2	8.1	-1.0	6.9
17.4	—	—	—	—	—	—	—	—	—

$\delta_f = 30$ deg

$C_T = 0$ $C_T = 0.536$

α_R (deg)	$(C_M)_{i_h=-1.2}$	$C_{M_{TO}}$	$C_{L_{T-0}}$	$(C_M)_{i_h=-1.2}$	$C_{M_{T-0}}$	$C_{L_{T-0}}$	α_R (deg)
-7.0	+0.35	-0.31	0.08	+0.270	-0.485	0.33	-6.0
-4.0	+0.25	-0.31	0.40	+0.265	-0.440	0.68	-3.2
-1.2	+0.15	-0.31	0.70	+0.250	-0.440	1.06	-0.3
+1.6	+0.06	-0.31	0.98	+0.250	-0.430	1.42	+2.5
+4.6	-0.05	-0.29	1.24	+0.215	-0.415	1.78	+5.2
+7.5	-0.15	-0.28	1.47	+0.190	-0.410	2.12	+8.4
+9.4	-0.23	-0.27	1.60	+0.140	-0.385	2.41	+11.2
+11.4	-0.31	-0.25	1.72	+0.120	-0.375	2.59	+14.5
+13.3	-0.38	-0.23	1.77	—	—	—	—

$C_T = 0$ $q_h/q = 1.00$

α_R (deg)	$C_{L_{T-0}}$	ΔC_{M_H}	α_H (deg)	ε (deg)
-7.0	0.08	0.66	-10.0	+1.8
-4.0	0.40	0.56	-8.5	+3.3
-1.2	0.70	0.46	-7.0	+4.6
+1.6	0.98	0.37	-5.6	+6.0
+4.6	1.24	0.24	-3.7	+7.1
+7.5	1.47	0.13	-2.0	+8.3
+9.4	1.60	0.04	-0.6	+8.8
+11.4	1.72	-0.06	+0.9	+9.3
+13.3	1.77	-0.15	+2.3	+9.8

C-160 $\delta_f = 30$ deg

$C_T = 0.536$ $\Delta V/V_o = 0.679$ $b_{max} = 0.414$

α_R (deg)	$C^*_{L_{T-0}} = C_{L_{T-0}} - C_T \sin\alpha_R$	ΔC_{M_H}	$\frac{h_{tot}}{D^*/2}$	b	$\frac{q_h}{q}$	α_h (deg)	ε (deg)	$\Delta\varepsilon$ (deg CALC.	ε (deg) CALC.
-6.0	0.39	0.755	1.60	0	1.000	-11.5	4.3	1.3	4.5
-3.2	0.71	0.705	1.41	0.004	1.008	-10.6	6.2	1.7	6.4
-0.3	1.06	0.690	1.23	0.021	1.042	-10.1	8.6	2.0	8.3
+2.5	1.40	0.680	1.06	0.046	1.094	-9.5	10.8	2.3	10.2
+5.2	1.73	0.630	0.89	0.087	1.182	-8.1	12.1	2.4	11.8
+8.4	2.04	0.600	0.69	0.166	1.360	-6.7	13.9	2.2	13.1
+11.2	2.31	0.525	0.51	0.211	1.467	-5.4	15.4	1.9	14.0
+14.5	2.46	0.495	0.32	0.385	1.918	-3.9	17.2	1.3	14.1

$\delta_f = 60$ deg

$C_T = 0$ $C_T = 0.826$

α_R (deg)	$(C_M)_{i_h=-1.2\text{deg}}$	$C_{M_{T-0}}$	$C_{L_{T-0}}$	$(C_M)_{i_h=-1.2\text{deg}}$	$C_{M_{T-0}}$	$C_{L_{T-0}}$	α_R (deg)
-7.4	+0.360	-0.51	1.04	0.070	-0.855	1.68	-6.5
-4.4	0.300	-0.50	1.30	0.110	-0.840	2.04	-3.5
-1.6	0.200	-0.50	1.57	0.150	-0.830	2.45	-0.8
+1.4	0.095	-0.50	1.80	0.140	-0.820	2.85	+2.0
+4.2	-0.025	-0.49	2.06	0.115	-0.865	3.31	+4.8
+7.3	-0.125	-0.46	2.28	0.110	-0.890	3.42	+6.6
+9.2	-0.200	-0.44	2.38	0.115	-0.900	3.64	+8.7

$C_T = 0.$ $q_h/q = 1.00$

α_R (deg)	$C_{L_{T-0}}$	ΔC_{M_H}	α_H (deg)	ε (deg)
-7.4	1.04	0.880	-13.4	+4.8
-4.4	1.30	0.800	-12.2	6.6
-1.6	1.57	0.700	-10.7	7.9
+1.4	1.80	0.595	-9.0	9.2
+4.2	2.06	0.465	-7.1	10.1
+7.3	2.28	0.335	-5.1	11.2
+9.2	2.38	0.240	-3.7	11.7

C-160 $\delta_f = 60$ deg.

$\Delta V/V_0 = 0.948$

$C_T = 0.826$

α_R (deg)	$C^*_{L_{T-0}} = C_{L_{T-0}} - C_T \sin\alpha_R$	ΔC_{M_H}	$\frac{h_{tot}}{D^*/2}$	b	$\frac{q_h}{q}$	α_H (deg)	ε (deg)	$\Delta\varepsilon$ (deg) CALC.	ε (deg) CALC.
-6.5	1.77	0.925	2.43	0	1.00	-14.1	6.4	0	8.8
-3.5	2.09	0.950	2.29	0	1.00	-14.5	9.8	0.2	10.5
-0.8	2.46	0.980	2.17	0	1.00	-14.9	12.9	0.3	12.3
2.0	2.82	0.960	2.05	0	1.00	-14.6	15.4	0.6	14.3
4.8	3.26	0.980	1.93	0	1.00	-14.9	18.5	0.8	16.6
6.6	3.33	1.000	1.84	0	1.00	-15.2	20.6	1.1	17.2
8.7	3.52	1.050	1.74	0	1.00	–	–	1.3	18.3

This data is also presented in figures on page XV- and XV

Table IX Downwash Characteristics (IV)

No	Conf.	h_h/c	i_w (deg)	z_h/D	δ_f (deg)	α_R (deg)	$C_f \sin\delta_f$	$\Delta\alpha_{0,f}$ (deg)	C_T	$\Delta V/V_0$	$C_{L\,P.0\,TEST}$	$\Delta C_{L_S\,TEST}$	C_L^*	D_{prop}	D^*	C_S	C_f	
		(78)	(79)	(80)	(81)	(82)	(83)	(89) = (15)	(85)	(86)	(87) = (38)	(88) = (59)	(89) = (87)×(88)	(90) = (9)	(91) = (42)	(92) = (4)	(93)	
13	C-160 Transall	3.99	2.0		0	0	0	0	0.242	0.349	0	0	0	0.289	0.270	0.254	0.084	$C_L = 0.059/\alpha_H$ deg
					0	6.0	0				0.48	0.10	0.58					
		3.99	2.0		0	13.0	0	0	0.242	0.349	0.98	0.21	1.19	0.289	0.270	0.254	0.084	$A_H = 4.80$
		3.99	2.0		30	-2.0	0.042	-16.8	0.537	0.679	0.61	0.18	0.79	0.289	0.258	0.254	0.084	$\bar{V}_H = 1.113$
					30	4.0	0.042				1.19	0.41	1.60					
		3.99	2.0		30	10.0	0.042	-16.8	0.537	0.679	1.64	0.65	2.29	0.289	0.258	0.254	0.084	
		3.99	2.0		60	-4.0	0.073	-33.6	0.826	0.948	1.33	0.46	1.79	0.289	0.251	0.254	0.0804	
					60	2.0	0.073				1.86	0.78	2.64					
		3.99	2.0		60	8.0	0.073	-33.6	0.826	0.948	2.32	1.28	3.60	0.289	0.251	0.254	0.0804	

No	Conf	l_h	h_t	$x_{cc}-x_{pr.}$	l_h^*	$(\Delta h_t)_\alpha$	$(\Delta h_t)_{upw.}$	$d\varepsilon/dC_L$	K_ε	$\left(\frac{dC_L}{d\alpha/1.0}\right)_{C_T=0}$ (1/deg)	ΔC_{L_S}	$\varepsilon_{\alpha=0}$	M	N	O	P	α_R (deg)	dim
		(94)	(95)	(96)	(97)	(98)	(99)	(100)	(101)	(102)	(88) = (59)	(104)	(105)	(106)	(107)	(108)	(82)	
13	C-160 Transall	0.827	0.020	0.277	0.688	0	0	4.70	1.5	0.080	0	1.9	0	0	2.85	0.034	0	m
						-0.029	0				0.10		3.38	0.21	2.85	0.084	6.0	m
		0.827	0.020	0.277	0.688	-0.062	0	4.70	1.5	0.080	0.21	1.9	7.33	1.48	2.85	0.142	13.0	m
		0.827	0.020	0.277	0.677	0.010	-0.020	4.70	1.5	0.098	0.18	5.2	-1.38	1.27	7.80	0.091	-2.0	m
						-0.019	-0.020				0.41		2.76	2.89	7.80	0.162	4.0	m
		0.827	0.020	0.277	0.677	-0.048	-0.020	4.70	1.5	0.098	0.65	5.2	6.91	4.58	7.80	0.237	10.0	m
		0.827	0.020	0.277	0.666	+0.019	-0.038	4.70	1.5	0.087	0.46	8.5	-2.45	3.24	12.75	0.160	-4.0	m
						-0.010	-0.038				0.78		1.23	5.50	12.75	0.236	2.0	m
		0.827	0.020	0.277	0.666	-0.039	-0.038	4.70	1.5	0.087	1.28	8.5	4.91	9.02	12.75	0.335	8.0	m

Table IX Downwash Characteristics (IV) (Concluded)

No	Conf	δ_f (deg) (81)	α_R (deg) (82)	h_{tot} CALC (109)	h_{tot} TEST (110)	$\frac{h_{tot}}{D^*/2}$ CALC (111)	b_{s_h} (112)	C_{s_h} (113)	S_{s_h} (114)	S_h (115)	$\frac{q_s}{q}$ CALC. (116)	b_{max} CALC. (117)	$b = \left(\frac{\Delta V}{V_0}\right)_{AV}$ CALC (122)	$\frac{q_h}{q}$ CALC. (123)	$\frac{q_h}{q}$ TEST (120)	$\frac{b}{b_{max}}$ CALC (124)	$\left(\frac{q_h}{q}\right)_{max}$ CALC (125)
13	C-160	0	0	0.054	—	0.40		0.129		0.121	1.820	0.213	0.177	1.383	—	0.83	1.471
	Transall	0	6.0	-0.017	—	-0.13							0.222	1.492	—	1.04	
		0	13.0	-0.102	—	-0.76		0.129		0.121	1.820	0.213	0.066	1.136	—	0.31	1.471
		30.0	-2.0	0.174	—	1.35		0.129		0.121	2.819	0.414	0.017	1.000	—	0.04	2.000
		30.0	4.0	0.124	—	0.96							0.070	1.042	—	0.17	
		30.0	10.0	0.076	—	0.59		0.129		0.121	2.819	0.414	0.215	1.173	—	0.52	2.000
		60.0	-4.0	0.295	—	2.32		0.129		0.121	3.795	0.580	0	1.000	—	0.00	2.496
		60.0	2.0	0.250	—	2.04							0	1.000	—	0.00	
		60.0	8.0	0.227	—	1.77		0.129		0.121	3.795	0.580	0	1.000	—	0.00	2.496

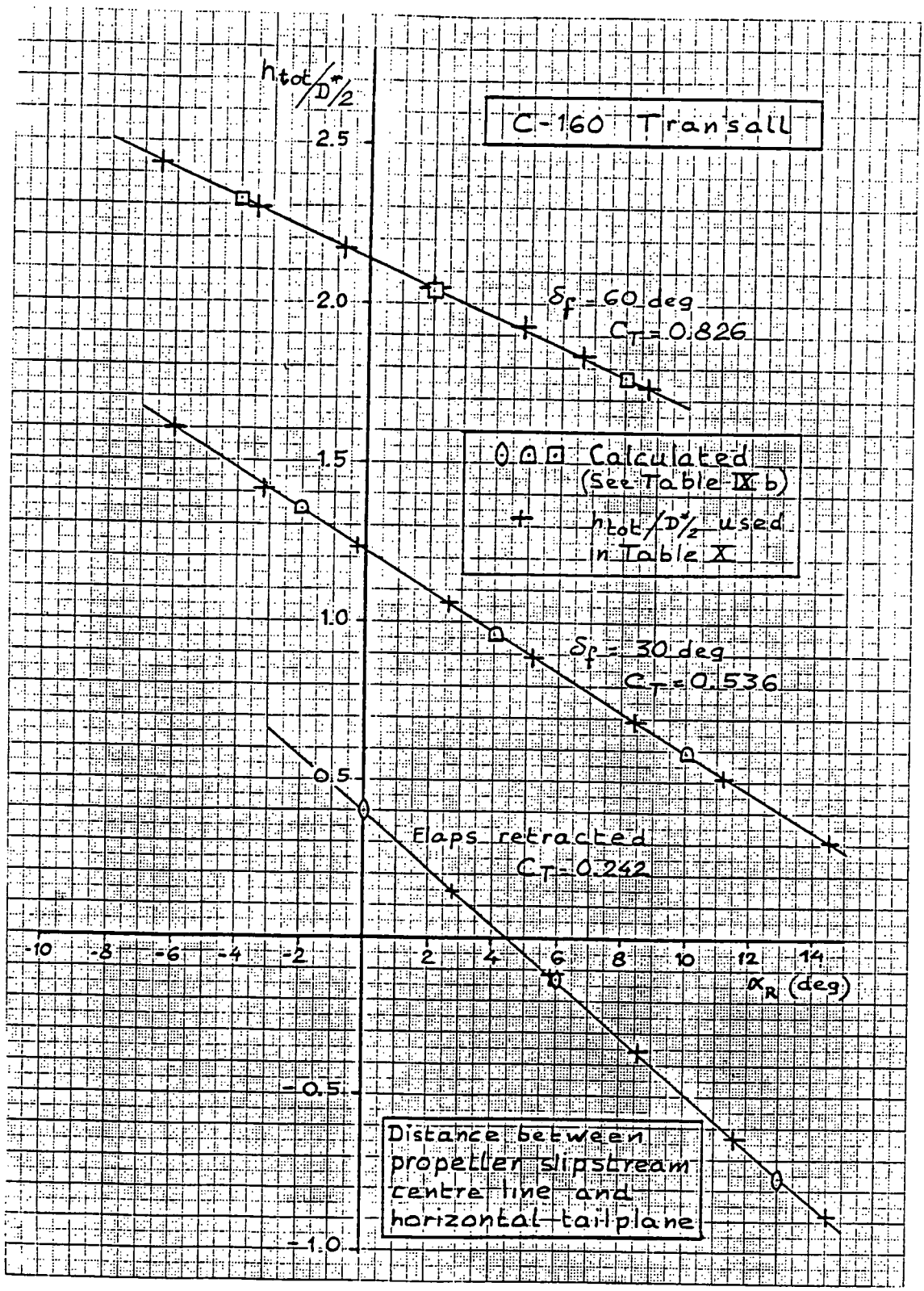
$h_{tot}/D^r/2$
C-160 Transall
2.5
2.0
1.5
1.0
0.5
δ_f = 60 deg
C_T = 0.826
Calculated
(See Table IX b)
$h_{tot}/D^r/2$ used
in Table X
δ_f = 30 deg
C_T = 0.536
Flaps retracted
C_T = 0.242
-10
-8
-6
-4
-2
2
4
6
8
10
12
14
α_R (deg)
-0.5
-1.0
Distance between
propeller slipstream
centre line and
horizontal tailplane

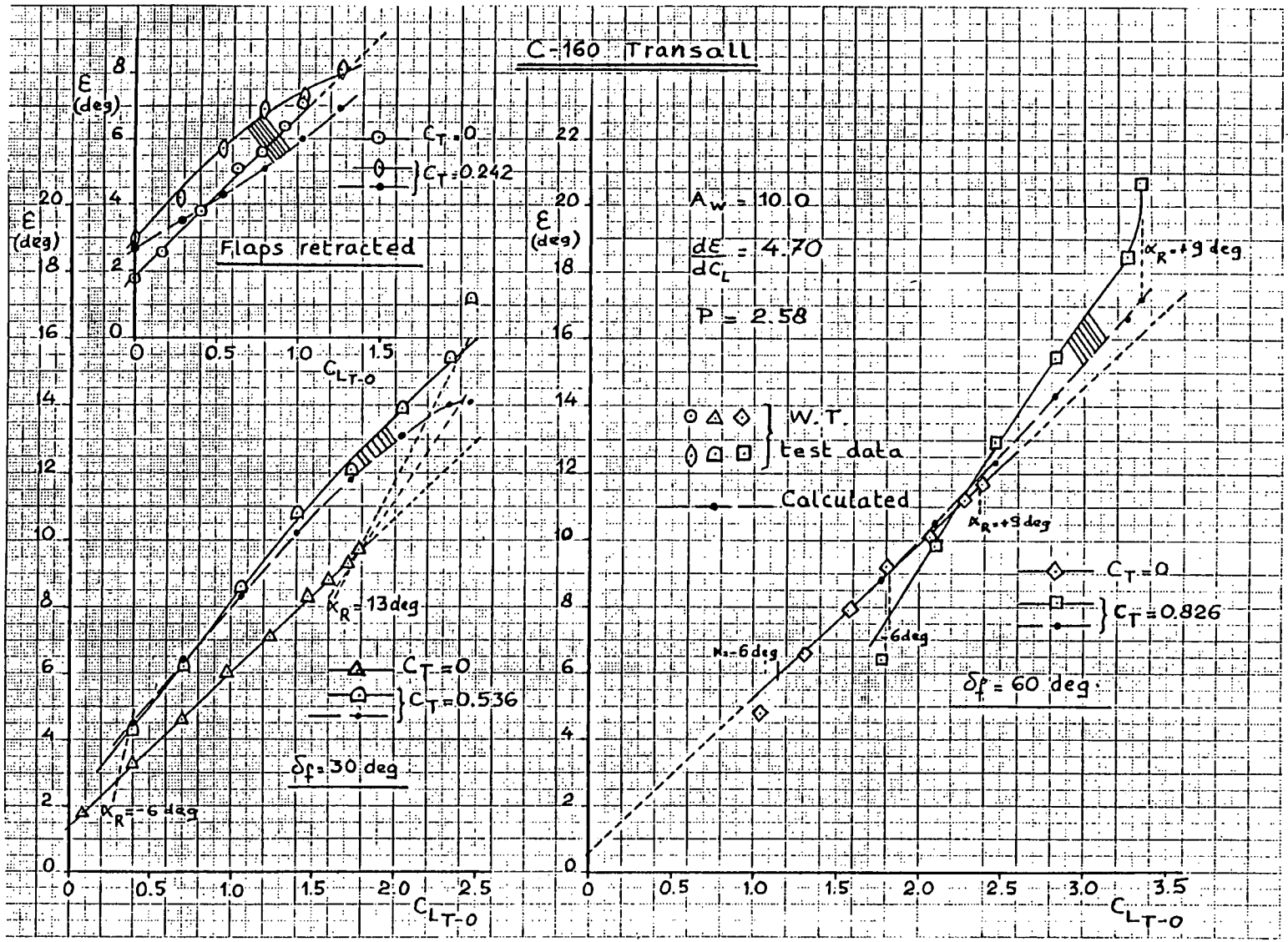
C-160 Transall
Flaps retracted
δ_f = 30 deg
δ_f = 60 deg
C_T = 0
C_T = 0.242
C_T = 0.536
C_T = 0.826
α_R = 13 deg
α_R = -6 deg
α_R = +9 deg
A_w = 10.0
$\frac{d\varepsilon}{dC_L}$ = 4.70
P = 2.58
W.T.
test data
Calculated
ε (deg)
C_{LT-O}

3. Breguet 1150 Atlantique

At constant α_R:

$$(\Delta C_M)_H = C_{M_{Tail\text{-}on}} - C_{M_{Tail\text{-}off}}$$

$$\alpha_H = \frac{(\Delta C_M)_H}{C_{L\alpha_H} \times \bar{V}_H \times \frac{q_H}{q}}$$

$A_H = 4.81$

$C_{L\alpha_H} = 0.0572/\text{deg}.$

$C_{L\delta_e} = 0.0340/\text{deg}.$

$\bar{V}_H = 1.012$

When $(\Delta C_M)_H = 0$, then $\alpha_H = 0$

$\varepsilon = \alpha_R - \alpha_H + i_h$,

So, when $\Delta C_M = 0$, then

$$\boxed{\varepsilon = \alpha_R + i_h}$$

$$C_{L\delta_e} / C_{L\alpha_H} = 0.586$$

$(\Delta C_M)_H$ as a function of i_h is presented on pages XIV-21 to XIV-23 for a number of α_R's and C_T's.

Downwash is presented on page XIV-24.

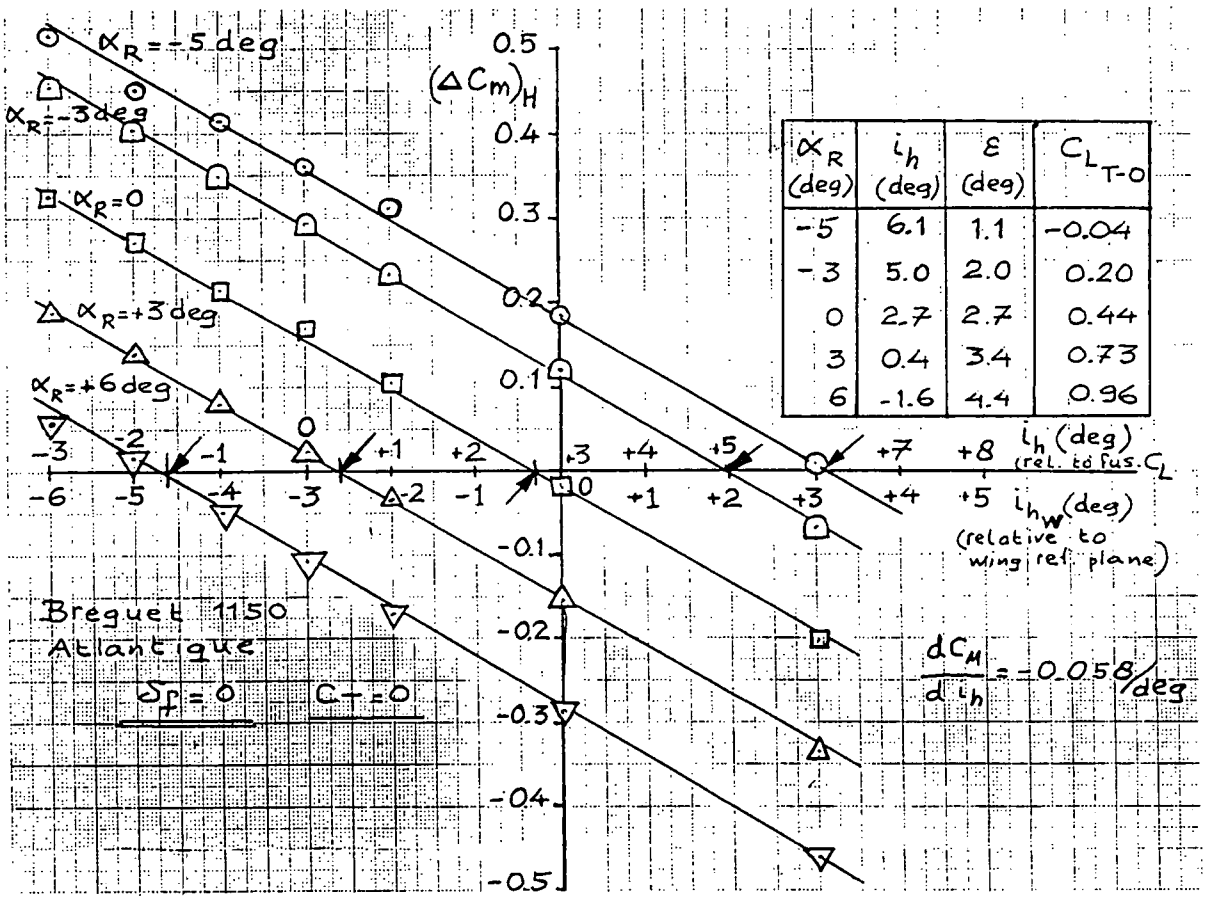

α_R (deg)	i_h (deg)	ε (deg)	$C_{L_{T-O}}$
-5	6.1	1.1	-0.04
-3	5.0	2.0	0.20
0	2.7	2.7	0.44
3	0.4	3.4	0.73
6	-1.6	4.4	0.96

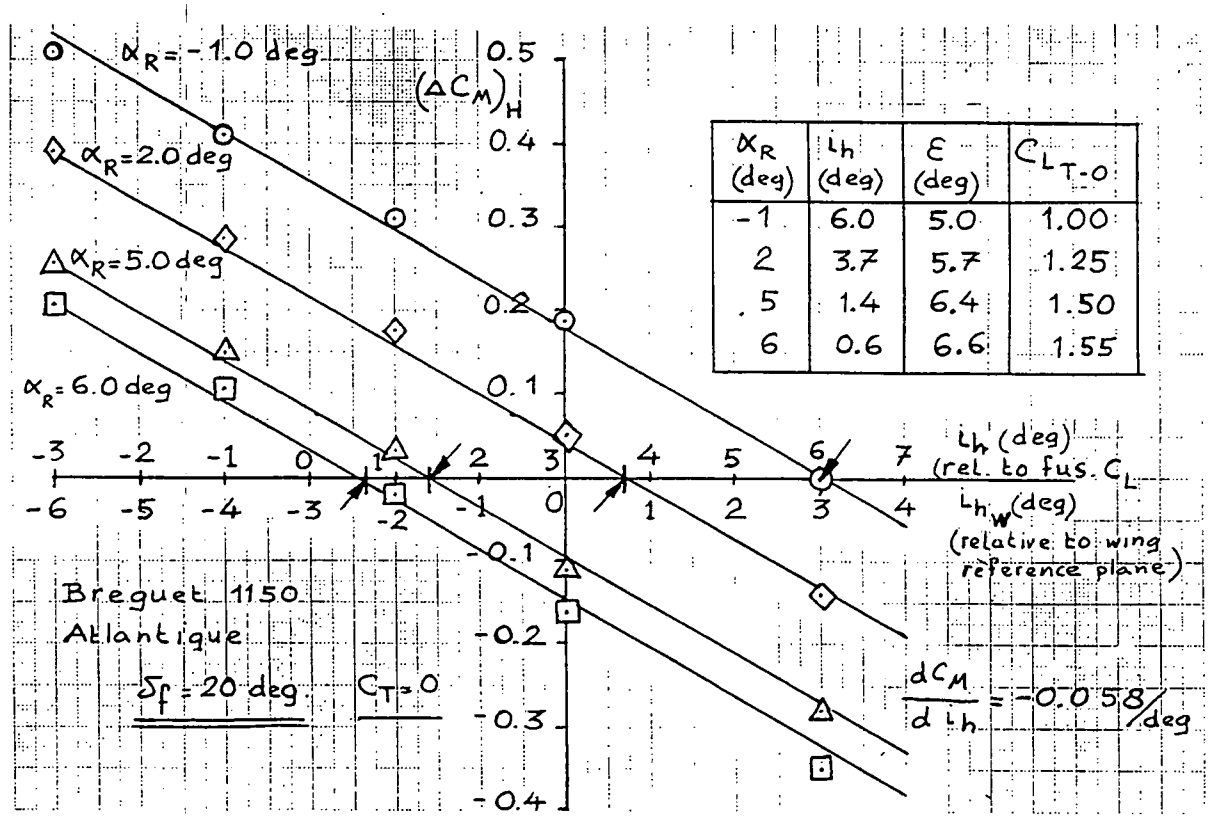

α_R (deg)	i_h (deg)	ε (deg)	$C_{L_{T-O}}$
-1	6.0	5.0	1.00
2	3.7	5.7	1.25
5	1.4	6.4	1.50
6	0.6	6.6	1.55

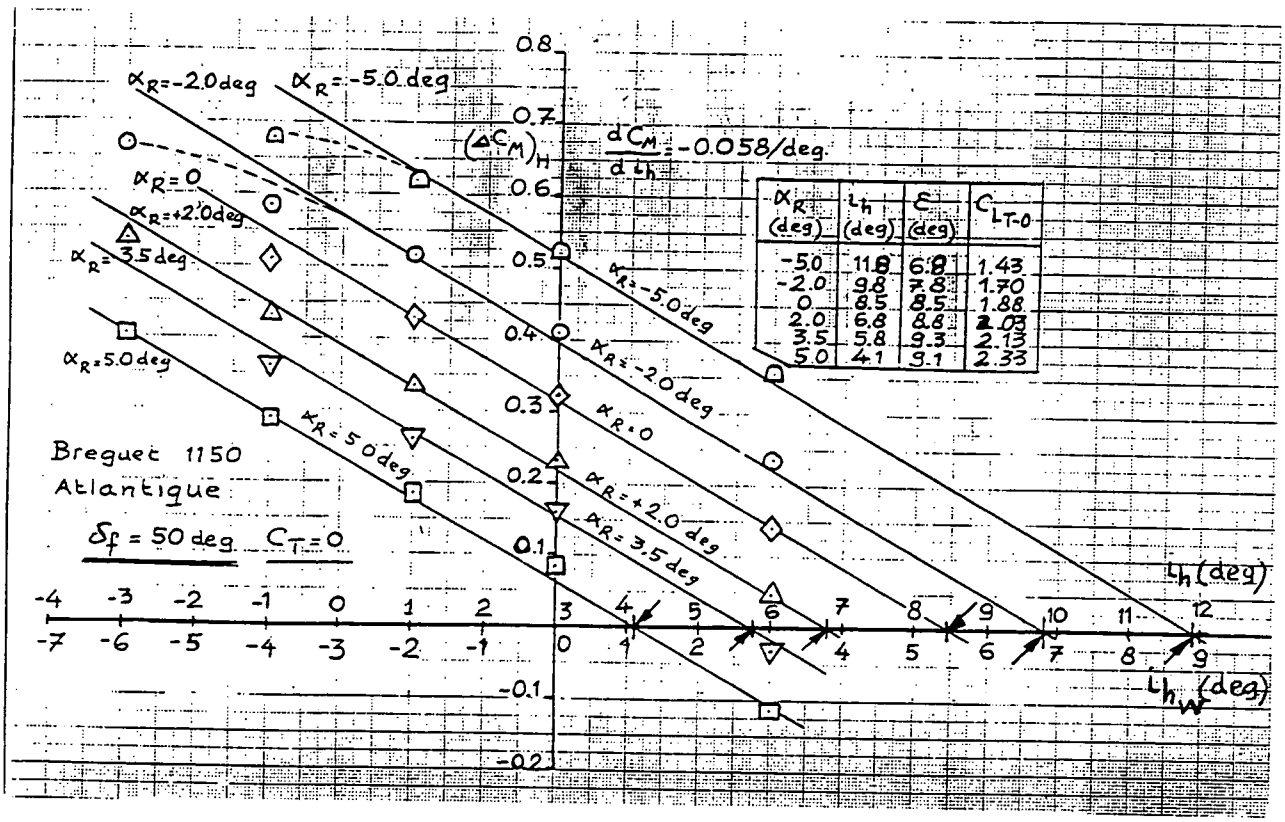

α_R (deg)	i_h (deg)	ε (deg)	$C_{L_{T-0}}$
-5.0	11.8	6.8	1.43
-2.0	9.8	7.8	1.70
0	8.5	8.5	1.88
2.0	6.8	8.8	2.03
3.5	5.8	9.3	2.13
5.0	4.1	9.1	2.33

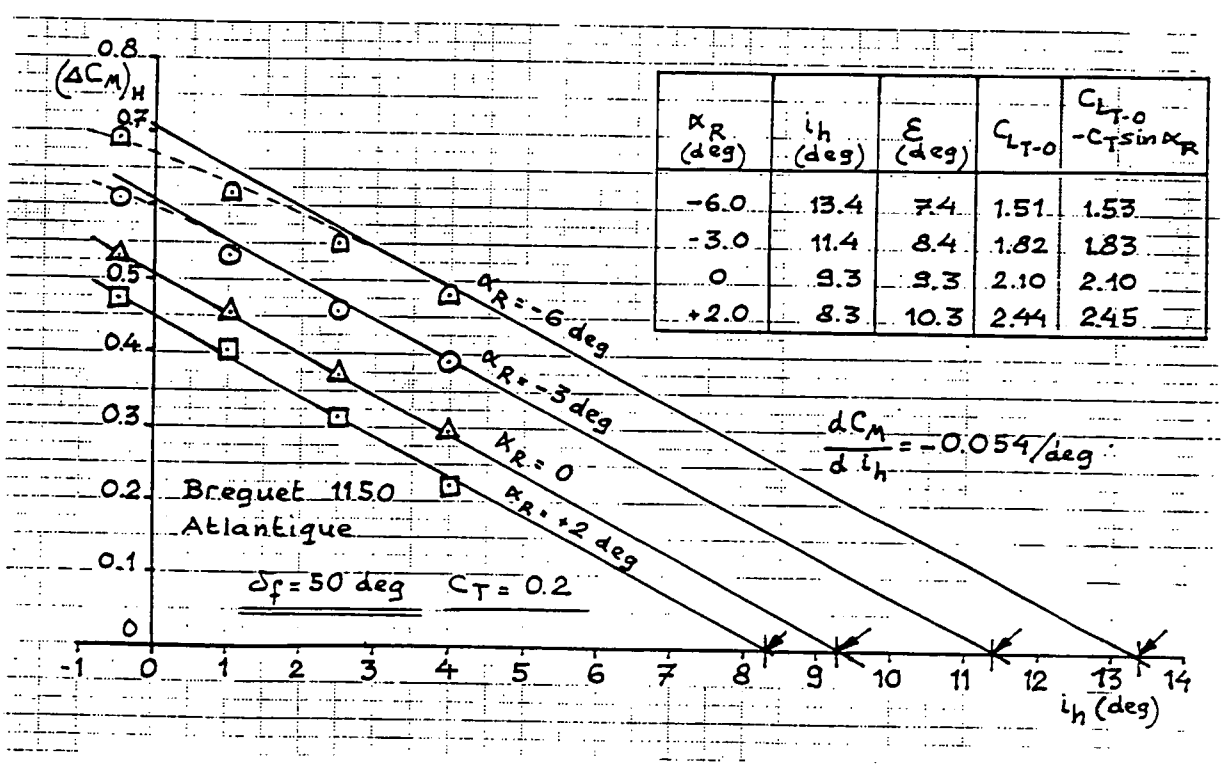

α_R (deg)	i_h (deg)	ε (deg)	$C_{L_{T-0}}$	$C_{L_{T-0}} - C_T \sin\alpha_R$
-6.0	13.4	7.4	1.51	1.53
-3.0	11.4	8.4	1.82	1.83
0	9.3	9.3	2.10	2.10
+2.0	8.3	10.3	2.44	2.45

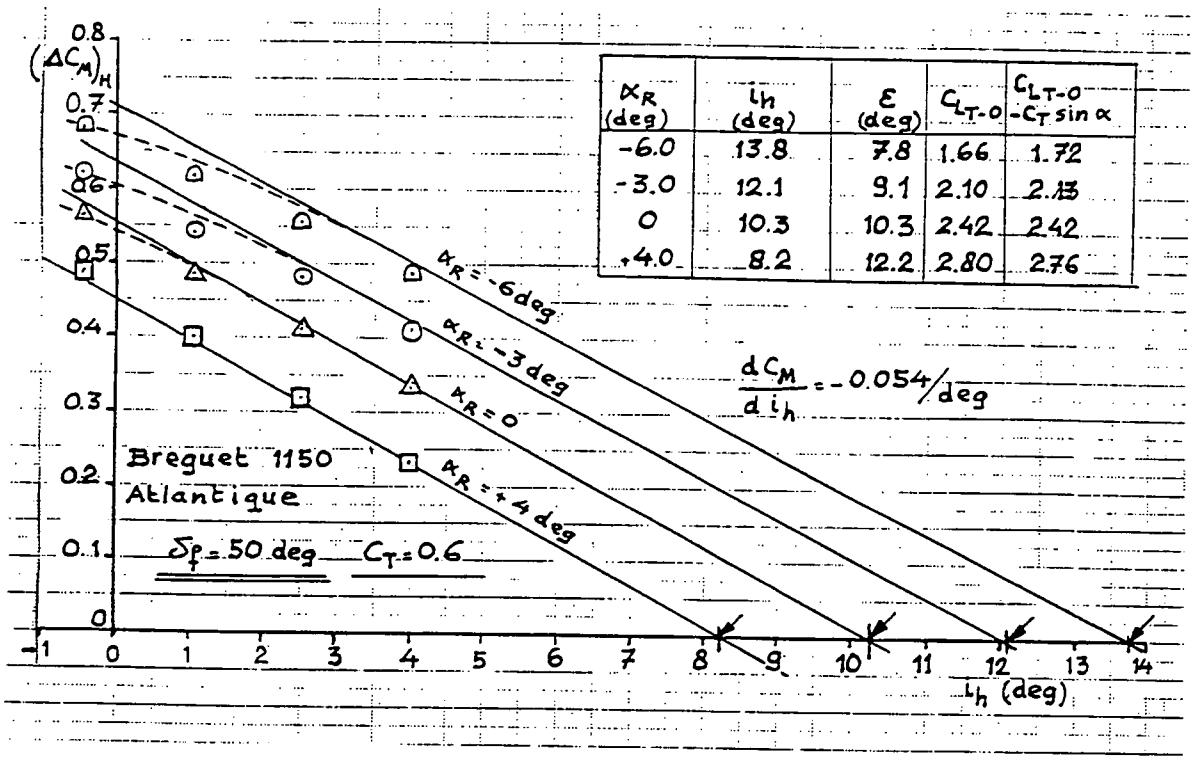

α_R (deg)	i_h (deg)	ε (deg)	$C_{L_{T-0}}$	$\frac{C_{L_{T-0}}}{-C_T \sin\alpha}$
-6.0	13.8	7.8	1.66	1.72
-3.0	12.1	9.1	2.10	2.13
0	10.3	10.3	2.42	2.42
+4.0	8.2	12.2	2.80	2.76

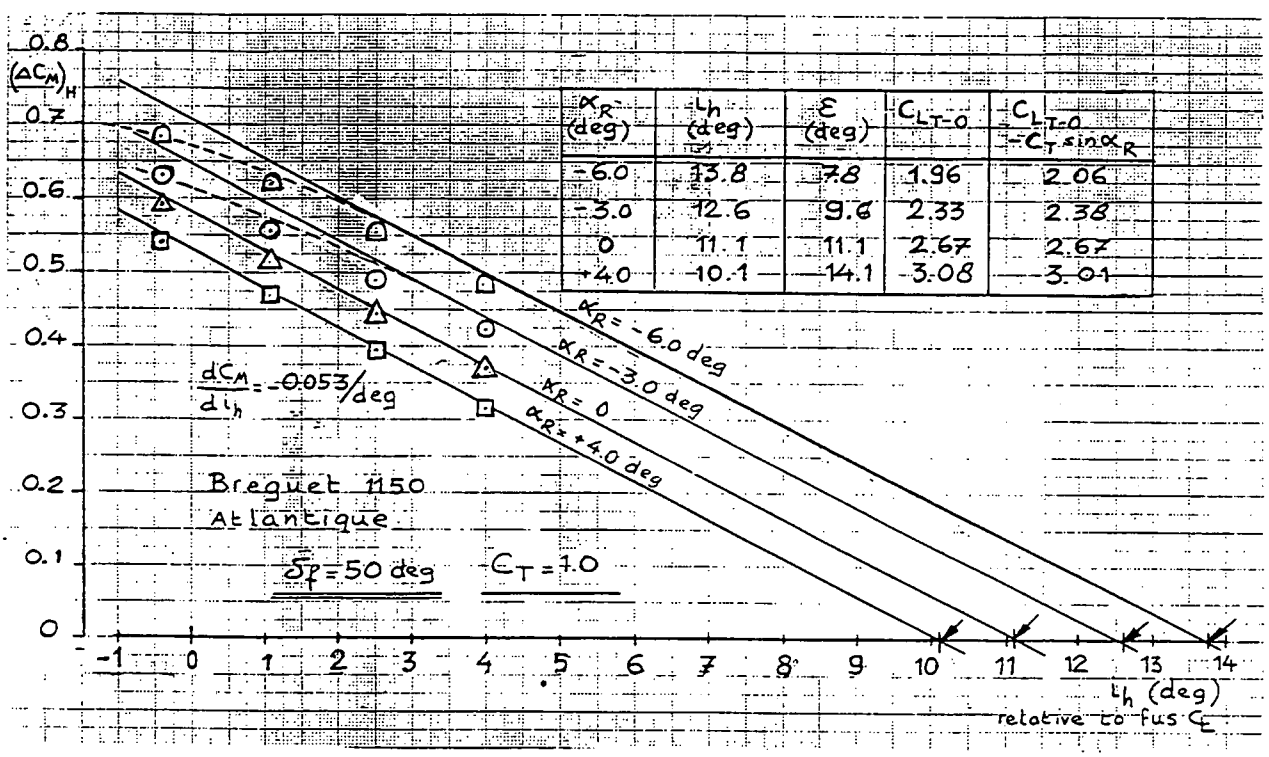

α_R (deg)	i_h (deg)	ε (deg)	$C_{L_{T-0}}$	$\frac{C_{L_{T-0}}}{-C_T \sin\alpha_R}$
-6.0	13.8	7.8	1.96	2.06
-3.0	12.6	9.6	2.33	2.38
0	11.1	11.1	2.67	2.67
+4.0	10.1	14.1	3.08	3.01

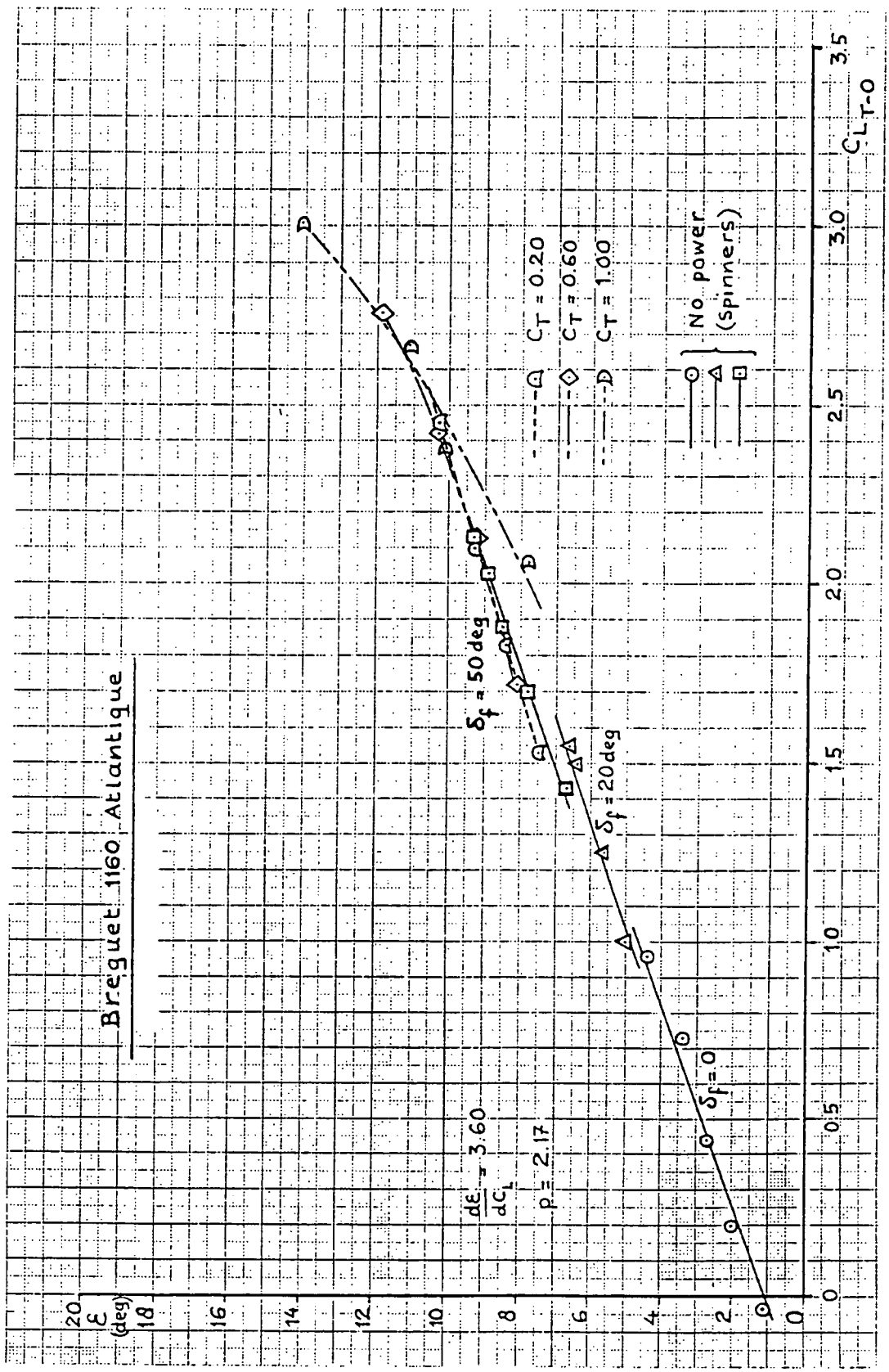
Breguet 1160 Atlantique
ε (deg)
dε/dC_L = 3.60
p = 2.17
δf = 50 deg
δf = 20 deg
δf = 0
CT = 0.20
CT = 0.60
CT = 1.00
No. power
(Spinners)
C_LT-O

Appendix XV

The effect of propeller slipstream on the tail-off pitching moment at small flap deflections ($\delta_f < 30$ deg)

As mentioned in Appendix V for tail-off aircraft configurations with flaps and slats retracted a good agreement between theory and testdata is found for the pitching moment when the effect of propeller slipstream is expressed as:

$$\Delta C_{M_s} = - \Delta C_{L_{s,\alpha}} \times \frac{\Delta X_{AC_{fus}}}{\overline{C}}$$

Thus, as is shown in figure 42 and on pages XV-2 to XV-4 the static stability dC_M/dC_L for aircraft configurations without tail and without flaps or slats is hardly affected by propeller slipstream effects.

For flap settings of 30 deg or above the best agreement between theory and test data on tail-off pitching moments is obtained when a term $\Delta C_{M_{FS}}$ is introduced where

$$\Delta C_{M_{FS}} = - \frac{\Delta X_{FS}}{\overline{C}} \Delta C_{L_{s,\alpha}}$$ (Chapter 6.2 of the main text)

Analysis of limited test data suggests that for flap settings below 30 deg best agreement between theory and test data is obtained when in the equations of chapter 6.2 instead of:

$$\Delta C_{M_{FS}} = - \frac{\Delta X_{FS}}{\overline{C}} \Delta C_{L_{s,\alpha}}$$

$$\Delta C^*_{M_{FS}} = - \left[\frac{\Delta X_{AC,fus}}{\overline{C}} + \left(\frac{\Delta X_{FS}}{\overline{C}} - \frac{\Delta X_{AC,fus}}{\overline{C}} \right) \frac{\delta_f}{30} \right] \Delta C_{L_{\alpha,s}}$$

is used.

The improvement in the comparison between the tail-off pitching moment for configurations with flap settings below 30 deg when using $\Delta C^*_{M_{FS}}$ instead of $\Delta C_{M_{FS}}$ is evident from a comparison of the data on page XV-5 and XV-6 with the data on page IX-9 and IX-14.

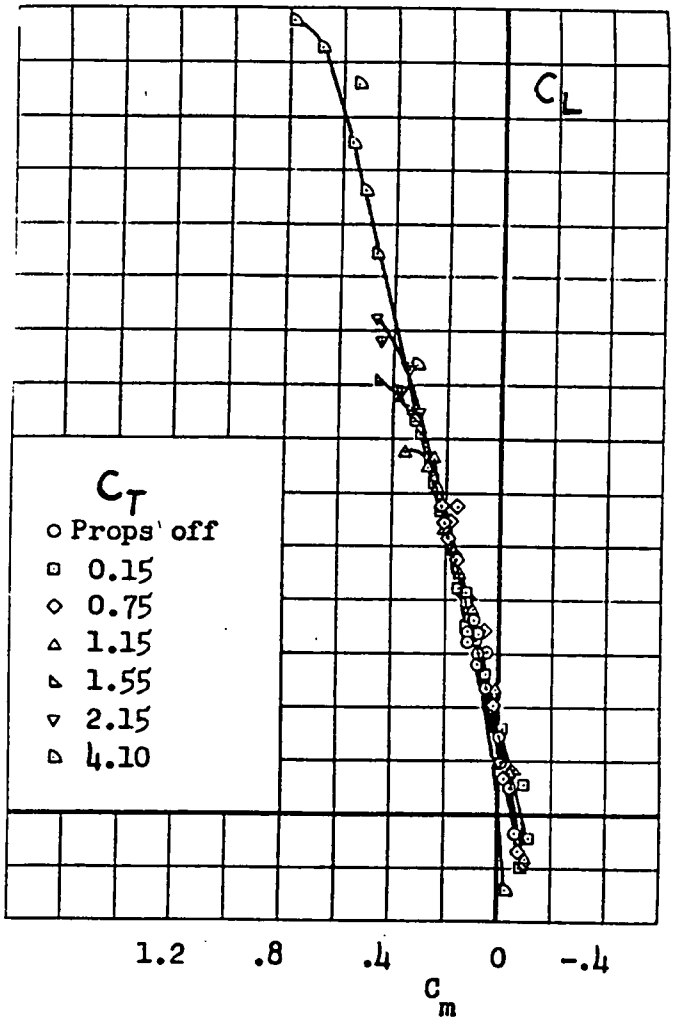

NASA

TN D-25

$\delta_f = \delta_a = 0^o$; tail off

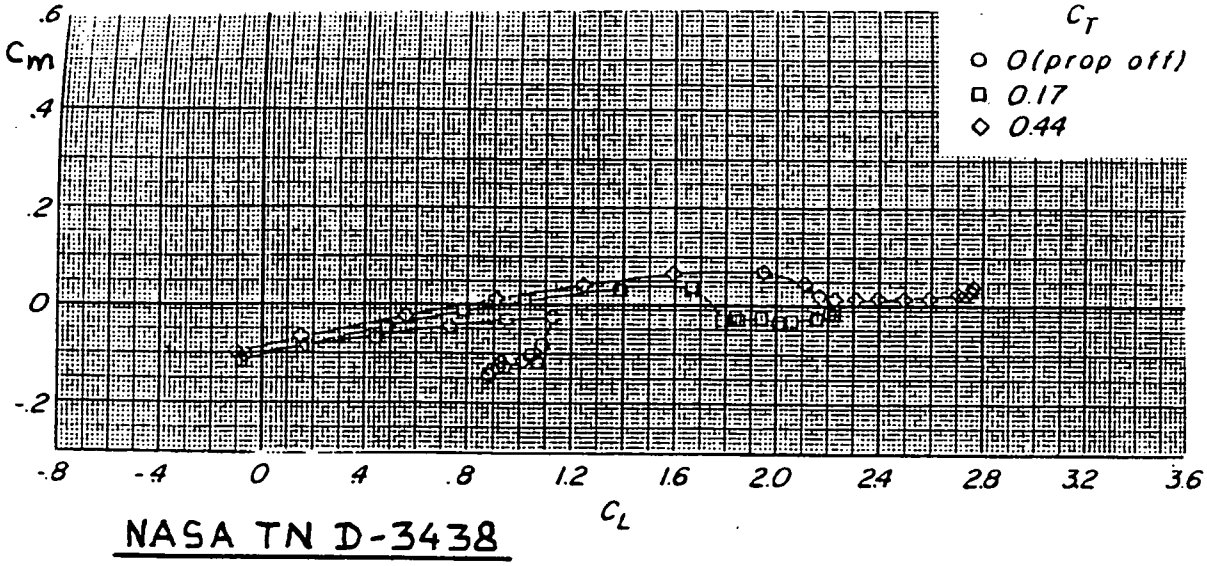

NASA TN D-3438

Variation of C_m with C_L.

NASA TN D-4448

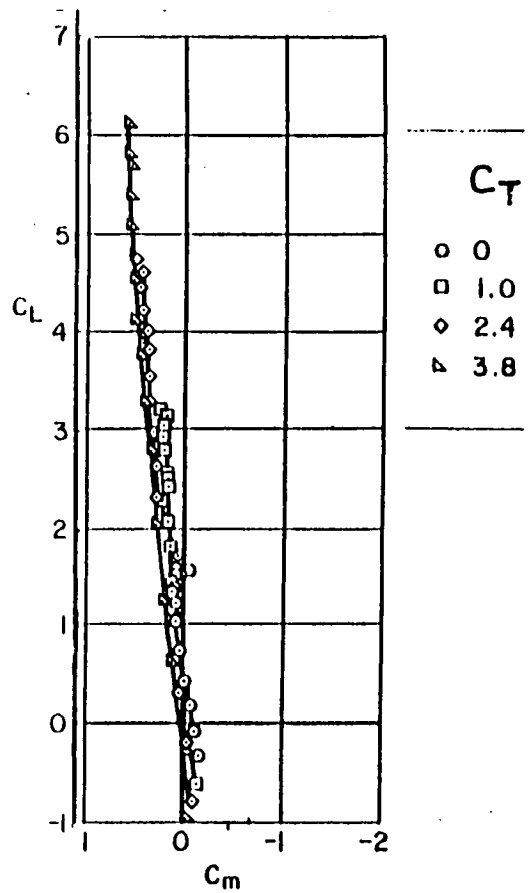

$\delta_f = 0^o$, clean leading edge.

model with the medium-span wing; tail off.

NASA TN D-6393

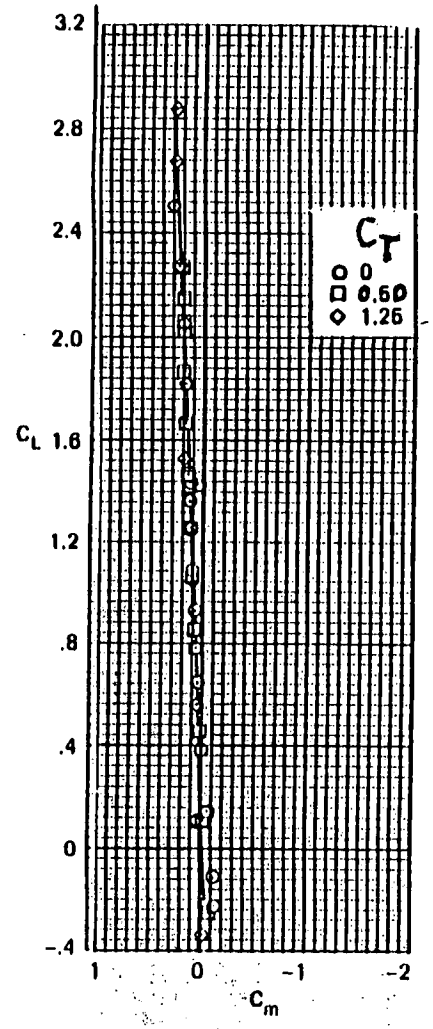

$\delta_f = 0°$, two propellers on.

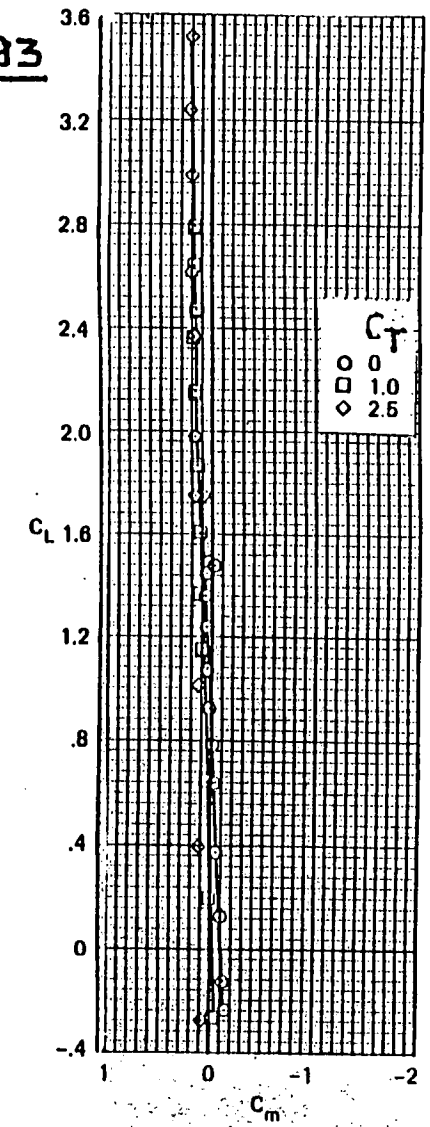

$\delta_f = 0°$, four propellers on.

Basic longitudinal characteristics; slats off, tail off.

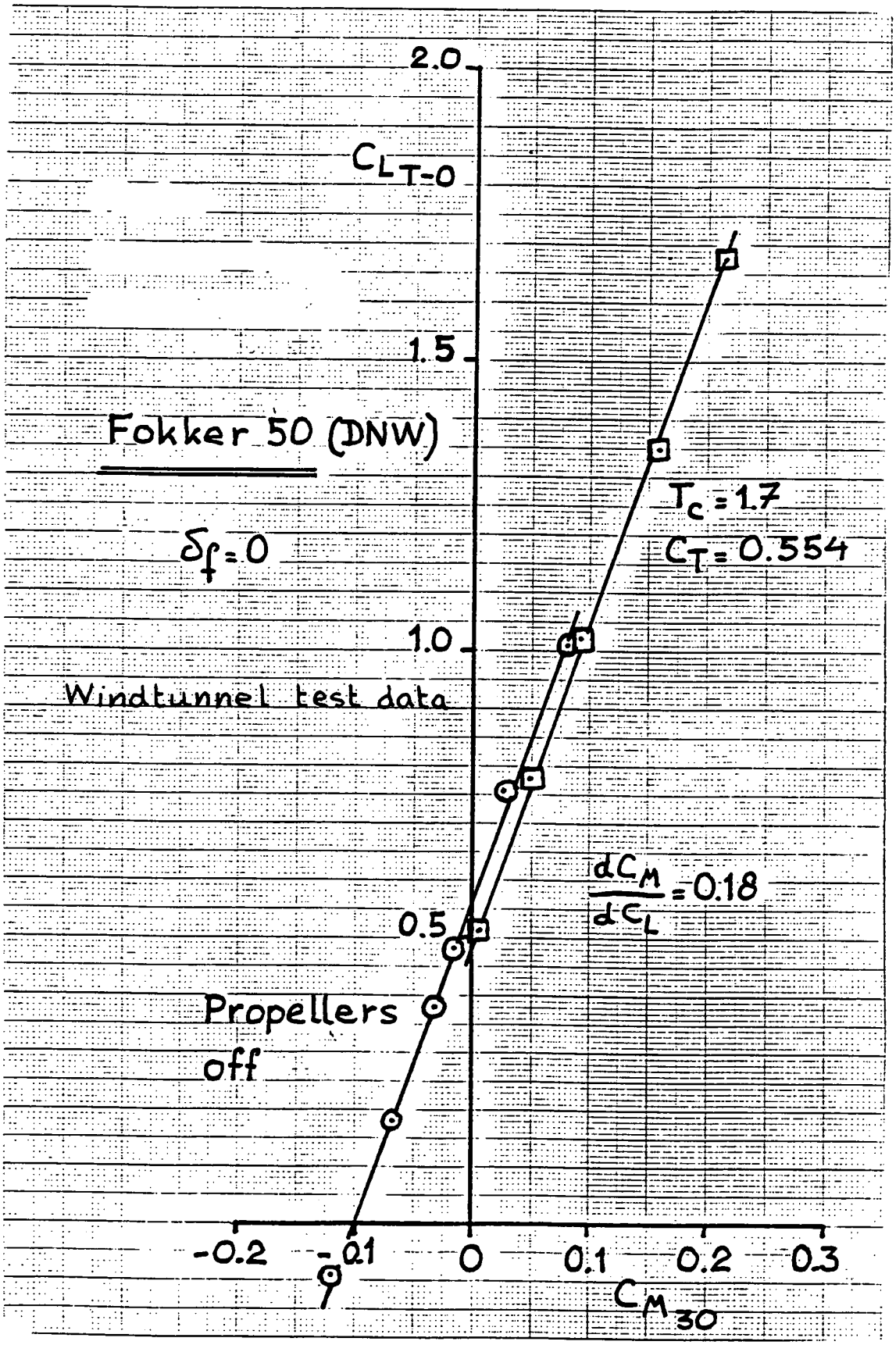
2.0
$C_{L_{T-O}}$
1.5
Fokker 50 (DNW)
$T_c = 1.7$
$C_T = 0.554$
$\delta_f = 0$
1.0
Windtunnel test data
$\frac{dC_M}{dC_L} = 0.18$
0.5
Propellers
off
-0.2
-0.1
0
0.1
0.2
0.3
$C_{M_{30}}$

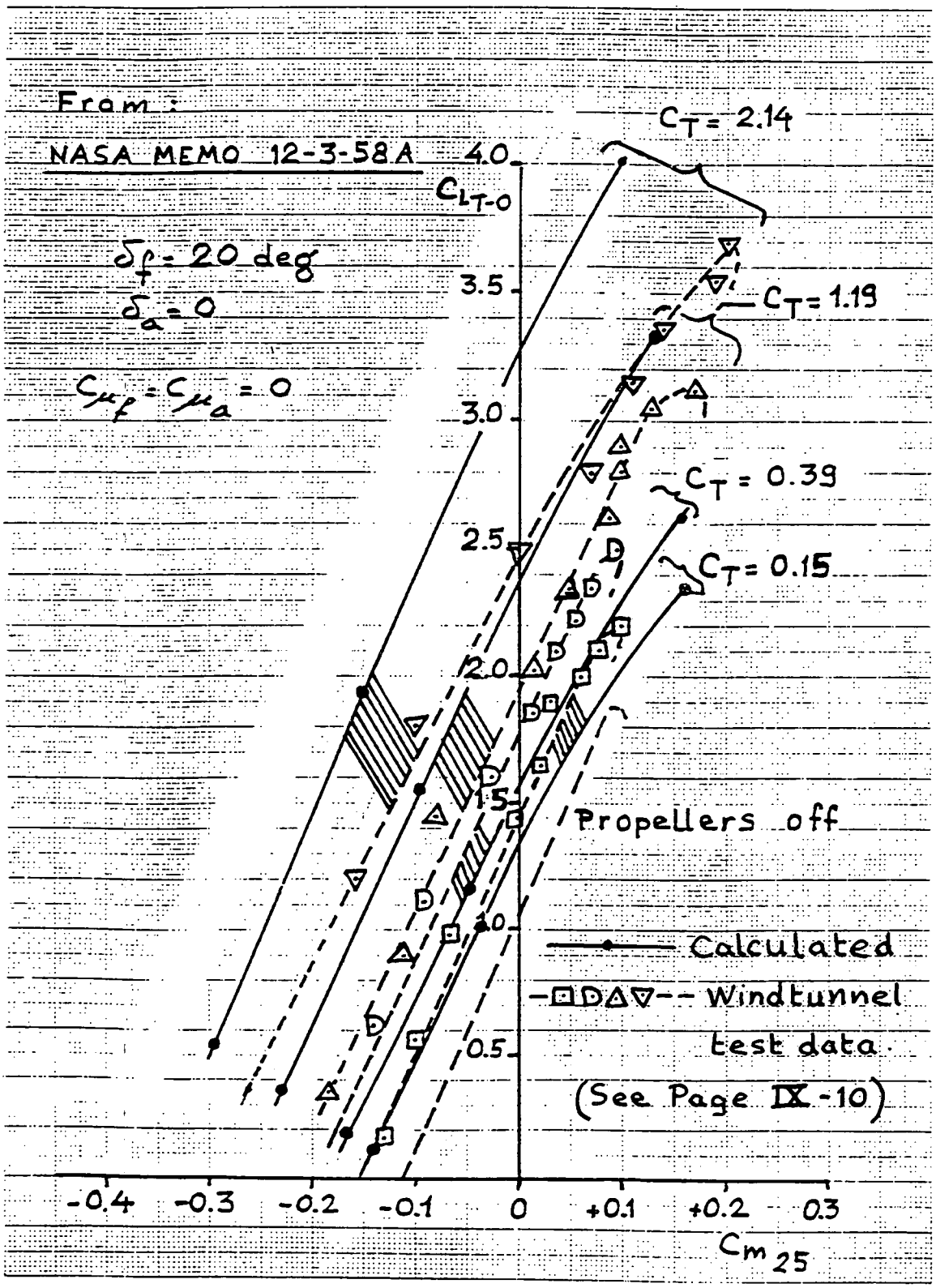
From :
NASA MEMO 12-3-58A
$\delta_f = 20$ deg
$\delta_a = 0$
$C_{\mu_f} = C_{\mu_a} = 0$
$C_{L_{T-0}}$
4.0
3.5
3.0
2.5
2.0
1.5
1.0
0.5
$C_T = 2.14$
$C_T = 1.19$
$C_T = 0.39$
$C_T = 0.15$
Propellers off
Calculated
Windtunnel test data
(See Page IX-10)
-0.4
-0.3
-0.2
-0.1
0
+0.1
+0.2
0.3
$C_{m_{25}}$

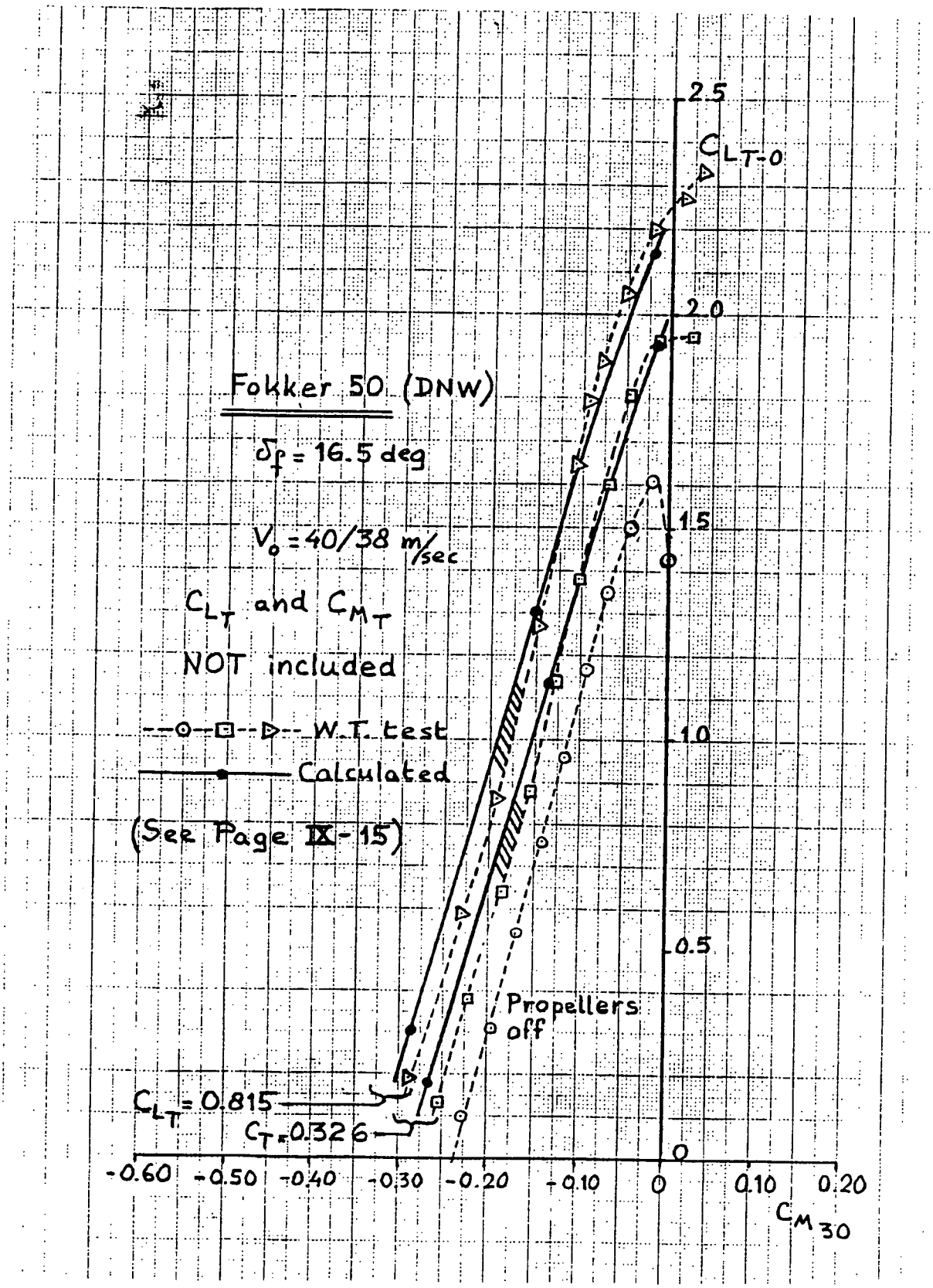
Fokker 50 (DNW)
δ_f = 16.5 deg
V_o = 40/38 m/sec
C_{L_T} and C_{M_T}
NOT included
W.T. test
Calculated
(See Page IX-15)
$C_{L_{T-O}}$
Propellers off
C_{L_T} = 0.815
C_T = 0.326
2.5
2.0
1.5
1.0
0.5
0
-0.60
-0.50
-0.40
-0.30
-0.20
-0.10
0
0.10
0.20
$C_{M_{30}}$

Appendix XVI

A comparison between the tail-on pitching moment curves of the aircraft configuration from Report NASA TN D-25 as calculated and as derived from windtunnel test data.

The tail-on pitching moment can be written as:

$$C_M = C_{M_{Tail-off}} + (\Delta C_M)_H \text{ , where}$$

$$(\Delta C_M)_H = -C_{L_{\alpha_H}} \overline{V_H} (\alpha_R - \varepsilon + i_h) \frac{q_h}{q}$$

with:

$C_{L_{\alpha_H}} = 0.052/deg$ $\quad$ $\bar{V}_H = 1.047$

$i_h = +4.3$ deg $\quad$ $(L_h/\bar{c} = 3.76)$

$(S_H/S_w = 0.275)$

$A_H = 4.55$

For the cruise configuration ($\delta_f = 0$) the calculation of C_M, both without and with tail are presented in Table X and in the figures on page XVI-5 to XIV-7.

For the landing configuration ($\delta_f = 60$ deg, $\delta_a = 30$ deg) the calculated tail-off data are presented in Table IV and in the figure on page IX-9. The tail-on data are presented in Table X and in the figures on page XIV-8.

The windtunnel test data both without and with tail surfaces are also presented in Tables IV and X and on pages IX-9, XVI-5 to XIV-8.

Table X Downwash Characteristics (V)

No.	Conf.	l_h/c (74)	i_w (deg) (79)	z_h/D (80)	δ_f (deg) (5)	α_R (deg) (19)	C_T (26)	$\Delta V/V_0$ (40)	$C_{L_{P-0}}$ TEST (38)	ΔC_{L_S} CALC (54)	C_L^* CALC (89) = (54)+(38)	$C_{L_{TOT}}$ CALC (87)	ε' (deg) (125)	D_{prop} (9)	D^* (42)	C_S (4)	C_f (93)	l_h (deg)	$C_{M_{0.25}}$ TEST
1	NASA TN D-25	3.76	8.3	0.32	0	-8.0	0.15	0.196	-0.12	+0.018	-0.102	-0.138	0.7	1.454	1.393	1.62	0.405	+4.3	
						0			0.55	0.068	0.618	0.622	2.4						
						8.0			1.25	0.115	1.365	1.406	6.5						
		3.76	8.3	0.32	0	12.0	0.15	0.196	1.55	0.139	1.689	1.748	7.8	1.454	1.393	1.62	0.405	+4.3	
		3.76	8.3	0.32	0	-8.0	1.15	1.074	-0.12	0.133	0.013	-0.163	0.9	1.454	1.252	1.62	0.405	+4.3	
						0			0.55	0.310	0.860	0.866	4.4						
						8.0			1.25	0.483	1.733	1.922	8.0						
		3.76	8.3	0.32	0	12.0	1.15	1.074	1.55	0.570	2.120	2.399	9.6	1.454	1.252	1.62	0.405	+4.3	
		3.76	8.3	0.32	0	-8.0	2.15	1.678	-0.12	0.252	0.132	-0.187	1.4	1.454	1.205	1.62	0.405	+4.3	
						0			0.55	0.489	1.039	1.047	5.15						
						8.0			1.25	0.694	1.944	2.278	8.9						
		3.76	8.3	0.32	0	12.0	2.15	1.678	1.55	0.841	2.391	2.886	10.7	1.454	1.205	1.62	0.405	+4.3	
		3.76	8.3	0.32	0	-8.0	4.10	2.576	-0.12	0.501	0.381	-0.214	2.6	1.454	1.163	1.62	0.405	+4.3	
						0			0.55	0.826	1.376	1.385	6.6						
						8.0			1.25	1.148	2.398	3.012	10.8						
		3.76	8.3	0.32	0	12.0	4.10	2.576	1.55	1.308	2.858	3.770	12.6	1.454	1.163	1.62	0.405	+4.3	
1	NASA TN D-25	3.76	8.3	0.32	60/δ_f=30	-8.0	0.15	0.196	2.05	0.238	2.288	2.312	6.9	1.454	1.393	1.62	0.405	+4.3	
						0			2.25	0.272	3.022	3.040	9.9						
		3.76	8.3	0.32	60/δ_f=30	8.0	0.15	0.196	3.35	0.302	3.652	3.706	12.5	1.454	1.393	1.62	0.405	+4.3	
		3.76	8.3	0.32	60/δ_f=30	-8.0	1.15	1.074	2.05	1.164	3.214	3.058	10.7	1.454	1.252	1.62	0.405	+4.3	
						0			2.25	1.298	4.048	4.075	14.1						
		3.76	8.3	0.32	60/δ_f=30	8.0	1.15	1.074	3.35	1.424	4.774	4.983	17.0	1.454	1.252	1.62	0.405	+4.3	
		3.76	8.3	0.32	60/δ_f=30	-8.0	2.15	1.678	2.05	1.902	3.804	3.794	13.0	1.454	1.205	1.62	0.405	+4.3	-0.160
						0			2.25	2.061	4.811	4.843	17.2						-0.100
		3.76	8.3	0.32	60/δ_f=30	8.0	2.15	1.678	3.35	2.231	5.581	5.939	20.3	1.454	1.205	1.62	0.405	+4.3	-0.050

Table X Downwash Characteristics (Continued)

No	Conf	l_h	h_t	$x_{0.25}-x_{pr}$	l_h^*	$(\Delta h_t)_\alpha$	$(\Delta h_t)_{upw.}$	$\frac{d\varepsilon}{dC_L}$	K_ε	$\left(\frac{dC_L}{d\bar{K}/r}\right)_{(1/deg)\,C_T=0}$	ΔC_{L_S} CALC	$\varepsilon_{\alpha=0}$	M	N	O	P	α_κ (deg)	$(\Delta h_t)_{\delta_f}$
		(94)	(95)	(96)	(97)	(98)	(99)	(100)	(101)	(102)	(103) $\equiv$ (58)	(104)	(105)	(106)	(107)	(108)	(82) $\equiv$ (18)	(83)
1	NASA TN D-25	5.55	0.575	1.45	4.41	0.202	0	4.10	1.5	0.082	0.018	3.0	-4.03	0.11	4.50	0.04	-8.0	0
						0					0.068		0	0.42		0.38	0	
						-0.202					0.115		4.03	0.71		0.72	8.0	
		5.55	0.575	1.45	4.41	-0.303	0	4.10	1.5	0.082	0.139	3.0	6.05	0.85	4.50	0.89	12.0	0
		5.55	0.575	1.45	4.41	0.202	0	4.10	1.5	0.082	0.133	3.0	-4.03	0.82	4.50	0.10	-8.0	0
						0					0.310		0	1.91		0.50	0	
						-0.202					0.483		4.03	2.92		0.90	8.0	
		5.55	0.555	1.45	4.41	-0.303	0	4.10	1.5	0.082	0.570	3.0	6.05	3.51	4.50	1.10	12.0	0
		5.55	0.555	1.45	4.41	0.202	0	4.10	1.5	0.082	0.252	3.0	-4.03	1.55	4.50	0.16	-8.0	0
						0					0.489		0	3.01		0.58	0	
						-0.202					0.694		4.03	4.27		1.00	8.0	
		5.55	0.555	1.45	4.41	-0.303	0	4.10	1.5	0.082	0.841	3.0	6.05	5.17	4.50	1.24	12.0	0
		5.55	0.555	1.45	4.41	0.202	0	4.10	1.5	0.082	0.501	3.0	-4.03	3.08	4.50	0.27	-8.0	0
						0					0.826		0	5.08		0.74	0	
						-0.202					1.148		4.03	7.06		1.23	8.0	
		5.55	0.575	1.45	4.41	-0.303	0	4.10	1.5	0.082	1.308	3.0	6.05	8.04	4.50	1.56	12.0	0
1	NASA TN D-25	5.55	0.575	1.45	4.41	0.202	-0.188	4.10	1.5	0.065	0.238	8.2	-3.20	1.46	13.05	0.88	-8.0	0.351
						0					0.272		0	1.67		1.16	0	
		5.55	0.575	1.45	4.41	-0.202	-0.188	4.10	1.5	0.065	0.302	8.2	3.20	1.86	13.05	1.44	8.0	0.351
		5.55	0.575	1.45	4.41	0.202	-0.188	4.10	1.5	0.065	1.164	8.2	-3.20	7.16	13.05	1.35	-8.0	0.351
						0					1.298		0	7.98		1.70	0	
		5.55	0.575	1.45	4.41	-0.202	-0.188	4.10	1.5	0.065	1.424	8.2	3.20	8.76	13.05	2.06	8.0	0.351
		5.55	0.575	1.45	4.41	0.202	-0.188	4.10	1.5	0.065	1.902	8.2	-3.20	11.70	13.05	1.74	-8.0	0.351
						0					2.061		0	12.68		2.13	0	
		5.55	0.575	1.45	4.41	-0.202	-0.188	4.10	1.5	0.065	2.231	8.2	3.20	13.72	13.05	2.54	8.0	0.351

Table X Downwash Characteristics (Concluded)

No	Conf	δ_f (deg) ⑥	α_R (deg) ⑧2 $\frac{⑤}{⑲}$	h_{tot} (109)	C_T (85)	$\frac{h_{tot}}{D^*/2}$ (111)	b_{s_h} (112)	C_{s_h} (113)	S_{s_h} (114)	S_h (115)	$\frac{q_s}{q}$ (116)	b_{max} (117)	$b=\frac{(\Delta v)_{av}}{(v_0)_{av}}$ (122)	$\frac{q_h}{q}$ (123)	$\Delta\varepsilon$ (deg) (126)	ε (deg) (127)	$(\Delta C_M)_h$ calc (128)	$C_{M_{0.25\bar{c}}}$ calc (129)
1	NASA TN D-25	0	-8.0	1.60	0.15	2.29	0	0.98	0	5.25	1.430	0.106	0	1.000	0.03	0.73	+0.241	+0.186
			0	0.96		1.37	0		0				0.002	1.004	0.53	3.93	-0.020	+0.005
			8.0	0.31		0.45	1.24		2.48				0.091	1.190	0.49	6.99	-0.344	-0.230
		0	12.0	-0.02	0.15	-0.03	1.39	0.98	2.72	5.25	1.430	0.106	0.106	1.223	0	7.80	-0.566	-0.420
		0	-8.0	1.66	1.15	2.65	0	0.98	0	5.25	4.301	0.595	0	1.000	0	0.90	+0.250	+0.182
			0	1.07		1.71	0		0				0	1.000	1.61	6.01	+0.093	+0.112
			8.0	0.49		0.78	0.78		1.53				0.179	1.390	3.71	11.71	-0.045	+0.070
		0	12.0	0.19	1.15	0.30	1.19	0.98	2.33	5.25	4.301	0.595	0.565	2.449	1.93	11.53	-0.636	-0.486
		0	-8.0	1.72	2.15	2.85	0	0.98	0	5.25	7.172	0.943	0	1.000	0	1.40	0.278	+0.203
			0	1.16		1.93	0		0				0	1.000	1.48	6.63	0.127	+0.145
			8.0	0.59		0.98	0		0				0.146	1.313	5.79	14.69	0.121	+0.286
		0	12.0	0.33	2.15	0.55	1.01	0.98	1.98	5.25	7.172	0.943	0.547	2.393	5.00	15.70	-0.078	+0.024
		0	-8.0	1.83	4.10	3.15	0	0.98	0	5.25	12.29	1.473	0	1.000	0	2.60	0.342	+0.250
			0	1.32		2.27	0		0				0	1.000	0.39	6.99	0.146	+0.150
			8.0	0.82		1.41	0		0				0.015	1.030	6.57	17.37	0.284	+0.393
		0	12.0	0.65	4.10	1.12	0	0.98	0	5.25	12.29	1.473	0.133	1.284	8.38	20.98	0.327	+0.477
1	NASA TN D-25	60/30	-8.0	2.60	0.15	3.73	0	0.98	0	5.25	1.430	0.106	0	1.000	0	6.90	0.577	-0.012
			0	1.90		2.73	0		0				0	1.000	0	9.90	0.305	-0.172
		60/30	8.0	1.20	0.15	1.72	0	0.98	0	5.25	1.430	0.106	0	1.000	0.28	12.78	0.026	-0.298
		60/30	-8.0	3.07	1.15	4.90	0	0.98	0	5.25	4.301	0.595	0	1.000	0	10.20	0.783	-0.005
			0	2.44		3.89	0		0				0	1.000	0	14.10	0.533	-0.140
		60/30	8.0	1.82	1.15	2.91	0	0.98	0	5.25	4.301	0.595	0	1.000	0	17.00	0.256	-0.263
		60/30	-8.0	3.46	2.15	5.74	0	0.98	0	5.25	7.172	0.943	0	1.000	0	13.00	0.908	-0.037
			0	2.86		4.76	0		0	5.25			0	1.000	0	17.20	0.701	-0.125
		60/30	8.0	2.30	2.15	3.81	0	0.98	0	5.25	7.172	0.943	0	1.000	0	20.30	0.435	-0.142

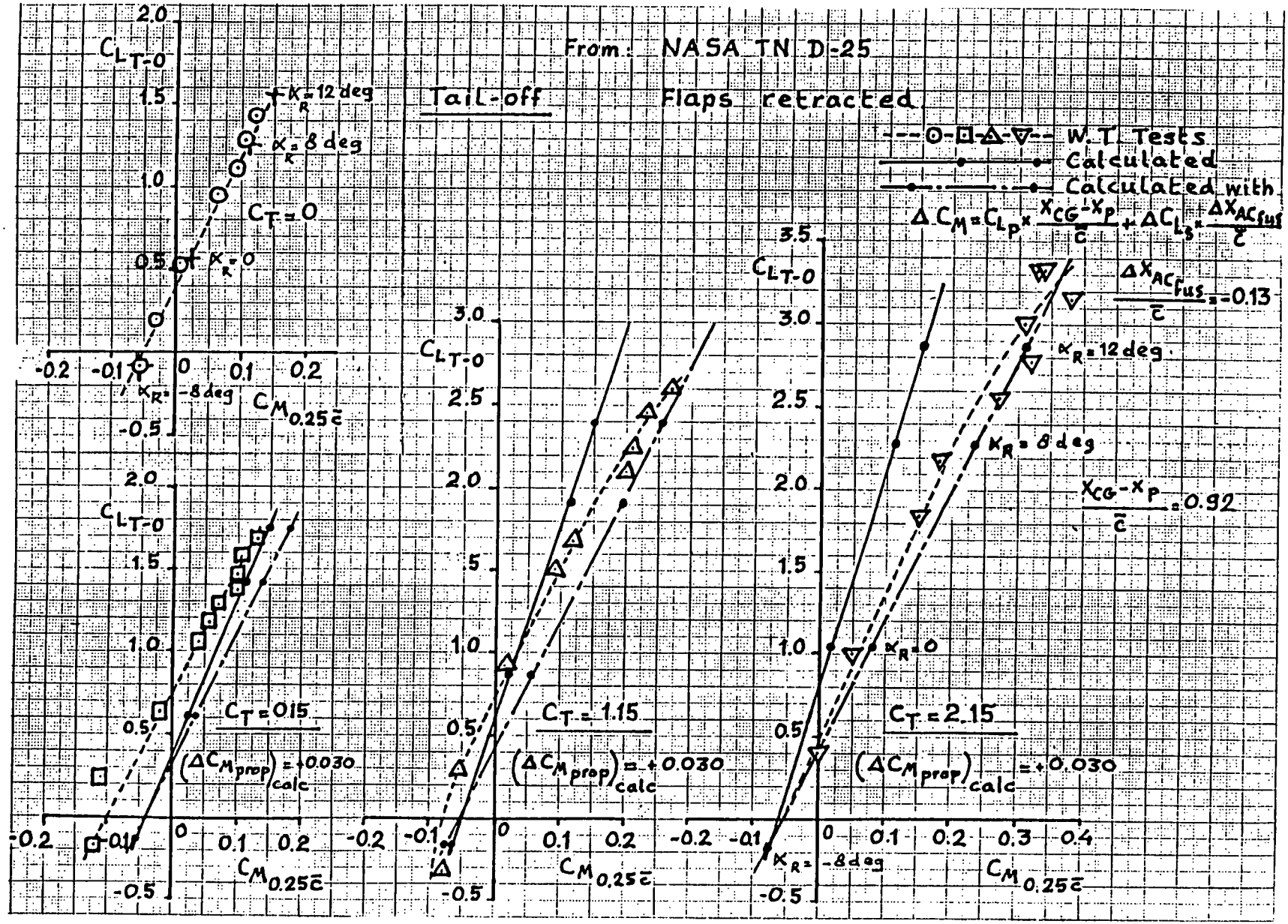
From: NASA TN D-25
Tail-off
Flaps retracted
W.T. Tests
Calculated
Calculated with
$\Delta C_M = C_{L_p} \frac{X_{CG}-X_p}{\bar{c}} + \Delta C_{L_3} \frac{\Delta X_{AC_{fus}}}{\bar{c}}$
$\frac{\Delta X_{AC_{fus}}}{\bar{c}} = 0.13$
$\frac{X_{CG}-X_p}{\bar{c}} = 0.92$
$C_{L_{T-0}}$
$C_{M_{0.25\bar{c}}}$
$\alpha_R = 12$ deg
$\alpha_R = 8$ deg
$\alpha_R = 0$
$\alpha_R = -8$ deg
$C_T = 0$
$C_T = 0.15$
$C_T = 1.15$
$C_T = 2.15$
$(\Delta C_{M_{prop}})_{calc} = +0.030$

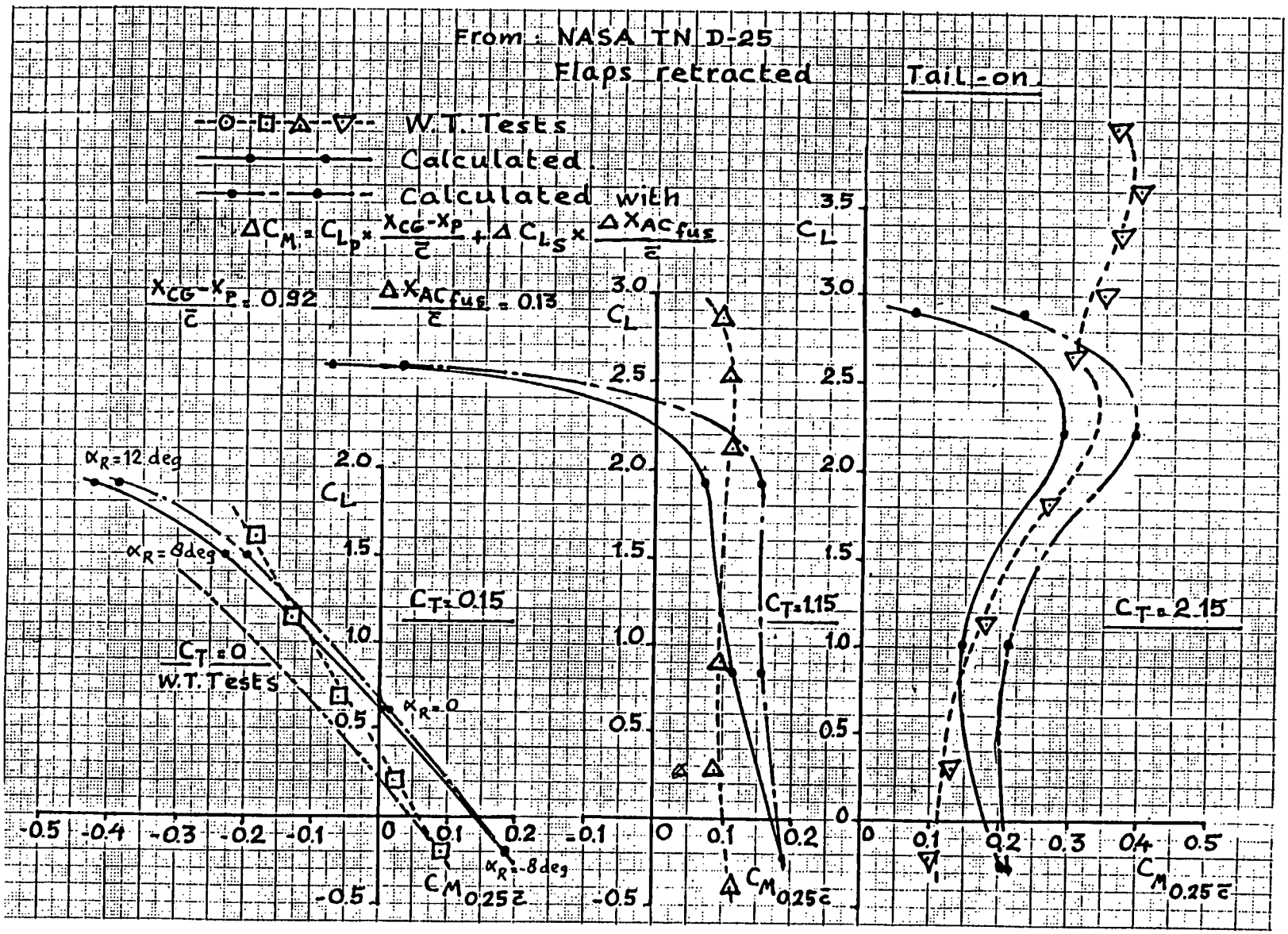
From NASA TN D-25
Flaps retracted
Tail-on
W.T. Tests
Calculated
Calculated with
$\Delta C_M = C_{L_p} \times \frac{X_{CG}-X_P}{\bar{c}} + \Delta C_{L_S} \times \frac{\Delta X_{AC_{fus}}}{\bar{c}}$
$\frac{X_{CG}-X_P}{\bar{c}} = 0.92$
$\frac{\Delta X_{AC_{fus}}}{\bar{c}} = 0.13$
$\alpha_R = 12$ deg
$\alpha_R = 8$ deg
$\alpha_R = 0$
$\alpha_R = -8$ deg
$C_T = 0$
W.T. Tests
$C_T = 0.15$
$C_T = 1.15$
$C_T = 2.15$
C_L
$C_{M_{0.25\bar{c}}}$
3.5
3.0
2.5
2.0
1.5
1.0
0.5
0
-0.5
-0.5
-0.4
-0.3
-0.2
-0.1
0.1
0.2
0.3
0.4
0.5

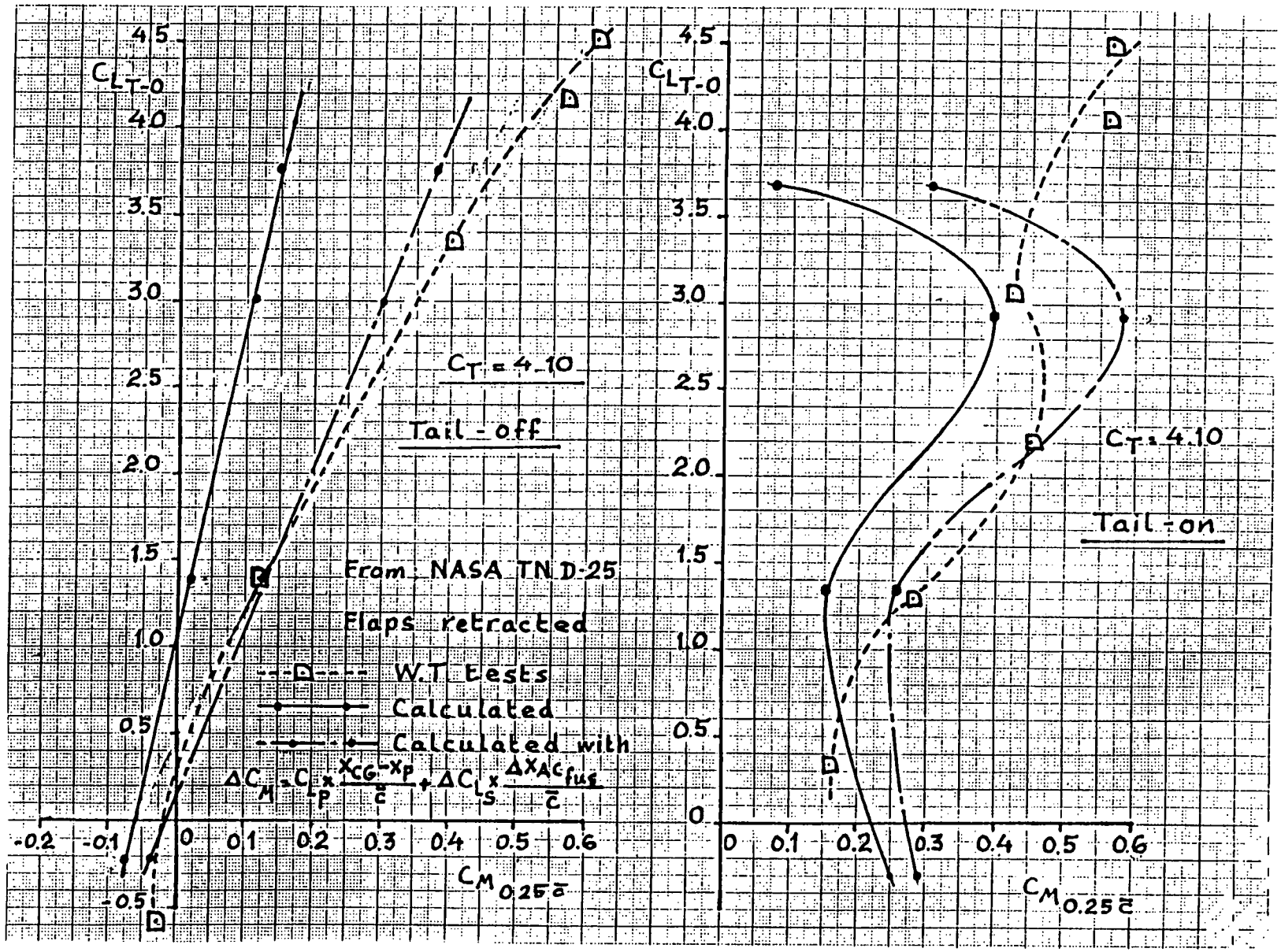
$C_{L_{T-0}}$
4.5
4.0
3.5
3.0
2.5
2.0
1.5
1.0
0.5
0
-0.5
-0.2
-0.1
0
0.1
0.2
0.3
0.4
0.5
0.6
$C_{M_{0.25\bar{c}}}$
$C_T = 4.10$
Tail - off
From NASA TN D-25
Flaps retracted
W.T Tests
Calculated
Calculated with
$\Delta C_M = C_{L_P} \times \frac{X_{CG} - X_P}{\bar{c}} + \Delta C_{L_S} \times \frac{\Delta X_{AC_{fus}}}{\bar{c}}$
Tail - on

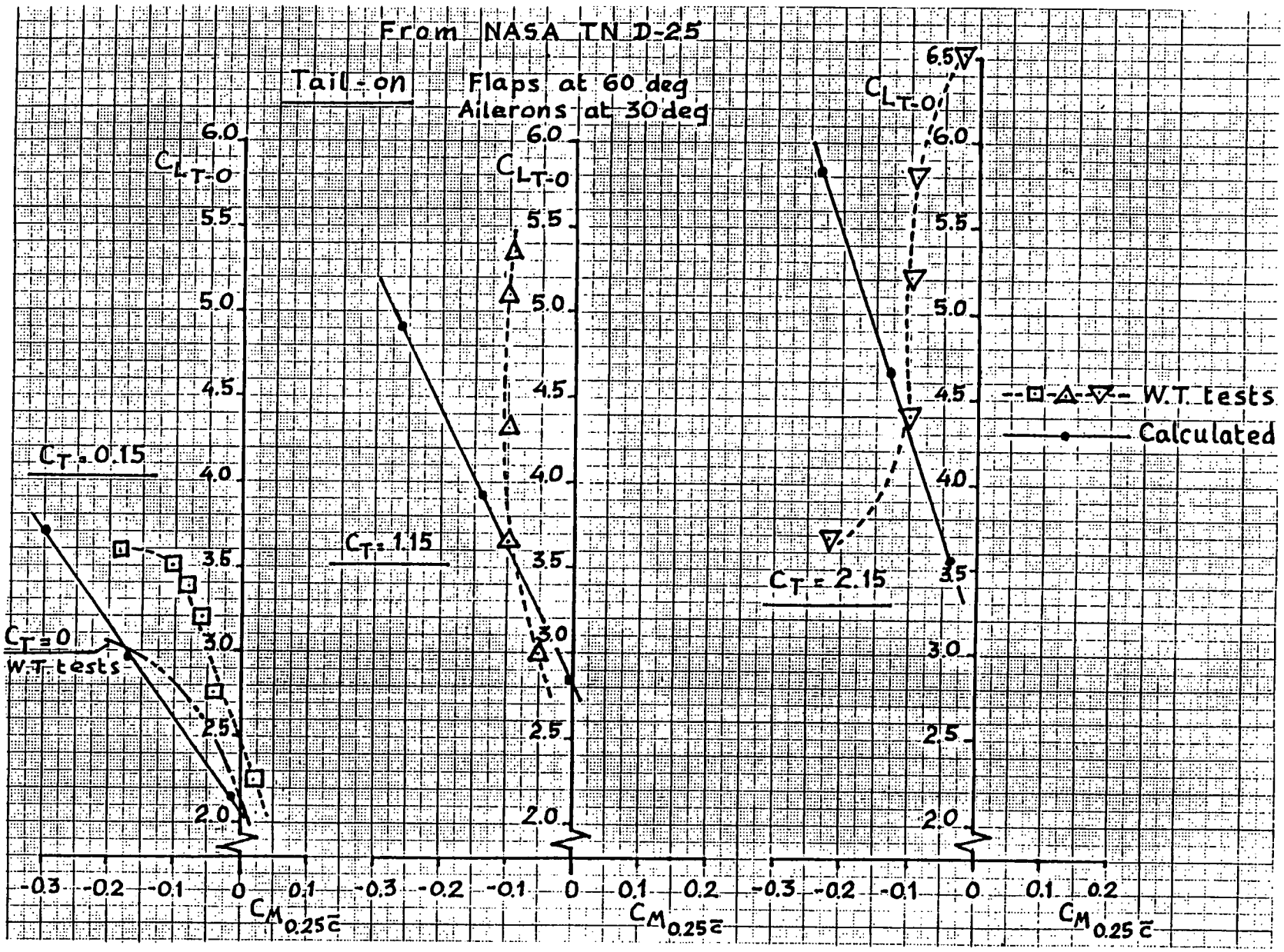
From NASA TN D-25
Tail-on
Flaps at 60 deg
Ailerons at 30 deg
$C_{L_{T-O}}$
$C_T = 0.15$
$C_T = 1.15$
$C_T = 2.15$
$C_T = 0$ W.T. tests
W.T. tests
Calculated
$C_{M_{0.25\bar{c}}}$

Appendix XVII

The effect of the ratio between the vertical distance between propeller axis and wing section chord and propeller diameter on lift due to propeller slipstream.

In the analysis of the effect of propeller slipstream on the aerodynamic characteristics of an aircraft as presented in the main body of this report the vertical location of the propeller axis relative to the wing has not been considered an important parameter because on most practical aircraft configurations this distance is small.

Also limited available test data suggested that this parameter only becomes important when this vertical distance with the propeller axis below the wing is of the order of 70% of half the propeller diameter or above (fig. 18 and ref. 5).

Recent test data show however that this relation between the vertical slipstream position and the wing is less unambiguous than thought before.

A first illustration of this statement is presented on pages XVII-3 and XVII-4. The figures on page XVII-3, show the test set-up for an experiment performed recently in the Low-Speed Tunnel of the Aerospace Faculty of the Delft University of Technology.
A wing half model, equipped with a 5-component balance at the root was investigated with a separately mounted propeller in front of the half model. This powered propeller was located at various vertical positions and operated at a thrust coefficient $C_T = 0.71$. When the wing angle of attack was varied the position of the propeller in the test section was changed accordingly keeping the distance Z_p constant.
On page XVII-4 test data are shown for the lift curve without propeller and the increase in lift due to slipstream at varying angle of attack for different values of the vertical distance Z_p.
The test data show a regular pattern with variations in ΔC_{LS} around $\alpha = 0$ and $Z_p = 0$ of the same order as at large α's and large values of Z_p. Note however that over the greater part of the range of α's and Z_p's the increase in lift due to slipstream ΔC_{LS} with increasing α is more or less constant, in particular for negative Z_p-values. This is in accordance with figure 18.

A second illustration is presented in the figures on pages XVII-5 to XVII-7 which show the test set-up and some test data from an experiment performed in the '70's at the National Aerospace Laboratory, NLR in the Netherlands.
A half model was constructed which was densely covered with pressure tappings allowing the determination of detailed pressure distributions, spanwise lift distributions and the overall lift.
In front of the wing half model two blowing nacelles were mounted producing a simulated slipstream at $C_T = 0$; 0.71 and 2.42.
The test data show trends which compare well with the data from page XVII-4. A downward shift of the slipstream of 0.50 D/2 decreases the lift by $\Delta(\Delta C_{LS}) \approx 0.15$ when $C_T = 0.81$ but the increase in lift with increasing angle of attack is hardly altered, both without and with flap deflected.

A third illustration is presented on pages XVII-8 to XVII-16. As indicated this example is taken from NASA TM 4541, dated April 1994. This test again concerns a half model, however with a powered nacelle with propeller mounted integrally with the wing half model.
In the example presented the propeller axis is positioned at 0.83 D/2 below the wing reference plane. In the clean configuration the lift at $\alpha = 0$ decreases by $\Delta\varepsilon \approx 0.25$ when the propeller thrust is increased from windmilling to $C_T = 1.10$. At $\alpha = 12$ deg the lift increases by $\Delta C_L \approx 0.40$ when $C_T = 1.10$. This is in reasonable agreement with the previous examples.
When the flaps are deflected to $\delta_f = 60$ deg however, the increase in lift is much larger than expected with the low thrust line position investigated. Apparently the low flap trailing edge position strongly affects the Kutta-Joukowski boundary-condition.

The conclusion of the present analysis must be that although with flaps retracted the effect of the vertical thrust line position seems reasonable clear,with flaps deflected this effect deserves further study.

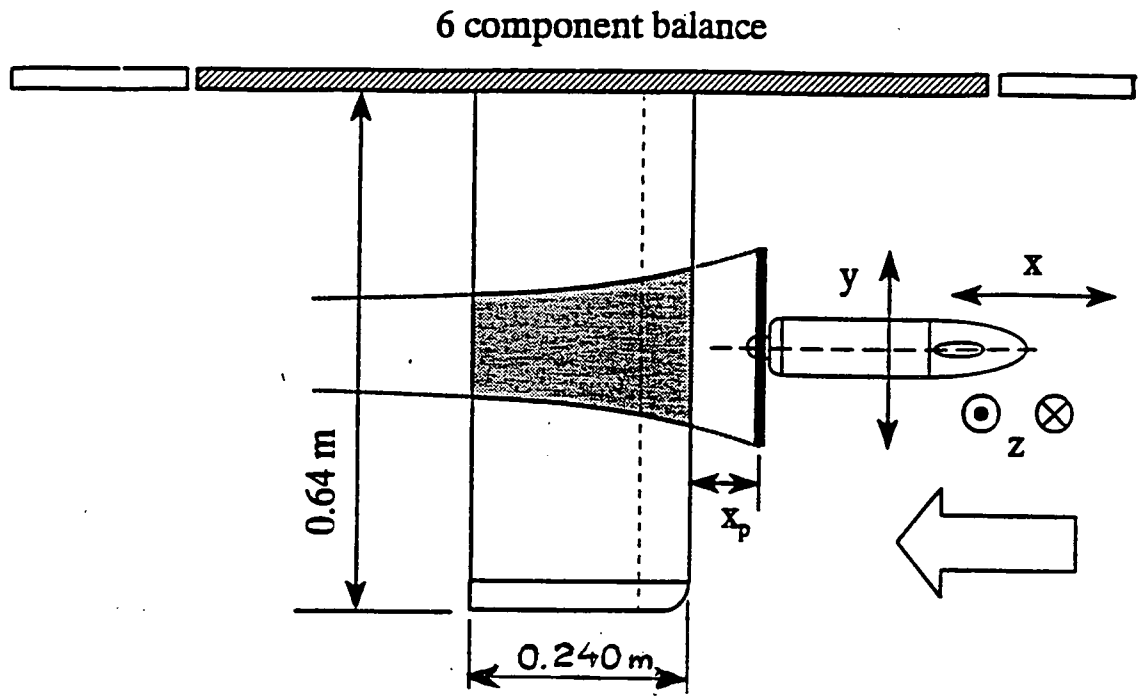

Airfoil section	: NACA64A015
A_w	: 5.33
D	: 0.236 m

Test set up for APROPOS tests (APROPOS = Adaptive PROpeller POsitioning System).

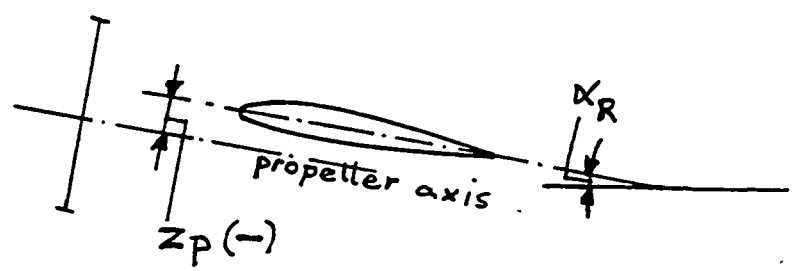

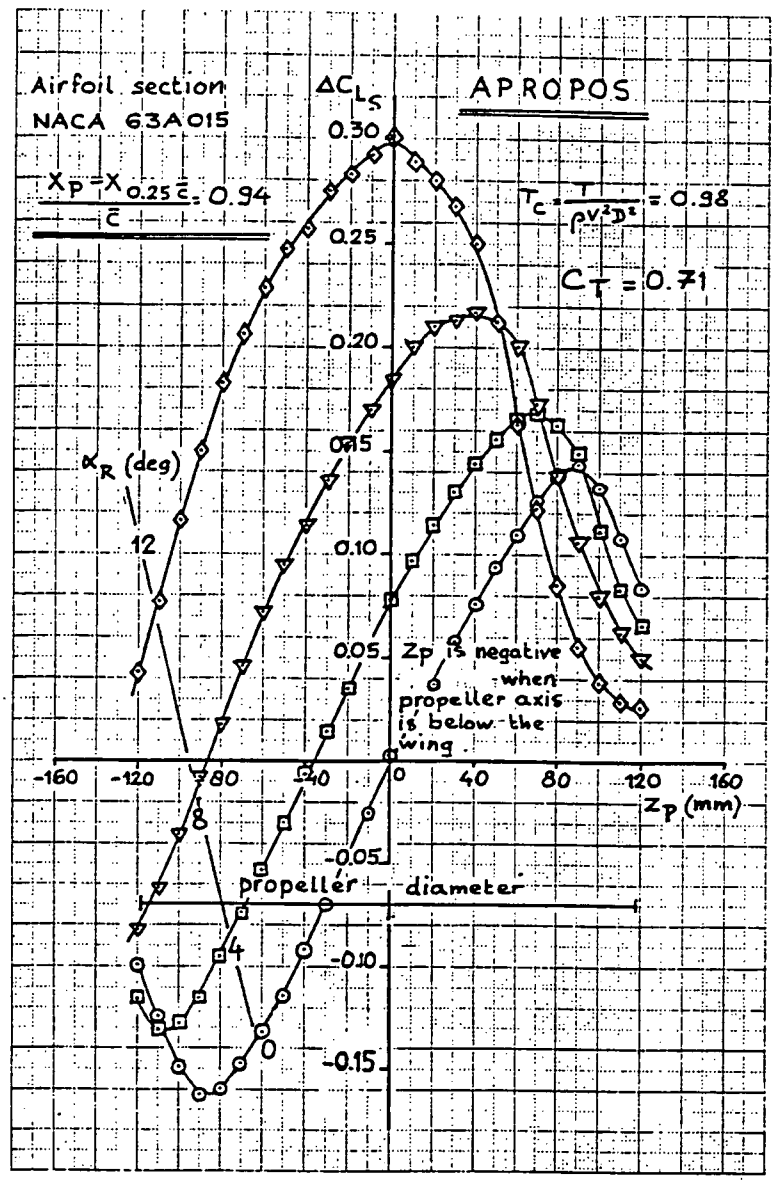
Airfoil section
NACA 63A015
$X_P = X_{0.25\bar{c}} = 0.94$
$\bar{c}$
ΔC_{L_S}
APROPOS
$T_c = \frac{T}{\rho V^2 D^2} = 0.98$
$C_T = 0.71$
0.30
0.25
0.20
0.15
0.10
0.05
α_R (deg)
12
8
4
0
Zp is negative when propeller axis is below the wing.
-160
-120
-80
-40
0
40
80
120
160
Z_P (mm)
-0.05
propeller diameter
-0.10
-0.15

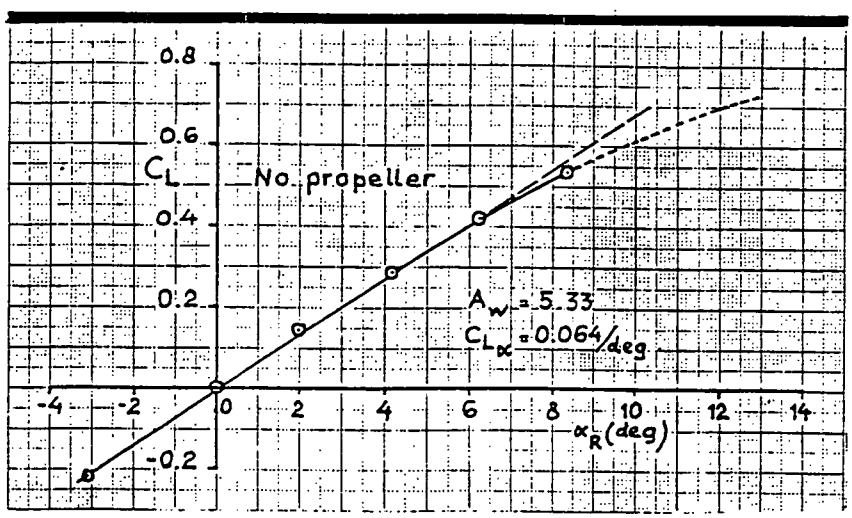
0.8
0.6
C_L
No propeller
0.4
0.2
$A_w = 5.33$
$C_{L_\alpha} = 0.064/\text{deg}$
-4
-2
0
2
4
6
8
10
12
14
α_R (deg)
-0.2

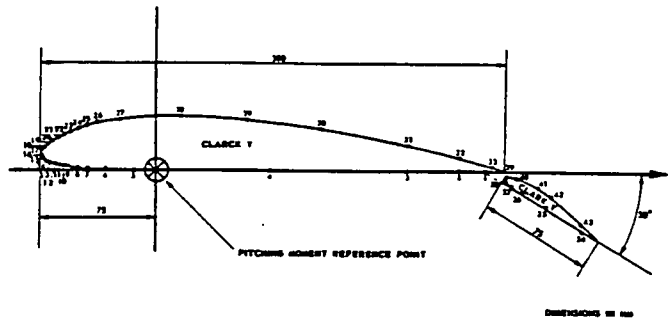

Cross-sectional view of wing-flap combination with indication of pressure hole locations

NLR 77...C

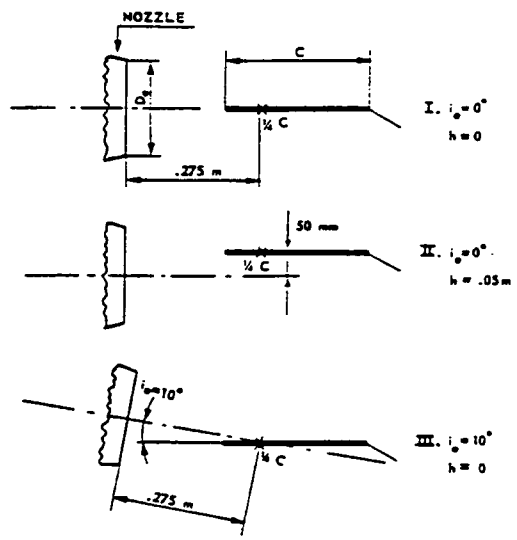

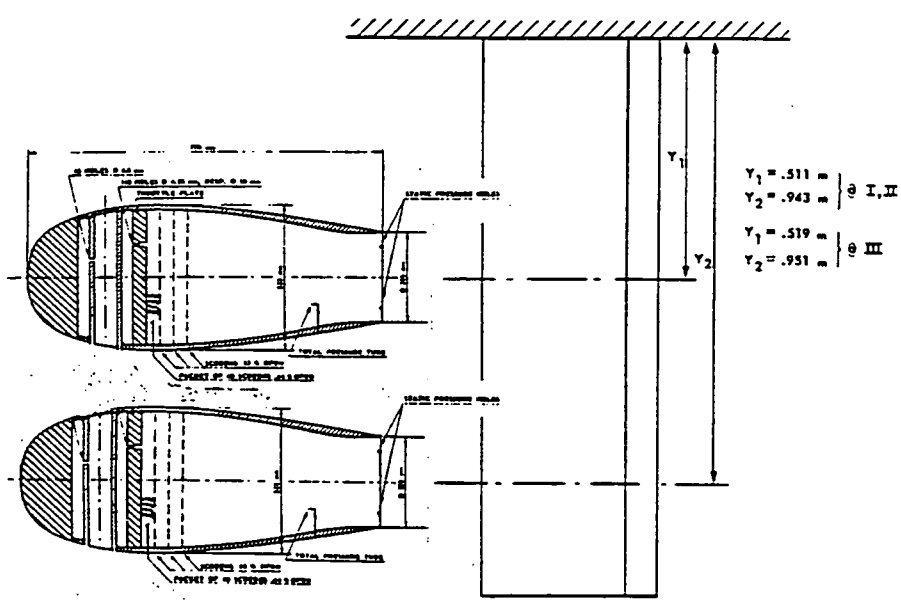

Nacelle positions relative to the wing model

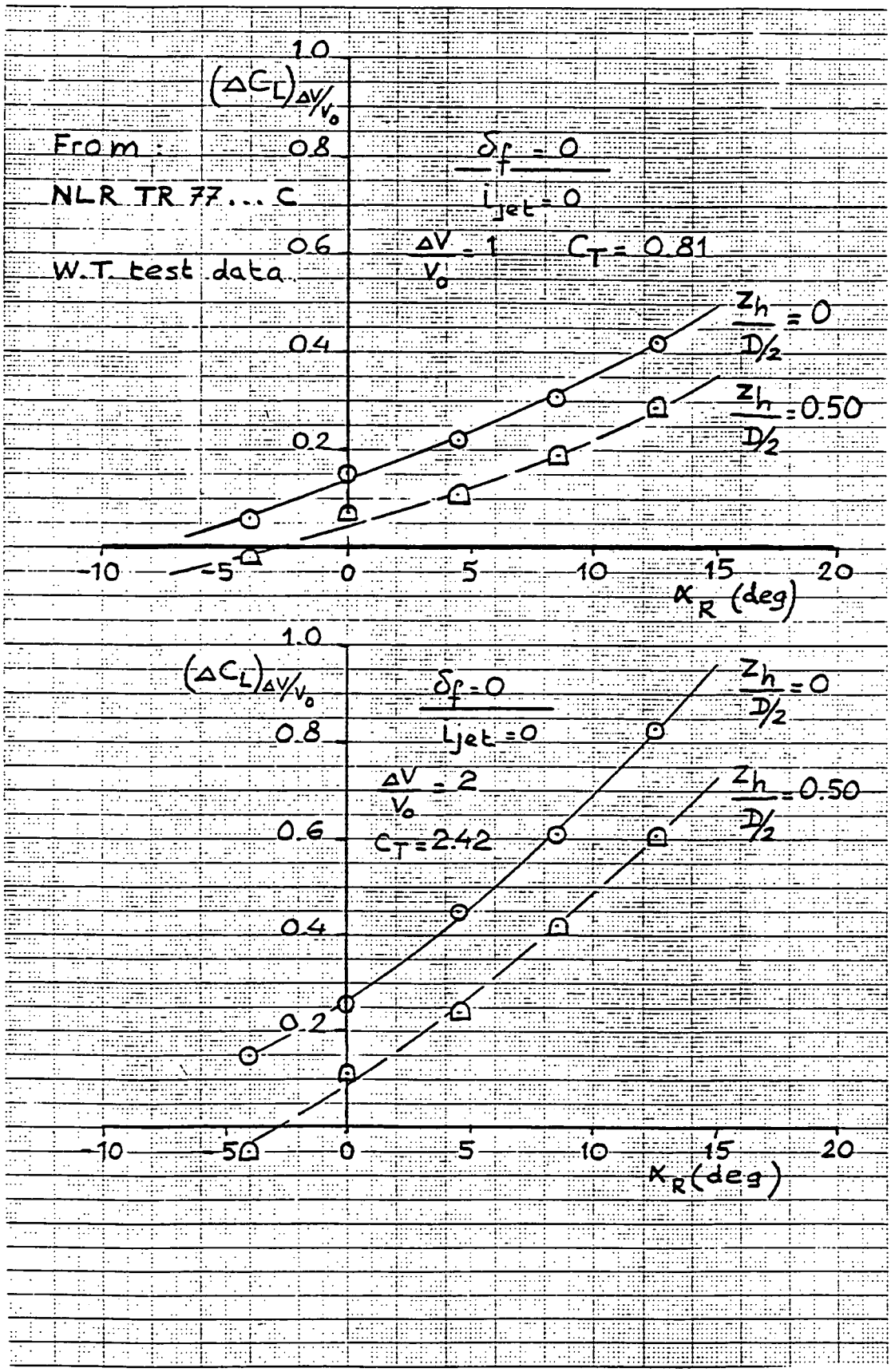
1.0
$(\Delta C_L)_{\Delta V/V_0}$
0.8
0.6
0.4
0.2
From :
NLR TR 77... C
W.T. test data
$\delta_f = 0$
$i_{jet} = 0$
$\frac{\Delta V}{V_0} = 1$
$C_T = 0.81$
$\frac{z_h}{D/2} = 0$
$\frac{z_h}{D/2} = 0.50$
-10
-5
0
5
10
15
20
α_R (deg)
1.0
$(\Delta C_L)_{\Delta V/V_0}$
0.8
0.6
0.4
0.2
$\delta_f = 0$
$i_{jet} = 0$
$\frac{\Delta V}{V_0} = 2$
$C_T = 2.42$
$\frac{z_h}{D/2} = 0$
$\frac{z_h}{D/2} = 0.50$
-10
-5
0
5
10
15
20
α_R (deg)

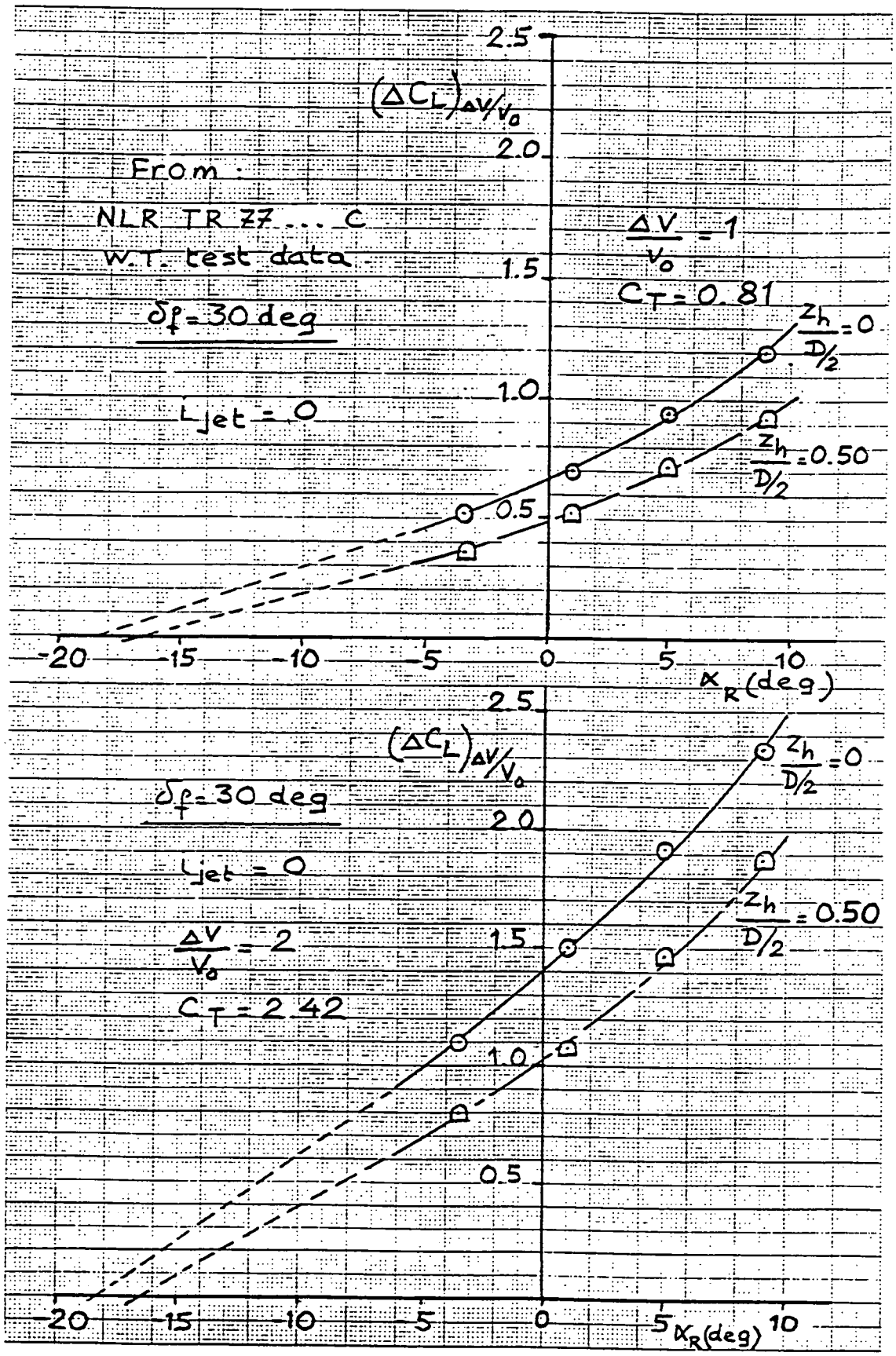
From :
NLR TR 77 ... C
W.T. test data
$\delta_f = 30$ deg
$L_{jet} = 0$
$\frac{\Delta V}{V_0} = 1$
$C_T = 0.81$
$\frac{z_h}{D/2} = 0$
$\frac{z_h}{D/2} = 0.50$
$(\Delta C_L)_{\Delta V/V_0}$
α_R (deg)
$\delta_f = 30$ deg
$L_{jet} = 0$
$\frac{\Delta V}{V_0} = 2$
$C_T = 2.42$
$\frac{z_h}{D/2} = 0$
$\frac{z_h}{D/2} = 0.50$
$(\Delta C_L)_{\Delta V/V_0}$
α_R (deg)

NASA Technical Memorandum 4541

Aerodynamic Characteristics of a Propeller-Powered High-Lift Semispan Wing

The 1-ft-diameter, eight-bladed propeller was a scale model of the SR–7L propeller designed and developed jointly by Hamilton Standard Propellers and NASA Lewis Research Center (ref. 9). The air motor that was used to power the propeller was a compact, high power-to-weight ratio, four-stage turbine designed to deliver approximately 150 hp at 19 000 rpm and was housed in the 5-in-diameter nacelle. The drive air was exhausted through a nozzle at the nacelle exit directly in the nacelle axial direction.

Experiments were conducted at a free-stream dynamic pressure of 15 lb/ft^2 (66.5 knots), which yielded a Reynolds number of 0.66×10^6 based on the wing reference chord of 20 in. Wing angle of attack was varied within the stall boundaries from −30° to 40°. The dynamic pressure and the propeller speeds of 11 000 and 14 000 rpm were selected to simulate highly loaded blade configurations

April 1994

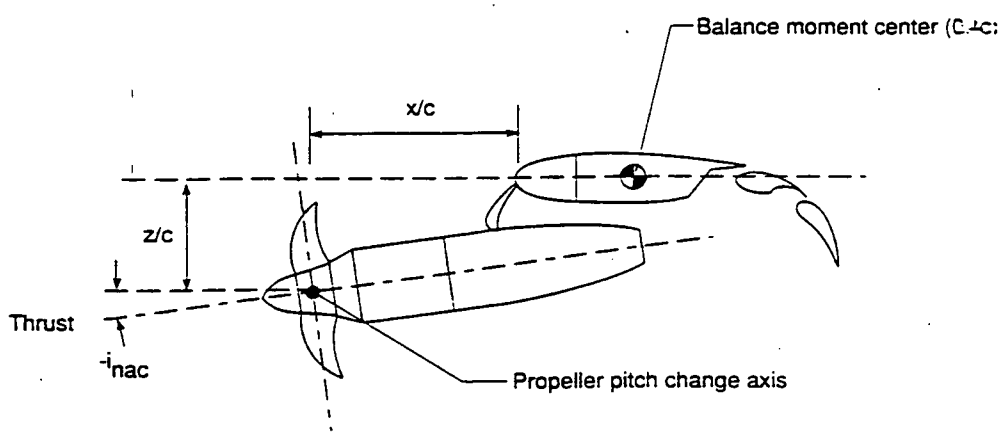

Figure 3. Schematic of propeller-nacelle position.

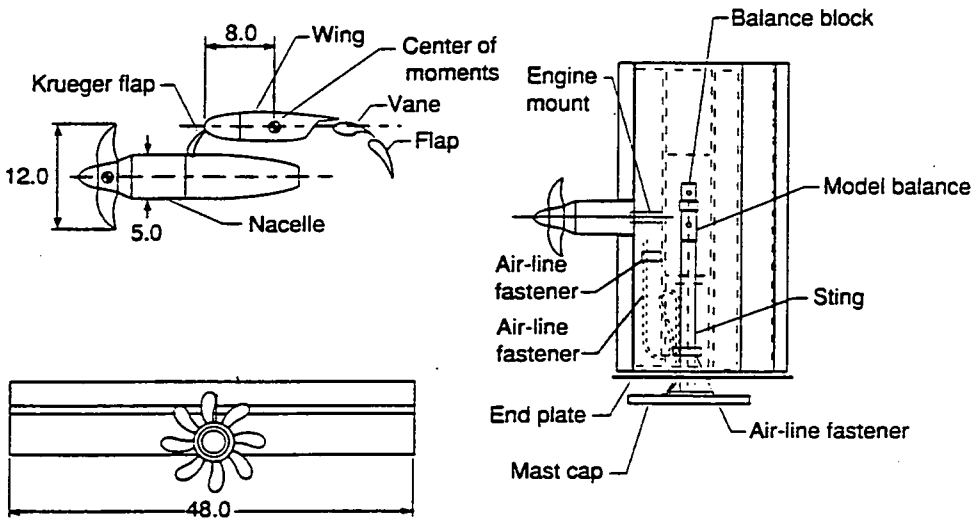

(a) Three-view sketch of semispan high-lift wing with propeller-nacelle assembly.

$\beta_{0.75} = 40$ deg

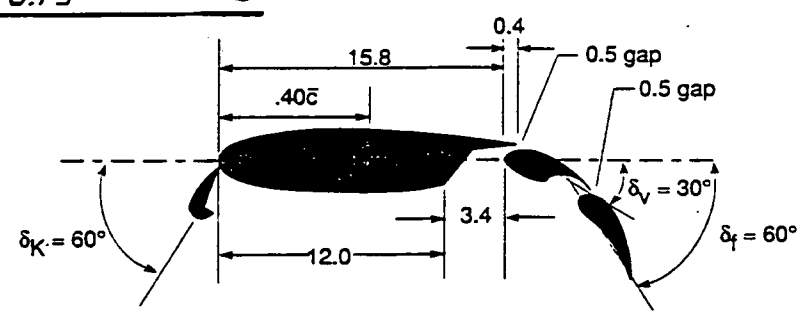

(b) High-lift configuration.

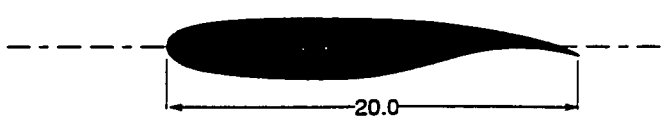

(c) Cruise configuration.

Figure 2. Schematics of test model. All dimensions are in inches.

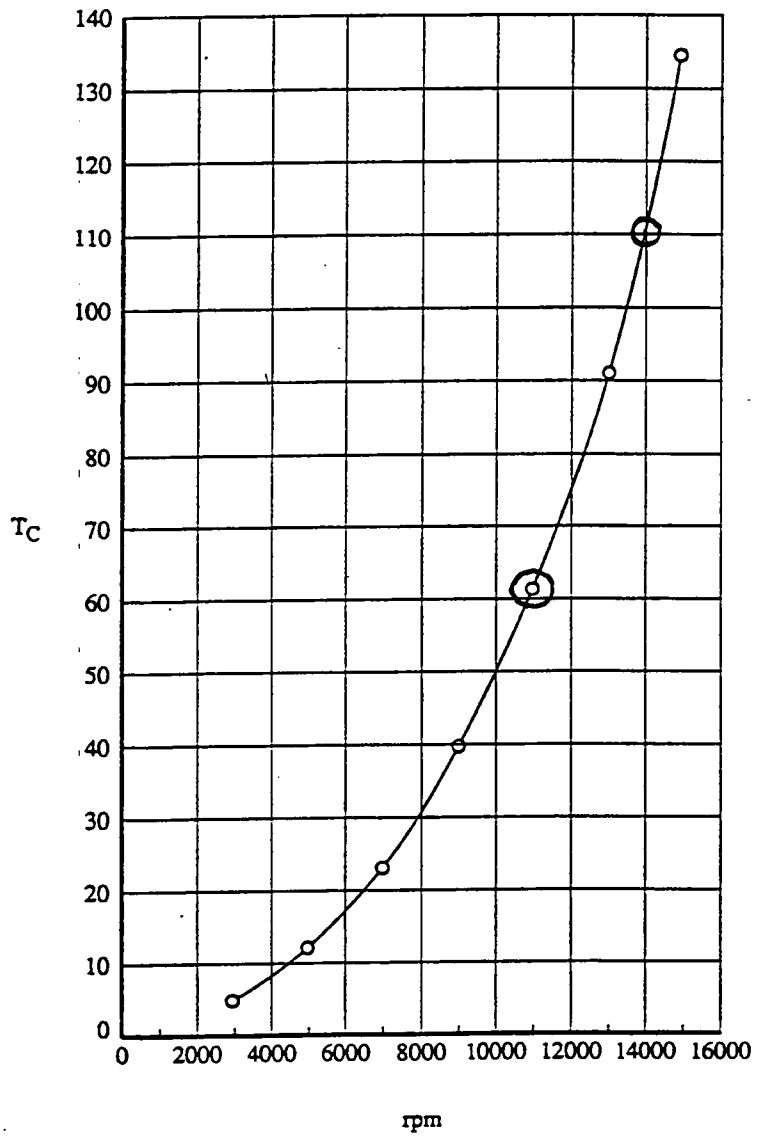

$q_{test} = 15$ lb/sq.ft

$S_w = 960$ sq.in.

Figure 16. Thrust variation with rpm for cruise configuration at static conditions.

If it is assumed that the thrust is constant between V = 0 and 66.5 kts, then:

At 11000 rpm T = 61 lb and $C_T = \frac{61}{15 \times 960/144} = 0.61$

At 14000 rpm T = 110 lb and $C_T = \frac{110}{15 \times 960/144} = 1.10$

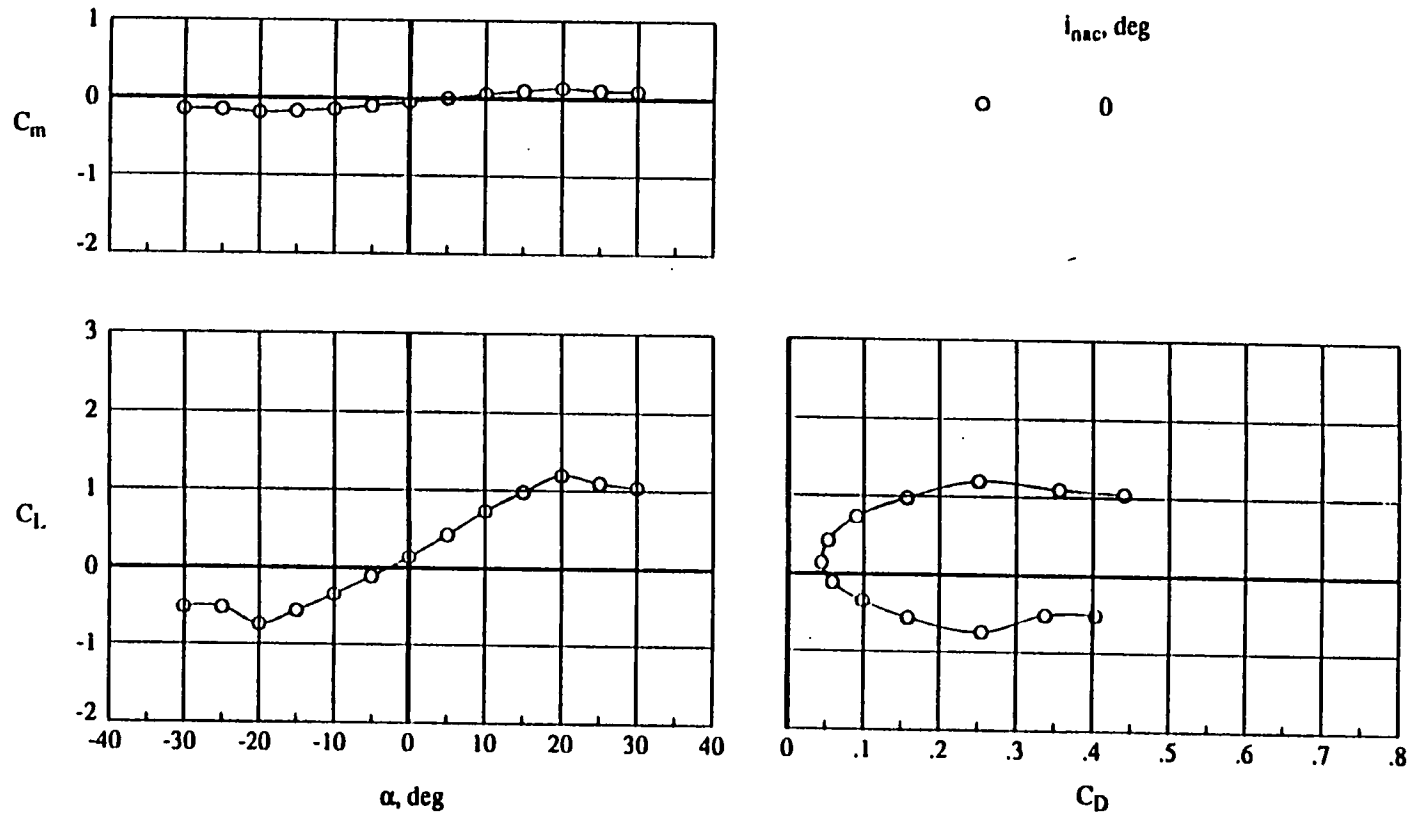

(a) Windmill conditions. $\frac{D/2}{\bar{c}} = 0.30$

Effect of nacelle inclination on aerodynamic characteristics for $q = 15$ lb/ft^2, $x/c = 0.60$, $z/c = 0.25$, and $\delta_f = 0°$.

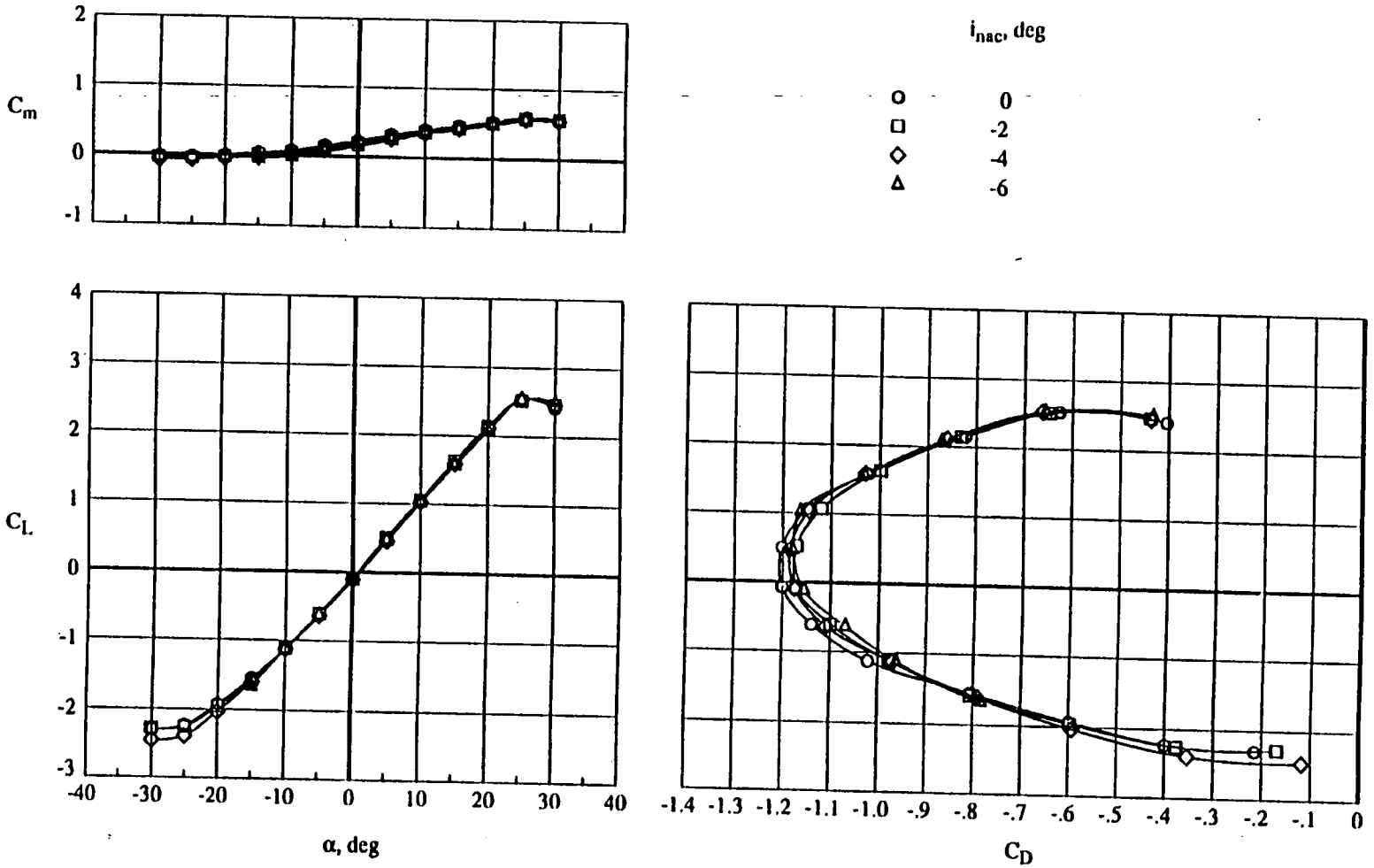

(c) Propeller speed = 14 000 rpm.

Figure 4. Concluded.

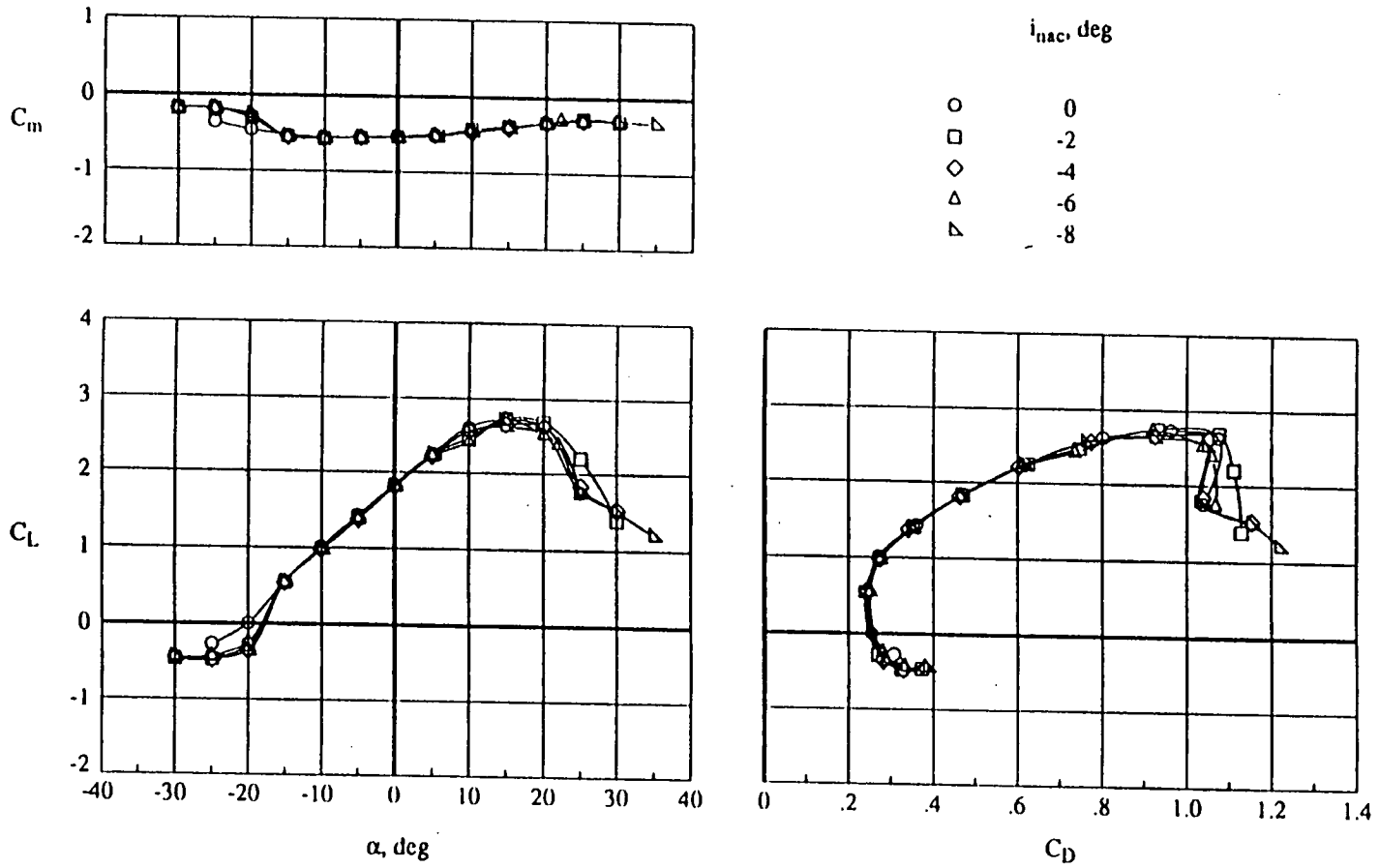

(a) Windmill conditions.

Figure 9. Effect of nacelle inclination on aerodynamic characteristics for $q = 15$ lb/ft^2, $x/c = 0.60$, $z/c = 0.30$, and $\delta_f = 60°$.

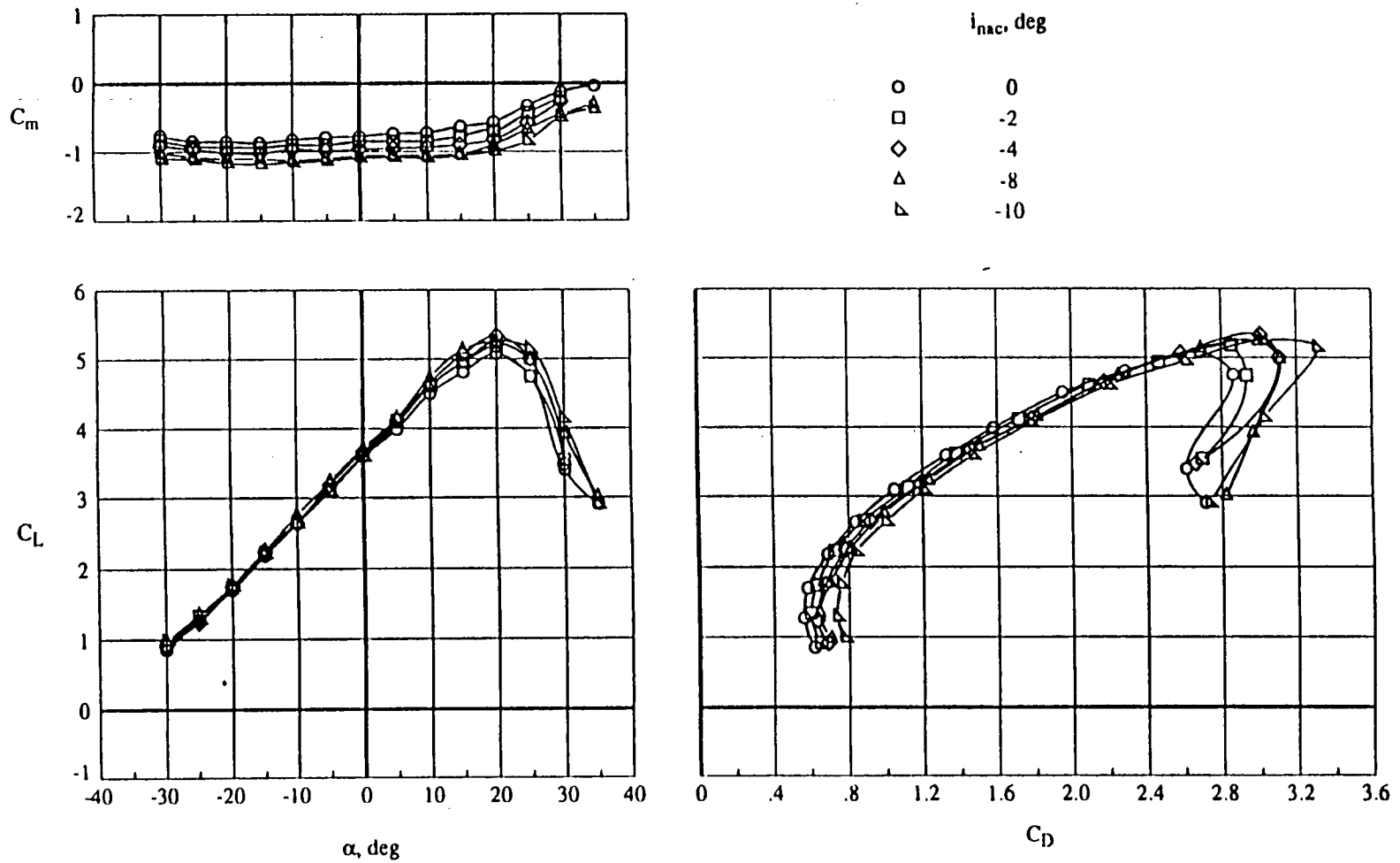

(b) Propeller speed = 14 000 rpm.

Effect of nacelle inclination on thrust-removed aerodynamic characteristics for $q = 15$ lb/ft^2, $\delta_f = 60°$, $x/c = 0.60$, and $z/c = 0.25$.

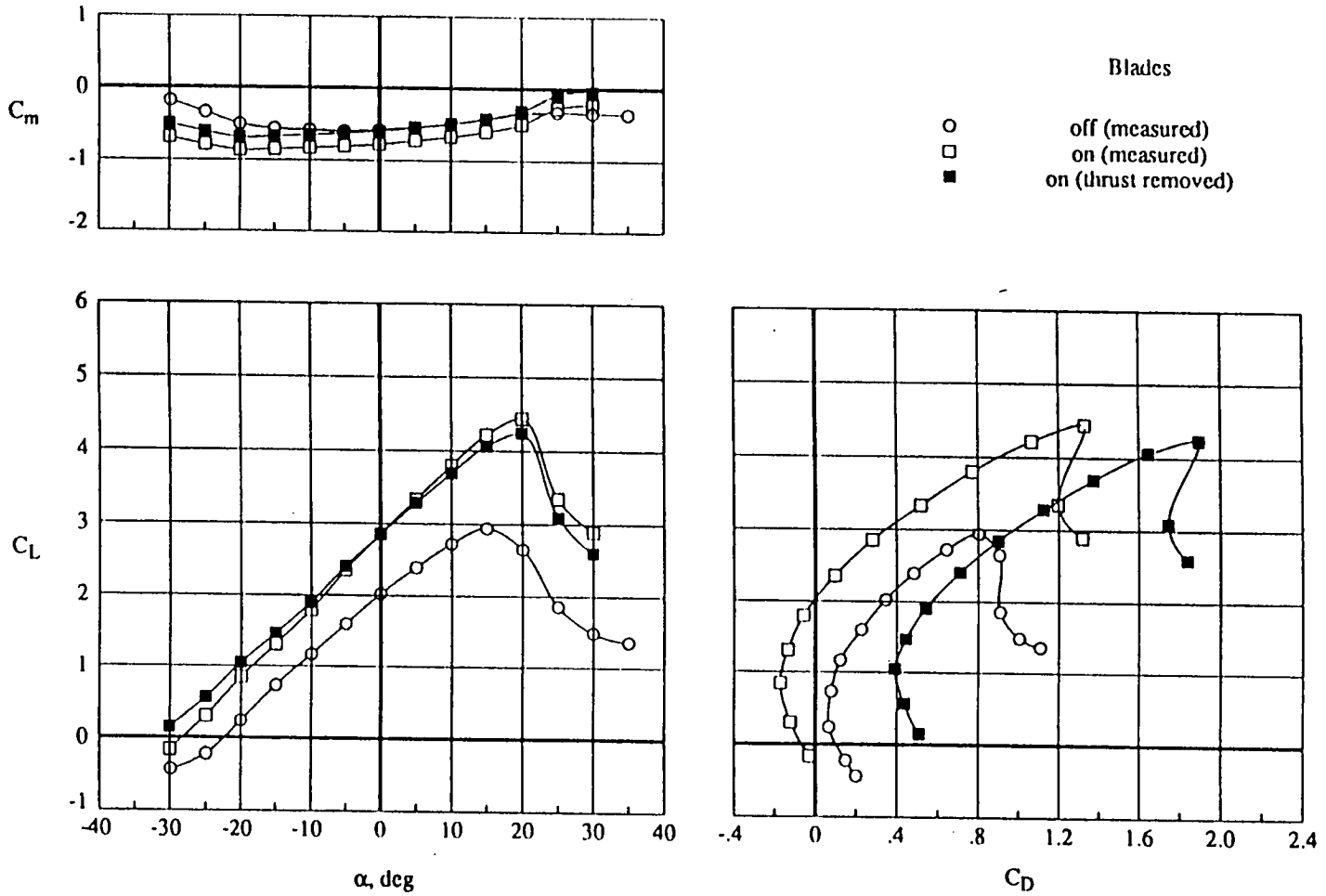

Figure 17. Propeller thrust and slipstream effects on wing aerodynamic characteristics with propeller blades on, and core pressure ratio matched to blades-off configuration for $q = 15$ lb/ft^2, $x/c = 0.60$, $z/c = 0.30$, $\delta_f = 60°$, and Propeller speed = 11 000 rpm.

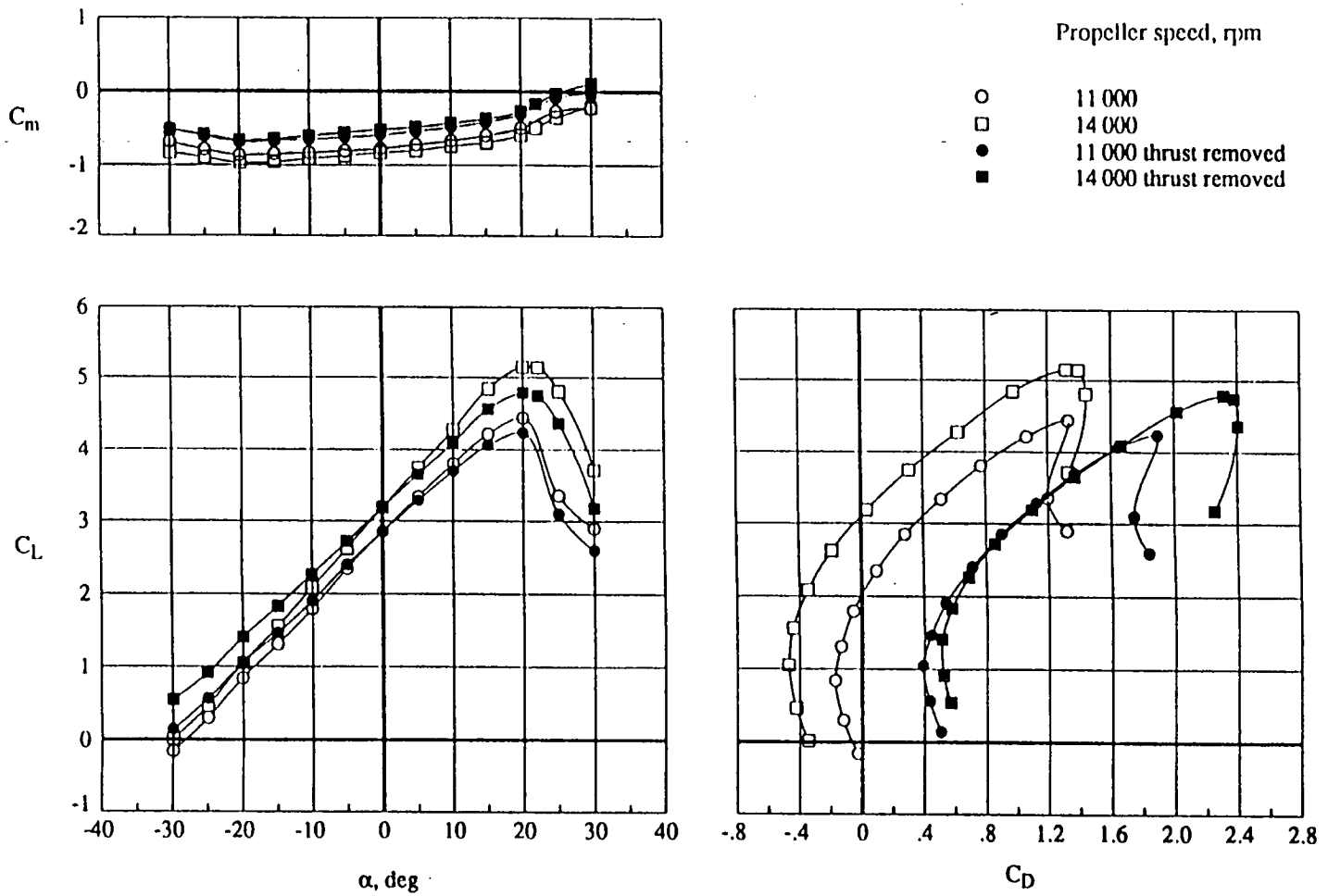

Figure 18. Effect of propeller rotational speed on wing aerodynamic performance for $q = 15$ lb/ft^2, $x/c = 0.60$, $z/c = 0.30$, $\delta_f = 60°$, and $i_{nac} = 0°$.

Appendix XVIII

The effect of the ratio between propeller diameter and wing chord on lift due to slipstream.

Already Smelt and Davies investigated in ref. 6 whether the increase in lift due to the slipstream of a given propeller at a certain thrust coefficient depends on the ratio between the average chord of the wing part submerged in the slipstream and the diameter of the (fully contracted) propeller slipstream.

Their conclusion was that for single propellers on clean wings with propeller-diameter-to-wing-chord ratios as low as $D^*/c_s = 0.58$ this ratio did not affect the lift due to slipstream. However when several propellers were mounted in front of the wing sufficiently close to each other so that their slipstreams merged the increase in lift due to slipstream approached double the increase in lift found with a single propeller at equal thrust.

Jameson, in ref. 31, analysed this question on a theoretical basis, albeit on a simplified mathematical model with a slipstream with square cross-sections. His conclusions agreed in general with those of Smelt and Davies.
He furthermore indicated that also when the slipstream of multiple propellers did not merge this configuration produced more lift than a single propeller at equal thrust. This was attributed to the smaller slipstream height-to-wing chord ratio.

In the present report the slipstream is considered as comparable to the flow around low-aspect-ratio wings as formulated by Jones (ref. 42) and De Young (ref. 43). As mentioned already in chapter 6.1 of the main body of this report the theory of refs. 42 and 43 states that the circulation on a wing with aspect-ratio approaching zero is exclusively determined by the flow angle of the trailing edge independent of the slope of the camber line. For all configurations analysed a better agreement between calculated and windtunnel test data were found however when the angle of attack of the wing part submerged in the slipstream was measured relative to the equivalent flat plate zero-lift angle.

For all cases however the ratio $D^*/c_s > 0.6$ except for the configuration from report NLR TR 77...C presented on page VI-10. On this "four-engined" configuration $D^*/c_s = 0.533$ with the flap extended and deflected to 30 deg.
On pages XVIII-3 and XVIII-4 lift curves both as calculated and as obtained from windtunnel tests are presented for this configuration for three slipstream-to-freestream velocity ratios.
The calculations were performed both according to the standard procedure where the slipstream downwash angle is related to the zero-lift angle and to a procedure related to the flap deflection angle.
Note that the test data lie halfway between the two sets of theoretical curves.

On pages XVIII-5 to XVIII-7 the increase in lift due to slipstream is presented for the configuration shown on page XVIII-7 as calculated according to the standard procedure and as derived from windtunnel tests. The two-engined model was tested with flaps retracted and at flapsettings of 20 and 40 degrees.
At the highest thrust coefficient investigated $D^*/c_s = 0.63$. Good agreement is shown between calculated and test data.
The data analysed in this appendix suggest that the procedure adopted for the determination of lift due to slipstream with flaps deflected is valid for $D^*/c_s > 0.60$.
For lower values of D^*/c_s the slipstream seems to resemble the flow over low-aspect-ratio wings even more. However a more detailed investigation into this subject seems justified before more definite conclusions can be drawn.

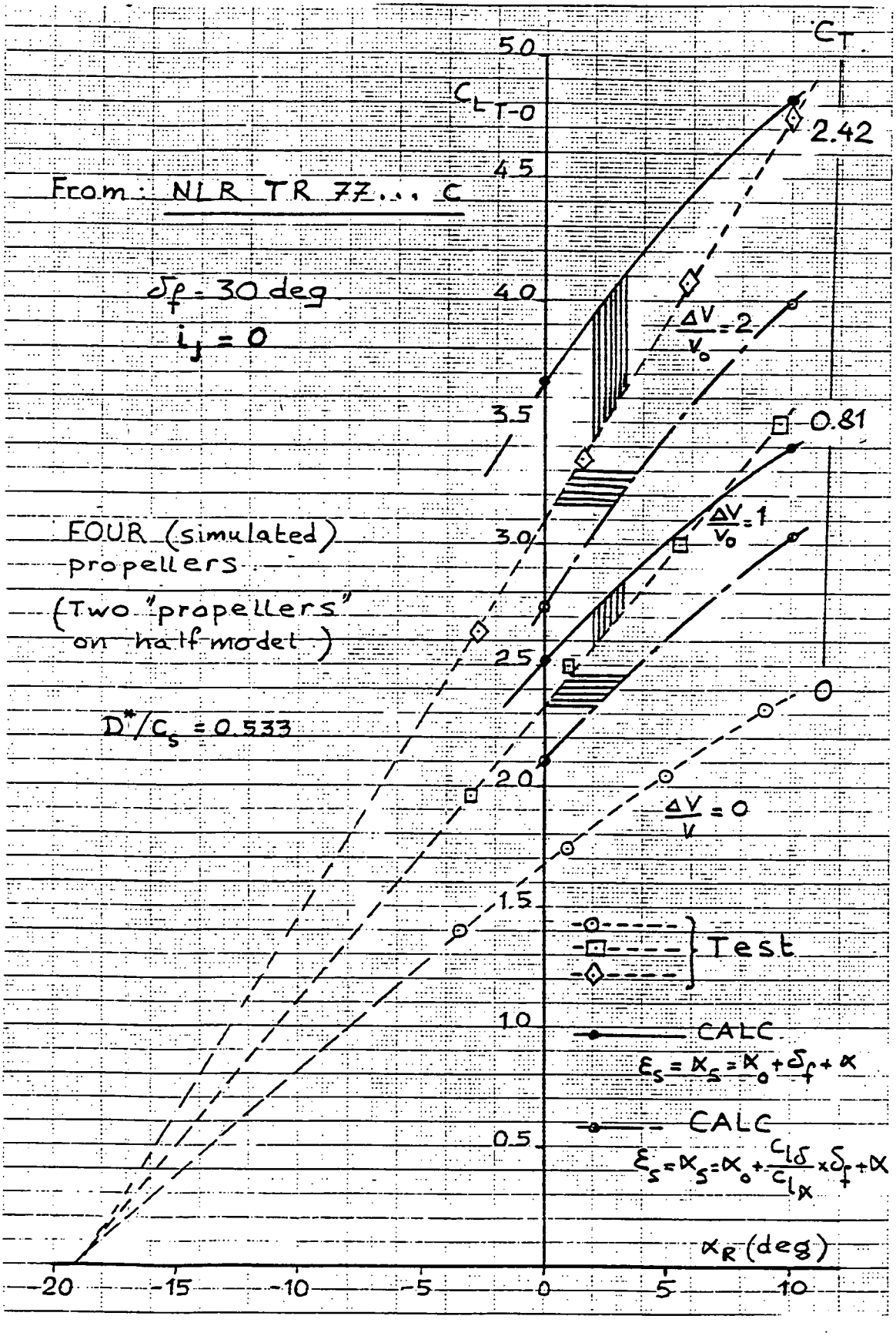
C_T
C_{LT-0}
5.0
4.5
4.0
3.5
3.0
2.5
2.0
1.5
1.0
0.5
2.42
0.81
0
From: NLR TR 77... C
δ_f = 30 deg
i_f = 0
$\frac{\Delta V}{V_0}$ = 2
$\frac{\Delta V}{V_0}$ = 1
$\frac{\Delta V}{V}$ = 0
FOUR (simulated) propellers
(Two "propellers" on half model)
D^*/C_s = 0.533
Test
CALC
$\varepsilon_s = \alpha_s = \alpha_0 + \delta_f + \alpha$
CALC
$\varepsilon_s = \alpha_s = \alpha_0 + \frac{c_{l\delta}}{c_{l\alpha}} \times \delta_f + \alpha$
α_R (deg)
-20
-15
-10
-5
0
5
10

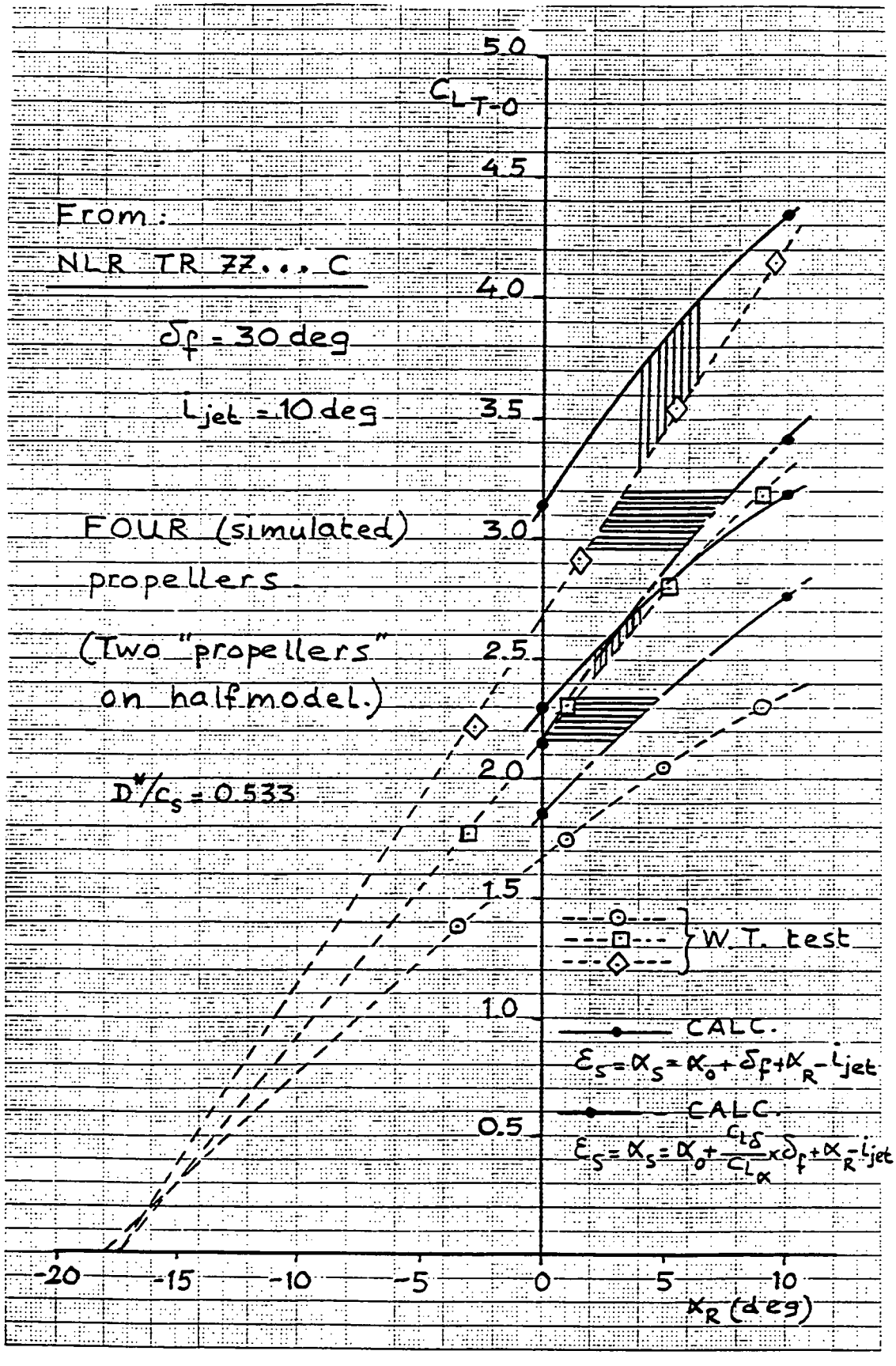
From:
NLR TR ZZ... C
δ_f = 30 deg
i_{jet} = 10 deg
FOUR (simulated) propellers
(Two "propellers" on halfmodel.)
D^*/c_s = 0.533
$C_{L_{T-0}}$
5.0
4.5
4.0
3.5
3.0
2.5
2.0
1.5
1.0
0.5
W.T. test
CALC.
$\varepsilon_s = \alpha_s = \alpha_0 + \delta_f + \alpha_R - i_{jet}$
CALC.
$\varepsilon_s = \alpha_s = \alpha_0 + \frac{C_{L\delta}}{C_{L\alpha}} \times \delta_f + \alpha_R - i_{jet}$
-20
-15
-10
-5
0
5
10
α_R (deg)

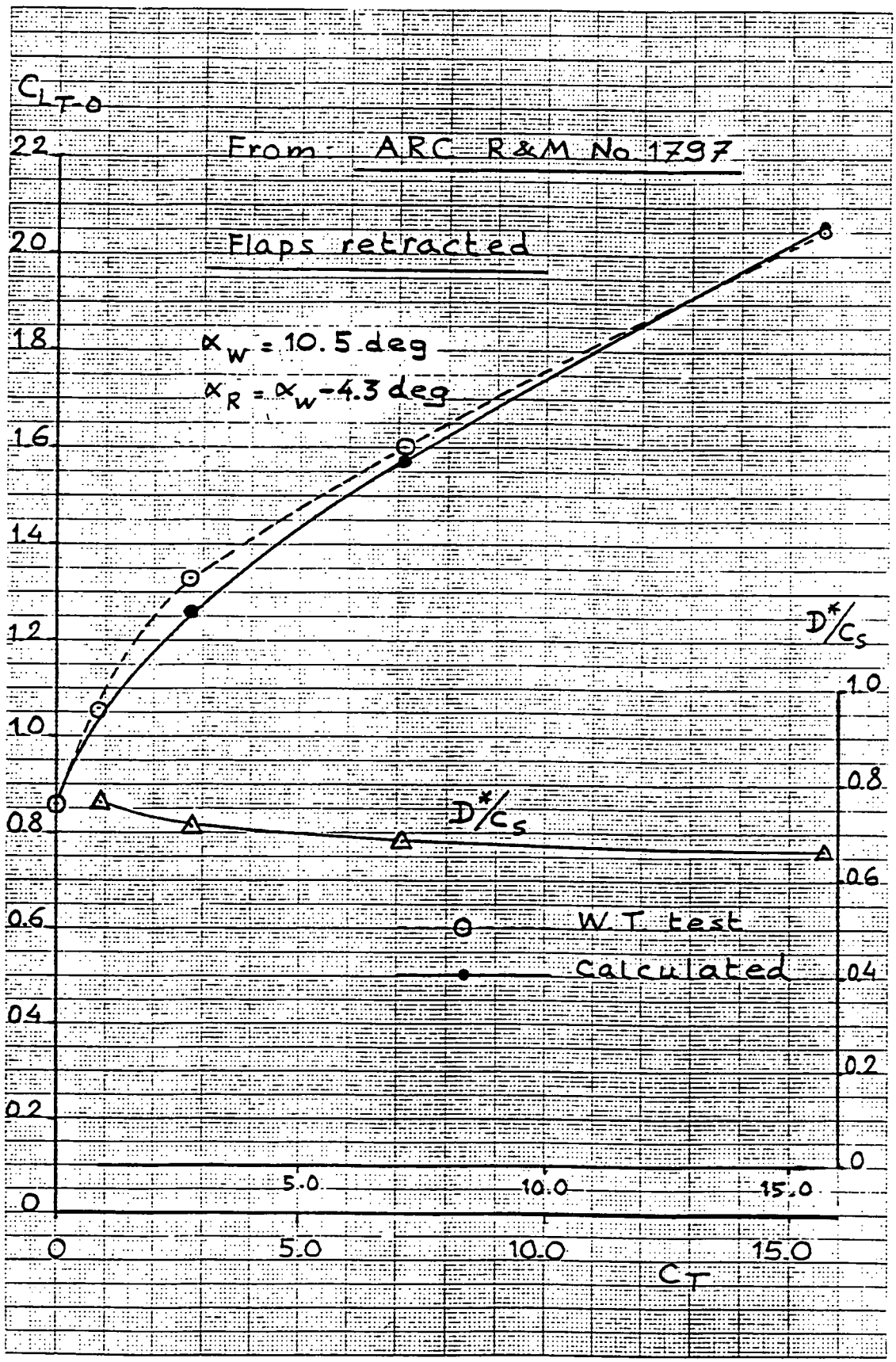
$C_{L_{T-0}}$
From ARC R&M No 1797
Flaps retracted
$\alpha_W = 10.5$ deg
$\alpha_R = \alpha_W - 4.3$ deg
D^*/C_S
D^*/C_S
W.T test
Calculated
C_T
22
20
18
16
14
12
10
0.8
0.6
04
02
0
5.0
10.0
15.0
1.0
0.8
0.6
04
0.2
0

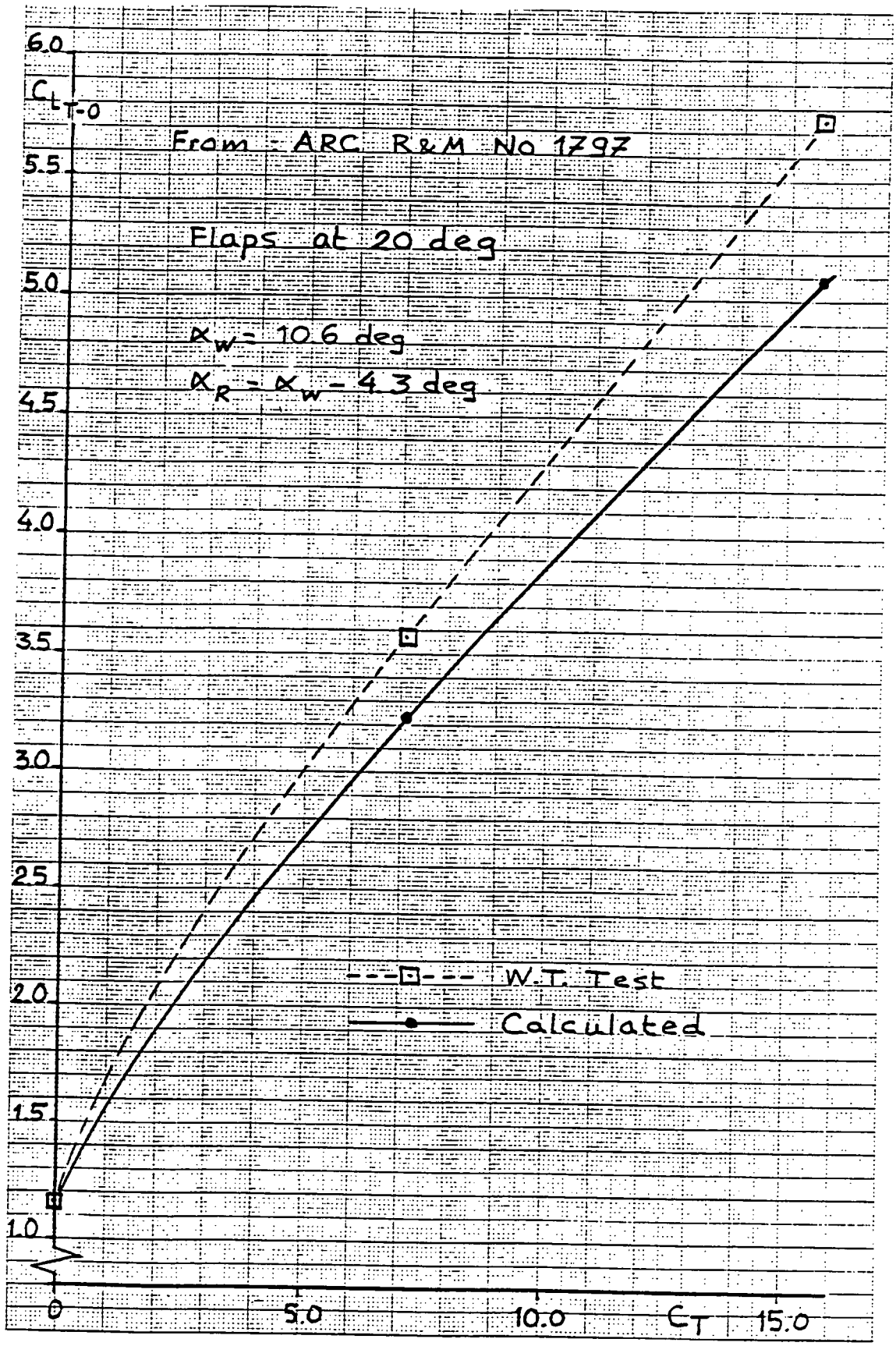
6.0
$C_{L_{T-0}}$
From - ARC. R&M No 1797
5.5
Flaps at 20 deg
5.0
α_W = 10.6 deg
$\alpha_R = \alpha_W - 4.3$ deg
4.5
4.0
3.5
3.0
2.5
2.0
W.T. Test
Calculated
1.5
1.0
0
5.0
10.0
C_T
15.0

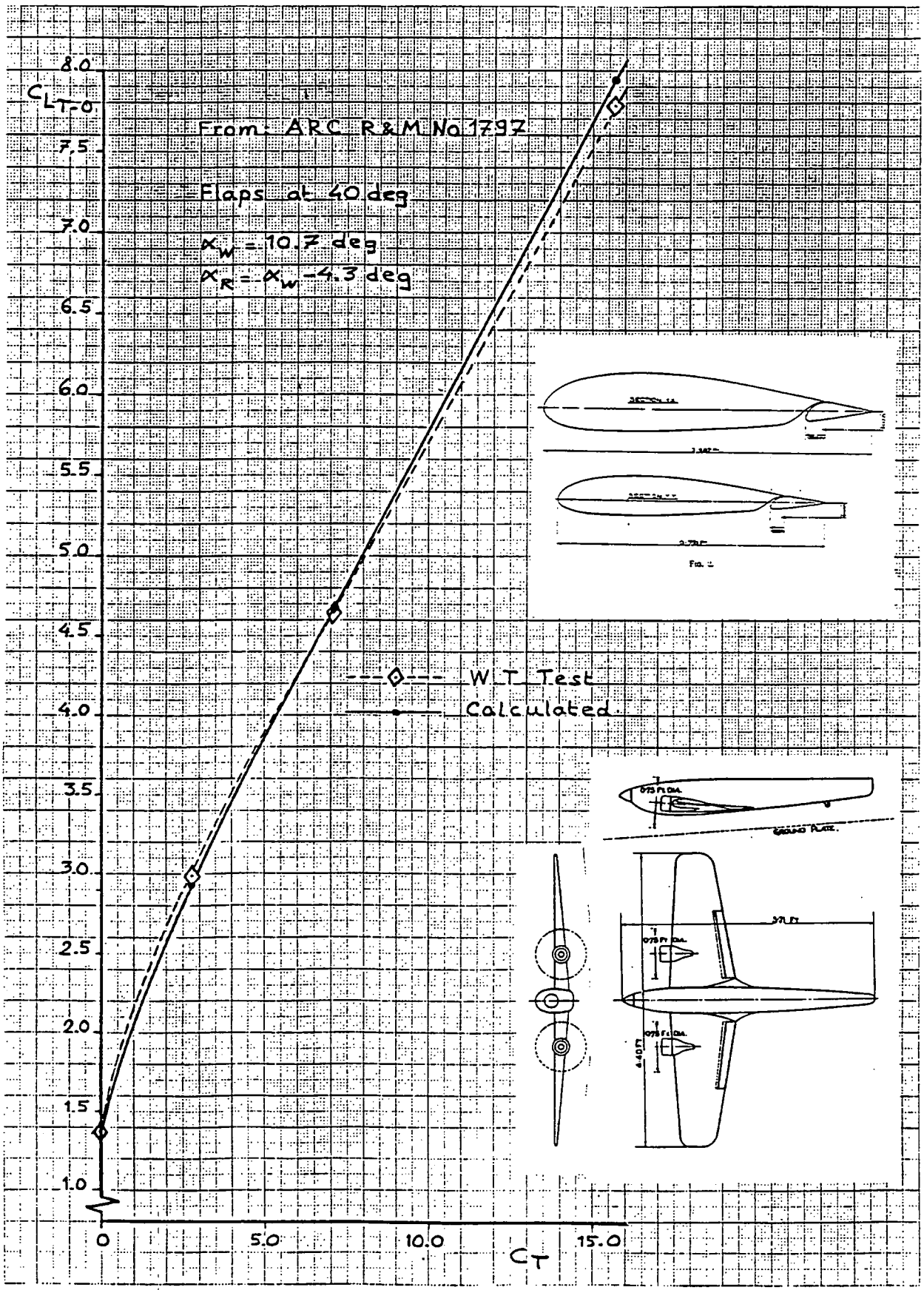
8.0
C_{LT-0}
7.5
7.0
6.5
6.0
5.5
5.0
4.5
4.0
3.5
3.0
2.5
2.0
1.5
1.0
0
5.0
10.0
15.0
C_T
From ARC R&M No 1797
Flaps at 40 deg
α_W = 10.7 deg
$\alpha_R = \alpha_W - 4.3$ deg
W.T. Test
Calculated